

Book: Quantum Mechanics in Chemistry
(Simons and Nichols)

This text is disseminated via the Open Education Resource (OER) LibreTexts Project (<https://LibreTexts.org>) and like the hundreds of other texts available within this powerful platform, it is freely available for reading, printing and "consuming." Most, but not all, pages in the library have licenses that may allow individuals to make changes, save, and print this book. Carefully consult the applicable license(s) before pursuing such effects.

Instructors can adopt existing LibreTexts texts or Remix them to quickly build course-specific resources to meet the needs of their students. Unlike traditional textbooks, LibreTexts' web based origins allow powerful integration of advanced features and new technologies to support learning.



The LibreTexts mission is to unite students, faculty and scholars in a cooperative effort to develop an easy-to-use online platform for the construction, customization, and dissemination of OER content to reduce the burdens of unreasonable textbook costs to our students and society. The LibreTexts project is a multi-institutional collaborative venture to develop the next generation of open-access texts to improve postsecondary education at all levels of higher learning by developing an Open Access Resource environment. The project currently consists of 14 independently operating and interconnected libraries that are constantly being optimized by students, faculty, and outside experts to supplant conventional paper-based books. These free textbook alternatives are organized within a central environment that is both vertically (from advance to basic level) and horizontally (across different fields) integrated.

The LibreTexts libraries are Powered by [NICE CXOne](#) and are supported by the Department of Education Open Textbook Pilot Project, the UC Davis Office of the Provost, the UC Davis Library, the California State University Affordable Learning Solutions Program, and Merlot. This material is based upon work supported by the National Science Foundation under Grant No. 1246120, 1525057, and 1413739.

Any opinions, findings, and conclusions or recommendations expressed in this material are those of the author(s) and do not necessarily reflect the views of the National Science Foundation nor the US Department of Education.

Have questions or comments? For information about adoptions or adaptations contact info@LibreTexts.org. More information on our activities can be found via Facebook (<https://facebook.com/Libretexts>), Twitter (<https://twitter.com/libretexts>), or our blog (<http://Blog.Libretexts.org>).

This text was compiled on 03/10/2025

TABLE OF CONTENTS

Licensing

1: The Basic Tools of Quantum Mechanics

- 1.1: Operators
- 1.2: Wavefunctions
- 1.3: The Schrödinger Equation
- 1.4: Free-Particle Motion in Two Dimensions
- 1.5: Particles in Boxes
- 1.6: One Electron Moving About a Nucleus
- 1.7: Harmonic Vibrational Motion
- 1.8: Rotational Motion for a Rigid Diatomic Molecule
- 1.9: The Physical Relevance of Wavefunctions, Operators and Eigenvalues

2: Approximation Methods

- 2.1: The Variational Method
- 2.2: Perturbation Theory
- 2.E: Approximation Methods (Exercises)

3: Nuclear Motion

- 3.1: The Born-Oppenheimer Separation of Electronic and Nuclear Motions
- 3.2: Time Scale Separation
- 3.3: Vibration/Rotation States for Each Electronic Surface
- 3.4: Rotation and Vibration of Diatomic Molecules
- 3.5: Separation of Vibration and Rotation
- 3.6: The Rigid Rotor and Harmonic Oscillator
- 3.7: The Morse Oscillator
- 3.8: Rotation of Polyatomic Molecules
- 3.9: Rotation of Linear Molecules
- 3.E: Exercises
- 3.10: Rotation of Non-Linear Molecules
- 3.11: Chapter Summary

4: Atomic Orbitals

- 4.1: Shapes of Atomic Orbitals
- 4.2: Directions of Atomic Orbitals
- 4.3: Sizes and Energies

5: Molecular Orbitals

- 5.1: Orbital Interaction Topology
- 5.2: Orbital Symmetry
- 5.3: Linear Molecules
- 5.4: Atoms

6: Quantum Mechanics in Reactions

- 6.1: Reduction in Symmetry Along Reaction Paths
- 6.2: Orbital Correlation Diagrams - Origins of the Woodward-Hoffmann Rules

7: Further Characterization of Molecular Orbitals

- 7.1: The LCAO-MO Expansion and the Orbital-Level Schrödinger Equation
- 7.2: Determining the Effective Potential
- 7.3: The Hückel Parameterization
- 7.4: The Extended Hückel Method

8: Electronic Configurations

- 8.1: Orbitals Do Not Provide the Complete Picture; Their Occupancy By the N Electrons Must Be Specified
- 8.2: Even N-Electron Configurations are Not Mother Nature's True Energy States
- 8.3: Mean-Field Models
- 8.4: Configuration Interaction (CI) Describes the Correct Electronic States
- 8.5: Summary

9: Symmetry of Electronic Wavefunctions

- 9.1: Electronic Configurations
- 9.2: Antisymmetric Wavefunctions

10: Angular Momentum and Group Symmetries of Electronic Wavefunctions

- 10.1: Angular Momentum Symmetry and Strategies for Angular Momentum Coupling
- 10.2: Electron Spin Angular Momentum
- 10.3: Coupling of Angular Momenta
- 10.4: Atomic Term Symbols and Wavefunctions
- 10.5: Atomic Configuration Wavefunctions
- 10.6: Inversion Symmetry
- 10.7: Review of Atomic Cases

11: Evaluating the Matrix Elements of N-electron Wavefunctions

- 11.1: Configuration State Functions can Express the Full N-Electron Wavefunction
- 11.2: The Slater-Condon Rules Give Expressions for the Operator Matrix Elements Among the CSFs
- 11.3: The Slater-Condon Rules
- 11.4: Examples of Applying the Slater-Condon Rules
- 11.S: Evaluating the Matrix Elements of N-electron Wavefunctions (Summary)

12: Quantum Mechanical Picture of Bond Making and Breaking Reactions

- 12.1: Concepts of Configuration and State Energies
- 12.2: Mixing of Covalent and Ionic Configurations
- 12.3: Various Types of Configuration Mixing

13: Molecular Rotation and Vibration

- 13.1: Rotational Motions of Rigid Molecules
- 13.2: Vibrational Motion Within the Harmonic Approximation
- 13.3: Anharmonicity

14: Time-dependent Quantum Dynamics

- 14.1: Time-Dependent Vector Potentials
- 14.2: Time-Dependent Perturbation Theory
- 14.3: Application to Electromagnetic Perturbations
- 14.4: The "Long-Wavelength" Approximation
- 14.5: The Kinetics of Photon Absorption and Emission

15: Spectroscopy

- 15.1: Rotational Transitions
- 15.2: Vibration-Rotation Transitions
- 15.3: Electronic-Vibration-Rotation Transitions
- 15.4: Time Correlation Function Expressions for Transition Rates

16: Collisions and Scattering

- 16.1: One Dimensional Scattering
- 16.2: Multichannel Problems
- 16.3: Classical Treatment of Nuclear Motion
- 16.4: Wavepackets

17: Higher Order Corrections to Electronic Structure

- 17.1: Orbitals, Configurations, and the Mean-Field Potential
- 17.2: Electron Correlation Requires Moving Beyond a Mean-Field Model
- 17.3: Moving from Qualitative to Quantitative Models
- 17.4: Atomic Units

18: Multiconfiguration Wavefunctions

- 18.1: Optimization of the Energy for a Multiconfiguration Wavefunction
- 18.2: The Single-Determinant Wavefunction
- 18.3: The Unrestricted Hartree-Fock Spin Impurity Problem
- 18.4: Atomic Orbital Basis Sets
- 18.5: The LCAO-MO Expansion
- 18.6: The Roothaan Matrix SCF Process
- 18.7: Observations on Orbitals and Orbital Energies

19: Multi-Determinant Wavefunctions

- 19.1: Introduction to Multi-Determinant Wavefunctions
- 19.2: Different Methods
- 19.3: Strengths and Weaknesses of Various Methods
- 19.4: Further Details on Implementing Multiconfigurational Methods

20: Response Theory

- 20.1: Calculations of Properties Other Than the Energy
- 20.2: Ab Initio, Semi-Empirical, and Empirical Force Field Methods

21: Problem Sets

22: Problems

- 22.1: The Basic Tools of Quantum Mechanics
 - 22.1.1: i. Review Exercises
 - 22.1.2: ii. Exercises
 - 22.1.3: iii. Problems 1-10
 - 22.1.4: iv. Problems 11-18
 - 22.1.5: v. Review Exercise Solutions
 - 22.1.6: vi. Exercise Solutions
- 22.2: Simple Molecular Orbital Theory
 - 22.2.1: i. Review Exercises
 - 22.2.2: ii. Exercises
 - 22.2.3: iii. Problems
 - 22.2.4: iv. Review Exercises Solutions
 - 22.2.5: v. Exercise Solution
 - 22.2.6: vi. Problem Solutions
- 22.3: Electronic Configurations, Term Symbols, and States
 - 22.3.1: i. Review Exercises
 - 22.3.2: ii. Exercises
 - 22.3.3: iii. Problems
 - 22.3.4: iv. Review Exercise Solutions
 - 22.3.5: v. Exercise Solutions
 - 22.3.6: vi. Problem Solutions
- 22.4: Molecular Rotation and Vibration
 - 22.4.1: i. Exercises
 - 22.4.2: ii. Problems
 - 22.4.3: iii. Exercise Solutions
 - 22.4.4: iv. Problem Solutions
- 22.5: Time Dependent Processes
 - 22.5.1: i. Exercises
 - 22.5.2: ii. Problems
 - 22.5.3: iii. Exercise Solutions
 - 22.5.4: iv. Problem Solutions
- 22.6: More Quantitative Aspects of Electronic Structure Calculations
 - 22.6.1: i. Review Exercises
 - 22.6.2: i. Review Exercises-
 - 22.6.3: ii. Exercises
 - 22.6.4: iii. Problems
 - 22.6.5: iv. Review Exercise Solutions
 - 22.6.6: v. Exercise Solutions
 - 22.6.7: vi. Problem Solutions

[Index](#)

[Glossary](#)

[Detailed Licensing](#)

Licensing

A detailed breakdown of this resource's licensing can be found in [Back Matter/Detailed Licensing](#).

CHAPTER OVERVIEW

1: The Basic Tools of Quantum Mechanics

Quantum Mechanics Describes Matter in Terms of Wavefunctions and Energy Levels and physical Measurements are Described in Terms of Operators Acting on Wavefunctions

- 1.1: Operators
- 1.2: Wavefunctions
- 1.3: The Schrödinger Equation
- 1.4: Free-Particle Motion in Two Dimensions
- 1.5: Particles in Boxes
- 1.6: One Electron Moving About a Nucleus
- 1.7: Harmonic Vibrational Motion
- 1.8: Rotational Motion for a Rigid Diatomic Molecule
- 1.9: The Physical Relevance of Wavefunctions, Operators and Eigenvalues

This page titled [1: The Basic Tools of Quantum Mechanics](#) is shared under a [CC BY-NC-SA 4.0](#) license and was authored, remixed, and/or curated by [Jack Simons](#) via [source content](#) that was edited to the style and standards of the LibreTexts platform.

1.1: Operators

Each physically measurable quantity has a corresponding operator. The eigenvalues of the operator tell the values of the corresponding physical property that can be observed

In quantum mechanics, any experimentally measurable physical quantity F (e.g., energy, dipole moment, orbital angular momentum, spin angular momentum, linear momentum, kinetic energy) whose classical mechanical expression can be written in terms of the cartesian positions $\{q_i\}$ and momenta $\{p_i\}$ of the particles that comprise the system of interest is assigned a corresponding quantum mechanical operator \mathbf{F} . Given F in terms of the $\{q_i\}$ and $\{p_i\}$, \mathbf{F} is formed by replacing p_j by $-i\hbar\frac{\partial}{\partial q_j}$ and leaving q_j untouched. For example, if

$$F = \sum_{i=1}^N \left(\frac{p_i^2}{2m_i} + \frac{1}{2}k(q_i - q_i^0)^2 + L(q_i - q_i^0) \right)$$

then

$$F = \sum_{i=1}^N \left(\frac{-\hbar^2}{2m_i} \frac{\partial^2}{\partial q_i^2} + \frac{1}{2}k(q_i - q_i^0)^2 + L(q_i - q_i^0) \right)$$

The x-component of the dipole moment for a collection of N particles has

$$F = \sum_{j=1}^N Z_j e x_j$$

and

$$F = \sum_{j=1}^N Z_j e x_j$$

where $Z_j e$ is the charge on the j^{th} particle.

The mapping from F to \mathbf{F} is straightforward only in terms of cartesian coordinates. To map a classical function F , given in terms of curvilinear coordinates (even if they are orthogonal), into its quantum operator is not at all straightforward. Interested readers are referred to Kemble's text on quantum mechanics which deals with this matter in detail. The mapping can always be done in terms of cartesian coordinates after which a transformation of the resulting coordinates and differential operators to a curvilinear system can be performed. The corresponding transformation of the kinetic energy operator to spherical coordinates is treated in detail in Appendix A. The text by EWK also covers this topic in considerable detail.

The relationship of these quantum mechanical operators to experimental measurement will be made clear later in this chapter. For now, suffice it to say that these operators define equations whose solutions determine the values of the corresponding physical property that can be observed when a measurement is carried out; only the values so determined can be observed. This should suggest the origins of quantum mechanics' prediction that some measurements will produce **discrete** or **quantized** values of certain variables (e.g., energy, angular momentum, etc.).

This page titled [1.1: Operators](#) is shared under a [CC BY-NC-SA 4.0](#) license and was authored, remixed, and/or curated by [Jack Simons](#) via [source content](#) that was edited to the style and standards of the LibreTexts platform.

1.2: Wavefunctions

The eigenfunctions of a quantum mechanical operator depend on the coordinates upon which the operator acts; these functions are called wavefunctions

In addition to operators corresponding to each physically measurable quantity, quantum mechanics describes the state of the system in terms of a wavefunction Ψ that is a function of the coordinates $\{q_j\}$ and of time t . The function $|\Psi(q_j, t)|^2 = \Psi^* \Psi$ gives the probability density for observing the coordinates at the values q_j at time t . For a many-particle system such as the H_2O molecule, the wavefunction depends on many coordinates. For the H_2O example, it depends on the x , y , and z (or r , q , and ϕ) coordinates of the ten electrons and the x , y , and z (or r , q , and ϕ) coordinates of the oxygen nucleus and of the two protons; a total of thirty-nine coordinates appear in Ψ .

In classical mechanics, the coordinates q_j and their corresponding momenta p_j are functions of time. The state of the system is then described by specifying $q_j(t)$ and $p_j(t)$. In quantum mechanics, the concept that q_j is known as a function of time is replaced by the concept of the probability density for finding q_j at a particular value at a particular time t : $|\Psi(q_j, t)|^2$. Knowledge of the corresponding momenta as functions of time is also relinquished in quantum mechanics; again, only knowledge of the probability density for finding p_j with any particular value at a particular time t remains.

This page titled [1.2: Wavefunctions](#) is shared under a [CC BY-NC-SA 4.0](#) license and was authored, remixed, and/or curated by [Jack Simons](#) via [source content](#) that was edited to the style and standards of the LibreTexts platform.

1.3: The Schrödinger Equation

The Time-Dependent Schrödinger Equation

How to extract from $\Psi(q_j, t)$ knowledge about momenta is treated, where the structure of quantum mechanics, the use of operators and wavefunctions to make predictions and interpretations about experimental measurements, and the origin of 'uncertainty relations' such as the well known Heisenberg uncertainty condition dealing with measurements of coordinates and momenta are also treated.

Before moving deeper into understanding what quantum mechanics 'means', it is useful to learn how the wavefunctions Ψ are found by applying the basic equation of quantum mechanics, the *Schrödinger equation*, to a few exactly soluble model problems. Knowing the solutions to these 'easy' yet chemically very relevant models will then facilitate learning more of the details about the structure of quantum mechanics because these model cases can be used as 'concrete examples'.

The Schrödinger equation is a differential equation depending on time and on all of the spatial coordinates necessary to describe the system at hand (thirty-nine for the H_2O example cited above). It is usually written

$$\mathbf{H}\Psi = i\hbar \frac{\partial \Psi}{\partial t}$$

where $\Psi(q_j, t)$ is the unknown wavefunction and \mathbf{H} is the operator corresponding to the total energy physical property of the system. This operator is called the Hamiltonian and is formed, as stated above, by first writing down the classical mechanical expression for the total energy (kinetic plus potential) in Cartesian coordinates and momenta and then replacing all classical momenta p_j by their quantum mechanical operators $p_j = -i\hbar \frac{\partial}{\partial q_j}$.

For the H_2O example used above, the classical mechanical energy of all thirteen particles is

$$E = \sum_i \left(\frac{p_i^2}{2m_e} + \frac{1}{2} \sum_j \frac{e^2}{r_{i,j}} - \sum_a Z_a \frac{e^2}{r_{i,a}} \right) + \sum_a \left(-\frac{\hbar^2}{2m_a} \frac{\partial^2}{\partial q_a^2} + \frac{1}{2} \sum_b Z_a Z_b \frac{e^2}{r_{a,b}} \right)$$

where the indices i and j are used to label the ten electrons whose thirty cartesian coordinates are $\{q_i\}$ and a and b label the three nuclei whose charges are denoted $\{Z_a\}$, and whose nine cartesian coordinates are $\{q_a\}$. The electron and nuclear masses are denoted m_e and $\{m_a\}$, respectively.

The corresponding Hamiltonian operator is

$$\mathbf{H} = \sum_i \left(-\left(\frac{\hbar^2}{2m_e} \right) \frac{\partial^2}{\partial q_i^2} + \frac{1}{2} \sum_j \frac{e^2}{r_{i,j}} - \sum_a Z_a \frac{e^2}{r_{i,a}} \right) + \sum_a \left(-\left(\frac{\hbar^2}{2m_a} \right) \frac{\partial^2}{\partial q_a^2} + \frac{1}{2} \sum_b Z_a Z_b \frac{e^2}{r_{a,b}} \right).$$

Notice that \mathbf{H} is a second order differential operator in the space of the thirty-nine Cartesian coordinates that describe the positions of the ten electrons and three nuclei. It is a second order operator because the momenta appear in the kinetic energy as p_j^2 and p_a^2 , and the quantum mechanical operator for each momentum $\mathbf{p} = i\hbar \frac{\partial}{\partial q}$ is of first order.

The Schrödinger equation for the H_2O then reads

$$\begin{aligned} \sum_i \left[-\left(\frac{\hbar^2}{2m_e} \right) \frac{\partial^2}{\partial q_i^2} + \frac{1}{2} \sum_j \frac{e^2}{r_{i,j}} - \sum_a Z_a \frac{e^2}{r_{i,a}} \right] \Psi + \sum_a \left[-\left(\frac{\hbar^2}{2m_a} \right) \frac{\partial^2}{\partial q_a^2} + \frac{1}{2} \sum_b Z_a Z_b \frac{e^2}{r_{a,b}} \right] \Psi \\ = i\hbar \frac{\partial \Psi}{\partial t} \end{aligned}$$

*If the Hamiltonian operator contains the time variable explicitly, one must solve the time-dependent Schrödinger equation. If the Hamiltonian operator does **not** contain the time variable explicitly, one can solve the time-independent Schrödinger equation*

The Time-Independent Schrödinger Equation

In cases where the classical energy, and hence the quantum Hamiltonian, do **not** contain terms that are explicitly time dependent (e.g., interactions with time varying external electric or magnetic fields would add to the above classical energy expression time dependent terms discussed later in this text), the separations of variables techniques can be used to reduce the Schrödinger equation to a time-independent equation.

In such cases, H is not explicitly time dependent, so one can assume that $\Psi(q_j, t)$ is of the form

$$\Psi(q_j, t) = \Psi(q_j)F(t).$$

Substituting this 'ansatz' into the time-dependent Schrödinger equation gives

$$\Psi(q_j) i\hbar \frac{\partial F}{\partial t} = H \Psi(q_j) F(t).$$

Dividing by $\Psi(q_j)F(t)$ then gives

$$F^{-1} \left(i\hbar \frac{\partial F}{\partial t} \right) = \Psi^{-1} (H \Psi(q_j)).$$

Since $F(t)$ is only a function of time t , and $\Psi(q_j)$ is only a function of the spatial coordinates $\{q_j\}$, and because the left hand and right hand sides must be equal for all values of t and of $\{q_j\}$, both the left and right hand sides must equal a constant. If this constant is called E , the **two** equations that are embodied in this separated Schrödinger equation read as follows:

$$\begin{aligned} H \Psi(q_j) &= E \Psi(q_j), \\ i\hbar \frac{\partial F(t)}{\partial t} &= i\hbar \frac{dF(t)}{dt} = E F(t). \end{aligned} \tag{1.3.1}$$

Equation 1.3.1 is called the *time-independent Schrödinger Equation*; it is a so-called eigenvalue equation in which one is asked to find functions that yield a constant multiple of themselves when acted on by the Hamiltonian operator. Such functions are called eigenfunctions of H and the corresponding constants are called eigenvalues of H . For example, if H were of the form

$$\frac{-\hbar^2}{2M} \frac{\partial^2}{\partial \phi^2} = H$$

then functions of the form $e^{(im\phi)}$ would be eigenfunctions because

$$\left(\frac{-\hbar^2}{2M} \frac{\partial^2}{\partial \phi^2} \right) e^{im\phi} = \left(\frac{m^2 \hbar^2}{2M} \right) e^{(im\phi)}$$

In this case, $\left(\frac{m^2 \hbar^2}{2M} \right)$ is the eigenvalue.

When the Schrödinger equation can be separated to generate a time-independent equation describing the spatial coordinate dependence of the wavefunction, the eigenvalue E must be returned to the equation determining $F(t)$ to find the time dependent part of the wavefunction. By solving

$$i\hbar \frac{dF(t)}{dt} = E F(t)$$

once E is known, one obtains

$$F(t) = e^{\frac{-iEt}{\hbar}}$$

and the full wavefunction can be written as

$$\Psi(q_j, t) = \Psi(q_j) e^{\frac{-iEt}{\hbar}}$$

and the full wavefunction can be written as

$$\Psi(q_j, t) = \Psi(q_j) e^{\frac{-iEt}{\hbar}}$$

For the above example, the time dependence is expressed by

$$F(t) = e^{\left(\frac{-it}{\hbar} \frac{m^2 \hbar^2}{2M} \right)}$$

Having been introduced to the concepts of operators, wavefunctions, the Hamiltonian and its Schrödinger equation, it is important to now consider several examples of the applications of these concepts. The examples treated below were chosen to provide the learner with valuable experience in solving the Schrödinger equation; they were also chosen because the models they embody form the most elementary chemical models of electronic motions in conjugated molecules and in atoms, rotations of linear molecules, and vibrations of chemical bonds.

This page titled [1.3: The Schrödinger Equation](#) is shared under a [CC BY-NC-SA 4.0](#) license and was authored, remixed, and/or curated by [Jack Simons](#) via [source content](#) that was edited to the style and standards of the LibreTexts platform.

1.4: Free-Particle Motion in Two Dimensions

The Schrödinger Equation

The number of dimensions depends on the number of particles and the number of spatial (and other) dimensions needed to characterize the position and motion of each particle

Consider an electron of mass m and charge e moving on a two-dimensional surface that defines the x,y plane (perhaps the electron is constrained to the surface of a solid by a potential that binds it tightly to a narrow region in the z -direction), and assume that the electron experiences a constant potential V_0 at all points in this plane (on any real atomic or molecular surface, the electron would experience a potential that varies with position in a manner that reflects the periodic structure of the surface). The pertinent time independent Schrödinger equation is:

$$-\frac{\hbar^2}{2m} \left(\frac{\partial^2}{\partial x^2} + \frac{\partial^2}{\partial y^2} \right) \psi(x,y) + V_0 \psi(x,y) = E \psi(x,y)$$

Because there are no terms in this equation that **couple** motion in the x and y directions (e.g., no terms of the form $x^a y^b$ or $\frac{\partial}{\partial x} \frac{\partial}{\partial y}$ or $x \frac{\partial}{\partial y}$), separation of variables can be used to write ϕ as a product $\phi(x,y)=A(x)B(y)$. Substitution of this form into the Schrödinger equation, followed by collecting together all x -dependent and all y -dependent terms, gives;

$$-\frac{\hbar^2}{2m} A^{-1} \frac{\partial^2 A}{\partial x^2} - \frac{\hbar^2}{2m} B^{-1} \frac{\partial^2 B}{\partial y^2} = E - V_0$$

Since the first term contains no y -dependence and the second contains no x -dependence, both must actually be constant (these two constants are denoted E_x and E_y , respectively), which allows two separate Schrödinger equations to be written:

$$\begin{aligned} \frac{-\hbar^2}{2m} A^{-1} \frac{\partial^2 A}{\partial x^2} &= E_x, \text{ and} \\ \frac{-\hbar^2}{2m} B^{-1} \frac{\partial^2 B}{\partial y^2} &= E_y \end{aligned}$$

The total energy E can then be expressed in terms of these separate energies E_x and E_y as $E_x + E_y = E - V_0$. Solutions to the x - and y - Schrödinger equations are easily seen to be:

$$\begin{aligned} A(x) &= e^{ix\sqrt{\frac{2mE_x}{\hbar^2}}} \text{ and} \\ &e^{-ix\sqrt{\frac{2mE_x}{\hbar^2}}} \\ B(y) &= e^{iy\sqrt{\frac{2mE_y}{\hbar^2}}} \text{ and} \\ &e^{-iy\sqrt{\frac{2mE_y}{\hbar^2}}} \end{aligned}$$

Two independent solutions are obtained for each equation because the x - and y -space Schrödinger equations are both second order differential equations.

Boundary Conditions

The boundary conditions, not the Schrödinger equation, determine whether the eigenvalues will be discrete or continuous

If the electron is entirely unconstrained within the x,y plane, the energies E_x and E_y can assume any value; this means that the experimenter can 'inject' the electron onto the x,y plane with any total energy E and any components E_x and E_y along the two axes

as long as $E_x + E_y = E$. In such a situation, one speaks of the energies along both coordinates as being 'in the continuum' or 'not quantized'.

In contrast, if the electron is constrained to remain within a fixed area in the x,y plane (e.g., a rectangular or circular region), then the situation is qualitatively different. Constraining the electron to any such specified area gives rise to so-called boundary conditions that impose additional requirements on the above A and B functions. These constraints can arise, for example, if the potential $V_0(x,y)$ becomes very large for x,y values outside the region, in which case, the probability of finding the electron outside the region is very small. Such a case might represent, for example, a situation in which the molecular structure of the solid surface changes outside the enclosed region in a way that is highly repulsive to the electron.

For example, if motion is constrained to take place within a rectangular region defined by $0 \leq x \leq L_x$; $0 \leq y \leq L_y$, then the continuity property that all wavefunctions must obey (because of their interpretation as probability densities, which must be continuous) causes A(x) to vanish at 0 and at L_x . Likewise, B(y) must vanish at 0 and at L_y . To implement these constraints for

A(x), one must linearly combine the above two solutions $e^{ix\sqrt{\frac{2mE_x}{\hbar^2}}}$ and $e^{-ix\sqrt{\frac{2mE_x}{\hbar^2}}}$ to achieve a function that vanishes at x=0:

$$A(x) = e^{ix\sqrt{\frac{2mE_x}{\hbar^2}}} - e^{-ix\sqrt{\frac{2mE_x}{\hbar^2}}}$$

One is allowed to linearly combine solutions of the Schrödinger equation that have the same energy (i.e., are degenerate) because Schrödinger equations are linear differential equations. An analogous process must be applied to B(y) to achieve a function that vanishes at y=0:

$$B(y) = e^{iy\sqrt{\frac{2mE_y}{\hbar^2}}} - e^{-iy\sqrt{\frac{2mE_y}{\hbar^2}}}$$

Further requiring A(x) and B(y) to vanish, respectively, at $x=L_x$ and $y=L_y$, gives equations that can be obeyed only if E_x and E_y assume particular values:

$$e^{iL_x\sqrt{\frac{2mE_x}{\hbar^2}}} - e^{-iL_x\sqrt{\frac{2mE_x}{\hbar^2}}} = 0 \text{ and}$$

$$e^{iL_y\sqrt{\frac{2mE_y}{\hbar^2}}} - e^{-iL_y\sqrt{\frac{2mE_y}{\hbar^2}}} = 0$$

These equations are equivalent to

$$\sin\left(iL_x\sqrt{\frac{2mE_x}{\hbar^2}}\right) = \sin\left(iL_y\sqrt{\frac{2mE_y}{\hbar^2}}\right) = 0$$

Knowing that $\sin(\theta)$ vanishes at $\theta = n\pi$, for $n=1,2,3,\dots$, (although the $\sin(n\pi)$ function vanishes for $n=0$, this function vanishes for all x or y, and is therefore unacceptable because it represents zero probability density at all points in space) one concludes that the energies E_x and E_y can assume only values that obey:

$$L_x\sqrt{\frac{2mE_x}{\hbar^2}} = n_x\pi$$

$$L_y\sqrt{\frac{2mE_y}{\hbar^2}} = n_y\pi, \text{ or}$$

$$E_x = \frac{n_x^2\pi^2\hbar^2}{2mL_x^2}, \text{ and}$$

$$E_y = \frac{n_y^2\pi^2\hbar^2}{2mL_y^2}, \text{ with } n_x \text{ and } n_y = 1,2,3,\dots$$

It is important to stress that it is the imposition of boundary conditions, expressing the fact that the electron is spatially constrained, that gives rise to quantized energies. In the absence of spatial confinement, or with confinement only at $x=0$ or L_x or only at $y=0$ or L_y , quantized energies would not be realized.

In this example, confinement of the electron to a finite interval along both the x and y coordinates yields energies that are quantized along both axes. If the electron were confined along one coordinate (e.g., between $0 \leq x \leq L_x$) but not along the other (i.e., $B(y)$ is either restricted to vanish at $y=0$ or at $y=L_y$ or at neither point), then the total energy E lies in the continuum; its E_x component is quantized but E_y is not. Such cases arise, for example, when a linear triatomic molecule has more than enough energy in one of its bonds to rupture it but not much energy in the other bond; the first bond's energy lies in the continuum, but the second bond's energy is quantized.

Perhaps more interesting is the case in which the bond with the higher dissociation energy is excited to a level that is not enough to break it but that is in excess of the dissociation energy of the weaker bond. In this case, one has two degenerate states- i. the strong bond having high internal energy and the weak bond having low energy (ψ_1), and ii. the strong bond having little energy and the weak bond having more than enough energy to rupture it (ψ_2). Although an experiment may prepare the molecule in a state that contains only the former component (i.e., $\psi = C_1\psi_1 + C_2\psi_2$ with $C_1 \ll C_2$), coupling between the two degenerate functions (induced by terms in the Hamiltonian \mathbf{H} that have been ignored in defining ψ_1 and ψ_2) usually causes the true wavefunction $\Psi = e^{\left(\frac{-itH}{\hbar}\right)}\psi$ to acquire a component of the second function as time evolves. In such a case, one speaks of internal vibrational energy flow giving rise to unimolecular decomposition of the molecule.

3. Energies and Wavefunctions for Bound States

For discrete energy levels, the energies are specified functions that depend on quantum numbers, one for each degree of freedom that is quantized

Returning to the situation in which motion is constrained along both axes, the resultant total energies and wavefunctions (obtained by inserting the quantum energy levels into the expressions for $A(x)B(y)$) are as follows:

$$E_x = \frac{n_x^2 \pi^2 \hbar^2}{2mL_x^2},$$

and

$$E_y = \frac{n_y^2 \pi^2 \hbar^2}{2mL_y^2},$$

$$E = E_x + E_y,$$

$$\psi(x, y) = \left(\sqrt{\frac{1}{2L_x}} \right) \left(\sqrt{\frac{1}{2L_y}} \right) \left[e^{\frac{in_x \pi x}{L_x}} - e^{\frac{-in_x \pi x}{L_x}} \right] \left[e^{\frac{in_y \pi y}{L_y}} - e^{\frac{-in_y \pi y}{L_y}} \right]$$

with n_x and $n_y = 1, 2, 3, \dots$

The two $\sqrt{\frac{1}{2L}}$ factors are included to guarantee that ψ is normalized:

$$\int |\psi(x, y)|^2 dx dy = 1.$$

Normalization allows $|\psi(x, y)|^2$ to be properly identified as a probability density for finding the electron at a point x, y .

4. Quantized Action Can Also be Used to Derive Energy Levels

There is another approach that can be used to find energy levels and is especially straightforward to use for systems whose Schrödinger equations are separable. The so-called classical **action** (denoted S) of a particle moving with momentum \mathbf{p} along a path leading from initial coordinate \mathbf{q}_i at initial time t_i to a final coordinate \mathbf{q}_f at time t_f is defined by:

$$S = \int_{\mathbf{q}_i, t_i}^{\mathbf{q}_f, t_f} \mathbf{p} \cdot d\mathbf{q}$$

Here, the momentum vector \mathbf{p} contains the momenta along all coordinates of the system, and the coordinate vector \mathbf{q} likewise contains the coordinates along all such degrees of freedom. For example, in the two-dimensional particle in a box problem considered above, $\mathbf{q} = (x, y)$ has two components as does $\mathbf{p} = (p_x, p_y)$, and the action integral is:

$$S = \int_{x_i, y_i, t_i}^{x_f, y_f, t_f} (p_x dx + p_y dy).$$

In computing such actions, it is essential to keep in mind the sign of the momentum as the particle moves from its initial to its final positions. An example will help clarify these matters.

For systems such as the above particle in a box example for which the Hamiltonian is separable, the action integral decomposed into a sum of such integrals, one for each degree of freedom. In this two-dimensional example, the additivity of H :

$$\begin{aligned} H &= H_x + H_y = \frac{p_x^2}{2m} + \frac{p_y^2}{2m} + V(x) + V(y) \\ &= \frac{-\hbar^2}{2m} \frac{\partial^2}{\partial x^2} + V(x) - \frac{\hbar^2}{2m} \frac{\partial^2}{\partial y^2} + V(y) \end{aligned}$$

means that p_x and p_y can be independently solved for in terms of the potentials $V(x)$ and $V(y)$ as well as the energies E_x and E_y associated with each separate degree of freedom:

$$\begin{aligned} p_x &= \pm \sqrt{2m(E_x - V(x))} \\ p_y &= \pm \sqrt{2m(E_y - V(y))}; \end{aligned}$$

the signs on p_x and p_y must be chosen to properly reflect the motion that the particle is actually undergoing. Substituting these expressions into the action integral yields:

$$\begin{aligned} S &= S_x + S_y \\ &= \int_{x_i, t_i}^{x_f, t_f} \pm \sqrt{2m(E_x - V(x))} dx + \int_{y_i, t_i}^{y_f, t_f} \pm \sqrt{2m(E_y - V(y))} dy. \end{aligned}$$

The relationship between these classical action integrals and existence of quantized energy levels has been shown to involve equating the classical action for motion on a closed path (i.e., a path that starts and ends at the same place after undergoing motion away from the starting point but eventually returning to the starting coordinate at a later time) to an integral multiple of Planck's constant:

$$S_{\text{closed}} = \int_{\mathbf{q}_i, t_i}^{\mathbf{q}_f = \mathbf{q}_i, t_f} \mathbf{p} \cdot d\mathbf{q} = nh \quad (n = 1, 2, 3, 4, \dots).$$

Applied to each of the independent coordinates of the two-dimensional particle in a box problem, this expression reads:

$$\begin{aligned} n_x h &= \int_{x=0}^{x=L_x} \sqrt{2m(E_x - V(x))} dx + \int_{x=L_x}^{x=0} -\sqrt{2m(E_x - V(x))} dx \\ n_y h &= \int_{y=0}^{y=L_y} \sqrt{2m(E_y - V(y))} dy + \int_{y=L_y}^{y=0} -\sqrt{2m(E_y - V(y))} dy. \end{aligned}$$

Notice that the sign of the momenta are positive in each of the first integrals appearing above (because the particle is moving from $x = 0$ to $x = L_x$, and analogously for y-motion, and thus has positive momentum) and negative in each of the second integrals (because the motion is from $x = L_x$ to $x = 0$ (and analogously for y-motion) and thus with negative momentum). Within the region bounded by $0 \leq x \leq L_x$; $0 \leq y \leq L_y$, the potential vanishes, so $V(x) = V(y) = 0$. Using this fact, and reversing the upper and lower limits, and thus the sign, in the second integrals above, one obtains:

$$n_x h = 2 \int_{x=0}^{x=L_x} \sqrt{2mE_x} dx = 2\sqrt{2mE_x} L_x$$
$$n_y h = 2 \int_{y=0}^{y=L_y} \sqrt{2mE_y} dy = 2\sqrt{2mE_y} L_y.$$

Solving for E_x and E_y , one finds:

$$E_x = \frac{(n_x h)^2}{8mL_x^2}$$
$$E_y = \frac{(n_y h)^2}{8mL_y^2}$$

These are the same quantized energy levels that arose when the wavefunction boundary conditions were matched at $x = 0$, $x = L_x$ and $y = 0$, $y = L_y$. In this case, one says that the Bohr-Sommerfeld quantization condition:

$$nh = \int_{\mathbf{q}_i; t_i}^{\mathbf{q}_f; t_f} \mathbf{q} \cdot d\mathbf{q}$$

has been used to obtain the result.

This page titled [1.4: Free-Particle Motion in Two Dimensions](#) is shared under a [CC BY-NC-SA 4.0](#) license and was authored, remixed, and/or curated by [Jack Simons](#) via [source content](#) that was edited to the style and standards of the LibreTexts platform.

1.5: Particles in Boxes

The particle-in-a-box problem provides an important model for several relevant chemical situations

The above 'particle in a box' model for motion in two dimensions can obviously be extended to three dimensions or to one. For two and three dimensions, it provides a crude but useful picture for electronic states on surfaces or in crystals, respectively. Free motion within a spherical volume gives rise to eigenfunctions that are used in nuclear physics to describe the motions of neutrons and protons in nuclei. In the so-called shell model of nuclei, the neutrons and protons fill separate s, p, d, etc orbitals with each type of nucleon forced to obey the Pauli principle. These orbitals are not the same in their radial 'shapes' as the s, p, d, etc orbitals of atoms because, in atoms, there is an additional radial potential

$$V(r) = -Z \frac{e^2}{r}$$

present. However, their angular shapes are the same as in atomic structure because, in both cases, the potential is independent of θ and ϕ . This same spherical box model has been used to describe the orbitals of valence electrons in clusters of mono-valent metal atoms such as Cs_n , Cu_n , Na_n and their positive and negative ions. Because of the metallic nature of these species, their valence electrons are sufficiently delocalized to render this simple model rather effective (see T. P. Martin, T. Bergmann, H. Göhlich, and T. Lange, J. Phys. Chem. **95**, 6421 (1991)).

One-dimensional free particle motion provides a qualitatively correct picture for π -electron motion along the p_π orbitals of a delocalized polyene. The one cartesian dimension then corresponds to motion along the delocalized chain. In such a model, the box length L is related to the carbon-carbon bond length R and the number N of carbon centers involved in the delocalized network $L = (N-1)R$. Below, such a conjugated network involving nine centers is depicted. In this example, the box length would be eight times the C-C bond length.

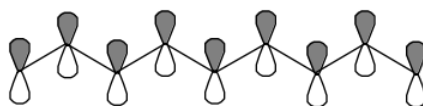


Figure 1.5.1: p-atomic orbitals in Nonanane

Conjugated π Network with 9 Centers Involved

The eigenstates $\psi_n(x)$ and their energies E_n represent orbitals into which electrons are placed. In the example case, if nine π electrons are present (e.g., as in the 1,3,5,7- nonatetraene radical), the ground electronic state would be represented by a total wavefunction consisting of a product in which the lowest four ψ 's are doubly occupied and the fifth ψ is singly occupied:

$$\Psi = \psi_1 \alpha \psi_1 \beta \psi_2 \alpha \psi_2 \beta \psi_3 \alpha \psi_3 \beta \psi_4 \alpha \psi_4 \beta \psi_5 \alpha.$$

A product wavefunction is appropriate because the total Hamiltonian involves the kinetic plus potential energies of nine electrons. To the extent that this total energy can be represented as the sum of nine separate energies, one for each electron, the Hamiltonian allows a separation of variables

$$H \cong \sum_j H(j)$$

in which each $H(j)$ describes the kinetic and potential energy of an individual electron. This (approximate) additivity of H implies that solutions of $H \Psi = E \Psi$ are products of solutions to

$$H(j)\psi(\mathbf{r}_j) = E_j\psi(\mathbf{r}_j).$$

The two lowest π -excited states would correspond to states of the form

$$\Psi^* = \psi_1 \alpha \psi_1 \beta \psi_2 \alpha \psi_2 \beta \psi_3 \alpha \psi_3 \beta \psi_4 \alpha \psi_5 \beta \psi_5 \alpha$$

and

$$\Psi'^* = \psi_1 \alpha \psi_1 \beta \psi_2 \alpha \psi_2 \beta \psi_3 \alpha \psi_3 \beta \psi_4 \alpha \psi_4 \beta \psi_6 \alpha,$$

where the spin-orbitals (orbitals multiplied by α or β) appearing in the above products depend on the coordinates of the various electrons. For example,

$$\psi_1\alpha\psi_1\beta\psi_2\alpha\psi_2\beta\psi_3\alpha\psi_3\beta\psi_4\alpha\psi_5\beta\psi_5\alpha$$

denotes

$$\psi_1\alpha(\mathbf{r}_1)\psi_1\beta(\mathbf{r}_2)\psi_2\alpha(\mathbf{r}_3)\psi_2\beta(\mathbf{r}_4)\psi_3\alpha(\mathbf{r}_5)\psi_3\beta(\mathbf{r}_6)\psi_4\alpha(\mathbf{r}_7)\psi_5\beta(\mathbf{r}_8)\psi_5\alpha(\mathbf{r}_9)$$

The electronic excitation energies within this model would be

$$\Delta E^* = \pi^2 \frac{\hbar^2}{2m} \left[\frac{5^2}{L^2} - \frac{4^2}{L^2} \right]$$

and

$$\Delta E'^* = \pi^2 \frac{\hbar^2}{2m} \left[\frac{6^2}{L^2} - \frac{5^2}{L^2} \right],$$

for the two excited-state functions described above. It turns out that this simple model of π -electron energies provides a qualitatively correct picture of such excitation energies.

This simple particle-in-a-box model does not yield orbital energies that relate to ionization energies unless the potential 'inside the box' is specified. Choosing the value of this potential V_0 such that

$$V_0 + \pi^2 \frac{\hbar^2}{2m} \left[\frac{5^2}{L^2} \right]$$

is equal to minus the lowest ionization energy of the 1,3,5,7-nonatetraene radical, gives energy levels (as $E = V_0 + \pi^2 \frac{\hbar^2}{2m} \left[\frac{n^2}{L^2} \right]$) which then are approximations to ionization energies.

The individual p-molecular orbitals

$$\psi_n = \sqrt{\frac{2}{L}} \sin\left(\frac{n\pi x}{L}\right)$$

are depicted in the figure below for a model of the 1,3,5 hexatriene π -orbital system for which the 'box length' L is five times the distance R_{CC} between neighboring pairs of Carbon atoms.

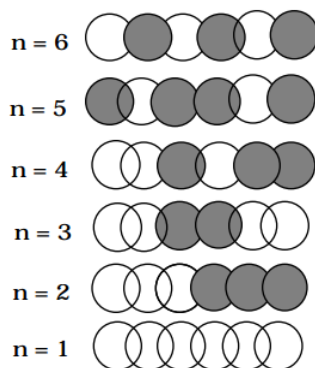


Figure 1.5.2: 1,3,5 hexatriene π -orbitals in order of increasing energy.

$$\sqrt{\frac{2}{L}} \sin\left(\frac{n\pi x}{L}\right); L = 5xR_{CC}$$

In this figure, positive amplitude is denoted by the clear spheres and negative amplitude is shown by the darkened spheres; the magnitude of the k^{th} C-atom centered atomic orbital in the n^{th} π -molecular orbital is given by

$$\sqrt{\frac{2}{L}} \sin\left(\frac{n\pi k R_{CC}}{L}\right).$$

This simple model allows one to estimate spin densities at each carbon center and provides insight into which centers should be most amenable to electrophilic or nucleophilic attack. For example, radical attack at the C_5 carbon of the nine-atom system described earlier would be more facile for the ground state Ψ than for either Ψ^* or Ψ'^* . In the former, the unpaired spin density resides in ψ_5 , which has non-zero amplitude at the C_5 site $x = \frac{L}{2}$; in Ψ^* and Ψ'^* , the unpaired density is in ψ_4 and ψ_6 , respectively, both of which have zero density at C_5 . These densities reflect the values

$$\sqrt{\frac{2}{L}} \sin\left(\frac{n\pi k R_{CC}}{L}\right)$$

of the amplitudes for this case in which $L = 8 \times R_{CC}$ for $n = 5, 4$, and 6 , respectively.

This page titled [1.5: Particles in Boxes](#) is shared under a [CC BY-NC-SA 4.0](#) license and was authored, remixed, and/or curated by [Jack Simons](#) via [source content](#) that was edited to the style and standards of the LibreTexts platform.

1.6: One Electron Moving About a Nucleus

The Schrödinger equation for a single particle of mass m moving in a central potential (one that depends only on the radial coordinate r) can be written as

$$-\frac{\hbar^2}{2\mu} \left(\frac{\partial^2}{\partial x^2} + \frac{\partial^2}{\partial y^2} + \frac{\partial^2}{\partial z^2} \right) \psi + V \left(\sqrt{x^2 + y^2 + z^2} \right) \psi = E\psi$$

This equation is not separable in cartesian coordinates (x, y, z) because of the way x, y , and z appear together in the square root. However, it is separable in spherical coordinates

$$\frac{\hbar^2}{2\mu r^2} \left(\frac{\partial}{\partial r} \left(r^2 \frac{\partial \psi}{\partial r} \right) \right) + \frac{1}{r^2 \sin \theta} \frac{\partial}{\partial \theta} \left(\sin \theta \frac{\partial \psi}{\partial \theta} \right) + \frac{1}{r^2 \sin^2 \theta} \frac{\partial^2 \psi}{\partial \phi^2} + V(r)\psi = E\psi.$$

Subtracting $V(r)\psi$ from both sides of the equation and multiplying by $\frac{-2\mu r^2}{\hbar^2}$ then moving the derivatives with respect to r to the right-hand side, one obtains

$$\frac{1}{\sin \theta} \frac{\partial}{\partial \theta} \left(\sin \theta \frac{\partial \psi}{\partial \theta} \right) + \frac{1}{\sin^2 \theta} \frac{\partial^2 \psi}{\partial \phi^2} = \frac{-2\mu r^2}{\hbar^2} (E - V(r))\psi - \frac{\partial}{\partial r} \left(r^2 \frac{\partial \psi}{\partial r} \right).$$

Notice that the right-hand side of this equation is a function of r only; it contains no θ or ϕ dependence. Let's call the entire right hand side $\mathbf{F}(r)$ to emphasize this fact.

To further separate the θ and ϕ dependence, we multiply by $\sin^2 \theta$ and subtract the θ derivative terms from both sides to obtain

$$\frac{\partial^2 \psi}{\partial \phi^2} = \mathbf{F}(r)\psi \sin^2 \theta - \sin \theta \frac{\partial}{\partial \theta} \left(\sin \theta \frac{\partial \psi}{\partial \theta} \right)$$

Now we have separated the ϕ dependence from the θ and r dependence. If we now substitute $\psi = \Phi(f)Q(r, \theta)$ and divide by ψ , we obtain

$$\frac{1}{\Phi} \frac{\partial^2 \Phi}{\partial \phi^2} = \frac{1}{Q} \left(\mathbf{F}(r) \sin^2 \theta - \sin \theta \frac{\partial}{\partial \theta} \left(\sin \theta \frac{\partial Q}{\partial \theta} \right) \right).$$

Now all of the ϕ dependence is isolated on the left hand side; the right hand side contains only r and θ dependence.

Whenever one has isolated the entire dependence on one variable as we have done above for the ϕ dependence, one can easily see that the left and right hand sides of the equation must equal a constant. For the above example, the left hand side contains no r or θ dependence and the right hand side contains no ϕ dependence. Because the two sides are equal, they both must actually contain no r , θ , or ϕ dependence; that is, they are constant.

For the above example, we therefore can set both sides equal to a so-called separation constant that we call $-m^2$. It will become clear shortly why we have chosen to express the constant in this form.

The Hydrogenic atom problem forms the basis of much of our thinking about atomic structure. To solve the corresponding Schrödinger equation requires separation of the r , θ , and ϕ variables

The Φ Equation

The resulting Φ equation reads

$$\Phi'' + m^2 \Phi = 0$$

which has as its most general solution

$$\Phi = Ae^{im\phi} + Be^{-im\phi}.$$

We must require the function Φ to be single-valued, which means that

$$\Phi(\phi) = \Phi(2\pi + \phi) \text{ or,}$$

$$Ae^{im\phi} (1 - e^{2im\pi}) + Be^{-im\phi} (1 - e^{-2im\pi}) = 0.$$

This is satisfied only when the separation constant is equal to an integer $m = 0, \pm 1, \pm 2, \dots$ and provides another example of the rule that quantization comes from the boundary conditions on the wavefunction. Here m is restricted to certain discrete values because the wavefunction must be such that when you rotate through 2π about the z -axis, you must get back what you started with.

The Θ Equation

Now returning to the equation in which the ϕ dependence was isolated from the r and θ dependence and rearranging the θ terms to the left-hand side, we have

$$\frac{1}{\sin\theta} \frac{\partial}{\partial\theta} \left(\sin\theta \frac{\partial Q}{\partial\theta} \right) - \frac{m^2 Q}{\sin^2\theta} = \mathbf{F}(r)Q.$$

In this equation we have separated θ and r variations so we can further decompose the wavefunction by introducing $Q = \Theta(\theta)R(r)$, which yields

$$\frac{1}{\Theta} \frac{1}{\sin\theta} \frac{\partial}{\partial\theta} \left(\sin\theta \frac{\partial\Theta}{\partial\theta} \right) - \frac{m^2}{\sin^2\theta} = \frac{\mathbf{F}(r)R}{R} = -\lambda,$$

where a second separation constant, $-\lambda$, has been introduced once the r and θ dependent terms have been separated onto the right and left hand sides, respectively.

We now can write the θ equation as

$$\frac{1}{\sin\theta} \frac{\partial}{\partial\theta} \left(\sin\theta \frac{\partial\Theta}{\partial\theta} \right) - \frac{m^2 \Theta}{\sin^2\theta} = -\lambda \Theta,$$

where m is the integer introduced earlier. To solve this equation for Θ , we make the substitutions $z = \cos\theta$ and $P(z) = \Theta(\theta)$, so $\sqrt{1-z^2} = \sin\theta$, and

$$\frac{\partial}{\partial\theta} = \frac{\partial z}{\partial\theta} \frac{\partial}{\partial z} = -\sin\theta \frac{\partial}{\partial z}$$

The range of values for θ was $0 \leq \theta < \pi$, so the range for z is $-1 < z < 1$. The equation for Θ , when expressed in terms of P and z , becomes

$$\frac{d}{dz} \left((1-z^2) \frac{dP}{dz} \right) - \frac{m^2 P}{1-z^2} + \lambda P = 0.$$

Now we can look for polynomial solutions for P , because z is restricted to be less than unity in magnitude. If $m = 0$, we first let

$$P = \sum_{k=0}^{\infty} a_k z^k,$$

and substitute into the differential equation to obtain

$$\sum_{k=1}^{\infty} (k+2)(k+1)a_{k+2}z^k - \sum_{k=0}^{\infty} (k+1)ka_kz^k + \lambda \sum_{k=0}^{\infty} a_kz^k = 0.$$

Equating like powers of z gives

$$a_{k+2} = \frac{a_k(k(k+1) - \lambda)}{(k+2)(k+1)}.$$

Note that for large values of k

$$\frac{a_{k+2}}{a_k} \rightarrow \frac{k^2 \left(1 + \frac{1}{k} \right)}{k^2 \left(1 + \frac{2}{k} \right) \left(1 + \frac{1}{k} \right)} = 1.$$

Since the coefficients do not decrease with k for large k , this series will diverge for $z = \pm 1$ unless it truncates at finite order. This truncation only happens if the separation constant λ obeys $\lambda = l(l+1)$, where l is an integer. So, once again, we see that a boundary condition (i.e., that the wavefunction be normalizable in this case) give rise to quantization. In this case, the values of λ are restricted to $l(l+1)$; before, we saw that m is restricted to $0, \pm 1, \pm 2, \dots$.

Since this recursion relation links every other coefficient, we can choose to solve for the even and odd functions separately. Choosing a_0 and then determining all of the even a_k in terms of this a_0 , followed by rescaling all of these a_k to make the function normalized generates an even solution. Choosing a_1 and determining all of the odd a_k in like manner, generates an odd solution.

For $l = 0$, the series truncates after one term and results in $P_0(z) = 1$. For $l = 1$ the same thing applies and $P_1(z) = z$. For $l = 2$, $a_2 = -6 \frac{a_0}{2} = -3a_0$, so one obtains $P_2 = 3z^2 - 1$, and so on. These polynomials are called Legendre polynomials.

For the more general case where $m \neq 0$, one can proceed as above to generate a polynomial solution for the Q function. Doing so, results in the following solutions:

$$P_l^m(z) = (1 - z^2)^{\frac{|m|}{2}} \frac{d^{|m|} P_l(z)}{dz^{|m|}}.$$

These functions are called [Associated Legendre polynomials](#), and they constitute the solutions to the Θ problem for non-zero m values.

The above P and $e^{im\phi}$ functions, when re-expressed in terms of θ and ϕ , yield the full angular part of the wavefunction for any centrosymmetric potential. These solutions are usually written as

$$Y_{l,m}(\theta, \phi) = P_l^m \frac{\cos\theta}{\sqrt{2\pi}} e^{im\phi}$$

These are called [spherical harmonics](#). They provide the angular solution of the r, θ, ϕ Schrödinger equation for any problem in which the potential depends only on the radial coordinate. Such situations include all one-electron atoms and ions (e.g., H, He^+ , Li^{++} , etc.), the rotational motion of a diatomic molecule (where the potential depends only on bond length r), the motion of a nucleon in a spherically symmetrical "box" (as occurs in the shell model of nuclei), and the scattering of two atoms (where the potential depends only on interatomic distance).

The R Equation

Let us now turn our attention to the radial equation, which is the only place that the explicit form of the potential appears. Using our derived results and specifying $V(r)$ to be the coulomb potential appropriate for an electron in the field of a nucleus of charge $+Ze$, yields:

$$\frac{1}{r^2} \frac{d}{dr} \left(r^2 \frac{dR}{dr} \right) + \left(\frac{2\mu}{\hbar^2} \left(E + \frac{Ze^2}{r} \right) - \frac{l(l+1)}{r^2} \right) R = 0.$$

We can simplify things considerably if we choose rescaled length and energy units because doing so removes the factors that depend on μ , \hbar , and e . We introduce a new radial coordinate ρ and a quantity σ as follows:

$$\rho = \sqrt{\frac{-8\mu E}{\hbar^2}} r$$

and

$$\sigma^2 = -\frac{\mu Z^2 e^4}{2E\hbar^2}.$$

Notice that if E is negative, as it will be for bound states (i.e., those states with energy below that of a free electron infinitely far from the nucleus and with zero kinetic energy), ρ is real. On the other hand, if E is positive, as it will be for states that lie in the continuum, ρ will be imaginary. These two cases will give rise to qualitatively different behavior in the solutions of the radial equation developed below.

We now define a function S such that

$$S(\rho) = R(r)$$

and substitute S for R to obtain:

$$\frac{1}{\rho^2} \frac{d}{d\rho} \left(\rho^2 \frac{dS}{d\rho} \right) + \left(-\frac{1}{4} - \frac{l(l+1)}{\rho^2} + \frac{\sigma}{\rho} \right) S = 0.$$

The differential operator terms can be recast in several ways using

$$\frac{1}{\rho^2} \frac{d}{d\rho} \left(\rho^2 \frac{dS}{d\rho} \right) = \frac{d^2 S}{d\rho^2} + \frac{2}{\rho} \frac{dS}{d\rho} = \frac{1}{\rho} \frac{d^2}{d\rho^2} (\rho S).$$

It is useful to keep in mind these three embodiments of the derivatives that enter into the radial kinetic energy; in various contexts it will be useful to employ various of these.

The strategy that we now follow is characteristic of solving second order differential equations. We will examine the equation for S at large and small ρ values. Having found solutions at these limits, we will use a power series in ρ to "interpolate" between these two limits.

Let us begin by examining the solution of the above equation at small values of ρ to see how the radial functions behave at small r . As $\rho \rightarrow 0$, the second term in the brackets will dominate. Neglecting the other two terms in the brackets, we find that, for small values of ρ (or r), the solution should behave like ρ^L and because the function must be normalizable, we must have $L \geq 0$. Since L can be any non-negative integer, this suggests the following more general form for $S(\rho)$:

$$S(\rho) \approx \rho^L e^{-a\rho}.$$

This form will insure that the function is normalizable since $S(\rho) \rightarrow 0$ as $\rho \rightarrow \infty$ for all L , as long as a is a real quantity. If ρ is imaginary, such a form may not be normalized (see below for further consequences).

Turning now to the behavior of S for large ρ , we make the substitution of $S(\rho)$ into the above equation and keep only the terms with the largest power of ρ (e.g., first term in brackets). Upon so doing, we obtain the equation

$$a^2 \rho^L e^{-a\rho} = \frac{1}{4} \rho^L e^{-a\rho},$$

which leads us to conclude that the exponent in the large- ρ behavior of S is $a = \frac{1}{2}$.

Having found the small- and large- ρ behaviors of $S(\rho)$, we can take S to have the following form to interpolate between large and small ρ -values:

$$S(\rho) = \rho^L e^{-\frac{\rho}{2}} P(\rho),$$

where the function L is expanded in an infinite power series in ρ as $P(\rho) = \sum a_k \rho^k$. Again Substituting this expression for S into the above equation we obtain

$$P'' \rho + P'(2L - \rho) + P(\sigma - L - 1) = 0,$$

and then substituting the power series expansion of P and solving for the a_k 's we arrive at:

$$a_{k+1} = \frac{(k - \sigma + L + 1)a_k}{(k+1)(k+2L+2)}.$$

For large k , the ratio of expansion coefficients reaches the limit $\frac{a_{k+1}}{a_k} = \frac{1}{k}$, which has the same behavior as the power series expansion of e^ρ . Because the power series expansion of P describes a function that behaves like e^ρ for large ρ , the resulting $S(\rho)$

function would not be normalizable because the $e^{-\frac{\rho}{2}}$ factor would be overwhelmed by this e^ρ dependence. Hence, the series expansion of P must truncate in order to achieve a normalizable S function. Notice that if ρ is imaginary, as it will be if E is in the continuum, the argument that the series must truncate to avoid an exponentially diverging function no longer applies. Thus, we see a key difference between bound (with r real) and continuum (with ρ imaginary) states. In the former case, the boundary condition of non-divergence arises; in the latter, it does not.

To truncate at a polynomial of order n' , we must have $n' - \sigma + L + 1 = 0$. This implies that the quantity σ introduced previously is restricted to $\sigma = n' + L + 1$, which is certainly an integer; let us call this integer n . If we label states in order of increasing $n = 1, 2, 3, \dots$, we see that doing so is consistent with specifying a maximum order (n') in the $P(\rho)$ polynomial $n' = 0, 1, 2, \dots$ after which the l -value can run from $l = 0$, in steps of unity up to $L = n - 1$.

Substituting the integer n for σ , we find that the energy levels are quantized because σ is quantized (equal to n):

$$E = -\frac{\mu Z^2 e^4}{2\hbar^2 n^2} : \text{ and } : \rho = \frac{Zr}{a_0 n}.$$

Here, the length a_0 is the so called Bohr radius $\left(a_0 = \frac{\hbar^2}{\mu e^2}\right)$; it appears once the above E -expression is substituted into the equation for ρ . Using the recursion equation to solve for the polynomial's coefficients a_k for any choice of n and l quantum numbers generates a so-called Laguerre polynomial; $P_{n-L-1}(\rho)$. They contain powers of ρ from zero through $n-l-1$.

This energy quantization does not arise for states lying in the continuum because the condition that the expansion of $P(\rho)$ terminate does not arise. The solutions of the radial equation appropriate to these scattering states (which relate to the scattering motion of an electron in the field of a nucleus of charge Z) are treated on p. 90 of EWK.

In summary, separation of variables has been used to solve the full r, θ, ϕ Schrödinger equation for one electron moving about a nucleus of charge Z . The θ and ϕ solutions are the spherical harmonics $Y_{L,m}(\theta, \phi)$. The bound-state radial solutions

$$R_{n,L}(r) = S(\rho) = \rho^L e^{-\frac{\rho}{2}} P_{n-L-1}(\rho)$$

depend on the n and l quantum numbers and are given in terms of the Laguerre polynomials (see EWK for tabulations of these polynomials).

Summary

To summarize, the quantum numbers l and m arise through boundary conditions requiring that $\psi(\theta)$ be normalizable (i.e., not diverge) and $\psi(\phi) = \psi(\phi + 2\pi)$. In the texts by Atkins, EWK, and McQuarrie the differential equations obeyed by the θ and ϕ components of $Y_{l,m}$ are solved in more detail and properties of the solutions are discussed. This differential equation involves the three-dimensional Schrödinger equation's angular kinetic energy operator. That is, the angular part of the above Hamiltonian is equal to $\hbar^2 \frac{L^2}{2mr^2}$, where L^2 is the square of the total angular momentum for the electron.

The radial equation, which is the only place the potential energy enters, is found to possess both bound-states (i.e., states whose energies lie below the asymptote at which the potential vanishes and the kinetic energy is zero) and continuum states lying energetically above this asymptote. The resulting hydrogenic wavefunctions (angular and radial) and energies are summarized in Appendix B for principal quantum numbers n ranging from 1 to 3 and in Pauling and Wilson for n up to 5.

There are both bound and continuum solutions to the radial Schrödinger equation for the attractive coulomb potential because, at energies below the asymptote the potential confines the particle between $r=0$ and an outer turning point, whereas at energies above the asymptote, the particle is no longer confined by an outer turning point (see the figure below).

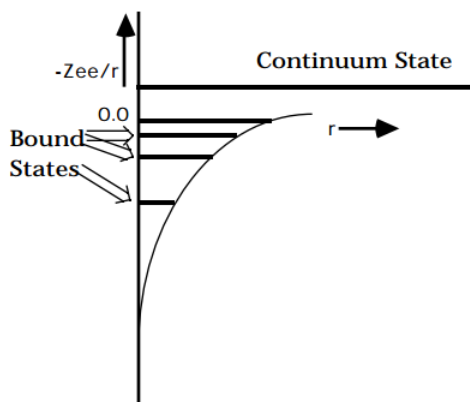


Figure 1.6.1: Insert caption here!

The solutions of this one-electron problem form the qualitative basis for much of atomic and molecular orbital theory. For this reason, the reader is encouraged to use Appendix B to gain a firmer understanding of the nature of the radial and angular parts of these wavefunctions. The orbitals that result are labeled by n , l , and m quantum numbers for the bound states and by l and m quantum numbers and the energy E for the continuum states. Much as the particle-in-a-box orbitals are used to qualitatively describe π - electrons in conjugated polyenes, these so-called hydrogen-like orbitals provide qualitative descriptions of orbitals of atoms with more than a single electron. By introducing the concept of screening as a way to represent the repulsive interactions among the electrons of an atom, an effective nuclear charge Z_{eff} can be used in place of Z in the $\psi_{n,l,m}$ and $E_{n,l}$ to generate approximate atomic orbitals to be filled by electrons in a many-electron atom. For example, in the crudest approximation of a carbon atom, the two 1s electrons experience the full nuclear attraction so $Z_{eff}=6$ for them, whereas the 2s and 2p electrons are screened by the two 1s electrons, so $Z_{eff}=4$ for them. Within this approximation, one then occupies two 1s orbitals with $Z=6$, two 2s orbitals with $Z=4$ and two 2p orbitals with $Z=4$ in forming the full six-electron wavefunction of the lowest-energy state of carbon.

This page titled [1.6: One Electron Moving About a Nucleus](#) is shared under a [CC BY-NC-SA 4.0](#) license and was authored, remixed, and/or curated by [Jack Simons](#) via [source content](#) that was edited to the style and standards of the LibreTexts platform.

1.7: Harmonic Vibrational Motion

The radial motion of a diatomic molecule in its lowest ($J=0$) rotational level can be described by the following Schrödinger equation:

$$\frac{-\hbar^2}{2\mu r^2} \frac{\partial}{\partial r} \left(r^2 \frac{\partial}{\partial r} \right) \psi + V(r)\psi = E\psi,$$

where μ is the reduced mass

$$\mu = \frac{m_1 m_2}{(m_1 + m_2)}$$

of the two atoms. By substituting $\psi = \frac{F(r)}{r}$ into this equation, one obtains an equation for $F(r)$ in which the differential operators appear to be less complicated:

$$\frac{-\hbar^2}{2\mu} \frac{d^2 F}{dr^2} + V(r)F = EF.$$

This equation is exactly the same as the equation seen above for the radial motion of the electron in the hydrogen-like atoms except that the reduced mass μ replaces the electron mass m and the potential $V(r)$ is **not** the Coulomb potential.

If the potential is approximated as a quadratic function of the bond displacement $x = r - r_e$ expanded about the point at which V is minimum:

$$V = \frac{1}{2}k(r - r_e)^2,$$

the resulting harmonic-oscillator equation can be solved exactly. Because the potential V grows without bound as x approaches ∞ or $-\infty$, only bound-state solutions exist for this model problem; that is, the motion is confined by the nature of the potential, so no continuum states exist.

This Schrödinger equation forms the basis for our thinking about bond stretching and angle bending vibrations as well as collective phonon motions in solids

In solving the radial differential equation for this potential (see Chapter 5 of McQuarrie), the large- r behavior is first examined. For large- r , the equation reads:

$$\frac{d^2 F}{dx^2} = \frac{1}{2}kx^2 \left(\frac{2\mu}{\hbar^2} \right) F,$$

where $x = r - r_e$ is the bond displacement away from equilibrium. Defining $\xi = \sqrt{\frac{\mu k}{\hbar^2}} x$ as a new scaled radial coordinate allows the solution of the large- r equation to be written as:

$$F_{\text{larger-}r} = e^{-\frac{\xi^2}{2}}$$

The general solution to the radial equation is then taken to be of the form:

$$F = e^{-\frac{\xi^2}{2}} \sum_{n=0}^{\infty} \xi^n C_n,$$

where the C_n are coefficients to be determined. Substituting this expression into the full radial equation generates a set of recursion equations for the C_n amplitudes. As in the solution of the hydrogen-like radial equation, the series described by these coefficients is divergent unless the energy E happens to equal specific values. It is this requirement that the wavefunction not diverge so it can be normalized that yields energy quantization. The energies of the states that arise are given by:

$$E_n = \hbar \sqrt{\frac{k}{\mu}} \left(n + \frac{1}{2} \right)$$

and the eigenfunctions are given in terms of the so-called [Hermite polynomials](#) $H_n(y)$ as follows:

$$\psi_n(x) = \frac{1}{\sqrt{n!2^n}} \sqrt{\frac{\alpha}{\pi}} \left(e^{-\frac{\alpha x^2}{2}} \right) H_n(\sqrt{\alpha}x),$$

where $\alpha = \left(\sqrt{\frac{k\mu}{\hbar^2}} \right)$. Within this harmonic approximation to the potential, the vibrational energy levels are evenly spaced:

$$\Delta E = E_{n+1} - E_n = \hbar \left(\frac{k}{\mu} \right).$$

In experimental data such evenly spaced energy level patterns are seldom seen; most commonly, one finds spacings $E_{n+1} - E_n$ that decrease as the quantum number n increases. In such cases, one says that the progression of vibrational levels displays anharmonicity.

Because the H_n are odd or even functions of x (depending on whether n is odd or even), the wavefunctions $\psi_n(x)$ are odd or even. This splitting of the solutions into two distinct classes is an example of the effect of symmetry; in this case, the symmetry is caused by the symmetry of the harmonic potential with respect to reflection through the origin along the x -axis. Throughout this text, many symmetries will arise; in each case, symmetry properties of the potential will cause the solutions of the Schrödinger equation to be decomposed into various symmetry groupings. Such symmetry decompositions are of great use because they provide additional quantum numbers (i.e., symmetry labels) by which the wavefunctions and energies can be labeled.

The harmonic oscillator energies and wavefunctions comprise the simplest reasonable model for vibrational motion. Vibrations of a polyatomic molecule are often characterized in terms of individual bond-stretching and angle-bending motions each of which is, in turn, approximated harmonically. This results in a total vibrational wavefunction that is written as a product of functions one for each of the vibrational coordinates.

Two of the most severe limitations of the harmonic oscillator model, the lack of anharmonicity (i.e., non-uniform energy level spacings) and lack of bond dissociation, result from the quadratic nature of its potential. By introducing model potentials that allow for proper bond dissociation (i.e., that do not increase without bound as $x \rightarrow \infty$), the major shortcomings of the harmonic oscillator picture can be overcome. The so-called Morse potential (see the figure below)

$$V(r) = D_e \left(1 - e^{-a(r-r_e)} \right)^2,$$

is often used in this regard.

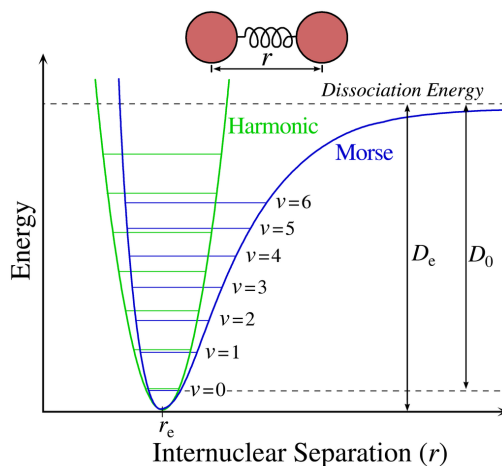


Figure 1.7.1: The Morse potential (blue) and harmonic oscillator potential (green). Unlike the energy levels of the harmonic oscillator potential, which are evenly spaced by $\hbar\omega$, the Morse potential level spacing decreases as the energy approaches the dissociation energy. The dissociation energy D_e is larger than the true energy required for dissociation D_0 due to the zero point energy of the lowest ($v = 0$) vibrational level. (CC-SA-BY-3.0; Somoza).

Here, D_e is the bond dissociation energy, r_e is the equilibrium bond length, and a is a constant that characterizes the 'steepness' of the potential and determines the vibrational frequencies. The advantage of using the Morse potential to improve upon harmonic

oscillator-level predictions is that its energy levels and wavefunctions are also known exactly. The energies are given in terms of the parameters of the potential as follows:

$$E_n = \hbar \sqrt{\frac{k}{\mu}} \left[\left(n + \frac{1}{2} \right) - \left(n + \frac{1}{2} \right)^2 \frac{\hbar}{4} \sqrt{\frac{k}{\mu}} D_e \right]$$

where the force constant k is $k = 2D_e a^2$. The Morse potential supports both bound states (those lying below the dissociation threshold for which vibration is confined by an outer turning point) and continuum states lying above the dissociation threshold. Its degree of anharmonicity is governed by the ratio of the harmonic energy $\hbar \sqrt{\frac{k}{\mu}}$ to the dissociation energy D_e .

This page titled [1.7: Harmonic Vibrational Motion](#) is shared under a [CC BY-NC-SA 4.0](#) license and was authored, remixed, and/or curated by [Jack Simons](#) via [source content](#) that was edited to the style and standards of the LibreTexts platform.

1.8: Rotational Motion for a Rigid Diatomic Molecule

A diatomic molecule with fixed bond length R rotating in the absence of any external potential is described by the following Schrödinger equation:

$$\frac{\hbar^2}{2\mu} \left[\frac{1}{R^2 \sin \theta} \frac{\partial}{\partial \theta} \left(\sin \theta \frac{\partial}{\partial \theta} \right) + \frac{1}{R^2 \sin^2 \theta} \frac{\partial^2}{\partial \phi^2} \right] \psi = E\psi$$

or

$$\frac{L^2 \psi}{2\mu R^2} = E\psi.$$

The angles θ and ϕ describe the orientation of the diatomic molecule's axis relative to a laboratory-fixed coordinate system, and μ is the reduced mass of the diatomic molecule

$$\mu = \frac{m_1 m_2}{m_1 + m_2}.$$

The differential operators can be seen to be exactly the same as those that arose in the hydrogen-like-atom case, and, as discussed above, these θ and ϕ differential operators are identical to the L^2 angular momentum operator whose general properties are analyzed in **Appendix G**. Therefore, the same spherical harmonics that served as the angular parts of the wavefunction in the earlier case now serve as the entire wavefunction for the so-called rigid rotor: $\psi = Y_{J,M}(\theta, \phi)$. As detailed later in this text, the eigenvalues corresponding to each such eigenfunction are given as:

$$E_J = \hbar^2 \frac{J(J+1)}{(2\mu R^2)} = BJ(J+1)$$

and are independent of M . Thus each energy level is labeled by J and is $2J+1$ -fold degenerate (because M ranges from $-J$ to J). The so-called rotational constant B (defined as $\frac{\hbar^2}{2\mu R^2}$) depends on the molecule's bond length and reduced mass. Spacings between successive rotational levels (which are of spectroscopic relevance because angular momentum selection rules often restrict ΔJ to 1, 0, and -1) are given by

$$\Delta E = B(J+1)(J+2) - BJ(J+1) = 2B(J+1).$$

These energy spacings are of relevance to microwave spectroscopy which probes the rotational energy levels of molecules.

This Schrödinger equation relates to the rotation of diatomic and linear polyatomic molecules. It also arises when treating the angular motions of electrons in any spherically symmetric potential.

Summary

The rigid rotor provides the most commonly employed approximation to the rotational energies and wavefunctions of linear molecules. As presented above, the model restricts the bond length to be fixed. Vibrational motion of the molecule gives rise to changes in R which are then reflected in changes in the rotational energy levels. The coupling between rotational and vibrational motion gives rise to rotational B constants that depend on vibrational state as well as dynamical couplings, called centrifugal distortions, that cause the total ro-vibrational energy of the molecule to depend on rotational and vibrational quantum numbers in a non-separable manner

This page titled [1.8: Rotational Motion for a Rigid Diatomic Molecule](#) is shared under a [CC BY-NC-SA 4.0](#) license and was authored, remixed, and/or curated by [Jack Simons](#) via [source content](#) that was edited to the style and standards of the LibreTexts platform.

1.9: The Physical Relevance of Wavefunctions, Operators and Eigenvalues

Quantum mechanics has a set of 'rules' that link operators, wavefunctions, and eigenvalues to physically measurable properties. These rules have been formulated not in some arbitrary manner nor by derivation from some higher subject. Rather, the rules were designed to allow quantum mechanics to mimic the experimentally observed facts as revealed in mother nature's data. The extent to which these rules seem difficult to understand usually reflects the presence of experimental observations that do not fit in with our common experience base.

The structure of quantum mechanics (QM) relates the wavefunction Ψ and operators \mathbf{F} to the 'real world' in which experimental measurements are performed through a set of rules. Some of these rules have already been introduced above. Here, they are presented in total as follows:

1: The Time Evolution

The time evolution of the wavefunction Ψ is determined by solving the time-dependent Schrödinger equation (see pp 23-25 of EWK for a rationalization of how the Schrödinger equation arises from the classical equation governing waves, Einstein's $E = h\nu$, and deBroglie's postulate that $\lambda = \frac{h}{p}$)

$$i\hbar \frac{\partial \Psi}{\partial t} = \mathbf{H}\Psi,$$

where \mathbf{H} is the Hamiltonian operator corresponding to the total (kinetic plus potential) energy of the system. For an isolated system (e.g., an atom or molecule not in contact with any external fields), \mathbf{H} consists of the kinetic and potential energies of the particles comprising the system. To describe interactions with an external field (e.g., an electromagnetic field, a static electric field, or the 'crystal field' caused by surrounding ligands), additional terms are added to \mathbf{H} to properly account for the system-field interactions.

If \mathbf{H} contains no explicit time dependence, then separation of space and time variables can be performed on the above Schrödinger equation $\Psi = \psi e^{\frac{-iEt}{\hbar}}$ to give

$$\mathbf{H}\psi = E\psi.$$

In such a case, the time dependence of the state is carried in the phase factor $e^{\frac{-Et}{\hbar}}$; the spatial dependence appears in $\psi(q_j)$.

The so called time independent Schrödinger equation $\mathbf{H}\psi = E\psi$ must be solved to determine the physically measurable energies E_k and wavefunctions ψ_k of the system. The most general solution to the full Schrödinger equation

$$i\hbar \frac{\partial \Psi}{\partial t} = \mathbf{H}\Psi$$

is then given by applying $e^{\frac{-i\mathbf{H}t}{\hbar}}$ to the wavefunction at some initial time ($t=0$)

$$\Psi = \sum_k C_k \psi_k$$

to obtain

$$\Psi(t) = \sum_k C_k \psi_k e^{\frac{-iE_k t}{\hbar}}.$$

The relative amplitudes C_k are determined by knowledge of the state at the initial time; this depends on how the system has been prepared in an earlier experiment. Just as Newton's laws of motion do not fully determine the time evolution of a classical system (i.e., the coordinates and momenta must be known at some initial time), the Schrödinger equation must be accompanied by initial conditions to fully determine $\Psi(q_j, t)$.

✓ Example 1.9.1:

Using the results of Problem 11 of this chapter to illustrate, the sudden ionization of N_2 in its $v=0$ vibrational state to generate N_2^+ produces a vibrational wavefunction

$$\Psi_0 = \sqrt{\frac{\alpha}{\pi}} e^{\frac{-\alpha x^2}{2}} = 3.53333 \frac{1}{\sqrt{\text{\AA}}}$$

that was created by the fast ionization of N_2 . Subsequent to ionization, this N_2 function is not an eigenfunction of the new vibrational Schrödinger equation appropriate to N_2^+ . As a result, this function will time evolve under the influence of the N_2^+ Hamiltonian. The time evolved wavefunction, according to this first rule, can be expressed in terms of the vibrational functions $\{\Psi_v\}$ and energies $\{E_v\}$ of the N_2^+ ion as

$$\Psi(t) = \sum_v C_v \Psi_v e^{\frac{-iE_v t}{\hbar}}.$$

The amplitudes C_v , which reflect the manner in which the wavefunction is prepared (at $t=0$), are determined by determining the component of each Ψ_v in the function Ψ at $t=0$. To do this, one uses

$$\int \Psi_{v'}^* \Psi(t=0) d\tau = C_{v'},$$

which is easily obtained by multiplying the above summation by $\Psi_{v'}^*$, integrating, and using the orthonormality of the $\{\Psi_v\}$ functions.

For the case at hand, this results shows that by forming integrals involving products of the N_2 $v=0$ function $\Psi(t=0)$

$$= \int_{-\infty}^{\infty} 3.47522 e^{-229.113(r^{-1.11642})^2} 3.53333 e^{-244.83(r^{-1.09769})^2} dr$$

As demonstrated in Problem 11, this integral reduces to 0.959. This means that the N_2 $v=0$ state, subsequent to sudden ionization, can be represented as containing $|0.959|^2 = 0.92$ fraction of the $v=0$ state of the N_2^+ ion.

Example 1.9.1 relates to the well known Franck-Condon principal of spectroscopy in which squares of 'overlaps' between the initial electronic state's vibrational wavefunction and the final electronic state's vibrational wavefunctions allow one to estimate the probabilities of populating various final-state vibrational levels.

In addition to initial conditions, solutions to the Schrödinger equation must obey certain other constraints in form. They must be continuous functions of all of their spatial coordinates and must be single valued; these properties allow $\Psi^* \Psi$ to be interpreted as a probability density (i.e., the probability of finding a particle at some position can not be multivalued nor can it be 'jerky' or discontinuous). The derivative of the wavefunction must also be continuous except at points where the potential function undergoes an infinite jump (e.g., at the wall of an infinitely high and steep potential barrier). This condition relates to the fact that the momentum must be continuous except at infinitely 'steep' potential barriers where the momentum undergoes a 'sudden' reversal.

2: Measurements are Eigenvalues

An experimental measurement of any quantity (whose corresponding operator is \mathbf{F}) must result in one of the eigenvalues f_j of the operator \mathbf{F} . These eigenvalues are obtained by solving

$$\mathbf{F}\phi_j = f_j\phi_j,$$

where the f_j are the eigenfunctions of \mathbf{F} . Once the measurement of \mathbf{F} is made, for that subpopulation of the experimental sample found to have the particular eigenvalue f_j , the wavefunction becomes ϕ_j .

The equation $\mathbf{H}\psi_k = E_k\psi_k$ is but a special case; it is an especially important case because much of the machinery of modern experimental chemistry is directed at placing the system in a particular energy quantum state by detecting its energy (e.g., by spectroscopic means). The reader is strongly urged to also study Appendix C to gain a more detailed and illustrated treatment of this and subsequent rules of quantum mechanics.

3: Operators that correspond to Measurables are Hermitian

The operators F corresponding to all physically measurable quantities are Hermitian; this means that their matrix representations obey (see Appendix C for a description of the 'bra' \langle and 'ket' \rangle notation used below):

$$\langle \chi_j | F | \chi_k \rangle = \langle \chi_k | F | \chi_j \rangle^* = \langle F \chi_j | \chi_k \rangle$$

in any basis $\{\chi_j\}$ of functions appropriate for the action of F (i.e., functions of the variables on which F operates). As expressed through equality of the first and third elements above, Hermitian operators are often said to 'obey the turn-over rule'. This means that F can be allowed to operate on the function to its right or on the function to its left if F is Hermitian.

Hermiticity assures that the eigenvalues $\{f_j\}$ are all real, that eigenfunctions $\{\chi_j\}$ having different eigenvalues are orthogonal and can be normalized $\langle \chi_j | \chi_k \rangle = \delta_{j,k}$, and that eigenfunctions having the same eigenvalues can be made orthonormal (these statements are proven in Appendix C).

4: Stationary states do not have varying Measurables

Once a particular value f_j is observed in a measurement of F , this same value will be observed in all subsequent measurements of F as long as the system remains undisturbed by measurements of other properties or by interactions with external fields. In fact, once f_i has been observed, the state of the system becomes an eigenstate of F (if it already was, it remains unchanged):

$$F\Psi = f_i\Psi.$$

This means that the measurement process itself may interfere with the state of the system and even determines what that state will be once the measurement has been made.

✓ Example 1.9.2:

Again consider the $v=0$ N_2 ionization treated in Problem 11 of this chapter. If, subsequent to ionization, the N_2^+ ions produced were probed to determine their internal vibrational state, a fraction of the sample equal to $|\langle \Psi(N_2; \nu=0) | \Psi(N_2^+; \nu=0) \rangle|^2 = 0.92$ would be detected in the $v=0$ state of the N_2^+ ion. For this sub-sample, the vibrational wavefunction becomes, and remains from then on,

$$\Psi(t) = \Psi(N_2^+; \nu=0) e^{\frac{-itE_{\nu=0}^+}{\hbar}},$$

where $E_{\nu=0}^+$ is the energy of the N_2^+ ion in its $\nu=0$ state. If, at some later time, this subsample is again probed, all species will be found to be in the $\nu=0$ state.

5: Probability of observed a specific Eigenvalue

The probability P_k of observing a particular value f_k when F is measured, given that the system wavefunction is Ψ prior to the measurement, is given by expanding Ψ in terms of the complete set of normalized eigenstates of F

$$\Psi = \sum_j |\phi_j\rangle \langle \phi_j | \Psi \rangle$$

and then computing $P_k = |\langle \phi_k | \Psi \rangle|^2$. For the special case in which Ψ is already one of the eigenstates of F (i.e., $\Psi = \phi_k$), the probability of observing f_j reduces to $P_j = \delta_{j,k}$. The set of numbers $C_j = \langle \phi_j | \Psi \rangle$ are called the expansion coefficients of Ψ in the basis of the $\{\phi_j\}$. These coefficients, when collected together in all possible products as $D_{j,i} = C_i^* C_j$ form the so-called density matrix $D_{j,i}$ of the wavefunction Ψ within the $\{\psi_j\}$ basis.

✓ Example 1.9.3:

If F is the operator for momentum in the x-direction and $\Psi(x, t)$ is the wave function for x as a function of time t , then the above expansion corresponds to a Fourier transform of Ψ

$$\Psi(x, t) = \frac{1}{2\pi} \int e^{ikx} \int e^{-ikx'} \Psi(x', t) dx' dk.$$

Here $\sqrt{\frac{1}{2\pi}} e^{ikx}$ is the normalized eigenfunction of $\mathbf{F} = -i\hbar \frac{\partial}{\partial x}$ corresponding to momentum eigenvalue $\hbar k$. These momentum eigenfunctions are orthonormal:

$$\frac{1}{2\pi} \int e^{-ikx} e^{ikx'} dx = \delta(x - x')$$

because \mathbf{F} is a Hermitian operator. The function $\int e^{-ikx'} \Psi(x', t) dx'$ is called the momentum-space transform of $\Psi(x, t)$ and is denoted $\Psi(k, t)$; it gives, when used as $\Psi^*(k, t) \Psi(k, t)$, the probability density for observing momentum values $\hbar k$ at time t .

✓ Example 1.9.4:

Take the initial ψ to be a superposition state of the form

$$\psi = a(2p_0 + 2p_{-1} - 2p_1) + b(3p_0 - 3p_{-1}),$$

where the a and b are amplitudes that describe the admixture of $2p$ and $3p$ functions in this wavefunction. Then:

a. If \mathbf{L}^2 were measured, the value $2\hbar^2$ would be observed with probability $3|a|^2 + 2|b|^2 = 1$, since all of the functions in ψ are p -type orbitals. After said measurement, the wavefunction would still be this same ψ because this entire ψ is an eigenfunction of \mathbf{L}^2 .

b. If \mathbf{L}_z were measured for this

$$\psi = a(2p_0 + 2p_{-1} - 2p_1) + b(3p_0 - 3p_{-1}),$$

the values $0\hbar$, $1\hbar$, and $-1\hbar$ would be observed (because these are the only functions with non-zero C_m coefficients for the L_z operator) with respective probabilities $|a|^2 + |b|^2$, $|a|^2$, and $|a|^2 + |b|^2$.

c. After L_z were measured, if the sub-population for which $-1\hbar$ had been detected were subjected to measurement of \mathbf{L}^2 the value $2\hbar^2$ would certainly be found because the new wavefunction

$$\psi' = [-a2p_{-1} - b3p_{-1}] \frac{1}{\sqrt{|a|^2 + |b|^2}}$$

is still an eigenfunction of \mathbf{L}^2 with this eigenvalue.

d. Again after \mathbf{L}_z were measured, if the sub-population for which $-1\hbar$ had been observed and for which the wavefunction is now

$$\psi' = [-a2p_{-1} - b3p_{-1}] \frac{1}{\sqrt{|a|^2 + |b|^2}}$$

were subjected to measurement of the energy (through the Hamiltonian operator), two values would be found. With probability $|a|^2 \frac{1}{|a|^2 + |b|^2}$ the energy of the $2p_{-1}$ orbital would be observed; with probability $|b|^2 \frac{1}{|a|^2 + |b|^2}$, the energy of the $3p_{-1}$ orbital would be observed.

If Ψ is a function of several variables (e.g., when Ψ describes more than one particle in a composite system), and if F is a property that depends on a subset of these variables (e.g., when F is a property of one of the particles in the composite system), then the expansion $\Psi = \sum_j |\phi_j\rangle \langle \phi_j | \Psi \rangle$ is viewed as relating only to Ψ 's dependence on the subset of variables related to F . In

this case, the integrals $\langle \phi_k | \Psi \rangle$ are carried out over only these variables; thus the probabilities $P_k = |\langle \phi_k | \Psi \rangle|^2$ depend parametrically on the remaining variables.

Suppose that $\Psi(r, \theta)$ describes the radial (r) and angular (θ) motion of a diatomic molecule constrained to move on a planar surface. If an experiment were performed to measure the component of the rotational angular momentum of the diatomic molecule perpendicular to the surface ($\mathbf{L}_z = -i\hbar \frac{\partial}{\partial \theta}$), only values equal to $m\hbar$ ($m=0, 1, -1, 2, -2, 3, -3, \dots$) could be observed, because these are the eigenvalues of \mathbf{L}_z :

$$\mathbf{L}_z \phi_m = -i\hbar \frac{\partial}{\partial \theta} \phi_m = m\hbar \phi_m, \text{ where}$$

$$\phi_m = \sqrt{\frac{1}{2\pi}} e^{im\theta}.$$

The quantization of \mathbf{L}_z arises because the eigenfunctions $\phi_m m(\theta)$ must be periodic in θ :

$$\phi(\theta + 2\pi) = \phi(\theta).$$

Such quantization (i.e., constraints on the values that physical properties can realize) will be seen to occur whenever the pertinent wavefunction is constrained to obey a so-called boundary condition (in this case, the boundary condition is $\phi(\theta + 2\pi) = \phi(\theta)$).

Expanding the θ -dependence of Ψ in terms of the ϕ_m

$$\Psi = \sum_m \langle \phi_m | \Psi \rangle \phi_m(\theta)$$

allows one to write the probability that $m\hbar$ is observed if the angular momentum \mathbf{L}_z is measured as follows:

$$P_m = |\langle \phi_m | \Psi \rangle|^2 = \left| \int \phi_m^*(\theta) \Psi(r, \theta) d\theta \right|^2.$$

If one is interested in the probability that $m\hbar$ be observed when L_z is measured regardless of what bond length r is involved, then it is appropriate to integrate this expression over the r -variable about which one does not care. This, in effect, sums contributions from all r values to obtain a result that is independent of the r variable. As a result, the probability reduces to:

$$P_m = \int \phi_m^*(\theta') \left[\Psi^*(r, \theta') \Psi(r, \theta) \right] \phi(\theta) d\theta' d\theta,$$

which is simply the above result integrated over r with a volume element $r dr$ for the twodimensional motion treated here. If, on the other hand, one were able to measure L_z values when r is equal to some specified bond length (this is only a hypothetical example; there is no known way to perform such a measurement), then the probability would equal:

$$P_m r dr = r dr \int \phi_m^*(\theta') \Psi^*(r, \theta') \Psi(r, \theta) \phi_m(\theta) d\theta' d\theta = |\langle \phi_m | \Psi \rangle|^2 r dr.$$

6. Commuting Operators

Two or more properties F, G, J whose corresponding Hermitian operators $\mathbf{F}, \mathbf{G}, \mathbf{J}$ commute

$$\mathbf{F}\mathbf{G} - \mathbf{G}\mathbf{F} = \mathbf{F}\mathbf{J} - \mathbf{J}\mathbf{F} = \mathbf{G}\mathbf{J} - \mathbf{J}\mathbf{G} = 0$$

have complete sets of simultaneous eigenfunctions (the proof of this is treated in Appendix C). This means that the set of functions that are eigenfunctions of one of the operators can be formed into a set of functions that are also eigenfunctions of the others:

$$\mathbf{F}\phi_j = f_j \phi_j \implies \mathbf{G}\phi_j = g_j \phi_j \implies \mathbf{J}\phi_j = j_j \phi_j.$$

✓ Example 1.9.5:

The p_x, p_y and p_z orbitals are eigenfunctions of the \mathbf{L}^2 angular momentum operator with eigenvalues equal to $L(L+1)\hbar^2 = 2\hbar^2$. Since \mathbf{L}^2 and \mathbf{L}_z commute and act on the same (angle) coordinates, they possess a complete set of simultaneous eigenfunctions.

Although the p_x, p_y and p_z orbitals are not eigenfunctions of \mathbf{L}_z , they can be combined to form three new orbitals: $p_0 = p_z, p_1 = \frac{1}{\sqrt{2}}[p_x + ip_y]$, and $p_{-1} = \frac{1}{\sqrt{2}}[p_x - ip_y]$ that are still eigenfunctions of \mathbf{L}^2 but are now eigenfunctions of \mathbf{L}_z also (with eigenvalues $0\hbar, 1\hbar$, and $-1\hbar$, respectively).

It should be mentioned that if two operators do not commute, they may still have some eigenfunctions in common, but they will not have a complete set of simultaneous eigenfunctions. For example, the L_z and L_x components of the angular momentum operator do not commute; however, a wavefunction with $L=0$ (i.e., an S-state) is an eigenfunction of both operators.

The fact that two operators commute is of great importance. It means that once a measurement of one of the properties is carried out, subsequent measurement of that property or of any of the other properties corresponding to mutually commuting operators can be made without altering the system's value of the properties measured earlier. Only subsequent measurement of another property whose operator does not commute with **F**, **G**, or **J** will destroy precise knowledge of the values of the properties measured earlier.

✓ Example 1.9.6:

Assume that an experiment has been carried out on an atom to measure its total angular momentum L^2 . According to quantum mechanics, only values equal to $L(L+1)\hbar^2$ will be observed. Further assume, for the particular experimental sample subjected to observation, that values of L^2 equal to $2\hbar^2$ and $0\hbar^2$ were detected in relative amounts of 64 % and 36 %, respectively. This means that the atom's original wavefunction ψ could be represented as:

$$\psi = 0.8P + 0.6S,$$

where P and S represent the P-state and S-state components of ψ . The squares of the amplitudes 0.8 and 0.6 give the 64 % and 36 % probabilities mentioned above.

Now assume that a subsequent measurement of the component of angular momentum along the lab-fixed z-axis is to be measured for that sub-population of the original sample found to be in the P-state. For that population, the wavefunction is now a pure P-function:

$$\psi' = P$$

However, at this stage we have no information about how much of this ψ' is of $m = 1, 0$, or -1 , nor do we know how much 2p, 3p, 4p, ... np components this state contains.

Because the property corresponding to the operator \mathbf{L}_z is about to be measured, we express the above ψ' in terms of the eigenfunctions of \mathbf{L}_z :

$$\psi' = P.$$

However, at this stage we have no information about how much of this ψ' is of $m = 1, 0$, or -1 , nor do we know how much 2p, 3p, 4p, ... np components this state contains.

Because the property corresponding to the operator \mathbf{L}_z is about to be measured, we express the above ψ' in terms of the eigenfunctions of \mathbf{L}_z :

$$\psi' = P = \sum_{m=1,0,-1} C'_m P_m.$$

When the measurement of L_z is made, the values $1\hbar, 0\hbar$, and $-1\hbar$ will be observed with probabilities given by $|C'_1|^2, |C'_0|^2$, and $|C'_{-1}|^2$, respectively. For that sub-population found to have, for example, L_z equal to $-1\hbar$, the wavefunction then becomes

$$\psi' = P_{-1}.$$

At this stage, we do not know how much of $2p_{-1}, 3p_{-1}, 4p_{-1}, \dots np_{-1}$ this wavefunction contains. To probe this question another subsequent measurement of the energy (corresponding to the H operator) could be made. Doing so would allow the amplitudes in the expansion of the above $\psi'' = P_{-1}$

$$\psi'' = P_{-1} = \sum_n C''_n n P_{-1}$$

to be found.

The kind of experiment outlined above allows one to find the content of each particular component of an initial sample's wavefunction. For example, the original wavefunction has $0.64|C''_n|^2|C'_m|^2$ fractional content of the various nP_m functions. It is analogous to the other examples considered above because all of the operators whose properties are measured commute.

✓ Example 1.9.7:

Let us consider an experiment in which we begin with a sample (with wavefunction ψ) that is first subjected to measurement of L_z and then subjected to measurement of L^2 and then of the energy. In this order, one would first find specific values (integer multiples of \hbar) of L_z and one would express ψ as

$$\psi = \sum_m D_m \psi_m.$$

At this stage, the nature of each ψ_m is unknown (e.g., the ψ_1 function can contain $\psi_{1,1}$, $\psi_{1,0}$, $\psi_{1,-1}$, etc. components); all that is known is that ψ_m has $m\hbar$ as its L_z value

Taking that sub-population ($|D_m|^2$ fraction) with a particular $m\hbar$ value for L_z and subjecting it to subsequent measurement of L^2 requires the current wavefunction ψ_m to be expressed as

$$\psi_m = \sum_L D_{L,m} \psi_{L,m}.$$

When L^2 is measured the value $L(L+1)\hbar^2$ will be observed with probability $|D_{m,L}|^2$, and the wavefunction for that particular sub-population will become

$$\psi'' = \psi_{L,m}.$$

At this stage, we know the value of L and of m , but we do not know the energy of the state. For example, we may know that the present sub-population has $L=1$, $m=-1$, but we have no knowledge (yet) of how much $2p-1$, $3p-1$, ... $np-1$ the system contains.

To further probe the sample, the above sub-population with $L=1$ and $m=-1$ can be subjected to measurement of the energy. In this case, the function $\psi_{1,-1}$ must be expressed as

$$\psi_{1,-1} = \sum_n D''_n n P_{-1}.$$

When the energy measurement is made, the state $n P_{-1}$ will be found $|D''_n|^2$ fraction of the time.

The fact that \mathbf{L}_z , \mathbf{L}^2 , and \mathbf{H} all commute with one another (i.e., are mutually commutative) makes the series of measurements described in the above examples more straightforward than if these operators did not commute.

In the first experiment, the fact that they are mutually commutative allowed us to expand the 64 % probable \mathbf{L}^2 eigenstate with $L=1$ in terms of functions that were eigenfunctions of the operator for which measurement was about to be made without destroying our knowledge of the value of L^2 . That is, because \mathbf{L}^2 and \mathbf{L}_z can have simultaneous eigenfunctions, the $L = 1$ function can be expanded in terms of functions that are eigenfunctions of both \mathbf{L}^2 and \mathbf{L}_z . This in turn, allowed us to find experimentally the sub-population that had, for example $-\hbar$ as its value of L_z while retaining knowledge that the state remains an eigenstate of \mathbf{L}^2 (the state at this time had $L = 1$ and $m = -1$ and was denoted P_{-1}). Then, when this P_{-1} state was subjected to energy measurement, knowledge of the energy of the sub-population could be gained without giving up knowledge of the L^2 and L_z information; upon carrying out said measurement, the state became $n P_{-1}$.

We therefore conclude that the act of carrying out an experimental measurement disturbs the system in that it causes the system's wavefunction to become an eigenfunction of the operator whose property is measured. If two properties whose corresponding operators commute are measured, the measurement of the second property does not destroy knowledge of the first property's value gained in the first measurement.

On the other hand, as detailed further in Appendix C, if the two properties (**F** and **G**) do not commute, the second measurement destroys knowledge of the first property's value. After the first measurement, Ψ is an eigenfunction of **F**; after the second measurement, it becomes an eigenfunction of **G**. If the two non-commuting operators' properties are measured in the opposite order, the wavefunction first is an eigenfunction of **G**, and subsequently becomes an eigenfunction of **F**.

It is thus often said that 'measurements for operators that do not commute interfere with one another'. The simultaneous measurement of the position and momentum along the same axis provides an example of two measurements that are incompatible. The fact that $\mathbf{x} = \mathbf{x}$ and $p_x = -i\hbar \frac{\partial}{\partial x}$ do not commute is straightforward to demonstrate:

$$\left[x \left(-i\hbar \frac{\partial}{\partial x} \right) - \left(-i\hbar \frac{\partial}{\partial x} \right) x \right] \chi = i\hbar \chi \neq 0.$$

Operators that commute with the Hamiltonian and with one another form a particularly important class because each such operator permits each of the energy eigenstates of the system to be labelled with a corresponding quantum number. These operators are called **symmetry operators**. As will be seen later, they include angular momenta (e.g., L^2, L_z, S^2, S_z , for atoms) and point group symmetries (e.g., planes and rotations about axes). Every operator that qualifies as a symmetry operator provides a quantum number with which the energy levels of the system can be labeled.

7: Expectation Values

If a property F is measured for a large number of systems all described by the same Ψ , the average value of $\langle F \rangle$ for such a set of measurements can be computed as

$$\langle F \rangle = \langle \Psi | \mathbf{F} | \Psi \rangle.$$

Expanding Ψ in terms of the complete set of eigenstates of \mathbf{F} allows $\langle F \rangle$ to be rewritten as follows:

$$\langle F \rangle = \sum_j f_j |\langle \phi_j | \Psi \rangle|^2,$$

which clearly expresses $\langle F \rangle$ as the product of the probability P_j of obtaining the particular value f_j when the property F is measured and the value f_j of the property in such a measurement. This same result can be expressed in terms of the density matrix $D_{i,j}$ of the state Ψ defined above as:

$$\begin{aligned} \langle F \rangle &= \sum_{i,j} \langle \Psi | \phi_i \rangle \langle \phi_i | \mathbf{F} | \phi_j \rangle \langle \phi_j | \Psi \rangle = \sum_{i,j} C_i^* \langle \phi_i | \mathbf{F} | \phi_j \rangle C_j \\ &= \sum_{i,j} D_{i,j} \langle \phi_i | \mathbf{F} | \phi_j \rangle = \text{Tr}(DF). \end{aligned}$$

Here, DF represents the matrix product of the density matrix $D_{j,i}$ and the matrix representation $F_{i,j} = \langle \phi_i | \mathbf{F} | \phi_j \rangle$ of the \mathbf{F} operator, both taken in the $\{\phi_j\}$ basis, and Tr represents the matrix trace operation.

As mentioned at the beginning of this Section, this set of rules and their relationships to experimental measurements can be quite perplexing. The structure of quantum mechanics embodied in the above rules was developed in light of new scientific observations (e.g., the photoelectric effect, diffraction of electrons) that could not be interpreted within the conventional pictures of classical mechanics. Throughout its development, these and other experimental observations placed severe constraints on the structure of the equations of the new quantum mechanics as well as on their interpretations. For example, the observation of discrete lines in the emission spectra of atoms gave rise to the idea that the atom's electrons could exist with only certain discrete energies and that light of specific frequencies would be given off as transitions among these quantized energy states took place.

Even with the assurance that quantum mechanics has firm underpinnings in experimental observations, students learning this subject for the first time often encounter difficulty. Therefore, it is useful to again examine some of the model problems for which the Schrödinger equation can be exactly solved and to learn how the above rules apply to such concrete examples.

The examples examined earlier in this Chapter and those given in the Exercises and Problems serve as useful models for chemically important phenomena: electronic motion in polyenes, in solids, and in atoms as well as vibrational and rotational motions. Their study thus far has served two purposes; it allowed the reader to gain some familiarity with applications of quantum mechanics and it introduced models that play central roles in much of chemistry. Their study now is designed to illustrate how the above seven rules of quantum mechanics relate to experimental reality.

An Example Illustrating Several of the Fundamental Rules

The physical significance of the time independent wavefunctions and energies treated in Section II as well as the meaning of the seven fundamental points given above can be further illustrated by again considering the simple two-dimensional electronic motion model.

If the electron were prepared in the eigenstate corresponding to $n_x = 1, n_y = 2$, its total energy would be

$$E = \pi^2 \frac{\hbar^2}{2m} \left[\frac{1^2}{L_x^2} + \frac{2^2}{L_y^2} \right].$$

If the energy were experimentally measured, this and only this value would be observed, and this same result would hold for all time as long as the electron is undisturbed.

If an experiment were carried out to measure the momentum of the electron along the y-axis, according to the second postulate above, only values equal to the eigenvalues of $-\hbar \frac{\partial}{\partial y}$ could be observed. The p_y eigenfunctions (i.e., functions that obey $p_y F = -\hbar \frac{\partial}{\partial y} F = cF$) are of the form

$$\sqrt{\frac{1}{L_y}} e^{ik_y y},$$

where the momentum $\hbar k_y$ can achieve any value; the $\sqrt{\frac{1}{L_y}}$ factor is used to normalize the eigenfunctions over the range $0 \leq y \leq L_y$. It is useful to note that the y-dependence of ψ as expressed above $\left[e^{\frac{i2\pi y}{L_y}} - e^{-\frac{i2\pi y}{L_y}} \right]$ is already written in terms of two such eigenstates of $-i\hbar \frac{\partial}{\partial y}$:

$$\begin{aligned} -\hbar \frac{\partial}{\partial y} \left(e^{\frac{i2\pi y}{L_y}} \right) &= \frac{2\hbar}{L_y} \left(e^{\frac{i2\pi y}{L_y}} \right), \text{ and} \\ -\hbar \frac{\partial}{\partial y} \left(e^{-\frac{i2\pi y}{L_y}} \right) &= -\frac{2\hbar}{L_y} \left(e^{-\frac{i2\pi y}{L_y}} \right). \end{aligned}$$

Thus, the expansion of ψ in terms of eigenstates of the property being measured dictated by the fifth postulate above is already accomplished. The only two terms in this expansion correspond to momenta along the y-axis of $\frac{2\hbar}{L_y}$ and $-\frac{2\hbar}{L_y}$; the probabilities of observing these two momenta are given by the squares of the expansion coefficients of ψ in terms of the normalized eigenfunctions of $-i\hbar \frac{\partial}{\partial y}$. The functions $\sqrt{\frac{1}{L_y}} \left(e^{\frac{i2\pi y}{L_y}} \right)$ and $\sqrt{\frac{1}{L_y}} \left(e^{-\frac{i2\pi y}{L_y}} \right)$ are such normalized eigenfunctions; the expansion coefficients of these functions in ψ are $\frac{1}{\sqrt{2}}$ and $-\frac{1}{\sqrt{2}}$, respectively. Thus the momentum $\frac{2\hbar}{L_y}$ will be observed with probability $\left(\frac{1}{\sqrt{2}} \right)^2 = \frac{1}{2}$ and $-\frac{2\hbar}{L_y}$ will be observed with probability $\left(\frac{1}{\sqrt{2}} \right)^2 = \frac{1}{2}$. If the momentum along the x-axis were experimentally measured, again only two values $\frac{1\hbar}{L_x}$ and $-\frac{1\hbar}{L_x}$ would be found, each with a probability of $\frac{1}{2}$.

The average value of the momentum along the x-axis can be computed either as the sum of the probabilities multiplied by the momentum values:

$$\langle p_x \rangle = \frac{1}{2} \left[\frac{1\hbar}{L_x} - \frac{1\hbar}{L_x} \right] = 0,$$

or as the so-called expectation value integral shown in the seventh postulate:

$$\langle p_x \rangle = \iint \psi^* \left(-\hbar \frac{\partial \psi}{\partial x} \right) dx dy.$$

Inserting the full expression for $\psi(x,y)$ and integrating over x and y from 0 to L_x and L_y , respectively, this integral is seen to vanish. This means that the result of a large number of measurements of p_x on electrons each described by the same ψ will yield zero net momentum along the x-axis.; half of the measurements will yield positive momenta and half will yield negative momenta of the same magnitude.

The time evolution of the full wavefunction given above for the $n_x=1, n_y=2$ state is easy to express because this ψ is an energy eigenstate:

$$\Psi(x, y, t) = \psi(x, y) e^{\frac{-iEt}{\hbar}}.$$

If, on the other hand, the electron had been prepared in a state $\psi(x, y)$ that is not a pure eigenstate (i.e., cannot be expressed as a single energy eigenfunction), then the time evolution is more complicated. For example, if at $t=0$ ψ were of the form

$$\psi = \sqrt{\frac{2}{L_x}} \sqrt{\frac{2}{L_y}} \left[a \sin\left(\frac{2\pi x}{L_x}\right) \sin\left(\frac{1\pi y}{L_y}\right) + b \sin\left(\frac{1\pi x}{L_x}\right) \sin\left(\frac{2\pi y}{L_y}\right) \right],$$

with a and b both real numbers whose squares give the probabilities of finding the system in the respective states, then the time

evolution operator $e^{\frac{-i\mathbf{H}t}{\hbar}}$ applied to ψ would yield the following time dependent function:

$$\Psi = \sqrt{\frac{2}{L_x}} \sqrt{\frac{2}{L_y}} \left[a e^{\frac{-iE_{2,1}t}{\hbar}} \sin\left(\frac{2\pi x}{L_x}\right) \sin\left(\frac{2\pi y}{L_y}\right) + b e^{\frac{-iE_{1,2}t}{\hbar}} \sin\left(\frac{1\pi x}{L_x}\right) \sin\left(\frac{2\pi y}{L_y}\right) \right],$$

where

$$E_{2,1} = \pi^2 \frac{\hbar^2}{2m} \left[\frac{2^2}{L_x^2} + \frac{1^2}{L_y^2} \right], \text{ and}$$

$$E_{1,2} = \pi^2 \frac{\hbar^2}{2m} \left[\frac{1^2}{L_x^2} + \frac{2^2}{L_y^2} \right], \text{ and}$$

The probability of finding $E_{2,1}$ if an experiment were carried out to measure energy would be $a |e^{\frac{-iE_{2,1}t}{\hbar}}|^2 = |a|^2$; the probability for finding $E_{1,2}$ would be $|b|^2$. The spatial probability distribution for finding the electron at points x, y will, in this case, be given by:

$$|\Psi|^2 = |a|^2 |\psi_{2,1}|^2 + |b|^2 |\psi_{1,2}|^2 + 2ab \psi_{2,1} \psi_{1,2} \cos\left(\frac{\Delta Et}{\hbar}\right),$$

where ΔE is $E_{2,1} - E_{1,2}$,

$$\psi_{2,1} = \sqrt{\frac{2}{L_x}} \sqrt{\frac{2}{L_y}} \sin\left(\frac{2\pi x}{L_x}\right) \sin\left(\frac{1\pi y}{L_y}\right),$$

and

$$\psi_{1,2} = \sqrt{\frac{2}{L_x}} \sqrt{\frac{2}{L_y}} \sin\left(\frac{1\pi x}{L_x}\right) \sin\left(\frac{2\pi y}{L_y}\right),$$

This spatial distribution is not stationary but evolves in time. So in this case, one has a wavefunction that is not a pure eigenstate of the Hamiltonian (one says that Ψ is a superposition state or a non-stationary state) whose average energy remains constant ($E = E_{2,1}|a|^2 + E_{1,2}|b|^2$) but whose spatial distribution changes with time.

Although it might seem that most spectroscopic measurements would be designed to prepare the system in an eigenstate (e.g., by focusing on the sample light whose frequency matches that of a particular transition), such need not be the case. For example, if very short laser pulses are employed, the Heisenberg uncertainty broadening ($\Delta E \Delta t \geq \hbar$) causes the light impinging on the sample to be very non-monochromatic (e.g., a pulse time of 1×10^{-12} sec corresponds to a frequency spread of approximately 5 cm^{-1}). This, in turn, removes any possibility of preparing the system in a particular quantum state with a resolution of better than 30 cm^{-1} because the system experiences time oscillating electromagnetic fields whose frequencies range over at least 5 cm^{-1} .

Essentially all of the model problems that have been introduced in this Chapter to illustrate the application of quantum mechanics constitute widely used, highly successful 'starting-point' models for important chemical phenomena. As such, it is important that students retain working knowledge of the energy levels, wavefunctions, and symmetries that pertain to these models.

Thus far, exactly soluble model problems that represent one or more aspects of an atom or molecule's quantum-state structure have been introduced and solved. For example, electronic motion in polyenes was modeled by a particle-in-a-box. The harmonic oscillator and rigid rotor were introduced to model vibrational and rotational motion of a diatomic molecule

As chemists, we are used to thinking of electronic, vibrational, rotational, and translational energy levels as being (at least approximately) separable. On the other hand, we are aware that situations exist in which energy can flow from one such degree of freedom to another (e.g., electronic-to-vibrational energy flow occurs in radiationless relaxation and vibration-rotation couplings are important in molecular spectroscopy). It is important to understand how the simplifications that allow us to focus on electronic or vibrational or rotational motion arise, how they can be obtained from a first-principles derivation, and what their limitations and range of accuracy are.

This page titled [1.9: The Physical Relevance of Wavefunctions, Operators and Eigenvalues](#) is shared under a [CC BY-NC-SA 4.0](#) license and was authored, remixed, and/or curated by [Jack Simons](#) via [source content](#) that was edited to the style and standards of the LibreTexts platform.

CHAPTER OVERVIEW

2: Approximation Methods

Approximation methods can be used when exact solutions to the Schrödinger equation cannot be found. In applying quantum mechanics to 'real' chemical problems, one is usually faced with a Schrödinger differential equation for which, to date, no one has found an analytical solution. This is equally true for electronic and nuclear-motion problems. It has therefore proven essential to develop and efficiently implement mathematical methods which can provide approximate solutions to such eigenvalue equations. Two methods are widely used in this context- the variational method and perturbation theory. These tools, whose use permeates virtually all areas of theoretical chemistry, are briefly outlined here, and the details of perturbation theory are amplified in Appendix D

[2.1: The Variational Method](#)

[2.2: Perturbation Theory](#)

[2.E: Approximation Methods \(Exercises\)](#)

This page titled [2: Approximation Methods](#) is shared under a [CC BY-NC-SA 4.0](#) license and was authored, remixed, and/or curated by [Jack Simons](#) via [source content](#) that was edited to the style and standards of the LibreTexts platform.

2.1: The Variational Method

For the kind of potentials that arise in atomic and molecular structure, the Hamiltonian H is a Hermitian operator that is bounded from below (i.e., it has a lowest eigenvalue). Because it is Hermitian, it possesses a complete set of orthonormal eigenfunctions $\{|\psi_j\rangle\}$. Any function Φ that depends on the same spatial and spin variables on which H operates and obeys the same boundary conditions that the $\{\Psi_j\}$ obey can be expanded in this complete set

$$\Phi = \sum_j C_j |\psi_j\rangle.$$

The expectation value of the Hamiltonian for any such function can be expressed in terms of its C_j coefficients and the **exact** energy levels E_j of H as follows:

$$\langle \Phi | H | \Phi \rangle = \sum_{ij} C_i C_j \langle \psi_i | H | \psi_j \rangle = \sum_j |C_j|^2 E_j.$$

If the function Φ is normalized, the sum $\sum_j |C_j|^2$ is equal to unity. Because H is bounded from below, all of the E_j must be greater than or equal to the lowest energy E_0 . Combining the latter two observations allows the energy expectation value of Φ to be used to produce a very important inequality:

$$\langle \Phi | H | \Phi \rangle \geq E_0.$$

The equality can hold only if Φ is equal to ψ_0 ; if Φ contains components along any of the other ψ_j , the energy of Φ will exceed E_0 .

This upper-bound property forms the basis of the so-called **variational method** in which 'trial wavefunctions' Φ are constructed:

1. To guarantee that Φ obeys all of the boundary conditions that the exact Ψ_j do and that Φ is of the proper spin and space symmetry and is a function of the same spatial and spin coordinates as the Ψ_j ;
2. With parameters embedded in Φ whose 'optimal' values are to be determined by making $\langle \Phi | H | \Phi \rangle$ a minimum.

It is perfectly acceptable to vary any parameters in Φ to attain the lowest possible value for $\langle \Phi | H | \Phi \rangle$ because the proof outlined above constrains this expectation value to be above the true lowest eigenstate's energy E_0 for **any** Φ . The philosophy then is that the Φ that gives the lowest $\langle \Phi | H | \Phi \rangle$ is the best because its expectation value is closest to the exact energy.

Linear Variational Calculations

Quite often a **trial wavefunction** is expanded as a linear combination of other functions (not the eigenvalues of the Hamiltonian, since they are not known)

$$\Phi = \sum_J^N C_J |\Phi_J\rangle. \quad (2.1.1)$$

In these cases, one says that a 'linear variational' calculation is being performed. The set of functions $\{\Phi_J\}$ are usually constructed to obey all of the boundary conditions that the exact state Ψ obeys, to be functions of the the same coordinates as Ψ , and to be of the same spatial and spin symmetry as Ψ . Beyond these conditions, the $\{\Phi_J\}$ are nothing more than members of a set of functions that are convenient to deal with (e.g., convenient to evaluate Hamiltonian matrix elements $\langle \Phi_I | H | \Phi_J \rangle$ that can, in principle, be made complete if more and more such functions are included in the expansion in Equation 2.1.1 (i.e., increase N).

For such a trial wavefunction, the energy depends quadratically on the 'linear variational' C_J coefficients:

$$\langle \Phi | H | \Phi \rangle = \sum_{I,J}^{N,N} C_I C_J \langle \Phi_I | H | \Phi_J \rangle.$$

Minimization of this energy with the constraint that Φ remain normalized, i.e.,

$$\langle \Phi | \Phi \rangle = \sum_{IJ} C_I C_J \langle \Phi_I | \Phi_J \rangle = 1$$

gives rise to a so-called **secular** or **eigenvalue-eigenvector** problem:

$$\sum_J [\langle \Phi_I | H | \Phi_J \rangle - E \langle \Phi_I | \Phi_J \rangle] C_J = \sum_J [H_{IJ} - E S_{IJ}] C_J = 0.$$

If the functions $\{|\Phi_J\rangle\}$ are orthonormal, then the overlap matrix S reduces to the unit matrix and the above generalized eigenvalue problem reduces to the more familiar form:

$$\sum_J^N H_{IJ} C_J = E C_I.$$

The secular problem, in either form, has as many eigenvalues E_i and eigenvectors $\{C_{iJ}\}$ as the dimension of the H_{IJ} matrix as Φ . It can also be shown that between successive pairs of the eigenvalues obtained by solving the secular problem at least one exact eigenvalue must occur (i.e., $E_{i+1} > E_{exact} > E_i$, for all i). This observation is referred to as 'the bracketing theorem'.

Variational methods, in particular the linear variational method, are the most widely used approximation techniques in quantum chemistry. To implement such a method one needs to know the Hamiltonian H whose energy levels are sought and one needs to construct a trial wavefunction in which some 'flexibility' exists (e.g., as in the linear variational method where the C_J coefficients can be varied). In Section 6 this tool will be used to develop several of the most commonly used and powerful molecular orbital methods in chemistry.

This page titled [2.1: The Variational Method](#) is shared under a [CC BY-NC-SA 4.0](#) license and was authored, remixed, and/or curated by [Jack Simons](#) via [source content](#) that was edited to the style and standards of the LibreTexts platform.

2.2: Perturbation Theory

Perturbation theory is the second most widely used approximation method in quantum chemistry. It allows one to estimate the splittings and shifts in energy levels and changes in wavefunctions that occur when an external field (e.g., an electric or magnetic field or a field that is due to a surrounding set of 'ligands'- a crystal field) or a field arising when a previously-ignored term in the Hamiltonian is applied to a species whose 'unperturbed' states are known. These 'perturbations' in energies and wavefunctions are expressed in terms of the (complete) set of unperturbed eigenstates.

Assuming that all of the wavefunctions ϕ_k and energies E_k^0 belonging to the unperturbed Hamiltonian H^0 are known

$$H^0 \Phi_k = E_k^0 \Phi_k,$$

and given that one wishes to find eigenstates (ψ_k and E_k) of the perturbed Hamiltonian

$$H = H^0 + \lambda V,$$

perturbation theory expresses ψ_k and E_k as power series in the perturbation strength λ :

$$\psi_k = \sum_{n=0}^{\infty} \lambda^n \psi_k^{(n)}$$

$$E_k = \sum_{n=0}^{\infty} \lambda^n E_k^{(n)}.$$

The systematic development of the equations needed to determine the $E_k^{(n)}$ and the $\psi_k^{(n)}$ is presented in Appendix D. Here, we simply quote the few lowest-order results.

The zeroth-order wavefunctions and energies are given in terms of the solutions of the unperturbed problem as follows:

$$\psi_k^{(0)} = \Phi_k$$

and

$$E_k^{(0)} = E_k^0.$$

This simply means that one must be willing to identify one of the unperturbed states as the 'best' approximation to the state being sought. This, of course, implies that one must therefore strive to find an unperturbed model problem, characterized by H^0 that represents the true system as accurately as possible, so that one of the Φ_k will be as close as possible to ψ_k .

The first-order energy correction is given in terms of the zeroth-order (i.e., unperturbed) wavefunction as:

$$E_k^{(1)} = \langle \Phi_k | V | \Phi_k \rangle,$$

which is identified as the average value of the perturbation taken with respect to the unperturbed function Φ_k . The so-called **first-order wavefunction** $\psi_k^{(1)}$ expressed in terms of the complete set of unperturbed functions $\{\Phi_j\}$ is:

$$\psi_k^{(1)} = \sum_{j \neq k} \frac{\langle \Phi_j | V | \Phi_k \rangle}{[E_k^0 - E_j^0]} |\Phi_j\rangle.$$

and the second-order correction to the wavefunction is expressed as

$$\psi_k^{(2)} = \sum_{j \neq k} \frac{1}{[E_k^0 - E_j^0]} \sum_{l \neq k} \left[\langle \Phi_j | V | \Phi_l \rangle - \delta_{j,i} E_k^{(1)} \right]$$

$$\langle \Phi_l | V | \Phi_k \rangle \frac{1}{E_k^0 - E_l^0} |\Phi_j\rangle.$$

An essential point about perturbation theory is that the energy corrections $E_k^{(n)}$ and wavefunction corrections $\psi_k^{(n)}$ are expressed in terms of integrals over the unperturbed wavefunctions Φ_k involving the perturbation (i.e., $\langle \Phi_j | V | \Phi_l \rangle$) and the unperturbed energies E_j^0 . Perturbation theory is most useful when one has, in hand, the solutions to an unperturbed Schrödinger equation that is

reasonably 'close' to the full Schrödinger equation whose solutions are being sought. In such a case, it is likely that low-order corrections will be adequate to describe the energies and wavefunctions of the full problem.

It is important to stress that although the solutions to the full 'perturbed' Schrödinger equation are expressed, as above, in terms of sums over all states of the unperturbed Schrödinger equation, it is improper to speak of the perturbation as creating excited-state species. For example, the polarization of the 1s orbital of the Hydrogen atom caused by the application of a static external electric field of strength E along the z-axis is described, in first-order perturbation theory, through the sum

$$\sum_{n=2,\infty} \phi_{np_0} \frac{\langle \phi_{np_0} | E e r \cos\theta | 1s \rangle}{E_{1s} - E_{np_0}}$$

over all $p_z = p_0$ orbitals labeled by principal quantum number n . The coefficient multiplying each p_0 orbital depends on the energy gap corresponding to the 1s-to- np 'excitation' as well as the electric dipole integral $\langle \phi_{np_0} | E e r \cos\theta | 1s \rangle$ between the 1s orbital and the np_0 orbital.

This sum describes the polarization of the 1s orbital in terms of functions that have p_0 symmetry; by combining an s orbital and p_0 orbitals, one can form a 'hybrid-like' orbital that is nothing but a distorted 1s orbital. The appearance of the excited np_0 orbitals has nothing to do with forming excited states; these np_0 orbitals simply provide a set of functions that can describe the response of the 1s orbital to the applied electric field.

The relative strengths and weaknesses of perturbation theory and the variational method, as applied to studies of the electronic structure of atoms and molecules, are discussed in Section 6.

This page titled [2.2: Perturbation Theory](#) is shared under a [CC BY-NC-SA 4.0](#) license and was authored, remixed, and/or curated by [Jack Simons](#) via [source content](#) that was edited to the style and standards of the LibreTexts platform.

2.E: Approximation Methods (Exercises)

Your page has been created!

Remove this content and add your own.

Edit page

Click the Edit page button in your user bar. You will see a suggested structure for your content. Add your content and hit Save.

Tips:

Drag and drop

Drag one or more image files from your computer and drop them onto your browser window to add them to your page.

Classifications

Tags are used to link pages to one another along common themes. Tags are also used as markers for the dynamic organization of content in the CXone Expert framework.

Working with templates

CXone Expert [templates](#) help guide and organize your documentation, making it flow easier and more uniformly. Edit existing templates or create your own.

 [Visit for all help topics.](#)

This page titled [2.E: Approximation Methods \(Exercises\)](#) is shared under a [CC BY-NC-SA 4.0](#) license and was authored, remixed, and/or curated by [Jack Simons](#) via [source content](#) that was edited to the style and standards of the LibreTexts platform.

CHAPTER OVERVIEW

3: Nuclear Motion

The Application of the Schrödinger Equation to the Motions of Electrons and Nuclei in a Molecule Lead to the Chemists' Picture of Electronic Energy Surfaces on Which Vibration and Rotation Occurs and Among Which Transitions Take Place.

[3.1: The Born-Oppenheimer Separation of Electronic and Nuclear Motions](#)

[3.2: Time Scale Separation](#)

[3.3: Vibration/Rotation States for Each Electronic Surface](#)

[3.4: Rotation and Vibration of Diatomic Molecules](#)

[3.5: Separation of Vibration and Rotation](#)

[3.6: The Rigid Rotor and Harmonic Oscillator](#)

[3.7: The Morse Oscillator](#)

[3.8: Rotation of Polyatomic Molecules](#)

[3.9: Rotation of Linear Molecules](#)

[3.E: Exercises](#)

[3.10: Rotation of Non-Linear Molecules](#)

[3.11: Chapter Summary](#)

This page titled [3: Nuclear Motion](#) is shared under a [CC BY-NC-SA 4.0](#) license and was authored, remixed, and/or curated by [Jack Simons](#) via [source content](#) that was edited to the style and standards of the LibreTexts platform.

3.1: The Born-Oppenheimer Separation of Electronic and Nuclear Motions

Many elements of chemists' pictures of molecular structure hinge on the point of view that separates the electronic motions from the vibrational/rotational motions and treats couplings between these (approximately) separated motions as 'perturbations'. It is essential to understand the origins and limitations of this separated-motions picture.

To develop a framework in terms of which to understand when such separability is valid, one thinks of an atom or molecule as consisting of a collection of N electrons and M nuclei each of which possesses kinetic energy and among which coulombic potential energies of interaction arise. To properly describe the motions of all these particles, one needs to consider the full Schrödinger equation $H\Psi = E\Psi$, in which the Hamiltonian H contains the sum (denoted H_e) of the kinetic energies of all N electrons and the coulomb potential energies among the N electrons and the M nuclei as well as the kinetic energy T of the M nuclei

$$T = \sum_{a=1,M} \left(\frac{-\hbar^2}{2m_a} \right) \nabla_a^2,$$

$$H = H_e + T$$

$$H_e = \sum_j \left[\frac{-\hbar^2}{2m_e} \nabla_j^2 - \sum_a \frac{Z_a e^2}{r_{j,a}} \right] + \sum_{j < k} \frac{e^2}{r_{j,k}} + \sum_{a < b} Z_a Z_b \frac{e^2}{R_{a,b}}.$$

Here, m_a is the mass of the nucleus a , $Z_a e^2$ is its charge, and ∇_a^2 is the Laplacian with respect to the three cartesian coordinates of this nucleus (this operator ∇_a^2 is given in spherical polar coordinates in Appendix A); $r_{j,a}$ is the distance between the j^{th} electron and the a^{th} nucleus, $r_{j,k}$ is the distance between the j^{th} and k^{th} electrons, m_e is the electron's mass, and $R_{a,b}$ is the distance from nucleus a to nucleus b .

The full Hamiltonian H thus contains differential operators over the $3N$ electronic coordinates (denoted r as a shorthand) and the $3M$ nuclear coordinates (denoted R as a shorthand). In contrast, the electronic Hamiltonian H_e is a Hermitian differential operator in r -space but **not** in R -space. Although H_e is indeed a function of the R -variables, it is not a differential operator involving them.

Because H_e is a Hermitian operator in r -space, its eigenfunctions $\Psi_i(r|R)$ obey $H_e \Psi_i(r|R) = E_i(R) \Psi_i(r|R)$

for any values of the R -variables, and form a **complete set** of functions of r for any values of R . These eigenfunctions and their eigenvalues $E_i(R)$ depend on R only because the potentials appearing in H_e depend on R . The Ψ_i and E_i are the **electronic wavefunctions** and **electronic energies** whose evaluations are treated in the next three Chapters.

The fact that the set of $\{\Psi_i\}$ is, in principle, complete in r -space allows the full (electronic and nuclear) wavefunction Ψ to have its r -dependence expanded in terms of the Ψ_i :

$$\Psi(r, R) = \sum_i \Psi_i(r|R) \Xi_i(R).$$

The $\Xi_i(R)$ functions, carry the remaining R -dependence of Ψ and are determined by insisting that Ψ as expressed here obey the full Schrödinger equation:

$$(H_e + T - E) \sum_i \Psi_i(r|R) \Xi_i(R) = 0.$$

Projecting this equation against $\langle \Psi_j(r|R) |$ (integrating only over the electronic coordinates because the Ψ_j are orthonormal only when so integrated) gives:

$$[(E_j(R) - E) \Xi_j(R) + T \Xi_j(R)] = - \sum_i \left[\langle \Psi_j | T | \Psi_i \rangle (R) \Xi_i(R) + \sum_{a=1,M} \frac{-\hbar^2}{m_a} \langle \Psi_j | \nabla_a | \Psi_i \rangle (R) \cdot \nabla_a \Xi_i(R) \right],$$

where the (R) notation in $\langle \Psi_j | T | \Psi_i \rangle (R)$ and $\langle \Psi_j | \nabla_a | \Psi_i \rangle (R)$ has been used to remind one that the integrals $\langle \dots \rangle$ are carried out only over the r coordinates and, as a result, still depend on the R coordinates.

In the **Born-Oppenheimer** (BO) approximation, one neglects the so-called nonadiabatic or non-BO couplings on the right-hand side of the above equation. Doing so yields the following equations for the $\Xi_i(R)$ functions:

$$[(E_j(R) - E)\Xi_j^0(R) + T\Xi_j^0(R)] = 0,$$

where the superscript in $\Xi_j^0(R)$ is used to indicate that these functions are solutions within the BO approximation only.

These BO equations can be recognized as the equations for the **translational, rotational, and vibrational** motion of the nuclei on the 'potential energy surface' $E_j(R)$. That is, within the BO picture, the electronic energies $E_j(R)$, considered as functions of the nuclear positions R , provide the potentials on which the nuclei move. The electronic and nuclear-motion aspects of the Schrödinger equation are thereby separated.

This page titled [3.1: The Born-Oppenheimer Separation of Electronic and Nuclear Motions](#) is shared under a [CC BY-NC-SA 4.0](#) license and was authored, remixed, and/or curated by [Jack Simons](#) via [source content](#) that was edited to the style and standards of the LibreTexts platform.

3.2: Time Scale Separation

The physical parameters that determine under what circumstances the BO approximation is accurate relate to the motional time scales of the electronic and vibrational/rotational coordinates.

The range of accuracy of this separation can be understood by considering the differences in time scales that relate to electronic motions and nuclear motions under ordinary circumstances. In most atoms and molecules, the electrons orbit the nuclei at speeds much in excess of even the fastest nuclear motions (the vibrations). As a result, the electrons can adjust 'quickly' to the slow motions of the nuclei. This means it should be possible to develop a model in which the electrons 'follow' smoothly as the nuclei vibrate and rotate.

This picture is that described by the BO approximation. Of course, one should expect large corrections to such a model for electronic states in which 'loosely held' electrons exist. For example, in molecular Rydberg states and in anions, where the outer valence electrons are bound by a fraction of an electron volt, the natural orbit frequencies of these electrons are not much faster (if at all) than vibrational frequencies. In such cases, significant breakdown of the BO picture is to be expected.

This page titled [3.2: Time Scale Separation](#) is shared under a [CC BY-NC-SA 4.0](#) license and was authored, remixed, and/or curated by [Jack Simons](#) via [source content](#) that was edited to the style and standards of the LibreTexts platform.

3.3: Vibration/Rotation States for Each Electronic Surface

The BO picture is what gives rise to the concept of a manifold of potential energy surfaces on which vibrational/rotational motions occur.

Even within the BO approximation, motion of the nuclei on the various electronic energy surfaces is different because the nature of the chemical bonding differs from surface to surface. That is, the vibrational/rotational motion on the ground-state surface is certainly not the same as on one of the excited-state surfaces. However, there are a complete set of wavefunctions $\chi_{j,m}^0(R)$ and energy levels $E_{j,m}^0$ for **each** surface $E_j(R)T + E_j(R)$ is a Hermitian operator in R-space for each surface (labelled j):

$$[T + E_j(R)]\chi_{j,m}^0(R) = E_{j,m}^0 \chi_{j,m}^0.$$

The eigenvalues $E_{j,m}^0$ must be labelled by the electronic surface (j) on which the motion occurs as well as to denote the particular state (m) on that surface.

This page titled [3.3: Vibration/Rotation States for Each Electronic Surface](#) is shared under a [CC BY-NC-SA 4.0](#) license and was authored, remixed, and/or curated by [Jack Simons](#) via [source content](#) that was edited to the style and standards of the LibreTexts platform.

3.4: Rotation and Vibration of Diatomic Molecules

For a diatomic species, the vibration-rotation $\left(\frac{V}{R}\right)$ kinetic energy operator can be expressed as follows in terms of the bond length R and the angles θ and ϕ that describe the orientation of the bond axis relative to a laboratory-fixed coordinate system:

$$T_{V/R} = \frac{-\hbar^2}{2\mu} \left[\frac{1}{R^2} \frac{\partial}{\partial R} \left(R^2 \frac{\partial}{\partial R} \right) - \left(\frac{L}{R\hbar} \right)^2 \right],$$

where the square of the rotational angular momentum of the diatomic species is

$$L^2 = \hbar^2 \left[\frac{1}{\sin\theta} \frac{\partial}{\partial \theta} \left(\sin\theta \frac{\partial}{\partial \theta} \right) + \frac{1}{\sin^2\theta} \frac{\partial^2}{\partial \phi^2} \right].$$

Because the potential $E_j(R)$ depends on R but not on θ or ϕ , the $\frac{V}{R}$ function $X_{j,n}^0$ can be written as a product of an angular part and an R -dependent part; moreover, because L^2 contains the full angle-dependence of $T_{V/R}$, $X_{j,n}^0$ can be written as

$$\Xi_{j,n}^0 = Y_{J,M}(\theta, \phi) F_{j,J,v}(R).$$

The general subscript n , which had represented the state in the full set of 3M-3 R -space coordinates, is replaced by the three quantum numbers J, M , and v (i.e., once one focuses on the three specific coordinates R, θ , and ϕ , a total of three quantum numbers arise in place of the symbol n).

Substituting this product form for $\Xi_{j,n}^0$ into the $\frac{V}{R}$ equation gives:

$$\frac{-\hbar^2}{2\mu} \left[\frac{1}{R^2} \frac{\partial}{\partial R} \left(R^2 \frac{\partial}{\partial R} \right) - \frac{J(J+1)}{R^2 \hbar^2} \right] F_{j,J,v}(R) + E_j(R) F_{j,J,v}(R) = E_{j,J,v}^0 F_{j,J,v}$$

as the equation for the vibrational (i.e., R -dependent) wavefunction within electronic state j and with the species rotating with $J(J+1)\hbar^2$ as the square of the total angular momentum and a projection along the laboratory-fixed Z -axis of $M\hbar$. The fact that the $F_{j,J,v}$ functions do not depend on the M quantum number derives from the fact that the $T_{V/R}$ kinetic energy operator does not explicitly contain J_Z ; only J^2 appears in $T_{V/R}$.

The solutions for which $J=0$ correspond to vibrational states in which the species has no rotational energy; they obey

$$\frac{-\hbar^2}{2\mu} \left[\frac{1}{R^2} \frac{\partial}{\partial R} \left(R^2 \frac{\partial}{\partial R} \right) \right] F_{j,0,v}(R) + E_j(R) F_{j,0,v}(R) = E_{j,0,v}^0 F_{j,0,v}.$$

The differential-operator parts of this equation can be simplified somewhat by substituting $F = \frac{\chi}{R}$ and thus obtaining the following equation for the new function χ :

$$\frac{-\hbar^2}{2\mu} \frac{\partial}{\partial R} \frac{\partial}{\partial R} \chi_{j,0,v}(R) + E_j(R) \chi_{j,0,v}(R) = E_{j,0,v}^0 \chi_{j,0,v}.$$

Solutions for which $J \neq 0$ require the vibrational wavefunction and energy to respond to the presence of the 'centrifugal potential' given by $\frac{\hbar^2 J(J+1)}{2\mu R^2}$; these solutions obey the full coupled V/R equations given above.

This page titled [3.4: Rotation and Vibration of Diatomic Molecules](#) is shared under a [CC BY-NC-SA 4.0](#) license and was authored, remixed, and/or curated by [Jack Simons](#) via [source content](#) that was edited to the style and standards of the LibreTexts platform.

3.5: Separation of Vibration and Rotation

It is common, in developing the working equations of diatomic-molecule rotational/vibrational spectroscopy, to treat the coupling between the two degrees of freedom using perturbation theory as developed later in this chapter. In particular, one can expand the centrifugal coupling $\hbar^2 \frac{J(J+1)}{2\mu R^2}$ around the equilibrium geometry R_e (which depends, of course, on J):

$$\begin{aligned}\hbar^2 \frac{J(J+1)}{2\mu R^2} &= \hbar^2 \frac{J(J+1)}{2\mu [R_e^2 (1 + \Delta R)^2]} \\ &\hbar^2 \frac{J(J+1)}{2\mu R_e^2} [1 - 2\Delta R + \dots],\end{aligned}$$

and treat the terms containing powers of the bond length displacement ΔR^k as perturbations. The zeroth-order equations read:

$$\frac{-\hbar^2}{2\mu} \left[\frac{1}{R^2} \frac{\partial}{\partial R} \left(R^2 \frac{\partial}{\partial R} \right) \right] F_{j,J,v}^0(R) + E_j(R) F_{j,J,v}^0(R) + \hbar^2 \frac{J(J+1)}{2\mu R_e^2} F_{j,J,v}^0 F_{j,J,v}^0,$$

and have solutions whose energies separate

$$E_{j,J,v}^0 = \hbar^2 \frac{J(J+1)}{2\mu R_e^2} + E_{j,v}$$

and whose wavefunctions are independent of J (because the coupling is not R -dependent in zeroth order)

$$F_{j,J,v}^0(R) = F_{j,v}(R).$$

Perturbation theory is then used to express the corrections to these zeroth order solutions as indicated in Appendix D.

This page titled [3.5: Separation of Vibration and Rotation](#) is shared under a [CC BY-NC-SA 4.0](#) license and was authored, remixed, and/or curated by [Jack Simons](#) via [source content](#) that was edited to the style and standards of the LibreTexts platform.

3.6: The Rigid Rotor and Harmonic Oscillator

Treatment of the rotational motion at the zeroth-order level described above introduces the so-called 'rigid rotor' energy levels and wavefunctions: $E_J = \hbar^2 \frac{J(J+1)}{2\mu R_e^2}$ and $Y_{J,M}(\theta, \phi)$; these same quantities arise when the diatomic molecule is treated as a rigid rod of length R_e . The spacings between successive rotational levels within this approximation are

$$\Delta E_{J+1,J} = 2hcB(J+1),$$

where the so-called rotational constant B is given in cm^{-1} as

$$B = \frac{h}{8\pi^2 c \mu R_e^2}.$$

The rotational level J is $(2J+1)$ -fold degenerate because the energy E_J is independent of the M quantum number of which there are $(2J+1)$ values for each J: $M = -J, -J+1, -J+2, \dots, J-2, J-1, J$.

The explicit form of the zeroth-order vibrational wavefunctions and energy levels, $F_{j,v}^0$ and $E_{j,v}^0$, depends on the description used for the electronic potential energy surface $E_j(R)$. In the crudest useful approximation, $E_j(R)$ is taken to be a so-called harmonic potential

$$E_j(R) \approx \frac{1}{2} k_j (R - R_e)^2;$$

as a consequence, the wavefunctions and energy levels reduce to

$$E_{j,v}^0 = E_j(R_e) + \hbar \frac{\sqrt{k}}{\mu} \left(v + \frac{1}{2} \right), \text{ and}$$

$$F_{j,v}^0(R) = \frac{1}{\sqrt{2^v v!}} \sqrt{\frac{\alpha}{\pi}} e^{\frac{-\alpha(R-R_e)^2}{2}} H_v \sqrt{\alpha} (R - R_e),$$

where $\alpha = \frac{\sqrt{k_j \mu}}{\hbar}$ and $H_v(y)$ denotes the Hermite polynomial defined by:

$$H_v(y) = (-1)^v e^{y^2} \frac{d^v}{dy^v} e^{-y^2}.$$

The solution of the vibrational differential equation

$$\frac{-\hbar^2}{2\mu} \left[\frac{1}{R^2} \frac{\partial}{\partial R} \left(R^2 \frac{\partial}{\partial R} \right) \right] F_{j,v}(R) + E_j(R) F_{j,v}(R) = E_{j,v} F_{j,v}$$

is treated in EWK, Atkins, and McQuarrie.

These harmonic-oscillator solutions predict evenly spaced energy levels (i.e., no anharmonicity) that persist for all v . It is, of course, known that molecular vibrations display anharmonicity (i.e., the energy levels move closer together as one moves to higher v) and that quantized vibrational motion ceases once the bond dissociation energy is reached.

This page titled [3.6: The Rigid Rotor and Harmonic Oscillator](#) is shared under a [CC BY-NC-SA 4.0](#) license and was authored, remixed, and/or curated by [Jack Simons](#) via [source content](#) that was edited to the style and standards of the LibreTexts platform.

3.7: The Morse Oscillator

The Morse oscillator model is often used to go beyond the harmonic oscillator approximation. In this model, the potential $E_j(R)$ is expressed in terms of the bond dissociation energy D_e and a parameter a related to the second derivative k of $E_j(R)$ at R_e $k = \frac{d^2 E_j}{dR^2} = 2a^2 D_e$ as follows:

$$E_j(R) - E_j(R_e) = D_e \left[1 - e^{-a(R-R_e)} \right]^2.$$

The Morse oscillator energy levels are given by

$$E_{j,v}^0 = E_j(R_e) + \hbar \frac{\sqrt{k}}{\mu} \left(v + \frac{1}{2} \right) - \frac{\hbar^2}{4} \left(\frac{k}{\mu D_e} \right) \left(v + \frac{1}{2} \right)^2$$

the corresponding eigenfunctions are also known analytically in terms of hypergeometric functions (see, for example, [Handbook of Mathematical Functions](#), M. Abramowitz and I. A. Stegun, Dover, Inc. New York, N. Y. (1964)). Clearly, the Morse solutions display anharmonicity as reflected in the negative term proportional to $(v + \frac{1}{2})^2$.

This page titled [3.7: The Morse Oscillator](#) is shared under a [CC BY-NC-SA 4.0](#) license and was authored, remixed, and/or curated by [Jack Simons](#) via [source content](#) that was edited to the style and standards of the LibreTexts platform.

3.8: Rotation of Polyatomic Molecules

For a non-linear polyatomic molecule, again with the centrifugal couplings to the vibrations evaluated at the equilibrium geometry, the following terms form the rotational part of the nuclear-motion kinetic energy:

$$T_{rot} = \sum_{i=a,b,c} \left(\frac{J_i^2}{2I_i} \right).$$

Here, I_i is the eigenvalue of the moment of inertia tensor:

$$I_{x,x} = \sum_a m_a [(R_a - R_{CoM})^2 - (x_a - x_{CoM})^2]$$

$$I_{x,y} = \sum_a m_a [(x_a - x_{CoM})(y_a - y_{CoM})]$$

expressed originally in terms of the cartesian coordinates of the nuclei (a) and of the center of mass in an arbitrary molecule-fixed coordinate system (and similarly for $I_{z,z}$, $I_{y,y}$, $I_{x,z}$ and $I_{y,z}$). The operator J_i corresponds to the component of the total rotational angular momentum \mathbf{J} along the direction belonging to the i^{th} eigenvector of the moment of inertia tensor.

Molecules for which all three principal moments of inertia (the I'_i 's) are equal are called 'spherical tops'. For these species, the rotational Hamiltonian can be expressed in terms of the square of the total rotational angular momentum J^2 :

$$T_{rot} = \frac{J^2}{2I},$$

as a consequence of which the rotational energies once again become

$$E_J = \hbar^2 \frac{J(J+1)}{2I}.$$

However, the $Y_{J,M}$ are not the corresponding eigenfunctions because the operator J^2 now contains contributions from rotations about three (no longer two) axes (i.e., the three principal axes). The proper rotational eigenfunctions are the $D_{M,K}^J(\alpha, \beta, \gamma)$ functions known as 'rotation matrices' (see Sections 3.5 and 3.6 of Zare's book on angular momentum) these functions depend on three angles (the three Euler angles needed to describe the orientation of the molecule in space) and three quantum numbers- J, M, and K. The quantum number M labels the projection of the total angular momentum (as $M\hbar$) along the laboratory-fixed z-axis; $K\hbar$ is the projection along one of the internal principal axes (in a spherical top molecule, all three axes are equivalent, so it does not matter which axis is chosen).

The energy levels of spherical top molecules are $(2J+1)^2$ -fold degenerate. Both the M and K quantum numbers run from -J, in steps of unity, to J; because the energy is independent of M and of K, the degeneracy is $(2J+1)^2$.

Molecules for which two of the three principal moments of inertia are equal are called symmetric top molecules. Prolate symmetric tops have $I_a < I_b = I_c$; oblate symmetric tops have $I_a = I_b < I_c$ (it is convention to order the moments of inertia as $I_a \leq I_b \leq I_c$). The rotational Hamiltonian can now be written in terms of J^2 and the component of \mathbf{J} along the unique moment of inertia's axis as:

$$T_{rot} = J_a^2 \left(\frac{1}{2I_a} - \frac{1}{2I_b} \right) + \frac{J^2}{2I_b}$$

for prolate tops, and

$$T_{rot} = J_c^2 \left(\frac{1}{2I_c} - \frac{1}{2I_b} \right) + \frac{J^2}{2I_b}$$

for oblate tops. Again, the $D_{M,K}^J(\alpha, \beta, \gamma)$ are the eigenfunctions, where the quantum number K describes the component of the rotational angular momentum \mathbf{J} along the unique molecule-fixed axis (i.e., the axis of the unique moment of inertia). The energy levels are now given in terms of J and K as follows:

$$E_{J,K} \hbar^2 \frac{J(J+1)}{2I_b} + \hbar^2 K^2 \left(\frac{1}{2I_a} - \frac{1}{2I_b} \right)$$

for prolate tops, and

$$E_{J,K} = \hbar^2 \frac{J(J+1)}{2I_b} + \hbar^2 K^2 \left(\frac{1}{2I_c} - \frac{1}{2I_b} \right)$$

for oblate tops.

Because the rotational energies now depend on K (as well as on J), the degeneracies are lower than for spherical tops. In particular, because the energies do not depend on M and depend on the square of K, the degeneracies are (2J+1) for states with K=0 and 2(2J+1) for states with |K| > 0; the extra factor of 2 arises for |K| > 0 states because pairs of states with K = |K| and K = -|K| are degenerate.

This page titled [3.8: Rotation of Polyatomic Molecules](#) is shared under a [CC BY-NC-SA 4.0](#) license and was authored, remixed, and/or curated by [Jack Simons](#) via [source content](#) that was edited to the style and standards of the LibreTexts platform.

3.9: Rotation of Linear Molecules

The rotational motion of a linear polyatomic molecule can be treated as an extension of the diatomic molecule case. One obtains the $Y_{J,M}(\theta, \phi)$ as rotational wavefunctions and, within the approximation in which the centrifugal potential is approximated at the equilibrium geometry of the molecule (R_e), the energy levels are:

$$E_J^0 = \hbar^2 \frac{J(J+1)}{2I}.$$

Here the total moment of inertia I of the molecule takes the place of μR_e^2 in the diatomic molecule case

$$I = \sum_a m_a (R_a - R_{CoM})^2;$$

m_a is the mass of atom a whose distance from the center of mass of the molecule is $(R_a - R_{CoM})$. The rotational level with quantum number J is $(2J+1)$ -fold degenerate again because there are $(2J+1)$ M - values.

This page titled [3.9: Rotation of Linear Molecules](#) is shared under a [CC BY-NC-SA 4.0](#) license and was authored, remixed, and/or curated by [Jack Simons](#) via [source content](#) that was edited to the style and standards of the LibreTexts platform.

3.E: Exercises

Your page has been created!

Remove this content and add your own.

Edit page

Click the Edit page button in your user bar. You will see a suggested structure for your content. Add your content and hit Save.

Tips:

[Drag and drop](#)

Drag one or more image files from your computer and drop them onto your browser window to add them to your page.

[Classifications](#)

Tags are used to link pages to one another along common themes. Tags are also used as markers for the dynamic organization of content in the CXone Expert framework.

[Working with templates](#)

CXone Expert [templates](#) help guide and organize your documentation, making it flow easier and more uniformly. Edit existing templates or create your own.

 [Visit for all help topics.](#)

This page titled [3.E: Exercises](#) is shared under a [CC BY-NC-SA 4.0](#) license and was authored, remixed, and/or curated by [Jack Simons](#) via [source content](#) that was edited to the style and standards of the LibreTexts platform.

3.10: Rotation of Non-Linear Molecules

For a non-linear polyatomic molecule, again with the centrifugal couplings to the vibrations evaluated at the equilibrium geometry, the following terms form the rotational part of the nuclear-motion kinetic energy:

$$T_{rot} = \sum_{i=a,b,c} \left(\frac{J_i^2}{2I_i} \right).$$

Here, I_i is the eigenvalue of the moment of inertia tensor:

$$I_{x,x} = \sum_a m_a [(R_a - R_{CoM})^2 - (x_a - x_{CoM})^2]$$

$$I_{x,y} = \sum_a m_a [(x_a - x_{CoM})(y_a - y_{CoM})]$$

expressed originally in terms of the cartesian coordinates of the nuclei (a) and of the center of mass in an arbitrary molecule-fixed coordinate system (and similarly for $I_{z,z}$, $I_{y,y}$, $I_{x,z}$ and $I_{y,z}$). The operator J_i corresponds to the component of the total rotational angular momentum \mathbf{J} along the direction belonging to the i^{th} eigenvector of the moment of inertia tensor.

Molecules for which all three principal moments of inertia (the I'_i 's) are equal are called 'spherical tops'. For these species, the rotational Hamiltonian can be expressed in terms of the square of the total rotational angular momentum J^2 :

$$T_{rot} = \frac{J^2}{2I},$$

as a consequence of which the rotational energies once again become

$$E_J = \hbar^2 \frac{J(J+1)}{2I}.$$

However, the $Y_{J,M}$ are not the corresponding eigenfunctions because the operator J^2 now contains contributions from rotations about three (no longer two) axes (i.e., the three principal axes). The proper rotational eigenfunctions are the $D_{M,K}^J(\alpha, \beta, \gamma)$ functions known as 'rotation matrices' (see Sections 3.5 and 3.6 of Zare's book on angular momentum) these functions depend on three angles (the three Euler angles needed to describe the orientation of the molecule in space) and three quantum numbers- J, M, and K. The quantum number M labels the projection of the total angular momentum (as $M\hbar$) along the laboratory-fixed z-axis; $K\hbar$ is the projection along one of the internal principal axes (in a spherical top molecule, all three axes are equivalent, so it does not matter which axis is chosen).

The energy levels of spherical top molecules are $(2J+1)^2$ -fold degenerate. Both the M and K quantum numbers run from -J, in steps of unity, to J; because the energy is independent of M and of K, the degeneracy is $(2J+1)^2$.

Molecules for which two of the three principal moments of inertia are equal are called symmetric top molecules. Prolate symmetric tops have $I_a < I_b = I_c$; oblate symmetric tops have $I_a = I_b < I_c$ (it is convention to order the moments of inertia as $I_a \leq I_b \leq I_c$). The rotational Hamiltonian can now be written in terms of J^2 and the component of \mathbf{J} along the unique moment of inertia's axis as:

$$T_{rot} = J_a^2 \left(\frac{1}{2I_a} - \frac{1}{2I_b} \right) + \frac{J^2}{2I_b}$$

for prolate tops, and

$$T_{rot} = J_c^2 \left(\frac{1}{2I_c} - \frac{1}{2I_b} \right) + \frac{J^2}{2I_b}$$

for oblate tops. Again, the $D_{M,K}^J(\alpha, \beta, \gamma)$ are the eigenfunctions, where the quantum number K describes the component of the rotational angular momentum \mathbf{J} along the unique molecule-fixed axis (i.e., the axis of the unique moment of inertia). The energy levels are now given in terms of J and K as follows:

$$E_{J,K} \hbar^2 \frac{J(J+1)}{2I_b} + \hbar^2 K^2 \left(\frac{1}{2I_a} - \frac{1}{2I_b} \right)$$

for prolate tops, and

$$E_{J,K} = \hbar^2 \frac{J(J+1)}{2I_b} + \hbar^2 K^2 \left(\frac{1}{2I_c} - \frac{1}{2I_b} \right)$$

for oblate tops.

Because the rotational energies now depend on K (as well as on J), the degeneracies are lower than for spherical tops. In particular, because the energies do not depend on M and depend on the square of K, the degeneracies are (2J+1) for states with K=0 and 2(2J+1) for states with |K| > 0; the extra factor of 2 arises for |K| > 0 states because pairs of states with K = |K| and K = -|K| are degenerate.

This page titled [3.10: Rotation of Non-Linear Molecules](#) is shared under a [CC BY-NC-SA 4.0](#) license and was authored, remixed, and/or curated by [Jack Simons](#) via [source content](#) that was edited to the style and standards of the LibreTexts platform.

3.11: Chapter Summary

This Chapter has shown how the solution of the Schrödinger equation governing the motions and interparticle potential energies of the nuclei and electrons of an atom or molecule (or ion) can be decomposed into two distinct problems:

- i. solution of the **electronic** Schrödinger equation for the electronic wavefunctions and energies, both of which depend on the nuclear geometry and
- ii. solution of the **vibration/rotation** Schrödinger equation for the motion of the nuclei on any one of the electronic energy surfaces.

This decomposition into approximately separable electronic and nuclear motion problems remains an important point of view in chemistry. It forms the basis of many of our models of molecular structure and our interpretation of molecular spectroscopy. It also establishes how we approach the computational simulation of the energy levels of atoms and molecules; we first compute electronic energy levels at a 'grid' of different positions of the nuclei, and we then solve for the motion of the nuclei on a particular energy surface using this grid of data.

The treatment of electronic motion is treated in detail in Sections 2, 3, and 6 where molecular orbitals and configurations and their computer evaluation is covered. The vibration/rotation motion of molecules on BO surfaces is introduced above, but should be treated in more detail in a subsequent course in molecular spectroscopy.

This page titled [3.11: Chapter Summary](#) is shared under a [CC BY-NC-SA 4.0](#) license and was authored, remixed, and/or curated by [Jack Simons](#) via [source content](#) that was edited to the style and standards of the LibreTexts platform.

CHAPTER OVERVIEW

4: Atomic Orbitals

Valence atomic orbitals on neighboring atoms combine to form bonding, non-bonding and antibonding molecular orbitals. In Section 1 the Schrödinger equation for the motion of a single electron moving about a nucleus of charge Z was explicitly solved. The energies of these orbitals relative to an electron infinitely far from the nucleus with zero kinetic energy were found to depend strongly on Z and on the principal quantum number n , as were the radial "sizes" of these hydrogenic orbitals. Closed analytical expressions for the r, θ , and ϕ dependence of these orbitals are given in Appendix B. The reader is advised to also review this material before undertaking study of this section.

[4.1: Shapes of Atomic Orbitals](#)

[4.2: Directions of Atomic Orbitals](#)

[4.3: Sizes and Energies](#)

This page titled [4: Atomic Orbitals](#) is shared under a [CC BY-NC-SA 4.0](#) license and was authored, remixed, and/or curated by [Jack Simons](#) via [source content](#) that was edited to the style and standards of the LibreTexts platform.

4.1: Shapes of Atomic Orbitals

Shapes of atomic orbitals play central roles in governing the types of directional bonds an atom can form.

All atoms have sets of bound and continuum s, p, d, f, g, etc. orbitals. Some of these orbitals may be unoccupied in the atom's low energy states, but they are still present and able to accept electron density if some physical process (e.g., photon absorption, electron attachment, or Lewis-base donation) causes such to occur. For example, the Hydrogen atom has 1s, 2s, 2p, 3s, 3p, 3d, etc. orbitals. Its negative ion H^- has states that involve $1s2s$, $2p^2$, $3s^2$, $3p^2$, etc. orbital occupancy. Moreover, when an H atom is placed in an external electronic field, its charge density polarizes in the direction of the field. This polarization can be described in terms of the orbitals of the isolated atom being combined to yield distorted orbitals (e.g., the 1s and 2p orbitals can "mix" or combine to yield sp hybrid orbitals, one directed toward increasing field and the other directed in the opposite direction). Thus in many situations it is important to keep in mind that each atom has a full set of orbitals available to it even if some of these orbitals are not occupied in the lowest energy state of the atom.

This page titled [4.1: Shapes of Atomic Orbitals](#) is shared under a [CC BY-NC-SA 4.0](#) license and was authored, remixed, and/or curated by [Jack Simons](#) via [source content](#) that was edited to the style and standards of the LibreTexts platform.

4.2: Directions of Atomic Orbitals

Atomic orbital directions also determine what directional bonds an atom will form.

Each set of p orbitals has three distinct directions or three different angular momentum m-quantum numbers as discussed in Appendix G. Each set of d orbitals has five distinct directions or m-quantum numbers, etc; s orbitals are unidirectional in that they are spherically symmetric, and have only $m = 0$. Note that the degeneracy of an orbital $(2l+1)$, which is the number of distinct spatial orientations or the number of m-values, grows with the angular momentum quantum number l of the orbital without bound.

It is because of the **energy degeneracy** within a set of orbitals, that these distinct directional orbitals (e.g., x, y, z for p orbitals) may be combined to give new orbitals which no longer possess specific spatial directions but which have specified angular momentum characteristics. The act of combining these degenerate orbitals does not change their energies. For example, the $\frac{1}{\sqrt{2}}(p_x + ip_y)$ and $\frac{1}{\sqrt{2}}(p_x - ip_y)$ combinations no longer point along the x and y axes, but instead correspond to specific angular momenta $(+1\hbar$ and $-1\hbar)$ about the z axis. The fact that they are angular momentum eigenfunctions can be seen by noting that the x and y orbitals contain ϕ dependences of $\cos(\phi)$ and $\sin(\phi)$, respectively. Thus the above combinations contain $e^{i\phi}$ and $e^{-i\phi}$, respectively. The sizes, shapes, and directions of a few s, p, and d orbitals are illustrated below (the light and dark areas represent positive and negative values, respectively).

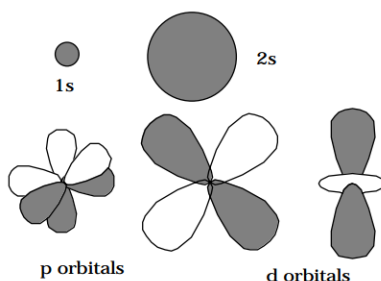


Figure 4.3.1: Insert caption here!

This page titled [4.2: Directions of Atomic Orbitals](#) is shared under a [CC BY-NC-SA 4.0](#) license and was authored, remixed, and/or curated by [Jack Simons](#) via [source content](#) that was edited to the style and standards of the LibreTexts platform.

4.3: Sizes and Energies

The size (e.g., average value or expectation value of the distance from the atomic nucleus to the electron) of an atomic orbital is determined primarily by its principal quantum number n and by the strength of the potential attracting an electron in this orbital to the atomic center (which has some l -dependence too). The energy (with negative energies corresponding to bound states in which the electron is attached to the atom with positive binding energy and positive energies corresponding to unbound scattering states) is also determined by n and by the electrostatic potential produced by the nucleus and by the other electrons. Each atom has an infinite set of orbitals of each l quantum number ranging from those with low energy and small size to those with higher energy and larger size.

Atomic orbitals are solutions to an orbital-level Schrödinger equation in which an electron moves in a potential energy field provided by the nucleus and all the other electrons. Such one-electron Schrödinger equations are discussed, as they pertain to qualitative and semi-empirical models of electronic structure in Appendix F. The spherical symmetry of the one-electron potential appropriate to atoms and atomic ions is what makes sets of the atomic orbitals degenerate. Such degeneracies arise in molecules too, but the extent of degeneracy is lower because the molecule's nuclear coulomb and electrostatic potential energy has lower symmetry than in the atomic case. As will be seen, it is the symmetry of the potential experienced by an electron moving in the orbital that determines the kind and degree of orbital degeneracy which arises.

Symmetry operators leave the electronic Hamiltonian \mathbf{H} invariant because the potential and kinetic energies are not changed if one applies such an operator R to the coordinates and momenta of **all** the electrons in the system. Because symmetry operations involve reflections through planes, rotations about axes, or inversions through points, the application of such an operation to a product such as $\mathbf{H}\psi$ gives the product of the operation applied to each term in the original product. Hence, one can write:

$$R(\mathbf{H}\psi) = (R\mathbf{H})(R\psi).$$

Now using the fact that \mathbf{H} is invariant to R , which means that $(R\mathbf{H}) = \mathbf{H}$, this result reduces to:

$$R(\mathbf{H}\psi) = \mathbf{H}(R\psi),$$

which says that R commutes with \mathbf{H} :

$$[R, \mathbf{H}] = 0$$

Because symmetry operators commute with the electronic Hamiltonian, the wavefunctions that are eigenstates of \mathbf{H} can be labeled by the symmetry of the point group of the molecule (i.e., those operators that leave \mathbf{H} invariant). It is for this reason that one constructs symmetry-adapted atomic basis orbitals to use in forming molecular orbitals.

This page titled [4.3: Sizes and Energies](#) is shared under a [CC BY-NC-SA 4.0](#) license and was authored, remixed, and/or curated by [Jack Simons](#) via [source content](#) that was edited to the style and standards of the LibreTexts platform.

CHAPTER OVERVIEW

5: Molecular Orbitals

Molecular orbitals possess specific topology, symmetry, and energy-level patterns.

[5.1: Orbital Interaction Topology](#)

[5.2: Orbital Symmetry](#)

[5.3: Linear Molecules](#)

[5.4: Atoms](#)

This page titled [5: Molecular Orbitals](#) is shared under a [CC BY-NC-SA 4.0](#) license and was authored, remixed, and/or curated by [Jack Simons](#) via [source content](#) that was edited to the style and standards of the LibreTexts platform.

5.1: Orbital Interaction Topology

The orbital interactions determine how many and which molecular orbitals will have low (bonding), intermediate (non-bonding), and higher (antibonding) energies, with all energies viewed relative to those of the constituent atomic orbitals. **The general patterns** that are observed in most compounds can be summarized as follows:

1. If the energy splittings among a given atom's atomic orbitals with the same principal quantum number are small, hybridization can easily occur to produce hybrid orbitals that are directed toward (and perhaps away from) the other atoms in the molecule. In the first-row elements (Li, Be, B, C, N, O, and F), the 2s-2p splitting is small, so hybridization is common. In contrast, for Ca, Ga, Ge, As, and Br it is less common, because the 4s-4p splitting is larger. Orbitals directed toward other atoms can form bonding and antibonding mo; those directed toward no other atoms will form nonbonding molecular orbitals.
2. In attempting to gain a qualitative picture of the electronic structure of any given molecule, it is advantageous to begin by hybridizing the atomic orbitals of those atoms which contain more than one ao in their valence shell. Only those atomic orbitals that are not involved in p-orbital interactions should be so hybridized.
3. Atomic or hybrid orbitals that are not directed in a s-interaction manner toward other atomic orbitals or hybrids on neighboring atoms can be involved in p-interactions or in nonbonding interactions.
4. Pairs of atomic orbitals or hybrid orbitals on neighboring atoms directed toward one another interact to produce bonding and antibonding orbitals. The more the bonding orbital lies below the lower-energy ao or hybrid orbital involved in its formation, the higher the antibonding orbital lies above the higher-energy ao or hybrid orbital.

For example, in formaldehyde, H_2CO , one forms sp^2 hybrids on the C atom; on the O atom, either sp hybrids (with one p orbital "reserved" for use in forming the π and π^* orbitals and another p orbital to be used as a non-bonding orbital lying in the plane of the molecule) or sp^2 hybrids (with the remaining p orbital reserved for the π and π^* orbitals) can be used. The H atoms use their 1s orbitals since hybridization is not feasible for them. The C atom clearly uses its sp^2 hybrids to form two CH and one CO σ bonding - antibonding orbital pairs.

The O atom uses one of its sp or sp^2 hybrids to form the CO σ bond and antibond. When sp hybrids are used in conceptualizing the bonding, the other sp hybrid forms a lone pair orbital directed away from the CO bond axis; one of the atomic p orbitals is involved in the CO π and π^* orbitals, while the other forms an in-plane non-bonding orbital. Alternatively, when sp^2 hybrids are used, the two sp^2 hybrids that do not interact with the C-atom sp^2 orbital form the two non-bonding orbitals. Hence, the final picture of bonding, non-bonding, and antibonding orbitals does not depend on which hybrids one uses as intermediates.

As another example, the 2s and 2p orbitals on the two N atoms of N_2 can be formed into pairs of sp hybrids on each N atom plus a pair of p_π atomic orbitals on each N atom. The sp hybrids directed toward the other N atom give rise to bonding σ and antibonding σ^* orbitals, and the sp hybrids directed away from the other N atom yield nonbonding σ orbitals. The p_π orbitals, which consist of 2p orbitals on the N atoms directed perpendicular to the N-N bond axis, produce bonding π and antibonding π^* orbitals.

5. In general, σ interactions for a given pair of atoms interacting are stronger than π interactions (which, in turn, are stronger than δ interactions, etc.) for any given sets (i.e., principal quantum number) of atomic orbitals that interact. Hence, σ bonding orbitals (originating from a given set of aos) lie below π bonding orbitals, and σ^* orbitals lie above π^* orbitals that arise from the same sets of aos. In the N_2 example, the σ bonding orbital formed from the two sp hybrids lies below the π bonding orbital, but the π^* orbital lies below the σ^* orbital. In the H_2CO example, the two CH and the one CO bonding orbitals have low energy; the CO π bonding orbital has the next lowest energy; the two O-atom non-bonding orbitals have intermediate energy; the CO π^* orbital has somewhat higher energy; and the two CH and one CO antibonding orbitals have the highest energies.
6. If a given ao or hybrid orbital interacts with or is coupled to orbitals on more than a single neighboring atom, multicenter bonding can occur. For example, in the allyl radical the central carbon atom's p_π orbital is coupled to the p_π orbitals on both neighboring atoms; in linear Li_3 , the central Li atom's 2s orbital interacts with the 2s orbitals on both terminal Li atoms; in triangular Cu_3 , the 2s orbitals on each Cu atom couple to each of the other two atoms' 4s orbitals.
7. Multicenter bonding that involves "linear" chains containing N atoms (e.g., as in conjugated polyenes or in chains of Cu or Na atoms for which the valence orbitals on one atom interact with those of its neighbors on both sides) gives rise to mo energy patterns in which there are $N/2$ (if N is even) or $N/2 - 1$ non-degenerate bonding orbitals and the same number of antibonding orbitals (if N is odd, there is also a single non-bonding orbital).

8. Multicenter bonding that involves "cyclic" chains of N atoms (e.g., as in cyclic conjugated polyenes or in rings of Cu or Na atoms for which the valence orbitals on one atom interact with those of its neighbors on both sides and the entire net forms a closed cycle) gives rise to mo energy patterns in which there is a lowest non-degenerate orbital and then a progression of doubly degenerate orbitals. If N is odd, this progression includes $(N-1)/2$ levels; if N is even, there are $(N-2)/2$ doubly degenerate levels and a final nondegenerate highest orbital. These patterns and those that appear in linear multicenter bonding are summarized in the Figures shown below.

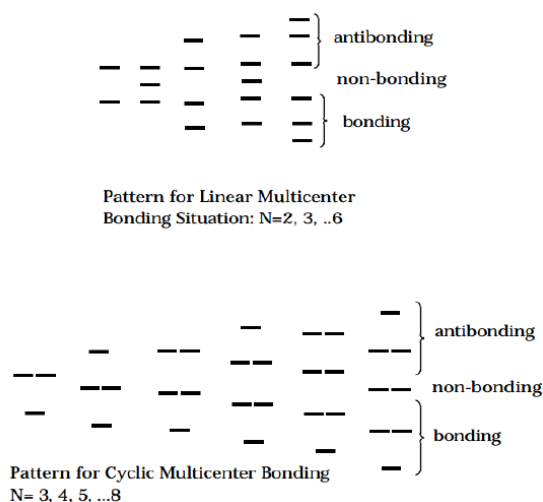


Figure 5.1.1: Insert caption here!

1. In extended systems such as solids, atom-based orbitals combine as above to form so called 'bands' of molecular orbitals. These bands are continuous rather than discrete as in the above cases involving small polyenes. The energy 'spread' within a band depends on the overlap among the atom-based orbitals that form the band; large overlap gives rise to a large band width, while small overlap produces a narrow band. As one moves from the bottom (i.e., the lower energy part) of a band to the top, the number of nodes in the corresponding band orbital increases, as a result of which its bonding nature decreases. In the figure shown below, the bands of a metal such as Ni (with 3d, 4s, and 4p orbitals) is illustrated. The d-orbital band is narrow because the 3d orbitals are small and hence do not overlap appreciably; the 4s and 4p bands are wider because the larger 4s and 4p orbitals overlap to a greater extent. The d-band is split into σ , π , and δ components corresponding to the nature of the overlap interactions among the constituent atomic d orbitals. Likewise, the p-band is split into σ and π components. The widths of the σ components of each band are larger than those of the π components because the corresponding σ overlap interactions are stronger. The intensities of the bands at energy E measure the densities of states at that E. The total integrated intensity under a given band is a measure of the total number of atomic orbitals that form the band.

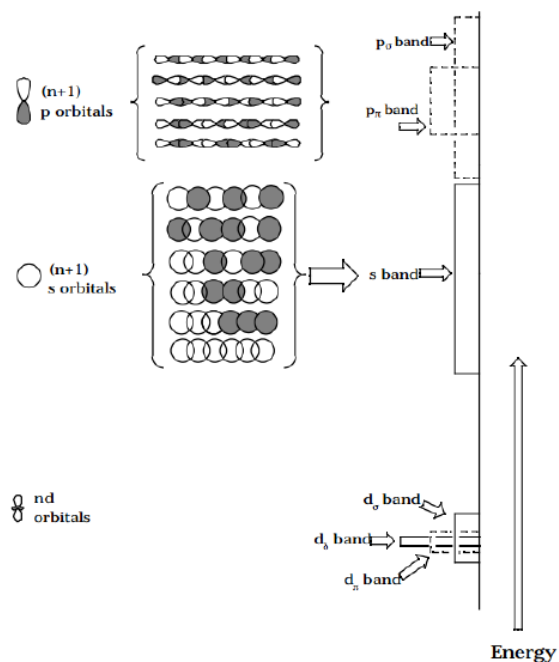


Figure 5.1.2: Insert caption here!

This page titled [5.1: Orbital Interaction Topology](#) is shared under a [CC BY-NC-SA 4.0](#) license and was authored, remixed, and/or curated by [Jack Simons](#) via [source content](#) that was edited to the style and standards of the LibreTexts platform.

5.2: Orbital Symmetry

Symmetry provides additional quantum numbers or labels to use in describing the molecular orbitals. Each such quantum number further sub-divides the collection of all molecular orbitals into sets that have vanishing Hamiltonian matrix elements among members belonging to different sets.

Orbital interaction "topology" as discussed above plays a most- important role in determining the orbital energy level patterns of a molecule. Symmetry also comes into play, but in a different manner. **Symmetry** can be used to characterize the core, bonding, nonbonding, and antibonding molecular orbitals. Much of this chapter is devoted to how this can be carried out in a systematic manner. Once the various molecular orbitals have been labeled according to symmetry, it may be possible to recognize additional degeneracies that may not have been apparent on the basis of orbital-interaction considerations alone. Thus, topology provides the basic energy ordering pattern and then symmetry enters to identify additional degeneracies.

For example, the three NH bonding and three NH antibonding orbitals in NH_3 , when symmetry adapted within the C_{3v} point group, cluster into a_1 and e molecular orbitals as shown in the Figure below. The N-atom localized non-bonding lone pair orbital and the N-atom 1s core orbital also belong to a_1 symmetry.

In a second example, the three CH bonds, three CH antibonds, CO bond and antibond, and three O-atom non-bonding orbitals of the methoxy radical $H_3C - O$ also cluster into a_1 and e orbitals as shown below. In these cases, point group symmetry allows one to identify degeneracies that may not have been apparent from the structure of the orbital interactions alone.

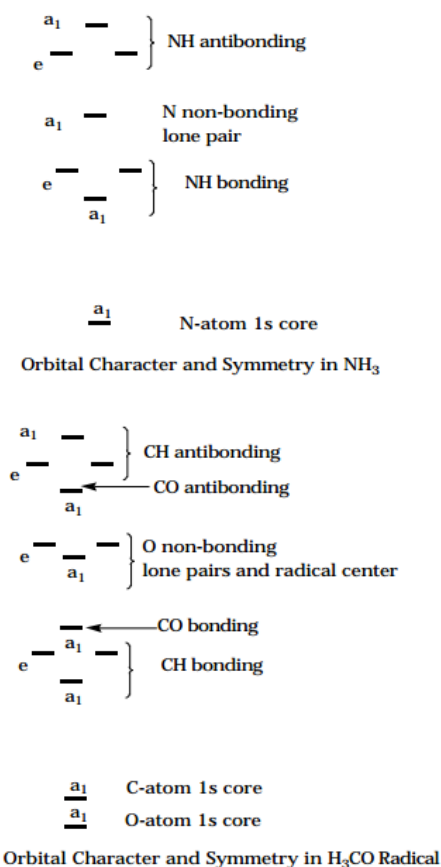


Figure 5.2.1: Insert caption here!

The three resultant molecular orbital energies are, of course, identical to those obtained without symmetry above. The three LCAO-MO coefficients, now expressing the molecular orbitals in terms of the symmetry adapted orbitals are $C_{is} = (0.707, 0.707, 0.0)$ for the bonding orbital, $(0.0, 0.0, 1.00)$ for the nonbonding orbital, and $(0.707, -0.707, 0.0)$ for the antibonding orbital. These coefficients, when combined with the symmetry adaptation coefficients C_{sa} given earlier, express the three molecular orbitals in terms of the three atomic orbitals as

$$\phi_i = \sum_{sa} C_{is} C_{sa} \chi_a$$

The sum

$$\sum_s C_{is} C_{sa}$$

gives the LCAO-MO coefficients C_{ia} which, for example, for the bonding orbital, are $(0.707^2, 0.707, 0.707^2)$, in agreement with what was found earlier without using symmetry.

The low energy orbitals of the H_2O molecule can be used to illustrate the use of symmetry within the primitive ao basis as well as in terms of hybrid orbitals. The 1s orbital on the Oxygen atom is clearly a nonbonding core orbital. The Oxygen 2s orbital and its three 2p orbitals are of valence type, as are the two Hydrogen 1s orbitals. In the absence of symmetry, these six valence orbitals would give rise to a 6x6 secular problem. By combining the two Hydrogen 1s orbitals into $0.707(1s_L + 1s_R)$ and $0.707(1s_L - 1s_R)$ symmetry adapted orbitals (labeled a_1 and b_2 within the C_{2v} point group; see the Figure below), and recognizing that the Oxygen 2s and $2p_z$ orbitals belong to a_1 symmetry (the z axis is taken as the C_2 rotation axis and the x axis is taken to be perpendicular to the plane in which the three nuclei lie) while the $2p_x$ orbital is b_1 and the $2p_y$ orbital is b_2 , allows the 6x6 problem to be decomposed into a 3x3 (a_1) secular problem, a 2x2 (b_2) secular problem and a 1x1 (b_1) problem. These decompositions allow one to conclude that there is one nonbonding b_1 orbital (the Oxygen $2p_x$ orbital), bonding and antibonding b_2 orbitals (the O-H bond and antibond formed by the Oxygen $2p_y$ orbital interacting with $0.707(1s_L - 1s_R)$), and, finally, a set of bonding, nonbonding, and antibonding a_1 orbitals (the O-H bond and antibond formed by the Oxygen 2s and $2p_z$ orbitals interacting with $0.707(1s_L + 1s_R)$ and the nonbonding orbital formed by the Oxygen 2s and $2p_z$ orbitals combining to form the "lone pair" orbital directed along the z-axis away from the two Hydrogen atoms).

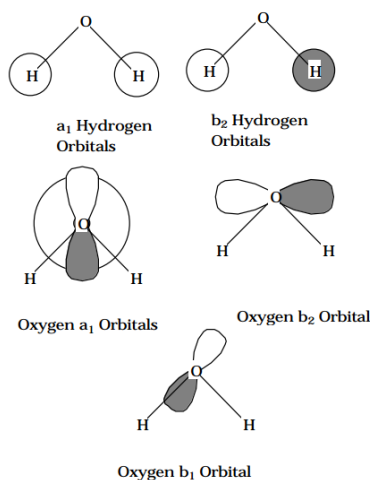


Figure 5.2.2: Insert caption here!

Alternatively, to analyze the H_2O molecule in terms of hybrid orbitals, one first combines the Oxygen 2s, $2p_z$, $2p_x$ and $2p_y$ orbitals to form four sp^3 hybrid orbitals. The valence-shell electron-pair repulsion (VSEPR) model of chemical bonding (see R. J. Gillespie and R. S. Nyholm, Quart. Rev. 11, 339 (1957) and R. J. Gillespie, J. Chem. Educ. 40, 295 (1963)) directs one to involve all of the Oxygen valence orbitals in the hybridization because four σ -bond or nonbonding electron pairs need to be accommodated about the Oxygen center; no π orbital interactions are involved, of course. Having formed the four sp^3 hybrid orbitals, one proceeds as with the primitive atomic orbitals; one forms symmetry adapted orbitals. In this case, the two Hydrogen 1s orbitals are combined exactly as above to form

$$0.707(1s_L + 1s_R)$$

and

$$0.707(1s_L - 1s_R).$$

The two sp^3 hybrids which lie in the plane of the H and O nuclei (label them L and R) are combined to give symmetry adapted hybrids: $0.707(L+R)$ and $0.707(L-R)$, which are of a_1 and b_2 symmetry, respectively (Figure Figure 5.2.3). The two sp^3 hybrids that lie above and below the plane of the three nuclei (label them T and B) are also symmetry adapted to form $0.707(T+ B)$ and

0.707(TB), which are of a_1 and b_1 symmetry, respectively. Once again, one has broken the 6x6 secular problem into a 3x3 a_1 block, a 2x2 b_2 block and a 1x1 b_1 block. Although the resulting bonding, nonbonding and antibonding a_1 orbitals, the bonding and antibonding b_2 orbitals and the nonbonding b_1 orbital are now viewed as formed from symmetry adapted Hydrogen orbitals and four Oxygen sp^3 orbitals, they are, of course, **exactly the same** molecular orbitals as were obtained earlier in terms of the symmetry adapted primitive aos. The formation of hybrid orbitals was an intermediate step which could not alter the final outcome.

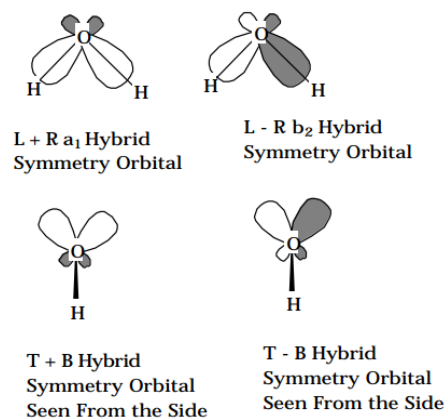


Figure 5.2.3: Insert caption here!

That no degenerate molecular orbitals arose in the above examples is a result of the fact that the C_{2v} point group to which H_2O and the allyl system belong (and certainly the C_s subgroup which was used above in the allyl case) has no degenerate representations. Molecules with higher symmetry such as NH_3 , CH_4 , and benzene have energetically degenerate orbitals because their molecular point groups have degenerate representations.

This page titled [5.2: Orbital Symmetry](#) is shared under a [CC BY-NC-SA 4.0](#) license and was authored, remixed, and/or curated by [Jack Simons](#) via [source content](#) that was edited to the style and standards of the LibreTexts platform.

5.3: Linear Molecules

Linear molecules belong to the axial rotation group. Their symmetry is intermediate in complexity between nonlinear molecules and atoms.

For linear molecules, the symmetry of the electrostatic potential provided by the nuclei and the other electrons is described by either the $C_{\infty v}$ or $D_{\infty h}$ group. The essential difference between these symmetry groups and the finite point groups which characterize the non-linear molecules lies in the fact that the electrostatic potential which an electron feels is invariant to rotations of **any** amount about the molecular axis (i.e., $V(\gamma + \delta\gamma) = V(\gamma)$, for any angle increment $\delta\gamma$). This means that the operator $C_{\delta\gamma}$ which generates a rotation of the electron's azimuthal angle γ by an amount $\delta\gamma$ about the molecular axis commutes with the Hamiltonian $[H, C_{\delta\gamma}] = 0$. $C_{\delta\gamma}$ can be written in terms of the quantum mechanical operator $L_z = -i\hbar \frac{\partial}{\partial \gamma}$ describing the orbital angular momentum of the electron about the molecular (z) axis:

$$C_{\delta\gamma} = e^{i\delta\gamma \frac{L_z}{\hbar}}.$$

Because $C_{\delta\gamma}$ commutes with the Hamiltonian and $C_{\delta\gamma}$ can be written in terms of L_z , L_z must commute with the Hamiltonian. As a result, the molecular orbitals ϕ of a linear molecule must be eigenfunctions of the z-component of angular momentum L_z :

$$-i\hbar \frac{\partial}{\partial \gamma} |\phi\rangle = m\hbar |\phi\rangle.$$

The electrostatic potential is not invariant under rotations of the electron about the x or y axes (those perpendicular to the molecular axis), so L_x and L_y do not commute with the Hamiltonian. Therefore, only L_z provides a "good quantum number" in the sense that the operator L_z commutes with the Hamiltonian.

In summary, the molecular orbitals of a linear molecule can be labeled by their m quantum number, which plays the same role as the point group labels did for non-linear polyatomic molecules, and which gives the eigenvalue of the angular momentum of the orbital about the molecule's symmetry axis. Because the kinetic energy part of the Hamiltonian contains $\frac{\hbar^2}{2m_e r^2} \frac{\partial^2}{\partial \gamma^2}$, whereas the potential energy part is independent of γ , the energies of the molecular orbitals depend on the **square** of the m quantum number. Thus, pairs of orbitals with $m = \pm 1$ are energetically degenerate; pairs with $m = \pm 2$ are degenerate, and so on. The absolute value of m, which is what the energy depends on, is called the λ quantum number. Molecular orbitals with $\lambda = 0$ are called σ orbitals; those with $\lambda = 1$ are π orbitals; and those with $\lambda = 2$ are δ orbitals.

Just as in the non-linear polyatomic-molecule case, the atomic orbitals which constitute a given molecular orbital must have the same symmetry as that of the molecular orbital. This means that σ , π , and δ molecular orbitals are formed, via LCAO-MO, from $m=0$, $m=\pm 1$, and $m=\pm 2$ atomic orbitals, respectively. In the diatomic N_2 molecule, for example, the core orbitals are of σ symmetry as are the molecular orbitals formed from the 2s and $2p_z$ atomic orbitals (or their hybrids) on each Nitrogen atom. The molecular orbitals formed from the atomic $2p_{-1} = (2p_x - i2p_y)$ and the $2p_{+1} = (2p_x + i2p_y)$ orbitals are of p symmetry and have $m = -1$ and $+1$.

For homonuclear diatomic molecules and other linear molecules which have a center of symmetry, the inversion operation (in which an electron's coordinates are inverted through the center of symmetry of the molecule) is also a symmetry operation. Each resultant molecular orbital can then also be labeled by a quantum number denoting its parity with respect to inversion. The symbols g (for gerade or even) and u (for ungerade or odd) are used for this label. Again for N_2 , the core orbitals are of σ_g and σ_u symmetry, and the bonding and antibonding σ orbitals formed from the 2s and $2p_\sigma$ orbitals on the two Nitrogen atoms are of σ_g and σ_u symmetry.

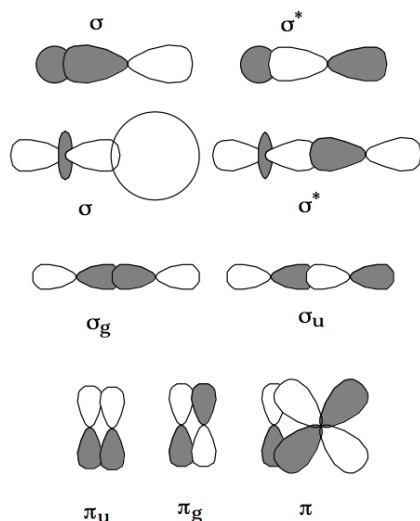


Figure 5.4.1: Insert caption here!

The bonding π molecular orbital pair (with $m = +1$ and -1) is of π_u symmetry whereas the corresponding antibonding orbital is of π_g symmetry. Examples of such molecular orbital symmetries are shown above.

The use of hybrid orbitals can be illustrated in the linear-molecule case by considering the N_2 molecule. Because two π bonding and antibonding molecular orbital pairs are involved in N_2 (one with $m = +1$, one with $m = -1$), VSEPR theory guides one to form sp hybrid orbitals from each of the Nitrogen atom's $2s$ and $2p_z$ (which is also the $2p$ orbital with $m = 0$) orbitals. Ignoring the core orbitals, which are of σ_g and σ_u symmetry as noted above, one then symmetry adapts the four sp hybrids (two from each atom) to build one σ_g orbital involving a bonding interaction between two sp hybrids pointed toward one another, an antibonding σ_u orbital involving the same pair of sp orbitals but coupled with opposite signs, a nonbonding σ_g orbital composed of two sp hybrids pointed away from the interatomic region combined with like sign, and a nonbonding σ_u orbital made of the latter two sp hybrids combined with opposite signs. The two $2p_m$ orbitals ($m = +1$ and -1) on each Nitrogen atom are then symmetry adapted to produce a pair of bonding π_u orbitals (with $m = +1$ and -1) and a pair of antibonding π_g orbitals (with $m = +1$ and -1). This hybridization and symmetry adaptation thereby reduces the 8×8 secular problem (which would be 10×10 if the core orbitals were included) into a 2×2 σ_g problem (one bonding and one nonbonding), a 2×2 σ_u problem (one bonding and one nonbonding), an identical pair of 1×1 π_u problems (bonding), and an identical pair of 1×1 π_g problems (antibonding).

Another example of the equivalence among various hybrid and atomic orbital points of view is provided by the CO molecule. Using, for example, sp hybrid orbitals on C and O, one obtains a picture in which there are: two core σ orbitals corresponding to the O-atom $1s$ and C-atom $1s$ orbitals; one CO bonding, two non-bonding, and one CO antibonding orbitals arising from the four sp hybrids; a pair of bonding and a pair of antibonding π orbitals formed from the two p orbitals on O and the two p orbitals on C. Alternatively, using sp^2 hybrids on both C and O, one obtains: the two core σ orbitals as above; a CO bonding and antibonding orbital pair formed from the sp^2 hybrids that are directed along the CO bond; and a single π bonding and antibonding π^* orbital set. The remaining two sp^2 orbitals on C and the two on O can then be symmetry adapted by forming \pm combinations within each pair to yield: an a_1 non-bonding orbital (from the $+$ combination) on each of C and O directed away from the CO bond axis; and a p_π orbital on each of C and O that can subsequently overlap to form the second π bonding and π^* antibonding orbital pair.

It should be clear from the above examples, that no matter what particular hybrid orbitals one chooses to utilize in conceptualizing a molecule's orbital interactions, symmetry ultimately returns to force one to form proper symmetry adapted combinations which, in turn, renders the various points of view equivalent. In the above examples and in several earlier examples, symmetry adaptation of, for example, sp^2 orbital pairs (e.g., $sp_L^2 \pm sp_R^2$) generated orbitals of pure spatial symmetry. In fact, symmetry combining hybrid orbitals in this manner amounts to forming other hybrid orbitals. For example, the above \pm combinations of sp^2 hybrids directed to the left (L) and right (R) of some bond axis generate a new sp hybrid directed along the bond axis but opposite to the sp^2 hybrid used to form the bond and a non-hybridized p orbital directed along the L-to-R direction. In the CO example, these combinations of sp^2 hybrids on O and C produce sp hybrids on O and C and p_π orbitals on O and C.

This page titled [5.3: Linear Molecules](#) is shared under a [CC BY-NC-SA 4.0](#) license and was authored, remixed, and/or curated by [Jack Simons](#) via [source content](#) that was edited to the style and standards of the LibreTexts platform.

5.4: Atoms

Atoms belong to the full rotation symmetry group; this makes their symmetry analysis the most complex to treat.

In moving from linear molecules to atoms, additional symmetry elements arise. In particular, the potential field experienced by an electron in an orbital becomes invariant to rotations of arbitrary amounts about the x, y, and z axes; in the linear-molecule case, it is invariant only to rotations of the electron's position about the molecule's symmetry axis (the z axis). These invariances are, of course, caused by the spherical symmetry of the potential of any atom. This additional symmetry of the potential causes the Hamiltonian to commute with all three components of the electron's angular momentum:

- $[L_x, H] = 0$
- $[L_y, H] = 0$
- $[L_z, H] = 0$

It is straightforward to show that H also commutes with the operator L^2 , defined as the sum of the squares of the three individual components of the angular momentum

$$L^2 = L_x^2 + L_y^2 + L_z^2$$

Because L_x , L_y , and L_z do not commute with one another, orbitals which are eigenfunctions of H **cannot** be simultaneous eigenfunctions of all three angular momentum operators. However, because L_x , L_y , and L_z do commute with L^2 , orbitals can be found which are eigenfunctions of H, of L^2 and of any one component of \mathbf{L} ; it is convention to select L_z as the operator which, along with H and L^2 , form a mutually commutative operator set of which the orbitals are simultaneous eigenfunctions.

So, for any atom, the orbitals can be labeled by both l and m quantum numbers, which play the role that point group labels did for non-linear molecules and λ did for linear molecules. Because (i) the kinetic energy operator in the electronic Hamiltonian explicitly contains $\frac{L^2}{2m_e r^2}$, (ii) the Hamiltonian does not contain additional L_z , L_x , or L_y factors, and (iii) the potential energy part of the Hamiltonian is spherically symmetric (and commutes with L^2 and L_z), the energies of atomic orbitals depend upon the l quantum number and are independent of the m quantum number. This is the source of the $2l+1$ - fold degeneracy of atomic orbitals.

The angular part of the atomic orbitals is described in terms of the spherical harmonics $Y_{l,m}$; that is, each atomic orbital ϕ can be expressed as

$$\phi_{n,l,m} = Y_{l,m}(\theta, \varphi) R_{n,l}(r).$$

The explicit solutions for the $Y_{l,m}$ and for the radial wavefunctions $R_{n,l}$ are given in Appendix B. The variables r, θ, φ give the position of the electron in the orbital in spherical coordinates. These angular functions are, as discussed earlier, related to the cartesian (i.e., spatially oriented) orbitals by simple transformations; for example, the orbitals with $l=2$ and $m=2,1,0,-1,-2$ can be expressed in terms of the d_{xy} , d_{xz} , d_{yz} , d_{xx-yy} , and d_{zz} orbitals. Either set of orbitals is acceptable in the sense that each orbital is an eigenfunction of H; transformations within a degenerate set of orbitals do not destroy the Hamiltonian- eigenfunction feature. The orbital set labeled with l and m quantum numbers is most useful when one is dealing with isolated atoms (which have spherical symmetry), because m is then a valid symmetry label, or with an atom in a local environment which is axially symmetric (e.g., in a linear molecule) where the m quantum number remains a useful symmetry label. The cartesian orbitals are preferred for describing an atom in a local environment which displays lower than axial symmetry (e.g., an atom interacting with a diatomic molecule in C_{2v} symmetry).

The radial part of the orbital $R_{n,l}(r)$ as well as the orbital energy $\varepsilon_{n,l}$ depend on l because the Hamiltonian itself contains $\frac{l(l+1)\hbar^2}{2m_e r^2}$; they are independent of m because the Hamiltonian has no m-dependence. For bound orbitals, $R_{n,l}(r)$ decays exponentially for large r (as $e^{-2r\sqrt{2\varepsilon_{n,l}}}$), and for unbound (scattering) orbitals, it is oscillatory at large r with an oscillation period related to the deBroglie wavelength of the electron. In $R_{n,l}(r)$ there are $(n-l-1)$ radial nodes lying between $r=0$ and $r = \infty$. These nodes provide differential stabilization of low-l orbitals over high-l orbitals of the same principal quantum number n. That is, penetration of outer shells is greater for low-l orbitals because they have more radial nodes; as a result, they have larger amplitude near the atomic nucleus and thus experience enhanced attraction to the positive nuclear charge.

The average size (i.e., $\langle r \rangle$):

$$\langle r \rangle = \int R_{n,l}^2 r r^2 dr)$$

of an orbital depends strongly on n , weakly on l and is independent of m . It also depends strongly on the nuclear charge and on the potential produced by the other electrons. This potential is often characterized qualitatively in terms of an effective nuclear charge Z_{eff} which is the true nuclear charge of the atom Z minus a screening component Z_{sc} which describes the repulsive effect of the electron density lying radially inside the electron under study. Because, for a given n , low- l orbitals penetrate closer to the nucleus than do high- l orbitals, they have higher Z_{eff} values (i.e., smaller Z_{sc} values) and correspondingly smaller average sizes and larger binding energies.

This page titled [5.4: Atoms](#) is shared under a [CC BY-NC-SA 4.0](#) license and was authored, remixed, and/or curated by [Jack Simons](#) via [source content](#) that was edited to the style and standards of the LibreTexts platform.

CHAPTER OVERVIEW

6: Quantum Mechanics in Reactions

Along "reaction paths", orbitals can be connected one-to-one according to their symmetries and energies. This is the origin of the Woodward-Hoffmann rules.

[6.1: Reduction in Symmetry Along Reaction Paths](#)

[6.2: Orbital Correlation Diagrams - Origins of the Woodward-Hoffmann Rules](#)

This page titled [6: Quantum Mechanics in Reactions](#) is shared under a [CC BY-NC-SA 4.0](#) license and was authored, remixed, and/or curated by [Jack Simons](#) via [source content](#) that was edited to the style and standards of the LibreTexts platform.

6.1: Reduction in Symmetry Along Reaction Paths

As fragments are brought together to form a larger molecule, the symmetry of the nuclear framework (recall the symmetry of the Coulombic potential experienced by electrons depends on the locations of the nuclei) changes. However, in some cases, certain symmetry elements persist throughout the path connecting the fragments and the product molecule. These preserved symmetry elements can be used to label the orbitals throughout the 'reaction'.

The point-group, axial- and full-rotation group symmetries which arise in nonlinear molecules, linear molecules, and atoms, respectively, are seen to provide quantum numbers or symmetry labels which can be used to characterize the orbitals appropriate for each such species. In a physical event such as interaction with an external electric or magnetic field or a chemical process such as collision or reaction with another species, the atom or molecule can experience a change in environment which causes the electrostatic potential which its orbitals experience to be of lower symmetry than that of the isolated atom or molecule. For example, when an atom interacts with another atom to form a diatomic molecule or simply to exchange energy during a collision, each atom's environment changes from being spherically symmetric to being axially symmetric. When the formaldehyde molecule undergoes unimolecular decomposition to produce $\text{CO} + \text{H}_2$ along a path that preserves C_{2v} symmetry, the orbitals of the CO moiety evolve from C_{2v} symmetry to axial symmetry.

It is important, therefore to be able to label the orbitals of atoms, linear, and nonlinear molecules in terms of their full symmetries as well in terms of the groups appropriate to lower-symmetry situations. This can be done by knowing how the representations of a higher symmetry group decompose into representations of a lower group. For example, the $Y_{l,m}$ functions appropriate for spherical symmetry, which belong to a $2l+1$ fold degenerate set in this higher symmetry, decompose into doubly degenerate pairs of functions $Y_{l,l}$, $Y_{l,-l}$; $Y_{l,l-1}$, $Y_{l,-l+1}$; etc., plus a single non-degenerate function $Y_{l,0}$, in axial symmetry. Moreover, because L^2 no longer commutes with the Hamiltonian whereas L_z does, orbitals with different l -values but the same m -values can be coupled. As the N_2 molecule is formed from two N atoms, the $2s$ and $2p_z$ orbitals, both of which belong to the same (σ) symmetry in the axial rotation group but which are of different symmetry in the isolated-atom spherical symmetry, can mix to form the σ_g bonding orbital, the σ_u antibonding, as well as the σ_g and σ_u nonbonding lone-pair orbitals. The fact that $2s$ and $2p$ have different l -values no longer uncouples these orbitals as it did for the isolated atoms, because l is no longer a "good" quantum number.

Another example of reduced symmetry is provided by the changes that occur as H_2O fragments into OH and H. The σ bonding orbitals (a_1 and b_2) and in-plane lone pair (a_1) and the σ^* antibonding (a_1 and b_2) of H_2O become a' orbitals (see the Figure below); the out-of-plane b_1 lone pair orbital becomes a'' (in Appendix IV of [Electronic Spectra and Electronic Structure of Polyatomic Molecules](#), G. Herzberg, Van Nostrand Reinhold Co., New York, N.Y. (1966) tables are given which allow one to determine how particular symmetries of a higher group evolve into symmetries of a lower group).

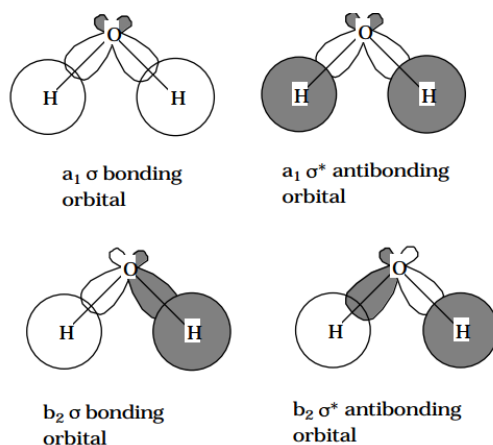
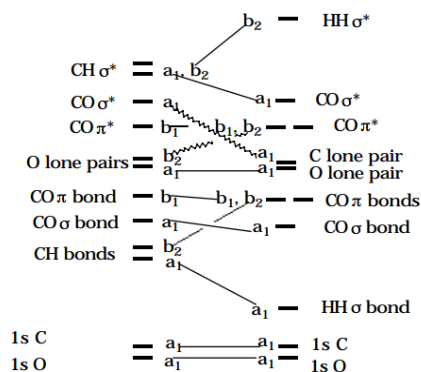


Figure 6.1.1: Insert caption here!

To further illustrate these points dealing with orbital symmetry, consider the insertion of CO into H_2 along a path which preserves C_{2v} symmetry. As the insertion occurs, the degenerate π bonding orbitals of CO become b_1 and b_2 orbitals. The antibonding π^* orbitals of CO also become b_1 and b_2 . The σ_g bonding orbital of H_2 becomes a_1 , and the σ_u antibonding H_2 orbital becomes b_2 . The orbitals of the reactant H_2CO are energy-ordered and labeled according to C_{2v} symmetry in the Figure shown below as are the orbitals of the product $H_2 + CO$.



$H_2CO \Rightarrow H_2 + CO$ Orbital Correlation Diagram in C_{2v} Symmetry

Figure 6.1.2: Insert caption here!

When these orbitals are connected according to their symmetries as shown above, one reactant orbital to one product orbital starting with the low-energy orbitals and working to increasing energy, an orbital correlation diagram (OCD) is formed. These diagrams play essential roles in analyzing whether reactions will have symmetry-imposed energy barriers on their potential energy surfaces along the reaction path considered in the symmetry analysis. The essence of this analysis, which is covered in detail in Chapter 12, can be understood by noticing that the sixteen electrons of ground-state H_2CO do not occupy their orbitals with the same occupancy pattern, symmetry-by-symmetry, as do the sixteen electrons of ground-state $H_2 + CO$. In particular, H_2CO places a pair of electrons in the second b_2 orbital while $H_2 + CO$ does not; on the other hand, $H_2 + CO$ places two electrons in the sixth a_1 orbital while H_2CO does not. The mismatch of the orbitals near the $5a_1$, $6a_1$, and $2b_2$ orbitals is the source of the mismatch in the electronic configurations of the ground-states of H_2CO and $H_2 + CO$. These mismatches give rise, as shown in Chapter 12, to symmetry-caused energy barriers on the $H_2CO \rightarrow H_2 + CO$ reaction potential energy surface.

This page titled [6.1: Reduction in Symmetry Along Reaction Paths](#) is shared under a [CC BY-NC-SA 4.0](#) license and was authored, remixed, and/or curated by [Jack Simons](#) via [source content](#) that was edited to the style and standards of the LibreTexts platform.

6.2: Orbital Correlation Diagrams - Origins of the Woodward-Hoffmann Rules

Connecting the energy-ordered orbitals of reactants to those of products according to symmetry elements that are preserved throughout the reaction produces an orbital correlation diagram.

In each of the examples cited above, symmetry reduction occurred as a molecule or atom approached and interacted with another species. The "path" along which this approach was thought to occur was characterized by symmetry in the sense that it preserved certain symmetry elements while destroying others. For example, the collision of two Nitrogen atoms to produce N_2 clearly occurs in a way which destroys spherical symmetry but preserves axial symmetry. In the other example used above, the formaldehyde molecule was postulated to decompose along a path which preserves C_{2v} symmetry while destroying the axial symmetries of CO and H_2 . The actual decomposition of formaldehyde may occur along some other path, but **if** it were to occur along the proposed path, then the symmetry analysis presented above would be useful.

The symmetry reduction analysis outlined above allows one to see new orbital interactions that arise (e.g., the $2s$ and $2p_z$ interactions in the $N + N \rightarrow N_2$ example) as the interaction increases. It also allows one to construct orbital correlation diagrams (OCD's) in which the orbitals of the "reactants" and "products" are energy ordered and labeled by the symmetries which are preserved throughout the "path", and the orbitals are then correlated by drawing lines connecting the orbitals of a given symmetry, one-by-one in increasing energy, from the reactants side of the diagram to the products side. As noted above, such orbital correlation diagrams play a central role in using symmetry to predict whether photochemical and thermal chemical reactions will experience activation barriers along proposed reaction paths (this subject is treated in Chapter 12).

To again illustrate the construction of an OCD, consider the p orbitals of 1,3-butadiene as the molecule undergoes disrotatory closing (notice that this is where a particular path is postulated; the actual reaction may or may not occur along such a path) to form cyclobutene. Along this path, the plane of symmetry which bisects and is perpendicular to the $C_2 - C_3$ bond is preserved, so the orbitals of the reactant and product are labeled as being even-e or odd-o under reflection through this plane. It is **not** proper to label the orbitals with respect to their symmetry under the plane containing the four C atoms; although this plane is indeed a symmetry operation for the reactants and products, it does not remain a valid symmetry throughout the reaction path.

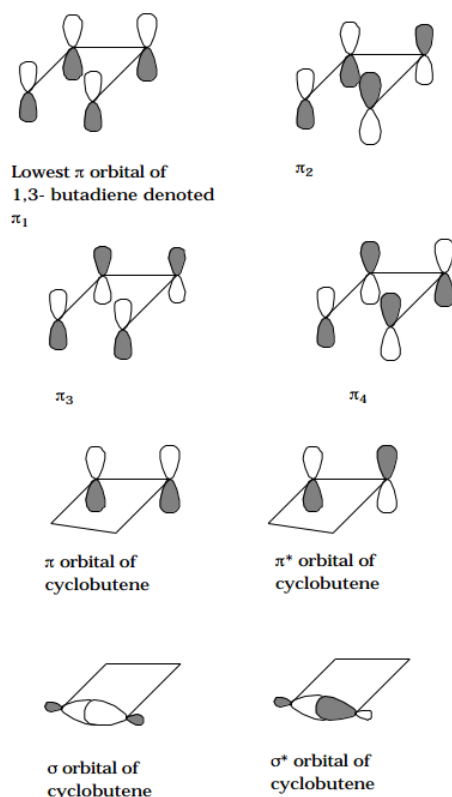


Figure 6.2.1: Insert caption here!

The four π orbitals of 1,3-butadiene are of the following symmetries under the preserved plane (see the orbitals in the Figure above): $\pi_1 = e, \pi_2 = 0, \pi_3 = e, \pi_4 = 0$. The π and π^* and σ and σ^* orbitals of cyclobutane which evolve from the four active orbitals of the 1,3-butadiene are of the following symmetry and energy order: $\sigma = e, \pi = e, \pi^* = 0, \sigma^* = 0$. Connecting these orbitals by symmetry, starting with the lowest energy orbital and going through the highest energy orbital, gives the following OCD:

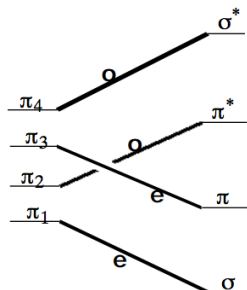


Figure 6.2.2: Insert caption here!

The fact that the lowest two orbitals of the reactants, which are those occupied by the four π electrons of the reactant, do not correlate to the lowest two orbitals of the products, which are the orbitals occupied by the two σ and two π electrons of the products, will be shown later in Chapter 12 to be the origin of the activation barrier for the thermal disrotatory rearrangement (in which the four active electrons occupy these lowest two orbitals) of 1,3-butadiene to produce cyclobutene.

If the reactants could be prepared, for example by photolysis, in an excited state having orbital occupancy $\pi_1^2 \pi_2^1 \pi_3^1$, then reaction along the path considered would not have any symmetry-imposed barrier because this singly excited configuration correlates to a singly-excited configuration $\sigma^2 \pi^1 \pi^{*1}$ of the products. The fact that the reactant and product configurations are of equivalent excitation level causes there to be no symmetry constraints on the photochemically induced reaction of 1,3-butadiene to produce cyclobutene. In contrast, the thermal reaction considered first above has a symmetry-imposed barrier because the orbital occupancy is forced to rearrange (by the occupancy of two electrons) from the ground-state wavefunction of the reactant to smoothly evolve into that of the product.

It should be stressed that although these symmetry considerations may allow one to anticipate barriers on reaction potential energy surfaces, they have nothing to do with the thermodynamic energy differences of such reactions. Symmetry says whether there will be symmetry-imposed barriers above and beyond any thermodynamic energy differences. The enthalpies of formation of reactants and products contain the information about the reaction's overall energy balance.

As another example of an OCD, consider the $N + N \rightarrow N_2$ recombination reaction mentioned above. The orbitals of the atoms must first be labeled according to the axial rotation group (including the inversion operation because this is a homonuclear molecule). The core 1s orbitals are symmetry adapted to produce $1\sigma_g$ and $1\sigma_u$ orbitals (the number 1 is used to indicate that these are the lowest energy orbitals of their respective symmetries); the 2s orbitals generate $2\sigma_g$ and $2\sigma_u$ orbitals; the 2p orbitals combine to yield $3\sigma_g$, a pair of $1\pi_u$ orbitals, a pair of $1\pi_g$ orbitals, and the $3\sigma_u$ orbital, whose bonding, nonbonding, and antibonding nature was detailed earlier. In the two separated Nitrogen atoms, the two orbitals derived from the 2s atomic orbitals are degenerate, and the six orbitals derived from the Nitrogen atoms' 2p orbitals are degenerate. At the equilibrium geometry of the N_2 molecule, these degeneracies are lifted. Only the degeneracies of the $1\pi_u$ and $1\pi_g$ orbitals, which are dictated by the degeneracy of $+m$ and $-m$ orbitals within the axial rotation group, remain.

As one proceeds inward past the equilibrium bond length of N_2 , toward the unitedatom limit in which the two Nitrogen nuclei are fused to produce a Silicon nucleus, the energy ordering of the orbitals changes. Labeling the orbitals of the Silicon atom according to the axial rotation group, one finds the 1s is σ_g , the 2s is σ_g , the 2p orbitals are σ_u and π_u , the 3s orbital is σ_g , the 3p orbitals are σ_u and π_u , and the 3d orbitals are σ_g, π_g , and δ_g . The following OCD is obtained when one connects the orbitals of the two separated Nitrogen atoms (properly symmetry adapted) to those of the N_2 molecule and eventually to those of the Silicon atom.

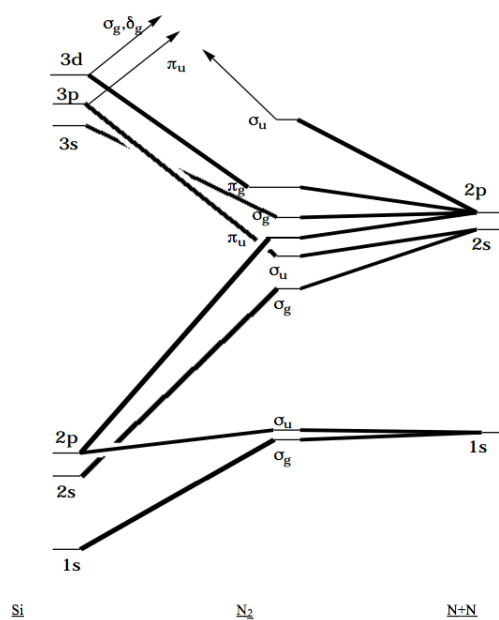


Figure 6.2.3: *Insert caption here!*

The fact that the separated-atom and united-atom limits involve several crossings in the OCD can be used to explain barriers in the potential energy curves of such diatomic molecules which occur at short internuclear distances. It should be noted that the Silicon atom's 3p orbitals of π_u symmetry and its 3d orbitals of σ_g and δ_g symmetry correlate with higher energy orbitals of N_2 not with the valence orbitals of this molecule, and that the 3s antibonding orbital of N_2 correlates with a higher energy orbital of Silicon (in particular, its 4p orbital).

This page titled [6.2: Orbital Correlation Diagrams - Origins of the Woodward-Hoffmann Rules](#) is shared under a [CC BY-NC-SA 4.0](#) license and was authored, remixed, and/or curated by [Jack Simons](#) via [source content](#) that was edited to the style and standards of the LibreTexts platform.

CHAPTER OVERVIEW

7: Further Characterization of Molecular Orbitals

The most elementary molecular orbital models contain symmetry, nodal pattern, and approximate energy information

[7.1: The LCAO-MO Expansion and the Orbital-Level Schrödinger Equation](#)

[7.2: Determining the Effective Potential](#)

[7.3: The Hückel Parameterization](#)

[7.4: The Extended Hückel Method](#)

This page titled [7: Further Characterization of Molecular Orbitals](#) is shared under a [CC BY-NC-SA 4.0](#) license and was authored, remixed, and/or curated by [Jack Simons](#) via [source content](#) that was edited to the style and standards of the LibreTexts platform.

7.1: The LCAO-MO Expansion and the Orbital-Level Schrödinger Equation

In the simplest picture of chemical bonding, the valence molecular orbitals ϕ_i are constructed as linear combinations of valence atomic orbitals χ_μ according to the LCAOMO formula:

$$\phi_i = \sum_{\mu} C_{i\mu} \chi_{\mu}.$$

The core electrons are not explicitly included in such a treatment, although their effects are felt through an electrostatic potential V that has the following properties:

1. V contains contributions from all of the nuclei in the molecule exerting coulombic attractions on the electron, as well as coulombic repulsions and exchange interactions exerted by the other electrons on this electron;
2. As a result of the (assumed) cancellation of attractions from distant nuclei and repulsions from the electron clouds (i.e., the core, lone-pair, and valence orbitals) that surround these distant nuclei, the effect of V on any particular mo ϕ_i depends primarily on the atomic charges and local bond polarities of the atoms over which ϕ_i is delocalized.

As a result of these assumptions, qualitative molecular orbital models can be developed in which one assumes that each mo ϕ_i obeys a one-electron Schrödinger equation

$$h\phi_i = \varepsilon_i \phi_i.$$

Here the orbital-level hamiltonian h contains the kinetic energy of motion of the electron and the potential V mentioned above:

$$\left[\frac{-\hbar^2}{2m_e \nabla^2} \right] \phi_i = \varepsilon_i \phi_i.$$

Expanding the mo ϕ_i in the LCAO-MO manner, substituting this expansion into the above Schrödinger equation, multiplying on the left by χ_ν^* , and integrating over the coordinates of the electron generates the following orbital-level eigenvalue problem:

$$\sum_{\mu} \langle \chi_\nu | \frac{-\hbar^2}{2m_e} \nabla^2 + V | \chi_\mu \rangle C_{i\mu} = \varepsilon \sum_{\mu} \langle \chi_\nu | \chi_\mu \rangle C_{i\mu}.$$

If the constituent atomic orbitals $\{\chi_\mu\}$ have been orthonormalized as discussed earlier in this chapter, the overlap integrals $\langle \chi_\nu | \chi_\mu \rangle$ reduce to $\delta_{\mu,\nu}$.

This page titled [7.1: The LCAO-MO Expansion and the Orbital-Level Schrödinger Equation](#) is shared under a [CC BY-NC-SA 4.0](#) license and was authored, remixed, and/or curated by [Jack Simons](#) via [source content](#) that was edited to the style and standards of the LibreTexts platform.

7.2: Determining the Effective Potential

In the most elementary models of orbital structure, the quantities that explicitly define the potential V are not computed from first principles as they are in so-called [ab initio methods](#). Rather, either experimental data or results of **ab initio** calculations are used to determine the parameters in terms of which V is expressed. The resulting empirical or semi-empirical methods discussed below differ in the sophistication used to include electron-electron interactions as well as in the manner experimental data or ab initio computational results are used to specify V .

If experimental data is used to parameterize a semi-empirical model, then the model should not be extended beyond the level at which it has been parameterized. For example, experimental bond energies, excitation energies, and ionization energies may be used to determine molecular orbital energies which, in turn, are summed to compute total energies. In such a parameterization it would be incorrect to subsequently use these molecular orbitals to form a wavefunction, as in Sections 3 and 6, that goes beyond the simple 'product of orbitals' description. To do so would be inconsistent because the more sophisticated wavefunction would duplicate what using the experimental data (which already contains mother nature's electronic correlations) to determine the parameters had accomplished.

Alternatively, if results of **ab initio** theory at the single-configuration orbital-product wavefunction level are used to define the parameters of a semi-empirical model, it would then be proper to use the semi-empirical orbitals in a subsequent higher-level treatment of electronic structure as done in Section 6.

This page titled [7.2: Determining the Effective Potential](#) is shared under a [CC BY-NC-SA 4.0](#) license and was authored, remixed, and/or curated by [Jack Simons](#) via [source content](#) that was edited to the style and standards of the LibreTexts platform.

7.3: The Hückel Parameterization

In the most simplified embodiment of the above orbital-level model, the following additional approximations are introduced.

Approximation 1: Diagonal Component

The diagonal values $\langle \chi_\mu | \frac{-\hbar^2}{2m_e} \nabla^2 + V | \chi_\mu \rangle$, which are usually denoted α_μ , are taken to be equal to the energy of an electron in the atomic orbital χ_μ and, as such, are evaluated in terms of atomic ionization energies (IP's) and electron affinities (EA's):

$$\langle \chi_\mu | \frac{-\hbar^2}{2m_e} \nabla^2 + V | \chi_\mu \rangle = -IP_\mu,$$

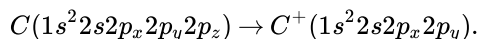
for atomic orbitals that are occupied in the atom, and

$$\langle \chi_\mu | \frac{-\hbar^2}{2m_e} \nabla^2 + V | \chi_\mu \rangle = -EA_\mu,$$

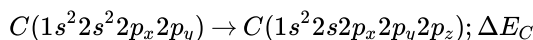
for atomic orbitals that are not occupied in the atom.

These approximations assume that contributions in V arising from coulombic attraction to nuclei other than the one on which χ_μ is located, and repulsions from the core, lone-pair, and valence electron clouds surrounding these other nuclei cancel to an extent that $\langle \chi_\mu | V | \chi_\mu \rangle$ contains only potentials from the atom on which χ_μ sits.

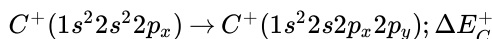
It should be noted that the IP's and EA's of valence-state orbitals are not identical to the experimentally measured IP's and EA's of the corresponding atom, but can be obtained from such information. For example, the 2p valence-state IP (VSIP) for a Carbon atom is the energy difference associated with the hypothetical process



If the energy differences for the "promotion" of C



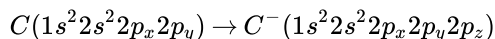
and for the promotion of C^+



are known, the desired VSIP is given by:

$$IP_{2p_z} = IP_C + \Delta E_C + -\Delta E_C^+.$$

The EA of the 2p orbital is obtained from the



energy gap, which means that $EA_{2p_z} = EA_C$. Some common IP's of valence 2p orbitals in eV are as follows: C (11.16), N (14.12), N^+ (28.71), O (17.70), O^+ (31.42), F^+ (37.28).

Approximation 2: Nearest Neighbors Approximation

The off-diagonal elements $\langle \chi_\nu | \frac{-\hbar^2}{2m_e} \nabla^2 + V | \chi_\mu \rangle$ are taken as zero if χ_μ and χ_ν belong to the same atom because the atomic orbitals are assumed to have been constructed to diagonalize the one-electron hamiltonian appropriate to an electron moving in that atom. They are set equal to a parameter denoted $\beta_{\mu,\nu}$ if χ_μ and χ_ν reside on neighboring atoms that are chemically bonded. If c_m and c_n reside on atoms that are not bonded neighbors, then the off-diagonal matrix element is set equal to zero.

Approximation 3: Off-Diagonal Component

The geometry dependence of the $\beta_{\mu,\nu}$ parameters is often approximated by assuming that $\beta_{\mu,\nu}$ is proportional to the overlap $S_{\mu,\nu}$ between the corresponding atomic orbitals:

$$\beta_{\mu,\nu} = \beta_{\mu,\nu}^o S_{\mu,\nu}.$$

Here $\beta_{\mu,\nu}^0$ is a constant (having energy units) characteristic of the bonding interaction between χ_μ and χ_ν ; its value is usually determined by forcing the molecular orbital energies obtained from such a qualitative orbital treatment to yield experimentally correct ionization potentials, bond dissociation energies, or electronic transition energies.

It is sometimes assumed that the overlap matrix S is the identity matrix. This means that overlap between the orbitals is neglected

The three approximations above form the basis of the so-called **Hückel model**. Its implementation requires knowledge of the atomic α_μ and $\beta_{\mu,\nu}^0$ values, which are eventually expressed in terms of experimental data, as well as a means of calculating the geometry dependence of the $\beta_{\mu,\nu}$'s (e.g., some method for computing overlap matrices $S_{\mu,\nu}$).

This page titled [7.3: The Hückel Parameterization](#) is shared under a [CC BY-NC-SA 4.0](#) license and was authored, remixed, and/or curated by [Jack Simons](#) via [source content](#) that was edited to the style and standards of the LibreTexts platform.

7.4: The Extended Hückel Method

It is well known that bonding and antibonding orbitals are formed when a pair of atomic orbitals from neighboring atoms interact. The energy splitting between the bonding and antibonding orbitals depends on the overlap between the pair of atomic orbitals. Also, the energy of the antibonding orbital lies higher above the arithmetic mean $E_{ave} = E_A + E_B$ of the energies of the constituent atomic orbitals (E_A and E_B) than the bonding orbital lies below E_{ave} . If overlap is ignored, as in conventional Hückel theory (except in parameterizing the geometry dependence of $\beta_{\mu,\nu}$), the differential destabilization of antibonding orbitals compared to stabilization of bonding orbitals can not be accounted for.

By parameterizing the off-diagonal Hamiltonian matrix elements in the following overlap-dependent manner:

$$h_{\nu,\mu} = \langle \chi_\nu | \frac{-\hbar^2}{2m_e} \nabla^2 + V | \chi_\mu \rangle = 0.5K(h_{\mu,\mu} + h_{\nu,\nu})S_{\mu,\nu},$$

and explicitly treating the overlaps among the constituent atomic orbitals $\{\chi_\mu\}$ in solving the orbital-level Schrödinger equation

$$\sum_\mu \langle \chi_\nu | \frac{-\hbar^2}{2m_e} \nabla^2 + V | \chi_\mu \rangle C_{i\mu} = \epsilon_i \sum_\mu \langle \chi_\nu | \chi_\mu \rangle C_{i\mu},$$

Hoffmann introduced the so-called extended Hückel method. He found that a value for $K = 1.75$ gave optimal results when using Slater-type orbitals as a basis (and for calculating the $S_{\mu\nu}$). The diagonal $h_{\mu,\mu}$ elements are given, as in the conventional Hückel method, in terms of valence-state IP's and EA's. Cusachs later proposed a variant of this parameterization of the off-diagonal elements:

$$h_{\nu,\mu} = 0.5K(h_{\mu,\mu})S_{\mu,\nu}(2 - |S_{\mu,\nu}|).$$

For first- and second-row atoms, the 1s or (2s, 2p) or (3s, 3p, 3d) valence-state ionization energies (α'_μ), the number of valence electrons (#Elec.) as well as the orbital exponents (e_s , e_p and e_d) of Slater-type orbitals used to calculate the overlap matrix elements $S_{m,n}$ corresponding are given below.

Atom	# Elec.	$e_s=e_p$	e_d	$\alpha_s(\text{eV})$	$\alpha_p(\text{eV})$	$\alpha_d(\text{eV})$
H	1	1.3		-13.6		
Li	1	0.650		-5.4	-3.5	
Be	2	0.975		-10.0	-6.0	
B	3	1.300		-15.2	-8.5	
C	4	1.625		-21.4	-11.4	
N	5	1.950		-26.0	-13.4	
O	6	2.275		-32.3	-14.8	
F	7	2.425		-40.0	-18.1	
Na	1	0.733		-5.1	-3.0	
Mg	2	0.950		-9.0	-4.5	
Al	3	1.167		-12.3	-6.5	
Si	4	1.383	1.383	-17.3	-9.2	-6.0
P	5	1.600	1.400	-18.6	-14.0	-7.0
S	6	1.817	1.500	-20.0	-13.3	-8.0
Cl	7	2.033	2.033	-30.0	-15.0	-9.0

Table 7.4.1: Insert caption here!

In the Hückel or extended Hückel methods no explicit reference is made to electron-electron interactions although such contributions are absorbed into the V potential, and hence into the α_μ and $\beta_{\mu,\nu}$ parameters of Hückel theory or the $h_{\mu,\mu}$ and $h_{\mu,\nu}$ parameters of extended Hückel theory. As electron density flows from one atom to another (due to electronegativity differences), the electron-electron repulsions in various atomic orbitals changes. To account for such charge-density-dependent coulombic energies, one must use an approach that includes explicit reference to inter-orbital coulomb and exchange interactions. There exists a large family of semi-empirical methods that permit explicit treatment of electronic interactions; some of the more commonly used approaches are discussed in Appendix F.

This page titled [7.4: The Extended Hückel Method](#) is shared under a [CC BY-NC-SA 4.0](#) license and was authored, remixed, and/or curated by [Jack Simons](#) via [source content](#) that was edited to the style and standards of the LibreTexts platform.

CHAPTER OVERVIEW

8: Electronic Configurations

One of the goals of quantum chemistry is to allow practicing chemists to use knowledge of the electronic states of fragments (atoms, radicals, ions, or molecules) to predict and understand the behavior (i.e., electronic energy levels, geometries, and reactivities) of larger molecules. In the preceding Section, orbital correlation diagrams were introduced to connect the orbitals of the fragments along a 'reaction path' leading to the orbitals of the products. In this Section, analogous connections are made among the fragment and product electronic states, again labeled by appropriate symmetries. To realize such connections, one must first write down N-electron wavefunctions that possess the appropriate symmetry; this task requires combining symmetries of the occupied orbitals to obtain the symmetries of the resulting states.

[8.1: Orbitals Do Not Provide the Complete Picture; Their Occupancy By the N Electrons Must Be Specified](#)

[8.2: Even N-Electron Configurations are Not Mother Nature's True Energy States](#)

[8.3: Mean-Field Models](#)

[8.4: Configuration Interaction \(CI\) Describes the Correct Electronic States](#)

[8.5: Summary](#)

This page titled [8: Electronic Configurations](#) is shared under a [CC BY-NC-SA 4.0](#) license and was authored, remixed, and/or curated by [Jack Simons](#) via [source content](#) that was edited to the style and standards of the LibreTexts platform.

8.1: Orbitals Do Not Provide the Complete Picture; Their Occupancy By the N Electrons Must Be Specified

Knowing the orbitals of a particular species provides one information about the sizes, shapes, directions, symmetries, and energies of those regions of space that are **available** to the electrons (i.e., the complete set of orbitals that are available). This knowledge does **not** determine into which orbitals the electrons are placed. It is by describing the electronic configurations (i.e., orbital occupancies such as $1s^2 2s^2 2p^2$ or $1s^2 2s^2 2p^1 3s^1$) appropriate to the energy range under study that one focuses on how the electrons occupy the orbitals. Moreover, a given configuration may give rise to several energy levels whose energies differ by chemically important amounts. for example, the $1s^2 2s^2 2p^2$ configuration of the Carbon atom produces nine degenerate 3P states, five degenerate 1D states, and a single 1S state. These three energy levels differ in energy by 1.5 eV and 1.2 eV, respectively.

This page titled [8.1: Orbitals Do Not Provide the Complete Picture; Their Occupancy By the N Electrons Must Be Specified](#) is shared under a [CC BY-NC-SA 4.0](#) license and was authored, remixed, and/or curated by [Jack Simons](#) via [source content](#) that was edited to the style and standards of the LibreTexts platform.

8.2: Even N-Electron Configurations are Not Mother Nature's True Energy States

Moreover, even single-configuration descriptions of atomic and molecular structure (e.g., $1s^2 2s^2 2p^4$ for the Oxygen atom) do not provide fully correct or highly accurate representations of the respective electronic wavefunctions. As will be shown in this Section and in more detail in Section 6, the picture of N electrons occupying orbitals to form a configuration is based on a so-called "mean field" description of the coulomb interactions among electrons. In such models, an electron at \mathbf{r} is viewed as interacting with an "averaged" charge density arising from the N-1 remaining electrons:

$$V_{\text{mean field}} = \int \rho_{N-1}(\mathbf{r}') \frac{e^2}{|\mathbf{r} - \mathbf{r}'|} d\mathbf{r}'.$$

Here $\rho_{N-1}(\mathbf{r}')$ represents the probability density for finding electrons at \mathbf{r}' , and $\frac{e^2}{|\mathbf{r} - \mathbf{r}'|}$ is the mutual Coulomb repulsion between electron density at \mathbf{r} and \mathbf{r}' . Analogous mean-field models arise in many areas of chemistry and physics, including electrolyte theory (e.g., [the Debye-Hückel theory](#)), statistical mechanics of dense gases (e.g., where the **Mayer-Mayer cluster** expansion is used to improve the ideal-gas mean field model), and chemical dynamics (e.g., the vibrationally averaged potential of interaction).

In each case, the mean-field model forms only a starting point from which one attempts to build a fully correct theory by effecting systematic corrections (e.g., using [perturbation theory](#)) to the mean-field model. The ultimate value of any particular meanfield model is related to its accuracy in describing experimental phenomena. If predictions of the mean-field model are far from the experimental observations, then higher-order corrections (which are usually difficult to implement) must be employed to improve its predictions. In such a case, one is motivated to search for a better model to use as a starting point so that lower-order perturbative (or other) corrections can be used to achieve chemical accuracy (e.g., ± 1 kcal/mole).

In electronic structure theory, the single-configuration picture (e.g., the $1s^2 2s^2 2p^4$ description of the oxygen atom) forms the mean-field starting point; the configuration interaction (CI) or perturbation theory techniques are then used to systematically improve this level of description.

The single-configuration mean-field theories of electronic structure neglect correlations among the electrons. That is, in expressing the interaction of an electron at \mathbf{r} with the N-1 other electrons, they use a probability density $\rho_{N-1}(\mathbf{r}')$ that is independent of the fact that another electron resides at \mathbf{r} .

The single-configuration mean-field theories of electronic structure neglect correlations among the electrons.

In fact, the so-called conditional probability density for finding one of N-1 electrons at \mathbf{r}' , given that an electron is at \mathbf{r} certainly depends on \mathbf{r} . As a result, the mean-field coulomb potential felt by a $2p_x$ orbital's electron in the $1s^2 2s^2 2p_x 2p_y$ single-configuration description of the Carbon atom is:

$$V_{\text{mean field}} = 2 \int |1s(\mathbf{r}')|^2 \frac{e^2}{|\mathbf{r} - \mathbf{r}'|} d\mathbf{r}' + 2 \int |2s(\mathbf{r}')|^2 \frac{e^2}{|\mathbf{r} - \mathbf{r}'|} d\mathbf{r}' + \int |2p_y(\mathbf{r}')|^2 \frac{e^2}{|\mathbf{r} - \mathbf{r}'|} d\mathbf{r}'.$$

In this example, the density $\rho_{N-1}(\mathbf{r}')$ is the sum of the charge densities of the orbitals occupied by the five other electrons $2|1s(\mathbf{r}')|^2 + 2|2s(\mathbf{r}')|^2 + |2p_y(\mathbf{r}')|^2$, and is not dependent on the fact that an electron resides at \mathbf{r} .

This page titled [8.2: Even N-Electron Configurations are Not Mother Nature's True Energy States](#) is shared under a [CC BY-NC-SA 4.0](#) license and was authored, remixed, and/or curated by [Jack Simons](#) via [source content](#) that was edited to the style and standards of the LibreTexts platform.

8.3: Mean-Field Models

The Mean-Field Model, Which Forms the Basis of Chemists' Pictures of Electronic Structure of Molecules, Is Not Very Accurate

The magnitude and "shape" of such a mean-field potential is shown below for the Beryllium atom. In this figure, the nucleus is at the origin, and one electron is placed at a distance from the nucleus equal to the maximum of the 1s orbital's radial probability density (near 0.13 Å). The radial coordinate of the second is plotted as the abscissa; this second electron is arbitrarily constrained to lie on the line connecting the nucleus and the first electron (along this direction, the inter-electronic interactions are largest). On the ordinate, there are two quantities plotted: (i) the Self-Consistent Field (SCF) mean-field potential $\int |1s(\mathbf{r}')|^2 \frac{e^2}{|\mathbf{r}-\mathbf{r}'|} d\mathbf{r}'$, and (ii) the so-called Fluctuation potential (F), which is the true coulombic $\frac{e^2}{|\mathbf{r}-\mathbf{r}'|}$ interaction potential minus the SCF potential.

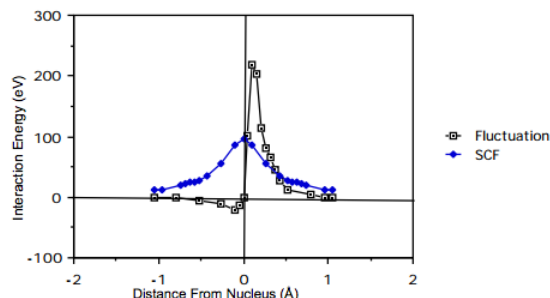


Figure 8.3.1: Insert caption here!

As a function of the inter-electron distance, the fluctuation potential decays to zero more rapidly than does the SCF potential. For this reason, approaches in which F is treated as a perturbation and corrections to the mean-field picture are computed perturbatively might be expected to be rapidly convergent (whenever perturbations describing long-range interactions arise, convergence of perturbation theory is expected to be slow or not successful). However, the magnitude of F is quite large and remains so over an appreciable range of inter-electron distances. The resultant corrections to

The resultant corrections to the SCF picture are therefore quite large when measured in kcal/mole. For example, the differences ΔE between the true (state-of-the-art quantum chemical calculation) energies of interaction among the four electrons in Be and the SCF mean-field estimates of these interactions are given in the table shown below in eV (recall that 1 eV = 23.06 kcal/mole).

Orb. Pair	1s α 1s β	1s α 2s α	1s α 2s β	1s β 2s α	1s β 2s β	2s α 2s β
ΔE in eV	1.126	0.022	0.058	0.058	0.022	1.234

Table 8.3.1: Insert caption here!

To provide further insight why the SCF mean-field model in electronic structure theory is of limited accuracy, it can be noted that the average value of the kinetic energy plus the attraction to the Be nucleus plus the SCF interaction potential for one of the 2s orbitals of Be with the three remaining electrons in the $1s^2 2s^2$ configuration is:

$$\langle 2s | \frac{-\hbar^2}{2m_e} \nabla^2 - \frac{4e^2}{r} + V_{SCF} | 2s \rangle = -15.4 eV;$$

the analogous quantity for the 2p orbital in the $1s^2 2s^2 p$ configuration is:

$$\langle 2p | \frac{-\hbar^2}{2m_e} \nabla^2 - \frac{4e^2}{r} + V_{SCF} | 2p \rangle = -12.28 eV;$$

the corresponding value for the 1s orbital is (negative and) of even larger magnitude. The SCF average coulomb interaction between the two 2s orbitals of $1s^2 2s^2$ Be is:

$$\int |2s(\mathbf{r})|^2 |2s(\mathbf{r}')|^2 \frac{e^2}{|\mathbf{r}-\mathbf{r}'|} d\mathbf{r} d\mathbf{r}' = 5,95 eV.$$

This data clearly shows that corrections to the SCF model (see the above table) represent significant fractions of the inter-electron interaction energies (e.g., 1.234 eV compared to 5.95- 1.234 = 4.72 eV for the two 2s electrons of Be), and that the interelectron interaction energies, in turn, constitute significant fractions of the total energy of each orbital (e.g., 5.95 -1.234 eV = 4.72 eV out of -15.4 eV for a 2s orbital of Be).

The task of describing the electronic states of atoms and molecules from first principles and in a chemically accurate manner (± 1 kcal/mole) is clearly quite formidable. The orbital picture and its accompanying SCF potential take care of "most" of the interactions among the N electrons (which interact via long-range coulomb forces and whose dynamics requires the application of quantum physics and permutational symmetry). However, the residual fluctuation potential, although of shorter range than the bare coulomb potential, is large enough to cause significant corrections to the mean-field picture. This, in turn, necessitates the use of more sophisticated and computationally taxing techniques (e.g., high order perturbation theory or large variational expansion spaces) to reach the desired chemical accuracy.

Mean-field models are obviously approximations whose accuracy must be determined so scientists can know to what degree they can be "trusted". For electronic structures of atoms and molecules, they require quite substantial corrections to bring them into line with experimental fact. Electrons in atoms and molecules undergo dynamical motions in which their coulomb repulsions cause them to "avoid" one another at every instant of time, not only in the average-repulsion manner that the mean-field models embody. The inclusion of instantaneous spatial correlations among electrons is necessary to achieve a more accurate description of atomic and molecular electronic structure.

This page titled [8.3: Mean-Field Models](#) is shared under a [CC BY-NC-SA 4.0](#) license and was authored, remixed, and/or curated by [Jack Simons](#) via [source content](#) that was edited to the style and standards of the LibreTexts platform.

8.4: Configuration Interaction (CI) Describes the Correct Electronic States

The most commonly employed tool for introducing such spatial correlations into electronic wavefunctions is called configuration interaction (CI); this approach is described briefly later in this Section and in considerable detail in [Section 6](#). Briefly, one employs the (in principle, complete as shown by P. O. Löwdin, Rev. Mod. Phys. 32 , 328 (1960)) set of N-electron configurations that

- can be formed by placing the N electrons into orbitals of the atom or molecule under study, and that
- possess the spatial, spin, and angular momentum symmetry of the electronic state of interest.

This set of functions is then used, in a linear variational function, to achieve, via the CI technique, a more accurate and dynamically correct description of the electronic structure of that state. For example, to describe the ground $1S$ state of the Be atom, the $1s2s2$ configuration (which yields the mean-field description) is augmented by including other configurations such as $1s^23s^2$, $1s^22p^2$, $1s^23p^2$, $1s^22s^3s$, $3s^22s^2$, $2p^22s^2$, etc., all of which have overall 1S spin and angular momentum symmetry. The excited 1S states are also combinations of all such configurations. Of course, the ground-state wavefunction is dominated by the $|1s^22s^2|$ and excited states contain dominant contributions from $|1s^22s3s|$, etc. configurations. The resultant CI wavefunctions are formed as shown in Section 6 as linear combinations of all such configurations.

To clarify the physical significance of mixing such configurations, it is useful to consider what are found to be the two most important such configurations for the ground $1S$ state of the Be atom:

$$\Psi \cong C_1 |1s^22s^2| - C_2 [|1s^22p_x^2| + |1s^22p_y^2| + |1s^22p_z^2|].$$

As proven in Chapter 13.III, this two-configuration description of Be's electronic structure is equivalent to a description in which two electrons reside in the $1s$ orbital (with opposite, α and β spins) while the other pair reside in $2s$ - $2p$ hybrid orbitals (more correctly, polarized orbitals) in a manner that instantaneously correlates their motions:

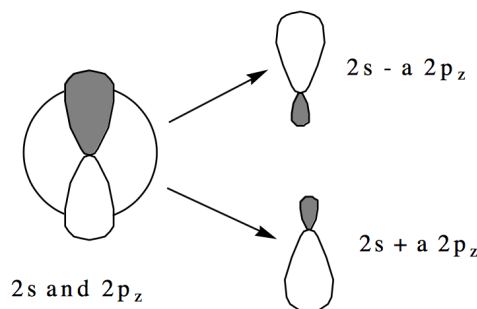
$$\Psi \cong \frac{1}{6} C_1 |1s^2| \{ [(2s - a2p_x)\alpha(2s + a2p_x)\beta - (2s - a2p_x)\beta(2s + a2p_x)\alpha] \quad (8.4.1)$$

$$+ [(2s - a2p_y)\alpha(2s + a2p_y)\beta - (2s - a2p_y)\beta(2s + a2p_y)\alpha] \quad (8.4.2)$$

$$+ [(2s - a2p_z)\alpha(2s + a2p_z)\beta - (2s - a2p_z)\beta(2s + a2p_z)\alpha] \}, \quad (8.4.3)$$

where $a = \sqrt{3 \frac{C_2}{C_1}}$.

The so-called polarized orbital pairs ($2s \pm a2p_{x,y, \text{ or } z}$) are formed by mixing into the $2s$ orbital an amount of the $2p_{x,y, \text{ or } z}$ orbital, with the mixing amplitude determined by the ratio of C_2 to C_1 . As will be detailed in Section 6, this ratio is proportional to the magnitude of the coupling $\langle |1s^22s^2| H |1s^22p^2| \rangle$ between the two configurations and inversely proportional to the energy difference $[\langle |1s^22s^2| H |1s^22s^2| \rangle - \langle |1s^22p^2| H |1s^22p^2| \rangle]$ for these configurations. So, in general, configurations that have similar energies (Hamiltonian expectation values) and couple strongly give rise to strongly mixed polarized orbital pairs. The result of forming such polarized orbital pairs are described pictorially below.



Polarized Orbital $2s$ and $2p_z$ Pairs

In each of the three equivalent terms in this wavefunction, one of the valence electrons moves in a $2s+a2p$ orbital polarized in one direction while the other valence electron moves in the $2s-a2p$ orbital polarized in the opposite direction. For example, the first term $[(2s - a2p_x)\alpha(2s + a2p_x)\beta - (2s - a2p_x)\beta(2s + a2p_x)\alpha]$ describes one electron occupying a $2s - a2p_x$ polarized

orbital while the other electron occupies the $2s + a2p_x$ orbital. In this picture, the electrons reduce their mutual coulomb repulsion by occupying different regions of space; in the SCF mean-field picture, both electrons reside in the same $2s$ region of space. In this particular example, the electrons undergo angular correlation to "avoid" one another. The fact that equal amounts of x , y , and z orbital polarization appear in Y is what preserves the 1S symmetry of the wavefunction.

The fact that the CI wavefunction

$$\Psi \cong C_1 |1s^2 2s^2| - C_2 [|1s^2 2p_x^2| + |1s^2 2p_y^2| + |1s^2 2p_z^2|]$$

mixes its two configurations with **opposite sign** is of significance. As will be seen later in Section 6, solution of the Schrödinger equation using the CI method in which two configurations (e.g., $|1s^2 2s^2|$ and $|1s^2 2p^2|$) are employed gives rise to two solutions. One approximates the ground state wave function; the other approximates an excited state. The former is the one that mixes the two configurations with opposite sign.

To understand why the latter is of higher energy, it suffices to analyze a function of the form

$$\Psi' \cong C_1 |1s^2 2s^2| + C_2 [|1s^2 2p_x^2| + |1s^2 2p_y^2| + |1s^2 2p_z^2|]$$

in a manner analogous to above. In this case, it can be shown that

$$\Psi' \cong \frac{1}{6} C_1 |1s^2| \{ [(2s - ia2p_x)\alpha(2s + ia2p_x)\beta - (2s - ia2p_x)\beta(2s + ia2p_x)\alpha] \quad (8.4.4)$$

$$+ [(2s - ia2p_y)\alpha(2s + ia2p_y)\beta - (2s - ia2p_y)\beta(2s + ia2p_y)\alpha] \quad (8.4.5)$$

$$+ [(2s - ia2p_z)\alpha(2s + ia2p_z)\beta - (2s - ia2p_z)\beta(2s + ia2p_z)\alpha] \}. \quad (8.4.6)$$

There is a fundamental difference, however, between the polarized orbital pairs introduced earlier $\phi_{\pm} = (2s \pm a2p_{x,y, \text{ or } z})$ and the corresponding functions $\phi'_{\pm} = (2s \pm ia2p_{x,y, \text{ or } z})$ appearing here. The probability densities embodied in the former

$$|\phi_{\pm}|^2 = |2s|^2 + a^2|p|^2 \pm 2a(2s p_{x,y \text{ or } z})$$

describe constructive (for the + case) and destructive (for the - case) superposition of the probabilities of the $2s$ and $2p$ orbitals. The probability densities of ϕ'_{\pm} are

$$|\phi'_{\pm}|^2 = (2s \pm ia2p_{x,y \text{ or } z}) * (2s \pm ia2p_{x,y \text{ or } z}) \quad (8.4.7)$$

$$= |2s|^2 + a^2|2p_{x,y \text{ or } z}|^2. \quad (8.4.8)$$

These densities are identical to one another and do not describe polarized orbital densities. Therefore, the CI wavefunction which mixes the two configurations with like sign, when analyzed in terms of orbital pairs, places the electrons into orbitals $\phi'_{\pm} = (2s \pm ia2p_{x,y, \text{ or } z})$ whose densities do not permit the electrons to avoid one another. Rather, both orbitals have the same spatial density $|2s|^2 + a^2|2p_{x,y, \text{ or } z}|^2$, which gives rise to higher coulombic interaction energy for this state.

This page titled [8.4: Configuration Interaction \(CI\) Describes the Correct Electronic States](#) is shared under a [CC BY-NC-SA 4.0](#) license and was authored, remixed, and/or curated by [Jack Simons](#) via [source content](#) that was edited to the style and standards of the LibreTexts platform.

8.5: Summary

In summary, the dynamical interactions among electrons give rise to instantaneous spatial correlations that must be handled to arrive at an accurate picture of atomic and molecular structure. The simple, single-configuration picture provided by the mean-field model is a useful starting point, but improvements are often needed. In Section 6, methods for treating electron correlation will be discussed in greater detail.

For the remainder of this Section, the primary focus is placed on forming proper N-electron wavefunctions by occupying the orbitals available to the system in a manner that guarantees that the resultant N-electron function is an eigenfunction of those operators that commute with the N-electron Hamiltonian.

For polyatomic molecules, these operators include point-group symmetry operators (which act on all N electrons) and the spin angular momentum (S^2 and S_z) of all of the electrons taken as a whole (this is true in the absence of spin-orbit coupling which is treated later as a perturbation). For linear molecules, the point group symmetry operations involve rotations R_z of all N electrons about the principal axis, as a result of which the total angular momentum L_z of the N electrons (taken as a whole) about this axis commutes with the Hamiltonian, H. Rotation of all N electrons about the x and y axes does not leave the total coulombic potential energy unchanged, so L_x and L_y do not commute with H. Hence for a linear molecule, L_z , S^2 , and S_z are the operators that commute with H. For atoms, the corresponding operators are L^2 , L_z , S^2 , and S_z (again, in the absence of spin-orbit coupling) where each operator pertains to the total orbital or spin angular momentum of the N electrons.

To construct N-electron functions that are eigenfunctions of the spatial symmetry or orbital angular momentum operators as well as the spin angular momentum operators, one has to "couple" the symmetry or angular momentum properties of the individual spinorbitals used to construct the N-electrons functions. This coupling involves forming direct product symmetries in the case of polyatomic molecules that belong to finite point groups, it involves vector coupling orbital and spin angular momenta in the case of atoms, and it involves vector coupling spin angular momenta and axis coupling orbital angular momenta when treating linear molecules. Much of this Section is devoted to developing the tools needed to carry out these couplings.

This page titled [8.5: Summary](#) is shared under a [CC BY-NC-SA 4.0](#) license and was authored, remixed, and/or curated by [Jack Simons](#) via [source content](#) that was edited to the style and standards of the LibreTexts platform.

CHAPTER OVERVIEW

9: Symmetry of Electronic Wavefunctions

Electronic wavefunctions must be constructed to have permutational antisymmetry because the N electrons are indistinguishable Fermions

[9.1: Electronic Configurations](#)

[9.2: Antisymmetric Wavefunctions](#)

This page titled [9: Symmetry of Electronic Wavefunctions](#) is shared under a [CC BY-NC-SA 4.0](#) license and was authored, remixed, and/or curated by [Jack Simons](#) via [source content](#) that was edited to the style and standards of the LibreTexts platform.

9.1: Electronic Configurations

Atoms, linear molecules, and non-linear molecules have orbitals which can be labeled either according to the symmetry appropriate for that isolated species or for the species in an environment which produces lower symmetry. These orbitals should be viewed as regions of space in which electrons can move, with, of course, at most two electrons (of opposite spin) in each orbital. Specification of a particular occupancy of the set of orbitals available to the system gives an **electronic configuration**. For example, $1s^2 2s^2 2p^4$ is an electronic configuration for the Oxygen atom (and for the F^{+1} ion and the N^{-1} ion); $1s^2 2s^2 2p^3 3p^1$ is another configuration for O, F^{+1} , or N^{-1} . These configurations represent situations in which the electrons occupy low-energy orbitals of the system and, as such, are likely to contribute strongly to the true ground and low-lying excited states and to the low-energy states of molecules formed from these atoms or ions.

Specification of an electronic configuration does not, however, specify a particular electronic state of the system. In the above $1s^2 2s^2 2p^4$ example, there are many ways (fifteen, to be precise) in which the 2p orbitals can be occupied by the four electrons. As a result, there are a total of fifteen states which cluster into three energetically distinct **levels**, lying within this single configuration. The $1s^2 2s^2 2p^3 3p^1$ configuration contains thirty-six states which group into six distinct energy levels (the word **level** is used to denote one or more state with the same energy). Not all states which arise from a given electronic configuration have the same energy because various states occupy the degenerate (e.g., 2p and 3p in the above examples) orbitals differently. That is, some states have orbital occupancies of the form

$$2p_1^2 2p_0^1 2p_{-1}^1$$

while others have

$$2p_1^2 2p_0^2 2p_{-1}^0$$

as a result, the states can have quite different coulombic repulsions among the electrons (the state with two doubly occupied orbitals would lie higher in energy than that with two singly occupied orbitals). Later in this Section and in Appendix G techniques for constructing wavefunctions for each state contained within a particular configuration are given in detail. Mastering these tools is an important aspect of learning the material in this text.

In summary, an atom or molecule has many orbitals (core, bonding, non-bonding, Rydberg, and antibonding) available to it; occupancy of these orbitals in a particular manner gives rise to a configuration. If some orbitals are partially occupied in this configuration, more than one state will arise; these states can differ in energy due to differences in how the orbitals are occupied. In particular, if degenerate orbitals are partially occupied, many states can arise and have energies which differ substantially because of differences in electron repulsions arising in these states. Systematic procedures for extracting all states from a given configuration, for labeling the states according to the appropriate symmetry group, for writing the wavefunctions corresponding to each state and for evaluating the energies corresponding to these wavefunctions are needed. Much of [Chapters 10](#) and [11](#) are devoted to developing and illustrating these tools.

This page titled [9.1: Electronic Configurations](#) is shared under a [CC BY-NC-SA 4.0](#) license and was authored, remixed, and/or curated by [Jack Simons](#) via [source content](#) that was edited to the style and standards of the LibreTexts platform.

9.2: Antisymmetric Wavefunctions

General Concepts

The total electronic Hamiltonian

$$\hat{H} = \sum_i \left(\frac{-\hbar^2}{2m_e} \nabla_i^2 - \sum_a \frac{Z_a e^2}{r_{ia}} \right) + \sum_{i>j} \frac{e^2}{r_{ij}} + \sum_{a>b} \frac{Z_a Z_b e^2}{r_{ab}}$$

where i and j label electrons and a and b label the nuclei (whose charges are denoted Z_a), commutes with the operators P_{ij} which permute the names of the electrons i and j . This, in turn, requires eigenfunctions of \hat{H} to be eigenfunctions of \hat{P}_{ij} . In fact, the set of such permutation operators form a group called [the symmetric group](#). In the present text, we will not exploit the full group theoretical nature of these operators; we will focus on the simple fact that all wavefunctions must be eigenfunctions of the \hat{P}_{ij} operator.

Because \hat{P}_{ij} obeys

$$\hat{P}_{ij}^* \hat{P}_{ij} = 1$$

the eigenvalues of the \hat{P}_{ij} operators must be +1 or -1. Electrons are Fermions (i.e., they have half-integral spin) and they must have wavefunctions which are **odd** under permutation of any pair:

$$\hat{P}_{ij} \Psi = -\Psi$$

Bosons such as photons or deuterium nuclei (i.e., species with integral spin quantum numbers) have wavefunctions, which are **even** under permutation and obey

$$\hat{P}_{ij} \Psi = +\Psi$$

These permutational symmetries are not only characteristics of the exact eigenfunctions of H belonging to any atom or molecule containing more than a single electron, but they are also conditions which **must** be placed on any acceptable model or trial wavefunction (e.g., in a variational sense) which one constructs.

In particular, within the orbital model of electronic structure (discussed in [Section 6](#)), one can not construct trial wavefunctions which are simple spin-orbital products (i.e., an orbital multiplied by an α or β spin function for each electron) such as

$$1s\alpha 1s\beta 2s\alpha 2s\beta 2p1\alpha 2p0\alpha.$$

Such spin-orbital product functions must be made permutationally antisymmetric if the N -electron trial function is to be properly antisymmetric. This can be accomplished for any such product wavefunction by applying the following antisymmetrizer operator:

$$A = \frac{1}{\sqrt{N!}} \sum p s p P$$

where N is the number of electrons, P runs over all $N!$ permutations, and $s p$ is +1 or -1 depending on whether the permutation P contains an even or odd number of pairwise permutations (e.g., 231 can be reached from 123 by two pairwise permutations:

$$123 \rightarrow 213 \rightarrow 231$$

so 231 would have $s p = 1$). The permutation operator P in A acts on a product wavefunction and permutes the ordering of the spin-orbitals.

For example,

$$A\phi_1\phi_2\phi_3 = \frac{1}{\sqrt{6}} [\phi_1\phi_2\phi_3 - \phi_1\phi_3\phi_2 - \phi_3\phi_2\phi_1 - \phi_2\phi_1\phi_3 + \phi_3\phi_1\phi_2 + \phi_2\phi_3\phi_1]$$

where the convention is that electronic coordinates r_1, r_2 , and r_3 correspond to the orbitals as they appear in the product (e.g., the term $\phi_3\phi_2\phi_1$ represents $\phi_3(r_1)\phi_2(r_2)\phi_1(r_3)$).

It turns out that the permutations \hat{P} can be allowed either to act on the "names" or labels of the electrons, keeping the order of the spin-orbitals fixed, or to act on the spin-orbitals, keeping the order and identity of the electrons' labels fixed. The resultant wavefunction, which contains $N!$ terms, is exactly the same regardless of how one allows the permutations to act. Because we wish to use the above convention in which the order of the electronic labels remains fixed as 1, 2, 3, ... N , we choose to think of the permutations acting on the names of the spin-orbitals. It should be noted that the effect of A on any spin-orbital product is to produce a function that is a sum of $N!$ terms. In each of these terms the same spin-orbitals appear, but the order in which they appear differs from term to term.

Antisymmetrization does not alter the overall orbital occupancy; it simply "scrambles" any knowledge of which electron is in which spin-orbital.

The antisymmetrized orbital product $A\varphi_1\varphi_2\varphi_3$ is represented by the short hand $|\varphi_1\varphi_2\varphi_3|$ and is referred to as a [Slater determinant](#). The origin of this notation can be made clear by noting that $(1/\sqrt{N!})$ times the determinant of a matrix whose rows are labeled by the index i of the spin-orbital φ_i and whose columns are labeled by the index j of the electron at r_j is equal to the above function:

$$A\varphi_1\varphi_2\varphi_3 = (1/\sqrt{3!})\det(\varphi_i(r_j)).$$

The general structure of such Slater determinants is illustrated below:

$$\frac{1}{\sqrt{N!}}\det\varphi_j(r_i) = \frac{1}{\sqrt{N}}\varphi_1(1)\varphi_2(1)\varphi_3(1)\dots\varphi_k(1)\dots\dots\varphi_N(1)\varphi_1(2)\varphi_2(2)\varphi_3(2)\dots\varphi_k(2)\dots\dots\varphi_N(2)\dots\dots\varphi_1(N)\varphi_2(N)\varphi_3(N)\dots\varphi_k(N)\dots\dots\varphi_N(N)$$

The antisymmetry of many-electron spin-orbital products places constraints on any acceptable model wavefunction, which give rise to important physical consequences. For example, it is antisymmetry that makes a function of the form $|1s\alpha 1s\alpha|$ vanish (thereby enforcing the [Pauli exclusion principle](#)) while $|1s\alpha 2s\alpha|$ does not vanish, except at points r_1 and r_2 where $1s(r_1) = 2s(r_2)$, and hence is acceptable. The Pauli principle is embodied in the fact that if any two or more columns (or rows) of a determinant are identical, the determinant vanishes. Antisymmetry also enforces indistinguishability of the electrons in that

$$|1s\alpha 1s\beta 2s\alpha 2s\beta| = -|1s\alpha 1s\beta 2s\beta 2s\alpha|.$$

That is, two wavefunctions which differ simply by the ordering of their spin-orbitals are equal to within a sign (+/- 1); such an overall sign difference in a wavefunction has no physical consequence because all physical properties depend on the product $\Psi^* \Psi$, which appears in any expectation value expression.

The antisymmetry of many-electron spin-orbital products places constraints on any acceptable model wavefunction.

Physical Consequences of Antisymmetry

Once the rules for evaluating energies of determinantal wavefunctions and for forming functions which have proper spin and spatial symmetries have been put forth (in [Chapter 11](#)), it will be clear that antisymmetry and electron spin considerations, in addition to orbital occupancies, play substantial roles in determining energies and that it is precisely these aspects that are responsible for energy splittings among states arising from one configuration. A single example may help illustrate this point. Consider the $\pi^1\pi^{*1}$ configuration of ethylene (ignore the other orbitals and focus on the properties of these two). As will be shown below when spin angular momentum is treated in full, the triplet spin states (e.g., $S = 1$) of this configuration are:

$$|S = 1, M_S = 1\rangle = |\pi\alpha\pi^*\alpha|$$

$$|S = 1, M_S = -1\rangle = |\pi\beta\pi^*\beta|,$$

and

$$|S = 1, M_S = 0\rangle = \frac{1}{\sqrt{2}}[|\pi\alpha\pi^*\beta| + |\pi\beta\pi^*\alpha|].$$

The singlet spin state is:

$$|S = 0, M_S = 0\rangle = \frac{1}{\sqrt{2}}[|\pi\alpha\pi^*\beta| - |\pi\beta\pi^*\alpha|].$$

To understand how the three triplet states have the same energy and why the singlet state has a different energy, and an energy different than the $M_S = 0$ triplet even though these two states are composed of the same two determinants, we proceed as follows:

- Step 1. We express the bonding π and antibonding π^* orbitals in terms of the atomic p-orbitals from which they are formed:

$$\pi = \frac{1}{\sqrt{2}}[L + R]$$

and

$$\pi^* = \frac{1}{\sqrt{2}}[L - R],$$

where R and L denote the p-orbitals on the left and right carbon atoms, respectively.

- Step 2. We substitute these expressions into the Slater determinants that form the singlet and triplet states and collect terms and throw out terms for which the determinants vanish.
- Step 3. This then gives the singlet and triplet states in terms of atomic-orbital occupancies where it is easier to see the energy equivalences and differences. Let us begin with the triplet states:

$$|\pi\alpha\pi^*\alpha| = \frac{1}{2}[|L\alpha L\alpha| - |R\alpha R\alpha| + |R\alpha L\alpha| - |L\alpha R\alpha|] \quad (9.2.1)$$

$$= |R\alpha L\alpha|; \quad (9.2.2)$$

$$\frac{1}{\sqrt{2}}[|\pi\alpha\pi^*\beta| + |\pi\beta\pi^*\alpha|] = \frac{1}{\sqrt{2}}\frac{1}{2}[|L\alpha L\beta| - |R\alpha R\beta| + |R\alpha L\beta| - |L\alpha R\beta| + |L\beta L\alpha| - |R\beta R\alpha| + |R\beta L\alpha| - |L\beta R\alpha|] \quad (9.2.3)$$

$$= \frac{1}{\sqrt{2}}[|R\alpha L\beta| + |R\beta L\alpha|]; \quad (9.2.4)$$

$$|\pi\beta\pi^*\beta| = \frac{1}{2}[|L\beta L\beta| - |R\beta R\beta| + |R\beta L\beta| - |L\beta R\beta|] \quad (9.2.5)$$

$$= |R\beta L\beta|. \quad (9.2.6)$$

The singlet state can be reduced in like fashion:

$$\frac{1}{\sqrt{2}}[|\pi\alpha\pi^*\beta| - |\pi\beta\pi^*\alpha|] = \frac{1}{\sqrt{2}}\frac{1}{2}[|L\alpha L\beta| - |R\alpha R\beta| + |R\alpha L\beta| - |L\alpha R\beta| - |L\beta L\alpha| + |R\beta R\alpha| - |R\beta L\alpha| + |L\beta R\alpha|] \quad (9.2.7)$$

$$= \frac{1}{\sqrt{2}}[|L\alpha L\beta| - |R\beta R\alpha|]. \quad (9.2.8)$$

Notice that all three triplet states involve atomic orbital occupancy in which one electron is on one atom while the other is on the second carbon atom. In contrast, the singlet state places both electrons on one carbon (it contains two terms; one with the two electrons on the left carbon and the other with both electrons on the right carbon). In a "valence bond" analysis of the physical content of the singlet and triplet $\pi^1\pi^{*1}$ states, it is clear that the energy of the triplet states will lie below that of the singlet because the singlet contains "zwitterion" components that can be denoted C^+C^- and C^-C^+ , while the three triplet states are purely "covalent". This case provides an excellent example of how the spin and permutational symmetries of a state "conspire" to qualitatively affect its energy and even electronic character as represented in its atomic orbital occupancies. Understanding this should provide ample motivation for learning how to form proper antisymmetric spin (and orbital) angular momentum eigenfunctions for atoms and molecules.

The energy of the triplet states will lie below that of the singlet

– dekscript –

This page titled [9.2: Antisymmetric Wavefunctions](#) is shared under a [CC BY-NC-SA 4.0](#) license and was authored, remixed, and/or curated by [Jack Simons](#) via [source content](#) that was edited to the style and standards of the LibreTexts platform.

CHAPTER OVERVIEW

10: Angular Momentum and Group Symmetries of Electronic Wavefunctions

Electronic wavefunctions must also possess proper symmetry. These include angular momentum and point group symmetries

[10.1: Angular Momentum Symmetry and Strategies for Angular Momentum Coupling](#)

[10.2: Electron Spin Angular Momentum](#)

[10.3: Coupling of Angular Momenta](#)

[10.4: Atomic Term Symbols and Wavefunctions](#)

[10.5: Atomic Configuration Wavefunctions](#)

[10.6: Inversion Symmetry](#)

[10.7: Review of Atomic Cases](#)

This page titled [10: Angular Momentum and Group Symmetries of Electronic Wavefunctions](#) is shared under a [CC BY-NC-SA 4.0](#) license and was authored, remixed, and/or curated by [Jack Simons](#) via [source content](#) that was edited to the style and standards of the LibreTexts platform.

10.1: Angular Momentum Symmetry and Strategies for Angular Momentum Coupling

Because the total Hamiltonian of a many-electron atom or molecule forms a mutually commutative set of operators with S^2 , S_z , and $A = (\hat{O}1/N!) \text{Sp sp P}$, the exact eigenfunctions of H must be eigenfunctions of these operators. Being an eigenfunction of A forces the eigenstates to be odd under all P_{ij} . Any acceptable model or trial wavefunction should be constrained to also be an eigenfunction of these symmetry operators.

If the atom or molecule has additional symmetries (e.g., full rotation symmetry for atoms, axial rotation symmetry for linear molecules and point group symmetry for nonlinear polyatomics), the trial wavefunctions should also conform to these spatial symmetries. This Chapter addresses those operators that commute with H , P_{ij} , S^2 , and S_z and among one another for atoms, linear, and non-linear molecules. As treated in detail in Appendix G, the full non-relativistic N-electron Hamiltonian of an atom or molecule

$$H = \sum_j \left(\frac{-\hbar^2}{2m} \nabla_j^2 - \sum_a \frac{Z_a e^2}{r_{j,a}} \right) + \sum_{j < k} \frac{e^2}{r_{j,k}}$$

commutes with the following operators:

- i. The inversion operator i and the three components of the total orbital angular momentum $L_z = \sum_j L_z(j)$, L_y , L_x , as well as the components of the total spin angular momentum S_z , S_x , and S_y for atoms (but not the individual electrons' $L_z(j)$, $S_z(j)$, etc). Hence, L^2 , L_z , S^2 , S_z are the operators we need to form eigenfunctions of, and L , M_L , S , and M_S are the "good" quantum numbers.
- ii. $L_z = \sum_j L_z(j)$, as well as the N-electron S_x , S_y , and S_z for linear molecules (also i , if the molecule has a center of symmetry). Hence, L_z , S^2 , and S_z are the operators we need to form eigenfunctions of, and M_L , S , and M_S are the "good" quantum numbers; L no longer is! iii.
- iii. S_x , S_y , and S_z as well as all point group operations for **non-linear polyatomic molecules**. Hence S^2 , S_z , and the point group operations are used to characterize the functions we need to form. When we include spin-orbit coupling into H (this adds another term to the potential that involves the spin and orbital angular momenta of the electrons), L^2 , L_z , S^2 , S_z no longer commute with H . However, $J_z = S_z + L_z$ and $J^2 = (\mathbf{L} + \mathbf{S})^2$ now do commute with H .

This page titled [10.1: Angular Momentum Symmetry and Strategies for Angular Momentum Coupling](#) is shared under a [CC BY-NC-SA 4.0](#) license and was authored, remixed, and/or curated by [Jack Simons](#) via [source content](#) that was edited to the style and standards of the LibreTexts platform.

10.2: Electron Spin Angular Momentum

Individual electrons possess intrinsic spin characterized by angular momentum quantum numbers s and m_s ; for electrons, $s = 1/2$ and $m_s = 1/2$, or $-1/2$. The $m_s = 1/2$ spin state of the electron is represented by the symbol α and the $m_s = -1/2$ state is represented by β . These spin functions obey:

$$S^2\alpha = \frac{1}{2}\left(\frac{1}{2} + 1\right)\hbar^2\alpha,$$

$$S_z\alpha = \frac{1}{2}\hbar\alpha$$

$$S^2\beta = \frac{1}{2}\left(\frac{1}{2} + 1\right)\hbar^2\beta$$

and

$$S_z\beta = -\frac{1}{2}\hbar\beta.$$

The α and β spin functions are connected via lowering S_- and raising S_+ operators, which are defined in terms of the x and y components of S as follows:

$$S_+ = S_x + iS_y$$

and

$$S_- = S_x - iS_y.$$

In particular $S_+\beta = \hbar\alpha$, $S_+\alpha = 0$, $S_-\alpha = \hbar\beta$, and $S_-\beta = 0$. These expressions are examples of the more general relations (these relations are developed in detail in Appendix G) which all angular momentum operators and their eigenstates obey:

$$J^2|j, m\rangle = j(j+1)\hbar^2|j, m\rangle$$

$$J_z|j, m\rangle = m\hbar|j, m\rangle$$

$$J_+|j, m\rangle = \hbar\sqrt{j(j+1) - m(m+1)}|j, m+1\rangle$$

and

$$J_-|j, m\rangle = \hbar\sqrt{j(j+1) - m(m-1)}|j, m-1\rangle$$

In a many-electron system, one must combine the spin functions of the individual electrons to generate eigenfunctions of the total $S_z = \sum_i S_z(i)$ (expressions for $S_x = \sum_i S_x(i)$ and $S_y = \sum_i S_y(i)$ also follow from the fact that the total angular momentum of a collection of particles is the sum of the angular momenta, component-by-component, of the individual angular momenta) and total S^2 operators because only these operators commute with the full Hamiltonian, H, and with the permutation operators P_{ij} . No longer are the individual $S^2(i)$ and $S_z(i)$ good quantum numbers; these operators do not commute with P_{ij} .

Spin states which are eigenfunctions of the total S^2 and S_z can be formed by using angular momentum coupling methods or the explicit construction methods detailed in Appendix (G). In the latter approach, one forms, consistent with the given electronic configuration, the spin state having maximum S_z eigenvalue (which is easy to identify as shown below and which corresponds to a state with S equal to this maximum S_z eigenvalue) and then generating states of lower S_z values and lower S values using the angular momentum raising and lowering operators

$$S_- = \sum_i S_-(i) \text{ and } S_+ = \sum_i S_+(i).$$

To illustrate, consider a three-electron example with the configuration $1s2s3s$. Starting with the determinant $|1s\alpha 2s\alpha 3s\alpha|$, which has the maximum $M_s = \frac{3}{2}$ and hence has $S = \frac{3}{2}$ (this function is denoted $|\frac{3}{2}, \frac{3}{2}\rangle$), apply S_- in the additive form $S_- = \sum_i S_-(i)$ to generate the following combination of three determinants:

$$\hbar [|1s\beta 2s\alpha 3s\alpha| + |1s\alpha 2s\beta 3s\alpha| + |1s\alpha 2s\alpha 3s\beta|],$$

which, according to the above identities, must equal

$$\hbar \sqrt{\frac{3}{2} \left(\frac{3}{2} + 1 \right) - \frac{3}{2} \left(\frac{3}{2} - 1 \right)} \left| \frac{3}{2}, \frac{1}{2} \right\rangle.$$

So the state $\left| \frac{3}{2}, \frac{1}{2} \right\rangle$ with $S = \frac{3}{2}$ and $M_S = \frac{1}{2}$ can be solved for in terms of the three determinants to give

$$\left| \frac{3}{2}, \frac{1}{2} \right\rangle = \frac{1}{\sqrt{3}} [|1s\beta 2s\alpha 3s\alpha| + |1s\alpha 2s\beta 3s\alpha| + |1s\alpha 2s\alpha 3s\beta|].$$

The states with $S = \frac{3}{2}$ and $M_S = \frac{-1}{2}$ and $\frac{-3}{2}$ can be obtained by further application of S_- to $\left| \frac{3}{2}, \frac{1}{2} \right\rangle$ (actually, the $M_S = \frac{-3}{2}$ can be identified as the "spin flipped" image of the state with $M_S = \frac{3}{2}$ and the one with $M_S = \frac{-1}{2}$ can be formed by interchanging all a's and b's in the $M_S = \frac{1}{2}$ state).

Of the eight total spin states (each electron can take on either α or β spin and there are three electrons, so the number of states is 2^3), the above process has identified proper combinations which yield the four states with $S = \frac{3}{2}$. Doing so consumed the determinants with $M_S = \frac{3}{2}$ and $\frac{-3}{2}$, one combination of the three determinants with $M_S = \frac{1}{2}$, and one combination of the three determinants with $M_S = \frac{-1}{2}$. There still remain two combinations of the $M_S = \frac{1}{2}$ and two combinations of the $M_S = \frac{-1}{2}$ determinants to deal with. These functions correspond to two sets of $S = \frac{1}{2}$ eigenfunctions having $M_S = \frac{1}{2}$ and $\frac{-1}{2}$. Combinations of the determinants must be used in forming the $S = \frac{1}{2}$ functions to keep the $S = \frac{1}{2}$ eigenfunctions orthogonal to the above $S = \frac{3}{2}$ functions (which is required because S^2 is a hermitian operator whose eigenfunctions belonging to different eigenvalues must be orthogonal). The two independent $S = \frac{1}{2}, M_S = \frac{3}{2}$ states can be formed by simply constructing combinations of the above three determinants with $M_S = \frac{1}{2}$ which are orthogonal to the $S = \frac{3}{2}$ combination given above and orthogonal to each other. For example,

$$\left| \frac{1}{2}, \frac{1}{2} \right\rangle = \frac{1}{\sqrt{2}} [|1s\beta 2s\alpha 3s\alpha| - |1s\alpha 2s\beta 3s\alpha| + 0x|1s\alpha 2s\alpha 3s\beta|],$$

$$\left| \frac{1}{2}, \frac{1}{2} \right\rangle = \frac{1}{\sqrt{6}} [|1s\beta 2s\alpha 3s\alpha| + |1s\alpha 2s\beta 3s\alpha| - 2x|1s\alpha 2s\alpha 3s\beta|],$$

are acceptable (as is any combination of these two functions generated by a unitary transformation). A pair of independent orthonormal states with $S = \frac{1}{2}$ and $M_S = \frac{-1}{2}$ can be generated by applying S_- to each of these two functions (or by constructing a pair of orthonormal functions which are combinations of the three determinants with $M_S = \frac{-1}{2}$ and which are orthogonal to the $S = \frac{3}{2}, M_S = \frac{-1}{2}$ function obtained as detailed above).

The above treatment of a three-electron case shows how to generate quartet (spin states are named in terms of their spin degeneracies $2S+1$) and doublet states for a configuration of the form $1s2s3s$. Not all three-electron configurations have both quartet and doublet states; for example, the $1s^2 2s$ configuration only supports one doublet state. The methods used above to generate $S = \frac{3}{2}$ and $S = \frac{1}{2}$ states are valid for any three-electron situation; however, some of the determinantal functions vanish if doubly occupied orbitals occur as for $1s^2 2s$. In particular, the $|1s\alpha 1s\alpha 2s\alpha|$ and $|1s\beta 1s\beta 2s\beta|$ with $M_S = \frac{3}{2}, \frac{-3}{2}$ and $|1s\alpha 1s\alpha 2s\beta|$ and $|1s\beta 1s\beta 2s\alpha|$ with $M_S = \frac{1}{2}, \frac{-1}{2}$ determinants vanish because they violate the Pauli principle; only $|1s\alpha 1s\beta 2s\alpha|$ and $|1s\alpha 1s\beta 2s\beta|$ do not vanish. These two remaining determinants form the $S = \frac{1}{2}, M_S = \frac{1}{2}, \frac{-1}{2}$ doublet spin functions which pertain to the $1s^2 2s$ configuration. It should be noted that all closed-shell components of a configuration (e.g., the $1s^2$ part of $1s^2 2s$ or the $1s^2 2s^2 2p^6$ part of $1s^2 2s^2 2p^6 3s^1 3p^1$) must involve α and β spin functions for each doubly occupied orbital and, as such, can contribute nothing to the total M_S value; only the open-shell components need to be treated with the angular momentum operator tools to arrive at proper total-spin eigenstates.

In summary, proper spin eigenfunctions must be constructed from antisymmetric (i.e., determinantal) wavefunctions as demonstrated above because the **total** S^2 and **total** S_z remain valid symmetry operators for many-electron systems. Doing so results in the spinadapted wavefunctions being expressed as combinations of determinants with coefficients determined via spin angular momentum techniques as demonstrated above. In configurations with closed-shell components, not all spin functions are possible because of the antisymmetry of the wavefunction; in particular, any closed-shell parts must involve $\alpha\beta$ spin pairings for each of the doubly occupied orbitals, and, as such, contribute zero to the total M_S .

This page titled [10.2: Electron Spin Angular Momentum](#) is shared under a [CC BY-NC-SA 4.0](#) license and was authored, remixed, and/or curated by [Jack Simons](#) via [source content](#) that was edited to the style and standards of the LibreTexts platform.

10.3: Coupling of Angular Momenta

Vector Coupling

Given two angular momenta (of any kind) \mathbf{L}_1 and \mathbf{L}_2 , when one generates states that are eigenstates of their vector sum $\mathbf{L} = \mathbf{L}_1 + \mathbf{L}_2$, one can obtain L values of

$$L_1 + L_2, L_1 + L_2 - 1, \dots, |L_1 - L_2|.$$

This can apply to two electrons for which the total spin S can be 1 or 0 as illustrated in detail above, or to a p and a d orbital for which the total orbital angular momentum L can be 3, 2, or 1. Thus for a $p^1 d^1$ electronic configuration, 3F , 1F , 3D , 1D , 3P , and 1P energy levels (and corresponding wavefunctions) arise. Here the term symbols are specified as the spin degeneracy ($2S+1$) and the letter that is associated with the L -value. If spin-orbit coupling is present, the 3F level further splits into $J=4, 3$, and 2 levels which are denoted 3F_4 , 3F_3 , and 3F_2 .

This simple "vector coupling" method applies to any angular momenta. However, if the angular momenta are "equivalent" in the sense that they involve indistinguishable particles that occupy the same orbital shell (e.g., $2p^3$ involves 3 equivalent electrons; $2p^1 3p^1 4p^1$ involves 3 non-equivalent electrons; $2p^2 3p^1$ involves 2 equivalent electrons and one non-equivalent electron), the Pauli principle eliminates some of the expected term symbols (i.e., when the corresponding wavefunctions are formed, some vanish because their Slater determinants vanish). Later in this section, techniques for dealing with the equivalent-angular momenta case are introduced. These techniques involve using the above tools to obtain a list of candidate term symbols after which Pauli-violating term symbols are eliminated.

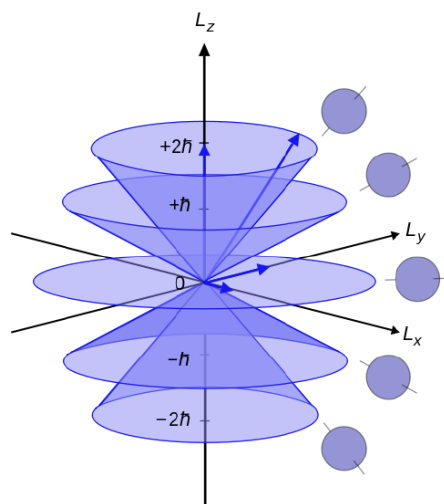


Figure 10.3.1: Illustration of the vector model of orbital angular momentum. Image used with permission (Public Domain; Maschen)

Non-Vector Coupling

For linear molecules, one does **not** vector couple the orbital angular momenta of the individual electrons (because only L_z not L^2 commutes with H), but one does vector couple the electrons' spin angular momenta. Coupling of the electrons' orbital angular momenta involves simply considering the various L_z eigenvalues that can arise from adding the L_z values of the individual electrons. For example, coupling two p orbitals (each of which can have $m = \pm 1$) can give

$$M_L = 1+1, 1-1, -1+1, \text{ and } -1-1, \text{ or } 2, 0, 0, \text{ and } -2.$$

The level with $M_L = \pm 2$ is called a D state (much like an orbital with $m = \pm 2$ is called a d orbital), and the two states with $M_L = 0$ are called S states. States with L_z eigenvalues of M_L and $-M_L$ are degenerate because the total energy is independent of which direction the electrons are moving about the linear molecule's axis (just a π_{+1} and π_{-1} orbitals are degenerate). Again, if the two electrons are non-equivalent, all possible couplings arise (e.g., a $\pi^1 \pi'^1$ configuration yields $^3\Delta$, $^3\Sigma$, $^3\Sigma$, $^1\Delta$, $^1\Sigma$, and $^1\Sigma$ states). In contrast, if the two electrons are equivalent, certain of the term symbols are Pauli forbidden. Again, techniques for dealing with such cases are treated later in this Chapter.

Direct Products for Non-Linear Molecules

For non-linear polyatomic molecules, one vector couples the electrons' spin angular momenta but their orbital angular momenta are not even considered. Instead, their point group symmetries must be combined, by forming direct products, to determine the symmetries of the resultant spin-orbital product states. For example, the $b_1^1 b_2^1$ configuration in C_{2v} symmetry gives rise to 3A_2 and 1A_2 term symbols. The $e^1 e'^1$ configuration in C_{3v} symmetry gives 3E , 3A_2 , 3A_1 , 1E , 1A_2 , and 1A_1 term symbols. For two equivalent electrons such as in the e^2 configuration, certain of the 3E , 3A_2 , 3A_1 , 1E , 1A_2 , and 1A_1 term symbols are Pauli forbidden. Once again, the methods needed to identify which term symbols arise in the equivalent-electron case are treated later.

One needs to learn how to tell which term symbols will be Pauli excluded, and to learn how to write the spin-orbit product wavefunctions corresponding to each term symbol and to evaluate the corresponding term symbols' energies.

This page titled [10.3: Coupling of Angular Momenta](#) is shared under a [CC BY-NC-SA 4.0](#) license and was authored, remixed, and/or curated by [Jack Simons](#) via [source content](#) that was edited to the style and standards of the LibreTexts platform.

10.4: Atomic Term Symbols and Wavefunctions

Non-Equivalent Orbital Term Symbols

When coupling non-equivalent angular momenta (e.g., a spin and an orbital angular momenta or two orbital angular momenta of non-equivalent electrons), one vector couples using the fact that the coupled angular momenta range from the sum of the two individual angular momenta to the absolute value of their difference. For example, when coupling the spins of two electrons, the total spin S can be 1 or 0; when coupling a p and a d orbital, the total orbital angular momentum can be 3, 2, or 1. Thus for a $p^1 d^1$ electronic configuration, 3F , 1F , 3D , 1D , 3P , and 1P energy levels (and corresponding wavefunctions) arise. The energy differences among these levels has to do with the different electron-electron repulsions that occur in these levels; that is, their wavefunctions involve different occupancy of the p and d orbitals and hence different repulsion energies. If spin-orbit coupling is present, the L and S angular momenta are further vector coupled. For example, the 3F level splits into $J=4, 3$, and 2 levels which are denoted 3F_4 , 3F_3 , and 3F_2 . The energy differences among these J -levels are caused by spin-orbit interactions.

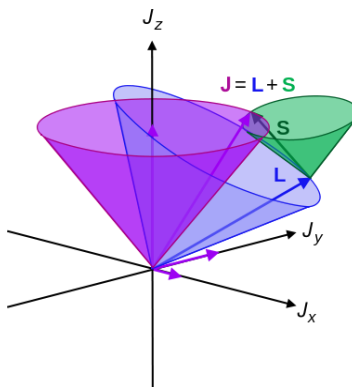


Figure 10.4.1: Illustration of L-S coupling. Total angular momentum J is purple, orbital L is blue, and spin S is green.

Equivalent Orbital Term Symbols

If equivalent angular momenta are coupled (e.g., to couple the orbital angular momenta of a p^2 or d^3 configuration), one must use the "box" method to determine which of the term symbols, that would be expected to arise if the angular momenta were nonequivalent, violate the Pauli principle. To carry out this step, one forms all possible unique (determinantal) product states with non-negative M_L and M_S values and arranges them into groups according to their M_L and M_S values. For example, the boxes appropriate to the p^2 orbital occupancy are shown below:

	M_L	2	1	0
M_S	1		$ p_1\alpha p_0\alpha $	$ p_1\alpha p_{-1}\alpha $
	0	$ p_1\alpha p_1\beta $	$ p_1\alpha p_0\beta , p_0\alpha p_1\beta $	$ p_1\alpha p_{-1}\beta ,$ $ p_{-1}\alpha p_1\beta ,$ $ p_0\alpha p_0\beta $

Figure 10.4.1: Insert caption here!

There is no need to form the corresponding states with negative M_L or negative M_S values because they are simply "mirror images" of those listed above. For example, the state with $M_L = -1$ and $M_S = -1$ is $|p_{-1}\beta p_0\beta|$, which can be obtained from the $M_L = 1, M_S = 1$ state $|p_1\alpha p_0\alpha|$ by replacing α by β and replacing p_1 by p_{-1} .

Given the box entries, one can identify those term symbols that arise by applying the following procedure over and over until all entries have been accounted for:

1. One identifies the highest M_S value (this gives a value of the total spin quantum number that arises, S) in the box. For the above example, the answer is $S = 1$.
2. For all product states of **this** M_S value, one identifies the highest M_L value (this gives a value of the total orbital angular momentum, L , that can arise **for this** S). For the above example, the highest M_L within the $M_S = 1$ states is $M_L = 1$ (not $M_L = 2$), hence $L = 1$.
3. Knowing an S, L combination, one knows the first term symbol that arises from this configuration. In the p^2 example, this is 3P .

- Because the level with this L and S quantum numbers contains $(2L+1)(2S+1)$ states with M_L and M_S quantum numbers running from $-L$ to L and from $-S$ to S , respectively, one must remove from the original box this number of product states. To do so, one simply erases from the box one entry with each such M_L and M_S value. Actually, since the box need only show those entries with non-negative M_L and M_S values, only these entries need be explicitly deleted. In the 3P example, this amounts to deleting nine product states with M_L, M_S values of 1,1; 1,0; 1,-1; 0,1; 0,0; 0,-1; -1,1; -1,0; -1,-1.
- After deleting these entries, one returns to step 1 and carries out the process again. For the p^2 example, the box after deleting the first nine product states looks as follows (those that appear in italics should be viewed as already cancelled in counting all of the 3P states):

M_L	2	1	0
M_S	1	<i>$p_1\alpha p_0\alpha\rangle$</i>	<i>$p_1\alpha p_{-1}\alpha\rangle$</i>
0	<i>$p_1\alpha p_1\beta\rangle$</i>	<i>$p_1\alpha p_0\beta\rangle$</i> , <i>$p_0\alpha p_1\beta\rangle$</i>	<i>$p_1\alpha p_{-1}\beta\rangle$</i> , <i>$p_{-1}\alpha p_1\beta\rangle$</i> , <i>$p_0\alpha p_0\beta\rangle$</i>

Figure 10.4.2: Insert caption here!

It should be emphasized that the process of deleting or crossing off entries in various M_L, M_S boxes involves only **counting** how many states there are; by no means do we identify the particular L, S, M_L, M_S wavefunctions when we cross out any particular entry in a box. For example, when the $|p_1\alpha p_0\beta\rangle$ product is deleted from the $M_L = 1, M_S = 0$ box in accounting for the states in the 3P level, we do not claim that $|p_1\alpha p_0\beta\rangle$ itself is a member of the 3P level; the $|p_0\alpha p_1\beta\rangle$ product state could just as well been eliminated when accounting for the 3P states. As will be shown later, the 3P state with $M_L = 1, M_S = 0$ will be a combination of $|p_1\alpha p_0\beta\rangle$ and $|p_0\alpha p_1\beta\rangle$.

Returning to the p^2 example at hand, after the 3P term symbol's states have been accounted for, the highest M_S value is 0 (hence there is an $S=0$ state), and within this M_S value, the highest M_L value is 2 (hence there is an $L=2$ state). This means there is a 1D level with five states having $M_L = 2, 1, 0, -1, -2$. Deleting five appropriate entries from the above box (again denoting deletions by italics) leaves the following box:

M_L	2	1	0
M_S	1	<i>$p_1\alpha p_0\alpha\rangle$</i>	<i>$p_1\alpha p_{-1}\alpha\rangle$</i>
0	<i>$p_1\alpha p_1\beta\rangle$</i>	<i>$p_1\alpha p_0\beta\rangle$</i> , <i>$p_0\alpha p_1\beta\rangle$</i>	<i>$p_1\alpha p_{-1}\beta\rangle$</i> , <i>$p_{-1}\alpha p_1\beta\rangle$</i> , <i>$p_0\alpha p_0\beta\rangle$</i>

Figure 10.4.3: Insert caption here!

The only remaining entry, which thus has the highest M_S and M_L values, has $M_S = 0$ and $M_L = 0$. Thus there is also a 1S level in the p^2 configuration.

Thus, unlike the non-equivalent $^2p^1 3p^1$ case, in which $^3P, ^1P, ^3D, ^1D, ^3S$, and 1S levels arise, only the $^3P, ^1D$, and 1S arise in the p^2 situation. This "box method" is necessary to carry out whenever one is dealing with equivalent angular momenta.

If one has mixed equivalent and non-equivalent angular momenta, one can determine **all** possible couplings of the equivalent angular momenta using this method and then use the simpler vector coupling method to add the non-equivalent angular momenta to **each** of these coupled angular momenta. For example, the $p^2 d^1$ configuration can be handled by vector coupling (using the straightforward non-equivalent procedure) $L=2$ (the d orbital) and $S = \frac{1}{2}$ (the third electron's spin) to **each** of $^3P, ^1D$, and 1S . The result is $^4F, ^4D, ^4P, ^2F, ^2D, ^2P, ^2G, ^2F, ^2D, ^2P, ^2S$, and 2D .

This page titled [10.4: Atomic Term Symbols and Wavefunctions](#) is shared under a [CC BY-NC-SA 4.0](#) license and was authored, remixed, and/or curated by [Jack Simons](#) via [source content](#) that was edited to the style and standards of the LibreTexts platform.

10.5: Atomic Configuration Wavefunctions

To express, in terms of Slater determinants, the wavefunctions corresponding to each of the states in each of the levels, one proceeds as follows:

1. For each M_S, M_L combination for which one can write down only one product function (i.e., in the non-equivalent angular momentum situation, for each case where only one product function sits at a given box row and column point), that product function **itself** is one of the desired states. For the p^2 example, the $|p_1\alpha p_0\alpha\rangle$ and $|p_1\alpha p_{-1}\alpha\rangle$ (as well as their four other M_L and M_S "mirror images") are members of the 3P level (since they have $M_S = \pm 1$) and $|p_1\alpha p_1\beta\rangle$ and its M_L mirror image are members of the 1D level (since they have $M_L = \pm 2$).
2. After identifying as many such states as possible by inspection, one uses L_{\pm} and S_{\pm} to generate states that belong to the same term symbols as those already identified but which have higher or lower M_L and/or M_S values.
3. If, after applying the above process, there are term symbols for which states have not yet been formed, one may have to construct such states by forming linear combinations that are orthogonal to all those states that have thus far been found.

To illustrate the use of raising and lowering operators to find the states that can not be identified by inspection, let us again focus on the p^2 case. Beginning with three of the 3P states that are easy to recognize, $|p_1\alpha p_0\alpha\rangle$, $|p_1\alpha p_{-1}\alpha\rangle$, and $|p_{-1}\alpha p_0\alpha\rangle$, we apply S_- to obtain the $M_S = 0$ functions:

$$\begin{aligned} S_-^3 P(M_L = 1, M_S = 1) &= [S_-(1) + S_-(2)] |p_1\alpha p_0\alpha\rangle \\ &= \hbar\sqrt{1(2) - 1(0)} \, ^3P(M_L = 1, M_S = 0) \\ &= \hbar\sqrt{\frac{1}{2}\left(\frac{3}{2} - \frac{1}{2}\left(-\frac{1}{2}\right)\right)} |p_1\beta p_0\alpha\rangle + \hbar\sqrt{1} |p_1\alpha p_0\beta\rangle, \end{aligned}$$

so,

$$^3P(M_L = 1, M_S = 0) = \frac{1}{\sqrt{2}} [|p_1\beta p_0\alpha\rangle + |p_1\alpha p_0\beta\rangle].$$

The same process applied to $|p_1\alpha p_{-1}\alpha\rangle$ and $|p_{-1}\alpha p_0\alpha\rangle$ gives

$$\frac{1}{\sqrt{2}} [|p_1\alpha p_{-1}\beta\rangle + |p_1\beta p_{-1}\alpha\rangle]$$

and

$$\frac{1}{\sqrt{2}} [|p_{-1}\beta p_0\beta\rangle + |p_{-1}\beta p_0\alpha\rangle],$$

respectively.

The $^3P(M_L = 1, M_S = 0) = \frac{1}{\sqrt{2}} [|p_1\beta p_0\alpha\rangle + |p_1\alpha p_0\beta\rangle]$ function can be acted on with L_- to generate $^3P(M_L = 0, M_S = 0)$:

$$\begin{aligned} L_-^3 P(M_L = 1, M_S = 0) &= [L_-(1) + L_-(2)] \frac{1}{\sqrt{2}} [|p_1\beta p_0\alpha\rangle + |p_1\alpha p_0\beta\rangle] \\ &= \hbar\sqrt{1(2) - 1(0)} \, ^3P(M_L = 0, M_S = 0) \\ &= \hbar\sqrt{\frac{1(2) - 1(0)}{2}} [|p_0\beta p_0\alpha\rangle + |p_0\alpha p_0\beta\rangle] + \hbar\sqrt{\frac{1(2) - 0(-1)}{2}} [|p_1\beta p_{-1}\alpha\rangle + |p_1\alpha p_{-1}\beta\rangle], \end{aligned}$$

so,

$$^3P(M_L = 0, M_S = 0) = \frac{1}{\sqrt{2}} [|p_1\beta p_{-1}\alpha\rangle + |p_1\alpha p_{-1}\beta\rangle].$$

The 1D term symbol is handled in like fashion. Beginning with the $M_L = 2$ state $|p_1\alpha p_1\beta|$, one applies L_- to generate the $M_L = 1$ state:

$$\begin{aligned} L_-^1 D(M_L = 2, M_S = 0) &= [L_-(1) + L_-(1)]|p_1\alpha p_1\beta| \\ &= \hbar\sqrt{2(3) - 2(1)}^1 D(M_L = 1, M_S = 0) \\ &= \hbar\sqrt{1(2) - 1(0)}[|p_0\alpha p_1\beta| + |p_1\alpha p_0\beta|], \end{aligned}$$

so,

$$^1D(M_L = 1, M_S = 0) = \frac{1}{\sqrt{2}}[|p_0\alpha p_1\beta| + |p_1\alpha p_0\beta|]$$

Applying L_- once more generates the $^1D(M_L = 0, M_S = 0)$ state:

$$\begin{aligned} L_-^1 D(M_L, M_S = 0) &= \frac{[L_-(1) + L_-(2)]}{\sqrt{2}}[|p_0\alpha p_1\beta| + |p_1\alpha p_0\beta|] \\ &= \hbar\sqrt{2(3) - 1(0)}^1 D(M_L = 0, M_S = 0) \\ &= \sqrt{\frac{1(2) - 0(-1)}{2}}[|p_{-1}\alpha p_1\beta| + |p_1\alpha p_{-1}\beta|] + \hbar\sqrt{\frac{1(2) - 1(0)}{2}}[|p_0\alpha p_0\beta| + |p_0\alpha p_0\beta|] \end{aligned}$$

so,

$$^1D(M_L = 0, M_S = 0) = \frac{1}{\sqrt{6}}[2|p_0\alpha p_0\beta| + |p_{-1}\alpha p_1\beta| + |p_1\alpha p_{-1}\beta|].$$

Notice that the $M_L = 0, M_S = 0$ states of 3P and of 1D are given in terms of the three determinants that appear in the "center" of the p^2 box diagram:

$$\begin{aligned} ^1D(M_L = 0, M_S = 0) &= \frac{1}{\sqrt{6}}[2|p_0\alpha p_0\beta| + |p_{-1}\alpha p_1\beta| + |p_1\alpha p_{-1}\beta|], \\ ^3P(M_L = 0, M_S = 0) &= \frac{1}{\sqrt{2}}[|p_1\beta p_{-1}\alpha| + |p_1\alpha p_{-1}\beta|] \\ &\quad - \frac{1}{\sqrt{2}}[|p_{-1}\alpha p_1\beta| + |p_1\alpha p_{-1}\beta|]. \end{aligned}$$

The only state that has eluded us thus far is the 1S state, which also has $M_L = 0$ and $M_S = 0$. To construct this state, which must also be some combination of the three determinants with $M_L = 0$ and $M_S = 0$, we use the fact that the 1S wavefunction **must** be orthogonal to the 3P and 1D functions because $^1S, ^3P$, and 1D are eigenfunctions of the hermitian operator L^2 having different eigenvalues. The state that is normalized and is a combination of $|p_0\alpha p_0\beta|$, $|p_{-1}\alpha p_1\beta|$, and $|p_1\alpha p_{-1}\beta|$ is given as follows:

$$^1S = \frac{1}{\sqrt{3}}[|p_0\alpha p_0\beta| - |p_{-1}\alpha p_1\beta| - |p_1\alpha p_{-1}\beta|].$$

This page titled [10.5: Atomic Configuration Wavefunctions](#) is shared under a [CC BY-NC-SA 4.0](#) license and was authored, remixed, and/or curated by [Jack Simons](#) via [source content](#) that was edited to the style and standards of the LibreTexts platform.

10.6: Inversion Symmetry

One more quantum number, that relating to the inversion (i) symmetry operator can be used in atomic cases because the total potential energy V is unchanged when **all** of the electrons have their position vectors subjected to inversion (i.e., $i\mathbf{r} = -\mathbf{r}$). This quantum number is straightforward to determine. Because each L, S, M_L, M_S, H state discussed previously consists of a few (or, in the case of configuration interaction several) symmetry adapted combinations of Slater determinant functions, the effect of the inversion operator on such a wavefunction Ψ can be determined by:

- i. applying i to each orbital occupied in Ψ thereby generating a ± 1 factor for each orbital (+1 for s, d, g, i, etc orbitals; -1 for p, f, h, j, etc orbitals),
- ii. multiplying these ± 1 factors to produce an overall sign for the character of Ψ under \hat{i} .

When this overall sign is positive, the function Ψ is termed "even" and its term symbol is appended with an "e" superscript (e.g., the 3P level of the O atom, which has $1s^2 2s^2 2p^4$ occupancy is labeled $^3P^e$); if the sign is negative Ψ is called "odd" and the term symbol is so amended (e.g., the 3P level of $1s^2 2s^1 2p^1 B^+$ ion is labeled 3P_o).

This page titled [10.6: Inversion Symmetry](#) is shared under a [CC BY-NC-SA 4.0](#) license and was authored, remixed, and/or curated by [Jack Simons](#) via [source content](#) that was edited to the style and standards of the LibreTexts platform.

10.7: Review of Atomic Cases

The orbitals of an atom are labeled by l and m_l quantum numbers; the orbitals belonging to a given energy and l value are $2l + 1$ -fold degenerate. The many-electron Hamiltonian, H , of an atom and the antisymmetrizer operator $A = \left(\sqrt{\frac{1}{N!}}\right) \sum_p s_p P$ commute with total $L_z = \sum_i L_z(i)$, as in the linear-molecule case. The additional symmetry present in the spherical atom reflects itself in the fact that L_x , and L_y now also commute with H and A . However, since L_z does **not** commute with L_x or L_y , new quantum numbers can not be introduced as symmetry labels for these other components of L . A new symmetry label does arise when

$$L^2 = L_z^2 + L_x^2 + L_y^2$$

is introduced; L^2 commutes with H , A , and L_z , so proper eigenstates (and trial wavefunctions) can be labeled with L , M_L , S , M_S , and H quantum numbers.

To identify the states which arise from a given atomic configuration and to construct properly symmetry-adapted determinantal wave functions corresponding to these symmetries, one must employ L and M_L and S and M_S angular momentum tools. One first identifies those determinants with maximum M_S (this then defines the maximum S value that occurs); within that set of determinants, one then identifies the determinant(s) with maximum M_L (this identifies the highest L value). This determinant has S and L equal to its M_S and M_L values (this can be verified, for example for L , by acting on this determinant with L_2 in the form

$$L^2 = L_- L_+ + L_z^2 + \hbar L_z$$

and realizing that L_+ acting on the state must vanish); other members of this L, S energy level can be constructed by sequential application of S_- and $L_- = \sum_i L_-(i)$. Having exhausted a set of $(2L+1)(2S+1)$ combinations of the determinants belonging to the given configuration, one proceeds to apply the same procedure to the remaining determinants (or combinations thereof). One identifies the maximum M_S and, within it, the maximum M_L which thereby specifies another S, L label and a new "maximum" state. The determinantal functions corresponding to these L, S (and various M_L, M_S) values can be constructed by applying S_- and L_- to this "maximum" state. This process is continued until all of the states and their determinantal wave functions are obtained.

As illustrated above, any p^2 configuration gives rise to $^3P^e, ^1D^e$, and $^1S^e$ levels which contain nine, five, and one state respectively. The use of L and S angular momentum algebra tools allows one to identify the wavefunctions corresponding to these states. As shown in detail in Appendix G, in the event that **spin-orbit** coupling causes the Hamiltonian, H , not to commute with L or with S but only with their vector sum $\mathbf{J} = \mathbf{L} + \mathbf{S}$, then these $L^2 S^2 L_z S_z$ eigenfunctions must be coupled (i.e., recombined) to generate $J^2 J_z$ eigenstates. The steps needed to effect this coupling are developed and illustrated for the above p^2 configuration case in Appendix G.

In the case of a pair of **non-equivalent** p orbitals (e.g., in a $2p^1 3p^1$ configuration), even more states would arise. They can also be found using the tools provided above. Their symmetry labels can be obtained by vector coupling (see Appendix G) the spin and orbital angular momenta of the two subsystems. The orbital angular momentum coupling with $l = 1$ and $l = 1$ gives $L = 2, 1$, and 0 or D, P , and S states. The spin angular momentum coupling with $s = 1/2$ and $s = 1/2$ gives $S = 1$ and 0 , or triplet and singlet states. So, vector coupling leads to the prediction that $^3D^e, ^1D^e, ^3P^e, ^1P^e, ^3S^e$, and $^1S^e$ states can be formed from a pair of non-equivalent p orbitals. It is seen that more states arise when non-equivalent orbitals are involved; for equivalent orbitals, some determinants vanish, thereby decreasing the total number of states that arise.

This page titled [10.7: Review of Atomic Cases](#) is shared under a [CC BY-NC-SA 4.0](#) license and was authored, remixed, and/or curated by [Jack Simons](#) via [source content](#) that was edited to the style and standards of the LibreTexts platform.

CHAPTER OVERVIEW

11: Evaluating the Matrix Elements of N-electron Wavefunctions

One must be able to evaluate the matrix elements among properly symmetry adapted N-electron configuration functions for any operator, the electronic Hamiltonian in particular. The Slater-Condon rules provide this capability

[11.1: Configuration State Functions can Express the Full N-Electron Wavefunction](#)

[11.2: The Slater-Condon Rules Give Expressions for the Operator Matrix Elements Among the CSFs](#)

[11.3: The Slater-Condon Rules](#)

[11.4: Examples of Applying the Slater-Condon Rules](#)

[11.S: Evaluating the Matrix Elements of N-electron Wavefunctions \(Summary\)](#)

This page titled [11: Evaluating the Matrix Elements of N-electron Wavefunctions](#) is shared under a [CC BY-NC-SA 4.0](#) license and was authored, remixed, and/or curated by [Jack Simons](#) via [source content](#) that was edited to the style and standards of the LibreTexts platform.

11.1: Configuration State Functions can Express the Full N-Electron Wavefunction

It has been demonstrated that a given electronic configuration can yield several space- and spin- adapted determinantal wavefunctions; such functions are referred to as configuration state functions (CSFs). These CSF wavefunctions are **not** the exact eigenfunctions of the many-electron Hamiltonian, H ; they are simply functions which possess the space, spin, and permutational symmetry of the exact eigenstates. As such, they comprise an acceptable set of functions to use in, for example, a [linear variational treatment](#) of the true states.

In such variational treatments of electronic structure, the N-electron wavefunction Ψ is expanded as a sum over **all** CSFs that possess the desired spatial and spin symmetry:

$$\Psi = \sum_J C_J \Phi_J.$$

Here, the Φ_J represent the CSFs that are of the correct symmetry, and the C_J are their expansion coefficients to be determined in the variational calculation. If the spin-orbitals used to form the determinants, that in turn form the CSFs $\{\Phi_J\}$, are orthonormal one electron functions (i.e., $\langle \phi_k | \phi_j \rangle = \delta_{k,j}$), then the CSFs can be shown to be orthonormal functions of N electrons

$$\langle \Phi_J | \Phi_K \rangle = \delta_{J,K}.$$

In fact, the Slater determinants themselves also are orthonormal functions of N electrons whenever orthonormal spin-orbitals are used to form the determinants.

The above expansion of the full N-electron wavefunction is termed a "[configuration-interaction](#)" (CI) expansion. It is, in principle, a mathematically rigorous approach to expressing Ψ because the set of **all** determinants that can be formed from a complete set of spin-orbitals can be shown to be complete. In practice, one is limited to the number of orbitals that can be used and in the number of CSFs that can be included in the CI expansion. Nevertheless, the CI expansion method forms the basis of the most commonly used techniques in quantum chemistry.

In general, the optimal variational (or perturbative) wavefunction for any (i.e., the ground or excited) state will include contributions from spin-and space-symmetry adapted determinants derived from all possible configurations. For example, although the determinant with $L = 1$, $S = 1$, $M_L = 1$, $M_S = 1$ arising from the $1s^2 2s^2 2p^2$ configuration may contribute strongly to the true ground electronic state of the Carbon atom, there will be contributions from all configurations which can provide these L, S, M_L , and M_S values (e.g., the $1s^2 2s^2 2p^1 3p^1$ and $2s^2 2p^4$ configurations will also contribute, although the $1s^2 2s^2 2p^1 3s^1$ and $1s^2 2s^1 2p^2 3p^1$ will not because the latter two configurations are odd under inversion symmetry whereas the state under study is even).

The mixing of CSFs from many configurations to produce an optimal description of the true electronic states is referred to as configuration interaction (CI). Strong CI (i.e., mixing of CSFs with large amplitudes appearing for more than one dominant CSF) can occur, for example, when two CSFs from different electronic configurations have nearly the same Hamiltonian expectation value. For example, the $1s^2 2s^2$ and $1s^2 2p^2 {}^1S$ configurations of Be and the analogous ns^2 and np^2 configurations of all alkaline earth atoms are close in energy because the ns-np orbital energy splitting is small for these elements; the π^2 and π^{2*} configurations of ethylene become equal in energy, and thus undergo strong CI mixing, as the CC π bond is twisted by 90° in which case the π and π^* orbitals become degenerate.

Within a variational treatment, the relative contributions of the spin-and space symmetry adapted CSFs are determined by solving a secular problem for the eigenvalues (E_i) and eigenvectors (C_i) of the matrix representation H of the full many-electron Hamiltonian \mathbf{H} within this CSF basis:

$$\sum_L H_{K,L} C_{i,L} = E_i C_{i,K}.$$

The eigenvalue E_i gives the variational estimate for the energy of the i^{th} state, and the entries in the corresponding eigenvector $C_{i,K}$ give the contribution of the K^{th} CSF to the i^{th} wavefunction Ψ_i in the sense that

$$\Psi_i = \sum_K C_{i,K} \Phi_K,$$

where Φ_K is the K^{th} CSF.

This page titled [11.1: Configuration State Functions can Express the Full N-Electron Wavefunction](#) is shared under a [CC BY-NC-SA 4.0](#) license and was authored, remixed, and/or curated by [Jack Simons](#) via [source content](#) that was edited to the style and standards of the LibreTexts platform.

11.2: The Slater-Condon Rules Give Expressions for the Operator Matrix Elements Among the CSFs

To form the $H_{K,L}$ matrix, one uses the so-called **Slater-Condon rules** which express all non-vanishing determinantal matrix elements involving either one- or two- electron operators (one-electron operators are additive and appear as

$$F = \sum_i f(i);$$

two-electron operators are pairwise additive and appear as

$$G = \sum_{ij} g(i, j).$$

Because the CSFs are simple linear combinations of determinants with coefficients determined by space and spin symmetry, the $H_{I,J}$ matrix in terms of determinants can be used to generate the $H_{K,L}$ matrix over CSFs.

The Slater-Condon rules give the matrix elements between two determinants

$$|> = |\phi_1 \phi_2 \phi_3 \dots \phi_N|$$

and

$$|>' = |\phi'_1 \phi'_2 \phi'_3 \dots \phi'_N|$$

for **any** quantum mechanical operator that is a sum of one- and two- electron operators ($F + G$). It expresses these matrix elements in terms of one- and two-electron integrals involving the spin-orbitals that appear in $|>$ and $|>'$ and the operators f and g .

As a first step in applying these rules, one must examine $|>$ and $|>'$ and determine by how many (if any) spin-orbitals $|>$ and $|>'$ differ. In so doing, one may have to reorder the spin-orbitals in one of the determinants to achieve maximal coincidence with those in the other determinant; it is essential to keep track of the number of permutations (N_p) that one makes in achieving maximal coincidence. The results of the Slater-Condon rules given below are then multiplied by $(-1)^{N_p}$ to obtain the matrix elements between the original $|>$ and $|>'$. The final result does not depend on whether one chooses to permute $|>$ or $|>'$.

Once maximal coincidence has been achieved, the Slater-Condon (SC) rules provide the following prescriptions for evaluating the matrix elements of any operator $F + G$ containing a one-electron part $F = \sum_i f(i)$ and a two-electron part $G = \sum_{ij} g(i, j)$ (the

Hamiltonian is, of course, a specific example of such an operator; the electric dipole operator $\sum_i e r_i$ and the electronic kinetic

energy $\frac{\hbar^2}{2m_e} \sum_i \nabla_i^2$ are examples of one-electron operators (for which one takes $g = 0$); the electron-electron coulomb interaction

$\sum_{i>j} \frac{e^2}{r_{ij}}$ is a two-electron operator (for which one takes $f = 0$)):

The Slater-Condon rules express integrals of one- and two-body operators over wavefunctions constructed as Slater determinants of orthonormal orbitals in terms of the individual orbitals. In doing so, the original integrals involving N -electron wavefunctions are reduced to sums over integrals involving at most two molecular orbitals, or in other words, the original $3N$ dimensional integral is expressed in terms of many three- and six-dimensional integrals.

This page titled [11.2: The Slater-Condon Rules Give Expressions for the Operator Matrix Elements Among the CSFs](#) is shared under a [CC BY-NC-SA 4.0](#) license and was authored, remixed, and/or curated by [Jack Simons](#) via [source content](#) that was edited to the style and standards of the LibreTexts platform.

11.3: The Slater-Condon Rules

The Slater-Condon rules express integrals of one- and two-body operators over wavefunctions constructed as Slater determinants of orthonormal orbitals in terms of the individual orbitals. In doing so, the original integrals involving N-electron wavefunctions are reduced to sums over integrals involving at most two molecular orbitals

i. If $|\rangle$ and $|\rangle$ are identical, then

$$\langle |F + G| \rangle = \sum_i \langle \phi_i | f | \phi_i \rangle + \sum_{i>j} [\langle \phi_i \phi_j | g | \phi_i \phi_j \rangle - \langle \phi_i \phi_j | g | \phi_j \phi_i \rangle],$$

where the sums over i and j run over all spin-orbitals in $|\rangle$;

ii. If $|\rangle$ and $|\rangle$ differ by a single spin-orbital mismatch ($\phi_p \neq \phi'_p$),

$$\langle |F + G|' \rangle = \langle \phi_p | f | \phi'_p \rangle + \sum_j [\langle \phi_p \phi_j | g | \phi'_p \phi_j \rangle - \langle \phi_p \phi_j | g | \phi_j \phi'_p \rangle],$$

where the sum over j runs over all spin-orbitals in $|\rangle$ except ϕ_p ;

iii. If $|\rangle$ and $|\rangle$ differ by two spin-orbitals ($\phi_p \neq \phi'_p$ and $\phi_q \neq \phi'_q$),

$$\langle |F + G|' \rangle = \langle \phi_p \phi_q | g | \phi'_p \phi'_q \rangle - \langle \phi_p \phi_q | g | \phi'_q \phi'_p \rangle$$

(note that the F contribution vanishes in this case);

iv. If $|\rangle$ and $|\rangle$ differ by three or more spin orbitals, then

$$\langle |F + G|' \rangle = 0;$$

v. For the identity operator I, the matrix elements $\langle |I|' \rangle = 0$ if $|\rangle$ and $|\rangle$ differ by one or more spin-orbitals (i.e., the Slater determinants are orthonormal if their spin-orbitals are).

Recall that each of these results is subject to multiplication by a factor of $(-1)^{N_p}$ to account for possible ordering differences in the spin-orbitals in $|\rangle$ and $|\rangle$.

In these expressions,

$$\langle \phi_i | f | \phi_j \rangle$$

is used to denote the one-electron integral

$$\int \phi_i^*(r) f(r) \phi_j(r) dr$$

and $\langle \phi_i \phi_j | g | \phi_k \phi_l \rangle$ (or in short hand notation $\langle ij | kl \rangle$) represents the two-electron integral

$$\int \phi_i^*(r) \phi_j^*(r') g(r, r') \phi_k(r) \phi_l(r') dr dr'$$

The notation $\langle ij | kl \rangle$ introduced above gives the two-electron integrals for the $g(r, r')$ operator in the so-called Dirac notation, in which the i and k indices label the spin-orbitals that refer to the coordinates r and the j and l indices label the spin-orbitals referring to coordinates r'. The r and r' denote r, θ, ϕ, σ and $r', \theta', \phi', \sigma'$ (with σ and σ' being the α or β spin functions). The fact that r and r' are integrated and hence represent 'dummy' variables introduces index permutational symmetry into this list of integrals. For example,

$$\langle ij | kl \rangle = \langle ji | lk \rangle = \langle kl | ij \rangle^* = \langle lk | ji \rangle^*;$$

the final two equivalences are results of the Hermitian nature of $g(r, r')$.

It is also common to represent these same two-electron integrals in a notation referred to as Mulliken notation in which:

$$\int \phi_i^*(r) \phi_j^*(r') g(r, r') \phi_k(r) \phi_l(r') dr dr' = (ik | jl).$$

Here, the indices i and k , which label the spin-orbital having variables r are grouped together, and j and l , which label spin-orbitals referring to the r' variables appear together. The above permutational symmetries, when expressed in terms of the Mulliken integral list read:

$$(ik|jl) = (jl|ik) = (ki|lj)^* = (lj|ki)^*.$$

If the operators f and g do not contain any electron spin operators, then the spin integrations implicit in these integrals (all of the ϕ_i are spin-orbitals, so each ϕ is accompanied by an α or β spin function and each ϕ^* involves the adjoint of one of the α or β spin functions) can be carried out as $\langle \alpha|\alpha \rangle = 1$, $\langle \alpha|\beta \rangle = 0$, $\langle \beta|\alpha \rangle = 0$, $\langle \beta|\beta \rangle = 1$, thereby yielding integrals over spatial orbitals. These spin integration results follow immediately from the general properties of angular momentum eigenfunctions detailed in Appendix G; in particular, because α and β are eigenfunctions of S_Z with different eigenvalues, they must be orthogonal $\langle \alpha|\beta \rangle = \langle \beta|\alpha \rangle = 0$.

The essential results of the Slater-Condon rules are:

1. The full $N!$ terms that arise in the N -electron Slater determinants do not have to be treated explicitly, nor do the $N!(N! + 1)/2$ Hamiltonian matrix elements among the $N!$ terms of one Slater determinant and the $N!$ terms of the same or another Slater determinant
2. All such matrix elements, for **any** one- and/or two-electron operator can be expressed in terms of one- or two-electron integrals over the spin-orbitals that appear in the determinants.
3. The integrals over orbitals are three or six dimensional integrals, regardless of how many electrons N there are.
4. These integrals over mo's can, through the LCAO-MO expansion, ultimately be expressed in terms of one- and two-electron integrals over the primitive atomic orbitals. It is only these ao-based integrals that can be evaluated explicitly (on high speed computers for all but the smallest systems).

This page titled [11.3: The Slater-Condon Rules](#) is shared under a [CC BY-NC-SA 4.0](#) license and was authored, remixed, and/or curated by [Jack Simons](#) via [source content](#) that was edited to the style and standards of the LibreTexts platform.

11.4: Examples of Applying the Slater-Condon Rules

It is wise to gain some experience using the Slater-Condon rules, so let us consider a few illustrative example problems.

1. What is the contribution to the total energy of the 3P level of Carbon made by the two 2p orbitals alone? Of course, the two 1s and two 2s spin-orbitals contribute to the total energy, but we artificially ignore all such contributions in this example to simplify the problem.

Because all nine of the 3P states have the same energy, we can calculate the energy of any one of them; it is therefore prudent to choose an "easy" one

$$^3P(M_L = 1, M_S = 1) = |p_1\alpha p_0\alpha|.$$

The energy of this state is $\langle p_1\alpha p_0\alpha | H | p_1\alpha p_0\alpha \rangle$. The SC rules tell us this equals:

$$I_{2p_1} + I_{2p_0} + \langle 2p_1 2p_0 | 2p_1 2p_0 \rangle - \langle 2p_1 2p_0 | 2p_0 2p_1 \rangle,$$

where the short hand notation $\langle I_j | f | j \rangle$ is introduced.

If the contributions from the two 1s and two 2s spin-orbitals are now taken into account, one obtains a **total** energy that also contains $2I_{1s} + 2I_{2s} + \langle 1s1s | 1s1s \rangle + 4 \langle 1s2s | 1s2s \rangle - 2 \langle 1s2s | 2s1s \rangle + \langle 2s2s | 2s2s \rangle + 2 \langle 1s2p_1 | 1s2p_1 \rangle - \langle 1s2p_1 | 2p_11s \rangle + 2 \langle 1s2p_0 | 1s2p_0 \rangle - \langle 1s2p_0 | 2p_01s \rangle + 2 \langle 2s2p_1 | 2s2p_1 \rangle - \langle 2s2p_1 | 2p_12s \rangle + 2 \langle 2s2p_0 | 2s2p_0 \rangle - \langle 2s2p_0 | 2p_02s \rangle$.

2. Is the energy of another 3P state equal to the above state's energy? Of course, but it may prove informative to prove this. Consider the $M_S = 0, M_L = 1$ state whose energy is:

$$\begin{aligned} \frac{1}{\sqrt{2}} \langle [p_1\alpha p_0\beta] + [p_1\beta p_0\alpha] | H | [p_1\alpha p_0\beta] + [p_1\beta p_0\alpha] \rangle &= \frac{1}{\sqrt{2}} \\ &= \frac{1}{2} [I_{2p_1} + I_{2p_0} + \langle 2p_1 2p_0 | 2p_1 2p_0 \rangle + I_{2p_1} + I_{2p_0} + \langle 2p_1 2p_0 | 2p_1 2p_0 \rangle] \\ &\quad - \frac{1}{2} [\langle 2p_1 2p_0 | 2p_0 2p_1 \rangle + \langle 2p_1 2p_0 | 2p_0 2p_1 \rangle] \\ &= I_{2p_1} + I_{2p_0} + \langle 2p_1 2p_0 | 2p_1 2p_0 \rangle - \langle 2p_1 2p_0 | 2p_0 2p_1 \rangle. \end{aligned}$$

Which is, indeed, the same as the other 3P energy obtained above

3. What energy would the singlet state $\frac{1}{\sqrt{2}} \langle [p_1\alpha p_0\beta] - [p_1\beta p_0\alpha] \rangle$ have?

The $^3P_{M_S=0}$ example can be used (changing the sign on the two determinants) to give

$$E = I_{2p_1} + I_{2p_0} + \langle 2p_1 2p_0 | 2p_1 2p_0 \rangle + \langle 2p_1 2p_0 | 2p_0 2p_1 \rangle.$$

Note, this is the $M_L = 1$ component of the 1D state; it is, of course, not a $1P$ state because no such state exists for two equivalent p electrons

4. What is the CI matrix element coupling $|1s^2 2s^2|$ and $|1s^2 3s^2|$?

These two determinants differ by two spin-orbitals, so

$$\langle 1s\alpha 1s\beta 2s\alpha 2s\beta | H | 1s\alpha 1s\beta 3s\alpha 3s\beta \rangle = \langle 2s2s | 3s3s \rangle = \langle 2s3s | 3s2s \rangle$$

(note, this is an exchange-type integral).

5. What is the CI matrix element coupling $|\pi\alpha\pi\beta\rangle$ and $|\pi^*\alpha\pi^*\beta\rangle$?

These two determinants differ by two spin-orbitals, so

$$\langle \pi\alpha\pi\beta | H | \pi^*\alpha\pi^*\beta \rangle = \langle \pi\pi | \pi^*\pi^* \rangle = \langle \pi\pi^* | \pi^*\pi \rangle$$

(note, again this is an exchange-type integral).

6. What is the Hamiltonian matrix element coupling $|\pi\alpha\pi\beta\rangle$ and $\frac{1}{\sqrt{2}}[|\pi\alpha\pi^*\beta\rangle - |\pi\beta\pi^*\alpha\rangle]$?

The first determinant differs from the π^2 determinant by one spin-orbital, as does the second (after it is placed into maximal coincidence by making one permutation), so

$$\begin{aligned} & \langle \pi\alpha\pi\beta | H | \frac{1}{\sqrt{2}}[|\pi\alpha\pi^*\beta\rangle - |\pi\beta\pi^*\alpha\rangle] \rangle \\ &= \frac{1}{\sqrt{2}} \left[\langle \pi | f | \pi^* \rangle + \langle \pi\pi | \pi^*\pi \rangle \right] - (-1) \frac{1}{\sqrt{2}} \left[\langle \pi | f | \pi^* \rangle + \langle \pi\pi | \pi^*\pi \rangle \right] \\ &= \sqrt{2} [\langle \pi | f | \pi^* \rangle + \langle \pi\pi | \pi^*\pi \rangle]. \end{aligned}$$

7. What is the element coupling $|\pi\alpha\pi\beta\rangle$ and $\frac{1}{\sqrt{2}}[|\pi\alpha\pi^*\beta\rangle + |\pi\beta\pi^*\alpha\rangle]$?

$$\begin{aligned} & \langle \pi\alpha\pi\beta | H | \frac{1}{\sqrt{2}}[|\pi\alpha\pi^*\beta\rangle + |\pi\beta\pi^*\alpha\rangle] \rangle = \frac{1}{\sqrt{2}} \left[\langle \pi | f | \pi^* \rangle + \langle \pi\pi | \pi^*\pi \rangle \right] \\ &+ (-1) \frac{1}{\sqrt{2}} \left[\langle \pi | f | \pi^* \rangle + \langle \pi\pi | \pi^*\pi \rangle \right] = 0. \end{aligned}$$

This result should not surprise you because $|\pi\alpha\pi\beta\rangle$ is an $S=0$ singlet state while $\frac{1}{\sqrt{2}}[|\pi\alpha\pi^*\beta\rangle + |\pi\beta\pi^*\alpha\rangle]$ is the $M_S = 0$ component of the $S=1$ triplet state.

8. What is the $\mathbf{r} = \sum_j e\mathbf{r}_j$ electric dipole matrix element between $|p_1\alpha p_1\beta\rangle$ and $\frac{1}{\sqrt{2}}[|p_1\alpha p_0\beta\rangle + |p_0\alpha p_1\beta\rangle]$? Is the second function a singlet or triplet? It is a singlet in disguise; by interchanging the $p_0\alpha$ and $p_1\beta$ and thus introducing a (-1) , this function is clearly identified as $\frac{1}{\sqrt{2}}[|p_1\alpha p_0\beta\rangle - |p_1\alpha p_0\alpha\rangle]$ which is a singlet.

The first determinant differs from the latter two by one spin orbital in each case, so

$$\langle p_1\alpha p_1\beta | \mathbf{r} | \frac{1}{\sqrt{2}}[|p_1\alpha p_0\beta\rangle + |p_0\alpha p_1\beta\rangle] \rangle = \frac{1}{\sqrt{2}} [\langle p_1 | \mathbf{r} | p_0 \rangle + \langle p_1 | \mathbf{r} | p_0 \rangle] = \frac{1}{\sqrt{2}} \langle p_1 | \mathbf{r} | p_0 \rangle.$$

9. What is the electric dipole matrix elements between the $^1\Delta = |\pi_1\alpha\pi_1\beta\rangle$ state and the $^1\Sigma = \frac{1}{\sqrt{2}}[|\pi_1\alpha\pi_{-1}\beta\rangle + |\pi_{-1}\alpha\pi_1\beta\rangle]$ state?

$$\begin{aligned} & \langle \frac{1}{\sqrt{2}}[|\pi_1\alpha\pi_{-1}\beta\rangle + |\pi_{-1}\alpha\pi_1\beta\rangle] | \mathbf{r} | \pi_1\alpha\pi_1\beta \rangle \\ &= \frac{1}{\sqrt{2}} [\langle \pi_{-1} | \mathbf{r} | \pi_1 \rangle + \langle \pi_{-1} | \mathbf{r} | \pi_1 \rangle] \\ &= \sqrt{2} \langle \pi_{-1} | \mathbf{r} | \pi_1 \rangle. \end{aligned}$$

10. As another example of the use of the SC rules, consider the configuration interaction which occurs between the $1s^2 2s^2$ and $1s^2 2p^2$ CSFs in the Be atom.

The CSFs corresponding to these two configurations are as follows:

$$\Phi_1 = |1s\alpha 1s\beta 2s\alpha 2s\beta|$$

and

$$\Phi_2 = \frac{1}{\sqrt{3}} [|1s\alpha 1s\beta 2p_0\alpha 2p_0\beta| - |1s\alpha 1s\beta 2p_1\alpha 2p_{-1}\beta| - |1s\alpha 1s\beta 2p_{-1}\alpha 2p_1\beta|].$$

The determinantal Hamiltonian matrix elements needed to evaluate the 2×2 $H_{K,L}$ matrix appropriate to these two CSFs are evaluated via the SC rules. The first such matrix element is:

$$\langle 1s\alpha 1s\beta 2s\alpha 2s\beta | H | 1s\alpha 1s\beta 2s\alpha 2s\beta \rangle = 2h_{1s} + 2h_{2s} + J_{1s,2s} + 4J_{1s,2s} + J_{2s,2s} - 2K_{1s,2s},$$

where

$$h_i = \langle \phi_i | \left(-\frac{\hbar^2}{2m_e} \nabla^2 - \frac{4e^2}{r} \right) | \phi_i \rangle,$$

$$J_{i,j} = \langle \phi_i \phi_j | \frac{e^2}{r_{12}} | \phi_i \phi_j \rangle,$$

and

$$K_{ij} = \langle \phi_i \phi_j | \frac{e^2}{r_{12}} | \phi_j \phi_i \rangle$$

are the orbital-level **one-electron**, **coulomb**, and **exchange integrals**, respectively.

Coulomb integrals J_{ij} describe the coulombic interaction of one charge density (ϕ_i^2 above) with another charge density (ϕ_j^2 above); exchange integrals K_{ij} describe the interaction of an **overlap** charge density (i.e., a density of the form $\phi_i \phi_j$) with itself ($\phi_i \phi_j$ with $\phi_i \phi_j$ in the above).

The spin functions α and β which accompany each orbital in $|1s\alpha 1s\beta 2s\alpha 2s\beta|$ have been eliminated by carrying out the spin integrations as discussed above. Because H contains no spin operators, this is straightforward and amounts to keeping integrals $\langle \phi_i | f | \phi_j \rangle$ only if ϕ_i and ϕ_j are of the same spin and integrals $\langle \phi_i \phi_j | g | \phi_k \phi_l \rangle$ only if ϕ_i and ϕ_k are of the same spin **and** ϕ_j and ϕ_l are of the same spin. The physical content of the above energy (i.e., Hamiltonian expectation value) of the $|1s\alpha 1s\beta 2s\alpha 2s\beta|$ determinant is clear: $2h_{1s} + 2h_{2s}$ is the sum of the expectation values of the one-electron (i.e., kinetic energy and electron-nuclear coulomb interaction) part of the Hamiltonian for the four occupied spin-orbitals; $J_{1s,1s} + 4J_{1s,2s} + J_{2s,2s} - 2K_{1s,2s}$ contains the coulombic repulsions among all pairs of occupied spin-orbitals minus the exchange interactions among pairs of spin-orbitals with like spin.

The determinantal matrix elements linking Φ_1 and Φ_2 are as follows:

$$\langle 1s\alpha 1s\beta 2s\alpha 2s\beta | H | 1s\alpha 1s\beta 2p_0\alpha 2p_0\beta \rangle = \langle 2s2s | 2p_0 2p_0 \rangle,$$

$$\langle 1s\alpha 1s\beta 2s\alpha 2s\beta | H | 1s\alpha 1s\beta 2p_1\alpha 2p_{-1}\beta \rangle = \langle 2s2s | 2p_1 2p_{-1} \rangle,$$

$$\langle 1s\alpha 1s\beta 2s\alpha 2s\beta | H | 1s\alpha 1s\beta 2p_{-1}\alpha 2p_1\beta \rangle = \langle 2s2s | 2p_{-1}2p_1 \rangle,$$

where the Dirac convention has been introduced as a shorthand notation for the two electron integrals (e.g., $\langle 2s2s | 2p_0 2p_0 \rangle$ represents $\int 2s^*(r_1)2s^*(r_2)\frac{e^2}{r_{12}}2p_0(r_1)2p_0(r_2)dr_1dr_2$).

The three integrals shown above can be seen to be equal and to be of the exchange integral form by expressing the integrals in terms of integrals over cartesian functions and recognizing identities due to the equivalence of the $2p_x$, $2p_y$, and $2p_z$ orbitals. For example,

$$\begin{aligned} \langle 2s2s | 2p_1 2p_{-1} \rangle &= \frac{1}{\sqrt{2}} [\langle 2s2s | [2p_x + i2p_y][2p_x - i2p_y] \rangle] = \\ \frac{1}{2} [\langle 2s2s | xx \rangle + \langle 2s2s | yy \rangle + i \langle 2s2s | yx \rangle - i \langle 2s2s | xy \rangle] &= \langle 2s2s | xx \rangle = K_{2s,x} \end{aligned}$$

(here the two imaginary terms cancel and the two remaining real integrals are equal);

$$\langle 2s2s 2p_0 2p_0 \rangle = \langle 2s2s | zz \rangle = \langle 2s2s | xx \rangle = K_{2s,x}$$

this is because $K_{2s,z} = K_{2s,x} = K_{2s,y}$;

$$\begin{aligned} \langle 2s2s | 2p_{-1} 2p_1 \rangle &= \frac{1}{2} [\langle 2s2s | [2p_x - i2p_y][2p_x + i2p_y] \rangle] = \\ \langle 2s2s | xx \rangle &= \int 2s^*(r_1)2s^*(r_2)\frac{e^2}{r_{12}}2p_x(r_1)2p_x(r_2)dr_1dr_2 = K_{2s,x}. \end{aligned}$$

These integrals are clearly of the exchange type because they involve the coulombic interaction of the $2s2p_{x,y,orz}$ overlap charge density with itself.

Moving on, the matrix elements among the three determinants in Φ_2 are given as follows:

$$\langle 1s\alpha 1s\beta 2p_0\alpha 2p_0\beta | H | 1s\alpha 1s\beta 2p_0\alpha 2p_0\beta \rangle = 2h_{1s} + 2h_{2p} + J_{1s,1s} + 4J_{1s,2p} - 2K_{1s,2p}$$

($J_{1s,2p}$ and $K_{1s,2p}$ are independent of whether the $2p$ orbital is $2p_x$, $2p_y$, or $2p_z$);

$$\langle 1s\alpha 1s\beta 2p_1\alpha 2p_{-1}\beta | H | 1s\alpha 1s\beta 2p_1\alpha 2p_{-1}\beta \rangle = 2h_{1s} + 2h_{2p} + J_{1s,1s} + 4J_{1s,2p} - 2K_{1s,2p} + \langle 2p_1 2p_{-1} | 2p_1 2p_{-1} \rangle;$$

$$\langle 1s\alpha 1s\beta 2p_{-1}\alpha 2p_1\beta | H | 1s\alpha 1s\beta 2p_{-1}\alpha 2p_1\beta \rangle = 2h_{1s} + 2h_{2p} + J_{1s,1s} + 4J_{1s,2p} - 2K_{1s,2p} + \langle 2p_{-1} 2p_1 | 2p_{-1} 2p_1 \rangle;$$

$$\langle 1s\alpha 1s\beta 2p_0\alpha 2p_0\beta | H | 1s\alpha 1s\beta 2p_1\alpha 2p_{-1}\beta \rangle = \langle 2p_0 2p_0 | 2p_1 2p_{-1} \rangle$$

$$\langle 1s\alpha 1s\beta 2p_0\alpha 2p_0\beta | H | 1s\alpha 1s\beta 2p_{-1}\alpha 2p_1\beta \rangle = \langle 2p_0 2p_0 | 2p_{-1} 2p_1 \rangle$$

$$\langle 1s\alpha 1s\beta 2p_1\alpha 2p_{-1}\beta | H | 1s\alpha 1s\beta 2p_{-1}\alpha 2p_1\beta \rangle = \langle 2p_1 2p_{-1} | 2p_{-1} 2p_1 \rangle$$

Certain of these integrals can be recast in terms of cartesian integrals for which equivalences are easier to identify as follows:

$$\langle 2p_0 2p_0 | 2p_1 2p_{-1} \rangle = \langle 2p_0 2p_0 | 2p_{-1} 2p_1 \rangle = \langle zz | xx \rangle = K_{z,x};$$

$$\langle 2p_1 2p_{-1} | 2p_{-1} 2p_1 \rangle = \langle xx | yy \rangle + \frac{1}{2} [\langle xx | xx \rangle - \langle xy | xy \rangle]$$

$$= K_{x,y} + \frac{1}{2} [J_{x,x} - J_{x,y}];$$

$$\langle 2p_1 2p_{-1} | 2p_1 2p_{-1} \rangle = \langle 2p_{-1} 2p_1 | 2p_{-1} 2p_1 \rangle = \frac{1}{2} [J_{x,x} + J_{x,y}].$$

Finally, the 2x2 CI matrix corresponding to the CSFs Ψ_1 and Ψ_2 can be formed from the above determinantal matrix elements; this results in:

$$H_{11} = 2h_{1s} + 2h_{2s} + J_{1s,1s} + 4J_{1s,2s} + J_{2s,2s} - 2K_{1s,2s};$$

$$H_{12} = \frac{-K_{2s,x}}{\sqrt{3}};$$

$$H_{22} = 2h_{1s} + 2h_{2p} + J_{1s,1s} + 4J_{1s,2p} - 2K_{1s,2p} + J_{Z,Z} - \frac{2}{3}K_{Z,X}.$$

The lowest eigenvalue of this matrix provides this CI calculation's estimate of the groundstate 1S energy of Be; its eigenvector provides the CI amplitudes for Φ_1 and Φ_2 in this ground-state wavefunction. The other root of the 2x2 secular problem gives an approximation to another 1S state of higher energy, in particular, a state dominated by the $\frac{1}{\sqrt{3}} [|1s\alpha 1s\beta 2p_0\alpha 2p_0\beta| - |1s\alpha 1s\beta 2p_1\alpha 2p_{-1}\beta| - |1s\alpha 1s\beta 2p_{-1}\alpha 2p_1\beta|]$ CSF.

11. As another example, consider the matrix elements which arise in electric dipole transitions between two singlet electronic states:

$\langle \Psi_1 | \mathbf{E} \cdot \sum_i e\mathbf{r}_i | \Psi_2 \rangle$. Here $\mathbf{E} \cdot \sum_i e\mathbf{r}_i$ is the one-electron operator describing the interaction of an electric field of magnitude and polarization \mathbf{E} with the instantaneous dipole moment of the electrons (the contribution to the dipole operator arising from the nuclear charges $-\sum_a Z_a e^2 \mathbf{R}_a$ does not contribute because, when placed between Ψ_1 and Ψ_2 , this zero-electron operator yields a vanishing integral because Ψ_1 and Ψ_2 are orthogonal).

When the states Ψ_1 and Ψ_2 are described as linear combinations of CSFs as introduced earlier ($\Psi_i = \sum_K C_{iK} \Psi_K$), these matrix elements can be expressed in terms of CSF-based matrix elements $\langle \Psi_K | \sum_i e\mathbf{r}_i | \Psi_L \rangle$. The fact that the electric dipole operator is a one-electron operator, in combination with the SC rules, guarantees that only states for which the dominant determinants differ by at most a single spin-orbital (i.e., those which are "singly excited") can be connected via electric dipole transitions through first order (i.e., in a one-photon transition to which the $\langle \Psi_1 | \sum_i e\mathbf{r}_i | \Psi_2 \rangle$ matrix elements pertain). It is for this reason that light with energy adequate to ionize or excite deep core electrons in atoms or molecules usually causes such ionization or excitation rather than double ionization or excitation of valence-level electrons; the latter are two-electron events.

In, for example, the $\pi \rightarrow \pi^*$ excitation of an olefin, the ground and excited states are dominated by CSFs of the form (where all but the "active" π and π^* orbitals are not explicitly written) :

$$\Psi_1 = |\dots \pi \alpha \pi \beta|$$

and

$$\Phi_2 = \frac{1}{\sqrt{2}} [|\dots \pi \alpha \pi^* \beta| - |\dots \pi \beta \pi^* \alpha|].$$

The electric dipole matrix element between these two CSFs can be found, using the SC rules, to be

$$\frac{e}{\sqrt{2}} \left[\langle \pi | \mathbf{r} | \pi^* \rangle + \langle \pi | \mathbf{r} | \pi^* \rangle \right] = \sqrt{2} e \langle \pi | \mathbf{r} | \pi^* \rangle.$$

Notice that in evaluating the second determinantal integral $\langle |\dots \pi \alpha \pi \beta| e \mathbf{r} | \dots \pi \beta \pi^* \alpha \rangle$, a sign change occurs when one puts the two determinants into maximum coincidence; this sign change then makes the minus sign in Φ_2 yield a positive sign in the final result.

This page titled [11.4: Examples of Applying the Slater-Condon Rules](#) is shared under a [CC BY-NC-SA 4.0](#) license and was authored, remixed, and/or curated by [Jack Simons](#) via [source content](#) that was edited to the style and standards of the LibreTexts platform.

11.S: Evaluating the Matrix Elements of N-electron Wavefunctions (Summary)

In all of the examples in [Chapter 11](#), the Slater-Condon rules were used to reduce matrix elements of one- or two- electron operators between determinantal functions to one- or two- electron integrals over the orbitals which appear in the determinants. In any **ab initio** electronic structure computer program there must exist the capability to form symmetry-adapted CSFs and to evaluate, using these SC rules, the Hamiltonian and other operators' matrix elements among these CSFs in terms of integrals over the Molecular Orbitals that appear in the CSFs. The Slater-Condon rules provide not only the tools to compute quantitative matrix elements; they allow one to understand in qualitative terms the strengths of interactions among CSFs. In the following section, the SC rules are used to explain why chemical reactions in which the reactants and products have dominant CSFs that differ by two spin-orbital occupancies often display activation energies that exceed the reaction endoergicity.

This page titled [11.S: Evaluating the Matrix Elements of N-electron Wavefunctions \(Summary\)](#) is shared under a [CC BY-NC-SA 4.0](#) license and was authored, remixed, and/or curated by [Jack Simons](#) via [source content](#) that was edited to the style and standards of the LibreTexts platform.

CHAPTER OVERVIEW

12: Quantum Mechanical Picture of Bond Making and Breaking Reactions

Along "reaction paths", configurations can be connected one-to-one according to their symmetries and energies. This is another part of the Woodward-Hoffmann rules

[12.1: Concepts of Configuration and State Energies](#)

[12.2: Mixing of Covalent and Ionic Configurations](#)

[12.3: Various Types of Configuration Mixing](#)

This page titled [12: Quantum Mechanical Picture of Bond Making and Breaking Reactions](#) is shared under a [CC BY-NC-SA 4.0](#) license and was authored, remixed, and/or curated by [Jack Simons](#) via [source content](#) that was edited to the style and standards of the LibreTexts platform.

12.1: Concepts of Configuration and State Energies

Plots of CSF Energies Give Configuration Correlation Diagrams

The energy of a particular electronic state of an atom or molecule has been expressed in terms of Hamiltonian matrix elements, using the Slater-Condon rules, over the various spin-and spatially adapted determinants or CSFs which enter into the state wavefunction.

$$E = \sum_{I,J} \langle \Phi_I | H | \Phi_J \rangle C_I C_J.$$

The diagonal matrix elements of H in the CSF basis multiplied by the appropriate CI amplitudes $\langle \Phi_I | H | \Phi_I \rangle C_I C_I$ represent the energy of the I^{th} CSF weighted by the strength (C_I^2) of that CSF in the wavefunction. The off-diagonal elements represent the effects of mixing among the CSFs; mixing is strongest whenever two or more CSFs have nearly the same energy (i.e., $\langle \Phi_I | H | \Phi_I \rangle \neq \langle \Phi_J | H | \Phi_J \rangle$) and there is strong coupling (i.e., $\langle \Phi_I | H | \Phi_J \rangle$ is large). Whenever the CSFs are widely separated in energy, each wavefunction is dominated by a single CSF.

CSFs Interact and Couple to Produce States and State Correlation Diagrams

Just as orbital energies connected according to their symmetries and plotted as functions of geometry constitute an orbital correlation diagram, plots of the **diagonal CSF energies**, connected according to symmetry, constitute a **configuration correlation diagram** (CCD). If, near regions where energies of CSFs of the same symmetry cross (according to the direct product rule of group theory discussed in Appendix E, only CSFs of the same symmetry mix because only they have non-vanishing $\langle \Phi_I | H | \Phi_J \rangle$ matrix elements), CI mixing is allowed to couple the CSFs to give rise to "avoided crossings", then the CCD is converted into a so-called **state correlation diagram** (SCD).

CSFs that Differ by Two Spin-Orbitals Interact Less Strongly than CSFs that Differ by One Spin-Orbital

The strengths of the couplings between pairs of CSFs whose energies cross are evaluated through the Slater-Condon rules. CSFs that differ by more than two spin-orbital occupancies do not couple; the Slater-Condon rules give vanishing Hamiltonian matrix elements for such pairs. Pairs that differ by two spin-orbitals (e.g. $|\dots \phi_a \dots \phi_b \dots | vs | \dots \phi_{a'} \dots \phi_{b'} \dots |$) have interaction strengths determined by the two-electron integrals $\langle ab | a'b' \rangle - \langle ab | b'a' \rangle$. Pairs that differ by a single spin-orbital (e.g. $|\dots \phi_a \dots | vs | \dots \phi_{a'} \dots |$) are coupled by the one- and two- electron parts of H : $\langle a | f | b \rangle + \sum_j [\langle a j | b j \rangle - \langle a j | j b \rangle]$. Usually, couplings among CSFs that differ by two spin-orbitals are much weaker

than those among CSFs that differ by one spin-orbital. In the latter case, the full strength of H is brought to bear, whereas in the former, only the electron-electron coulomb potential is operative.

State Correlation Diagrams

In the SCD, the energies are connected by symmetry but the configurational nature as reflected in the C_I coefficients changes as one passes through geometries where crossings in the CCD occur. The SCD is the ultimate product of an orbital and configuration symmetry and energy analysis and gives one the most useful information about whether reactions will or will not encounter barriers on the ground and excited state surfaces.

As an example of the application of CCD's and SCD's, consider the disrotatory closing of 1,3-butadiene to produce cyclobutene. The OCD given earlier for this proposed reaction path is reproduced below.

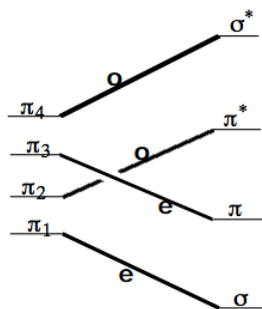


Figure 12.1.1: Insert caption here!

Recall that the symmetry labels e and o refer to the symmetries of the orbitals under reflection through the one C_v plane that is **preserved** throughout the proposed disrotatory closing. Low-energy configurations (assuming one is interested in the thermal or low-lying photochemically excited-state reactivity of this system) for the reactant molecule and their overall space and spin symmetry are as follows:

- $\pi_1^2 \pi_2^2 = 1e^2 1o^2$, ¹ Even
- $\pi_1^2 \pi_2^1 \pi_3^1 = 1e^2 1o^1 2e^1$, ³ Odd and ¹ Odd.

For the product molecule, on the other hand, the low-lying states are

- $\sigma^2 \pi^2 = 1e^2 2e^2$, ¹ Even
- $\sigma^2 \pi^1 \pi^{*1} = 1e^2 2e^1 o^1$, ³ Odd, ¹ Odd.

Notice that although the lowest energy configuration at the reactant geometry $\pi_1^2 \pi_2^2 = 1e^2 1o^2$ and the lowest energy configuration at the product geometry $\sigma^2 \pi^2 = 1e^2 2e^2$ are both of 1Even symmetry, they are **not** the same configurations; they involve occupancy of different symmetry orbitals.

In constructing the CCD, one must trace the energies of all four of the above CSFs (actually there are more because the singlet and triplet excited CSFs must be treated independently) along the proposed reaction path. In doing so, one must realize that the $1e^2 1o^2$ CSF has low energy on the reactant side of the CCD because it corresponds to $\pi_1^2 \pi_2^2$ orbital occupancy, but on the product side, it corresponds to $\sigma^2 \pi^{*2}$ orbital occupancy and is thus of very high energy. Likewise, the $1e^2 2e^2$ CSF has low energy on the product side where it is $\sigma^2 \pi^2$ but high energy on the reactant side where it corresponds to $\pi_1^2 \pi_3^2$. The low-lying singly excited CSFs are $1e^2 2e^1 1o^1$ at both reactant and product geometries; in the former case, they correspond to $\pi_1^2 \pi_2^1 \pi_3^1$ occupancy and at the latter to $\sigma^2 \pi^1 \pi^{*1}$ occupancy. Plotting the energies of these CSFs along the disrotatory reaction path results in the CCD shown below.

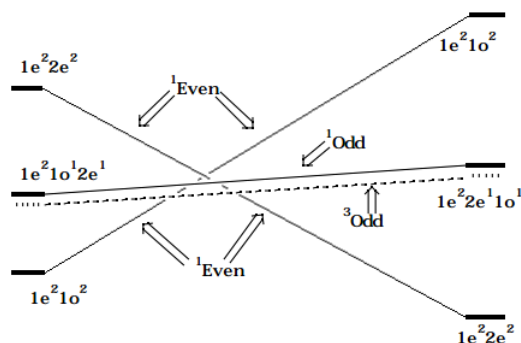


Figure 12.1.2: Insert caption here!

If the two ¹Even CSFs which cross are allowed to interact (the Slater-Condon rules give their interaction strength in terms of the exchange integral $\langle 1e^2 1o^2 | H | 1e^2 2e^2 \rangle = \langle 1o1o | 2e2e \rangle = K_{1o,2e}$) to produce states which are combinations of the two 1Even CSFs, the following SCD results:

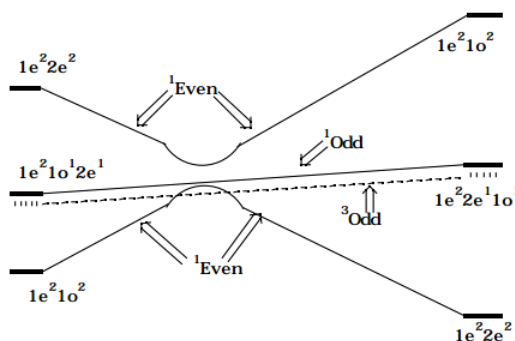


Figure 12.1.3: Insert caption here!

This SCD predicts that the thermal (i.e., on the ground electronic surface) disrotatory rearrangement of 1,3-butadiene to produce cyclobutene will experience a **symmetry-imposed barrier** which arises because of the avoided crossing of the two 1Even configurations; this avoidance occurs because the orbital occupancy pattern (i.e., the configuration) which is best for the ground state of the reactant is not identical to that of the product molecule. The SCD also predicts that there should be no symmetry-imposed barrier for the singlet or triplet excited-state rearrangement, although the reaction leading from excited 1,3-butadiene to excited cyclobutene may be endothermic on the grounds of bond strengths alone.

It is also possible to infer from the SCD that excitation of the lowest singlet $\pi\pi^*$ state of 1,3-butadiene would involve a low quantum yield for producing cyclobutene and would, in fact, produce ground-state butadiene. As the reaction proceeds along the singlet $\pi\pi^*$ surface this 1Odd state intersects the ground 1Even surface on the **reactant side** of the diagram; internal conversion (i.e., quenching from the 1Odd to the 1Even surfaces induced by using a vibration of odd symmetry to "digest" the excess energy (much like vibronic borrowing in spectroscopy) can lead to production of ground-state reactant molecules. Some fraction of such events will lead to the system remaining on the 1Odd surface until, further along the reaction path, the 1Odd surface again intersects the 1Even surface on the **product side** at which time quenching to produce ground-state products can occur. Although, in principle, it is possible for some fraction of the events to follow the 1Odd surface beyond this second intersection and to thus lead to 1Odd product molecules that might fluoresce, quenching is known to be rapid in most polyatomic molecules; as a result, reactions which are chemiluminescent are rare. An appropriate introduction to the use of OCD's, CCD's, and SCD's as well as the radiationless processes that can occur in thermal and photochemical reactions is given in the text **Energetic Principles of Chemical Reactions**, J. Simons, Jones and Bartlett, Boston (1983).

This page titled [12.1: Concepts of Configuration and State Energies](#) is shared under a [CC BY-NC-SA 4.0](#) license and was authored, remixed, and/or curated by [Jack Simons](#) via [source content](#) that was edited to the style and standards of the LibreTexts platform.

12.2: Mixing of Covalent and Ionic Configurations

As chemists, much of our intuition concerning chemical bonds is built on simple models introduced in undergraduate chemistry courses. The detailed examination of the H_2 molecule via the valence bond and molecular orbital approaches forms the basis of our thinking about bonding when confronted with new systems. Let us examine this model system in further detail to explore the electronic states that arise by occupying two orbitals (derived from the two 1s orbitals on the two hydrogen atoms) with two electrons.

In total, there exist **six** electronic states for all such two-orbital, two-electron systems. The heterolytic fragments $X + Y$: and $X: + Y$ produce two singlet states; the homolytic fragments $X\cdot + Y\cdot$ produce one singlet state and a set of three triplet states having $M_S = 1, 0$, and -1 . Understanding the relative energies of these six states, their bonding and antibonding characters, and which molecular state dissociates to which asymptote are important.

Before proceeding, it is important to clarify the notation (*e. g.*, $X\cdot$, $Y\cdot$, $X, Y:$, *etc.*), which is designed to be applicable to neutral as well as charged species. In all cases considered here, only two electrons play active roles in the bond formation. These electrons are represented by the dots. The symbols $X\cdot$ and $Y\cdot$ are used to denote species in which a single electron is attached to the respective fragment. By $X:$, we mean that both electrons are attached to the X- fragment; Y means that neither electron resides on the Y- fragment. Let us now examine the various bonding situations that can occur; these examples will help illustrate and further clarify this notation.

The H_2 Case in Which Homolytic Bond Cleavage is Favored

To consider why the two-orbital two-electron single bond formation case can be more complex than often thought, let us consider the H_2 system in more detail. In the molecular orbital description of H_2 , both bonding sg and antibonding su mos appear. There are two electrons that can both occupy the sg mo to yield the ground electronic state $H_2(1S_g^+, S_g^2)$; however, they can also occupy both orbitals to yield $^3S_u + (sg^1s_u^1)$ and $^1S_u + (s_g^1s_u^1)$, or both can occupy the su mo to give the $1S_g + (su^2)$ state. As demonstrated explicitly below, these latter two states dissociate heterolytically to $X + Y: = H^+ + H^-$, and are sufficiently high in energy relative to $X\cdot + Y\cdot = H + H$ that we ordinarily can ignore them. However, their presence and character are important in the development of a full treatment of the molecular orbital model for H_2 and are **essential** to a proper treatment of cases in which heterolytic bond cleavage is favored.

Cases in Which Heterolytic Bond Cleavage is Favored

For some systems one or both of the heterolytic bond dissociation asymptotes (*e.g.*, $X + Y:$ or $X: + Y$) may be **lower** in energy than the homolytic bond dissociation asymptote. Thus, the states that are analogues of the $^1\sum_u^+(\sigma_g^1\sigma_u^1)$ and $^1\sum_g^+(\sigma_u^2)$ states of H_2 can no longer be ignored in understanding the valence states of the XY molecules. This situation arises quite naturally in systems involving transition metals, where interactions between empty metal or metal ion orbitals and 2-electron donor ligands are ubiquitous.

Two classes of systems illustrate cases for which heterolytic bond dissociation lies lower than the homolytic products. The first involves transition metal dimer cations, M_2^+ . Especially for metals to the right side of the periodic table, such cations can be considered to have ground-state electron configurations with $\sigma^2 d^n d^{n+1}$ character, where the d electrons are not heavily involved in the bonding and the s bond is formed primarily from the metal atom s orbitals. If the σ bond is homolytically broken, one forms $X\cdot + Y\cdot = M(s^1 d^{n+1}) + M^+(s^1 d^n)$. For most metals, this dissociation asymptote lies higher in energy than the heterolytic products $X: + Y = M(s^2 d^n) + M^+(s^0 d^{n+1})$, since the latter electron configurations correspond to the ground states for the neutrals and ions, respectively. A prototypical species which fits this bonding picture is Ni_2^+ .

The second type of system in which heterolytic cleavage is favored arises with a metal-ligand complex having an atomic metal ion (with a $s^0 d^{n+1}$ configuration) and a two electron donor, L: . A prototype is $(Ag C_6H_6)^+$ which was observed to photodissociate to form $X\cdot + Y\cdot = Ag(^2S, s^1 d^{10}) + C_6H_6 + (^2B_1)$ rather than the lower energy (heterolytically cleaved) dissociation limit $Y + X: = Ag(^1S, s^0 d^{10}) + C_6H_6(^1A_1)$.

Analysis of Two-Electron, Two-Orbital, Single-Bond Formation

The resultant family of six electronic states can be described in terms of the six configuration state functions (CSFs) that arise when one occupies the pair of bonding σ and antibonding σ^* molecular orbitals with two electrons. The CSFs are combinations of Slater determinants formed to generate proper spin- and spatial symmetry- functions.

The spin- and spatial- symmetry adapted N-electron functions referred to as CSFs can be formed from one or more Slater determinants. For example, to describe the singlet CSF corresponding to the closed-shell σ^2 orbital occupancy, a single Slater determinant

$$\Sigma(0) = |\sigma\alpha\sigma\beta| = \frac{1}{\sqrt{2}}[\sigma\alpha(1)\sigma\beta(2) - \sigma\beta(1)\sigma\alpha(2)]$$

suffices. An analogous expression for the $(\sigma^*)^2$ CSF is given by

$$^1\Sigma^{**}(0) = |\sigma^*\alpha\sigma^*\beta| = \frac{1}{\sqrt{2}}[\sigma^*\alpha(1)\sigma^*\beta(2) - \sigma^*\alpha(2)\sigma^*\beta(1)].$$

This page titled [12.2: Mixing of Covalent and Ionic Configurations](#) is shared under a [CC BY-NC-SA 4.0](#) license and was authored, remixed, and/or curated by [Jack Simons](#) via [source content](#) that was edited to the style and standards of the LibreTexts platform.

12.3: Various Types of Configuration Mixing

Essential CI

The above examples of the use of CCD's show that, as motion takes place along the proposed reaction path, geometries may be encountered at which it is **essential** to describe the electronic wavefunction in terms of a linear combination of more than one CSF:

$$\Psi = \sum_I C_I \Phi_I$$

where the Φ_I are the CSFs which are undergoing the avoided crossing. Such essential configuration mixing is often referred to as treating "**essential CI**".

Dynamical CI

To achieve reasonable chemical accuracy (e.g., ± 5 kcal/mole) in electronic structure calculations it is necessary to use a multiconfigurational Ψ even in situations where no obvious strong configuration mixing (e.g., crossings of CSF energies) is present. For example, in describing the π^2 bonding electron pair of an olefin or the ns^2 electron pair in alkaline earth atoms, it is important to mix in doubly excited CSFs of the form $(\pi^*)^2$ and np^2 , respectively. The reasons for introducing such a CI-level treatment were treated for an alkaline earth atom earlier in this chapter.

Briefly, the physical importance of such doubly-excited CSFs can be made clear by using the identity:

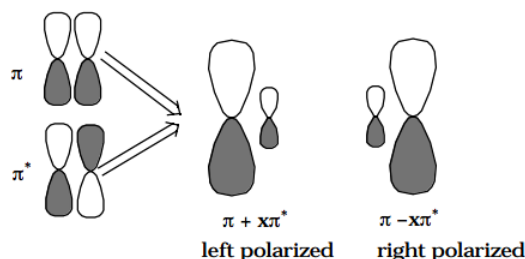
$$C_I | \dots \phi \alpha \phi \beta \dots | - C_2 | \dots \phi' \alpha \phi' \beta \dots | \\ = \frac{C_I}{2} [| \dots (\phi - x\phi') \alpha (\phi + x\phi') \beta \dots | - | \dots (\phi - x\phi') \beta (\phi + x\phi') \alpha \dots |],$$

where

$$x = \sqrt{\frac{C_2}{C_1}}$$

This allows one to interpret the combination of two CSFs which differ from one another by a double excitation from one orbital (ϕ) to another (ϕ') as equivalent to a singlet coupling of two different (non-orthogonal) orbitals ($\phi - x\phi'$) and $(\phi + x\phi')$. This picture is closely related to the so-called generalized valence bond (GVB) model that W. A. Goddard and his co-workers have developed (see W. A. Goddard and L. B. Harding, *Annu. Rev. Phys. Chem.* **29**, 363 (1978)). In the simplest embodiment of the GVB model, each electron pair in the atom or molecule is correlated by mixing in a CSF in which that electron pair is "doubly excited" to a correlating orbital. The direct product of all such pair correlations generates the GVB-type wavefunction. In the GVB approach, these electron correlations are not specified in terms of double excitations involving CSFs formed from orthonormal spin orbitals; instead, explicitly non-orthogonal GVB orbitals are used as described above, but the result is the same as one would obtain using the direct product of doubly excited CSFs.

In the olefin example mentioned above, the two non-orthogonal "polarized orbital pairs" involve mixing the π and π^* orbitals to produce two left-right polarized orbitals as depicted below:



In this case, one says that the π^2 electron pair undergoes left-right correlation when the $(\pi^*)^2$ CSF is mixed into the CI wavefunction.

In the alkaline earth atom case, the polarized orbital pairs are formed by mixing the ns and np orbitals (actually, one must mix in equal amounts of p_1 , p_{-1} , and p_0 orbitals to preserve overall 1S symmetry in this case), and give rise to angular correlation of the electron pair. Use of an $(n+1)s^2$ CSF for the alkaline earth calculation would contribute in-out or radial correlation because, in this case, the polarized orbital pair formed from the ns and (n+1)s orbitals would be radially polarized.

The use of doubly excited CSFs is thus seen as a mechanism by which Ψ can place electron **pairs**, which in the single-configuration picture occupy the same orbital, into different regions of space (i.e., one into a member of the polarized orbital pair) thereby lowering their mutual coulombic repulsions. Such electron correlation effects are referred to as "**dynamical electron correlation**"; they are extremely important to include if one expects to achieve chemically meaningful accuracy (i.e., ± 5 kcal/mole).

This page titled [12.3: Various Types of Configuration Mixing](#) is shared under a [CC BY-NC-SA 4.0](#) license and was authored, remixed, and/or curated by [Jack Simons](#) via [source content](#) that was edited to the style and standards of the LibreTexts platform.

CHAPTER OVERVIEW

13: Molecular Rotation and Vibration

Treating the full internal nuclear-motion dynamics of a polyatomic molecule is complicated. It is conventional to examine the rotational movement of a hypothetical "rigid" molecule as well as the vibrational motion of a non-rotating molecule, and to then treat the rotation-vibration couplings using perturbation theory.

[13.1: Rotational Motions of Rigid Molecules](#)

[13.2: Vibrational Motion Within the Harmonic Approximation](#)

[13.3: Anharmonicity](#)

This page titled [13: Molecular Rotation and Vibration](#) is shared under a [CC BY-NC-SA 4.0](#) license and was authored, remixed, and/or curated by [Jack Simons](#) via [source content](#) that was edited to the style and standards of the LibreTexts platform.

13.1: Rotational Motions of Rigid Molecules

In Chapter 3 and Appendix G the energy levels and wavefunctions that describe the rotation of rigid molecules are described. Therefore, in this Chapter these results will be summarized briefly and emphasis will be placed on detailing how the corresponding rotational Schrödinger equations are obtained and the assumptions and limitations underlying them.

Linear Molecules

As given in Chapter 3, the Schrödinger equation for the angular motion of a rigid (i.e., having fixed bond length R) diatomic molecule is

$$\frac{\hbar^2}{2\mu} \left[\frac{1}{R^2 \sin \theta} \frac{\partial}{\partial \theta} \left(\sin \theta \frac{\partial}{\partial \theta} \right) + \left(\frac{1}{R^2 \sin^2 \theta} \right) \frac{\partial^2}{\partial \phi^2} \right] \psi = E\psi$$

or more succinctly in terms of the angular momentum operator as

$$\frac{L^2 \psi}{2\mu R^2} = E\psi$$

The Hamiltonian in this problem contains only the kinetic energy of rotation; no potential energy is present because the molecule is undergoing unhindered "free rotation". The angles θ and ϕ describe the orientation of the diatomic molecule's axis relative to a laboratory-fixed coordinate system, and μ is the reduced mass of the diatomic molecule

$$\mu = \frac{m_1 m_2}{m_1 + m_2}.$$

The Eigenfunctions and Eigenvalues

The eigenvalues corresponding to each eigenfunction are straightforward to find because H_{rot} is proportional to the L^2 operator whose eigenvalues have already been determined. The resultant rotational energies are given as:

$$E_J = \hbar^2 \frac{J(J+1)}{(2\mu R^2)} = BJ(J+1)$$

and are *independent* of M . Thus each energy level is labeled by J and is $2J+1$ -fold degenerate (because M ranges from $-J$ to J). The rotational constant B (defined as $\hbar^2/2\mu R^2$) depends on the molecule's bond length and reduced mass. Spacings between successive rotational levels (which are of spectroscopic relevance because angular momentum selection rules often restrict ΔJ to 1, 0, and -1) are given by

$$\Delta E = B(J+1)(J+2) - BJ(J+1) = 2B(J+1).$$

Within this "rigid rotor" model, the absorption spectrum of a rigid diatomic molecule should display a series of peaks, each of which corresponds to a specific $J \rightarrow J+1$ transition. The energies at which these peaks occur should grow linearly with J . An example of such a progression of rotational lines is shown in the figure below.

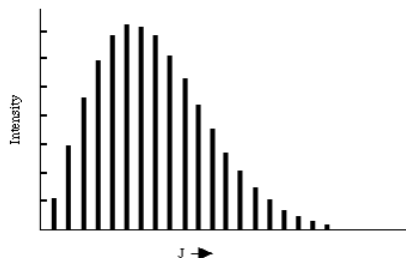


Figure 13.1.1: Insert caption here!

The energies at which the rotational transitions occur appear to fit the $\Delta E = 2B(J+1)$ formula rather well. The intensities of transitions from level J to level $J+1$ vary strongly with J primarily because the population of molecules in the absorbing level varies with J . These populations P_J are given, when the system is at equilibrium at temperature T , in terms of the degeneracy $(2J+1)$ of the J^{th} level and the energy of this level $B J(J+1)$:

$$P_J = Q^{-1} (2J+1) e^{\frac{-BJ(J+1)}{kT}},$$

where Q is the [rotational partition function](#):

$$Q = \sum_J (2J+1) e^{\frac{-BJ(J+1)}{kT}}.$$

For low values of J , the degeneracy is low and the $e^{\frac{-BJ(J+1)}{kT}}$ factor is near unity. As J increases, the degeneracy grows linearly but the $e^{\frac{-BJ(J+1)}{kT}}$ factor decreases more rapidly. As a result, there is a value of J , given by taking the derivative of $(2J+1)e^{\frac{-BJ(J+1)}{kT}}$ with respect to J and setting it equal to zero,

$$2J_m a x + 1 = \sqrt{\frac{2kT}{B}}$$

at which the intensity of the rotational transition is expected to reach its maximum.

The eigenfunctions belonging to these energy levels are the spherical harmonics $Y_{L,M}(\theta, \phi)$ which are normalized according to

$$\int_0^\pi \int_0^{2\pi} Y_{L,M}^*(\theta, \phi) Y_{L',M'}(\theta, \phi) \sin\theta d\theta d\phi = \delta_{L,L'} \delta_{M,M'}.$$

These functions are identical to those that appear in the solution of the angular part of Hydrogen-like atoms. The above energy levels and eigenfunctions also apply to the rotation of rigid linear polyatomic molecules; the only difference is that the moment of inertia I entering into the rotational energy expression is given by

$$I = \sum_a m_a R_a^2$$

where m_a is the mass of the a^{th} atom and R_a is its distance from the center of mass of the molecule. This moment of inertia replaces mR^2 in the earlier rotational energy level expressions.

Non-Linear Molecules

The rotational kinetic energy operator for a rigid polyatomic molecule is shown in Appendix G to be

$$H_{rot} = \frac{J_b^2}{2I_a} + \frac{J_b^2}{2I_b} + \frac{J_c^2}{2I_c}$$

where the I_k ($k = a, b, c$) are the three principal moments of inertia of the molecule (the eigenvalues of the moment of inertia tensor). This tensor has elements in a Cartesian coordinate system ($K, K' = X, Y, Z$) whose origin is located at the center of mass of the molecule that are computed as:

$$I_{K,K} = \sum_j m_j (R_j^2 - R_{K,j}^2) \text{ (for } K = K') \\ I_{K,K'} = - \sum_j m_j R_{K,j} R_{K',j} \text{ (for } K \neq K').$$

The components of the quantum mechanical angular momentum operators along the three principal axes are:

$$J_a = -i\hbar \cos\chi \left[\cot\theta \frac{\partial}{\partial\chi} - \frac{1}{\sin\theta} \frac{\partial}{\partial\phi} \right] - i\hbar \sin\chi \frac{\partial}{\partial\theta} \\ J_b = i\hbar \sin\chi \left[\cot\theta \frac{\partial}{\partial\chi} - \frac{1}{\sin\theta} \frac{\partial}{\partial\phi} \right] - i\hbar \cos\chi \frac{\partial}{\partial\theta} \\ J_c = -i\hbar \frac{\partial}{\partial\chi}.$$

The angles θ , ϕ , and χ are the Euler angles needed to specify the orientation of the rigid molecule relative to a laboratory-fixed coordinate system. The corresponding square of the total angular momentum operator J^2 can be obtained as

$$J^2 = J_a^2 + J_b^2 + J_c^2 = -\frac{\partial^2}{\partial \theta^2} - \cot \theta \frac{\partial}{\partial \theta} - \frac{1}{\sin \theta} \left(\frac{\partial^2}{\partial \phi^2} + \frac{\partial^2}{\partial \chi^2} - 2 \cos \theta \frac{\partial^2}{\partial \phi \partial \chi} \right),$$

and the component along the lab-fixed Z axis J_Z is $-i\hbar \frac{\partial}{\partial \phi}$.

The Eigenfunctions and Eigenvalues for Special Cases

Spherical Tops

When the three principal moment of inertia values are identical, the molecule is termed a **spherical top**. In this case, the total rotational energy can be expressed in terms of the total angular momentum operator J^2

$$H_{rot} = \frac{J^2}{2I}$$

As a result, the eigenfunctions of H_{rot} are those of J^2 (and J_a as well as J_Z both of which commute with J^2 and with one another; J_Z is the component of \mathbf{J} along the lab-fixed Z-axis and commutes with J_a because $J_Z = -i\hbar \frac{\partial}{\partial \phi}$ and $J_a = -i\hbar \frac{\partial}{\partial \chi}$ act on different angles). The energies associated with such eigenfunctions are

$$E(J, M, K) = \hbar^2 \frac{J(J+1)}{2I^2},$$

for all K (i.e., J_a quantum numbers) ranging from -J to J in unit steps and for all M (i.e., J_Z quantum numbers) ranging from -J to J. Each energy level is therefore $(2J+1)^2$ degenerate because there are $2J+1$ possible K values and $2J+1$ possible M values for each J.

The eigenfunctions of J^2 , J_Z and J_a , $|J, M, K\rangle$ are given in terms of the set of rotation matrices $D_{J,M,K}$:

$$|J, M, K\rangle = \sqrt{\frac{2J+1}{8\pi^2}} D_{J,M,K}^*(\theta, \phi, \chi)$$

which obey

$$J^2 |J, M, K\rangle = \hbar^2 J(J+1) |J, M, K\rangle,$$

$$J_a |J, M, K\rangle = \hbar K |J, M, K\rangle,$$

$$J_Z |J, M, K\rangle = \hbar M |J, M, K\rangle.$$

Symmetric Tops

Molecules for which two of the three principal moments of inertia are equal are called **symmetric tops**. Those for which the unique moment of inertia is smaller than the other two are termed **prolate** symmetric tops; if the unique moment of inertia is larger than the others, the molecule is an **oblate** symmetric top. Again, the rotational kinetic energy, which is the full rotational Hamiltonian, can be written in terms of the total rotational angular momentum operator J^2 and the component of angular momentum along the axis with the unique principal moment of inertia:

$$H_{rot} = \frac{J^2}{2I} + J_a^2 \left[\frac{1}{2I_a} - \frac{1}{2I} \right]$$

for prolate tops and

$$H_{rot} = \frac{J^2}{2I} + J_c^2 \left[\frac{1}{2I_c} - \frac{1}{2I} \right]$$

for oblate tops.

As a result, the eigenfunctions of H_{rot} are those of J^2 and J_a or J_c (and of J_Z), and the corresponding energy levels are:

$$E(J, K, M) = \hbar^2 \frac{J(J+1)}{2I^2} + \hbar^2 K^2 \left[\frac{1}{2I_a} - \frac{1}{2I} \right],$$

for prolate tops

$$E(J, K, M) = \hbar^2 \frac{J(J+1)}{2I^2} + \hbar^2 K^2 \left[\frac{1}{2I_a} - \frac{1}{2I} \right],$$

for oblate tops, again for K and M (i.e., J_a or J_c and J_z quantum numbers, respectively) ranging from -J to J in unit steps. Since the energy now depends on K, these levels are only $2J + 1$ degenerate due to the $2J + 1$ different M values that arise for each J value. The eigenfunctions $|J, M, K\rangle$ are the same rotation matrix functions as arise for the spherical-top case.

Asymmetric Tops

The rotational eigenfunctions and energy levels of a molecule for which all three principal moments of inertia are distinct (a so-called **asymmetric top**) can not easily be expressed in terms of the angular momentum eigenstates and the J, M, and K quantum numbers. However, given the three principal moments of inertia I_a, I_b , and I_c , a matrix representation of each of the three contributions to the rotational Hamiltonian

$$H_{rot} = \frac{J_a^2}{2I_a} + \frac{J_b^2}{2I_b} + \frac{J_c^2}{2I_c}$$

can be formed within a basis set of the $\{|J, M, K\rangle\}$ rotation matrix functions. This matrix will not be diagonal because the $|J, M, K\rangle$ functions are not eigenfunctions of the asymmetric top H_{rot} . However, the matrix can be formed in this basis and subsequently brought to diagonal form by finding its eigenvectors $\{C_{n,J,M,K}\}$ and its eigenvalues $\{E_n\}$. The vector coefficients express the asymmetric top eigenstates as

$$\Psi_n(\theta, \phi, \chi) = \sum_{J,M,K} C_{n,J,M,K} |J, M, K\rangle.$$

Because the total angular momentum J^2 still commutes with H_{rot} , each such eigenstate will contain only one J-value, and hence Ψ_n can also be labeled by a J quantum number:

$$\Psi_{n,J}(\theta, \phi, \chi) = \sum_{M,K} C_{n,J,M,K} |J, M, K\rangle.$$

To form the only non-zero matrix elements of H_{rot} within the $|J, M, K\rangle$ basis, one can use the following properties of the rotation-matrix functions:

$$\langle J, M, K | J_a^2 | J, M, K \rangle = \langle J, M, K | J_b^2 | J, M, K \rangle = \frac{1}{2} \langle J, M, K | J^2 - J_c^2 | J, M, K \rangle = \hbar^2 [J(J+1) - K^2],$$

$$\langle J, M, K | J_c^2 | J, M, K \rangle = \hbar^2 K^2,$$

$$\begin{aligned} \langle J, M, K | J_a^2 | J, M, K \pm 2 \rangle &= -\langle J, M, K | J_b^2 | J, M, K \pm 2 \rangle \\ &= \hbar^2 \sqrt{J(J+1) - K(K \pm 1)} \sqrt{J(J+1) - (K \pm 1)(K \pm 2)} \end{aligned}$$

$$\langle J, M, K | J_c^2 | J, M, K \pm 2 \rangle = 0.$$

Each of the elements of J_c^2 , J_a^2 , and J_b^2 must, of course, be multiplied, respectively, by $\frac{1}{2I_c}$, $\frac{1}{2I_a}$ and $\frac{1}{2I_b}$ summed together to form the matrix representation of H_{rot} . The diagonalization of this matrix then provides the asymmetric top energies and wavefunctions.

This page titled [13.1: Rotational Motions of Rigid Molecules](#) is shared under a [CC BY-NC-SA 4.0](#) license and was authored, remixed, and/or curated by [Jack Simons](#) via [source content](#) that was edited to the style and standards of the LibreTexts platform.

13.2: Vibrational Motion Within the Harmonic Approximation

The simple harmonic motion of a diatomic molecule was treated in Chapter 1, and will not be repeated here. Instead, emphasis is placed on polyatomic molecules whose electronic energy's dependence on the 3N Cartesian coordinates of its N atoms can be written (approximately) in terms of a Taylor series expansion about a stable local minimum. We therefore assume that the molecule of interest exists in an electronic state for which the geometry being considered is stable (i.e., not subject to spontaneous geometrical distortion).

The Taylor series expansion of the electronic energy is written as:

$$V(q_k) = V(0) + \sum_k \left(\frac{\partial V}{\partial q_k} \right) q_k + \frac{1}{2} \sum_{j,k} q_j H_{j,k} + \dots,$$

where $V(0)$ is the value of the electronic energy at the stable geometry under study, q_k is the **displacement** of the k_{th} Cartesian coordinate away from this starting position, $\left(\frac{\partial V}{\partial q_k} \right)$ is the gradient of the electronic energy along this direction, and the $H_{j,k}$ are the second derivative or **Hessian** matrix elements along these directions $H_{j,k} = \left(\frac{\partial^2 V}{\partial q_j \partial q_k} \right)$. If the starting geometry corresponds to a stable species, the gradient terms will all vanish (meaning this geometry corresponds to a minimum, maximum, or saddle point), and the Hessian matrix will possess 3N - 5 (for linear species) or 3N - 6 (for non-linear molecules) positive eigenvalues and 5 or 6 zero eigenvalues (corresponding to 3 translational and 2 or 3 rotational motions of the molecule). If the Hessian has one negative eigenvalue, the geometry corresponds to a transition state (these situations are discussed in detail in Chapter 20).

From now on, we assume that the geometry under study corresponds to that of a stable minimum about which vibrational motion occurs. The treatment of unstable geometries is of great importance to chemistry, but this Chapter deals with vibrations of stable species. For a good treatment of situations under which geometrical instability is expected to occur, see Chapter 2 of the text **Energetic Principles of Chemical Reactions** by J. Simons. A discussion of how local minima and transition states are located on electronic energy surfaces is provided in Chapter 20 of the present text.

The Newton Equations of Motion for Vibration

The Kinetic and Potential Energy Matrices

Truncating the Taylor series at the quadratic terms (assuming these terms dominate because only small displacements from the equilibrium geometry are of interest), one has the so-called **harmonic** potential:

$$V(q_k) = V(0) + \frac{1}{2} \sum_{j,k} q_j H_{j,k} q_k.$$

The classical mechanical equations of motion for the 3N $\{q_k\}$ coordinates can be written in terms of the above potential energy and the following kinetic energy function:

$$T = \frac{1}{2} \sum_j m_j \dot{q}_j^2,$$

where \dot{q}_j denotes the time rate of change of the coordinate q_j and m_j is the mass of the atom on which the j^{th} Cartesian coordinate resides. The Newton equations thus obtained are:

$$m_j \ddot{q}_j = - \sum_k H_{j,k} q_k$$

where the force along the j^{th} coordinate is given by minus the derivative of the potential V along this coordinate $\frac{\partial V}{\partial q_j} = \sum_k H_{j,k} q_k$ within the harmonic approximation.

These classical equations can more compactly be expressed in terms of the time evolution of a set of so-called **mass weighted** Cartesian coordinates defined as:

$$x_j = q_j \sqrt{m_j},$$

in terms of which the Newton equations become

$$\ddot{x}_j = - \sum_k H'_{j,k} x_k$$

and the **mass-weighted Hessian** matrix elements are

$$H'_{j,k} = H_{j,k} \frac{1}{\sqrt{m_j m_k}}.$$

The Harmonic Vibrational Energies and Normal Mode Eigenvectors

Assuming that the x_j undergo some form of sinusoidal time evolution:

$$x_j(t) = x_j(0) \cos(\omega t),$$

and substituting this into the Newton equations produces a matrix eigenvalue equation:

$$\omega^2 x_j = \sum_k H'_{j,k} x_k$$

in which the eigenvalues are the squares of the so-called **normal mode** vibrational frequencies and the eigenvectors give the amplitudes of motion along each of the 3N mass weighted Cartesian coordinates that belong to each mode.

Within this harmonic treatment of vibrational motion, the total vibrational energy of the molecule is given as

$$E(v_1, v_2, \dots, v_{3N-5 \text{ or } 6}) = \sum_{j=1}^{3N-5 \text{ or } 6} \hbar \omega_j \left(v_j + \frac{1}{2} \right)$$

as a product of 3N-5 or 3N-6 harmonic oscillator functions $\Psi_{v_j}(x_j)$ are for each normal mode within this picture, the energy gap between one vibrational level and another in which one of the v_j quantum numbers is increased by unity (the origin of this "selection rule" is discussed in Chapter 15) is

$$\Delta E_{v_j} \rightarrow v_j + 1 = \hbar \omega_j$$

The harmonic model thus predicts that the "fundamental" ($v = 0 \rightarrow v = 1$) and "hot band" ($v = 1 \rightarrow v = 2$) transition should occur at the same energy, and the overtone ($v=0 \rightarrow v=2$) transitions should occur at exactly twice this energy.

The Use of Symmetry

Symmetry Adapted Modes

It is often possible to simplify the calculation of the normal mode frequencies and eigenvectors by exploiting molecular point group symmetry. For molecules that possess symmetry, the electronic potential $V(q_j)$ displays symmetry with respect to displacements of symmetry equivalent Cartesian coordinates. For example, consider the water molecule at its C_{2v} equilibrium geometry as illustrated in the figure below. A very small movement of the H_2O molecule's left H atom in the positive x direction (Δx_L) produces the same change in V as a correspondingly small displacement of the right H atom in the negative x direction ($-\Delta x_R$). Similarly, movement of the left H in the positive y direction (Δy_L) produces an energy change identical to movement of the right H in the positive y direction (Δy_R).

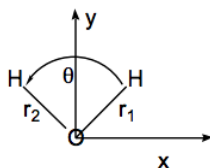


Figure 13.2.1: Insert caption here!

The equivalence of the pairs of Cartesian coordinate displacements is a result of the fact that the displacement vectors are connected by the point group operations of the C_{2v} group. In particular, reflection of Δx_L through the yz plane produces $-\Delta x_R$, and reflection of Δy_L through this same plane yields Δy_R .

More generally, it is possible to combine sets of Cartesian displacement coordinates $\{q_k\}$ into so-called symmetry adapted coordinates $\{Q_{\Gamma,j}\}$, where the index Γ labels the irreducible representation and j labels the particular combination of that

symmetry. These symmetry adapted coordinates can be formed by applying the point group projection operators to the individual Cartesian displacement coordinates.

To illustrate, again consider the H_2O molecule in the coordinate system described above. The $3N = 9$ mass weighted Cartesian displacement coordinates $(X_L, Y_L, Z_L, X_O, Y_O, Z_O, X_R, Y_R, Z_R)$ can be symmetry adapted by applying the following four projection operators:

$$P_{A_1} = 1 + \sigma_{yz} + \sigma_{xy} + C_2$$

$$P_{b_1} = 1 + \sigma_{yz} + \sigma_{xy} - C_2$$

$$P_{b_2} = 1 - \sigma_{yz} + \sigma_{xy} - C_2$$

$$P_{a_2} = 1 - \sigma_{yz} - \sigma_{xy} + C_2$$

to each of the 9 original coordinates. Of course, one will **not** obtain $9 \times 4 = 36$ independent symmetry adapted coordinates in this manner; many identical combinations will arise, and only 9 will be independent.

The independent combination of a_1 symmetry (normalized to produce vectors of unit length) are

$$Q_{a_1,1} = \frac{1}{\sqrt{2}}[X_L - X_R]$$

$$Q_{a_1,2} = \frac{1}{\sqrt{2}}[Y_L - Y_R]$$

$$Q_{a_1,3} = [Y_O]$$

Those of b_2 symmetry are

$$Q_{b_2,1} = \frac{1}{\sqrt{2}}[X_L + X_R]$$

$$Q_{b_2,2} = \frac{1}{\sqrt{2}}[Y_L - Y_R]$$

$$Q_{b_2,3} = [X_O]$$

and the combinations

$$Q_{b_1,1} = \frac{1}{\sqrt{2}}[Z_L + Z_R]$$

$$Q_{b_1,2} = [Z_O]$$

are of b_1 symmetry, whereas

$$Q_{a_2,1} = \frac{1}{\sqrt{2}}[Z_L - Z_R]$$

is of a_2 symmetry.

Point Group Symmetry of the Harmonic Potential

These nine $Q_{\Gamma,j}$ are expressed as unitary transformations of the original mass weighted Cartesian coordinates:

$$Q_{\Gamma,j} = \sum_k C_{\Gamma,j,k} X_k$$

These transformation coefficients $\{C_{\Gamma,j,k}\}$ can be used to carry out a unitary transformation of the 9×9 mass-weighted Hessian matrix. In so doing, we need only form blocks

$$H_{j,1}^{\Gamma} = \sum_{kk'} C_{\Gamma,j,k} H_{k,k'} \frac{1}{\sqrt{m_k m_{k'}}} C_{\Gamma,1,k'}$$

within which the symmetries of the two modes are identical. The off-diagonal elements

$$H_{j1}^{\Gamma\Gamma'} = {}_{kk'} C_{\Gamma,j,k} H_{k,k'} \frac{1}{\sqrt{m_k m'_k}} C_{\Gamma',1,k'}$$

vanish because the potential $V(q_j)$ (and the full vibrational Hamiltonian $H = T + V$) commutes with the C_{2v} point group symmetry operations.

As a result, the 9x9 mass-weighted Hessian eigenvalue problem can be sub divided into two 3x3 matrix problems (of a_1 and b_2 symmetry), one 2x2 matrix of b_1 symmetry and one 1x1 matrix of a_2 symmetry. For example, the a_1 symmetry block $H_{jl}^{a_1}$ is formed as follows:

$$\begin{bmatrix} \frac{1}{\sqrt{2}} & -\frac{1}{\sqrt{2}} & 0 \\ \frac{1}{\sqrt{2}} & \frac{1}{\sqrt{2}} & 0 \\ 0 & 0 & 1 \end{bmatrix} \begin{bmatrix} m^{-1} H \frac{\partial^2 V}{\partial x_L^2} & m^{-1} H \frac{\partial^2 V}{\partial x_L \partial x_R} & (m_H m_O)^{-1/2} \frac{\partial^2 V}{\partial x_L \partial x_O} \\ m^{-1} H \frac{\partial^2 V}{\partial x_R \partial x_L} & m^{-1} H \frac{\partial^2 V}{\partial x_R^2} & (m_H m_O)^{-1/2} \frac{\partial^2 V}{\partial x_R \partial x_O} \\ (m_H m_O)^{-1/2} \frac{\partial^2 V}{\partial x_O \partial x_L} & (m_H m_O)^{-1/2} \frac{\partial^2 V}{\partial x_O \partial x_R} & m^{-1} O \frac{\partial^2 V}{\partial x_O^2} \end{bmatrix} \begin{bmatrix} \frac{1}{\sqrt{2}} & \frac{1}{\sqrt{2}} & 0 \\ \frac{1}{\sqrt{2}} & -\frac{1}{\sqrt{2}} & 0 \\ 0 & 0 & 1 \end{bmatrix}$$

The b_2 , b_1 and a_2 blocks are formed in a similar manner. The eigenvalues of each of these blocks provide the squares of the harmonic vibrational frequencies, the eigenvectors provide the normal mode displacements as linear combinations of the symmetry adapted $\{Q_j^\Gamma\}$.

Regardless of whether symmetry is used to block diagonalize the mass-weighted Hessian, six (for non-linear molecules) or five (for linear species) of the eigenvalues will equal zero. The eigenvectors belonging to these zero eigenvalues describe the 3 translations and 2 or 3 rotations of the molecule. For example,

$$\begin{aligned} \frac{1}{\sqrt{3}}[X_L + X_R + X_O] \\ \frac{1}{\sqrt{3}}[Y_L + Y_R + Y_O] \\ \frac{1}{\sqrt{3}}[Z_L + Z_R + Z_O] \end{aligned}$$

are three translation eigenvectors of b_2 , a_1 and b_1 symmetry, and

$$\frac{1}{\sqrt{2}}(Z_L - Z_R)$$

is a rotation (about the Y-axis in the figure shown above) of a_2 symmetry. This rotation vector can be generated by applying the a_2 projection operator to Z_L or to Z_R . The fact that rotation about the Y-axis is of a_2 symmetry is indicated in the right-hand column of the C_{2v} character table of Appendix E via the symbol R_Z (n.b., care must be taken to realize that the axis convention used in the above figure is different than that implied in the character table; the latter has the Z-axis out of the molecular plane, while the figure calls this the X-axis). The other two rotations are of b_1 and b_2 symmetry (see the C_{2v} character table of Appendix E) and involve spinning of the molecule about the X- and Z- axes of the figure drawn above, respectively.

So, of the 9 cartesian displacements, 3 are of a_1 symmetry, 3 of b_2 , 2 of b_1 , and 1 of a_2 . Of these, there are three translations (a_1 , b_2 , and b_1) and three rotations (b_2 , b_1 , and a_2). This leaves two vibrations of a_1 and one of b_2 symmetry. For the H_2O example treated here, the three non zero eigenvalues of the mass-weighted Hessian are therefore of a_1 , b_2 , and a_1 symmetry. They describe the symmetric and asymmetric stretch vibrations and the bending mode, respectively as illustrated below.

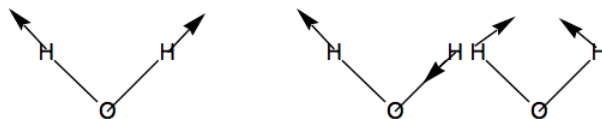


Figure 13.2.2: Insert caption here!

The method of vibrational analysis presented here can work for any polyatomic molecule. One knows the mass-weighted Hessian and then computes the non-zero eigenvalues which then provide the squares of the normal mode vibrational frequencies. Point

group symmetry can be used to block diagonalize this Hessian and to label the vibrational modes according to symmetry.

This page titled [13.2: Vibrational Motion Within the Harmonic Approximation](#) is shared under a [CC BY-NC-SA 4.0](#) license and was authored, remixed, and/or curated by [Jack Simons](#) via [source content](#) that was edited to the style and standards of the LibreTexts platform.

13.3: Anharmonicity

The electronic energy of a molecule, ion, or radical at geometries near a stable structure can be expanded in a Taylor series in powers of displacement coordinates as was done in the preceding section of this Chapter. This expansion leads to a picture of uncoupled harmonic vibrational energy levels

$$E(v_1 \dots v_{3N-5 \text{ or } 6}) = \sum_{j=1}^{3N-5 \text{ or } 6} \hbar \omega_j \left(v_j + \frac{1}{2} \right)$$

and wavefunctions

$$\Psi(x_1 \dots x_{3N-5 \text{ or } 6}) = \prod_{j=1}^{3N-5 \text{ or } 6} \Psi_{v_j}(x_j).$$

The spacing between energy levels in which one of the normal-mode quantum numbers increases by unity

$$\Delta E_{vj} = E(\dots v_j + 1 \dots) - E(\dots v_j \dots) = \hbar \omega_j$$

is predicted to be independent of the quantum number v_j . This picture of evenly spaced energy levels

$$\Delta E_0 = \Delta E_1 = \Delta E_2 = \dots$$

is an incorrect aspect of the harmonic model of vibrational motion, and is a result of the quadratic model for the potential energy surface $V(x_j)$.

The Expansion of $E(v)$ in Powers of $\left(v + \frac{1}{2}\right)$.

Experimental evidence clearly indicates that significant deviations from the harmonic oscillator energy expression occur as the quantum number v_j grows. In Chapter 1 these deviations were explained in terms of the diatomic molecule's true potential $V(R)$ deviating strongly from the harmonic $\frac{1}{2k}(E - E_e)^2$ potential at higher energy (and hence larger $|R - R_e|$) as shown in the following figure.

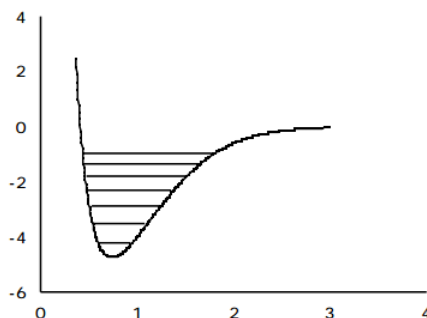


Figure 13.3.1: Insert caption here!

At larger bond lengths, the true potential is "softer" than the harmonic potential, and eventually reaches its asymptote which lies at the dissociation energy D_e above its minimum. This negative deviation of the true $V(R)$ from $\frac{1}{2k}(R - R_e)^2$ causes the true vibrational energy levels to lie below the harmonic predictions.

It is convention to express the experimentally observed vibrational energy levels, along each of the $3N-5$ or 6 independent modes, as follows:

$$E(v_j) = \hbar \left[\omega_j \left(v_j + \frac{1}{2} \right) - (\omega x)_j \left(v_j + \frac{1}{2} \right)^2 + (\omega y)_j \left(v_j + \frac{1}{2} \right)^3 + (\omega z)_j \left(v_j + \frac{1}{2} \right)^4 + \dots \right]$$

The first term is the harmonic expression. The next is termed the first anharmonicity; it (usually) produces a negative contribution to $E(v_j)$ that varies as $\left(v_j + \frac{1}{2}\right)^2$. The spacings between successive $v_j \rightarrow v_j + 1$ energy levels is then given by:

$$\Delta E_{vj} = E(v_j + 1) - E(v_j)$$

$$= \hbar[\omega_j - 2(\omega x)_j(v_j + 1) + \dots]$$

A plot of the spacing between neighboring energy levels versus v_j should be linear for values of v_j where the harmonic and first overtone terms dominate. The slope of such a plot is expected to be $-2\hbar(\omega x)_j$ and the small $-v_j$ intercept should be $\hbar[\omega_j - 2(\omega x)_j]$. Such a plot of experimental data, which clearly can be used to determine the ω_j and $(\omega x)_j$ parameter of the vibrational mode of study, is shown in the figure below.

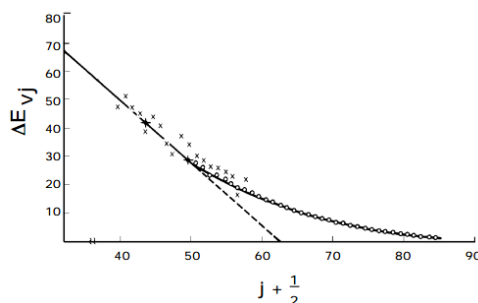


Figure 13.3.2: Insert caption here!

The Birge-Spinner Extrapolation

These so-called Birge-Spinner plots can also be used to determine dissociation energies of molecules. By linearly extrapolating the plot of experimental ΔE_{v_j} values to large v_j values, one can find the value of v_j at which the spacing between neighboring vibrational levels goes to zero. This value $v_{j, \max}$ specifies the quantum number of the last bound vibrational level for the particular potential energy function $V(x_j)$ of interest. The dissociation energy D_e can then be computed by adding to $\frac{1}{2}\hbar\omega_j$ (the zero point energy along this mode) the sum of the spacings between neighboring vibrational energy levels from $v_j = 0$ to $v_j = v_{j, \max}$:

$$D_e = \frac{1}{2}\hbar\omega_j + \sum_{v_j=0}^{v_{j, \max}} \Delta E_{v_j}.$$

Since experimental data are not usually available for the entire range of v_j values (from 0 to $v_{j, \max}$), this sum must be computed using the anharmonic expression for ΔE_{v_j} :

$$\Delta E_{v_j} = \hbar \left[\omega_j - 2(\omega x)_j \left(v_j + \frac{1}{2} + \dots \right) \right].$$

Alternatively, the sum can be computed from the Birge-Spinner graph by measuring the area under the straight-line fit to the graph of ΔE_{v_j} or v_j from $v_j = 0$ to $v_j = v_{j, \max}$.

This completes our introduction to the subject of rotational and vibrational motions of molecules (which applies equally well to ions and radicals). The information contained in this Section is used again in Section 5 where photon-induced transitions between pairs of molecular electronic, vibrational, and rotational eigenstates are examined. More advanced treatments of the subject matter of this Section can be found in the text by Wilson, Decius, and Cross, as well as in Zare's text on angular momentum.

This page titled [13.3: Anharmonicity](#) is shared under a [CC BY-NC-SA 4.0](#) license and was authored, remixed, and/or curated by [Jack Simons](#) via [source content](#) that was edited to the style and standards of the LibreTexts platform.

CHAPTER OVERVIEW

14: Time-dependent Quantum Dynamics

The interaction of a molecular species with electromagnetic fields can cause transitions to occur among the available molecular energy levels (electronic, vibrational, rotational, and nuclear spin). Collisions among molecular species likewise can cause transitions to occur. Time-dependent perturbation theory and the methods of molecular dynamics can be employed to treat such transitions.

[14.1: Time-Dependent Vector Potentials](#)

[14.2: Time-Dependent Perturbation Theory](#)

[14.3: Application to Electromagnetic Perturbations](#)

[14.4: The "Long-Wavelength" Approximation](#)

[14.5: The Kinetics of Photon Absorption and Emission](#)

This page titled [14: Time-dependent Quantum Dynamics](#) is shared under a [CC BY-NC-SA 4.0](#) license and was authored, remixed, and/or curated by [Jack Simons](#) via [source content](#) that was edited to the style and standards of the LibreTexts platform.

14.1: Time-Dependent Vector Potentials

The full N-electron non-relativistic Hamiltonian H discussed earlier in this text involves the kinetic energies of the electrons and of the nuclei and the mutual Coulombic interactions among these particles

$$H = \sum_{a=1,M} -\left(\frac{\hbar^2}{2m_a}\right) \nabla_a^2 + \sum_j \left[\left(-\frac{\hbar^2}{2m_e}\right) \nabla_j^2 - \sum_a Z_a \frac{e^2}{r_{j,a}} \right] + \sum_{j < k} \frac{e^2}{r_{j,k}} + \sum_{a < b} Z_a Z_b \frac{e^2}{R_{a,b}}.$$

When an electromagnetic field is present, this is not the correct Hamiltonian, but it can be modified straightforwardly to obtain the proper H .

The Time-Dependent Vector $\mathbf{A}(\mathbf{r}, t)$ Potential

The only changes required to achieve the Hamiltonian that describes the same system in the presence of an electromagnetic field are to replace the momentum operators \mathbf{P}_a and \mathbf{p}_j for the nuclei and electrons, respectively, by $(\mathbf{P}_a - Z_a e/c \mathbf{A}(\mathbf{R}_a, t))$ and $(\mathbf{p}_j - e/c \mathbf{A}(\mathbf{r}_j, t))$. Here $Z_a e$ is the charge on the a th nucleus, $-e$ is the charge of the electron, and c is the speed of light.

The vector potential \mathbf{A} depends on time t and on the spatial location \mathbf{r} of the particle in the following manner:

$$\mathbf{A}(\mathbf{r}, t) = 2\mathbf{A}_0 \cos(\omega t - \mathbf{k} \cdot \mathbf{r}).$$

The circular frequency of the radiation ω (radians per second) and the wave vector \mathbf{k} (the magnitude of \mathbf{k} is $|\mathbf{k}| = \frac{2\pi}{\lambda}$, where λ is the wavelength of the light) control the temporal and spatial oscillations of the photons. The vector \mathbf{A}_0 characterizes the strength (through the magnitude of \mathbf{A}_0) of the field as well as the direction of the \mathbf{A} potential; the direction of propagation of the photons is given by the unit vector $\mathbf{k}/|\mathbf{k}|$. The factor of 2 in the definition of \mathbf{A} allows one to think of \mathbf{A}_0 as measuring the strength of both $e^{i(\omega t - \mathbf{k} \cdot \mathbf{r})}$ and $e^{-i(\omega t - \mathbf{k} \cdot \mathbf{r})}$ components of the $\cos(\omega t - \mathbf{k} \cdot \mathbf{r})$ function.

The Electric $\mathbf{E}(\mathbf{r}, t)$ and Magnetic $\mathbf{H}(\mathbf{r}, t)$ Fields

The electric $\mathbf{E}(\mathbf{r}, t)$ and magnetic $\mathbf{H}(\mathbf{r}, t)$ fields of the photons are expressed in terms of the vector potential \mathbf{A} as

$$\mathbf{E}(\mathbf{r}, t) = -\frac{1}{c} \frac{\partial \mathbf{A}}{\partial t} = \frac{\omega}{c} \mathbf{A}_0 \sin(\omega t - \mathbf{k} \cdot \mathbf{r})$$

$$\mathbf{H}(\mathbf{r}, t) = \nabla \times \mathbf{A} = \mathbf{k} \times \mathbf{A}_0 \sin(\omega t - \mathbf{k} \cdot \mathbf{r}).$$

The \mathbf{E} field lies parallel to the \mathbf{A}_0 vector, and the \mathbf{H} field is perpendicular to \mathbf{A}_0 ; both are perpendicular to the direction of propagation of the light $\mathbf{k}/|\mathbf{k}|$. \mathbf{E} and \mathbf{H} have the same phase because they both vary with time and spatial location as $\sin(\omega t - \mathbf{k} \cdot \mathbf{r})$. The relative orientations of these vectors are shown below.



Figure 14.1.1: Insert caption here!

The Resulting Hamiltonian

Replacing the nuclear and electronic momenta by the modifications shown above in the kinetic energy terms of the full electronic and nuclear-motion hamiltonian results in the following **additional** factors appearing in H :

$$H_{int} = \sum_j \left[\frac{ie\hbar}{m_e c} \mathbf{A}(\mathbf{r}_j, t) \cdot \nabla_j + \left(\frac{e^2}{2m_e c^2} \right) |\mathbf{A}(\mathbf{r}_j, t)|^2 \right] + \sum_a \left[\left(iZ_a \frac{e\hbar}{m_a c} \right) \mathbf{A}(\mathbf{R}_a, t) \cdot \nabla_a + \left(\frac{Z_a^2 e^2}{2m_a c^2} \right) |\mathbf{A}(\mathbf{R}_a, t)|^2 \right].$$

These so-called interaction perturbations H_{int} are what induces transitions among the various electronic/vibrational/rotational states of a molecule. The one-electron additive nature of H_{int} plays an important role in determining the kind of transitions that H_{int} can induce. For example, it causes the most intense electronic transitions to involve excitation of a single electron from one orbital to another (e.g., the [Slater-Condon rules](#)).

This page titled [14.1: Time-Dependent Vector Potentials](#) is shared under a [CC BY-NC-SA 4.0](#) license and was authored, remixed, and/or curated by [Jack Simons](#) via [source content](#) that was edited to the style and standards of the LibreTexts platform.

14.2: Time-Dependent Perturbation Theory

The mathematical machinery needed to compute the rates of transitions among molecular states induced by such a time-dependent perturbation is contained in time dependent perturbation theory (TDPT). The development of this theory proceeds as follows. One first assumes that one has in-hand **all** of the eigenfunctions $\{\Phi_k\}$ and eigenvalues $\{E_k^0\}$ that characterize the Hamiltonian H^0 of the molecule in the absence of the external perturbation:

$$H^0 \Phi_k = E_k^0 \Phi_k.$$

One then writes the time-dependent Schrödinger equation

$$i\hbar \frac{\partial \Psi}{\partial t} = (H^0 + H_{int})\Psi$$

in which the full Hamiltonian is explicitly divided into a part that governs the system in the absence of the radiation field and H_{int} which describes the interaction with the field.

Perturbative Solution

By treating H^0 as of zeroth order (in the field strength $|\mathbf{A}_0|$), expanding Ψ order-by order in the field-strength parameter:

$$\Psi = \Psi^0 + \Psi^1 + \Psi^2 + \Psi^3 + \dots,$$

realizing that H_{int} contains terms that are both first- and second- order in $|\mathbf{A}_0|$

$$H_{int}^1 = \sum_j \left[\left(\frac{ie\hbar}{m_e c} \right) \mathbf{A}(r_j, t) \cdot \nabla_j \right] + \sum_a \sum_a \left[\left(\frac{iZ_a e\hbar}{m_a c} \right) \mathbf{A}(R_a, t) \cdot \nabla_a \right],$$

$$H_{int}^2 = \sum_j \left[\left(\frac{e^2}{2m_e c^2} \right) |\mathbf{A}(r_j, t)|^2 \right] + \sum_a \left[\left(\frac{Z_a^2 e^2}{2m_a c^2} \right) |\mathbf{A}(R_a, t)|^2 \right],$$

and then collecting together all terms of like power of $|\mathbf{A}_0|$, one obtains the set of time dependent perturbation theory equations. The lowest order such equations read:

$$i\hbar \frac{\partial \Psi^0}{\partial t} = H^0 \Psi^0$$

$$i\hbar \frac{\partial \Psi^1}{\partial t} = (H^0 \Psi^1 + H_{int}^1 \Psi^0)$$

$$i\hbar \frac{\partial \Psi^2}{\partial t} = (H^0 \Psi^2 + H_{int}^2 \Psi^0 + H_{int}^1 \Psi^1).$$

The zeroth order equations can easily be solved because H^0 is independent of time. Assuming that at $t = -\infty$, $\Psi = \psi_i$ (we use the index i to denote the initial state), this solution is:

$$\Psi^0 = \Phi_i e^{\frac{-iE_i^0 t}{\hbar}}.$$

The first-order correction to Ψ^0 , Ψ^1 can be found by (i) expanding Ψ^1 in the complete set of zeroth-order states $\{\Phi_f\}$:

$$\Psi^1 = \sum_f \Phi_f \langle \Phi_f | \Psi^1 \rangle = \sum_f \Phi_f C_f^1,$$

(ii) using the fact that

$$H^0 \Phi_f = E_f^0 \Phi_f$$

,

and (iii) substituting all of this into the equation that Ψ^1 obeys. The resultant equation for the coefficients that appear in the first-order equation can be written as

$$i\hbar \frac{\partial C_f^1}{\partial t} = \sum_k [E_k^0 C_k^1 \delta_{f,k}] + \langle \Phi_f | H_{int}^1 | \Phi_i \rangle e^{\frac{-iE_i^0 t}{\hbar}},$$

or

$$i\hbar \frac{\partial C_f^1}{\partial t} = E_f^0 C_f^1 + \langle \Phi_f | H_{int}^1 | \Phi_i \rangle e^{\frac{-iE_i^0 t}{\hbar}}.$$

Defining

$$C_f^1(t) = D_f^1(t) e^{\frac{-iE_f^0 t}{\hbar}}.$$

this equation can be cast in terms of an easy-to-solve equation for the D_f^1 coefficients:

$$i\hbar \frac{\partial D_f^1}{\partial t} = \langle \Phi_f | H_{int}^1 | \Phi_i \rangle e^{\frac{i[E_f^0 - E_i^0]t}{\hbar}}.$$

Assuming that the electromagnetic field $\mathbf{A}(\mathbf{r}, t)$ is turned on at $t=0$, and remains on until $t = T$, this equation for D_f^1 can be integrated to yield:

$$D_f^1(t) = \frac{1}{(i\hbar)} \int_0^T \langle \Phi_f | H_{int}^1 | \Phi_i \rangle e^{\frac{i[E_f^0 - E_i^0]t'}{\hbar}} dt'.$$

This page titled [14.2: Time-Dependent Perturbation Theory](#) is shared under a [CC BY-NC-SA 4.0](#) license and was authored, remixed, and/or curated by [Jack Simons](#) via [source content](#) that was edited to the style and standards of the LibreTexts platform.

14.3: Application to Electromagnetic Perturbations

First-Order Fermi-Wentzel "Golden Rule"

Using the earlier expressions for H_{int}^1 and for $\mathbf{A}(\mathbf{r}, t)$

$$H_{int}^1 = \sum_j \left[\left(\frac{ie\hbar}{m_e c} \right) \mathbf{A}(\mathbf{r}_j, t) \cdot \nabla_j \right] + \sum_a \left[\left(\frac{iZ_a e\hbar}{m_a c} \right) \mathbf{A}(\mathbf{R}_a, t) \cdot \nabla_a \right]$$

and

$$2\mathbf{A}_0 \cos(\omega t - \mathbf{k} \cdot \mathbf{r}) = \mathbf{A}_0 \left[e^{i(\omega t - \mathbf{k} \cdot \mathbf{r})} + e^{-i(\omega t - \mathbf{k} \cdot \mathbf{r})} \right],$$

it is relatively straightforward to carry out the above time integration to achieve a final expression for $D_f^1(t)$, which can then be substituted into $C_f^1(t) = D_f^1(t)e^{(-\frac{iE_f^0 t}{\hbar})}$ to obtain the final expression for the first-order estimate of the probability amplitude for the molecule appearing in the state $\Phi_f e^{(-\frac{iE_f^0 t}{\hbar})}$ after being subjected to electromagnetic radiation from $t = 0$ until $t = T$. This final expression reads:

$$C_f^1(T) = \frac{1}{i\hbar} e^{\frac{-iE_f^0 T}{\hbar}} \left[\langle \Phi_f | \sum_j \left[\left(\frac{ie\hbar}{m_e c} \right) e^{-i\mathbf{k} \cdot \mathbf{r}_j} \mathbf{A}_0 \cdot \nabla_j + \sum_a \left(\frac{iZ_a e\hbar}{m_a c} \right) e^{-i\mathbf{k} \cdot \mathbf{R}_a} \mathbf{A}_0 \cdot \nabla_a | \Phi_i \rangle \right] \frac{e^{i(\omega + \omega_{f,i})T} - 1}{i(\omega + \omega_{f,i})} \right] \\ + \frac{1}{i\hbar} e^{\frac{-iE_f^0 T}{\hbar}} \left[\langle \Phi_f | \sum_j \left[\left(\frac{ie\hbar}{m_e c} \right) e^{i\mathbf{k} \cdot \mathbf{r}_j} \mathbf{A}_0 \cdot \nabla_j + \sum_a \left(\frac{iZ_a e\hbar}{m_a c} \right) e^{i\mathbf{k} \cdot \mathbf{R}_a} \mathbf{A}_0 \cdot \nabla_a | \Phi_i \rangle \right] \frac{e^{i(-\omega + \omega_{f,i})T} - 1}{i(-\omega + \omega_{f,i})} \right]$$

where

$$\omega_{f,i} = \frac{[E_f^0 - E_i^0]}{\hbar}$$

is the resonance frequency for the transition between "initial" state Φ_i and "final" state Φ_f

Defining the time-independent parts of the above expression as

$$\alpha_{f,i} = \langle \Phi_f | \sum_j \left[\left(\frac{e}{m_e c} \right) e^{-i\mathbf{k} \cdot \mathbf{r}_j} \mathbf{A}_0 \cdot \nabla_j + \sum_a \left(\frac{Z_a e}{m_a c} \right) e^{-i\mathbf{k} \cdot \mathbf{R}_a} \mathbf{A}_0 \cdot \nabla_a | \Phi_i \rangle \right],$$

this result can be written as

$$C_f^1(T) = e^{\frac{-iE_f^0 T}{\hbar}} \left[\alpha_{f,i} \frac{e^{i(\omega + \omega_{f,i})T} - 1}{i(\omega + \omega_{f,i})} + \alpha_{f,i}^* \frac{e^{-i(\omega - \omega_{f,i})T} - 1}{-i(\omega - \omega_{f,i})} \right].$$

The modulus squared $|C_f^1(T)|^2$ gives the probability of finding the molecule in the final state Φ_f at time T , given that it was in Φ_i at time $t = 0$. If the light's frequency ω is tuned close to the transition frequency $\omega_{f,i}$ of a particular transition, the term whose denominator contains $(\omega - \omega_{f,i})$ will dominate the term with $(\omega + \omega_{f,i})$ in its denominator. Within this "near-resonance" condition, the above probability reduces to:

$$|C_f^1|^2 = 2|\alpha_{f,i}|^2 \frac{1 - \cos(\omega - \omega_{f,i})T}{(\omega - \omega_{f,i})^2} \\ = 4|\alpha_{f,i}|^2 \frac{\sin^2(1/2(\omega - \omega_{f,i})T)}{(\omega - \omega_{f,i})^2}.$$

This is the final result of the first-order time-dependent perturbation theory treatment of light-induced transitions between states Φ_i and Φ_f .

The so-called sinc-function

$$\frac{\sin^2(1/2(\omega - \omega_{f,i})T)}{(\omega - \omega_{f,i})^2}$$

as shown in the figure below is strongly peaked near $\omega = \omega_{f,i}$, and displays secondary maxima (of decreasing amplitudes) near $\omega = \omega_{f,i} + 2\frac{n\pi}{T}$, $n = 1, 2, \dots$. In the $T \rightarrow \infty$ limit, this function becomes narrower and narrower, and the area under it

$$\int_{-\infty}^{\infty} \frac{\sin^2(1/2(\omega - \omega_{f,i})T)}{(\omega - \omega_{f,i})^2} d\omega = \frac{T}{2} \int_{-\infty}^{\infty} \frac{\sin^2(1/2(\omega - \omega_{f,i})T)}{1/4T^2(\omega - \omega_{f,i})^2} d\left(\omega \frac{T}{2}\right) = \frac{T}{2} \int_{-\infty}^{\infty} \frac{\sin^2(x)}{x^2} = \pi \frac{T}{2}$$

grows with T. Physically, this means that when the molecules are exposed to the light source for long times (large T), the sinc function emphasizes ω values near $\omega_{f,i}$ (i.e., the on-resonance ω values). These properties of the sinc function will play important roles in what follows.

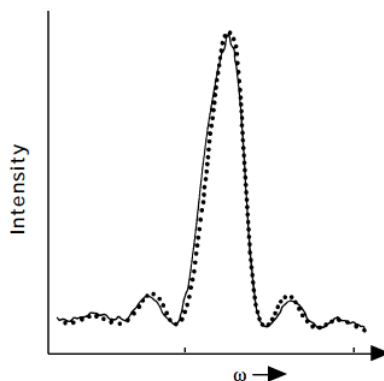


Figure 14.3.1: Insert caption here!

In most experiments, light sources have a "spread" of frequencies associated with them; that is, they provide photons of various frequencies. To characterize such sources, it is common to introduce the spectral source function $g(\omega) d\omega$ which gives the probability that the photons from this source have frequency somewhere between ω and $\omega + d\omega$. For narrow-band lasers, $g(\omega)$ is a sharply peaked function about some "nominal" frequency ω_0 ; broader band light sources have much broader $g(\omega)$ functions.

When such non-monochromatic light sources are used, it is necessary to average the above formula for $|C_f^1(T)|^2$ over the $g(\omega) d\omega$ probability function in computing the probability of finding the molecule in state Φ_f after time T, given that it was in Φ_i up until $t = 0$, when the light source was turned on. In particular, the proper expression becomes:

$$\begin{aligned} |C_f^1(T)|_{ave}^2 &= 4|\alpha_{fi}|^2 \int g(\omega) \frac{\sin^2(1/2(\omega - \omega_{f,i})T)}{(\omega - \omega_{f,i})^2} d\omega \\ &= 2|\alpha_{fi}|^2 T \int_{-\infty}^{\infty} g(\omega) \frac{2\sin^2(1/2(\omega - \omega_{f,i})T)}{1/4T^2(\omega - \omega_{f,i})^2} d\left(\omega \frac{T}{2}\right) \end{aligned}$$

If the light-source function is "tuned" to peak near $\omega = \omega_{f,i}$ and if $g(\omega)$ is much broader (in ω -space) than the $\frac{\sin^2(1/2(\omega - \omega_{f,i})T)}{(\omega - \omega_{f,i})^2}$ function, $g(\omega)$ can be replaced by its value at the peak of the $\frac{\sin^2(1/2(\omega - \omega_{f,i})T)}{(\omega - \omega_{f,i})^2}$ function, yielding:

$$\begin{aligned} |C_f^1(T)|_{ave} &= 2g(\omega_{f,i})|\alpha_{fi}|^2 T \int_{-\infty}^{\infty} \frac{\sin^2(1/2(\omega - \omega_{f,i})T)}{1/4T^2(\omega - \omega_{f,i})^2} d\left(\omega \frac{T}{2}\right) = 2g(\omega_{f,i})|\alpha_{fi}|^2 T \int_{-\infty}^{\infty} \frac{\sin^2(x)}{x^2} dx \\ &= 2\pi g(\omega_{f,i})|\alpha_{fi}|^2 T. \end{aligned}$$

The fact that the **probability** of excitation from Φ_i to Φ_f grows linearly with the time T over which the light source is turned on implies that the **rate** of transitions between these two states is constant and given by:

$$\mathbf{R}_{i,f} = 2\pi g(\omega_{f,i}) |\alpha_{f,i}|^2;$$

this is the so-called first-order Fermi-Wentzel "**golden rule**" expression for such transition rates. It gives the rate as the square of a transition matrix element between the two states involved, of the first order perturbation multiplied by the light source function $g(\omega)$ evaluated at the transition frequency $\omega_{f,i}$.

Higher Order Results

Solution of the second-order time-dependent perturbation equations,

$$i\hbar \frac{\partial \Psi^2}{\partial t} = (H^0 \Psi^2 + H_{int}^2 \Psi^0 + H_{int}^1 \Psi^1)$$

which will not be treated in detail here, gives rise to two distinct types of contributions to the transition probabilities between Φ_i and Φ_f :

There will be matrix elements of the form

$$\langle \Phi_f | \sum_j \left[\left(\frac{e^2}{2m_e c^2} \right) |\mathbf{A}(\mathbf{r}_j, t)|^2 \right] + \sum_a \left[\left(\frac{Z_a^2 e^2}{2m_a c^2} \right) |\mathbf{A}(R_a, t)|^2 \right] | \Phi_i \rangle$$

arising when H_{int}^2 couples Φ_i to Φ_f .

There will be matrix elements of the form

$$\begin{aligned} \sum_k \langle \Phi_f | \sum_j \left[\left(\frac{ie\hbar}{m_e c} \right) \mathbf{A}(\mathbf{r}_j, t) \cdot \nabla_j \right] + \sum_a \left[\left(\frac{iZ_a e\hbar}{m_a c} \right) \mathbf{A}(R_a, t) \cdot \nabla_a \right] | \Phi_k \rangle \\ \langle \Phi_k | \sum_j \left[\left(\frac{ie\hbar}{m_e c} \right) \mathbf{A}(\mathbf{r}_j, t) \cdot \nabla_j \right] + \sum_a \left[\left(\frac{iZ_a e\hbar}{m_a c} \right) \mathbf{A}(R_a, t) \cdot \nabla_a \right] | \Phi_i \rangle \end{aligned}$$

arising from expanding $H_{int}^1 \Psi^1 = \sum_k C_k^1 H_{int}^1 | \Phi_k \rangle$ and using the earlier result for the first-order amplitudes C_k^1 . Because both types of second-order terms vary quadratically with the $\mathbf{A}(\mathbf{r}, t)$ potential, and because \mathbf{A} has time dependence of the form $\cos(\omega t - \mathbf{k} \cdot \mathbf{r})$, these terms contain portions that vary with time as $\cos(2\omega t)$. As a result, transitions between initial and final states Φ_i and Φ_f whose transition frequency is $\omega_{f,i}$ can be induced when $2\omega = \omega_{f,i}$; in this case, one speaks of coherent two-photon induced transitions in which the electromagnetic field produces a perturbation that has twice the frequency of the "nominal" light source frequency ω .

This page titled [14.3: Application to Electromagnetic Perturbations](#) is shared under a [CC BY-NC-SA 4.0](#) license and was authored, remixed, and/or curated by [Jack Simons](#) via [source content](#) that was edited to the style and standards of the LibreTexts platform.

14.4: The "Long-Wavelength" Approximation

To make progress in further analyzing the first-order results obtained above, it is useful to consider the wavelength λ of the light used in most visible/ultraviolet, infrared, or microwave spectroscopic experiments. Even the shortest such wavelengths (ultraviolet) are considerably longer than the spatial extent of all, but the largest molecules (i.e., polymers and biomolecules for which the approximations we introduce next are not appropriate).

In the definition of the essential coupling matrix element $\alpha_{f,i}$

$$\alpha_{f,i} = \langle \Phi_f | \sum_j \left(\frac{e}{m_e c} \right) e^{-i\mathbf{k} \cdot \mathbf{r}_j} \mathbf{A}_0 \cdot \nabla_j + \sum_a \left(\frac{Z_a e}{m_a c} \right) e^{-i\mathbf{k} \cdot \mathbf{R}_a} \mathbf{A}_0 \cdot \nabla_a | \Phi_i \rangle,$$

the factors $e^{-i\mathbf{k} \cdot \mathbf{r}_j}$ and $e^{-i\mathbf{k} \cdot \mathbf{R}_a}$ can be expanded as:

$$e^{-i\mathbf{k} \cdot \mathbf{r}_j} = 1 + (-i\mathbf{k} \cdot \mathbf{r}_j) + \frac{1}{2}(-i\mathbf{k} \cdot \mathbf{r}_j)^2 + \dots$$

$$e^{-i\mathbf{k} \cdot \mathbf{R}_a} = 1 + (-i\mathbf{k} \cdot \mathbf{R}_a) + \frac{1}{2}(-i\mathbf{k} \cdot \mathbf{R}_a)^2 + \dots$$

Because $|\mathbf{k}| = 2\pi/\lambda$, and the scales of \mathbf{r}_j and \mathbf{R}_a are of the dimension of the molecule, $\mathbf{k} \cdot \mathbf{r}_j$ and $\mathbf{k} \cdot \mathbf{R}_a$ are less than unity in magnitude, within this so-called "long-wavelength" approximation.

Electric Dipole Transitions

Introducing these expansions into the expression for $\alpha_{f,i}$ gives rise to terms of various powers in $1/\lambda$. The lowest order terms are:

$$\alpha_{f,i}(E1) = \langle \Phi_f | \sum_j \left(\frac{e}{m_e c} \right) \mathbf{A}_0 \cdot \nabla_j + \sum_a \left(\frac{Z_a e}{m_a c} \right) \mathbf{A}_0 \cdot \nabla_a | \Phi_i \rangle$$

and are called "electric dipole" terms, and are denoted E1. To see why these matrix elements are termed E1, we use the following identity (see Chapter 1) between the momentum operator $-i\hbar\nabla$ and the corresponding position operator \mathbf{r} :

$$\nabla_j = - \left(\frac{m_e}{\hbar^2} \right) [H, \mathbf{r}_j]$$

$$\nabla_a = - \left(\frac{m_a}{\hbar^2} \right) [H, \mathbf{R}_a]$$

This derives from the fact that H contains ∇_j and ∇_a in its kinetic energy operators (as ∇_a^2 and ∇_j^2). Substituting these expressions into the above $\alpha_{f,i}(E1)$ equation and using $H\Phi_{i \text{ or } f} = E_{i \text{ or } f}^0 \Phi_{i \text{ or } f}$, one obtains:

$$\begin{aligned} \alpha_{f,i}(E1) &= (E_f^0 - E_i^0) \mathbf{A}_0 \cdot \langle \Phi_f | \sum_j \left(\frac{e}{\hbar^2 c} \right) \mathbf{r}_j + \sum_a \left(\frac{Z_a e}{\hbar^2 c} \right) \mathbf{R}_a | \Phi_i \rangle \\ &= \omega_{f,i} \mathbf{A}_0 \cdot \langle \Phi_f | \sum_j \left(\frac{e}{\hbar c} \right) \mathbf{r}_j + \sum_a \left(\frac{Z_a e}{\hbar c} \right) \mathbf{R}_a | \Phi_i \rangle \\ &= \left(\frac{\omega_{f,i}}{\hbar c} \right) \mathbf{A}_0 \cdot \langle \Phi_f | \mu | \Phi_i \rangle, \end{aligned}$$

where μ is the electric dipole moment operator for the electrons and nuclei:

$$\mu = \sum_j e \mathbf{r}_j + \sum_a Z_a e \mathbf{R}_a.$$

The fact that the E1 approximation to $\alpha_{f,i}$ contains matrix elements of the electric dipole operator between the initial and final states makes it clear why this is called the **electric dipole contribution** to $\alpha_{f,i}$; within the E1 notation, the E stands for electric moment and the 1 stands for the first such moment (i.e., the dipole moment).

Within this approximation, the overall rate of transitions is given by:

$$R_{i,f} = 2\pi g(\omega_{f,i}) |\alpha_{f,i}|^2$$

$$2\pi g(\omega_{f,i}) \left(\frac{\omega_{f,i}}{\hbar c} \right)^2 |\mathbf{A}_0 \cdot \langle \Phi_f | \boldsymbol{\mu} | \Phi_i \rangle|^2.$$

Recalling that $\mathbf{E}(\mathbf{r}, t) = -\frac{1}{c} \frac{\partial \mathbf{A}}{\partial t} = \frac{\omega}{c} \mathbf{A}_0 \sin(\omega t - \mathbf{k} \cdot \mathbf{r})$,

the magnitude of \mathbf{A}_0 can be replaced by that of \mathbf{E} , and this rate expression becomes

$$R_{i,f} = \left(\frac{2\pi}{\hbar^2} \right) g(\omega_{f,i}) |\mathbf{E}_0 \cdot \langle \Phi_f | \boldsymbol{\mu} | \Phi_i \rangle|^2.$$

This expresses the widely used E1 approximation to the [Fermi-Wentzel golden rule](#).

Magnetic Dipole and Electric Quadrupole Transitions

When E1 predictions for the rates of transitions between states vanish (e.g., for symmetry reasons as discussed below), it is essential to examine higher order contributions to $\alpha_{f,i}$. The next terms in the above long-wavelength expansion vary as $\frac{1}{\lambda}$ and have the form:

$$\alpha_{f,i}(E2 + M1) = \langle \Phi_f | \sum_j \left(\frac{e}{m_e c} \right) [-i\mathbf{k} \cdot \mathbf{r}_j] \mathbf{A}_0 \cdot \nabla_j + \sum_a \left(\frac{Z_a e}{m_a c} \right) [-i\mathbf{k} \cdot \mathbf{R}_a] \mathbf{A}_0 \cdot \nabla_a | \Phi_i \rangle.$$

For reasons soon to be shown, they are called electric quadrupole (E2) and magnetic dipole (M1) terms. Clearly, higher and higher order terms can be so generated. Within the longwavelength regime, however, successive terms should decrease in magnitude because of the successively higher powers of $\frac{1}{\lambda}$ that they contain.

To further analyze the above E2 + M1 factors, let us label the propagation direction of the light as the z-axis (the axis along which \mathbf{k} lies) and the direction of \mathbf{A}_0 as the x-axis. These axes are so-called "lab-fixed" axes because their orientation is determined by the direction of the light source and the direction of polarization of the light source's \mathbf{E} field, both of which are specified by laboratory conditions. The molecule being subjected to this light can be oriented at arbitrary angles relative to these lab axes. With the x, y, and z axes so defined, the above expression for $\alpha_{f,i}$ (E2+M1) becomes

$$\alpha_{f,i}(E2 + M1) = -i \left(\frac{A_0 2\pi}{\lambda} \right) \langle \Phi_f | \sum_j \left(\frac{e}{m_e c} \right) z_j \frac{\partial}{\partial x_j} + \sum_a \left(\frac{Z_a e}{m_a c} \right) z_a \frac{\partial}{\partial x_a} | \Phi_i \rangle.$$

Now writing (for both z_j and z_a)

$$z \frac{\partial}{\partial x} = \frac{1}{2} \left(z \frac{\partial}{\partial x} - x \frac{\partial}{\partial z} + z \frac{\partial}{\partial x} + x \frac{\partial}{\partial z} \right),$$

and using

$$\begin{aligned} \nabla_j &= - \left(\frac{m_e}{\hbar^2} \right) [H, \mathbf{r}_j] \\ \nabla_a &= - \left(\frac{m_a}{\hbar^2} \right) [H, \mathbf{R}_a], \end{aligned}$$

the contributions of $\frac{1}{2} \left(z \frac{\partial}{\partial x} + x \frac{\partial}{\partial z} \right)$ (E2+M1) can be rewritten as

$$\alpha_{f,i}(E2) = -i \frac{(A_0 e 2\pi \omega_{f,i})}{c \lambda \hbar} \langle \Phi_f | \sum_j z_j x_j + \sum_a Z_a z_a x_a | \Phi_i \rangle.$$

The operator $\sum_i z_i x_i + \sum_a Z_a z_a x_a$ that appears above is the z,x element of the electric quadrupole moment operator $Q_{z,x}$; it is for this reason that this particular component is labeled E2 and denoted the electric quadrupole contribution.

The remaining $\frac{1}{2} \left(z \frac{\partial}{\partial x} - x \frac{\partial}{\partial z} \right)$ contribution to $\alpha_{f,i}$ (E2+M1) can be rewritten in a form that makes its content more clear by first noting that

$$\frac{1}{2} \left(z \frac{\partial}{\partial x} - x \frac{\partial}{\partial z} \right) = \left(\frac{i}{2\hbar} \right) (z p_x - x p_z) = \left(\frac{i}{2\hbar} \right) L_y$$

contains the y-component of the angular momentum operator. Hence, the following contribution to $\alpha_{f,i}$ (E2+M1) arises:

$$\alpha_{f,i}(MI) = \frac{A_0 2\pi e}{2\lambda c \hbar} \langle \Phi_f | \sum_j \frac{L_{y_j}}{m_e} + \sum_a Z_a \frac{L_{y_a}}{m_a} | \Phi_i \rangle.$$

The magnetic dipole moment of the electrons about the y axis is

$$\mu_{y, \text{electrons}} = \sum_j \left(\frac{e}{2m_e c} \right) L_{y_j};$$

that of the nuclei is

$$\mu_{y, \text{nuclei}} = \sum_a \left(\frac{Z_a e}{2m_a c} \right) L_{y_a}.$$

The $\alpha_{f,i}$ (M1) term thus describes the interaction of the magnetic dipole moments of the electrons and nuclei with the magnetic field (of strength $|H| = A_0 k$) of the light (which lies along the y axis):

$$\alpha_{f,i}(M1) = \frac{|H|}{\hbar} \langle \Phi_f | \mu_{y, \text{electrons}} + \mu_{y, \text{nuclei}} | \Phi_i \rangle.$$

The total rate of transitions from Φ_i to Φ_f is given, through first-order in perturbation theory, by

$$R_{i,f} = 2\pi g(\omega_{f,i}) |\alpha_{f,i}|^2,$$

where $\alpha_{f,i}$ is a sum of its E1, E2, M1, etc. pieces. In the next chapter, molecular symmetry will be shown to be of use in analyzing these various pieces. It should be kept in mind that the contributions caused by E1 terms will dominate, within the long-wavelength approximation, unless symmetry causes these terms to vanish. It is primarily under such circumstances that consideration of M1 and E2 transitions is needed.

This page titled [14.4: The "Long-Wavelength" Approximation](#) is shared under a [CC BY-NC-SA 4.0](#) license and was authored, remixed, and/or curated by [Jack Simons](#) via [source content](#) that was edited to the style and standards of the LibreTexts platform.

14.5: The Kinetics of Photon Absorption and Emission

The Phenomenological Rate Laws

Before closing this chapter, it is important to emphasize the context in which the transition rate expressions obtained here are most commonly used. The perturbative approach used in the above development gives rise to various contributions to the overall rate coefficient for transitions from an initial state Φ_i to a final state Φ_f ; these contributions include the electric dipole, magnetic dipole, and electric quadrupole first order terms as well contributions arising from second (and higher) order terms in the perturbation solution.

In principle, once the rate expression

$$R_{i,f} = 2\pi g(\omega_{f,i}) |\alpha_{f,i}|^2$$

has been evaluated through some order in perturbation theory and including the dominant electromagnetic interactions, one can make use of these **state-to-state rates**, which are computed on a per-molecule basis, to describe the time evolution of the populations of the various energy levels of the molecule under the influence of the light source's electromagnetic fields.

For example, given two states, denoted i and f , between which transitions can be induced by photons of frequency $\omega_{f,i}$, the following kinetic model is often used to describe the time evolution of the numbers of molecules n_i and n_f in the respective states:

$$\begin{aligned}\frac{dn_i}{dt} &= -R_{i,f}n_i + R_{f,i}n_f \\ \frac{dn_f}{dt} &= -R_{f,i}n_f + R_{i,f}n_i.\end{aligned}$$

Here, $R_{i,f}$ and $R_{f,i}$ are the rates (per molecule) of transitions for the $i \rightarrow f$ and $f \rightarrow i$ transitions respectively. As noted above, these rates are proportional to the intensity of the light source (i.e., the photon intensity) at the resonant frequency and to the square of a matrix element connecting the respective states. This matrix element square is $|\alpha_{i,f}|^2$ in the former case and $|\alpha_{f,i}|^2$ in the latter. Because the perturbation operator whose matrix elements are $\alpha_{i,f}$ and $\alpha_{f,i}$ is Hermitian (this is true through all orders of perturbation theory and for all terms in the long-wavelength expansion), these two quantities are complex conjugates of one another, and, hence $|\alpha_{i,f}|^2 = |\alpha_{f,i}|^2$, from which it follows that $R_{i,f} = R_{f,i}$. This means that the state-to-state absorption and stimulated emission rate coefficients (i.e., the rate per molecule undergoing the transition) are identical. This result is referred to as the principle of **microscopic reversibility**.

Quite often, the states between which transitions occur are members of levels that contain more than a single state. For example, in rotational spectroscopy a transition between a state in the $J = 3$ level of a diatomic molecule and a state in the $J = 4$ level involve such states; the respective levels are $2J+1 = 7$ and $2J+1 = 9$ fold degenerate, respectively.

To extend the above kinetic model to this more general case in which degenerate levels occur, one uses the number of molecules in each **level** (N_i and N_f for the two levels in the above example) as the time dependent variables. The kinetic equations then governing their time evolution can be obtained by summing the state-to-state equations over all states in each level

$$\begin{aligned}\sum_{i \text{ in level } I} \left(\frac{dn_i}{dt} \right) &= \frac{dN_I}{dt} \\ \sum_{f \text{ in level } F} \left(\frac{dn_f}{dt} \right) &= \frac{dN_F}{dt}\end{aligned}$$

and realizing that each state within a given level can undergo transitions to all states within the other level (hence the total rates of production and consumption must be summed over all states to or from which transitions can occur). This generalization results in a set of rate laws for the populations of the respective levels:

$$\begin{aligned}\frac{dN_i}{dt} &= -g_f R_{i,f} N_i + g_i R_{f,i} N_f \\ \frac{dN_f}{dt} &= -g_i R_{f,i} N_f + g_f R_{i,f} N_i.\end{aligned}$$

Here, g_i and g_f are the degeneracies of the two levels (i.e., the number of states in each level) and the $R_{i,f}$ and $R_{f,i}$, which are equal as described above, are the state-to-state rate coefficients introduced earlier.

Spontaneous and Stimulated Emission

It turns out (the development of this concept is beyond the scope of this text) that the rate at which an excited level can emit photons and decay to a lower energy level is dependent on two factors:

- i. the rate of **stimulated** photon emission as covered above and
- ii. the rate of **spontaneous** photon emission.

The former rate $g_f R_{i,f}$ (per molecule) is proportional to the light intensity $g(\omega_{f,i})$ at the resonance frequency. It is conventional to separate out this intensity factor by defining an intensity independent rate coefficient $B_{i,f}$ for this process as:

$$g_f R_{i,f} = g(\omega_{f,i}) B_{i,f}.$$

Clearly, $B_{i,f}$ embodies the final-level degeneracy factor g_f , the perturbation matrix elements, and the 2π factor in the earlier expression for $R_{i,f}$. The spontaneous rate of transition from the excited to the lower level is found to be **independent** of photon intensity, because it deals with a process that does not require collision with a photon to occur, and is usually denoted $A_{i,f}$. The rate of photon-stimulated upward transitions from state f to state i ($g_i R_{f,i} = g_i R_{i,f}$ in the present case) is also proportional to $g(\omega_{f,i})$, so it is written by convention as:

$$g_i R_{f,i} = g(\omega_{f,i}) B_{f,i}.$$

An important relation between the $B_{i,f}$ and $B_{f,i}$ parameters exists and is based on the identity $R_{i,f} = R_{f,i}$ that connects the state-to-state rate coefficients:

$$\frac{(B_{i,f})}{(B_{f,i})} = \frac{(g_f R_{i,f})}{(g_i R_{f,i})} = \frac{g_f}{g_i}.$$

This relationship will prove useful in the following sections.

Saturated Transitions and Transparency

Returning to the kinetic equations that govern the time evolution of the populations of two levels connected by photon absorption and emission, and adding in the term needed for spontaneous emission, one finds (with the initial level being of the lower energy):

$$\begin{aligned}\frac{dN_i}{dt} &= -gB_{i,f}N_i + (A_{f,i} + gB_{f,i})N_f \\ \frac{dN_f}{dt} &= -(A_{f,i} + gB_{f,i})N_f + gB_{i,f}N_i\end{aligned}$$

where $g = g(\omega)$ denotes the light intensity at the resonance frequency. At steady state, the populations of these two levels are given by setting

$$\begin{aligned}\frac{dN_i}{dt} &= \frac{dN_f}{dt} = 0 : \\ \frac{N_f}{N_i} &= \frac{(gB_{i,f})}{(A_{f,i} + gB_{f,i})}.\end{aligned}$$

When the light source's intensity is so large as to render $gB_{f,i} \gg A_{f,i}$ (i.e., when the rate of spontaneous emission is small compared to the stimulated rate), this population ratio reaches $(B_{i,f}/B_{f,i})$, which was shown earlier to equal (g_f/g_i) . In this case, one says that the populations have been **saturated** by the intense light source. Any further increase in light intensity will result in **zero** increase in the rate at which photons are being absorbed. Transitions that have had their populations saturated by the application of intense light sources are said to display optical **transparency** because they are unable to absorb (nor emit) any further photons because of their state of saturation.

Equilibrium and Relations Between A and B Coefficients

When the molecules in the two levels being discussed reach **equilibrium** (at which time the $\frac{dN_i}{dt} = \frac{dN_f}{dt} = 0$ also holds) with a photon source that itself is in **equilibrium** characterized by a temperature T , we must have:

$$\frac{N_f}{N_i} = \frac{g_f}{g_i} e^{\frac{-(E_f - E_i)}{kT}} = \frac{g_f}{g_i} e^{\frac{\hbar\omega}{kT}}$$

where g_f and g_i are the degeneracies of the states labeled f and i . The photon source that is characterized by an equilibrium temperature T is known as a **black body** radiator, whose intensity profile $g(\omega)$ (in $\text{erg cm}^{-3} \text{ sec}$) is known to be of the form:

$$g(\omega) = \frac{2(\hbar\omega)^3}{\pi c^3 \hbar^2} \left(e^{\frac{\hbar\omega}{kT}} - 1 \right)^{-1}.$$

Equating the kinetic result that must hold at equilibrium:

$$\frac{N_f}{N_i} = \frac{(gB_{i,f})}{(A_{f,i} + gB_{f,i})}$$

to the thermodynamic result:

$$\frac{N_f}{N_i} = \frac{g_f}{g_i} e^{\frac{\hbar\omega}{kT}},$$

and using the above black body $g(\omega)$ expression and the identity

$$\frac{B_{i,f}}{B_{f,i}} = \frac{g_f}{g_i},$$

one can solve for the $A_{f,i}$ rate coefficient in terms of the $B_{f,i}$ coefficient. Doing so yields:

$$A_{f,i} = B_{f,i} \frac{2(\hbar\omega)^3}{\pi^3 \hbar^2}$$

Summary

In summary, the so-called **Einstein A and B rate coefficients** connecting a lower-energy initial state i and a final state f are related by the following conditions:

$$B_{i,f} = \frac{g_f}{g_i} B_{f,i}$$

and

$$A_{f,i} = \frac{2(\hbar\omega)^3}{\pi c^3 \hbar^2} B_{f,i}.$$

These phenomenological level-to-level rate coefficients are related to the state-to-state $R_{i,f}$ coefficients derived by applying perturbation theory to the electromagnetic perturbation through

$$g_f R_{i,f} = g(\omega_{f,i}) B_{i,f}.$$

The A and B coefficients can be used in a kinetic equation model to follow the time evolution of the populations of the corresponding levels:

$$\begin{aligned} \frac{dN_i}{dt} &= -gB_{i,f}N_i + (A_{f,i} + gB_{f,i})N_f \\ \frac{dN_f}{dt} &= -(A_{f,i} + gB_{f,i})N_f + gB_{i,f}N_i. \end{aligned}$$

These equations possess steady state solutions

$$\frac{N_f}{N_i} = \frac{(gB_{i,f})}{(A_{f,i} + gB_{f,i})}$$

which, for large $g(\omega)$, produce saturation conditions:

$$\frac{N_f}{N_i} = \frac{(B_{i,f})}{(B_{f,i})} = \frac{g_f}{g_i}.$$

This page titled [14.5: The Kinetics of Photon Absorption and Emission](#) is shared under a [CC BY-NC-SA 4.0](#) license and was authored, remixed, and/or curated by [Jack Simons](#) via [source content](#) that was edited to the style and standards of the LibreTexts platform.

CHAPTER OVERVIEW

15: Spectroscopy

The tools of time-dependent perturbation theory can be applied to transitions among electronic, vibrational, and rotational states of molecules.

[15.1: Rotational Transitions](#)

[15.2: Vibration-Rotation Transitions](#)

[15.3: Electronic-Vibration-Rotation Transitions](#)

[15.4: Time Correlation Function Expressions for Transition Rates](#)

This page titled [15: Spectroscopy](#) is shared under a [CC BY-NC-SA 4.0](#) license and was authored, remixed, and/or curated by [Jack Simons](#) via [source content](#) that was edited to the style and standards of the LibreTexts platform.

15.1: Rotational Transitions

Within the approximation that the electronic, vibrational, and rotational states of a molecule can be treated as independent, the total molecular wavefunction of the "initial" state is a product

$$\Phi_i = \psi_{ei} \chi_{vi} \phi_{ri}$$

of an electronic function ψ_{ei} , a vibrational function χ_{vi} , and a rotational function ϕ_{ri}

. A similar product expression holds for the "final" wavefunction Φ_f .

In microwave spectroscopy, the energy of the radiation lies in the range of fractions of a cm^{-1} through several cm^{-1} ; such energies are adequate to excite rotational motions of molecules but are not high enough to excite any but the weakest vibrations (e.g., those of weakly bound Van der Waals complexes). In rotational transitions, the electronic and vibrational states are thus left unchanged by the excitation process; hence $\psi_{ei} = \psi_{ef}$ and $\chi_{vi} = \chi_{vf}$.

Applying the first-order electric dipole transition rate expressions

$$R_{i,f} = 2\pi g(\omega_{f,i}) |\alpha_{f,i}|^2$$

obtained in [Chapter 14](#) to this case requires that the E1 approximation

$$R_{i,f} = \left(\frac{2\pi}{\hbar^2} \right) g(\omega_{f,i}) |\mathbf{E}_0 \cdot \langle \Phi_f | \boldsymbol{\mu} | \Phi_i \rangle|^2$$

be examined in further detail. Specifically, the electric dipole matrix elements $\langle \Phi_f | \boldsymbol{\mu} | \Phi_i \rangle$ with $\boldsymbol{\mu} = \sum_j e \mathbf{r}_j + \sum_a Z_a e \mathbf{R}_a$ must be analyzed for Φ_i and Φ_f being of the product form shown above.

The integrations over the electronic coordinates contained in $\langle \Phi_f | \boldsymbol{\mu} | \Phi_i \rangle$, as well as the integrations over vibrational degrees of freedom yield "expectation values" of the electric dipole moment operator because the electronic and vibrational components of Φ_i and Φ_f are identical:

$$\langle \psi_{ei} | \boldsymbol{\mu} | \psi_{ei} \rangle = \boldsymbol{\mu}(\mathbf{R})$$

is the dipole moment of the initial electronic state (which is a function of the internal geometrical degrees of freedom of the molecule, denoted \mathbf{R}); and

$$\langle \chi_{vi} | \boldsymbol{\mu}(\mathbf{R}) | \chi_{vi} \rangle = \boldsymbol{\mu}_{ave}$$

is the vibrationally averaged dipole moment for the particular vibrational state labeled χ_{vi} . The vector $\boldsymbol{\mu}_{ave}$ has components along various directions and can be viewed as a vector "locked" to the molecule's internal coordinate axis (labeled a, b, c as below).

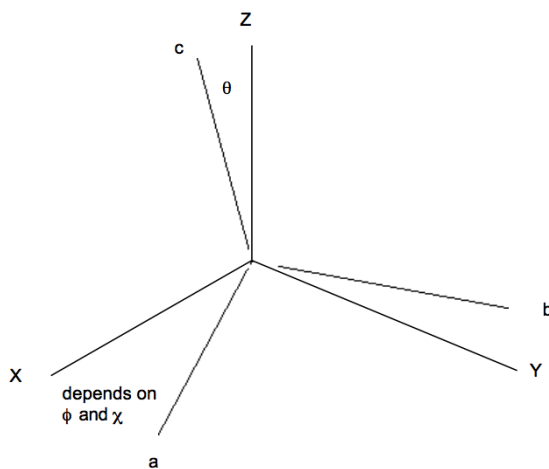


Figure 15.1.1: Insert caption here!

The rotational part of the $\langle \Phi_f | \boldsymbol{\mu} | \Phi_i \rangle$ integral is not of the expectation value form because the initial rotational function ϕ_{ir} is not the same as the final ϕ_{fr} . This integral has the form:

$$\langle \Phi_{ir} | \mu_{ave} | \Phi_{fr} \rangle = \int (Y_{L,M}^*(\theta, \phi)) \mu_{ave} Y_{L',M'}(\theta, \phi) \sin\theta \, d\theta \, d\phi$$

or linear molecules whose initial and final rotational wavefunctions are $Y_{L,M}$ and $Y_{L',M'}$, respectively, and

$$\langle \phi_{ir} | \mu_{ave} | \phi_{fr} \rangle = \sqrt{\frac{2L+1}{8\pi^2}} \sqrt{\frac{2L'+1}{8\pi^2}} \int (D_{L,M,K}(\theta, \phi, \chi) \mu_{ave} D_{L',M',K'}^*(\theta, \phi, \chi) \sin\theta \, d\theta \, d\phi \, d\chi)$$

for spherical or symmetric top molecules (here, $\sqrt{\frac{2L+1}{8\pi^2}} D_{L,M,K}^*(\theta, \phi, \chi)$ are the normalized rotational wavefunctions described in Chapter 13 and in Appendix G). The angles θ , ϕ , and χ refer to how the molecule-fixed coordinate system is oriented with respect to the space-fixed X, Y, Z axis system.

Linear Molecules

For linear molecules, the vibrationally averaged dipole moment μ_{ave} lies along the molecular axis; hence its orientation in the lab-fixed coordinate system can be specified in terms of the same angles (θ and ϕ) that are used to describe the rotational functions $Y_{L,M}(\theta, \phi)$. Therefore, the three components of the $\langle \phi_{ir} | \mu_{ave} | \phi_{fr} \rangle$ integral can be written as:

$$\langle \phi_{ir} | \mu_{ave} | \phi_{fr} \rangle_x = \mu \int Y_{L,M}^*(\theta, \phi) \sin\theta \cos\phi Y_{L',M'}(\theta, \phi) \sin\theta \, d\theta \, d\phi$$

$$\langle \phi_{ir} | \mu_{ave} | \phi_{fr} \rangle_y = \mu \int Y_{L,M}^*(\theta, \phi) \sin\theta \sin\phi Y_{L',M'}(\theta, \phi) \sin\theta \, d\theta \, d\phi$$

$$\langle \phi_{ir} | \mu_{ave} | \phi_{fr} \rangle_z = \mu \int Y_{L,M}^*(\theta, \phi) \sin\theta \cos\phi Y_{L',M'}(\theta, \phi) \sin\theta \, d\theta \, d\phi$$

where μ is the magnitude of the averaged dipole moment. **If the molecule has no dipole moment**, all of the above electric dipole integrals vanish and the **intensity** of E1 rotational transitions **is zero**.

The three E1 integrals can be further analyzed by noting that $\cos\theta \propto Y_{1,0}$; $\sin\theta \cos\phi \propto Y_{1,1} + Y_{1,-1}$; and $\sin\theta \sin\phi \propto Y_{1,1} - Y_{1,-1}$ and using the angular momentum coupling methods illustrated in Appendix G. In particular, the result given in that appendix:

$$D_{J,M,M'} D_{l,n,n'} = \sum_{J,M,M'} \langle J, M | j, m; l, n \rangle \langle j, m'; l, n' | J, M' \rangle D_{J,M,M'}$$

when multiplied by $D_{J,M,M'}^*$ and integrated over $\sin\theta \, d\theta \, d\phi \, d\chi$, yields:

$$\begin{aligned} & \int D_{J,M,M'}^* D_{j,m} D_{l,n,n'} \sin\theta \, d\theta \, d\phi \, d\chi \\ &= \frac{8\pi^2}{2J+1} \langle J, M | j, m; l, n \rangle \langle j, m'; l, n' | J, M' \rangle \\ &= 8\pi^2 \left(\frac{j!J}{m!n - M} \right) \left(\frac{j!J}{m'n' - M'} \right) (-1)^{M+M'}. \end{aligned}$$

To use this result in the present linear-molecule case, we note that the $D_{J,M,K}$ functions and the $Y_{J,M}$ functions are related by:

$$Y_{J,M}(\theta, \phi) = \sqrt{\frac{2J+1}{4\pi}} D_{J,M,0}^*(\theta, \phi, \chi).$$

The normalization factor is now $\sqrt{\frac{2J+1}{4\pi}}$ rather than $\sqrt{\frac{2J+1}{8\pi^2}}$ because the $Y_{J,M}$ are no longer functions of χ , and thus the need to integrate over $0 \leq \chi \leq 1\pi$ disappears. Likewise, the χ -dependence of $D_{J,M,K}^*$ disappears for $K = 0$.

We now use these identities in the three E1 integrals of the form

$$\mu \int Y_{L,M}^*(\theta, \phi) Y_{1,m}(\theta, \phi) Y_{L',M'}(\theta, \phi) \sin\theta \, d\theta \, d\phi,$$

with $m = 0$ being the Z- axis integral, and the Y- and X- axis integrals being combinations of the $m = 1$ and $m = -1$ results. Doing so yields:

$$\begin{aligned} & \mu \int Y_{L,M}^*(\theta, \phi) Y_{1,m}(\theta, \phi) Y_{L',M'}(\theta, \phi) \sin\theta \, d\theta \, d\phi \\ &= \mu \sqrt{\frac{2L+1}{4\pi} \frac{2L'+1}{4\pi} \frac{3}{4\pi}} \int D_{L,M,0} \mathbf{D}_{1,m,0}^* \mathbf{D}_{L',M',0}^* \sin\theta \, d\theta \, d\phi \, d\frac{\chi}{2\pi}. \end{aligned}$$

The last factor of $1/2\pi$ is inserted to cancel out the integration over $d\chi$ that, because all K-factors in the rotation matrices equal zero, trivially yields 2π . Now, using the result shown above expressing the integral over three rotation matrices, these E1 integrals for the linearmolecule case reduce to:

$$\begin{aligned} & \mu \int Y_{L,M}^*(\theta, \phi) Y_{1,m}(\theta, \phi) Y_{L',M'}(\theta, \phi) \sin\theta \, d\theta \, d\phi \\ &= \mu \sqrt{\frac{2L+1}{4\pi} \frac{2L'+1}{4\pi} \frac{3}{4\pi} \frac{8\pi^2}{2\pi}} \left(\frac{L' 1 L}{M' m - M} \right) \left(\frac{L' 1 L}{0 0 - 0} \right) (-1)^M \\ & \mu \sqrt{(2L+1)(2L'+1) \frac{3}{4\pi}} \left(\frac{L' 1 L}{M' m - M} \right) \left(\frac{L' 1 L}{0 0 - 0} \right) (-1)^M. \end{aligned}$$

Applied to the z-axis integral (identifying $m = 0$), this result therefore vanishes unless:

$$M = M'$$

and

$$L = L' + 1 \text{ or } L' - 1.$$

Even though angular momentum coupling considerations would allow $L = L'$ (because coupling two angular momenta with $j = 1$ and $j = L'$ should give $L'+1$, L' , and $L'-1$), the 3-j symbol $\left(\frac{L' 1 L}{0 0 - 0} \right)$ vanishes for the $L = L'$ case since 3-j symbols have the following symmetry

$$\left(\frac{L' 1 L}{M' m - M} \right) = (-1)^{L+L'+1} \left(\frac{L' 1 L}{-M' -m M} \right)$$

with respect to the M , M' , and m indices. Applied to the $\left(\frac{L' 1 L}{0 0 - 0} \right)$ 3-j symbol, this means that this particular 3-j element vanishes for $L = L'$ since $L + L' + 1$ is odd and hence $(-1)^{L+L'+1}$ is -1.

Applied to the x- and y- axis integrals, which contain $m = \pm 1$ components, this same analysis yields:

$$\mu \sqrt{(2L+1)(2L'+1) \frac{3}{4\pi}} \left(\frac{L' 1 L}{M' \pm 1 - M} \right) \left(\frac{L' 1 L}{0 0 - 0} \right) (-1)^M$$

which then requires that

$$M = M' \pm 1$$

and

$$L = L' + 1, L' - 1$$

with $L = L'$ again being forbidden because of the second 3-j symbol.

These results provide so-called "**selection rules**" because the limit the L and M values of the final rotational state, given the L' , M' values of the initial rotational state. In the figure shown below, the $L = L' + 1$ absorption spectrum of NO at 120 °K is given. The intensities of the various peaks are related to the populations of the lower-energy rotational states which are, in turn, proportional to

$(2L' + 1)e^{(-L'(L'+1))\frac{\hbar^2}{8\pi^2IkT}}$. Also included in the intensities are so-called **line strength factors** that are proportional to the squares of the quantities:

$$\mu \sqrt{(2L+1)(2L'+1)\frac{3}{4\pi}} \left(\begin{matrix} L' & 1 & L \\ M' & m & -M \end{matrix} \right) \left(\begin{matrix} L' & 1 & L \\ 0 & 0 & -0 \end{matrix} \right) (-1)^M$$

which appear in the E1 integrals analyzed above (recall that the rate of photon absorption $R_{i,f} = \left(\frac{2\pi}{\hbar^2}\right) g(\omega_{f,i}) |\mathbf{E}_0 \cdot \langle \Phi_f | \mu | \Phi_i \rangle|^2$ involves the squares of these matrix elements). The book by Zare gives an excellent treatment of line strength factors' contributions to rotation, vibration, and electronic line intensities.

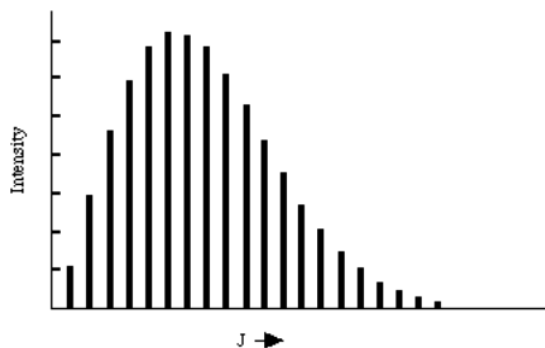


Figure 15.1.2: Insert caption here!

Non-Linear Molecules

For molecules that are non-linear and whose rotational wavefunctions are given in terms of the spherical or symmetric top functions $D_{L,M,K}^*$, the dipole moment μ_{ave} can have components along any or all three of the molecule's internal coordinates (e.g., the three molecule-fixed coordinates that describe the orientation of the principal axes of the moment of inertia tensor). For a spherical top molecule, $|\mu_{ave}|$ vanishes, so E1 transitions do not occur.

For symmetric top species, μ_{ave} lies along the symmetry axis of the molecule, so the orientation of μ_{ave} can again be described in terms of θ and ϕ , the angles used to locate the orientation of the molecule's symmetry axis relative to the lab-fixed coordinate system. As a result, the E1 integral again can be decomposed into three pieces:

$$\langle \phi_{ir} | \mu_{ave} | \phi_{fr} \rangle_x = \mu \int D_{L,M,K}(\theta, \phi, \chi) \cos\theta \cos\phi D_{L',M',K'}^*(\theta, \phi, \chi) \sin\theta d\theta d\phi d\chi$$

$$\langle \phi_{ir} | \mu_{ave} | \phi_{fr} \rangle_y = \mu \int D_{L,M,K}(\theta, \phi, \chi) \cos\theta \sin\phi D_{L',M',K'}^*(\theta, \phi, \chi) \sin\theta d\theta d\phi d\chi$$

$$\langle \phi_{ir} | \mu_{ave} | \phi_{fr} \rangle_z = \mu \int D_{L,M,K}(\theta, \phi, \chi) \cos\theta D_{L',M',K'}^*(\theta, \phi, \chi) \sin\theta d\theta d\phi d\chi$$

Using the fact that $\cos\theta \propto D_{1,0,0}^*$; $\sin\theta \cos\phi \propto D_{1,1,0}^* + D_{1,-1,0}^*$; and $\sin\theta \sin\phi \propto D_{1,1,0}^* - D_{1,-1,0}^*$ and the tools of angular momentum coupling allows these integrals to be expressed, as above, in terms of products of the following 3-j symbols:

$$\left(\begin{matrix} L' & 1 & L \\ M' & m & -M \end{matrix} \right) \left(\begin{matrix} L' & 1 & L \\ K' & 0 & -K \end{matrix} \right),$$

from which the following selection rules are derived:

$$L = L' + 1, L', L' - 1 \text{ (but not } L = L' = 0)$$

$$K = K'$$

$$M = M' + m,$$

with $m = 0$ for the Z-axis integral and $m = \pm 1$ for the X- and Y- axis integrals. In addition, if $K = K' = 0$, the $L = L'$ transitions are also forbidden by the second 3-j symbol vanishing.

This page titled [15.1: Rotational Transitions](#) is shared under a [CC BY-NC-SA 4.0](#) license and was authored, remixed, and/or curated by [Jack Simons](#) via [source content](#) that was edited to the style and standards of the LibreTexts platform.

15.2: Vibration-Rotation Transitions

When the initial and final electronic states are identical, but the respective vibrational and rotational states are not, one is dealing with transitions between vibration-rotation states of the molecule. These transitions are studied in infrared (IR) spectroscopy using light of energy in the 30 cm^{-1} (far IR) to 5000 cm^{-1} range. The electric dipole matrix element analysis still begins with the electronic dipole moment integral $\langle\psi_{ei}|\mu|\psi_{ei}\rangle = \mu(\mathbf{R})$, but the integration over internal vibrational coordinates no longer produces the vibrationally averaged dipole moment. Instead one forms the vibrational **transition dipole** integral:

$$\langle\chi_{vf}|\mu(\mathbf{R})|\chi_{vi}\rangle = \mu_{f,i}$$

between the initial χ_i and final χ_f vibrational states.

The Dipole Moment Derivatives

Expressing $\mu(\mathbf{R})$ in a power series expansion about the equilibrium bond length position (denoted \mathbf{R}_e collectively and $R_{a,e}$ individually):

$$\mu(\mathbf{R}) = \mu(\mathbf{R}_e) + \sum_a \frac{\partial\mu}{\partial R_a} (R_a - R_{a,e}) + \dots,$$

substituting into the $\langle\chi_{vf}|\mu(\mathbf{R})|\chi_{vi}\rangle$ integral, and using the fact that χ_i and χ_f are orthogonal (because they are eigenfunctions of vibrational motion on the same electronic surface and hence of the same vibrational Hamiltonian), one obtains:

$$\begin{aligned}\langle\chi_{vf}|\mu(\mathbf{R})|\chi_{vi}\rangle &= \mu(\mathbf{R}_e)\langle\chi_{vf}|\chi_{vi}\rangle + \sum_a \frac{\partial\mu}{\partial R_a} \langle\chi_{vf}|(R_a - R_{a,e})|\chi_{vi}\rangle + \dots \\ &= \sum_a \left(\frac{\partial\mu}{\partial R_a} \right) \langle\chi_{vf}|(\mathbf{R}_a - \mathbf{R}_{a,e})|\chi_{vi}\rangle + \dots\end{aligned}$$

This result can be interpreted as follows:

1. Each independent vibrational mode of the molecule contributes to the $\mu_{f,i}$ vector an amount equal to $\left(\frac{\partial\mu}{\partial R_a} \right) \langle\chi_{vf}|(\mathbf{R}_a - \mathbf{R}_{a,e})|\chi_{vi}\rangle + \dots$
2. Each such contribution contains one part $\left(\frac{\partial\mu}{\partial R_a} \right)$ that depends on how the molecule's dipole moment function varies with vibration along that particular mode (labeled a),
3. and a second part $\langle\chi_{vf}|(\mathbf{R}_a - \mathbf{R}_{a,e})|\chi_{vi}\rangle$ that depends on the character of the initial and final vibrational wavefunctions.

If the vibration does not produce a **modulation of the dipole moment** (e.g., as with the symmetric stretch vibration of the CO_2 molecule), its infrared intensity vanishes because $\left(\frac{\partial\mu}{\partial R_a} \right) = 0$. One says that such transitions are infrared "inactive".

Selection Rules on v in the Harmonic Approximation

If the vibrational functions are described within the harmonic oscillator approximation, it can be shown that the $\langle\chi_{vf}|(\mathbf{R}_a - \mathbf{R}_{a,e})|\chi_{vi}\rangle$ integrals vanish unless $v_f = v_i + 1$, $v_i - 1$ (and that these integrals are proportional to $\sqrt{v_i + 1}$ and $\sqrt{v_i}$ in the respective cases). Even when χ_{vf} and χ_{vi} are rather non-harmonic, it turns out that such $\Delta v = \pm 1$ transitions have the largest $\langle\chi_{vf}|(\mathbf{R}_a - \mathbf{R}_{a,e})|\chi_{vi}\rangle$ integrals and therefore the highest infrared intensities. For these reasons, transitions that correspond to $\Delta v = \pm 1$ are called "**fundamental**"; those with $\Delta v = \pm 2$ are called "**first overtone**" transitions.

In summary then, vibrations for which the molecule's dipole moment is modulated as the vibration occurs (i.e., for which $\left(\frac{\partial\mu}{\partial R_a} \right)$ is non-zero) **and** for which $\Delta v = \pm 1$ tend to have large infrared intensities; overtones of such vibrations tend to have smaller intensities, and those for which $\left(\frac{\partial\mu}{\partial R_a} \right) = 0$ have no intensity.

Rotational Selection Rules

The result of all of the vibrational modes' contributions to

$$\sum_a \left(\frac{\partial \mu}{\partial \mathbf{R}_a} \right) \langle \chi_{vf} | (\mathbf{R}_a - \mathbf{R}_{a,e}) | \chi_{vi} \rangle$$

is a vector μ_{trans} that is termed the vibrational "transition dipole" moment. This is a vector with components along, in principle, all three of the internal axes of the molecule. For each particular vibrational transition (i.e., each particular χ_i and χ_f) its orientation in space depends only on the orientation of the molecule; it is thus said to be locked to the molecule's coordinate frame. As such, its orientation relative to the lab-fixed coordinates (which is needed to effect a derivation of rotational selection rules as was done earlier in this Chapter) can be described much as was done above for the vibrationally averaged dipole moment that arises in purely rotational transitions. There are, however, important differences in detail. In particular,

1. For a linear molecule μ_{trans} can have components either along (e.g., when stretching vibrations are excited; these cases are denoted σ -cases) or perpendicular to (e.g., when bending vibrations are excited; they are denoted π cases) the molecule's axis.
2. For symmetric top species, μ_{trans} need not lie along the molecule's symmetry axis; it can have components either along or perpendicular to this axis.
3. For spherical tops, μ_{trans} will vanish whenever the vibration does not induce a dipole moment in the molecule. Vibrations such as the totally symmetric a_1 C-H stretching motion in CH_4 do not induce a dipole moment, and are thus infrared inactive; non-totally-symmetric vibrations can also be inactive if they induce no dipole moment.

As a result of the above considerations, the angular integrals

$$\langle \phi_{ir} | \mu_{trans} | \phi_{fr} \rangle = \int D_{L,M,K}(\theta, \phi, \chi) \mu_{trans} D_{L',M',K'}^*(\theta, \phi, \chi) \sin\theta d\theta d\phi d\chi$$

that determine the rotational selection rules appropriate to vibrational transitions produce similar, but not identical, results as in the purely rotational transition case.

The derivation of these selection rules proceeds as before, with the following additional considerations. The transition dipole moment's μ_{trans} components along the labfixed axes must be related to its molecule-fixed coordinates (that are determined by the nature of the vibrational transition as discussed above). This transformation, as given in Zare's text, reads as follows:

$$(\mu_{trans})_m = \sum_k D_{1,m,k}^*(\theta, \phi, \chi) (\mu_{trans})_k$$

where $(\mu_{trans})_m$ with $m = 1, 0, -1$ refer to the components along the lab-fixed (X, Y, Z) axes and $(\mu_{trans})_k$ with $k = 1, 0, -1$ refer to the components along the molecule-fixed (a, b, c) axes.

This relationship, when used, for example, in the symmetric or spherical top E1 integral:

$$\langle \phi_{ir} | \mu_{trans} | \phi_{fr} \rangle = \int D_{L,M,K}(\theta, \phi, \chi) \mu_{trans} D_{L',M',K'}^*(\theta, \phi, \chi) \sin\theta d\theta d\phi d\chi$$

gives rise to products of 3-j symbols of the form:

$$\left(\begin{matrix} L' & 1 & L \\ M' & m & -M \end{matrix} \right) \left(\begin{matrix} L' & 1 & L \\ K' & k & -K \end{matrix} \right).$$

The product of these 3-j symbols is nonvanishing only under certain conditions that provide the rotational selection rules applicable to vibrational lines of symmetric and spherical top molecules.

Both 3-j symbols will vanish unless

$$L = L' + 1, L', \text{ or } L' - 1.$$

In the special case in which $L = L' = 0$ (and hence with $M = M' = 0 = K = K'$, which means that $m = 0 = k$), these 3-j symbols again vanish. Therefore, transitions with

$$L = L' = 0$$

are again forbidden. As usual, the fact that the lab-fixed quantum number m can range over $m = 1, 0, -1$, requires that

$$M = M' + 1, M', \text{ or } M' - 1.$$

The selection rules for ΔK depend on the nature of the vibrational transition, in particular, on the component of μ_{trans} along the molecule-fixed axes. For the second 3-j symbol to not vanish, one must have

$$K = K' + k,$$

where $k = 0, 1$, and -1 refer to these molecule-fixed components of the transition dipole. Depending on the nature of the transition, various k values contribute.

Symmetric Tops

In a symmetric top molecule such as NH_3 , if the transition dipole lies along the molecule's symmetry axis, only $k = 0$ contributes. Such vibrations preserve the molecule's symmetry relative to this symmetry axis (e.g. the totally symmetric N-H stretching mode in NH_3). The additional selection rule $\Delta K = 0$ is thus obtained. Moreover, for $K = K' = 0$, all transitions with $\Delta L = 0$ vanish because the second 3-j symbol vanishes. In summary, one has:

$$\Delta K = 0; \Delta M = \pm 1, 0; \Delta L = \pm 1, 0 \text{ (but } L = L' = 0 \text{ is forbidden and all } \Delta L = 0 \text{ are forbidden for } K = K' = 0)$$

for symmetric tops with vibrations whose transition dipole lies along the symmetry axis.

If the transition dipole lies perpendicular to the symmetry axis, only $k = \pm 1$ contribute. In this case, one finds

$$\Delta K = \pm 1; \Delta M = \pm 1, 0; \Delta L = \pm 1, 0 \text{ (neither } L = L' = 0 \text{ nor } K = K' = 0 \text{ can occur for such transitions, so there are no additional constraints).}$$

Linear Molecules

When the above analysis is applied to a diatomic species such as HCl, only $k = 0$ is present since the only vibration present in such a molecule is the bond stretching vibration, which has σ symmetry. Moreover, the rotational functions are spherical harmonics (which can be viewed as $D_{L',M',K'}^*(\theta, \phi, \chi)$ functions with $K' = 0$), so the K and K' quantum numbers are identically zero. As a result, the product of 3-j symbols

$$\left(\begin{array}{ccc} L' & 1 & L \\ M' & n & -M \end{array} \right) \left(\begin{array}{ccc} L' & 1 & L \\ K' & k & -K \end{array} \right)$$

reduces to

$$\left(\begin{array}{ccc} L' & 1 & L \\ M' & m & -M \end{array} \right) \left(\begin{array}{ccc} L' & 1 & L \\ 0 & 0 & 0 \end{array} \right)$$

which will vanish unless

$$L = L' + 1, L' - 1,$$

but **not** $L = L'$ (since parity then causes the second 3-j symbol to vanish), and

$$M = M' + 1, M', M' - 1.$$

The $L = L' + 1$ transitions are termed **R-branch** absorptions and those obeying $L = L' - 1$ are called **P-branch** transitions. Hence, the selection rules

$$\Delta M = \pm 1, 0; \Delta L = \pm 1$$

are identical to those for purely rotational transitions.

When applied to linear polyatomic molecules, these same selection rules result if the vibration is of σ symmetry (i.e., has $k = 0$). If, on the other hand, the transition is of π symmetry (i.e., has $k = \pm 1$), so the transition dipole lies perpendicular to the molecule's axis, one obtains:

$$\Delta M = \pm 1, 0; \Delta L = \pm 1, 0.$$

These selection rules are derived by realizing that in addition to $k = \pm 1$, one has: (i) a linear-molecule rotational wavefunction that in the $v = 0$ vibrational level is described in terms of a rotation matrix $D_{L',M',0}(\theta, \phi, \chi)$ with no angular momentum along the molecular axis, $K' = 0$; (ii) a $v = 1$ molecule whose rotational wavefunction must be given by a rotation matrix $D_{L,M,1}(\theta, \phi, \chi)$ with one unit of angular momentum about the molecule's axis, $K = 1$. In the latter case, the angular momentum is produced by the degenerate π vibration itself. As a result, the selection rules above derive from the following product of 3-j symbols:

$$\begin{pmatrix} L' & 1 & L \\ M' & m & -M \end{pmatrix} \begin{pmatrix} L' & 1 & L \\ 0 & 1 & -1 \end{pmatrix}.$$

Because $\Delta L = 0$ transitions are allowed for π vibrations, one says that π vibrations possess **Q-branches** in addition to their R- and P- branches (with $\Delta L = 1$ and -1 , respectively).

In the figure shown below, the $v = 0 \rightarrow v = 1$ (fundamental) vibrational absorption spectrum of HCl is shown. Here the peaks at lower energy (to the right of the figure) belong to P-branch transitions and occur at energies given approximately by:

$$E = \hbar\omega_{\text{stretch}} + \left(\frac{h^2}{8\pi^2 I}\right) ((L-1)L - L(L+1)) = \hbar\omega_{\text{stretch}} - 2 \left(\frac{h^2}{8\pi^2 I}\right) L.$$

The R-branch transitions occur at higher energies given approximately by:

$$E = \hbar\omega_{\text{stretch}} + \left(\frac{h^2}{8\pi^2 I}\right) ((L+1)(L+2) - L(L+1)) = \hbar\omega_{\text{stretch}} + 2 \left(\frac{h^2}{8\pi^2 I}\right) (L+1).$$

The absorption that is "missing" from the figure below lying slightly below 2900 cm^{-1} is the **Q-branch** transition for which $L = L'$; it is absent because the selection rules forbid it.

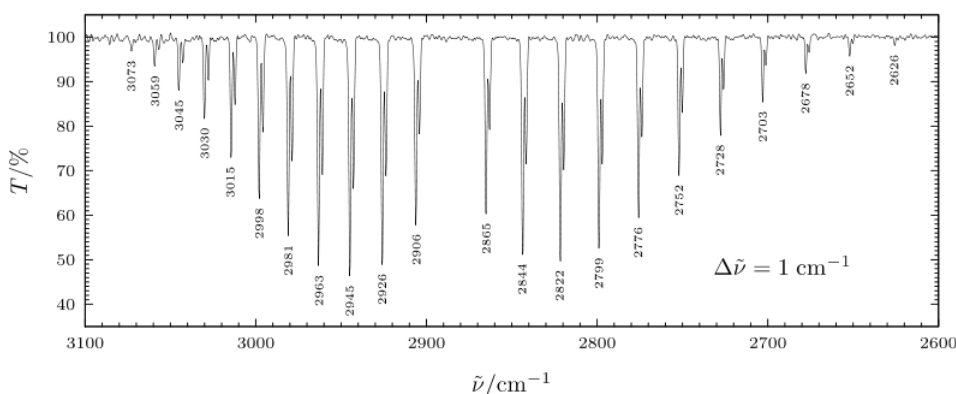


Figure 15.2.1: Infrared rotational-vibration spectrum of hydrochloric acid gas at room temperature. The P- and R- branches correspond, respectively, to $v=0$ and $v=1$. The IR absorption intensities depend on the isotopes present in the sample, e.g. $^1\text{H}-^{35}\text{Cl}$ vs. $^1\text{H}-^{37}\text{Cl}$. (CC BY-SA 2.5; mrtz)

It should be noted that the spacings between the experimentally observed peaks in HCl are not constant as would be expected based on the above P- and R- branch formulas. This is because the moment of inertia appropriate for the $v = 1$ vibrational level is different than that of the $v = 0$ level. These effects of vibration-rotation coupling can be modeled by allowing the $v = 0$ and $v = 1$ levels to have rotational energies written as

$$E = \hbar\omega_{\text{stretch}} \left(v + \frac{1}{2}\right) + \left(\frac{h^2}{8\pi^2 I_v}\right) (L(L+1))$$

where v and L are the vibrational and rotational quantum numbers. The P- and R- branch transition energies that pertain to these energy levels can then be written as:

$$E_P = \hbar\omega_{\text{stretch}} - \left[\left(\frac{h^2}{8\pi^2 I_1}\right) + \left(\frac{h^2}{8\pi^2 I_0}\right) \right] L + \left[\left(\frac{h^2}{8\pi^2 I_1}\right) - \left(\frac{h^2}{8\pi^2 I_0}\right) \right] L^2$$

$$E_R = \hbar\omega_{\text{stretch}} + 2 \left(\frac{h^2}{8\pi^2 I_1}\right) + 3 \left[\left(\frac{h^2}{8\pi^2 I_1}\right) - \left(\frac{h^2}{8\pi^2 I_0}\right) \right] L + \left[\left(\frac{h^2}{8\pi^2 I_1}\right) - \left(\frac{h^2}{8\pi^2 I_0}\right) \right] L^2.$$

Clearly, these formulas reduce to those shown earlier in the $I_1 = I_0$ limit.

If the vibrationally averaged bond length is longer in the $v = 1$ state than in the $v = 0$ state, which is to be expected, I_1 will be larger than I_0 , and therefore $\left[\left(\frac{h^2}{8\pi^2 I_1}\right) - \left(\frac{h^2}{8\pi^2 I_0}\right) \right]$ will be negative. In this case, the **spacing** between neighboring P-branch lines

will increase as shown above for HCl. In contrast, the fact that $\left[\left(\frac{h^2}{8\pi^2 I_1} \right) - \left(\frac{h^2}{8\pi^2 I_0} \right) \right]$ is negative causes the **spacing** between neighboring R- branch lines to decrease, again as shown for HCl.

This page titled [15.2: Vibration-Rotation Transitions](#) is shared under a [CC BY-NC-SA 4.0](#) license and was authored, remixed, and/or curated by [Jack Simons](#) via [source content](#) that was edited to the style and standards of the LibreTexts platform.

15.3: Electronic-Vibration-Rotation Transitions

The Electronic Transition Dipole and Use of Point Group Symmetry

Returning to the expression

$$R_{i,f} = \left(\frac{2\pi}{\hbar^2} \right) g(\omega_{f,i}) |\mathbf{E}_0 \cdot \langle \phi_f | \boldsymbol{\mu} | \phi_i \rangle|^2$$

for the rate of photon absorption, we realize that the electronic integral now involves

$$\langle \psi_{ef} | \boldsymbol{\mu} | \psi_{ei} \rangle = \boldsymbol{\mu}_{f,i}(\mathbf{R}),$$

a transition dipole matrix element between the initial $\phi_{e,i}$ and final $\phi_{e,f}$ electronic wavefunctions. This element is a function of the internal vibrational coordinates of the molecule, and again is a vector locked to the molecule's internal axis frame.

Molecular point-group symmetry can often be used to determine whether a particular transition's dipole matrix element will vanish and, as a result, the electronic transition will be "forbidden" and thus predicted to have zero intensity. If the direct product of the symmetries of the initial and final electronic states ψ_{ei} and ψ_{ef} do not match the symmetry of the electric dipole operator (which has the symmetry of its x, y, and z components; these symmetries can be read off the right most column of the character tables given in Appendix E), the matrix element will vanish.

For example, the formaldehyde molecule H_2CO has a ground electronic state (see Chapter 11) that has 1A_1 symmetry in the C_{2v} point group. Its $\pi \rightarrow \pi^*$ singlet excited state also has 1A_1 symmetry because both the π and π^* orbitals are of b_1 symmetry. In contrast, the lowest $n \rightarrow \pi^*$ singlet excited state is of 1A_2 symmetry because the highest energy oxygen centered n orbital is of b_2 symmetry and the π^* orbital is of b_1 symmetry, so the Slater determinant in which both the n and π^* orbitals are singly occupied has its symmetry dictated by the $b_2 \times b_1$ direct product, which is A_2 .

The $\pi \rightarrow \pi^*$ transition thus involves ground (1A_1) and excited (1A_1) states whose direct product ($A_1 \times A_1$) is of A_1 symmetry. This transition thus requires that the electric dipole operator possess a component of A_1 symmetry. A glance at the C_{2v} point group's character table shows that the molecular z-axis is of A_1 symmetry. Thus, if the light's electric field has a non-zero component along the C_2 symmetry axis (the molecule's z-axis), the $\pi \rightarrow \pi^*$ transition is predicted to be allowed. Light polarized along either of the molecule's other two axes cannot induce this transition.

In contrast, the $n \rightarrow \pi^*$ transition has a ground-excited state direct product of $B_2 \times B_1 = A_2$ symmetry. The C_{2v} 's point group character table clearly shows that the electric dipole operator (i.e., its x, y, and z components in the molecule-fixed frame) has no component of A_2 symmetry; thus, light of no electric field orientation can induce this $n \rightarrow \pi^*$ transition. We thus say that the $n \rightarrow \pi^*$ transition is E1 forbidden (although it is M1 allowed).

Beyond such electronic symmetry analysis, it is also possible to derive vibrational and rotational selection rules for electronic transitions that are E1 allowed. As was done in the vibrational spectroscopy case, it is conventional to expand $\boldsymbol{\mu}_{f,i}(\mathbf{R})$ in a power series about the equilibrium geometry of the initial electronic state (since this geometry is more characteristic of the molecular structure prior to photon absorption):

$$\boldsymbol{\mu}_{f,i}(\mathbf{R}) = \boldsymbol{\mu}_{f,i}(\mathbf{R}_e) + \sum_a \frac{\partial \boldsymbol{\mu}_{f,i}}{\partial R_a} (R_a - R_{a,e}) + \dots$$

The Franck-Condon Factors

The first term in this expansion, when substituted into the integral over the vibrational coordinates, gives $\boldsymbol{\mu}_{f,i}(\mathbf{R}_e) \langle \chi_{vf} | \chi_{vi} \rangle$, which has the form of the electronic transition dipole multiplied by the "overlap integral" between the initial and final vibrational wavefunctions. The $\boldsymbol{\mu}_{f,i}(\mathbf{R}_e)$ factor was discussed above; it is the electronic E1 transition integral evaluated at the equilibrium geometry of the absorbing state. Symmetry can often be used to determine whether this integral vanishes, as a result of which the E1 transition will be "forbidden".

Unlike the vibration-rotation case, the vibrational overlap integrals $\langle \chi_{vf} | \chi_{vi} \rangle$ do not necessarily vanish because χ_{vf} and χ_{vi} are no longer eigenfunctions of the same vibrational Hamiltonian. χ_{vf} is an eigenfunction whose potential energy is the **final** electronic state's energy surface; χ_{vi} has the **initial** electronic state's energy surface as its potential. The squares of these $\langle \chi_{vf} | \chi_{vi} \rangle$ integrals,

which are what eventually enter into the transition rate expression $R_{i,f} = \left(\frac{2\pi}{\hbar^2} \right) g(\omega_{f,i}) |\mathbf{E}_0 \cdot \langle \phi_f | \boldsymbol{\mu} | \phi_i \rangle|^2$, are called "**Franck-Condon factors**". Their relative magnitudes play strong roles in determining the relative intensities of various vibrational "bands" (i.e., peaks) within a particular electronic transition's spectrum.

Whenever an electronic transition causes a large change in the geometry (bond lengths or angles) of the molecule, the Franck-Condon factors tend to display the characteristic "broad progression" shown below when considered for one initial-state vibrational level v_i and various final-state vibrational levels v_f :

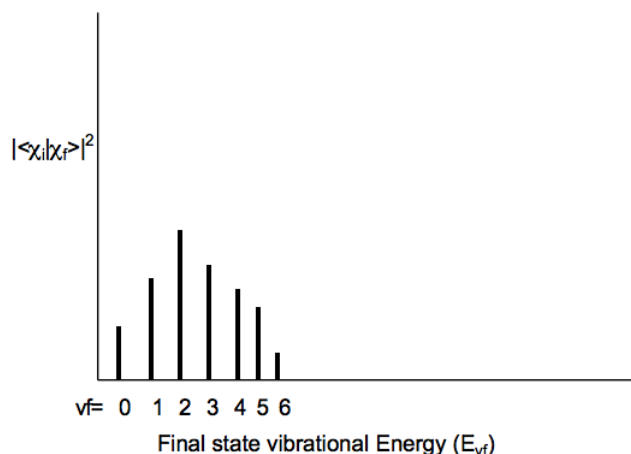


Figure 15.3.1: Insert caption here!

Notice that as one moves to higher v_f values, the energy spacing between the states ($E_{vf} - E_{vf-1}$) decreases; this, of course, reflects the anharmonicity in the excited state vibrational potential. For the above example, the transition to the $v_f = 2$ state has the largest Franck-Condon factor. This means that the overlap of the initial state's vibrational wavefunction χ_{vi} is largest for the final state's χ_{vf} function with $v_f = 2$.

As a qualitative rule of thumb, the larger the geometry difference between the initial and final state potentials, the broader will be the Franck-Condon profile (as shown above) and the larger the v_f value for which this profile peaks. Differences in harmonic frequencies between the two states can also broaden the Franck-Condon profile, although not as significantly as do geometry differences.

For example, if the initial and final states have very similar geometries and frequencies along the mode that is excited when the particular electronic excitation is realized, the following type of Franck-Condon profile may result:

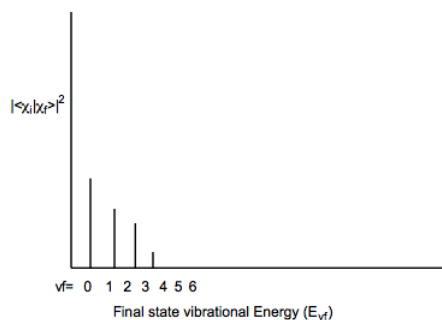


Figure 15.3.2: Insert caption here!

In contrast, if the initial and final electronic states have very different geometries and/or vibrational frequencies along some mode, a very broad Franck-Condon envelope peaked at high- v_f will result as shown below:

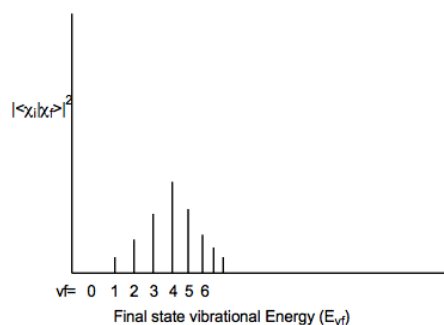


Figure 15.3.3: Insert caption here!

Vibronic Effects

The second term in the above expansion of the transition dipole matrix element $\sum_a \frac{\partial \mu_{f,i}}{\partial R_a} (R_a - R_{a,e})$ can become important to analyze when the first term $\mu_{f,i}(\mathbf{R}_e)$ vanishes (e.g., for reasons of symmetry). This dipole derivative term, when substituted into the integral over vibrational coordinates gives $\sum_a \frac{\partial \mu_{f,i}}{\partial R_a} \langle \chi_{vf} | (R_a - R_{a,e}) | \chi_{vi} \rangle$. Transitions for which $\mu_{f,i}(\mathbf{R}_e)$ vanishes but for which $\frac{\partial \mu_{f,i}}{\partial R_a}$ does not for the a^{th} vibrational mode are said to derive intensity through "vibronic coupling" with that mode. The intensities of such modes are dependent on how strongly the electronic dipole integral varies along the mode (i.e. on $\frac{\partial \mu_{f,i}}{\partial R_a}$) as well as on the magnitude of the vibrational integral $\langle \chi_{vf} | (R_a - R_{a,e}) | \chi_{vi} \rangle$.

An example of an E1 forbidden but "vibronically allowed" transition is provided by the singlet $n \rightarrow \pi^*$ transition of H_2CO that was discussed earlier in this section. As detailed there, the ground electronic state has 1A_1 symmetry, and the $n \rightarrow \pi^*$ state is of 1A_2 symmetry, so the E1 transition integral $\langle \psi_{ef} | \mu | \psi_{ei} \rangle$ vanishes for all three (x, y, z) components of the electric dipole operator μ . However, vibrations that are of b_2 symmetry (e.g., the H-C-H asymmetric stretch vibration) can induce intensity in the $n \rightarrow \pi^*$ transition as follows: (i) For such vibrations, the b_2 mode's $v_i = 0$ to $v_f = 1$ vibronic integral $\langle \chi_{vf} | (R_a - R_{a,e}) | \chi_{vi} \rangle$ will be non-zero and probably quite substantial (because, for harmonic oscillator functions these "fundamental" transition integrals are dominant- see earlier); (ii) Along these same b_2 modes, the electronic transition dipole integral **derivative** $\frac{\partial \mu_{f,i}}{\partial R_a}$ will be non-zero, even though the integral itself $\mu_{f,i}(\mathbf{R}_e)$ vanishes when evaluated at the initial state's equilibrium geometry.

To understand why the derivative $\frac{\partial \mu_{f,i}}{\partial R_a}$ can be non-zero for distortions (denoted R_a) of b_2 symmetry, consider this quantity in greater detail:

$$\frac{\partial \mu_{f,i}}{\partial R_a} = \frac{\partial}{\partial R} \langle \psi_{ef} | \mu | \psi_{ei} \rangle = \langle \frac{\partial \psi_{ef}}{\partial R_a} | \mu | \psi_{ei} \rangle + \langle \psi_{ef} | \mu | \frac{\partial \psi_{ei}}{\partial R_a} \rangle + \langle \psi_{ef} | \frac{\partial \mu}{\partial R_a} | \psi_{ei} \rangle.$$

The third integral vanishes because the derivative of the dipole operator itself $\mu = \sum_i e r_j + \sum_a Z_a e R_a$ with respect to the coordinates of atomic centers, yields an operator that contains only a sum of scalar quantities (the elementary charge e and the magnitudes of various atomic charges Z_a); as a result and because the integral over the electronic wavefunctions $\langle \psi + e f | \psi_{ei} \rangle$ vanishes, this contribution yields zero. The first and second integrals need not vanish by symmetry because the wavefunction derivatives $\frac{\partial \psi_{ef}}{\partial R_a}$ and $\frac{\partial \psi_{ei}}{\partial R_a}$ do **not** possess the same symmetry as their respective wavefunctions ψ_{ef} and ψ_{ei} . In fact, it can be shown that the symmetry of such a derivative is given by the direct product of the symmetries of its wavefunction and the symmetry of the vibrational mode that gives rise to the $\frac{\partial}{\partial R_a}$. For the H_2CO case at hand, the b_2 mode vibration can induce in the excited 1A_2 state a derivative component (i.e., $\frac{\partial \psi_{ef}}{\partial R_a}$) that is of 1B_1 symmetry) and this same vibration can induce in the 1A_1 ground state a derivative component of 1B_2 symmetry.

As a result, the contribution $\langle \frac{\partial \psi_{ef}}{\partial R_a} | \mu | \psi_{ei} \rangle$ to $\frac{\partial \mu_{f,i}}{\partial R_a}$ arising from vibronic coupling within the **excited** electronic state can be expected to be non-zero for components of the dipole operator μ that are of $(\frac{\partial \psi_{ef}}{\partial R_a} x \psi_{ei}) = (B_1 \times A_1) = B_1$ symmetry. Light polarized along the molecule's x-axis gives such a b_1 component to μ (see the C_{2v} character table in Appendix E). The second contribution

$\langle \psi_{ef} | \mu | \frac{\partial \psi_{ei}}{\partial R_a} \rangle$ can be non-zero for components of μ that are of $(\psi + ef \times \frac{\partial \psi_{ei}}{\partial R_a}) = (A_2 \times B_2) = B_1$ symmetry; again, light of x-axis polarization can induce such a transition.

In summary, electronic transitions that are E1 forbidden by symmetry can derive significant (e.g., in H_2CO the singlet $n \rightarrow \pi^*$ transition is rather intense) intensity through vibronic coupling. In such coupling, one or more vibrations (either in the initial or the final state) cause the respective electronic wavefunction to acquire (through $\frac{\partial \psi}{\partial R_a}$) a symmetry component that is different than that of ψ itself. The symmetry of $\frac{\partial \psi}{\partial R_a}$, which is given as the direct product of the symmetry of ψ and that of the vibration, can then cause the electric dipole integral $\langle \psi' | \mu | \frac{\partial \psi}{\partial R_a} \rangle$ to be non-zero even when $\langle \psi' | \mu | \psi \rangle$ is zero. Such vibronically allowed transitions are said to derive their intensity through vibronic borrowing.

Rotational Selection Rules for Electronic Transitions

Each vibrational peak within an electronic transition can also display rotational structure (depending on the spacing of the rotational lines, the resolution of the spectrometer, and the presence or absence of substantial line broadening effects such as those discussed later in this Chapter). The selection rules for such transitions are derived in a fashion that parallels that given above for the vibration-rotation case. The major difference between this electronic case and the earlier situation is that the vibrational transition dipole moment μ_{trans} appropriate to the former is replaced by $\mu_{f,i}(\mathbf{R}_e)$ for conventional (i.e., nonvibronic) transitions or $\frac{\partial \mu_{f,i}}{\partial R_a}$ (for vibronic transitions).

As before, when $\mu_{f,i}(\mathbf{R}_e)$ (or $\frac{\partial \mu_{f,i}}{\partial R_a}$) lies along the molecular axis of a linear molecule, the transition is denoted σ and $k = 0$ applies; when this vector lies perpendicular to the axis it is called π and $k = \pm 1$ pertains. The resultant **linear-molecule** rotational selection rules are the same as in the vibration-rotation case:

$$\Delta L = \pm 1, \text{ and } \Delta M = \pm 1, 0 \text{ (for } \sigma \text{ transitions).}$$

$$\Delta L = \pm 1, \text{ and } \Delta M = \pm 1, 0 \text{ (for } \pi \text{ transitions).}$$

In the latter case, the $L = L' = 0$ situation does not arise because a π transition has one unit of angular momentum along the molecular axis which would preclude both L and L' vanishing.

$$\Delta L = \pm 1, 0; \Delta M = \pm 1, 0; \text{ and } \Delta K = 0 \text{ (} L = L' = 0 \text{ is not allowed and all } \Delta L = 0 \text{ are forbidden when } K = K' = 0 \text{)}$$

which applies when $\mu_{f,i}(\mathbf{R}_e)$ or $\frac{\partial \mu_{f,i}}{\partial R_a}$ lies along the symmetry axis, and

$$\Delta L = \pm 1, 0; \Delta M = \pm 1, 0; \text{ and } \Delta K = \pm 1 \text{ (} L = L' = 0 \text{ is not allowed)}$$

which applies when $\mu_{f,i}(\mathbf{R}_e)$ or $\frac{\partial \mu_{f,i}}{\partial R_a}$ lies perpendicular to the symmetry axis.

This page titled [15.3: Electronic-Vibration-Rotation Transitions](#) is shared under a [CC BY-NC-SA 4.0](#) license and was authored, remixed, and/or curated by [Jack Simons](#) via [source content](#) that was edited to the style and standards of the LibreTexts platform.

15.4: Time Correlation Function Expressions for Transition Rates

The first-order E1 "golden-rule" expression for the rates of photon-induced transitions can be recast into a form in which certain specific physical models are easily introduced and insights are easily gained. Moreover, by using so-called equilibrium averaged time correlation functions, it is possible to obtain rate expressions appropriate to a large number of molecules that exist in a distribution of initial states (e.g., for molecules that occupy many possible rotational and perhaps several vibrational levels at room temperature).

State-to-State Rate of Energy Absorption or Emission

To begin, the expression obtained earlier

$$R_{i,f} = \left(\frac{2\pi}{\hbar^2} \right) g(\omega_{f,i}) |\mathbf{E}_0 \cdot \langle \phi_f | \mu | \Phi_i \rangle|^2,$$

that is appropriate to transitions between a particular initial state Φ_i and a specific final state Φ_f , is rewritten as

$$R_{i,f} = \left(\frac{2\pi}{\hbar^2} \right) \int g(\omega) |\mathbf{E}_0 \cdot \langle \phi_f | \mu | \phi_i \rangle|^2 \delta(\omega_{f,i} - \omega) d\omega.$$

Here, the $\delta(\omega_{f,i} - \omega)$ function is used to specifically enforce the "resonance condition" that resulted in the time-dependent perturbation treatment given in Chapter 14; it states that the photons' frequency ω must be resonant with the transition frequency $\omega_{f,i}$. It should be noted that by allowing ω to run over positive and negative values, the photon absorption (with $\omega_{f,i}$ positive and hence ω positive) and the stimulated emission case (with $\omega_{f,i}$ negative and hence ω negative) are both included in this expression (as long as $g(\omega)$ is defined as $g(|\omega|)$ so that the negative- ω contributions are multiplied by the light source intensity at the corresponding positive ω value).

The following integral identity can be used to replace the δ -function:

$$\delta(\omega_{f,i} - \omega) = \frac{1}{2\pi} \int_{-\infty}^{\infty} e^{i(\omega_{f,i} - \omega)t} dt$$

by a form that is more amenable to further development. Then, the state-to-state rate of transition becomes:

$$R_{i,f} = \left(\frac{1}{\hbar} \right) \int g(\omega) |\mathbf{E}_0 \cdot \langle \phi_f | \mu | \phi_i \rangle|^2 \int_{-\infty}^{\infty} e^{i(\omega_{f,i} - \omega)t} dt d\omega.$$

Averaging Over Equilibrium Boltzmann Population of Initial States

If this expression is then multiplied by the **equilibrium probability** ρ_i that the molecule is found in the state Φ_i and summed over all such initial states and summed over all final states Φ_f that can be reached from Φ_i with photons of energy $\hbar\omega$, the **equilibrium averaged rate of photon absorption** by the molecular sample is obtained:

$$R_{\text{eq.ave.}} = \left(\frac{1}{\hbar^2} \right) \sum_{i,f} \rho_i \int g(\omega) |\mathbf{E}_0 \cdot \langle \Phi_f | \mu | \Phi_i \rangle|^2 \int_{-\infty}^{\infty} e^{i(\omega_{f,i} - \omega)t} dt d\omega.$$

This expression is appropriate for an ensemble of molecules that can be in various initial states Φ_i with probabilities ρ_i . The corresponding result for transitions that originate in a particular state (Φ_i) but end up in any of the "allowed" (by energy and selection rules) final states reads:

$$R_{\text{state i.}} = \left(\frac{1}{\hbar^2} \right) \sum_f \int g(\omega) |\mathbf{E}_0 \cdot \langle \Phi_f | \mu | \Phi_i \rangle|^2$$

$$\int_{-\infty}^{\infty} e^{i(\omega_{f,i}-\omega)t} dt d\omega.$$

For a canonical ensemble, in which the number of molecules, the temperature, and the system volume are specified, ρ_i takes the form:

$$\phi_i = \frac{g_i}{Q} e^{-\frac{E_i^0}{kT}}$$

where Q is the canonical partition function of the molecules and g_i is the degeneracy of the state Φ_i whose energy is E_i^0 .

In the above expression for $R_{\text{eq.ave.}}$, a double sum occurs. Writing out the elements that appear in this sum in detail, one finds:

$$\sum_{i,f} \phi_i \mathbf{E}_0 \cdot \langle \Phi_i | \mu | \Phi_f \rangle \mathbf{E}_0 \cdot \langle \Phi_f | \mu | \Phi_i \rangle e^{i(\omega_{f,i})t}.$$

In situations in which one is interested in developing an expression for the intensity arising from transitions to **all** allowed final states, the sum over these final states can be carried out explicitly by first writing

$$\langle \Phi_f | \mu | \Phi_i \rangle e^{i(\omega_{f,i})t} = \langle \Phi_f | e^{\frac{iHt}{\hbar}} \mu e^{-\frac{iHt}{\hbar}} | \Phi_i \rangle$$

and then using the fact that the set of states $\{\Phi_k\}$ are complete and hence obey

$$\sum_k |\Phi_k\rangle \langle \Phi_k| = 1.$$

The result of using these identities as well as the **Heisenberg definition** of the time dependence of the dipole operator

$$\mu(t) = e^{\frac{iHt}{\hbar}} \mu e^{-\frac{iHt}{\hbar}},$$

is:

$$\sum_i \rho_i \langle \Phi | \mathbf{E}_0 \cdot \mu \mathbf{E}_0 \cdot \mu(t) | \Phi_i \rangle.$$

In this form, one says that the time dependence has been reduce to that of an equilibrium averaged (n.b., the $\sum_i \rho_i \langle \Phi_i | | \Phi_i \rangle$) **time correlation function** involving the component of the dipole operator along the external electric field at $t = 0$ ($\mathbf{E}_0 \cdot \mu$) and this component at a different time t ($\mathbf{E}_0 \cdot \mu(t)$).

Photon Emission and Absorption

If $\omega_{f,i}$ is positive (i.e., in the photon absorption case), the above expression will yield a non-zero contribution when multiplied by $e^{-i\omega t}$ and integrated over positive ω values. If $\omega_{f,i}$ is negative (as for stimulated photon emission), this expression will contribute, again when multiplied by $e^{-i\omega t}$, for negative ω -values. In the latter situation, ρ_i is the equilibrium probability of finding the molecule in the (excited) state from which emission will occur; this probability can be related to that of the lower state ρ_f by

$$\begin{aligned} \rho_{\text{excited}} &= \rho_{\text{lower}} e^{-\frac{(E_{\text{excited}}^0 - E_{\text{lower}}^0)}{kT}} \\ &= \rho_{\text{lower}} e^{-\frac{\hbar\omega}{kT}}. \end{aligned}$$

In this form, it is important to realize that the excited and lower states are treated as individual **states**, not as levels that might contain a degenerate set of states.

The absorption and emission cases can be combined into a single **net** expression for the rate of photon absorption by recognizing that the latter process leads to photon production, and thus must be entered with a negative sign. The resultant expression for the **net rate of decrease of photons** is:

$$R_{\text{eq.ave.net}} = \left(\frac{1}{\hbar^2} \right) \sum_i \rho_i \left(1 - e^{-\frac{\hbar\omega}{kT}} \right) \iint g(\omega) \langle \Phi_i | (\mathbf{E}_0 \cdot \boldsymbol{\mu}) \mathbf{E}_0 \cdot \boldsymbol{\mu}(t) | \Phi_i \rangle e^{-i\omega t} d\omega dt.$$

The Line Shape and Time Correlation Functions

Now, it is convention to introduce the so-called "line shape" function $I(\omega)$:

$$I(\omega) = \sum_i \rho_i \int \langle \Phi_i | (\mathbf{E}_0 \cdot \boldsymbol{\mu}) \mathbf{E}_0 \cdot \boldsymbol{\mu}(t) | \Phi_i \rangle e^{-i\omega t} dt$$

in terms of which the net photon absorption rate is

$$R_{\text{eq.ave.net}} = \left(\frac{1}{\hbar^2} \right) \left(1 - e^{-\hbar\omega/kT} \right) \int g(\omega) I(\omega) d\omega.$$

As stated above, the function

$$C(t) = \sum_i \rho_i \langle \Phi_i | \mathbf{E}_0 \cdot \boldsymbol{\mu} \mathbf{E}_0 \cdot \boldsymbol{\mu}(t) | \Phi_i \rangle$$

is called the equilibrium averaged **time correlation function** of the component of the electric dipole operator along the direction of the external electric field \mathbf{E}_0 . Its Fourier transform is $I(\omega)$, the **spectral line shape** function. The convolution of $I(\omega)$ with the light source's ($g(\omega)$) function, multiplied by $\left(1 - e^{-\frac{\hbar\omega}{kT}} \right)$, the correction for stimulated photon emission, gives the net rate of photon absorption.

This page titled [15.4: Time Correlation Function Expressions for Transition Rates](#) is shared under a [CC BY-NC-SA 4.0](#) license and was authored, remixed, and/or curated by [Jack Simons](#) via [source content](#) that was edited to the style and standards of the LibreTexts platform.

CHAPTER OVERVIEW

16: Collisions and Scattering

Collisions among molecules can also be viewed as a problem in time-dependent quantum mechanics. The perturbation is the "interaction potential" and the time dependence arises from the movement of the nuclear positions.

[16.1: One Dimensional Scattering](#)

[16.2: Multichannel Problems](#)

[16.3: Classical Treatment of Nuclear Motion](#)

[16.4: Wavepackets](#)

This page titled [16: Collisions and Scattering](#) is shared under a [CC BY-NC-SA 4.0](#) license and was authored, remixed, and/or curated by [Jack Simons](#) via [source content](#) that was edited to the style and standards of the LibreTexts platform.

16.1: One Dimensional Scattering

Atom-atom scattering on a single Born-Oppenheimer energy surface can be reduced to a one-dimensional Schrödinger equation by separating the radial and angular parts of the three-dimensional Schrödinger equation in the same fashion as used for the Hydrogen atom in Chapter 1. The resultant equation for the radial part $\psi(R)$ of the wavefunction can be written as:

$$-\left(\frac{\hbar^2}{2\mu}\right) \frac{1}{R^2} \frac{\partial}{\partial R} \left(R^2 \frac{\partial \psi}{\partial R} \right) + L(L+1) \frac{\hbar^2}{(2\mu R^2)} \psi + V(R)\psi = E\psi,$$

where L is the quantum number that labels the angular momentum of the colliding particles whose reduced mass is μ .

Defining $\Psi(R) = R\psi(R)$ and substituting into the above equation gives the following equation for Ψ :

$$\left(\frac{\hbar^2}{2\mu}\right) \frac{\partial^2 \Psi}{\partial R^2} + L(L+1) \frac{\hbar^2}{2\mu R^2} \Psi + V(R)\Psi = E\Psi.$$

The combination of the "centrifugal potential" $L(L+1) \frac{\hbar^2}{2\mu R^2}$ and the electronic potential $V(R)$ thus produce a total "effective potential" for describing the radial motion of the system.

The simplest reasonable model for such an effective potential is provided by the "square well" potential illustrated below. This model $V(R)$ could, for example, be applied to the $L = 0$ scattering of two atoms whose bond dissociation energy is D_e and whose equilibrium bond length for this electronic surface lies somewhere between $R = 0$ and $R = R_{\max}$.

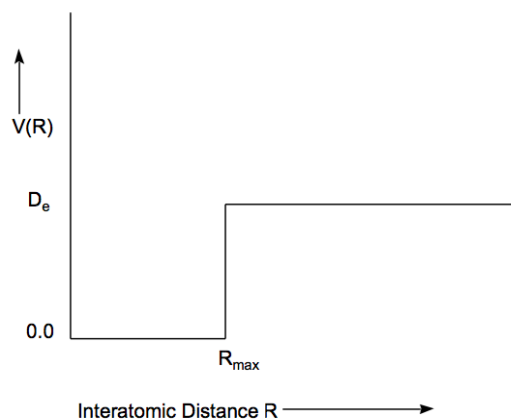


Figure 16.1.1: Insert caption here!

The piecewise constant nature of this particular $V(R)$ allows exact solutions to be written both for bound and scattering states because the Schrödinger equation

$$\begin{aligned} -\left(\frac{\hbar^2}{2\mu}\right) \frac{d^2 \Psi}{dR^2} &= E\Psi \quad (\text{for } 0 \leq R \leq R_{\max}) \\ -\left(\frac{\hbar^2}{2\mu}\right) \frac{d^2 \Psi}{dR^2} + D_e \Psi &= E\Psi \quad (R_{\max} \leq R < \infty) \end{aligned}$$

admits simple sinusoidal solutions.

Bound States

The **bound states** are characterized by having $E < D_e$. For the inner region, the two solutions to the above equation are

$$\Psi_1(R) = A \sin(kR)$$

and

$$\Psi_2(R) = B \cos(kR)$$

where

$$k = \sqrt{\frac{2\mu E}{\hbar^2}}$$

is termed the "local wave number" because it is related to the momentum values for the $e^{\pm ikR}$ components of such a function:

$$\frac{-i\hbar\partial e^{\pm ikR}}{\partial R} = \hbar k e^{\pm ikR}.$$

The $\cos(kR)$ solution must be excluded (i.e., its amplitude B in the general solution of the Schrödinger equation must be chosen equal to 0.0) because this function does not vanish at $R = 0$, where the potential moves to infinity and thus the wavefunction must vanish. This means that only the

$$\Psi = A \sin(kR)$$

term remains for this inner region.

Within the asymptotic region ($R > R_{max}$) there are also two solutions to the Schrödinger equation:

$$\Psi_3 = C e^{-\kappa R}$$

and

$$\Psi_4 = D e^{\kappa R}$$

where

$$\kappa = \sqrt{\frac{2\mu(D_e - E)}{\hbar^2}}.$$

Clearly, one of these functions is a decaying function of R for large R and the other Ψ_4 grows exponentially for large R . The latter's amplitude D must be set to zero because this function generates a probability density that grows larger and larger as R penetrates deeper and deeper into the classically forbidden region (where $E < V(R)$).

To connect Ψ_1 in the inner region to Ψ_3 in the outer region, we use the fact that Ψ and $\frac{d\Psi}{dR}$ must be continuous except at points R where $V(R)$ undergoes an infinite discontinuity (see Chapter 1). Continuity of Ψ at R_{max} gives:

$$A \sin(kR_{max}) = C e^{-\kappa R_{max}},$$

and continuity of $\frac{d\Psi}{dR}$ at R_{max} yields

$$A k \cos(kR_{max}) = -\kappa C e^{-\kappa R_{max}}$$

These two equations allow the ratio C/A as well as the energy E (which appears in κ and in k) to be determined:

$$\frac{A}{C} = \frac{-\kappa}{k} \frac{e^{-\kappa R_{max}}}{\cos(kR_{max})}.$$

The condition that determines E is based on the well known requirement that the determinant of coefficients must vanish for homogeneous linear equations to have non-trivial solutions (i.e., not $A = C = 0$):

$$\det \begin{pmatrix} \sin(kR_{max}) & -e^{-\kappa R_{max}} \\ k \cos(kR_{max}) & \kappa e^{-\kappa R_{max}} \end{pmatrix} = 0$$

The vanishing of this determinant can be rewritten as

$$\kappa \sin(kR_{max}) e^{-\kappa R_{max}} + k \cos(kR_{max}) e^{-\kappa R_{max}} = 0$$

or

$$\tan(kR_{max}) = \frac{-\kappa}{k}.$$

When employed in the expression for A/C , this result gives

$$\frac{A}{C} = \frac{e^{-\kappa R_{\max}}}{\sin(kR_{\max})}$$

For very large D_e compared to E , the above equation for E reduces to the familiar "particle in a box" energy level result since $\frac{k}{\kappa}$ vanishes in this limit, and thus $\tan(kR_{\max}) = 0$, which is equivalent to $\sin(kR_{\max}) = 0$, which yields the familiar $E = \frac{n^2 h^2}{8\mu R_{\max}^2}$ and $\frac{C}{A} = 0$, so $\Psi = A \sin(kR)$.

When D_e is not large compared to E , the full transcendental equation $\tan(kR_{\max}) = -\frac{k}{\kappa}$ must be solved numerically or graphically for the eigenvalues E_n , $n = 1, 2, 3, \dots$. These energy levels, when substituted into the definitions for k and κ give the wavefunctions:

$$\Psi = A \sin(kR) \text{ (for } 0 \leq R \leq R_{\max} \text{)}$$

$$\Psi = A \sin(kR_{\max}) e^{\kappa R_{\max}} e^{-\kappa R} \text{ (for } R_{\max} \leq R < \infty \text{)}.$$

The one remaining unknown A can be determined by requiring that the modulus squared of the wavefunction describe a probability density that is normalized to unity when integrated over all space:

$$\int_0^{\infty} |\Psi|^2 dR = 1.$$

Note that this condition is equivalent to

$$\int_0^{\infty} |\Psi|^2 R^2 dR = 1$$

which would pertain to the original radial wavefunction. In the case of an infinitely deep potential well, this normalization condition reduces to

$$\int_0^{R_{\max}} A^2 \sin^2(kR) dR = 1$$

which produces

$$A = \sqrt{\frac{2}{R_{\max}}}.$$

Scattering States

The **scattering states** are treated in much the same manner. The functions Ψ_1 and Ψ_2 arise as above, and the amplitude of Ψ_2 must again be chosen to vanish because Ψ must vanish at $R = 0$ where the potential moves to infinity. However, in the exterior region ($R > R_{\max}$), the two solutions are now written as:

$$\Psi_3 = C e^{ik'R}$$

$$\Psi_4 = D e^{-ik'R}$$

where the large- R local wavenumber

$$k' = \sqrt{\frac{2\mu(E - D_e)}{\hbar^2}}$$

arises because $E > D_e$ for scattering states.

The conditions that Ψ and $\frac{d\Psi}{dR}$ be continuous at R_{\max} still apply:

$$A \sin(kR_{\max}) = C e^{ik'R_{\max}} - ik'D e^{-ik'R_{\max}}.$$

and

$$k A \cos(kR_{\max}) = ik' C e^{ik'R_{\max}} - ik' D e^{-ik'R_{\max}}.$$

However, these two equations (in **three** unknowns A, C, and D) can no longer be solved to generate eigenvalues E and amplitude ratios. There are now three amplitudes as well as the E value but only these two equations plus a normalization condition to be used. The result is that the energy no longer is specified by a boundary condition; it can take on any value. We thus speak of scattering states as being "in the continuum" because the allowed values of E form a continuum beginning at $E = D_e$ (since the zero of energy is defined in this example as at the bottom of the potential well).

The $R > R_{\max}$ components of Ψ are commonly referred to as "incoming"

$$\Psi_{\text{in}} = D e^{-ik'R}$$

and "outgoing"

$$\Psi_{\text{out}} = C e^{ik'R}$$

because their radial momentum eigenvalues are $-\hbar k'$ and $\hbar k'$, respectively. It is a common convention to define the amplitude D so that the **flux** of incoming particles is unity.

Choosing

$$D = \sqrt{\frac{\mu}{\hbar k'}}$$

produces an incoming wavefunction whose current density is:

$$\begin{aligned} S(R) &= \frac{-i\hbar}{2\mu} \left[\Psi_{\text{in}}^* \left(\frac{d}{dR} \Psi_{\text{in}} \right) - \left(\frac{d\Psi_{\text{in}}}{dR} \right)^* \Psi_{\text{in}} \right] \\ &= |D|^2 \left(\frac{-i\hbar}{2\mu} \right) [-2ik'] \\ &= -1. \end{aligned}$$

This means that there is one unit of current density moving inward (this produces the minus sign) for all values of R at which Ψ_{in} is an appropriate wavefunction (i.e., $R > R_{\max}$). This condition takes the place of the probability normalization condition specified in the boundstate case when the modulus squared of the total wavefunction is required to be normalized to unity over all space. Scattering wavefunctions can not be so normalized because they do not decay at large R; for this reason, the flux normalization condition is usually employed. The magnitudes of the outgoing (C) and short range (A) wavefunctions relative to that of the incoming function (D) then provide information about the scattering and "trapping" of incident flux by the interaction potential.

Once D is so specified, the above two boundary matching equations are written as a set of two inhomogeneous linear equations in two unknowns (A and C):

$$A \sin(kR_{\max}) - C e^{ik'R_{\max}} = D e^{-ik'R_{\max}}$$

and

$$k A \cos(kR_{\max}) - ik' C e^{ik'R_{\max}} = -ik' D e^{-ik'R_{\max}}$$

or

$$\begin{pmatrix} \sin(kR_{\max}) & -e^{ik'R_{\max}} \\ k \cos(kR_{\max}) & -ik' e^{ik'R_{\max}} \end{pmatrix} \begin{pmatrix} A \\ C \end{pmatrix} = \begin{pmatrix} D e^{-ik'R_{\max}} \\ -ik' D e^{-ik'R_{\max}} \end{pmatrix}.$$

Non-trivial solutions for A and C will exist except when the determinant of the matrix on the left side vanishes:

$$-ik' \sin(kR_{\max}) + k \cos(kR_{\max}) = 0,$$

which can be true only if

$$\tan(kR_{\max}) = \frac{ik'}{k}.$$

This equation is not obeyed for any (real) value of the energy E , so solutions for A and C in terms of the specified D can always be found.

In summary, specification of unit incident flux is made by choosing D as indicated above. For any collision energy $E > D_e$, the 2×1 array on the right hand side of the set of linear equations written above can be formed, as can the 2×2 matrix on the left side. These linear equations can then be solved for A and C . The overall wavefunction for this E is then given by:

$$\begin{aligned}\Psi &= A \sin(kR) && (\text{for } 0 \leq R \leq R_{\max}) \\ \Psi &= C e^{ik'R} + D e^{-ik'R} && (\text{for } R_{\max} \leq R < \infty).\end{aligned}$$

Shape Resonance States

If the angular momentum quantum number L in the effective potential introduced earlier is non-zero, this potential has a repulsive component at large R . This repulsion can combine with short-range attractive interactions due, for example, to chemical bond forces, to produce an effective potential that one can model in terms of simple piecewise functions shown below.

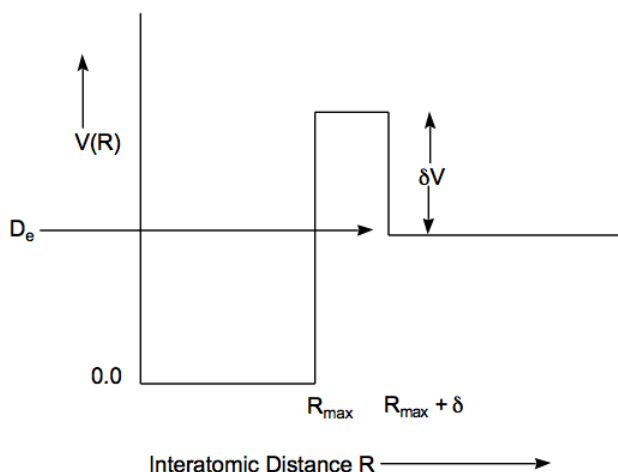


Figure 16.1.1: Insert caption here!

Again, the piecewise nature of the potential allows the one-dimensional Schrödinger equation to be solved analytically. For energies below D_e , one again finds bound states in much the same way as illustrated above (but with the exponentially decaying function $e^{-\kappa'R}$ used in the region $R_{\max} \leq R \leq R_{\max} + \delta$, with $\kappa' = \sqrt{2\mu(-D_e - \delta V - E)/\hbar^2}$).

For energies lying above $D_e + \delta V$, scattering states occur and the four amplitudes of the functions $(\sin(kR)$, $e^{(\pm ik'R)}$ with $k' = \sqrt{2\mu(D_e + \delta V + E)/\hbar^2}$, and $e^{(ik'R)}$) appropriate to each R -region are determined in terms of the amplitude of the incoming asymptotic function $D e^{(-ik'R)}$ from the four equations obtained by matching Ψ and $\frac{d\Psi}{dR}$ at R_{\max} and at $R_{\max} + \delta$.

For energies lying in the range $D_e < E < D_e + \delta V$, a qualitatively different class of scattering function exists. These so-called **shape resonance** states occur at energies that are determined by the condition that the amplitude of the wavefunction within the barrier (i.e., for $0 \leq R \leq R_{\max}$) be large so that incident flux successfully tunnels through the barrier and builds up, through constructive interference, large probability amplitude there. Let us now turn our attention to this specific energy regime.

The piecewise solutions to the Schrödinger equation appropriate to the shaperesonance case are easily written down:

$$\begin{aligned}\Psi &= A \sin(kR) && (\text{for } 0 \leq R \leq R_{\max}) \\ \Psi &= B_+ e^{\kappa'R} + B_- e^{-\kappa'R} && (\text{for } R_{\max} \leq R \leq R_{\max} + \delta) \\ \Psi &= C e^{ik'R} + D e^{-ik'R} && (\text{for } R_{\max} + \delta \leq R \leq \infty)\end{aligned}$$

Note that both exponentially growing and decaying functions are acceptable in the $R_{\max} \leq R \leq R_{\max} + \delta$ region because this region does not extend to $R = \infty$. There are four amplitudes (A , B_+ , B_- , and C) that must be expressed in terms of the specified

amplitude D of the incoming flux. Four equations that can be used to achieve this goal result when Ψ and $\frac{d\Psi}{dR}$ are matched at R_{max} and at $R_{max} + \delta$:

$$\begin{aligned} A \sin(kR_{max}) &= B_+ e^{\kappa' R_{max}} + B_- e^{-\kappa' R_{max}}, \\ A k \cos(kR_{max}) &= \kappa' B_+ e^{\kappa' R_{max}} - \kappa' B_- e^{-\kappa' R_{max}}, \\ B_+ e^{\kappa'(R_{max}+\delta)} + B_- e^{-\kappa'(R_{max}+\delta)} &= C e^{ik'(R_{max}+\delta)} + D e^{-ik'(R_{max}+\delta)}, \\ \kappa' B_+ e^{\kappa'(R_{max}+\delta)} - \kappa' B_- e^{-\kappa'(R_{max}+\delta)} &= ik' C e^{ik'(R_{max}+\delta)} - ik' D e^{-ik'(R_{max}+\delta)}. \end{aligned}$$

It is especially instructive to consider the value of A/D that results from solving this set of four equations in four unknowns because the modulus of this ratio provides information about the relative amount of amplitude that exists inside the centrifugal barrier in the attractive region of the potential compared to that existing in the asymptotic region as incoming flux.

The result of solving for A/D is:

$$\frac{A}{D} = \frac{4\kappa' e^{-ik'(R_{max}+\delta)}}{\left[\frac{e^{\kappa'\delta}(ik' - \kappa')(\kappa' \sin(kR_{max}) + k \cos(kR_{max}))}{ik'} + \frac{e^{-\kappa'\delta}(ik' + \kappa')(\kappa' \sin(kR_{max}) - k \cos(kR_{max}))}{ik'} \right]^{-1}}$$

Further, it is instructive to consider this result under conditions of a high (large $D_e + \delta V - E$) and thick (large δ) barrier. In such a case, the "tunnelling factor" $e^{-\kappa'\delta}$ will be very small compared to its counterpart $e^{\kappa'\delta}$, and so

$$\frac{A}{D} = 4 \frac{ik' \kappa'}{ik' - \kappa'} e^{-ik'(R_{max}+\delta)} \frac{e^{-\kappa'\delta}}{\kappa' \sin(kR_{max}) + k \cos(kR_{max})}.$$

The $e^{-\kappa'\delta}$ factor in A/D causes the magnitude of the wavefunction inside the barrier to be small in most circumstances; we say that incident flux must tunnel through the barrier to reach the inner region and that $e^{-\kappa'\delta}$ gives the probability of this tunnelling. The magnitude of the A/D factor could become large if the collision energy E is such that

$$\kappa' \sin(kR_{max}) + k \cos(kR_{max})$$

is small. In fact, if

$$\tan(kR_{max}) = \frac{-k}{\kappa'}$$

this denominator factor in A/D will vanish and A/D will become infinite. Note that the above condition is similar to the energy quantization condition

$$\tan(kR_{max}) = \frac{-k}{\kappa}$$

that arose when bound states of a finite potential well were examined earlier in this Chapter. There is, however, an important difference. In the bound-state situation

$$k = \sqrt{\frac{2\mu E}{\hbar^2}}$$

and

$$\kappa = \sqrt{\frac{2\mu(D_e - E)}{\hbar^2}};$$

in this shape-resonance case, k is the same, but

$$\kappa' = \sqrt{\frac{2\mu(D_e + \delta V - E)}{\hbar^2}}$$

rather than κ occurs, so the two $\tan(kR_{max})$ equations are not identical.

However, in the case of a very high barrier (so that κ' is much larger than k), the denominator

$$\kappa' \sin(kR_{max}) + k \cos(kR_{max}) \approx \kappa' \sin(kR_{max})$$

in A/D can become small if

$$\sin(kR_{max}) \approx 0.$$

This condition is nothing but the energy quantization condition that would occur for the particle-in-a-box potential shown below.

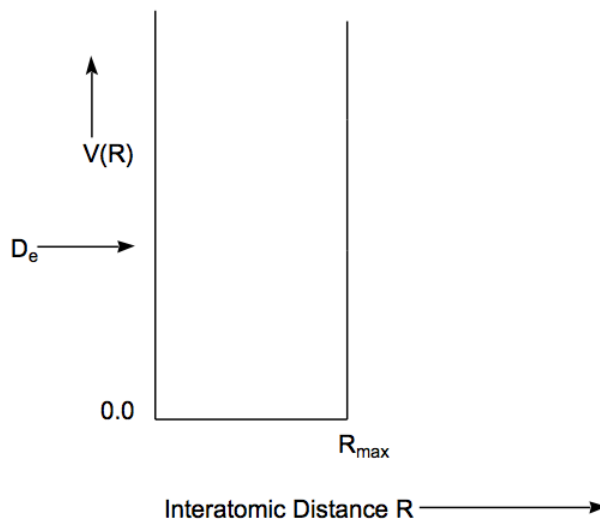


Figure 16.1.4: Insert caption here!

This potential is identical to the true effective potential for $0 \leq R \leq R_{max}$, but extends to infinity beyond R_{max} ; the barrier and the dissociation asymptote displayed by the true potential are absent.

In summary, when a barrier is present on a potential energy surface, at energies above the dissociation asymptote D_e but below the top of the barrier ($D_e + \delta V$ here), one can expect shape-resonance states to occur at "special" scattering energies E . These so-called resonance energies can often be approximated by the bound-state energies of a potential that is identical to the potential of interest in the inner region ($0 \leq R \leq R_{max}$ here) but that extends to infinity beyond the top of the barrier (i.e., beyond the barrier, it does not fall back to values below E).

The chemical significance of shape resonances is great. Highly rotationally excited molecules may have more than enough total energy to dissociate (D_e), but this energy may be "stored" in the rotational motion, and the vibrational energy may be less than D_e . In terms of the above model, high angular momentum may produce a significant barrier in the effective potential, but the system's vibrational energy may lie significantly below D_e . In such a case, and when viewed in terms of motion on an angular momentum modified effective potential, the lifetime of the molecule with respect to dissociation is determined by the rate of tunnelling through the barrier.

For the case at hand, one speaks of "rotational predissociation" of the molecule. The lifetime τ can be estimated by computing the frequency ν at which flux existing inside R_{max} strikes the barrier at R_{max}

$$\nu = \frac{\hbar k}{2\mu R_{max}} \text{ (sec}^{-1}\text{)}$$

and then multiplying by the probability P that flux tunnels through the barrier from R_{max} to $R_{max} + \delta$:

$$P = e^{-2\kappa'\delta}.$$

The result is that

$$\frac{1}{\tau} = \frac{\hbar k}{2\mu R_{max}} e^{-2\kappa'\delta}$$

with the energy E entering into k and κ' being determined by the resonance condition: $(\kappa' \sin(kR_{max}) + k \cos(kR_{max})) = \text{minimum}$.

Although the examples treated above involved piecewise constant potentials (so the Schrödinger equation and the boundary matching conditions could be solved exactly), many of the characteristics observed carry over to more chemically realistic situations. As discussed, for example, in ***Energetic Principles of Chemical Reactions*** , J. Simons, Jones and Bartlett, Portola Valley, Calif. (1983), one can often model chemical reaction processes in terms of:

1. motion along a "reaction coordinate" (s) from a region characteristic of reactant materials where the potential surface is positively curved in all direction and all forces (i.e., gradients of the potential along all internal coordinates) vanish,
2. to a transition state at which the potential surface's curvature along s is negative while all other curvatures are positive and all forces vanish,
3. onward to product materials where again all curvatures are positive and all forces vanish.

Within such a "reaction path" point of view, motion transverse to the reaction coordinate s is often modelled in terms of local harmonic motion although more sophisticated treatments of the dynamics is possible. In any event, this picture leads one to consider motion along a single degree of freedom (s), with respect to which much of the above treatment can be carried over, coupled to transverse motion along all other internal degrees of freedom taking place under an entirely positively curved potential (which therefore produces restoring forces to movement away from the "streambed" traced out by the reaction path s).

This page titled [16.1: One Dimensional Scattering](#) is shared under a [CC BY-NC-SA 4.0](#) license and was authored, remixed, and/or curated by [Jack Simons](#) via [source content](#) that was edited to the style and standards of the LibreTexts platform.

16.2: Multichannel Problems

When excited electronic states are involved, couplings between two or more electronic surfaces may arise. Dynamics occurring on an excited-state surface may evolve in a way that produces flux on another surface. For example, collisions between an electronically excited $1s2s(^3S)$ He atom and a ground-state $1s^2(^1S)$ He atom occur on a potential energy surface that is repulsive at large R (due to the repulsive interaction between the closed-shell $1s^2$ He and the large $2s$ orbital) but attractive at smaller R (due to the $\sigma^2\sigma^{*1}$ orbital occupancy arising from the three $1s$ -derived electrons). The ground-state potential energy surface for this system (pertaining to two $1s^2(^1S)$ He atoms) is repulsive at small R values (because of the $\sigma^2\sigma^{*2}$ nature of the electronic state). In this case, there are two Born-Oppenheimer electronic-nuclear motion states that are degenerate and thus need to be combined to achieve a proper description of the dynamics:

$$\Psi_1 = |\sigma^2\sigma^{*2}|\Psi_{\text{ground.}}(R, \theta, \phi)$$

pertaining to the ground electronic state and the scattering state $\Psi_{\text{ground.}}$ on this energy surface, and

$$\Psi_2 = |\sigma^2\sigma^{*1}2\sigma^1|\Psi_{\text{ex.}}(R, \theta, \phi)$$

pertaining to the excited electronic state and the nuclear-motion state $\Psi_{\text{ex.}}$ on this energy surface. Both of these wavefunctions can have the same energy E ; the former has high nuclear-motion energy and low electronic energy, while the latter has higher electronic energy and lower nuclear-motion energy.

A simple model that can be used to illustrate the two-state couplings that arise in such cases is introduced through the two one-dimensional piecewise potential surfaces shown below.

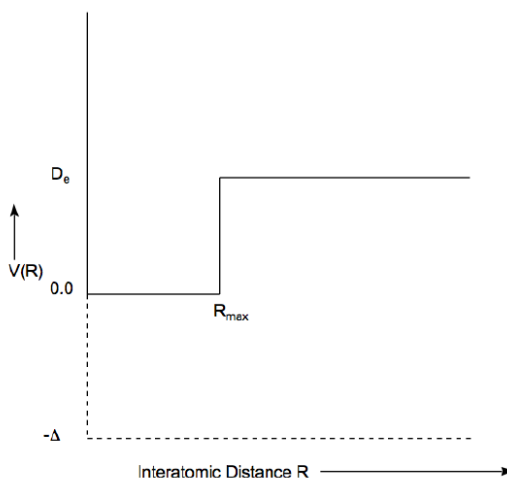


Figure 16.2.1: Insert Caption here!

The dashed energy surface

$$V(R) = -\Delta \text{ for } 0 \leq R < \infty$$

provides a simple representation of a repulsive lower-energy surface, and the solid-line plot represents the excited-state surface that has a well of depth D_e and whose well lies Δ above the ground-state surface.

In this case, and for energies lying above zero (for $E < 0$, only nuclear motion on the lower energy dashed surface is "open" (i.e., accessible)) yet below D_e , the nuclear motion wavefunction can have amplitudes belonging to both surfaces. That is, the total (electronic and nuclear) wavefunction consists of two portions that can be written as:

$$\Psi = A\phi\sin(kR) + \phi''A''\sin(k''R) \text{ (for } 0 \leq R \leq R_{\text{max}})$$

and

$$\Psi = A\phi\sin(kR_{\text{max}})e^{\kappa R_{\text{max}}}e^{-\kappa R} + \phi''A''\sin(k''R) \text{ (for } R_{\text{max}} \leq R < \infty),$$

where ϕ and ϕ'' denote the electronic functions belonging to the upper and lower energy surfaces, respectively. The wavenumbers k and k'' are defined as:

$$k = \sqrt{\frac{2\mu E}{\hbar^2}}$$

$$k'' = \sqrt{\frac{2\mu(E + \Delta)}{\hbar^2}}$$

and κ is as before

$$\kappa = \sqrt{\frac{2\mu(D_e - E)}{\hbar^2}}.$$

For the lower-energy surface, only the $\sin(k''R)$ function is allowed because the $\cos(k''R)$ function does not vanish at $R=0$.

The Coupled Channel Equations

In such cases, the relative amplitudes (A and A'') of the nuclear motion wavefunctions on each surface must be determined by substituting the above "two-channel" wavefunction (the word channel is used to denote separate asymptotic states of the system; in this case, the ϕ and ϕ'' electronic states) into the full Schrödinger equation. In Chapter 3, the couplings among Born-Oppenheimer states were so treated and resulted in the following equation:

$$[(E_j(R) - E)\Xi_j(R) + T\Xi_j(R)] = - \sum_i \left[\langle \Psi_j | T | \Psi_i \rangle (R) \Xi_i(R) + \sum_{a=1, M} \left(\frac{-\hbar^2}{m_a} \right) \langle \Psi_j | \nabla_a | \Psi_i \rangle (R) \cdot \nabla_a \Xi_i(R) \right]$$

where $E_j(R)$ and $\Xi_j(R)$ denote the electronic energy surfaces and nuclear-motion wavefunctions, Ψ_j denote the corresponding electronic wavefunctions, and the ∇_a represent derivatives with respect to the various coordinates of the nuclei. Changing to the notation used in the one-dimensional model problem introduced above, these so-called **coupled-channel** equations read:

$$\left[(-\Delta - E) - \frac{\hbar^2}{2\mu} \frac{d^2}{dR^2} \right] A'' \sin(k''R) = - \left[\langle \phi'' | - \frac{\hbar^2}{2\mu} \frac{d^2}{dR^2} | \phi'' \rangle A'' \sin(k''R) + \left(-\frac{\hbar^2}{\mu} \right) \langle \phi'' | \frac{d}{dR} | \phi \rangle \frac{d}{dR} A \sin(kR) \right]$$

(for $0 \leq R \leq R_{\max}$),

$$\left[(-\Delta - E) - \frac{\hbar^2}{2\mu} \frac{d^2}{dR^2} \right] A'' \sin(k''R) = - \left[\langle \phi'' | - \frac{\hbar^2}{2\mu} \frac{d^2}{dR^2} | \phi'' \rangle A'' \sin(k''R) + \left(-\frac{\hbar^2}{\mu} \right) \langle \phi'' | \frac{d}{dR} | \phi \rangle \frac{d}{dR} A \phi \sin(kR_{\max}) e^{\kappa R_{\max}} e^{-\kappa R} \right]$$

(for $0 \leq R < \infty$),

when the index j refers to the ground-state surfaces ($V(R) = -\Delta$, for $0 < R < \infty$), and

$$\left[(0 - E) - \frac{\hbar^2}{2\mu} \frac{d^2}{dR^2} \right] A \sin(kR) = - \left[\langle \phi | - \frac{\hbar^2}{2\mu} \frac{d^2}{dR^2} | \phi \rangle A \sin(kR) + \left(-\frac{\hbar^2}{\mu} \right) \langle \phi | \frac{d}{dR} | \phi'' \rangle \frac{d}{dR} A'' \sin(k''R) \right]$$

(for $0 \leq R \leq R_{\max}$)

$$\left[(D_e - E) - \frac{\hbar^2}{2\mu} \frac{d^2}{dR^2} \right] A \sin(kR_{\max}) e^{\kappa R_{\max}} e^{-\kappa R} = - \left[\langle \phi | - \frac{\hbar^2}{2\mu} \frac{d^2}{dR^2} | \phi \rangle A \sin(kR_{\max}) e^{\kappa R_{\max}} e^{-\kappa R} - \left(\frac{\hbar^2}{\mu} \right) \langle \phi | \frac{d}{dR} | \phi'' \rangle \frac{d}{dR} A'' \sin(k''R) \right]$$

(for $R_{\max} \leq R < \infty$)

when the index j refers to the excited-state surface (where $V(R) = 0$, for $0 < R \leq R_{\max}$ and $V(R) = D_e$ for $R_{\max} \leq R < \infty$).

Clearly, if the right-hand sides of the above equations are ignored, one simply recaptures the Schrödinger equations describing motion on the separate potential energy surfaces:

$$\left[(-\Delta - E) - \frac{\hbar^2}{2\mu} \frac{d^2}{dR^2} \right] A'' \sin(k''R) = 0$$

(for $0 \leq R \leq R_{\max}$),

$$\left[(-\Delta - E) - \frac{\hbar^2}{2\mu} \frac{d^2}{dR^2} \right] A'' \sin(k''R) = 0$$

(for $0 \leq R < \infty$);

that describe motion on the lower-energy surface, and

$$\left[(0 - E) - \frac{\hbar^2}{2\mu} \frac{d^2}{dR^2} \right] A \sin(kR) = 0$$

(for $0 \leq R \leq R_{\max}$),

$$\left[(D_e - E) - \frac{\hbar^2}{2\mu} \frac{d^2}{dR^2} \right] A \sin(kR_{\max}) e^{\kappa R_{\max}} e^{-\kappa R} = 0$$

(for $R_{\max} \leq R < \infty$)

describing motion on the upper surface on which the bonding interaction occurs. The terms on the right-hand sides provide the couplings that cause the true solutions to the Schrödinger equation to be combinations of solutions for the two separate surfaces.

In applications of the coupled-channel approach illustrated above, coupled sets of second order differential equations (two in the above example) are solved by starting with a specified flux in one of the channels and a chosen energy E . For example, one might specify the amplitude A to be unity to represent preparation of the system in a bound vibrational level (with $E < D_e$) of the excited electronic-state potential. One would then choose E to be one of the eigenenergies of that potential. Propagation methods could be used to solve the coupled differential equations subject to these choices of E and A . The result would be the determination of the amplitude A' of the wavefunction on the groundstate surface. The ratio A'/A provides a measure of the strength of coupling between the two Born-Oppenheimer states

Perturbative Treatment

Alternatively, one can treat the coupling between the two states via time dependent perturbation theory. For example, by taking $A = 1.0$ and choosing E to be one of the eigenenergies of the excited-state potential, one is specifying that the system is initially (just prior to $t = 0$) prepared in a state whose wavefunction is:

$$\begin{aligned} \Psi_{\text{ex}}^0 &= \phi \sin(kR) \text{ (for } 0 \leq R \leq R_{\max} \text{)} \\ \Psi_{\text{ex}}^0 &= \phi \sin(kR_{\max}) e^{\kappa R_{\max}} e^{-\kappa R} \text{ (for } R_{\max} \leq R \leq \infty \text{)}. \end{aligned}$$

From $t = 0$ on, the coupling to the other state

$$\Psi_{\text{ground}}^0 = \phi' \sin(k'R) \text{ (for } 0 \leq R < \infty$$

is induced by the "perturbation" embodied in the terms on the right-hand side of the coupled-channel equations

Within this time dependent perturbation theory framework, the rate of transition of probability amplitude from the initially prepared state (on the excited state surface) to the ground-state surface is proportional to the square of the perturbation matrix elements between these two states:

$$\begin{aligned} \text{Rate} \propto & \left| \int_0^{R_{\max}} \sin(kR) e^{\kappa R_{\max}} e^{-\kappa R} \left\langle \phi \left| \frac{d}{dR} \right| \phi'' \right\rangle \left(\frac{d}{dR} \sin(k'R) \right) dR + \int_{R_{\max}}^{\infty} \sin(kR_{\max}) e^{\kappa R_{\max}} e^{-\kappa R} \right. \\ & \left. \left\langle \phi \left| \frac{d}{dR} \right| \phi'' \right\rangle \left(\frac{d}{dR} \sin(k'R) \right) dR \right|^2 \end{aligned}$$

The matrix elements occurring here contain two distinct parts:

$$\langle \phi | \frac{d}{dR} | \phi'' \rangle$$

has to do with the electronic state couplings that are induced by radial movement of the nuclei; and both

$$\sin(kR) \frac{d}{dR} \sin(k'R)$$

relate to couplings between the two nuclear-motion wavefunctions induced by these same radial motions. For a transition to occur, both the electronic and nuclear-motion states must undergo changes. The initially prepared state (the bound state on the upper electronic surface) has high electronic and low nuclear-motion energy, while the state to which transitions may occur (the scattering state on the lower electronic surface) has low electronic energy and higher nuclear-motion energy.

Of course, in the above example, the integrals over R can be carried out if the electronic matrix elements $\langle \phi | \frac{d}{dR} | \phi'' \rangle$ can be handled. In practical chemical applications (for an introductory treatment see **Energetic Principles of Chemical Reactions**, J. Simons, Jones and Bartlett, Portola Valley, Calif. (1983)), the evaluation of these electronic matrix elements is a formidable task that often requires computation intensive techniques such as those discussed in Section 6.

Even when the electronic coupling elements are available (or are modelled or parameterized in some reasonable manner), the solution of the coupled-channel equations that govern the nuclear motion is a demanding task. For the purposes of this text, it suffices to note that:

1. couplings between motion on two or more electronic states can and do occur;
2. these couplings are essential to treat whenever the electronic energy difference (i.e., the spacing between pairs of Born-Oppenheimer potential surfaces) is small (i.e., comparable to vibrational or rotational energy level spacings);
3. there exists a rigorous theoretical framework in terms of which one can evaluate the rates of so-called radiationless transitions between pairs of such electronic, vibrational, rotational states. Expressions for such transitions involve (a) electronic matrix elements that depend on how strongly the electronic states are modulated by movement (hence the $\frac{d}{dR}$) of the nuclei, and (b) nuclear-motion integrals connecting the initial and final nuclear-motion wavefunctions, which also contain $\frac{d}{dR}$ because they describe the "recoil" of the nuclei induced by the electronic transition.

Chemical Relevance

As presented above, the most obvious situation of multichannel dynamics arises when electronically excited molecules undergo radiationless relaxation (e.g., internal conversion when the spin symmetry of the two states is the same or intersystem crossing when the two states differ in spin symmetry). These subjects are treated in some detail in the text **Energetic Principles of Chemical Reactions**, J. Simons, Jones and Bartlett, Portola Valley, Calif. (1983)) where radiationless transitions arising in photochemistry and polyatomic molecule reactivity are discussed.

Let us consider an example involving the chemical reactivity of electronically excited alkaline earth or $d^{10}s^2$ transition metal atoms with H_2 molecules. The particular case for $Cd^* + H_2 \rightarrow CdH + H$ has been studied experimentally and theoretically. In such systems, the potential energy surface connecting to ground-state $Cd(^1S) + H_2$ becomes highly repulsive as the collision partners approach (see the depiction provided in the Figure shown below). The three surfaces that correlate with the $Cd(^1P) + H_2$ species prepared by photo-excitation of $Cd(^1S)$ behave quite differently as functions of the Cd-to- H_2 distance because in each the singly occupied 6p orbital assumes a different orientation relative to the H_2 molecule's bond axis. For (near) C_{2v} orientations, these states are labeled 1B_2 , 1B_1 , and 1A_1 ; they have the 6p orbital directed as shown in the second Figure, respectively. The corresponding triplet surfaces that derive from $Cd(^3P) + H_2$ behave, as functions of the Cd-to- H_2 distance (R) in similar manner, except they are shifted to lower energy because $Cd(^3P)$ lies below $Cd(^1P)$ by ca. 37 kcal/mol.

Collisions between $Cd(^1P)$ and H_2 can occur on any of the three surfaces mentioned above. Flux on the 1A_1 surface is primarily reflected (at low collision energies characteristic of the thermal experiments) because this surface is quite repulsive at large R . Flux on the 1B_1 surface can proceed in to quite small R (ca. 2.4 Å) before repulsive forces on this surface reflect it. At geometries near $R = 2.0$ Å and $r_{HH} = 0.88$ Å, the highly repulsive 3A_1 surface intersects this 1B_1 surface from below. At and near this intersection, a combination of spin-orbit coupling (which is large for Cd) and non-adiabatic coupling may induce flux to evolve onto the 3A_1 surface, after which fragmentation to $Cd(^3P) + H_2$ could occur.

In contrast, flux on the 1B_2 surface propagates inward under attractive forces to $R = 2.25 \text{ \AA}$ and $r_{HH} = 0.79 \text{ \AA}$ where it may evolve onto the 3A_1 surface which intersects from below. At and near this intersection, a combination of spin-orbit coupling (which is large for Cd) and non-adiabatic coupling may induce flux to evolve onto the 3A_1 surface, after which fragmentation to $Cd(^3P) + H_2$ could occur. Flux that continues to propagate inward to smaller R values experiences even stronger attractive forces that lead, near $R = 1.69 \text{ \AA}$ and $r_{HH} = 1.54 \text{ \AA}$, to an intersection with the 1A_1 surface that connects to $Cd(^1S) + H_2$. Here, non-adiabatic couplings may cause flux to evolve onto the 1A_1 surface which may then lead to formation of ground state $Cd(^1S) + H_2$ or $Cd(^1S) + H + H$, both of which are energetically possible. Processes in which electronically excited atoms produce groundstate atoms through such collisions and surface hopping are termed "electronic quenching".

The nature of the non-adiabatic couplings that arise in the two examples given above are quite different. In the former case, when the 1B_1 and 3A_1 surfaces are in close proximity to one another, the first-order coupling element:

$$\langle \Psi(^1B_1) | \nabla_j | \Psi(^3A_1) \rangle$$

is non-zero only for nuclear motions (i.e., ∇_j) of $b_1 x_{a1} = b_1$ symmetry. For the CdH_2 collision complex being considered in (or near) C_{2v} symmetry, such a motion corresponds to rotational motion of the nuclei about an axis lying parallel to the H-H bond axis. In contrast, to couple the 3A_1 and 1B_2 electronic states through an element of the form

$$\langle \Psi(^1B_2) | \nabla_j | \Psi(^3A_1) \rangle,$$

the motion must be of $b_2 x_{a1} = b_2$ symmetry. This movement corresponds to asymmetric vibrational motion of the two Cd-H interatomic coordinates.

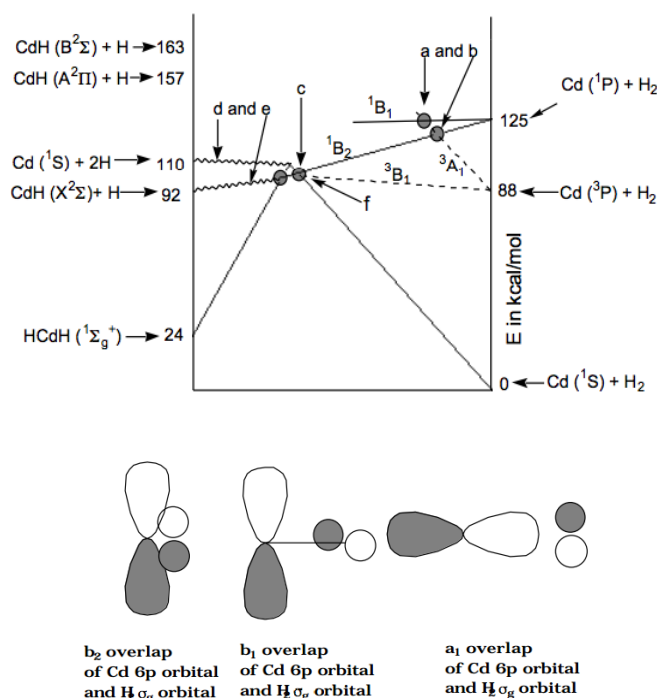
The implications of these observations are clear. For example, in so-called halfcollision experiments in which a van der Waals CdH_2 complex is probed, internal rotational motion would be expected to enhance $^1B_1 \rightarrow ^3A_1$ quenching, whereas asymmetric vibrational motion should enhance the $^1B_2 \rightarrow ^3A_1$ process.

Moreover, the production of ground-state $Cd(^1S) + H_2$ via $^1B_2 \rightarrow ^1A_1$ surface hopping (near $R = 1.69 \text{ \AA}$ and $r_{HH} = 1.54 \text{ \AA}$) should also be enhanced by asymmetric vibrational excitation. The 1B_2 and 1A_1 surfaces also provide, through their non-adiabatic couplings, a "gateway" to formation of the asymmetric bond cleavage products $CdH(^2\Sigma) + H$. It can be shown that the curvature (i.e., second energy derivative) of a potential energy surface consists of two parts: (i) one part that is always positive, and (ii) a second that can be represented in terms of the non-adiabatic coupling elements between the two surfaces and the energy gap ΔE between the two surfaces. Applied to the two states at hand, this second contributor to the curvature of the 1B_2 surface is:

$$\frac{|\langle \Psi(^1B_2) | \nabla_f | \Psi(^1A_1) \rangle|^2}{E(^1B_2) - E(^1A_1)}.$$

Clearly, when the 1A_1 state is higher in energy but strongly non-adiabatically coupled to the 1B_2 state, negative curvature along the asymmetric b_2 vibrational mode is expected for the 1B_2 state. When the 1A_1 state is lower in energy, negative curvature along the b_2 vibrational mode is expected for the 1A_1 state (because the above expression also expresses the curvature of the 1A_1 state).

Therefore, in the region of close-approach of these two states, state-to-state surface hopping can be facile. Moreover, one of the two states (the lower lying at each geometry) will likely possess negative curvature along the b_2 vibrational mode. It is this negative curvature that causes movement away from C_{2v} symmetry to occur spontaneously, thus leading to the $CdH(^2\Sigma) + H$ reaction products.



Coupled-state dynamics can also be used to describe situations in which vibrational rather than electronic-state transitions occur. For example, when van der Waals complexes such as HCl...Ar undergo so-called vibrational predissociation, one thinks in terms of movement of the Ar atom relative to the center of mass of the HCl molecule playing the role of the R coordinate above, and the vibrational state of HCl as playing the role of the quantized (electronic) state in the above example.

In such cases, a vibrationally excited HCl molecule (e.g., in $v = 1$) to which an Ar atom is attached via weak van der Waals attraction transfers its vibrational energy to the Ar atom, subsequently dropping to a lower (e.g., $v = 0$) vibrational level. Within the twocoupled-state model introduced above, the upper energy surface pertains to Ar in a bound vibrational level (having dissociation energy D_e) with HCl in an excited vibrational state (Δ being the $v = 0$ to $v = 1$ vibrational energy gap), and the lower surface describes an Ar atom that is free from the HCl molecule that is itself in its $v = 0$ vibrational state. In this case, the coordinate R is the Ar-to-HCl distance.

In analogy with the electronic-nuclear coupling example discussed earlier, the rate of transition from HCl ($v=1$) bound to Ar to HCl($v=0$) plus a free Ar atom depends on the strength of coupling between the Ar...HCl relative motion coordinate (R) and the HCl internal vibrational coordinate. The $\langle \phi | \frac{d}{dR} | \phi' \rangle$ coupling elements in this case are integrals over the HCl vibrational coordinate x involving the $v = 0$ (ϕ) and $v = 1$ (ϕ') vibrational functions. The integrals over the R coordinate in the earlier expression for the rate of radiationless transitions now involve integration over the distance R between the Ar atom and the center of mass of the HCl molecule.

This completes our discussion of dynamical processes in which more than one Born-Oppenheimer state is involved. There are many situations in molecular spectroscopy and chemical dynamics where consideration of such coupled-state dynamics is essential. These cases are characterized by

1. total energies E which may be partitioned in two or more ways among the internal degrees of freedom (e.g., electronic and nuclear motion or vibrational and ad-atom in the above examples),
2. Born-Oppenheimer potentials that differ in energy by a small amount (so that energy transfer from the other degree(s) of freedom is facile).

This page titled [16.2: Multichannel Problems](#) is shared under a [CC BY-NC-SA 4.0](#) license and was authored, remixed, and/or curated by [Jack Simons](#) via [source content](#) that was edited to the style and standards of the LibreTexts platform.

16.3: Classical Treatment of Nuclear Motion

For all but very elementary chemical reactions (e.g., $D + HH \rightarrow HD + H$ or $F + HH \rightarrow FH + H$) or scattering processes (e.g., $CO(v,J) + He \rightarrow CO(v',J') + He$), the above fully quantal coupled equations simply can not be solved even when modern supercomputers are employed. Fortunately, the Schrödinger equation can be replaced by a simple classical mechanics treatment of nuclear motions under certain circumstances.

For motion of a particle of mass μ along a direction R , the primary condition under which a classical treatment of nuclear motion is valid

$$\frac{\lambda}{4\pi} \left| \frac{1}{p} \frac{dp}{dR} \right| \ll 1$$

relates to the fractional change in the **local momentum** defined as:

$$p = \sqrt{2\mu(E - E_j(R))}$$

along R within the $3N - 5$ or $3N - 6$ dimensional internal coordinate space of the molecule, as well as to the **local de Broglie wavelength**

$$\lambda = \frac{2\pi\hbar}{|p|}.$$

The inverse of the quantity $\frac{1}{p} \left| \frac{dp}{dR} \right|$ can be thought of as the length over which the momentum changes by 100%. The above condition then states that the local de Broglie wavelength must be short with respect to the distance over which the potential changes appreciably. Clearly, whenever one is dealing with heavy nuclei that are moving fast (so $|p|$ is large), one should anticipate that the local de Broglie wavelength of those particles may be short enough to meet the above criteria for classical treatment.

It has been determined that for potentials characteristic of typical chemical bonding (whose depths and dynamic range of interatomic distances are well known), and for all but low-energy motions (e.g., zero-point vibrations) of light particles such as Hydrogen and Deuterium nuclei or electrons, the local de Broglie wavelengths are often short enough for the above condition to be met (because of the large masses μ of non-Hydrogenic species) except when their velocities approach zero (e.g., near classical turning points). It is therefore common to treat the nuclear-motion dynamics of molecules that do not contain H or D atoms in a purely classical manner, and to apply so-called semi-classical corrections near classical turning points. The motions of H and D atomic centers usually require quantal treatment except when their kinetic energies are quite high.

Classical Trajectories

To apply classical mechanics to the treatment of nuclear-motion dynamics, one solves Newtonian equations

$$m_k \frac{d^2 X_k}{dt^2} = - \frac{dE_j}{dX_k}$$

where X_k denotes one of the $3N$ cartesian coordinates of the atomic centers in the molecule, m_k is the mass of the atom associated with this coordinate, and $\frac{dE_j}{dX_k}$ is the derivative of the potential, which is the electronic energy $E_j(R)$, along the k^{th} coordinate's direction. Starting with coordinates $\{X_k(0)\}$ and corresponding momenta $\{P_k(0)\}$ at some initial time $t = 0$, and given the ability to compute the force $-\frac{dE_j}{dX_k}$ at any location of the nuclei, the Newton equations can be solved (usually on a computer) using finite-difference methods:

$$X_k(t + \delta t) = X_{k, \text{extk}}(t) + P_k(t) \frac{\delta t}{m_k}$$

$$P_k(t + \delta t) = P_k(t) - \frac{dE_j}{dX_k}(t) \delta t.$$

In so doing, one generates a sequence of coordinates $\{X_k(t_n)\}$ and momenta $\{P_k(t_n)\}$, one for each "time step" t_n . The histories of these coordinates and momenta as functions of time are called "**classical trajectories**". Following them from early times, characteristic of the molecule(s) at "reactant" geometries, through to late times, perhaps characteristic of "product" geometries,

allows one to monitor and predict the fate of the time evolution of the nuclear dynamics. Even for large molecules with many atomic centers, propagation of such classical trajectories is feasible on modern computers **if** the forces $-\frac{dE_j}{dX_k}$ can be computed in a manner that does not consume inordinate amounts of computer time.

In Section 6, methods by which such force calculations are performed using firstprinciples quantum mechanical methods (i.e., so-called **ab initio** methods) are discussed. Suffice it to say that these calculations are often the rate limiting step in carrying out classical trajectory simulations of molecular dynamics. The large effort involved in the **ab initio** determination of electronic energies and their gradients $-\frac{dE}{dX_k}$ motivate one to consider using empirical "force field" functions $V_j(R)$ in place of the ab initio electronic energy $E_j(R)$. Such model potentials $V_j(R)$, are usually constructed in terms of easy to compute and to differentiate functions of the interatomic distances and valence angles that appear in the molecule. The parameters that appear in the attractive and repulsive parts of these potentials are usually chosen so the potential is consistent with certain experimental data (e.g., bond dissociation energies, bond lengths, vibrational energies, torsion energy barriers).

For a large polyatomic molecule, the potential function V usually contains several distinct contributions:

$$V = V_{\text{bond}} + V_{\text{bend}} + V_{\text{vanderWaals}} + V_{\text{torsion}} + V_{\text{electrostatic}}$$

Here V_{bond} gives the dependence of V on stretching displacements of the bonds (i.e., interatomic distances between pairs of bonded atoms) and is usually modeled as a harmonic or Morse function for each bond in the molecule:

$$V_{\text{bond}} = \sum_J \frac{1}{2} k_J (R_J - R_{\text{eq},J})^2$$

or

$$V_{\text{bond}} = \sum_J D_{e,J} \left(1 - e^{-a_J(R_J - R_{\text{eq},J})} \right)^2$$

where the index J labels the bonds and the k_J , a_J and $R_{\text{eq},J}$ are the force constant and equilibrium bond length parameters for the J^{th} bond.

V_{bend} describes the bending potentials for each triplet of atoms (ABC) that are bonded in a A-B-C manner; it is usually modeled in terms of a harmonic potential for each such bend:

$$V_{\text{bend}} = \sum_J \frac{1}{2} k_J^\theta (\theta_J - \theta_{\text{eq},J})^2.$$

The $\theta_{\text{eq},J}$ and k_J^θ are the equilibrium angles and force constants for the J^{th} angle.

$V_{\text{vanderWaals}}$ represents the van der Waals interactions between all pairs of atoms that are not bonded to one another. It is usually written as a sum over all pairs of such atoms (labeled J and K) of a [Lennard-Jones 6-12 potential](#):

$$V_{\text{vanderWaals}} = \sum_{J < K} [a_{J,K} (R_{J,K})^{-12} - b_{J,K} (R_{J,K})^{-6}]$$

where $a_{J,K}$ and $b_{J,K}$ are parameters relating to the repulsive and dispersion attraction forces, respectively for the J^{th} and K^{th} atoms.

V_{torsion} contributions describe the dependence of V on angles of rotation about single bonds. For example, rotation of a CH_3 group around the single bond connecting the carbon atom to another group may have an angle dependence of the form:

$$V_{\text{torsion}} = V_0 (1 - \cos(3\theta))$$

where θ is the torsion rotation angle, and V_0 is the magnitude of the interaction between the C-H bonds and the group on the atom bonded to carbon.

$V_{\text{electrostatic}}$ contains the interactions among polar bonds or other polar groups (including any charged groups). It is usually written as a sum over pairs of atomic centers (J and K) of Coulombic interactions between fractional charges $\{Q_J\}$ (chosen to represent the bond polarity) on these atoms:

$$V_{\text{electrostatic}} = \sum_{J < K} \frac{Q_J Q_K}{R_{J,K}}$$

Although the total potential V as written above contains many components, each is a relatively simple function of the Cartesian positions of the atomic centers. Therefore, it is relatively straightforward to evaluate V and its gradient along all $3N$ Cartesian directions in a computationally efficient manner. For this reason, the use of such empirical force fields in so-called **molecular mechanics** simulations of classical dynamics is widely used for treating large organic and biological molecules.

Initial Conditions

No single trajectory can be used to simulate chemical reaction or collisions that relate to realistic experiments. To generate classical trajectories that are characteristic of particular experiments, one must choose many initial conditions (coordinates and momenta) the **collection** of which is representative of the experiment. For example, to use an ensemble of trajectories to simulate a molecular beam collision between H and Cl atoms at a collision energy E , one must follow many classical trajectories that have a range of "impact parameters" (b) from zero up to some maximum value b_{max} beyond which the H ...Cl interaction potential vanishes. The figure shown below describes the impact parameter as the distance of closest approach that a trajectory would have if no attractive or repulsive forces were operative.

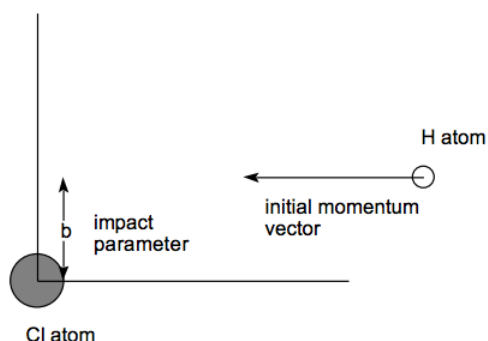


Figure 16.3.1: Insert caption here!

Moreover, if the energy resolution of the experiment makes it impossible to fix the collision energy closer than an amount δE , one must run collections of trajectories for values of E lying within this range.

If, in contrast, one wishes to simulate thermal reaction rates, one needs to follow trajectories with various E values and various impact parameters b from initiation at $t = 0$ to their conclusion (at which time the chemical outcome is interrogated). Each of these trajectories must have their outcome weighted by an amount proportional to a Boltzmann factor $e^{\frac{-E}{RT}}$, where R is the ideal gas constant and T is the temperature because this factor specifies the probability that a collision occurs with kinetic energy E .

As the complexity of the molecule under study increases, the number of parameters needed to specify the initial conditions also grows. For example, classical trajectories that relate to $F + H_2 \rightarrow HF + H$ need to be specified by providing (i) an impact parameter for the F to the center of mass of H_2 , (ii) the relative translational energy of the F and H_2 , (iii) the radial momentum and coordinate of the H_2 molecule's bond length, and (iv) the angular momentum of the H_2 molecule as well as the angle of the H-H bond axis relative to the line connecting the F atom to the center of mass of the H_2 molecule. Many such sets of initial conditions must be chosen and the resultant classical trajectories followed to generate an ensemble of trajectories pertinent to an experimental situation.

It should be clear that even the classical mechanical simulation of chemical experiments involves considerable effort because no single trajectory can represent the experimental situation. Many trajectories, each with different initial conditions selected so they represent, as an ensemble, the experimental conditions, must be followed and the outcome of all such trajectories must be averaged over the probability of realizing each specific initial condition.

Analyzing Final Conditions

Even after classical trajectories have been followed from $t = 0$ until the outcomes of the collisions are clear, one needs to properly relate the fate of each trajectory to the experimental situation. For the $F + H_2 \rightarrow HF + H$ example used above, one needs to examine each trajectory to determine, for example, (i) whether $HF + H$ products are formed or non-reactive collision to produce $F + H_2$ has occurred, (ii) the amount of rotational energy and angular momentum that is contained in the HF product molecule, (iii)

the amount of relative translational energy that remains in the H + FH products, and (iv) the amount of vibrational energy that ends up in the HF product molecule.

Because classical rather than quantum mechanical equations are used to follow the time evolution of the molecular system, there is no guarantee that the amount of energy or angular momentum found in degrees of freedom for which these quantities should be quantized will be so. For example, $\text{F} + \text{H}_2 \rightarrow \text{HF} + \text{H}$ trajectories may produce HF molecules with internal vibrational energy that is not a half integral multiple of the fundamental vibrational frequency ω of the HF bond. Also, the rotational angular momentum of the HF molecule may not fit the formula $J(J+1)\frac{\hbar^2}{8\pi^2I}$, where I is HF's moment of inertia.

To connect such purely classical mechanical results more closely to the world of quantized energy levels, a method known as "binning" is often used. In this technique, one assigns the outcome of a classical trajectory to the particular quantum state (e.g., to a vibrational state v or a rotational state J of the HF molecule in the above example) whose quantum energy is closest to the classically determined energy. For the HF example at hand, the classical vibrational energy $E_{\text{cl.vib}}$ is simply used to define, as the closest integer, a vibrational quantum number v according to:

$$v = \frac{E_{\text{cl.vib}}}{\hbar\omega} - \frac{1}{2}.$$

Likewise, a rotational quantum number J can be assigned as the closest integer to that determined by using the classical rotational energy $E_{\text{cl.rot}}$ in the formula:

$$J = \frac{1}{2} \left[\sqrt{1 + \frac{32\pi^2 I E_{\text{cl,rot}}}{h^2}} - 1 \right]$$

which is the solution of the quadratic equation $J(J+1)\frac{\hbar^2}{8\pi^2I} = E_{\text{cl,rot}}$. By following many trajectories and assigning vibrational and rotational quantum numbers to the product molecules formed in each trajectory, one can generate histograms giving the frequency with which each product molecule quantum state is observed for the ensemble of trajectories used to simulate the experiment of interest. In this way, one can approximately extract product-channel quantum state distributions from classical trajectory simulations.

This page titled [16.3: Classical Treatment of Nuclear Motion](#) is shared under a [CC BY-NC-SA 4.0](#) license and was authored, remixed, and/or curated by [Jack Simons](#) via [source content](#) that was edited to the style and standards of the LibreTexts platform.

16.4: Wavepackets

In an attempt to combine the attributes and strengths of classical trajectories, which allow us to "watch" the motions that molecules undergo, and quantum mechanical wavefunctions, which are needed if interference phenomena are to be treated, a hybrid approach is sometimes used. A popular and rather successful such point of view is provided by so called **coherent state wavepackets**.

A quantum mechanical wavefunction $\psi(\mathbf{x}|\mathbf{X}, \mathbf{P})$ that is a function of all pertinent degrees of freedom (denoted collectively by \mathbf{x}) and that depends on two sets of parameters (denoted \mathbf{X} and \mathbf{P} , respectively) is defined as follows:

$$\psi(\mathbf{x}|\mathbf{X}, \mathbf{P}) = \prod_{k=1}^N \frac{e^{\left[\frac{iP_k x_k}{\hbar} - \frac{(x_k - X_k)^2}{4\langle \Delta x_k \rangle^2} \right]}}{\sqrt{2\pi\langle \Delta x_k \rangle^2}}$$

Here, $\langle \Delta x_k \rangle^2$ is the uncertainty

$$\langle \Delta x_k \rangle^2 = \int |\psi|^2 (x_k - X_k)^2 d\mathbf{x}$$

along the k^{th} degree of freedom for this wavefunction, defined as the mean squared displacement away from the average coordinate

$$\int |\psi|^2 x_k d\mathbf{x} = X_k.$$

So, the parameter X_k specifies the **average value** of the coordinate x_k . In like fashion, it can be shown that the parameter P_k is equal to the **average value** of the momentum along the k^{th} coordinate:

$$\int \psi^* \left(-i\hbar \frac{\partial}{\partial x_k} - P_k \right)^2 \psi d\mathbf{x} = P_k$$

The uncertainty in the momentum along each coordinate:

$$\langle \Delta p_k \rangle^2 = \int \psi^* \left(-i\hbar \frac{\partial}{\partial x_k} - P_k \right)^2 \psi d\mathbf{x}$$

is given, for functions of the coherent state form, in terms of the coordinate uncertainty as

$$\langle \Delta p_k \rangle^2 \langle \Delta x_k \rangle^2 = \frac{\hbar^2}{4}$$

Of course, the general Heisenberg uncertainty condition

$$\langle \Delta p_k \rangle^2 \langle \Delta x_k \rangle^2 \geq \frac{\hbar^2}{4}$$

limits the coordinate and momentum uncertainty products for arbitrary wavefunctions. The coherent state wave packet functions are those for which this **uncertainty product is minimum**. In this sense, coherent state wave packets are seen to be as close to classical as possible since in classical mechanics there are no limits placed on the resolution with which one can observe coordinates and momenta

These wavepacket functions are employed as follows in the most straightforward treatments of combined quantal/classical mechanics:

1. Classical trajectories are used, as described in greater detail above, to generate a series of coordinates $X_k(t_n)$ and momenta $P_k(t_n)$ at a sequence of times denoted $\{t_n\}$.
2. These classical coordinates and momenta are used to **define** a wavepacket function as written above, whose \mathbf{X}_k and \mathbf{P}_k parameters are taken to be the coordinates and momenta of the classical trajectory. In effect, the wavepacket moves around "riding" the classical trajectory's coordinates and momenta as time evolves
3. At any time t_n , the quantum mechanical properties of the system are computed by forming the expectation values of the corresponding quantum operators for a wavepacket wavefunction of the form given above with X_k and P_k given by the

classical coordinates and momenta at that time t_n .

Such wavepackets are, of course, simple approximations to the true quantum mechanical functions of the system because they do not obey the Schrödinger equation appropriate to the system. They should be expected to provide accurate representations to the true wavefunctions for systems that are more classical in nature (i.e., when the local de Broglie wave lengths are short compared to the range over which the potentials vary appreciably). For species containing light particles (e.g., electrons or H atoms) or for low kinetic energies, the local de Broglie wave lengths will not satisfy such criteria, and these approaches can be expected to be less reliable. For further information about the use of coherent state wavepackets in molecular dynamics and molecular spectroscopy, see E. J. Heller, *Acc. Chem. Res.* 14, 368 (1981).

*This completes our treatment of the subjects of molecular dynamics and molecular collisions. Neither its depth nor its level was at the research level; rather, we intended to provide the reader with an introduction to many of the theoretical concepts and methods that arise when applying either the quantum Schrödinger equation or classical Newtonian mechanics to chemical reaction dynamics. Essentially none of the experimental aspects of this subject (e.g., molecular beam methods for preparing "cold" molecules, laser pump/probe methods for preparing reagents in specified quantum states and observing products in such states) have been discussed. An excellent introduction to both the experimental and theoretical foundations of modern chemical and collision dynamics is provided by the text **Molecular Reaction Dynamics and Chemical Reactivity** by R. D. Levine and R. B. Bernstein, Oxford Univ. Press (1987).*

This page titled [16.4: Wavepackets](#) is shared under a [CC BY-NC-SA 4.0](#) license and was authored, remixed, and/or curated by [Jack Simons](#) via [source content](#) that was edited to the style and standards of the LibreTexts platform.

CHAPTER OVERVIEW

17: Higher Order Corrections to Electronic Structure

Electrons interact via pairwise Coulomb forces; within the "orbital picture" these interactions are modelled by less difficult to treat "averaged" potentials. The difference between the true Coulombic interactions and the averaged potential is not small, so to achieve reasonable (ca. 1 kcal/mol) chemical accuracy, high-order corrections to the orbital picture are needed.

[17.1: Orbitals, Configurations, and the Mean-Field Potential](#)

[17.2: Electron Correlation Requires Moving Beyond a Mean-Field Model](#)

[17.3: Moving from Qualitative to Quantitative Models](#)

[17.4: Atomic Units](#)

This page titled [17: Higher Order Corrections to Electronic Structure](#) is shared under a [CC BY-NC-SA 4.0](#) license and was authored, remixed, and/or curated by [Jack Simons](#) via [source content](#) that was edited to the style and standards of the LibreTexts platform.

17.1: Orbitals, Configurations, and the Mean-Field Potential

The discipline of computational *ab initio* quantum chemistry is aimed at determining the electronic energies and wavefunctions of atoms, molecules, radicals, ions, solids, and all other chemical species. The phrase *ab initio* implies that one attempts to solve the Schrödinger equation from first principles, treating the molecule as a collection of positive nuclei and negative electrons moving under the influence of coulombic potentials, and not using any prior knowledge about this species' chemical behavior.

To make practical use of such a point of view requires that approximations be introduced; the full Schrödinger equation is too difficult to solve exactly for any but simple model problems. These approximations take the form of physical concepts (e.g., orbitals, configurations, quantum numbers, term symbols, energy surfaces, selection rules, etc.) that provide useful means of organizing and interpreting experimental data and computational methods that allow quantitative predictions to be made.

Essentially all *ab initio* quantum chemistry methods use, as a starting point from which improvements are made, a picture in which the electrons interact via a one-electron additive potential. These so-called **mean-field** potentials

$$V_{mf}(\mathbf{r}) = \sum_j V_{mf}(\mathbf{r}_j)$$

provide descriptions of atomic and molecular structure that are approximate. Their predictions must be improved to achieve reasonably accurate solutions to the true electronic Schrödinger equation. In so doing, three constructs that characterize essentially all *ab initio* quantum chemical methods are employed: **orbitals, configurations, and electron correlation**.

Since the electronic kinetic energy operator is one-electron additive

$$T = \sum_j T_j$$

the mean-field Hamiltonian

$$H^0 = T + V_{mf}$$

is also of this form. The additivity of H^0 implies that the mean-field wavefunctions $\{\Psi_k^0\}$ can be formed in terms of products of functions $\{\phi_k\}$ of the coordinates of the individual electrons, and that the corresponding energies $\{E_k^0\}$ are additive. Thus, it is the ansatz that V_{mf} is separable that leads to the concept of **orbitals**, which are the one-electron functions $\{\phi_j\}$. These orbitals are found by solving the one-electron Schrödinger equations:

$$(T_1 + V_{mf}(\mathbf{r}_1))\phi_j(\mathbf{r}_1) = \epsilon_j\phi_j(\mathbf{r}_1);$$

the eigenvalues $\{\epsilon_j\}$ are called **orbital energies**.

Because each of the electrons also possesses intrinsic spin, the one-electron functions $\{\phi_j\}$ used in this construction are taken to be eigenfunctions of $(T_1 + V_{mf}(\mathbf{r}_1))$ multiplied by either α or β . This set of functions is called the set of mean-field **spin-orbitals**.

Given the complete set of solutions to this one-electron equation, a complete set of N-electron mean-field wavefunctions can be written down. Each Ψ_k^0 is constructed by forming an antisymmetrized product of N spin-orbitals chosen from the set of $\{\phi_j\}$, allowing each spin-orbital in the list to be a function of the coordinates of one of the N electrons (e.g.,

$$\Psi_k^0 = |\phi_{k1}(\mathbf{r}_1)\phi_{k2}(\mathbf{r}_2)\phi_{k3}(\mathbf{r}_3)\cdots\phi_{k(N-1)}(\mathbf{r}_{N-1})\phi_{kN}(\mathbf{r}_N)|,$$

as above). The corresponding mean field energy is evaluated as the sum over those spin-orbitals that appear in Ψ_k^0 :

$$E_k^0 = \sum_{j=1,N} \epsilon_{kj}.$$

By choosing to place N electrons into specific spin-orbitals, one has specified a **configuration**. By making other choices of which N ϕ_j to occupy, one describes other configurations. Just as the one-electron mean-field Schrödinger equation has a complete set of spin-orbital solutions $\{\phi_j$ and $\epsilon_j\}$, the N-electron mean-field Schrödinger equation has a complete set of N-electron **configuration state functions** (CSFs) Ψ_k^0 and energies E_k^0 .

This page titled [17.1: Orbitals, Configurations, and the Mean-Field Potential](#) is shared under a [CC BY-NC-SA 4.0](#) license and was authored, remixed, and/or curated by [Jack Simons](#) via [source content](#) that was edited to the style and standards of the LibreTexts platform.

17.2: Electron Correlation Requires Moving Beyond a Mean-Field Model

To improve upon the mean-field picture of electronic structure, one must move beyond the single-configuration approximation. It is essential to do so to achieve higher accuracy, but it is also important to do so to achieve a **conceptually** correct view of chemical electronic structure. However, it is very disconcerting to be told that the familiar $1s^2 2s^2 2p^2$ configuration description of the carbon atom is inadequate and that instead one must think of the 3P ground state of this atom as a 'mixture' of multiple (often considered "excited-state") configurations:

- $1s^2 2s^2 2p^2$
- $1s^2 2s^2 3p^2$
- $1s^2 2s^2 3d^2$
- $2s^2 3s^2 2p^2$

and any other configurations whose angular momenta can be coupled to produce $L = 1$ and $S = 1$.

Although the picture of configurations in which N electrons occupy N spin-orbitals may be very familiar and useful for systematizing electronic states of atoms and molecules, these constructs are approximations to the true states of the system. They were introduced when the mean-field approximation was made, and neither orbitals nor configurations describe the proper eigenstates $\{\Psi_k, E_k\}$.

The picture of configurations in which N electrons occupy N spin-orbitals is very familiar and useful for systematizing electronic states of atoms and molecules, but these constructs are approximations to the true states of the system.

The inclusion of instantaneous spatial correlations among electrons is necessary to achieve a more accurate description of atomic and molecular electronic structure. **No** single spin-orbital product wavefunction is capable of treating electron correlation to **any** extent; its product nature renders it incapable of doing so.

This page titled 17.2: Electron Correlation Requires Moving Beyond a Mean-Field Model is shared under a CC BY-NC-SA 4.0 license and was authored, remixed, and/or curated by Jack Simons via source content that was edited to the style and standards of the LibreTexts platform.

17.3: Moving from Qualitative to Quantitative Models

The preceding Chapters introduced, in a qualitative manner, many of the concepts which are used in applying quantum mechanics to electronic structures of atoms and molecules. Atomic, bonding, non-bonding, antibonding, Rydberg, hybrid, and delocalized orbitals and the configurations formed by occupying these orbitals were discussed. Spin and spatial symmetry as well as permutational symmetry were treated, and properly symmetry-adapted configuration state functions were formed. The Slater-Condon rules were shown to provide expressions for Hamiltonian matrix elements (and those involving any one- or two-electron operator) over such CSFs in terms of integrals over the orbitals occupied in the CSFs. Orbital, configuration, and state correlation diagrams were introduced to allow one to follow the evolution of electronic structures throughout a 'reaction path'.

Section 6 addresses the **quantitative and computational implementation** of many of the above ideas. It is not designed to address all of the state-of-the-art methods which have been, and are still being, developed to calculate orbitals and state wavefunctions. The rapid growth in computer hardware and software power and the evolution of new computer architectures makes it difficult, if not impossible, to present an up-to-date overview of the techniques that are presently at the cutting edge in computational chemistry. Nevertheless, this Section attempts to describe the essential elements of several of the more powerful and commonly used methods; it is likely that many of these elements will persist in the next generation of computational chemistry techniques although the details of their implementation will evolve considerably. The text by Szabo and Ostlund provides excellent insights into many of the theoretical methods treated in this Section.

This page titled [17.3: Moving from Qualitative to Quantitative Models](#) is shared under a [CC BY-NC-SA 4.0](#) license and was authored, remixed, and/or curated by [Jack Simons](#) via [source content](#) that was edited to the style and standards of the LibreTexts platform.

17.4: Atomic Units

The electronic Hamiltonian is expressed, in this Section, in so-called atomic units (au)

$$H_e = \sum \left[-\frac{1}{2} \nabla_j^2 - \sum_a \frac{Z_a}{r_{j,a}} \right] + \sum_{j < k} \frac{1}{r_{j,k}}.$$

These units are introduced to remove all \hbar , e , and m_e factors from the equations.

To effect this unit transformation, one notes that the kinetic energy operator scales as r_j^{-2} whereas the coulombic potentials scale as r_j^{-1} and as $r_{j,k}^{-1}$. So, if each of the distances appearing in the cartesian coordinates of the electrons and nuclei were expressed as a unit of length a_0 multiplied by a dimensionless length factor, the kinetic energy operator would involve terms of the form $\left(-\frac{\hbar^2}{2(a_0)^2 m_e} \right) \nabla_j^2$, and the coulombic potentials would appear as $\frac{Z_a e^2}{(a_0) r_{j,a}}$ and $\frac{e^2}{(a_0) r_{j,k}}$. A factor of $\frac{e^2}{a_0}$ (which has units of energy since a_0 has units of length) can then be removed from the coulombic and kinetic energies, after which the kinetic energy terms appear as $-\frac{\hbar^2}{2(e^2 a_0) m_e} \nabla_j^2$ and the potential energies appear as $\frac{Z_a}{r_{j,a}}$ and $\frac{1}{r_{k,j}}$. Then, choosing $a_0 = \frac{\hbar^2}{e^2 m_e}$ changes the kinetic energy terms into $-\frac{1}{2} \nabla_j^2$; as a result, the entire electronic Hamiltonian takes the form given above in which no e^2 , m_e , or \hbar^2 factors appear. The value of the so-called Bohr radius $a_0 = \frac{\hbar^2}{e^2 m_e}$ is 0.529 Å, and the so-called Hartree energy unit $\frac{e^2}{a_0}$, which factors out of H_e , is 27.21 eV or 627.51 kcal/mol.

This page titled [17.4: Atomic Units](#) is shared under a [CC BY-NC-SA 4.0](#) license and was authored, remixed, and/or curated by [Jack Simons](#) via [source content](#) that was edited to the style and standards of the LibreTexts platform.

CHAPTER OVERVIEW

18: Multiconfiguration Wavefunctions

The single Slater determinant wavefunction (properly spin and symmetry adapted) is the starting point of the most common mean field potential. It is also the origin of the molecular orbital concept.

[18.1: Optimization of the Energy for a Multiconfiguration Wavefunction](#)

[18.2: The Single-Determinant Wavefunction](#)

[18.3: The Unrestricted Hartree-Fock Spin Impurity Problem](#)

[18.4: Atomic Orbital Basis Sets](#)

[18.5: The LCAO-MO Expansion](#)

[18.6: The Roothaan Matrix SCF Process](#)

[18.7: Observations on Orbitals and Orbital Energies](#)

This page titled [18: Multiconfiguration Wavefunctions](#) is shared under a [CC BY-NC-SA 4.0](#) license and was authored, remixed, and/or curated by [Jack Simons](#) via [source content](#) that was edited to the style and standards of the LibreTexts platform.

18.1: Optimization of the Energy for a Multiconfiguration Wavefunction

The Energy Expression

The most straightforward way to introduce the concept of optimal molecular orbitals is to consider a trial wavefunction of the form which was introduced earlier in Chapter 9.2. Consider a multi-electron wavefunction of the multiconfigurational form

$$\Psi = \sum_I^M C_I \Phi_I$$

where Φ_I is a space- and spin-adapted configuration state function (CSF) consisting of determinantal wavefunctions of spin-orbitals (ϕ_i):

$$\Phi_I = |\phi_{I1} \phi_{I2} \phi_{I3} \dots \phi_{IN}|.$$

The expectation value of the Hamiltonian with this wavefunction

$$E = \langle \Psi | \hat{H} | \Psi \rangle$$

can be expanded as:

$$E = \sum_{I=1}^M \sum_{J=1}^M C_I C_J \langle \Phi_I | \hat{H} | \Phi_J \rangle.$$

The spin- and space-symmetry of the Φ_I SCFs determine the symmetry of the state Ψ whose energy is to be optimized. In this form, it is clear that E is a quadratic function of the C_I amplitudes C_J ; it is a quartic functional of the spin-orbitals because the Slater-Condon rules express each $\langle \Phi_I | \hat{H} | \Phi_J \rangle$ CI matrix element in terms of one- and two-electron integrals $\langle \phi_i | f | \phi_j \rangle$ and $\langle \phi_i \phi_j | g | \phi_k \phi_l \rangle$ over these spin-orbitals.

The Fock and Secular Equations

The **variational** method can be used to optimize the above expectation value expression for the electronic energy (i.e., to make the functional stationary) as a function of the CI coefficients C_J and the LCAO-MO coefficients $\{C_{\nu,i}\}$ that characterize the spin-orbitals. However, in doing so the set of $\{C_{\nu,i}\}$ can not be treated as entirely independent variables. The fact that the spin-orbitals $\{\phi_i\}$ are assumed to be orthonormal imposes a set of constraints on the $\{C_{\nu,i}\}$:

$$\langle \phi_i | \phi_j \rangle = \delta_{i,j} = \sum_{\mu,\nu} C_{\mu,i}^* \langle \chi_\mu | \chi_\nu \rangle C_{\nu,j}$$

These constraints can be enforced within the variational optimization of the energy function mentioned above by introducing a set of Lagrange multipliers $\{\epsilon_{i,j}\}$, one for each constraint condition, and subsequently differentiating

$$E - \sum_{i,j} \epsilon_{i,j} \left[\delta_{i,j} - \sum_{\mu,\nu} C_{\mu,i}^* \langle \chi_\mu | \chi_\nu \rangle C_{\nu,j} \right]$$

with respect to each of the $C_{\nu,i}$ variables.

Upon doing so, the following set of equations is obtained (early references to the derivation of such equations include A. C. Wahl, J. Chem. Phys. 41,2600 (1964) and F. Grein and T. C. Chang, Chem. Phys. Lett. 12, 44 (1971) and R. Shepard, p 63, in Adv. in Chem. Phys. LXIX, K. P. Lawley, Ed., WileyInterscience, New York (1987); the subject is also treated in the textbook **Second Quantization Based Methods in Quantum Chemistry**, P. Jørgensen and J. Simons, Academic Press, New York (1981)):

$$\sum_{J=1}^M H_{I,J} C_J = E C_I \quad (18.1.1)$$

with $I = 1, 2, \dots M$ and

$$F \phi_i = \sum_j \epsilon_{i,j} \phi_j, \quad (18.1.2)$$

where the $\epsilon_{i,j}$ are Lagrange multipliers.

The set of equations in Equation 18.1.1 that govern the $\{C_J\}$ amplitudes are called the **CI-secular equations**. The set of equations in Equation 18.1.2 that determine the LCAO-MO coefficients of the spin-orbitals $\{\phi_j\}$ are called the **Fock equations**. The Fock operator F is given in terms of the one- and two-electron operators in H itself as well as the so-called one- and two-electron density matrices $\gamma_{i,j}$ and $\Gamma_{i,j,k,l}$ which are defined below. These density matrices reflect the averaged occupancies of the various spin orbitals in the CSFs of Ψ . The resultant expression for F is:

$$F\phi_i = \sum_j \gamma_{i,j} h\phi_j + \sum_{j,k,l} \Gamma_{i,j,k,l} J_{k,l}\phi_k,$$

where h is the one-electron component of the Hamiltonian (i.e., the kinetic energy operator and the sum of coulombic attractions to the nuclei). The operator $J_{j,l}$ is defined by:

$$J_{j,l}\phi_k(r) = \int \phi_j^*(r')\phi_l(r') \frac{1}{|r-r'|} d\tau \phi_k(r),$$

where the integration denoted $d\tau'$ is over the spatial and spin coordinates. The so-called spin integration simply means that the α or β spin function associated with ϕ_l must be the same as the α or β spin function associated with ϕ_j or the integral will vanish. This is a consequence of the orthonormality conditions $\langle\alpha|\alpha\rangle = \langle\beta|\beta\rangle = 1$, $\langle\alpha|\beta\rangle = \langle\beta|\alpha\rangle = 0$

One- and Two- Electron Density Matrices

The density matrices introduced above can most straightforwardly be expressed in terms of the CI amplitudes and the nature of the orbital occupancies in the CSFs of Ψ as follows:

1. $\gamma_{i,i}$ is the sum over all CSFs, in which ϕ_i is occupied, of the square of the CI coefficient of that CSF:

$$\gamma_{i,i} = \sum_I (\text{with } \phi_i \text{ occupied}) C_I^2.$$

2. $\gamma_{i,j}$ is the sum over pairs of CSFs which differ by a single spin-orbital occupancy (i.e., one having ϕ_i occupied where the other has ϕ_j occupied after the two are placed into maximal coincidence-the sign factor (sign) arising from bringing the two to maximal coincidence is attached to the final density matrix element):

$$\gamma_{i,j} = \sum_{I,J} (\text{sign})(\text{with } \phi_i \text{ occupied in } I \text{ where } \phi_j \text{ is in } J) C_I C_J.$$

The two-electron density matrix elements are given in similar fashion:

3. $\Gamma_{i,j,i,j} = \sum_I (\text{with both } \phi_i \text{ and } \phi_j \text{ occupied}) C_I C_I$

4. $\Gamma_{i,j,j,i} = -\sum_I (\text{with both } \phi_i \text{ and } \phi_j \text{ occupied}) C_I C_I = -\Gamma_{i,j,i,j}$ (it can be shown, in general that $\Gamma_{i,j,k,l}$ is odd under exchange of i and j , odd under exchange of k and l and even under $(i,j) \leftrightarrow (k,l)$ exchange; this implies that $\Gamma_{i,j,k,l}$ vanishes if $i = j$ or $k = l$);

5. $\Gamma_{i,j,k,j} = \sum_{I,J} (\text{sign})(\text{with } \phi_j \text{ in both } I \text{ and } J \text{ and } \phi_i \text{ in } I \text{ where } \phi_k \text{ is in } J) C_I C_J$

$$= \Gamma_{j,i,j,k} = -\Gamma_{i,j,j,k} = -\Gamma_{j,i,l,k};$$

6. $\Gamma_{i,j,k,l} = \sum_{I,J} (\text{sign})(\text{with } \phi_i \text{ in } I \text{ where } \phi_k \text{ is in } J \text{ and } \phi_j \text{ in } I \text{ where } \phi_l \text{ is in } J) C_I C_J$

$$= \Gamma_{j,i,l,k} = -\Gamma_{j,i,j,l} = -\Gamma_{i,j,l,k} = \Gamma_{j,i,l,k}.$$

These density matrices are themselves quadratic functions of the CI coefficients and they reflect all of the permutational symmetry of the determinantal functions used in constructing Ψ ; they are a compact representation of all of the Slater-Condon rules as applied to the particular CSFs which appear in Ψ . They contain all information about the spin-orbital occupancy of the CSFs in Ψ . The one- and two- electron integrals $\langle\phi_i|f|\phi_j\rangle$ and $\langle\phi_i\phi_j|g|\phi_k\phi_l\rangle$ contain all of the information about the magnitudes of the kinetic and Coulombic interaction energies.

This page titled [18.1: Optimization of the Energy for a Multiconfiguration Wavefunction](#) is shared under a [CC BY-NC-SA 4.0](#) license and was authored, remixed, and/or curated by [Jack Simons](#) via [source content](#) that was edited to the style and standards of the LibreTexts platform.

18.2: The Single-Determinant Wavefunction

The simplest trial function of the form given above is the single Slater determinant function:

$$|\Psi\rangle = |\phi_1 \phi_2 \phi_3 \dots \phi_N|.$$

For such a function, the CI part of the energy minimization is absent (the classic papers in which the SCF equations for closed- and open-shell systems are treated are C. C. J. Roothaan, Rev. Mod. Phys. 23, 69 (1951); 32, 179 (1960)) and the density matrices simplify greatly because only one spin-orbital occupancy is operative. In this case, the orbital optimization conditions reduce to:

$$\hat{F}\phi_i = \sum_j \epsilon_{i,j} \phi_j,$$

where the so-called Fock operator \hat{F} is given by

$$\hat{F}\phi_i = h\phi_i + \sum_{j(\text{occupied})} [\hat{J}_j - \hat{K}_j] \phi_i.$$

The coulomb (\hat{J}_j) and exchange (\hat{K}_j) operators are defined by the relations:

$$\hat{J}_j \phi_i = \int \phi_j^*(r') \phi_j(r') \frac{1}{|r - r'|} d\tau' \phi_i(r)$$

and

$$\hat{K}_j \phi_i = \int \phi_j^*(r') \phi_i(r') \frac{1}{|r - r'|} d\tau' \phi_j(r).$$

Again, the integration implies integration over the spin variables associated with the ϕ_j (and, for the exchange operator, ϕ_i), as a result of which the exchange integral vanishes unless the spin function of ϕ_j is the same as that of ϕ_i ; the coulomb integral is non-vanishing no matter what the spin functions of ϕ_j and ϕ_i .

The sum over coulomb and exchange interactions in the Fock operator runs only over those spin-orbitals that are occupied in the trial Ψ . Because a unitary transformation among the orbitals that appear in $|\Psi\rangle$ leaves the determinant unchanged (this is a property of determinants- $\det(UA) = \det(U) \det(A) = 1 \det(A)$, if U is a unitary matrix), it is possible to choose such a unitary transformation to make the $\epsilon_{i,j}$ matrix diagonal. Upon so doing, one is left with the so-called **canonical Hartree-Fock equations**:

$$\hat{F}\phi_i = \epsilon_i \phi_i,$$

where ϵ_i is the diagonal value of the $\epsilon_{i,j}$ matrix after the unitary transformation has been applied; that is, ϵ_i is an eigenvalue of the $\epsilon_{i,j}$ matrix. These equations are of the eigenvalue-eigenfunction form with the Fock operator playing the role of an effective one-electron Hamiltonian and the ϕ_i playing the role of the one-electron eigenfunctions.

It should be noted that the Hartree-Fock equations $\hat{F}\phi_i = \epsilon_i \phi_i$ possess solutions for the spin-orbitals which appear in Ψ (the so-called **occupied** spin-orbitals) as well as for orbitals which are not occupied in Ψ (the so-called **virtual** spin-orbitals). In fact, the F operator is hermitian, so it possesses a complete set of orthonormal eigenfunctions; only those which appear in Ψ appear in the coulomb and exchange potentials of the Fock operator. The physical meaning of the occupied and virtual orbitals will be clarified later in this Chapter (Section VII.A).

This page titled [18.2: The Single-Determinant Wavefunction](#) is shared under a [CC BY-NC-SA 4.0](#) license and was authored, remixed, and/or curated by [Jack Simons](#) via [source content](#) that was edited to the style and standards of the LibreTexts platform.

18.3: The Unrestricted Hartree-Fock Spin Impurity Problem

As formulated above in terms of spin-orbitals, the Hartree-Fock (HF) equations yield orbitals that do not guarantee that Ψ possesses proper spin symmetry. To illustrate the point, consider the form of the equations for an open-shell system such as the Lithium atom Li. If $1s\alpha$, $1s\beta$, and $2s\alpha$ spin-orbitals are chosen to appear in the trial function Ψ , then the Fock operator will contain the following terms:

$$F = h + J_{1s\alpha} + J_{1s\beta} + J_{2s\alpha} - [K_{1s\alpha} + K_{1s\beta} + K_{2s\alpha}].$$

Acting on an α spin-orbital $\phi_{k\alpha}$ with F and carrying out the spin interfrations, one obtains

$$F\phi_{k\alpha} = h\phi_{k\alpha} + (2J_{1s} + J_{2s})\phi_{k\alpha} - (K_{1s} + K_{2s})\phi_{k\alpha}.$$

In contrast, when acting on a β spin-orbital, one obtains

$$F\phi_{k\beta} = h\phi_{k\beta} + (2J_{1s} + J_{2s})\phi_{k\beta} - (K_{1s})\phi_{k\beta}.$$

Spin-orbitals of α and β type **do not** experience the same exchange potential in this model, which is clearly due to the fact that Ψ contains two α spin-orbitals and only one β spin-orbital.

One consequence of the spin-polarized nature of the effective potential in F is that the optimal $1s\alpha$ and $1s\beta$ spin-orbitals, which are themselves solutions of $F\phi_i = \epsilon_i\phi_i$, do not have identical orbital energies (i.e., $\epsilon_{1s\alpha} \neq \epsilon_{1s\beta}$) and are not spatially identical to one another (i.e., $\phi_{1s\alpha}$ and $\phi_{1s\beta}$ do not have identical LCAO-MO expansion coefficients). This resultant spin polarization of the orbitals in Ψ gives rise to spin impurities in Ψ . That is, the determinant $|1s\alpha 1s'\beta 2s\alpha|$ is not a pure doublet spin eigenfunction although it is an S_z eigenfunction with $M_s = \frac{1}{2}$; it contains both $S = \frac{1}{2}$ and $S = \frac{3}{2}$ components. If the $1s\alpha$ and $1s'\beta$ spin-orbitals were spatially identical, then $|1s\alpha 1s'\beta 2s\alpha|$ would be a pure spin eigenfunction with $S = \frac{1}{2}$.

The above single-determinant wavefunction is commonly referred to as being of the **unrestricted Hartree-Fock** (UHF) type because no restrictions are placed on the spatial nature of the orbitals which appear in Ψ . In general, UHF wavefunctions are not of pure spin symmetry for any open-shell system. Such a UHF treatment forms the starting point of early versions of the widely used and highly successful Gaussian 70 through Gaussian- 8X series of electronic structure computer codes which derive from J. A. Pople and coworkers (see, for example, M. J. Frisch, J. S. Binkley, H. B. Schlegel, K. Raghavachari, C. F. Melius, R. L. Martin, J. J. P. Stewart, F. W. Bobrowicz, C. M. Rohling, L. R. Kahn, D. J. Defrees, R. Seeger, R. A. Whitehead, D. J. Fox, E. M. Fleuder, and J. A. Pople, Gaussian 86, Carnegie-Mellon Quantum Chemistry Publishing Unit, Pittsburgh, PA (1984)).

The inherent spin-impurity problem is sometimes 'fixed' by using the orbitals which are obtained in the UHF calculation to subsequently form a properly spin-adapted wavefunction. For the above Li atom example, this amounts to forming a new wavefunction (after the orbitals are obtained via the UHF process) using the techniques detailed in Section 3 and Appendix G:

$$\Psi = \frac{1}{\sqrt{2}} [|1s\alpha 1s'\beta 2s\alpha| - |1s\beta 1s'\alpha 2s\alpha|].$$

This wavefunction is a pure $S = \frac{1}{2}$ state. This prescription for avoiding spin contamination (i.e., carrying out the UHF calculation and then forming a new spin-pure Ψ) is referred to as **spin-projection**.

It is, of course, possible to first form the above spin-pure Ψ as a trial wavefunction and to then determine the orbitals $1s$, $1s'$ and $2s$ which minimize its energy; in so doing, one is dealing with a spin-pure function from the start. The problem with carrying out this process, which is referred to as a **spin-adapted** Hartree-Fock calculation, is that the resultant $1s$ and $1s'$ orbitals still do not have identical spatial attributes. Having a set of orbitals ($1s$, $1s'$, $2s$, and the virtual orbitals) that form a non-orthogonal set ($1s$ and $1s'$ are neither identical nor orthogonal) makes it difficult to progress beyond the singleconfiguration wavefunction as one often wishes to do. That is, it is difficult to use a spinadapted wavefunction as a starting point for a correlated-level treatment of electronic motions.

Before addressing head-on the problem of how to best treat orbital optimization for open-shell species, it is useful to examine how the HF equations are solved in practice in terms of the LCAO-MO process.

This page titled [18.3: The Unrestricted Hartree-Fock Spin Impurity Problem](#) is shared under a [CC BY-NC-SA 4.0](#) license and was authored, remixed, and/or curated by [Jack Simons](#) via [source content](#) that was edited to the style and standards of the LibreTexts platform.

18.4: Atomic Orbital Basis Sets

The basis orbitals commonly used in the LCAO-MO-SCF process fall into two classes Slater-type orbitals and Cartesian Gaussian-type orbitals.

Slater-type orbitals (STO) are characterized by quantum numbers n , l , and m and exponents (which characterize the 'size' of the basis function) ξ :

$$\chi_{n,l,m}(r, \theta, \phi) = N_{n,l,m,\xi} Y_{l,m}(\theta, \phi) r^{n-1} e^{-\xi r},$$

and $N_{n,l,m,\xi}$ denotes the normalization constant.

Cartesian Gaussian-type orbitals (GTO) are characterized by quantum numbers a , b , and c which detail the angular shape and direction of the orbital and exponents α which govern the radial 'size' of the basis function akin to ξ in STOs.

$$\chi_{a,b,c}(r, \theta, \phi) = N'_{a,b,c,\alpha} x^a y^b z^c e^{-\alpha r^2},$$

For example, orbitals with a , b , and c values of 1,0,0 or 0,1,0 or 0,0,1 are p_x , p_y , and p_z orbitals; those with a , b , and c values of 2, 0, 0 or 0, 2, 0 or 0, 0, 2 and 1, 1, 0 or 0, 1, 1 or 1, 0, 1 span the space of five d orbitals and one s orbital (the sum of the 2, 0, 0 and 0, 2, 0 and 0, 0, 2 orbitals is an s orbital because $x^2 + y^2 + z^2 = r^2$ is independent of θ and ϕ).

For both types of orbitals, the coordinates r , θ , and ϕ refer to the position of the electron relative to a set of axes attached to the center on which the basis orbital is located.

The Utility of Gaussians

Although STOs are preferred on fundamental grounds (e.g., as demonstrated in Appendices A and B, the hydrogen atom orbitals are of this form and the exact solution of the many-electron Schrödinger equation can be shown to be of this form (in each of its coordinates) near the nuclear centers), STOs are used primarily for atomic and linear-molecule calculations because the multi-center integrals $\langle \chi_a \chi_b | g | \chi_c \chi_d \rangle$ (each basis orbital can be on a separate atomic center) which arise in polyatomic-molecule calculations can not efficiently be performed when STOs are employed. In contrast, such integrals can routinely be done when GTOs are used. This fundamental advantage of GTOs has led to the dominance of these functions in molecular quantum chemistry.

To understand why integrals over GTOs can be carried out when analogous STO based integrals are much more difficult, one must only consider the orbital products ($\chi_a \chi_c(r_1)$ and $\chi_b \chi_d(r_2)$) which arise in such integrals. For orbitals of the GTO form, such products involve $e^{-\alpha_a(r-R_a)^2} e^{-\alpha_c(r-R_c)^2}$. By completing the square in the exponent, this product can be rewritten as follows:

$$e^{-\alpha_a(r-R_a)^2} e^{-\alpha_c(r-R_c)^2} = e^{-(\alpha_a+\alpha_c)(r-R')^2} e^{-\alpha'(\mathbf{R}_a-\mathbf{R}_c)^2},$$

where

$$\mathbf{R}' = \frac{\alpha_a \mathbf{R}_a + \alpha_c \mathbf{R}_c}{\alpha_a + \alpha_c}$$

and

$$\alpha' = \frac{\alpha_a \alpha_c}{\alpha_a + \alpha_c}.$$

Thus, the product of two GTOs on different centers is equal to a single other GTO at a center \mathbf{R}' between the two original centers. As a result, even a four-center two-electron integral over GTOs can be written as, at most, a two-center two-electron integral; it turns out that this reduction in centers is enough to allow all such integrals to be carried out. A similar reduction does **not** arise for STOs because the product of two STOs can not be rewritten as a new STO at a new center.

To overcome the primary weakness of GTO functions, that they have incorrect behavior near the nuclear centers (i.e., their radial derivatives vanish at the nucleus whereas the derivatives of STOs are non-zero), it is common to combine two, three, or more GTOs, with combination coefficients which are fixed and **not** treated as LCAO-MO parameters, into new functions called contracted GTOs or CGTOs. Typically, a series of tight, medium, and loose GTOs (i.e., GTOs with large, medium, and small α values, respectively) are multiplied by so-called contraction coefficients and summed to produce a CGTO which appears to possess the proper 'cusp' (i.e., non-zero slope) at the nuclear center (although even such a combination can not because each GTO has zero slope at the nucleus).

Basis Set Libraries

Much effort has been devoted to developing sets of STO or GTO basis orbitals for main-group elements and the lighter transition metals. This ongoing effort is aimed at providing standard basis set libraries which:

1. Yield reasonable chemical accuracy in the resultant wavefunctions and energies.
2. Are cost effective in that their use in practical calculations is feasible.
3. Are relatively transferrable in the sense that the basis for a given atom is flexible enough to be used for that atom in a variety of bonding environments (where the atom's hybridization and local polarity may vary).

The Fundamental Core and Valence Basis

In constructing an atomic orbital basis to use in a particular calculation, one must choose from among several classes of functions. First, the size and nature of the primary core and valence basis must be specified. Within this category, the following choices are common:

1. A **minimal basis** in which the number of STO or CGTO orbitals is equal to the number of core and valence atomic orbitals in the atom.
2. A **double-zeta** (DZ) basis in which twice as many STOs or CGTOs are used as there are core and valence atomic orbitals. The use of more basis functions is motivated by a desire to provide additional variational flexibility to the LCAO-MO process. This flexibility allows the LCAO-MO process to generate molecular orbitals of variable diffuseness as the local electronegativity of the atom varies. Typically, double-zeta bases include pairs of functions with one member of each pair having a smaller exponent (ζ or α value) than in the minimal basis and the other member having a larger exponent.
3. A **triple-zeta** (TZ) basis in which three times as many STOs or CGTOs are used as the number of core and valence atomic orbitals.
4. Dunning has developed CGTO bases which range from approximately DZ to substantially beyond TZ quality (T. H. Dunning, J. Chem. Phys. 53, 2823 (1970); T. H. Dunning and P. J. Hay in **Methods of Electronic Structure Theory**, H. F. Schaefer, III Ed., Plenum Press, New York (1977)). These bases involve contractions of primitive GTO bases which Huzinaga had earlier optimized (S. Huzinaga, J. Chem. Phys. 42, 1293 (1965)) for use as uncontracted functions (i.e., for which Huzinaga varied the α values to minimize the energies of several electronic states of the corresponding atom). These Dunning bases are commonly denoted, for example, as follows for first-row atoms: (10s,6p/5s,4p), which means that 10 s-type primitive GTOs have been contracted to produce 5 separate s-type CGTOs and that 6 primitive p-type GTOs were contracted to generate 4 separate p-type CGTOs. More recent basis sets from the Dunning group are given in T. Dunning, J. Chem. Phys. 90, 1007 (1990).
5. Even-tempered basis sets (M. W. Schmidt and K. Ruedenberg, J. Chem. Phys. 71, 3961 (1979)) consist of GTOs in which the orbital exponents α_k belonging to series of orbitals consist of geometrical progressions: $\alpha_k = a \beta^k$, where α and β characterize the particular set of GTOs.
6. STO-3G bases were employed some years ago (W. J. Hehre, R. F. Stewart, and J. A. Pople, J. Chem. Phys. 51, 2657 (1969)) but are less popular recently. These bases are constructed by least squares fitting GTOs to STOs which have been optimized for various electronic states of the atom. When three GTOs are employed to fit each STO, a STO-3G basis is formed.
7. 4-31G, 5-31G, and 6-31G bases (R. Ditchfield, W. J. Hehre, and J. A. Pople, J. Chem. Phys. 54, 724 (1971); W. J. Hehre, R. Ditchfield, and J. A. Pople, J. Chem. Phys. 56, 2257 (1972); P. C. Hariharan and J. A. Pople, Theoret. Chim. Acta (Berl.) 28, 213 (1973); R. Krishnan, J. S. Binkley, R. Seeger, and J. A. Pople, J. Chem. Phys. 72, 650 (1980)) employ a single CGTO of contraction length 4, 5, or 6 to describe the core orbital. The valence space is described at the DZ level with the first CGTO constructed from 3 primitive GTOs and the second CGTO built from a single primitive GTO.

The values of the orbital exponents (ζ s or α s) and the GTO-to-CGTO contraction coefficients needed to implement a particular basis of the kind described above have been tabulated in several journal articles and in computer data bases (in particular, in the data base contained in the book **Handbook of Gaussian Basis Sets: A Compendium for Ab initio Molecular Orbital Calculations**, R. Poirer, R. Kari, and I. G. Csizmadia, Elsevier Science Publishing Co., Inc., New York, New York (1985)).

Several other sources of basis sets for particular atoms are listed in the Table shown below (here JCP and JACS are abbreviations for the Journal of Chemical Physics and the Journal of The American Chemical Society, respectively).

Literature Reference	Basis Type	Atoms
Hehre, W.J.; Stewart, R.F.; Pople, J.A. JCP 51 , 2657 (1969). Hehre, W.J.; Ditchfield, R.; Stewart, R.F.; Pople, J.A. JCP 52 , 2769 (1970).	STO - 3G	H-Ar
Binkley, J.S.; Pople, J.A.; Hehre, W.J. JACS 102 , 939 (1980).	3-21G	H-Ne
Gordon, M.S.; Binkley, J.S.; Pople, J.A.; Pietro, W.J.; Hehre, W.J. JACS 104 , 2797 (1982).	3-21G	Na-Ar
Dobbs, K.D.; Hehre, W.J., J. Comput. Chem. 7 , 359 (1986).	3-21G	K, Ca, C
Dobbs, K.D.; Hehre, W.J., J. Comput. Chem. 8, 880 (1987).	3-21G	Sc-Zn
Ditchfield, R.; Hehre, W.J.; Pople, J.A., JCP 54 , 724 (1971).	6-31G	H
Dill, J.D.; Pople, J.A., JCP 62 , 2921 (1975).	6-31G	Li, B
Binkley, J.S.; Pople, J.A., JCP 66 , 879 (1977)	6-31G	Be
Hehre, W.J.; Ditchfield, R.; Pople, J.A., JCP 56 , 2257 (1972).	6-31G	C-F
Franci, M.M.; Pietro, W.J.; Hehre, W.J.; Binkley, J.S.; Gordon, M.S.; DeFrees, D.J.; Pople, J.A. JCP 77 , 3654 (1982).	6-31G	Na-Ar
Dunning, T. JCP 53 , 2823 (1970).	(4s/2s)	H
	(4s/3s)	H
	(9s5p/3s2p)	B-F
	(9s5p/4s2p)	B-F
	(9s5p/5s3p)	B-F
Dunning, T. JCP 55 , 716 (1971).	(5s/3s)	H
	(10s/4s)	Li
	(10s/5s)	Be
	(10s6p/5s3p)	B-Ne
	(10s6p/5s4p)	B-Ne
Krishnan, R.; Binkley, J.S.; Seeger, R.; Pople, J.A. JCP 72 , 650 (1980).	6-311G	H-Ne
Dunning, unpublished VDZ.	(4s/2s)	H
	(9s5p/3s2)	Li, Be, C
	(12s8p/4s3p)	Na-Ar
Dunning, unpublished VTZ.	(5s/3s)	H
	(6s/3s)	H
	(12s6p/4s3p)	Li, Be, C
	(17s10p/5s4p)	Mg-Ar
	(17s10p/5s4p)	Mg-Ar
Dunning, unpublished VQZ.	(7s/4s)	H
	(8s/4s)	H
	(16s7p/5s4p)	B-Ne
Dunning, T. JCP 90 , 1007 (1989). (pVDZ,pVTZ,pVQZ correlation-consistent)	(4s1p/2s1p)	H
	(5s2p1d/3s2p1d)	H
	(6s3p1d1f/4s3p2d1f)	H
	(9s4p1d/3s2p1d)	B-Ne
	(10s5p2d1f/4s3p2d1f)	B-Ne
	(12s6p3d2f1g/5s4p3d2f1g)	B-Ne
	(12s6p3d2f1g/5s4p3d2f1g)	B-Ne
Huzinaga, S.; Klobukowski, M.; Tatewaki, H. Can. J. Chem. 63 , 1812 (1985).	(14s/2s)	Li, Be
	(14s9p/2s1p)	B-Ne
	(16s9p/3s1p)	Na-Mg
	(16s11p/3s2p)	Al-Ar
Huzinaga, S.; Klobukowski, M. THEOCHEM. 44 , 1 (1988).	(14s10p/2s1p)	B-Ne
	(17s10p/3s1p)	Na-Mg
	(17s13p/3s2p)	Al-Ar
	(20s13p/4s2p)	K-Ca
	(20s13p10d/4s2p1d)	Sc-Zn
	(20s14p9d/4s3d1d)	Ga
	(20s14p9d/4s3d1d)	Ga
McLean, A.D.; Chandler, G.S. JCP 72 , 5639 (1980).	(12s8p/4s2p)	Na-Ar, P ⁻ , S
	(12s8p/5s2p)	Na-Ar, P ⁻ , S
	(12s8p/6s4p)	Na-Ar, P ⁻ , S
	(12s9p/6s4p)	Na-Ar, P ⁻ , S
	(12s9p/6s5p)	Na-Ar, P ⁻ , S
Dunning, T.H.Jr.; Hay, P.J. Chapter 1 in 'Methods of Electronic Structure Theory', Schaefer, H.F.III, Ed., Plenum Press, N.Y., 1977.	(11s7p/6s4p)	Al-Cl
Hood, D.M.; Pitzer, R.M.; Schaefer, H.F.III, JCP 71 , 705 (1979).	(14s11p6d/10s8p3d)	Sc-Zn

Literature Reference	Basis Type	Atoms
Schmidt, M.W.; Ruedenberg, K. JCP 71 , 3951 (1979). (regular even-tempered)	([N]s), N=3-10	H
	([2N]s), N=3-10	He
	([2N]s), N=3-14	Li, Be
	([2N]s[N]p), N=3-11	B, N-N
	([2N]s[N]p), N=3-13	C
	([2N]s[N]p), N=4-12	Na, Mg
	([2N-6]s[N]p), N=7-15	Al-Ar

Polarization Functions

In addition to the fundamental core and valence basis described above, one usually adds a set of so-called **polarization functions** to the basis. Polarization functions are functions of one higher angular momentum than appears in the atom's valence orbital space (e.g. d-functions for C, N, and O and p-functions for H). These polarization functions have exponents (ζ or α) which cause their radial sizes to be similar to the sizes of the primary valence orbitals (i.e., the polarization p orbitals of the H atom are similar in size to the 1s orbital). Thus, they are **not** orbitals which provide a description of the atom's valence orbital with one higher l-value; such higher-l valence orbitals would be radially more diffuse and would therefore require the use of STOs or GTOs with smaller exponents.

The primary purpose of polarization functions is to give additional angular flexibility to the LCAO-MO process in forming the valence molecular orbitals. This is illustrated below where polarization d_π orbitals are seen to contribute to formation of the bonding π orbital of a carbonyl group by allowing polarization of the Carbon atom's p_π orbital toward the right and of the Oxygen atom's p_π orbital toward the left.

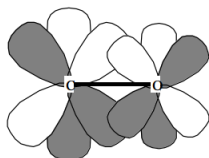


Figure 18.4.1: Insert caption here!

Polarization functions are essential in strained ring compounds because they provide the angular flexibility needed to direct the electron density into regions between bonded atoms.

Functions with higher l-values and with 'sizes' more in line with those of the lower-l orbitals are also used to introduce additional angular correlation into the calculation by permitting polarized orbital pairs (see Chapter 10) involving higher angular correlations to be formed. Optimal polarization functions for first and second row atoms have been tabulated (B. Roos and P. Siegbahn, Theoret. Chim. Acta (Berl.) 17 , 199 (1970); M. J. Frisch, J. A. Pople, and J. S. Binkley, J. Chem. Phys. 80, 3265 (1984)).

Diffuse Functions

When dealing with anions or Rydberg states, one must augment the above basis sets by adding so-called diffuse basis orbitals. The conventional valence and polarization functions described above do not provide enough radial flexibility to adequately describe either of these cases. Energy-optimized diffuse functions appropriate to anions of most lighter main group elements have been tabulated in the literature (an excellent source of Gaussian basis set information is provided in **Handbook of Gaussian Basis Sets**, R. Poirier, R. Kari, and I. G. Csizmadia, Elsevier, Amsterdam (1985)) and in data bases. Rydberg diffuse basis sets are usually created by adding to conventional valence-plus-polarization bases sequences of primitive GTOs whose exponents are smaller than that (call it α_{diff}) of the most diffuse GTO which contributes strongly to the valence CGTOs. As a 'rule of thumb', one can generate a series of such diffuse orbitals which are linearly independent yet span considerably different regions of radial space by introducing primitive GTOs whose exponents are $\frac{1}{3}\alpha_{\text{diff}}$, $\frac{1}{9}\alpha_{\text{diff}}$, $\frac{1}{27}\alpha_{\text{diff}}$, etc.

Once one has specified an atomic orbital basis for each atom in the molecule, the LCAO-MO procedure can be used to determine the $C_{\nu,i}$ coefficients that describe the occupied and virtual orbitals in terms of the chosen basis set. It is important to keep in mind that the basis orbitals are **not** themselves the true orbitals of the isolated atoms; even the proper atomic orbitals are combinations (with atomic values for the $C_{\nu,i}$ coefficients) of the basis functions. For example, in a minimal-basis-level treatment of the Carbon atom, the 2s atomic orbital is formed by combining, with opposite sign to achieve the radial node, the two CGTOs (or STOs); the more diffuse s-type basis function will have a larger $C_{\nu,\nu}$ coefficient in the 2s atomic orbital. The 1s atomic orbital is formed by combining the same two CGTOs but with the same sign and with the less diffuse basis function having a larger $C_{\nu,i}$ coefficient. The LCAO-MO-SCF process itself determines the magnitudes and signs of the $C_{\nu,i}$.

This page titled [18.4: Atomic Orbital Basis Sets](#) is shared under a [CC BY-NC-SA 4.0](#) license and was authored, remixed, and/or curated by [Jack Simons](#) via [source content](#) that was edited to the style and standards of the LibreTexts platform.

18.5: The LCAO-MO Expansion

The HF equations $F\phi_i = \epsilon_i\phi_i$ comprise a set of integro-differential equations; their differential nature arises from the kinetic energy operator in h , and the coulomb and exchange operators provide their integral nature. The solutions of these equations must be achieved iteratively because the J_i and K_i operators in F depend on the orbitals ϕ_i which are to be solved for. Typical iterative schemes begin with a 'guess' for those ϕ_i which appear in Ψ , which then allows F to be formed. Solutions to $F\phi_i = \epsilon_i\phi_i$ are then found, and those ϕ_i which possess the space and spin symmetry of the occupied orbitals of Ψ and which have the proper energies and nodal character are used to generate a new F operator (i.e., new J_i and K_i operators). The new \hat{F} operator then gives new ϕ_i and ϵ_i via solution of the new equations:

$$\hat{F}\phi_i = \epsilon_i\phi_i. \quad (18.5.1)$$

This iterative process is continued until the ϕ_i and ϵ_i do not vary significantly from one iteration to the next, at which time one says that the process has converged. This iterative procedure is referred to as the Hartree-Fock **self-consistent field** (SCF) procedure because iteration eventually leads to coulomb and exchange potential fields that are consistent from iteration to iteration.

In practice, solution of Equation 18.5.1 as an integro-differential equation can be carried out only for atoms (C. Froese-Fischer, Comp. Phys. Commun. 1, 152 (1970)) and linear molecules (P. A. Christiansen and E. A. McCullough, J. Chem. Phys. 67, 1877 (1977)) for which the angular parts of the ϕ_i can be exactly separated from the radial because of the axial- or full- rotation group symmetry (e.g., $\phi_i = Y_{l,m}R_{n,l}(r)$ for an atom and $\phi_i = e^{im\phi}R_{n,l,m}(r, \theta)$ for a linear molecule). In such special cases, $F\phi_i = \epsilon_i\phi_i$ gives rise to a set of coupled equations for the $R_{n,l}(r)$ or $R_{n,l,m}(r, \theta)$ which can and have been solved. However, for non-linear molecules, the HF equations have not yet been solved in such a manner because of the three-dimensional nature of the ϕ_i and of the potential terms in F .

In the most commonly employed procedures used to solve the HF equations for non-linear molecules, the ϕ_i are expanded in a basis of functions χ_m according to the LCAO-MO procedure:

$$\phi_i = \sum_{\mu} C_{\mu,i} \chi_{\mu}.$$

Doing so then reduces $F\phi_i = \epsilon_i\phi_i$ to a matrix eigenvalue-type equation of the form:

$$\sum_{\nu} F_{\mu,\nu} C_{\nu,i} = \epsilon_i \sum_{\nu} S_{\mu,\nu} C_{\nu,i},$$

where $S_{\mu,\nu} = \langle \chi_{\mu} | \chi_{\nu} \rangle$ is the overlap matrix among the atomic orbitals (aos) and

$$F_{\mu,\nu} = \langle \chi_{\mu} | h | \chi_{\nu} \rangle + \sum_{\delta,\kappa} \left[\gamma_{\delta,\kappa} \langle \chi_{\mu} \chi_{\delta} | g | \chi_{\nu} \chi_{\kappa} \rangle - \gamma_{\delta,\kappa}^{ex} \langle \chi_{\mu} \chi_{\delta} | g | \chi_{\kappa} \chi_{\nu} \rangle \right]$$

is the matrix representation of the Fock operator in the ao basis. The coulomb and exchange-density matrix elements in the ao basis are:

$$\gamma_{\delta,\kappa} = \sum_{i(\text{occupied})} C_{\delta,i} C_{\kappa,i}, \text{ and}$$

$$\gamma_{\delta,\kappa}^{ex} = \sum_{i(\text{occ., and same spin})} C_{\delta,i} C_{\kappa,i},$$

where the sum in $\gamma_{\delta,\kappa}^{ex}$ runs over those occupied spin-orbitals whose m_s value is equal to that for which the Fock matrix is being formed (for a closed-shell species, $\gamma_{\delta,\kappa}^{ex} = \frac{1}{2} \gamma_{\delta,\kappa}$).

It should be noted that by moving to a matrix problem, one does not remove the need for an iterative solution; the $F_{\mu,\nu}$ matrix elements depend on the $C_{\nu,i}$ LCAO-MO coefficients which are, in turn, solutions of the so-called Roothaan matrix Hartree-Fock equations:

$$\sum_{\nu} F_{\mu,\nu} C_{\nu,i} = \epsilon_i \sum_{\nu} S_{\mu,\nu} C_{\nu,i}. \quad (18.5.2)$$

One should also note that, just as $F\phi_i = \epsilon_i\phi_i$ possesses a complete set of eigenfunctions, the matrix $F_{\mu,\nu}$, whose dimension M is equal to the number of atomic basis orbitals used in the LCAO-MO expansion, has M eigenvalues ϵ_i and M eigenvectors whose elements are the $C_{\nu,i}$. Thus, there are occupied and virtual molecular orbitals (mos) each of which is described in the LCAO-MO form with $C_{\nu,i}$ coefficients obtained via solution of Equations [18.5.2](#)

This page titled [18.5: The LCAO-MO Expansion](#) is shared under a [CC BY-NC-SA 4.0](#) license and was authored, remixed, and/or curated by [Jack Simons](#) via [source content](#) that was edited to the style and standards of the LibreTexts platform.

18.6: The Roothaan Matrix SCF Process

The matrix SCF equations introduced earlier

$$\sum_{\nu} F_{\mu,\nu} C_{\nu,i} = \epsilon_i \sum_{\nu} S_{\mu,\nu} C_{\nu,i}$$

must be solved both for the occupied and virtual orbitals' energies ϵ_i and $C_{\nu,i}$ values. Only the occupied orbitals' $C_{\nu,i}$ coefficients enter into the Fock operator

$$F_{\mu,\nu} = \langle \chi_{\mu} | h | \chi_{\nu} \rangle + \sum_{\delta,\kappa} \left[\langle \chi_{\mu} \chi_{\delta} | g | \chi_{\nu} \chi_{\kappa} \rangle - \gamma_{\delta,\kappa}^{ex} \langle \chi_{\mu} \chi_{\delta} | g | \chi_{\kappa} \chi_{\nu} \rangle \right],$$

but both the occupied and virtual orbitals are solutions of the SCF equations. Once atomic basis sets have been chosen for each atom, the **one- and two-electron integrals** appearing in $F_{\mu,\nu}$ must be evaluated. Doing so is a time consuming process, but there are presently several highly efficient computer codes which allow such integrals to be computed for s, p, d, f, and even g, h, and i basis functions. After executing one of these **'integral packages'** for a basis with a total of N functions, one has available (usually on the computer's hard disk) of the order of $\frac{N^2}{2}$ one-electron and $\frac{N^4}{8}$ two-electron integrals over these atomic basis orbitals (the factors of $\frac{1}{2}$ and $\frac{1}{8}$ arise from permutational symmetries of the integrals). When treating extremely large atomic orbital basis sets (e.g., 200 or more basis functions), modern computer programs calculate the requisite integrals but never store them on the disk. Instead, their contributions to $F_{\mu,\nu}$ are accumulated 'on the fly' after which the integrals are discarded.

To begin the SCF process, one must input to the computer routine which computes $F_{\mu,\nu}$ **initial 'guesses'** for the $C_{\nu,i}$ values corresponding to the occupied orbitals. These initial guesses are typically made in one of the following ways:

1. If one has available $C_{\nu,i}$ values for the system from an SCF calculation performed earlier at a nearby molecular geometry, one can use these $C_{\nu,i}$ values to begin the SCF process.
2. If one has $C_{\nu,i}$ values appropriate to fragments of the system (e.g., for C and O atoms if the CO molecule is under study or for CH_2 and O if H_2CO is being studied), one can use these.
3. If one has no other information available, one can carry out one iteration of the SCF process in which the two-electron contributions to $F_{\mu,\nu}$ are ignored (i.e., take $F_{\mu,\nu} = \langle \chi_{\mu} | h | \chi_{\nu} \rangle$) and use the resultant solutions to $\sum_{\nu} F_{\mu,\nu} C_{\nu,i} = \epsilon_i \sum_{\nu} S_{\mu,\nu} C_{\nu,i}$ as initial guesses for the $C_{\nu,i}$. Using only the one-electron part of the Hamiltonian to determine initial values for the LCAO-MO coefficients may seem like a rather severe step; it is, and the resultant $C_{\nu,i}$ values are usually far from the converged values which the SCF process eventually produces. However, the initial $C_{\nu,i}$ obtained in this manner have proper symmetries and nodal patterns because the one-electron part of the Hamiltonian has the same symmetry as the full Hamiltonian.

Once initial guesses are made for the $C_{\nu,i}$ of the occupied orbitals, the full $F_{\mu,\nu}$ matrix is formed and new ϵ_i and $C_{\nu,i}$ values are obtained by solving $\sum_{\nu} F_{\mu,\nu} C_{\nu,i} = \epsilon_i \sum_{\nu} S_{\mu,\nu} C_{\nu,i}$. These new orbitals are then used to form a new $F_{\mu,\nu}$ matrix from which new ϵ_i and $C_{\nu,i}$ are obtained. This iterative process is carried on until the ϵ_i and $C_{\nu,i}$ do not vary (within specified tolerances) from iteration to iteration, at which time one says that the SCF process has converged and reached self-consistency.

As presented, the Roothaan SCF process is carried out in a fully *ab initio* manner in that all one- and two-electron integrals are computed in terms of the specified basis set; no experimental data or other input is employed. As described in Appendix F, it is possible to introduce approximations to the coulomb and exchange integrals entering into the Fock matrix elements that permit many of the requisite $F_{\mu,\nu}$ elements to be evaluated in terms of experimental data or in terms of a small set of 'fundamental' orbital-level coulomb interaction integrals that can be computed in an *ab initio* manner. This approach forms the basis of so-called 'semi-empirical' methods. Appendix F provides the reader with a brief introduction to such approaches to the electronic structure problem and deals in some detail with the well known Hückel and CNDO- level approximations.

This page titled [18.6: The Roothaan Matrix SCF Process](#) is shared under a [CC BY-NC-SA 4.0](#) license and was authored, remixed, and/or curated by [Jack Simons](#) via [source content](#) that was edited to the style and standards of the LibreTexts platform.

18.7: Observations on Orbitals and Orbital Energies

The Meaning of Orbital Energies

The physical content of the Hartree-Fock orbital energies can be seen by observing that $\hat{F}\phi = \epsilon_i\phi_i$ implies that ϵ_i can be written as:

$$\epsilon_i = \langle \phi_i | \hat{F} | \phi_i \rangle = \langle \phi_i | h | \phi_i \rangle + \sum_{j(\text{occupied})} \langle \phi_i | J_j - K_j | \phi_i \rangle = \langle \phi_i | h | \phi_i \rangle + \sum_{j(\text{occupied})} [\mathbf{J}_{i,j} - \mathbf{K}_{i,j}].$$

In this form, it is clear that ϵ_i is equal to the average value of the kinetic energy plus Coulombic attraction to the nuclei for an electron in ϕ_i plus the sum over all of the spin-orbitals occupied in Ψ of coulomb minus exchange interactions between ϕ_i and these occupied spin-orbitals.

- If ϕ_i itself is an occupied spin-orbital, the term $[\mathbf{J}_{i,i} - \mathbf{K}_{i,i}]$ disappears and the latter sum represents the coulomb minus exchange interaction of ϕ_i with all of the N-1 **other** occupied spin-orbitals.
- If ϕ_i is a virtual spin-orbital, this cancellation does not occur, and one obtains the coulomb minus exchange interaction of ϕ_i with all N of the occupied spin-orbitals.

In this sense, the orbital energies for occupied orbitals pertain to interactions which are appropriate to a total of N electrons, while the orbital energies of virtual orbitals pertain to a system with N+1 electrons. It is this fact that makes SCF virtual orbitals not optimal (in fact, not usually very good) for use in subsequent correlation calculations where, for instance, they are used, in combination with the occupied orbitals, to form polarized orbital pairs as discussed in Chapter 12. To correlate a pair of electrons that occupy a valence orbital requires double excitations into a virtual orbital that is not too dislike in size. Although the virtual SCF orbitals themselves suffer these drawbacks, the space they span can indeed be used for treating electron correlation. To do so, it is useful to recombine (in a unitary manner to preserve orthonormality) the virtual orbitals to 'focus' the correlating power into as few orbitals as possible so that the multiconfigurational wavefunction can be formed with as few CSFs as possible. Techniques for effecting such reoptimization or improvement of the virtual orbitals are treated later in this text.

Koopmans' Theorem

Further insight into the meaning of the energies of occupied and virtual orbitals can be gained by considering the following model of the vertical (i.e., at fixed molecular geometry) detachment or attachment of an electron to the original N-electron molecule:

1. In this model, **both** the parent molecule and the species generated by adding or removing an electron are treated at the single-determinant level.
2. In this model, the Hartree-Fock orbitals of the parent molecule are used to describe both the parent and the species generated by electron addition or removal. It is said that such a model neglects '**orbital relaxation**' which would accompany the electron addition or removal (i.e., the reoptimization of the spin-orbitals to allow them to become appropriate to the daughter species).

Within this simplified model, the energy difference between the daughter and the parent species can be written as follows (ϕ_k represents the particular spin-orbital that is added or removed):

1. For electron detachment:

$$\begin{aligned} E^{N-1} - E^N &= \langle \phi_1 \phi_2 \dots \phi_{k-1} \dots \phi_N | \mathbf{H} | \phi_1 \phi_2 \dots \phi_{k-1} \dots \phi_N \rangle - \langle \phi_1 \phi_2 \dots \phi_{k-1} \phi_k \dots \phi_N | \mathbf{H} | \phi_1 \phi_2 \dots \phi_{k-1} \phi_k \dots \phi_N \rangle \\ &= -\langle \phi_k | h | \phi_k \rangle - \sum_{j=(1, k-1, k+1, N)} [J_{k,j} - K_{k,j}] = -\epsilon_k; \end{aligned}$$

2. For electron attachment:

$$\begin{aligned} E^N - E^{N+1} &= \langle \phi_1 \phi_2 \dots \phi_N | \mathbf{H} | \phi_1 \phi_2 \dots \phi_N \rangle - \langle \phi_1 \phi_2 \dots \phi_N \phi_k \dots \phi_N | \mathbf{H} | \phi_1 \phi_2 \dots \phi_N \phi_k \dots \phi_N \rangle \\ &= -\langle \phi_k | h | \phi_k \rangle - \sum_{j=(1, N)} [J_{k,j} - K_{k,j}] = -\epsilon_k; \end{aligned}$$

So, within the limitations of the single-determinant, frozen-orbital model set forth, the ionization potentials (IPs) and electron affinities (EAs) are given as the negative of the occupied and virtual spin-orbital energies, respectively. This statement is referred to

as Koopmans' theorem (T. Koopmans, *Physica* 1, 104 (1933)); it is used extensively in quantum chemical calculations as a means for estimating IPs and EAs and often yields results that are at least qualitatively correct (i.e., ± 0.5 eV).

Koopmans' theorem argues that the ionization potentials and electron affinities are given as the negative of the occupied and virtual spin-orbital energies, respectively.

Orbital Energies and the Total Energy

For the N-electron species whose Hartree-Fock orbitals and orbital energies have been determined, the total SCF electronic energy can be written, by using the Slater-Condon rules, as:

$$E = \sum_{i(\text{occupied})} \langle \phi_i | h | \phi_i \rangle + \sum_{i>j(\text{occupied})} [J_{i,j} - K_{i,j}].$$

For this same system, the sum of the orbital energies of the occupied spin-orbitals is given by:

$$\sum_{i(\text{occupied})} \epsilon_i = \sum_{i(\text{occupied})} \langle \phi_i | h | \phi_i \rangle + \sum_{i,j(\text{occupied})} [J_{i,j} - K_{i,j}].$$

These two seemingly very similar expressions differ in a very important way; the sum of occupied orbital energies, when compared to the total energy, double counts the coulomb minus exchange interaction energies. Thus, within the Hartree-Fock approximation, the sum of the occupied orbital energies is **not** equal to the total energy. The total SCF energy can be computed in terms of the sum of occupied orbital energies by taking one-half of $\sum_{i(\text{occupied})} \epsilon_i$ and then adding to this one-half of $\sum_{i(\text{occupied})} \langle \phi_i | h | \phi_i \rangle$:

$$E = \frac{1}{2} \left[\sum_{i(\text{occupied})} \langle \phi_i | h | \phi_i \rangle + \sum_{i(\text{occupied})} \epsilon_i \right].$$

The fact that the sum of orbital energies is not the total SCF energy also means that as one attempts to develop a qualitative picture of the energies of CSFs along a reaction path, as when orbital and configuration correlation diagrams are constructed, one must be careful not to equate the sum of orbital energies with the total configurational energy; the former is higher than the latter by an amount equal to the sum of the coulomb minus exchange interactions.

The sum of orbital energies is not the total SCF energy.

The Brillouin Theorem

The condition that the SCF energy be stationary with respect to variations $\delta\phi_i$ in the occupied spin-orbitals (that preserve orthonormality) can be written

$$\langle \phi_1 \dots \delta\phi_i \dots \phi_N | H | \phi_1 \dots \phi_i \dots \phi_N \rangle = 0.$$

The infinitesimal variation of ϕ_i can be expressed in terms of its (small) components along the other occupied ϕ_j and along the virtual ϕ_m as follows:

$$\delta\phi_i = \sum_{j=\text{occ}} U_{ij} \phi_j + \sum_m U_{im} \phi_m.$$

When substituted into $\langle \phi_1 \dots \delta\phi_i \dots \phi_N |$, the terms $\sum_{j'=\text{occ}} \langle \phi_1 \dots \phi_{j'} \dots \phi_N | U_{ij}$ vanish because ϕ_j already appears in the original

Slater determinant $|\phi_1 \dots \phi_N\rangle$, so $|\phi_1 \dots \phi_j \dots \phi_N\rangle$ contains ϕ_j twice. Only the sum over virtual orbitals remains, and the stationary property written above becomes

$$\sum_m U_{im} \langle \phi_1 \dots \phi_m \dots \phi_N | H | \phi_1 \dots \phi_i \dots \phi_N \rangle = 0.$$

The Slater-Condon rules allow one to express the Hamiltonian matrix elements appearing here as

$$\langle \phi_1 \dots \phi_m \dots \phi_N | H | \phi_1 \dots \phi_i \dots \phi_N \rangle = \langle \phi_m | h | \phi_i \rangle + \sum_{j=\text{occ}, j \neq i} \langle \phi_m | [J_j - K_j] | \phi_i \rangle,$$

which (because the term with $j=i$ can be included since it vanishes) is equal to the following element of the Fock operator: $\langle \phi_m | F | \phi_i \rangle = \epsilon_i \delta_{im} = 0$. This result proves that Hamiltonian matrix elements between the SCF determinant and those that are singly excited relative to the SCF determinant vanish because they reduce to Fock-operator integrals connecting the pair of orbitals involved in the 'excitation'. This stability property of the SCF energy is known as the Brillouin theorem (i.e., that $|\phi_1 \phi_i \phi_N|$ and $|\phi_1 \dots \phi_m \dots \phi_N|$ have zero Hamiltonian matrix elements if the ϕ s are SCF orbitals). It is exploited in quantum chemical calculations in two manners:

1. When multiconfiguration wavefunctions are formed from SCF spin-orbitals, it allows one to neglect Hamiltonian matrix elements between the SCF configuration and those that are 'singly excited' in constructing the secular matrix.
2. A so-called generalized Brillouin theorem (GBT) arises when one deals with energy optimization for a multiconfigurational variational trial wavefunction for which the orbitals and CI mixing coefficients are simultaneously optimized. This GBT causes certain Hamiltonian matrix elements to vanish, which, in turn, simplifies the treatment of electron correlation for such wavefunctions. This matter is treated in more detail later in this text.

This page titled [18.7: Observations on Orbitals and Orbital Energies](#) is shared under a [CC BY-NC-SA 4.0](#) license and was authored, remixed, and/or curated by [Jack Simons](#) via [source content](#) that was edited to the style and standards of the LibreTexts platform.

CHAPTER OVERVIEW

19: Multi-Determinant Wavefunctions

Corrections to the mean-field model are needed to describe the instantaneous Coulombic interactions among the electrons. This is achieved by including more than one Slater determinant in the wavefunction.

[19.1: Introduction to Multi-Determinant Wavefunctions](#)

[19.2: Different Methods](#)

[19.3: Strengths and Weaknesses of Various Methods](#)

[19.4: Further Details on Implementing Multiconfigurational Methods](#)

This page titled [19: Multi-Determinant Wavefunctions](#) is shared under a [CC BY-NC-SA 4.0](#) license and was authored, remixed, and/or curated by [Jack Simons](#) via [source content](#) that was edited to the style and standards of the LibreTexts platform.

19.1: Introduction to Multi-Determinant Wavefunctions

Much of the development of the previous chapter pertains to the use of a single Slater determinant trial wavefunction. As presented, it relates to what has been called the unrestricted Hartree-Fock (UHF) theory in which each spin-orbital ϕ_i has its own orbital energy ϵ_i and LCAO-MO coefficients $C_{\nu,i}$; there may be different $C_{\nu,i}$ for α spin-orbitals than for β spin-orbitals. Such a wavefunction suffers from the *spin contamination* difficulty detailed earlier.

To allow for a properly spin- and space- symmetry adapted trial wavefunction and to permit Ψ to contain more than a single CSF, methods which are more flexible than the single-determinant HF procedure are needed. In particular, it may be necessary to use a combination of determinants to describe such a proper symmetry function. Moreover, as emphasized earlier, whenever two or more CSFs have similar energies (i.e., Hamiltonian expectation values) and can couple strongly through the Hamiltonian (e.g., at avoided crossings in configuration correlation diagrams), the wavefunction must be described in a multiconfigurational manner to permit the wavefunction to evolve smoothly from reactants to products. Also, whenever dynamical electron correlation effects are to be treated, a multiconfigurational Ψ must be used; in this case, CSFs that are **doubly excited** relative to one or more of the essential CSFs (i.e., the dominant CSFs that are included in the so-called reference wavefunction) are included to permit polarized-orbital-pair formation.

Multiconfigurational functions are needed not only to account for electron correlation but also to permit orbital readjustments to occur. For example, if a set of SCF orbitals is employed in forming a multi-CSF wavefunction, the variational condition that the energy is stationary with respect to variations in the LCAO-MO coefficients is no longer obeyed (i.e., the SCF energy functional is stationary when SCF orbitals are employed, but the MC-energy functional is generally not stationary if SCF orbitals are employed). For such reasons, it is important to include CSFs that are **singly excited** relative to the dominant CSFs in the reference wavefunction.

That singly excited CSFs allow for orbital relaxation can be seen as follows. Consider a wavefunction consisting of one CSF $|\phi_1 \dots \phi_i \dots \phi_N|$ to which singly excited CSFs of the form $|\phi_1 \dots \phi_m \dots \phi_N|$ have been added with coefficients $C_{i,m}$:

$$\Psi = \sum_m C_{i,m} |\phi_1 \dots \phi_m \dots \phi_N| + |\phi_1 \dots \phi_i \dots \phi_N|.$$

All of these determinants have all of their columns equal except the i^{th} column; therefore, they can be combined into a single new determinant:

$$\Psi = |\phi_1 \dots \phi'_i \dots \phi_N|,$$

where the relaxed orbital ϕ'_i

$$\phi'_i = \phi_i + \sum_m C_{i,m} \phi_m.$$

The sum of CSFs that are singly excited in the i^{th} spin-orbital with respect to $|\phi_1 \dots \phi_i \dots \phi_N|$ is therefore seen to allow the spin-orbital ϕ_i to relax into the new spin-orbital ϕ'_i . It is in this sense that singly excited CSFs allow for orbital reoptimization.

In summary, doubly excited CSFs are often employed to permit polarized orbital pair formation and hence to allow for electron correlations. Singly excited CSFs are included to permit orbital relaxation (i.e., orbital reoptimization) to occur.

This page titled [19.1: Introduction to Multi-Determinant Wavefunctions](#) is shared under a [CC BY-NC-SA 4.0](#) license and was authored, remixed, and/or curated by [Jack Simons](#) via [source content](#) that was edited to the style and standards of the LibreTexts platform.

19.2: Different Methods

There are numerous procedures currently in use for determining the 'best' wavefunction of the form:

$$\Psi = \sum_I C_I \Phi_I,$$

where Φ_I is a spin- and space- symmetry adapted CSF consisting of determinants of the form $|\phi_{I1}\phi_{I2}\phi_{I3}\dots\phi_{IN}|$. Excellent overviews of many of these methods are included in **Modern Theoretical Chemistry** Vols. 3 and 4, H. F. Schaefer, III Ed., Plenum Press, New York (1977) and in **Advances in Chemical Physics**, Vols. LXVII and LXIX, K. P. Lawley, Ed., Wiley-Interscience, New York (1987). Within the present Chapter, these two key references will be denoted MTC, Vols. 3 and 4, and ACP, Vols. 67 and 69, respectively.

In all such trial wavefunctions, there are two fundamentally different kinds of parameters that need to be determined- the CI coefficients C_I and the LCAO-MO coefficients describing the ϕ_{Ik} . The most commonly employed methods used to determine these parameters include:

1. The **multiconfigurational self-consistent field** (MCSCF) method in which the expectation value $\frac{\langle\Psi|\mathbf{H}|\Psi\rangle}{\langle\Psi|\Psi\rangle}$ is treated variationally and simultaneously made stationary with respect to variations in the C_I and $C_{n,i}$ coefficients subject to the constraints that the spin-orbitals and the full N-electron wavefunction remain normalized:

$$\langle\phi_i|\phi_j\rangle = \delta_{i,j} = \sum_{\nu,\mu} C_{\nu,i} S_{\nu,\mu} C_{\mu,i}, \text{ and}$$

$$\sum_I C_I^2 = 1.$$

The articles by H.-J. Werner and by R. Shepard in ACP Vol. 69 provide up to date reviews of the status of this approach. The article by A. C. Wahl and G. Das in MTC Vol. 3 covers the 'earlier' history on this topic. F. W. Bobrowicz and W. A. Goddard, III provide, in MTC Vol. 3, an overview of the GVB approach, which, as discussed in Chapter 12, can be viewed as a specific kind of MCSCF calculation.

2. The **configuration interaction** (CI) method in which the LCAO-MO coefficients are determined first (and independently) via either a singleconfiguration SCF calculation or an MCSCF calculation using a small number of CSFs. The CI coefficients are subsequently determined by making the expectation value $\frac{\langle\Psi|\mathbf{H}|\Psi\rangle}{\langle\Psi|\Psi\rangle}$ stationary with respect to variations in the C_I only. In this process, the optimizations of the orbitals and of the CSF amplitudes are done in separate steps. The articles by I. Shavitt and by B. O. Ross and P. E. M. Siegbahn in MTC, Vol. 3 give excellent early overviews of the CI method.
3. The **Møller-Plesset perturbation method** (MPPT) uses the single-configuration SCF process (usually the UHF implementation) to first determine a set of LCAO-MO coefficients and, hence, a set of orbitals that obey $F\phi_i = \epsilon_i\phi_i$. Then, using an unperturbed Hamiltonian equal to the sum of these Fock operators for each of the N electrons $H^0 = \sum_{i=1,N} F(i)$, perturbation theory (see Appendix D for an introduction to time-independent perturbation theory) is used to determine the CI amplitudes for the CSFs. The MPPT procedure is also referred to as the many-body perturbation theory (MBPT) method. The two names arose because two different schools of physics and chemistry developed them for somewhat different applications. Later, workers realized that they were identical in their working equations when the UHF H^0 is employed as the unperturbed Hamiltonian. In this text, we will therefore refer to this approach as MPPT/MBPT.

The amplitude for the so-called **reference** CSF used in the SCF process is taken as unity and the other CSFs' amplitudes are determined, relative to this one, by Rayleigh-Schrödinger perturbation theory using the full N-electron Hamiltonian minus the sum of Fock operators $H-H^0$ as the perturbation. The Slater-Condon rules are used for evaluating matrix elements of $(H-H^0)$ among these CSFs. The essential features of the MPPT/MBPT approach are described in the following articles: J. A. Pople, R. Krishnan, H. B. Schlegel, and J. S. Binkley, Int. J. Quantum Chem. 14, 545 (1978); R. J. Bartlett and D. M. Silver, J. Chem. Phys. 62, 3258 (1975); R. Krishnan and J. A. Pople, Int. J. Quantum Chem. 14, 91 (1978).

4. The **Coupled-Cluster method** expresses the CI part of the wavefunction in a somewhat different manner (the early work in chemistry on this method is described in J. Cizek, J. Chem. Phys. 45, 4256 (1966); J. Paldus, J. Cizek, and I. Shavitt, Phys.

Rev. A5 , 50 (1972); R. J. Bartlett and G. D. Purvis, Int. J. Quantum Chem. 14 , 561 (1978); G. D. Purvis and R. J. Bartlett, J. Chem. Phys. 76 , 1910 (1982));

$$\Psi = e^T \Phi,$$

where Φ is a single CSF (usually the UHF single determinant) which has been used to independently determine a set of spin-orbitals and LCAO-MO coefficients via the SCF process. The operator T generates, when acting on Φ , single, double, etc. 'excitations' (i.e., CSFs in which one, two, etc. of the occupied spin-orbitals in Φ have been replaced by virtual spin-orbitals). T is commonly expressed in terms of operators that effect such spin-orbital removals and additions as follows:

$$T = \sum_{i,m} t_i^m m^+ i + \sum_{i,j,m,n} t_{i,j}^{m,n} m^+ n^+ j i + \dots,$$

where the operator m^+ is used to denote creation of an electron in virtual spin-orbital ϕ_m and the operator j is used to denote **removal** of an electron from occupied spin-orbital ϕ_j .

The t_i^m , $t_{i,j}^{m,n}$, etc. amplitudes, which play the role of the CI coefficients in CC theory, are determined through the set of equations generated by projecting the Schrödinger equation in the form

$$e^{-T} H e^T \Phi = E \Phi$$

against CSFs which are single, double, etc. excitations relative to Φ . For example, for double excitations $\Phi_{i,j}^{m,n}$ the equations read:

$$\langle \Phi_{i,j}^{m,n} | e^{-T} e^T | \Phi \rangle = E \langle \Phi_{i,j}^{m,n} | \Phi \rangle = 0;$$

zero is obtained on the right hand side because the excited CSFs $|\Phi_{i,j}^{m,n}\rangle$ are orthogonal to the reference function $|\Phi\rangle$. The elements on the left hand side of the CC equations can be expressed, as described below, in terms of one- and two-electron integrals over the spin-orbitals used in forming the reference and excited CSFs.

Integral Transformations

All of the above methods require the evaluation of one- and two-electron integrals over the N atomic orbital basis: $\langle \chi_a | f | \chi_b \rangle$ and $\langle \chi_a \chi_b | g | \chi_c \chi_d \rangle$. Eventually, all of these methods provide their working equations and energy expressions in terms of one- and two electron integrals over the N final **molecular orbitals**: $\langle \phi_i | f | \phi_j \rangle$ and $\langle \chi_i \chi_j | g | \chi_k \chi_l \rangle$. The mo-based integrals can only be evaluated by **transforming** the AO-based integrals as follows:

$$\langle \phi_i \phi_j | g | \phi_k \phi_l \rangle = \sum_{a,b,c,d} C_{a,i} C_{b,j} C_{c,k} C_{d,l} \langle \chi_a \chi_b | g | \chi_c \chi_d \rangle,$$

and

$$\langle \phi_i | f | \phi_j \rangle = \sum_{a,b} C_{a,i} C_{b,j} \langle \chi_a | f | \chi_b \rangle.$$

It would seem that the process of evaluating all N^4 of the $\langle \phi_i \phi_j | g | \phi_k \phi_l \rangle$, each of which requires N^4 additions and multiplications, would require computer time proportional to N^8 . However, it is possible to perform the full transformation of the two-electron integral list in a time that scales as N^5 . This is done by first performing a transformation of the $\langle \chi_a \chi_b | g | \chi_c \chi_d \rangle$ to an intermediate array $\langle \chi_a \chi_b | g | \chi_c \phi_1 \rangle$ labeled as follows:

$$\langle \chi_a \chi_b | g | \chi_c \phi_1 \rangle = \sum_d C_{d,1} \langle \chi_a \chi_b | g | \chi_c \chi_d \rangle.$$

This partial transformation requires N^5 multiplications and additions. The list $\langle \chi_a \chi_b | g | \chi_c \phi_1 \rangle$ is then transformed to a second-level transformed array $\langle \chi_a \chi_b | g | \phi_k \phi_1 \rangle$:

$$\langle \chi_a \chi_b | g | \phi_k \phi_1 \rangle = \sum_c C_{c,k} \langle \chi_a \chi_b | g | \chi_c \phi_1 \rangle,$$

which requires another N^5 operations. This sequential, one-index-at-a-time transformation is repeated four times until the final $\langle \phi_i \phi_j | g | \phi_k \phi_l \rangle$ array is in hand. The entire transformation done this way requires $4N^5$ multiplications and additions.

Once the requisite one- and two-electron integrals are available in the molecular orbital basis, the multiconfigurational wavefunction and energy calculation can begin. These transformations consume a large fraction of the computer time used in most such calculations, and represent a severe bottleneck to progress in applying **ab initio** electronic structure methods to larger systems.

Configuration List Choices

Once the requisite one- and two-electron integrals are available in the molecular orbital basis, the multiconfigurational wavefunction and energy calculation can begin. Each of these methods has its own approach to describing the configurations $\{\Phi_J\}$ included in the calculation and how the $\{C_J\}$ amplitudes and the total energy E is to be determined.

The **number of configurations** (N_C) varies greatly among the methods and is an important factor to keep in mind when planning to carry out an *ab initio* calculation. Under certain circumstances (e.g., when studying Woodward-Hoffmann forbidden reactions where an avoided crossing of two configurations produces an activation barrier), it may be essential to use more than one electronic configuration. Sometimes, one configuration (e.g., the SCF model) is adequate to capture the qualitative essence of the electronic structure. In all cases, many configurations will be needed if highly accurate treatment of electron-electron correlations are desired.

The value of N_C determines how much computer time and memory is needed to solve the N_C -dimensional $\sum_J H_{IJ} C_J = E C_I$ secular problem in the CI and MCSCF methods. Solution of these matrix eigenvalue equations requires computer time that scales as N_C^2 (if few eigenvalues are computed) to N_C^3 (if most eigenvalues are obtained).

So-called **complete-active-space** (CAS) methods form **all** CSFs that can be created by distributing N valence electrons among P valence orbitals. For example, the eight noncore electrons of H_2O might be distributed, in a manner that gives $M_S = 0$, among six valence orbitals (e.g., two lone-pair orbitals, two OH σ bonding orbitals, and two OH σ^* antibonding orbitals). The number of configurations thereby created is 225. If the same eight electrons were distributed among ten valence orbitals 44,100 configurations results; for twenty and thirty valence orbitals, 23,474,025 and 751,034,025 configurations arise, respectively. Clearly, practical considerations dictate that CAS-based approaches be limited to situations in which a few electrons are to be correlated using a few valence orbitals. The primary advantage of CAS configurations is discussed below in Sec. II. C.

This page titled [19.2: Different Methods](#) is shared under a [CC BY-NC-SA 4.0](#) license and was authored, remixed, and/or curated by [Jack Simons](#) via [source content](#) that was edited to the style and standards of the LibreTexts platform.

19.3: Strengths and Weaknesses of Various Methods

Variational Methods Such as MCSCF, SCF, and CI Produce Energies that are Upper Bounds, but These Energies are not Size-Extensive

Methods that are based on making the energy functional $\frac{\langle \Psi | H | \Psi \rangle}{\langle \Psi | \Psi \rangle}$ stationary (i.e., variational methods) yield **upper bounds** to the lowest energy of the symmetry which characterizes the CSFs which comprise Ψ . These methods also can provide approximate excited-state energies and wavefunctions (e. g., in the form of other solutions of the secular equation $\sum_J H_{IJ} C_J = C_I$ that arises in the CI and MCSCF methods). Excited-state energies obtained in this manner can be shown to 'bracket' the true energies of the given symmetry in that between any two approximate energies obtained in the variational calculation, there exists at least one true eigenvalue. This characteristic is commonly referred to as the 'bracketing theorem' (E. A. Hylleraas and B. Undheim, Z. Phys. 65, 759 (1930); J. K. L. MacDonald, Phys. Rev. 43, 830 (1933)). These are strong attributes of the variational methods, as is the long and rich history of developments of analytical and computational tools for efficiently implementing such methods (see the discussions of the CI and MCSCF methods in MTC and ACP).

However, all variational techniques suffer from at least one serious drawback; they are not **size-extensive** (J. A. Pople, pg. 51 in **Energy, Structure, and Reactivity**, D. W. Smith and W. B. McRae, Eds., Wiley, New York (1973)). This means that the energy computed using these tools can not be trusted to scale with the size of the system. For example, a calculation performed on two CH_3 species at large separation may not yield an energy equal to twice the energy obtained by performing the same kind of calculation on a single CH_3 species. Lack of size-extensivity precludes these methods from use in extended systems (e.g., solids) where errors due to improper scaling of the energy with the number of molecules produce nonsensical results.

By carefully adjusting the kind of variational wavefunction used, it is possible to circumvent size-extensivity problems for selected species. For example, a CI calculation on Be_2 using **all** $1 \sum_g$ CSFs that can be formed by placing the four valence electrons into the orbitals $2\sigma_g, 2\sigma_u, 3\sigma_g, 3\sigma_u, 1\pi_u$, and $1\pi_g$ can yield an energy equal to twice that of the Be atom described by CSFs in which the two valence electrons of the Be atom are placed into the 2s and 2p orbitals in all ways consistent with a 1S symmetry. Such special choices of configurations give rise to what are called **complete-active-space** (CAS) MCSCF or CI calculations (see the article by B. O. Roos in ACP for an overview of this approach).

Let us consider an example to understand why the CAS choice of configurations works. The 1S ground state of the Be atom is known to form a wavefunction that is a strong mixture of CSFs that arise from the $2s^2$ and $2p^2$ configurations:

$$\Psi_{Be} = C_1 |1s^2 2s^2| + C_2 |1s^2 2p^2|,$$

where the latter CSF is a short-hand representation for the proper spin- and spacesymmetry adapted CSF

$$|1s^2 2p^2| = \frac{1}{\sqrt{3}} [|1s\alpha 1s\beta 2p_0\alpha 2p_0\beta| - |1s\alpha 1s\beta 2p_1\alpha 2p_{-1}\beta| - |1s\alpha 1s\beta 2p_{-1}\alpha 2p_1\beta|].$$

The reason the CAS process works is that the Be_2 CAS wavefunction has the flexibility to dissociate into the product of two CAS Be wavefunctions:

$$\Psi = \Psi_{Bea} \Psi_{Beb} = [C_1 |1s^2 2s^2| + C_2 |1s^2 2p^2|]_a [C_1 |1s^2 2s^2| + C_2 |1s^2 2p^2|]_b,$$

where the subscripts a and b label the two Be atoms, because the four electron CAS function distributes the four electrons in all ways among the $2\sigma_a, 2\sigma_b, 2\pi_a$, and $2\pi_b$ orbitals. In contrast, if the Be_2 calculation had been carried out using only the following CSFs: $|1\sigma_g^2 1\sigma_u^2 2\sigma_g^2 2\sigma_u^2|$ and all single and double excitations relative to this (dominant) CSF, which is a very common type of CI procedure to follow, the Be_2 wavefunction would not have contained the particular CSFs $|1\sigma^2 2\pi^2|_a |1\sigma^2 2\pi^2|_b$ because these CSFs are four-fold excited relative to the $|1\sigma_g^2 1\sigma_u^2 2\sigma_g^2 2\sigma_u^2|$ 'reference' CSF.

In general, one finds that if the 'monomer' uses CSFs that are K-fold excited relative to its dominant CSF to achieve an accurate description of its electron correlation, a size-extensive variational calculation on the 'dimer' will require the inclusion of CSFs that are 2K-fold excited relative to the dimer's dominant CSF. To perform a size-extensive variational calculation on a species containing M monomers therefore requires the inclusion of CSFs that are MxK-fold excited relative to the M-mer's dominant CSF.

Non-Variational Methods Such as MPPT/MBPT and CC do not Produce Upper Bounds, but Yield Size-Extensive Energies

In contrast to variational methods, perturbation theory and coupled-cluster methods achieve their energies from a 'transition formula' $\langle \Phi | H | \Psi \rangle$ rather than from an expectation value $\langle \Psi | H | \Psi \rangle$. It can be shown (H. P. Kelly, Phys. Rev. 131, 684 (1963)) that this difference allows non-variational techniques to yield size-extensive energies. This can be seen in the MPPT/MBPT case by considering the energy of two non-interacting Be atoms. The reference CSF is $\Phi = |s_g^2 2s_a^2 a s_b^2 2s_b^2|$; the Slater-Condon rules limit the CSFs in Ψ which can contribute to

$$E = \langle \Phi | H | \Psi \rangle = \langle \Phi | H \sum_J C_J \Phi_J \rangle.$$

to be Φ itself and those CSFs that are singly or doubly excited relative to Φ . These 'excitations' can involve atom a, atom b, or both atoms. However, any CSFs that involve excitations on both atoms (e.g., $|1s_a^2 2s_a 2p_a 1s_b^2 2s_b 2p_b|$) give rise, via the SC rules, to one- and two- electron integrals over orbitals on both atoms; these integrals (e.g., $\langle 2s_a 2p_a | g | 2s_b 2p_b \rangle$) vanish if the atoms are far apart, as a result of which the contributions due to such CSFs vanish in our consideration of size-extensivity. Thus, only CSFs that are excited on one or the other atom contribute to the energy:

$$E = \langle \Phi_a \Phi_b | H \sum_{Ja} C_{Ja} \Phi_{Ja}^* \Phi_b + \sum_{Jb} C_{Jb} \Phi_a \Phi_{Jb}^* \rangle,$$

where Φ_a and Φ_b as well as Φ_{Ja}^* and Φ_{Jb}^* are used to denote the a and b parts of the reference and excited CSFs, respectively.

This expression, once the SC rules are used to reduce it to one- and two- electron integrals, is of the additive form required of any size-extensive method:

$$E = \langle \Phi_a | H \sum_{Ja} C_{Ja} \Phi_{Ja} \rangle + \langle \Phi_b | H \sum_{Jb} C_{Jb} \Phi_{Jb} \rangle,$$

and will yield a size-extensive energy if the equations used to determine the C_{Ja} and C_{Jb} amplitudes are themselves separable. In MPPT/MBPT, these amplitudes are expressed, in first order, as:

$$C_{Ja} = \frac{\langle \Phi_a \Phi_b | H | \Phi_{Ja}^* \Phi_b \rangle}{E_a^0 + E_b^0 - E_{Ja}^* - E_b^0}$$

(and analogously for C_{Jb}). Again using the SC rules, this expression reduces to one that involves only atom a:

$$C_{Ja} = \frac{\langle H | \Phi_{Ja}^* \rangle}{E_a^0 - E_{Ja}^*}.$$

The additivity of E and the separability of the equations determining the C_J coefficients make the MPPT/MBPT energy size-extensive. This property can also be demonstrated for the Coupled-Cluster energy (see the references given above in Chapter 19. I.4). However, size-extensive methods have at least one serious weakness; their energies do **not** provide upper bounds to the true energies of the system (because their energy functional is not of the expectation-value form for which the upper bound property has been proven).

Which Method is Best?

At this time, it may not possible to say which method is preferred for applications where all are practical. Nor is it possible to assess, in a way that is applicable to most chemical species, the accuracies with which various methods predict bond lengths and energies or other properties. However, there are reasons to recommend some methods over others in specific cases. For example, certain applications require a size-extensive energy (e.g., extended systems that consist of a large or macroscopic number of units or studies of weak intermolecular interactions), so MBPT/MPPT or CC or CAS-based MCSCF are preferred. Moreover, certain chemical reactions (e.g., Woodward-Hoffmann forbidden reactions) and certain bond-breaking events require two or more 'essential' electronic configurations. For them, single-configuration-based methods such as conventional CC and MBTP/MPPT should not be used; MCSCF or CI calculations would be better. Very large molecules, in which thousands of atomic orbital basis functions are required, may be impossible to treat by methods whose effort scales as N^4 or higher; density functional methods would be better to use then.

For all calculations, the choice of atomic orbital basis set must be made carefully, keeping in mind the N^4 scaling of the one- and two-electron integral evaluation step and the N^5 scaling of the two-electron integral transformation step. Of course, basis functions that describe the essence of the states to be studied are essential (e.g., Rydberg or anion states require diffuse functions, and strained rings require polarization functions).

As larger atomic basis sets are employed, the size of the CSF list used to treat dynamic correlation increases rapidly. For example, most of the above methods use singly and doubly excited CSFs for this purpose. For large basis sets, the number of such CSFs, N_C , scales as the number of electrons squared, n_e^2 , times the number of basis functions squared, N^2 . Since the effort needed to solve the CI secular problem varies as N_C^2 or N_C^3 , a dependence as strong as N^4 to N^6 can result. To handle such large CSF spaces, all of the multiconfigurational techniques mentioned in this paper have been developed to the extent that calculations involving of the order of 100 to 5,000 CSFs are routinely performed and calculations using 10,000, 100,000, and even several million CSFs are practical

Other methods, most of which can be viewed as derivatives of the techniques introduced above, have been and are still being developed. This ongoing process has been, in large part, stimulated by the explosive growth in computer power and change in computer architecture that has been realized in recent years. All indications are that this growth pattern will continue, so *ab initio* quantum chemistry will likely have an even larger impact on future chemistry research and education (through new insights and concepts).

This page titled [19.3: Strengths and Weaknesses of Various Methods](#) is shared under a [CC BY-NC-SA 4.0](#) license and was authored, remixed, and/or curated by [Jack Simons](#) via [source content](#) that was edited to the style and standards of the LibreTexts platform.

19.4: Further Details on Implementing Multiconfigurational Methods

The MCSCF Method

The simultaneous optimization of the LCAO-MO and CI coefficients performed within an MCSCF calculation is a quite formidable task. The variational energy functional is a quadratic function of the CI coefficients, and so one can express the stationary conditions for these variables in the secular form:

$$\sum_J H_{I,J} C_J = E C_I.$$

However, E is a quartic function of the $C_{\nu,i}$ coefficients because each matrix element $\langle \Phi_I | H | \Phi_I \rangle$ involves one- and two-electron integrals over the mos ϕ_i , and the two-electron integrals depend quartically on the $C_{\nu,i}$ coefficients. The stationary conditions with respect to these $C_{\nu,i}$ parameters must be solved iteratively because of this quartic dependence.

It is well known that minimization of a function (E) of several non-linear parameters (the $C_{\nu,i}$) is a difficult task that can suffer from poor convergence and may locate local rather than global minima. In an MCSCF wavefunction containing many CSFs, the energy is only weakly dependent on the orbitals that are weakly occupied (i.e., those that appear in CSFs with small C_I values); in contrast, E is strongly dependent on the $C_{\nu,i}$ coefficients of those orbitals that appear in the CSFs with larger C_I values. One is therefore faced with minimizing a function of many variables (there may be as many $C_{\nu,i}$ as the square of the number of orbital basis functions) that depends strongly on several of the variables and weakly on many others. This is a very difficult job.

For these reasons, in the MCSCF method, the number of CSFs is usually kept to a small to moderate number (e.g., a few to several hundred) chosen to describe essential correlations (i.e., configuration crossings, proper dissociation) and important dynamical correlations (those electron-pair correlations of angular, radial, left-right, etc. nature that arise when low-lying 'virtual' orbitals are present). In such a compact wavefunction, only spin-orbitals with reasonably large occupations (e.g., as characterized by the diagonal elements of the one-particle density matrix $\gamma_{i,j}$) appear. As a result, the energy functional is expressed in terms of variables on which it is strongly dependent, in which case the nonlinear optimization process is less likely to be pathological.

Such a compact MCSCF wavefunction is designed to provide a good description of the set of strongly occupied spin-orbitals and of the CI amplitudes for CSFs in which only these spin-orbitals appear. It, of course, provides no information about the spin-orbitals that are not used to form the CSFs on which the MCSCF calculation is based. As a result, the MCSCF energy is invariant to a unitary transformation among these 'virtual' orbitals.

In addition to the references mentioned earlier in ACP and MTC, the following papers describe several of the advances that have been made in the MCSCF method, especially with respect to enhancing its rate and range of convergence: E. Dalgaard and P. Jørgensen, J. Chem. Phys. 69 , 3833 (1978); H. J. Aa. Jensen, P. Jørgensen, and H. Ågren, J. Chem. Phys. 87 , 457 (1987); B. H. Lengsfeld, III and B. Liu, J. Chem. Phys. 75 , 478 (1981).

The Configuration Interaction Method

In the [Configuration Interaction \(CI\) method](#), one usually attempts to realize a high-level treatment of electron correlation. A set of orthonormal molecular orbitals are first obtained from an SCF or MCSCF calculation (usually involving a small to moderate list of CSFs). The LCAO-MO coefficients of these orbitals are **no longer considered** as variational parameters in the subsequent CI calculation; only the C_I coefficients are to be further optimized.

The CI wavefunction

$$\psi = \sum_J C_J \Phi_J$$

is most commonly constructed from CSFs Φ_J that include:

1. All of the CSFs in the SCF (in which case only a single CSF is included) or MCSCF wavefunction that was used to generate the molecular orbitals ϕ_i . This set of CSFs are referred to as spanning the '**reference space**' of the subsequent CI calculation, and the particular combination of these CSFs used in this orbital optimization (i.e., the SCF or MCSCF wavefunction) is called the **reference function**.
2. CSFs that are generated by carrying out single, double, triple, etc. level 'excitations' (i.e., orbital replacements) relative to reference CSFs. CI wavefunctions limited to include contributions through various levels of excitation (e.g., single, double, etc.

) are denoted S (singly excited), D (doubly), SD (singly and doubly), SDT (singly, doubly, and triply), and so on.

The orbitals from which electrons are removed and those into which electrons are excited can be restricted to focus attention on correlations among certain orbitals. For example, if excitations out of core electrons are excluded, one computes a total energy that contains no correlation corrections for these core orbitals. Often it is possible to so limit the nature of the orbital excitations to focus on the energetic quantities of interest (e.g., the CC bond breaking in ethane requires correlation of the σ_{CC} orbital but the 1s Carbon core orbitals and the CH bond orbitals may be treated in a non-correlated manner).

Clearly, the number of CSFs included in the CI calculation can be far in excess of the number considered in typical MCSCF calculations; CI wavefunctions including 5,000 to 50,000 CSFs are routinely used, and functions with one to **several million** CSFs are within the realm of practicality (see, for example, J. Olsen, B. Roos, Poul Jørgensen, and H. J. Aa. Jensen, J. Chem. Phys. 89, 2185 (1988) and J. Olsen, P. Jørgensen, and J. Simons, Chem. Phys. Letters 169, 463 (1990)).

The need for such large CSF expansions should not come as a surprise once one considers that (i) each electron pair requires **at least** two CSFs (let us say it requires P of them, on average, a dominant one and P-1 others which are doubly excited) to form polarized orbital pairs, (ii) there are of the order of $N(N-1)/2 = X$ electron pairs in an atom or molecule containing N electrons, and (iii) that the number of terms in the CI wavefunction scales as P^X . So, for an H_2O molecule containing ten electrons, there would be P^{55} terms in the CI expansion. This is 3.6×10^{16} terms if $P=2$ and 1.7×10^{26} terms if $P=3$. Undoubtedly, this is an over estimate of the number of CSFs needed to describe electron correlation in H_2O , but it demonstrates how rapidly the number of CSFs can grow with the number of electrons in the system.

The $H_{I,J}$ matrices that arise in CI calculations are evaluated in terms of one- and two- electron integrals over the molecular orbitals using the equivalent of the Slater-Condon rules. For large CI calculations, the full $H_{I,J}$ matrix is not actually evaluated and stored in the computer's memory (or on its disk); rather, so-called 'direct CI' methods (see the article by Roos and Siegbahn in MTC) are used to compute and immediately sum contributions to the sum $\sum_I H_{I,J} C_I$ in terms of integrals, density matrix elements, and approximate values of the C_J amplitudes. Iterative methods (see, for example, E. R. Davidson, J. Comput. Phys. 17, 87 (1975)), in which approximate values for the C_J coefficients and energy E are refined through sequential application of $\sum_I H_{I,J}$ to the preceding estimate of the C_J vector, are employed to solve these large CI matrix eigenvalue problems.

The MPPT/MBPT Method

In the MPPT/MBPT method, once the reference CSF is chosen and the SCF orbitals belonging to this CSF are determined, the wavefunction ψ and energy E are determined in an order-by-order manner. This is one of the primary strengths of the MPPT/MBPT technique; it does not require one to make further (potentially arbitrary) choices once the basis set and dominant (SCF) configuration are specified. In contrast to the MCSCF and CI treatments, one need not make choices of CSFs to include in or exclude from ψ . The MPPT/MBPT perturbation equations determine what CSFs must be included through any particular order.

For example, the first-order wavefunction correction ψ^1 (i.e., $\psi = \Phi + \psi^1$ through first order) is given by:

$$\psi^1 = - \sum_{i < j, m > n} \frac{\langle \Phi_{i,j}^{m,n} | H - H^0 | \Phi \rangle}{\epsilon_m - \epsilon_i + \epsilon_n - \epsilon_j} | \Phi_{i,j}^{m,n} \rangle \quad (19.4.1)$$

$$= - \sum_{i < j, m < n} \frac{\langle i, j | g | m, n \rangle - \langle i, j | g | n, m \rangle}{\epsilon_m - \epsilon_i + \epsilon_n - \epsilon_j} | \Phi_{i,j}^{m,n} \rangle \quad (19.4.2)$$

where the SCF orbital energies are denoted ϵ_k and $\Phi_{i,j}^{m,n}$ represents a CSF that is **doubly excited** relative to Φ . Thus, only doubly **excited** CSFs contribute to the **first-order wavefunction**; as a result, the energy E is given through second order as:

$$E = \langle H^0 | \Phi \rangle + \langle \Phi | H - H^0 | \Phi \rangle + \langle \Phi | H - H^0 | \psi^1 \rangle \quad (19.4.3)$$

$$= \langle \Phi | H | \Phi \rangle - \sum_{i < j, m < n} \frac{|\langle \Phi_{i,j}^{m,n} | H - H^0 | \Phi \rangle|^2}{\epsilon_m - \epsilon_i + \epsilon_n - \epsilon_j} \quad (19.4.4)$$

$$= E_{SCF} - \sum_{i < j, m < n} \frac{|\langle i, j | g | m, n \rangle - \langle i, j | g | n, m \rangle|^2}{\epsilon_m - \epsilon_i + \epsilon_n - \epsilon_j} \quad (19.4.5)$$

$$= E^0 + E^1 + E^2. \quad (19.4.6)$$

These contributions have been expressed, using the SC rules, in terms of the two-electron integrals $\langle i,j|g|m,n\rangle$ coupling the excited spin-orbitals to the spin-orbitals from which electrons were excited as well as the orbital energy differences $[\epsilon_m - \epsilon_i + \epsilon_n - \epsilon_j]$ accompanying such excitations. In this form, it becomes clear that major contributions to the correlation energy of the pair of occupied orbitals $\phi_i\phi_j$ are made by double excitations into virtual orbitals $\phi_m\phi_n$ that have large coupling (i.e., large $\langle i,j|g|m,n\rangle$ integrals) and small orbital energy gaps, $[\epsilon_m - \epsilon_i + \epsilon_n - \epsilon_j]$.

In higher order corrections to the wavefunction and to the energy, contributions from CSFs that are singly, triply, etc. excited relative to Φ appear, and additional contributions from the doubly excited CSFs also enter. It is relatively common to carry MPPT/MBPT calculations (see the references given above in Chapter 19.I.3 where the contributions of the Pople and Bartlett groups to the development of MPPT/MBPT are documented) through to third order in the energy (whose evaluation can be shown to require only ψ^0 and ψ^1). The entire GAUSSIAN-8X series of programs, which have been used in thousands of important chemical studies, calculate E through third order in this manner.

In addition to being size-extensive and not requiring one to specify input beyond the basis set and the dominant CSF, the MPPT/MBPT approach is able to include the effect of **all** CSFs (that contribute to any given order) without having to find any eigenvalues of a matrix. This is an important advantage because matrix eigenvalue determination, which is necessary in MCSCF and CI calculations, requires computer time in proportion to the third power of the dimension of the $H_{I,J}$ matrix. Despite all of these advantages, it is important to remember the primary disadvantages of the MPPT/MBPT approach; its energy is not an upper bound to the true energy and it may not be able to treat cases for which two or more CSFs have equal or nearly equal amplitudes because it obtains the amplitudes of all but the dominant CSF from perturbation theory formulas that assume the perturbation is 'small'.

The Coupled-Cluster Method

The implementation of the Coupled-Cluster method begins much as in the MPPT/MBPT case; one selects a reference CSF that is used in the SCF process to generate a set of spin-orbitals to be used in the subsequent correlated calculation. The set of working equations of the Coupled-Cluster technique can be written explicitly by introducing the form of the so-called cluster operator T,

$$T = \sum_{i,m} t_i^m m^+ i + \sum_{i,j,m,n} t_{i,j}^{m,n} m^+ n^+ j i + \dots,$$

where the combination of operators $m^+ i$ denotes creation of an electron in virtual spin orbital ϕ_m and removal of an electron from occupied spin-orbital ϕ_i to generate a single excitation. The operation $m^+ n^+ j i$ therefore represents a double excitation from $\phi_i\phi_j$ to $\phi_m\phi_n$. Expressing the cluster operator T in terms of the amplitudes t_i^m , $t_{i,j}^{m,n}$, etc. for singly, doubly, etc. excited CSFs, and expanding the exponential operators in

$$e^{-T} H e^T$$

one obtains:

$$\begin{aligned} \langle \Phi_i^m | H + [H, T] + \frac{1}{2} [[H, T], T] + \frac{1}{6} [[[H, T], T], T] + \frac{1}{24} [[[[H, T], T], T], T] | \Phi \rangle &= 0; \\ \langle \Phi_{i,j}^{m,n} | H + [H, T] + \frac{1}{2} [[H, T], T] + \frac{1}{6} [[[H, T], T], T] + \frac{1}{24} [[[[H, T], T], T], T] | \Phi \rangle &= 0; \\ \langle \Phi_{i,j,k}^{m,n,p} | H + [H, T] + \frac{1}{2} [[H, T], T] + \frac{1}{6} [[[H, T], T], T] + \frac{1}{24} [[[[H, T], T], T], T] | \Phi \rangle &= 0; \end{aligned}$$

and so on for higher order excited CSFs. It can be shown, because of the one- and twoelectron operator nature of H, that the expansion of the exponential operators truncates exactly at the fourth power; that is terms such as $[[[[[H, T], T], T], T], T]$ and higher commutators vanish identically (this is demonstrated in Chapter 4 of **Second Quantization Based Methods in Quantum Chemistry**, P. Jørgensen and J. Simons, Academic Press, New York (1981).

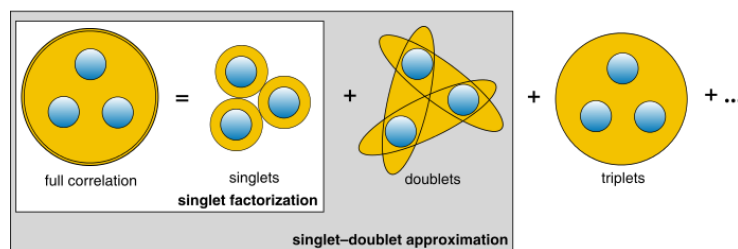


Figure 19.3.1: Schematic representation of the cluster-expansion-based classification. The full correlation is composed of singlets, doublets, triplets, and higher-order correlations, all uniquely defined by the cluster-expansion approach. Each blue sphere corresponds to one particle operator and yellow circles/ellipses to correlations. The number of spheres within a correlation identifies the cluster number. (CC SA-BY-3.0; Christoph N. Böttge, "Phonon-assistierte Lasertätigkeit in Mikroresonatoren").

As a result, the exact Coupled-Cluster equations are **quartic equations** for the t_i^m , $t_{i,j}^{m,n}$, etc. amplitudes. Although it is a rather formidable task to evaluate all of the commutator matrix elements appearing in the above Coupled-Cluster equations, it can be and has been done (the references given above to Purvis and Bartlett are especially relevant in this context). The result is to express each such matrix element, via the Slater-Condon rules, in terms of one- and twoelectron integrals over the spin-orbitals used in determining Φ , including those in Φ itself and the 'virtual' orbitals not in Φ .

In general, these quartic equations must then be solved in an iterative manner and are susceptible to convergence difficulties that are similar to those that arise in MCSCF-type calculations. In any such iterative process, it is important to start with an approximation (to the t amplitudes, in this case) which is reasonably close to the final converged result. Such an approximation is often achieved, for example, by neglecting all of the terms that are nonlinear in the t amplitudes (because these amplitudes are assumed to be less than unity in magnitude). This leads, for the Coupled-Cluster working equations obtained by projecting onto the doubly excited CSFs, to:

$$\langle i,j | g | m,n \rangle' + [\epsilon_m - \epsilon_i + \epsilon_n - \epsilon_j] t_{i,j}^{m,n} + \sum_{i',j',m',n'} \langle \Phi_{i,j}^{m,n} | H - H^0 | \Phi_{i',j'}^{m',n'} \rangle \Phi_{i',j'}^{m',n'} t_{i',j'}^{m',n'} = 0,$$

where the notation $\frac{\langle i,j | g | m,n \rangle'}{\epsilon_m - \epsilon_i + \epsilon_n - \epsilon_j}$ is used to denote the two-electron integral difference $\langle i,j | g | m,n \rangle - \langle i,j | g | n,m \rangle$. If, in addition, the factors that couple different doubly excited CSFs are ignored (i.e., the sum over i',j',m',n'), the equations for the t amplitudes reduce to the equations for the CSF amplitudes of the first-order MPPT/MBPT wavefunction:

$$t_{i,j}^{m,n} = - \frac{\langle i,j | g | m,n \rangle'}{\epsilon_m - \epsilon_i + \epsilon_n - \epsilon_j}$$

As Bartlett and Pople have both demonstrated, there is, in fact, close relationship between the MPPT/MBPT and Coupled-Cluster methods when the Coupled-Cluster equations are solved iteratively starting with such an MPPT/MBPT-like initial 'guess' for these double-excitation amplitudes.

The Coupled-Cluster method, as presented here, suffers from the same drawbacks as the MPPT/MBPT approach; its energy is not an upper bound and it may not be able to accurately describe wavefunctions which have two or more CSFs with approximately equal amplitude. Moreover, solution of the non-linear Coupled-Cluster equations may be difficult and slowly (if at all) convergent. It has the same advantages as the MPPT/MBPT method; its energy is size-extensive, it requires no large matrix eigenvalue solution, and its energy and wavefunction are determined once one specifies the basis and the dominant CSF.

Density Functional Methods

These approaches provide alternatives to the conventional tools of quantum chemistry. The CI, MCSCF, MPPT/MBPT, and CC methods move beyond the singleconfiguration picture by adding to the wave function more configurations whose amplitudes they each determine in their own way. This can lead to a very large number of CSFs in the correlated wave function, and, as a result, a need for extraordinary computer resources.

The density functional approaches are different. Here one solves a set of orbitallevel equations

$$\left[-\frac{\hbar^2}{2m_e} \nabla^2 - \sum_A \frac{Z_A e^2}{|\mathbf{r} - \mathbf{R}_A|} + \int \frac{\rho(\mathbf{r}' e^2)}{|\mathbf{r} - \mathbf{r}'|} d\mathbf{r}' + U(\mathbf{r}) \right] \phi_i = \epsilon_i \phi_i$$

in which the orbitals $\{\phi_i\}$ 'feel' potentials due to the nuclear centers (having charges Z_A), Coulombic interaction with the **total** electron density $\rho(\mathbf{r})$, and a so-called **exchange correlation** potential denoted $U(\mathbf{r})$. The particular electronic state for which the calculation is being performed is specified by forming a corresponding density $\rho(\mathbf{r})$. Before going further in describing how DFT calculations are carried out, let us examine the origins underlying this theory.

The so-called Hohenberg-Kohn theorem states that the **ground-state** electron density $\rho(\mathbf{r})$ describing an N-electron system uniquely determines the potential $V(\mathbf{r})$ in the Hamiltonian

$$H = \sum_j \frac{\hbar^2}{2m_e} \nabla_j^2 + V(\mathbf{r}_j) + \frac{e^2}{2} \sum_{j \neq k} \frac{1}{r_{j,k}},$$

and, because H determines the ground-state energy and wave function of the system, the ground-state density $\rho(\mathbf{r})$ determines the ground-state properties of the system. The proof of this theorem proceeds as follows:

- $\rho(\mathbf{r})$ determines N because $\int \rho(\mathbf{r}) d^3r = N$.
- Assume that there are two distinct potentials (aside from an additive constant that simply shifts the zero of total energy) $V(\mathbf{r})$ and $V'(\mathbf{r})$ which, when used in H and H' , respectively, to solve for a ground state produce

$$E_0, \psi(\mathbf{r}) \text{ and } E'_0, \psi'(\mathbf{r})$$

that have the same one-electron density:

$$\int |\psi|^2 d\mathbf{r}_2 d\mathbf{r}_3 \dots d\mathbf{r}_N = \rho(\mathbf{r}) = \int |\psi'|^2 d\mathbf{r}_2 d\mathbf{r}_3 \dots d\mathbf{r}_N$$

- If we think of ψ as trial variational wave function for the Hamiltonian H, we know that

$$E_0 < \langle \psi' | H | \psi' \rangle = \langle \psi' | H' | \psi' \rangle + \int \rho(\mathbf{r}) [V(\mathbf{r}) - V'(\mathbf{r})] d^3\mathbf{r} = E'_0 + \int \rho(\mathbf{r}) [V(\mathbf{r}) - V'(\mathbf{r})] d^3\mathbf{r} \quad (19.4.7)$$

- Similarly, taking ψ as a trial function for the H' Hamiltonian, one finds that

$$E'_0 < E_0 + \int \rho(\mathbf{r}) [V'(\mathbf{r}) - V(\mathbf{r})] d^3\mathbf{r}. \quad (19.4.8)$$

- Adding the Equations 19.4.7 and 19.4.8 gives

$$E_0 + E'_0 < E_0 + E'_0,$$

and a clear contradiction.

Hence, there cannot be two distinct potentials V and V' that give the same groundstate $\rho(\mathbf{r})$. So, the ground-state density $\rho(\mathbf{r})$ uniquely determines N and V , and thus H, and therefore ψ and E_0 . Furthermore, because ψ determines all properties of the ground state, then $\rho(\mathbf{r})$, in principle, determines all such properties. This means that even the kinetic energy and the electron-electron interaction energy of the ground-state are determined by $\rho(\mathbf{r})$. It is easy to see that $\int \rho(\mathbf{r}) V(\mathbf{r}) d^3\mathbf{r} = V[\rho]$ gives the average value of the electron nuclear (plus any additional one-electron additive potential) interaction in terms of the ground-state density $\rho(\mathbf{r})$, but how are the kinetic energy $T[\rho]$ and the electron-electron interaction $V_{ee}[\rho]$ energy expressed in terms of ρ ?

The main difficulty with DFT is that the **Hohenberg-Kohn theorem** shows that the **ground-state** values of T , V_{ee} , V , etc. are all unique functionals of the **ground-state** ρ (i.e., that they can, in principle, be determined once ρ is given), but it does not tell us what these functional relations are.

To see how it might make sense that a property such as the kinetic energy, whose operator $-\frac{\hbar^2}{2m_e} \nabla^2$ involves derivatives, can be related to the electron density, consider a simple system of N non-interacting electrons moving in a three-dimensional cubic "box" potential. The energy states of such electrons are known to be

$$E = \left(\frac{\hbar^2}{2m_e L^2} \right) (n_x^2 + n_y^2 + n_z^2),$$

where L is the length of the box along the three axes, and n_x , n_y , and n_z are the quantum numbers describing the state. We can view $n_x^2 + n_y^2 + n_z^2 = R^2$ as defining the squared radius of a sphere in three dimensions, and we realize that the density of quantum states in this space is one state per unit volume in the n_x, n_y, n_z space. Because n_x, n_y , and n_z must be positive

integers, the volume covering all states with energy less than or equal to a specified energy $E = \left(\frac{h^2}{2m_e L^2}\right) R^2$ is $\frac{1}{8}$ the volume of the sphere of radius R :

$$\Phi(E) = \frac{1}{8} \left(\frac{4\pi}{3}\right) R^3 = \left(\frac{\pi}{6}\right) \sqrt{9m_e E \frac{L^2}{h^2}}^3.$$

Since there is one state per unit of such volume, $\Phi(E)$ is also the number of states with energy less than or equal to E , and is called the **integrated density of states**. The number of states $g(E) dE$ with energy between E and $E+dE$, the **density of states**, is the derivative of Φ :

$$g(E) = \frac{d\Phi}{dE} = \frac{\pi}{4} \sqrt{8m_e \frac{L^2}{h^2}}^3 \sqrt{E}.$$

If we calculate the total energy for N electrons, with the states having energies up to the so-called **Fermi energy** (i.e., the energy of the highest occupied molecular orbital HOMO) doubly occupied, we obtain the ground-state energy:

$$E_0 = 2 \int_0^{E_F} g(E) E dE = \frac{8\pi}{5} \sqrt{\frac{2m_e}{h^2}}^3 L^3 \sqrt{E_F}^5.$$

The total number of electrons N can be expressed as

$$N = 2 \int_0^{E_F} g(E) dE = \frac{8\pi}{3} \sqrt{\frac{2m_e}{h^2}}^3 L^3 \sqrt{E_F}^3,$$

which can be solved for E_F in terms of N to then express E_0 in terms of N instead of E_F :

$$E_0 = \frac{3h^2}{10m_e} \sqrt{\frac{3}{8\pi}}^2 L^3 \sqrt{\frac{N}{L}}^5.$$

This gives the total energy, which is also the kinetic energy in this case because the potential energy is zero within the “box”, in terms of the electron density $\rho(x,y,z) = \left(\frac{N}{L^3}\right)$. It therefore may be plausible to express kinetic energies in terms of electron densities $\rho(\mathbf{r})$, but it is by no means clear how to do so for “real” atoms and molecules with electron-nuclear and electron-electron interactions operative.

In one of the earliest DFT models, the **Thomas-Fermi** theory, the kinetic energy of an atom or molecule is approximated using the above kind of treatment on a “local” level. That is, for each volume element in \mathbf{r} space, one assumes the expression given above to be valid, and then one integrates over all \mathbf{r} to compute the total kinetic energy:

$$T_{TF}[\rho] = \int \frac{3h^2}{10m_e} \sqrt{\frac{3}{8\pi}}^2 \sqrt{\rho(\mathbf{r})}^5 d^3\mathbf{r} = C_F \int \sqrt{\rho(\mathbf{r})}^5 d^3\mathbf{r},$$

where the last equality simply defines the C_F constant (which is 2.8712 in atomic units). Ignoring the correlation and exchange contributions to the total energy, this T is combined with the electron-nuclear V and Coulombic electron-electron potential energies to give the Thomas-Fermi total energy:

$$E_{0,TF}[\rho] = C_F \int \sqrt{\rho(\mathbf{r})}^5 d^3\mathbf{r} + \int V(\mathbf{r})\rho(\mathbf{r})d^3\mathbf{r} + \frac{e^2}{2} \int \rho(\mathbf{r}) \frac{\rho(\mathbf{r}')}{|\mathbf{r}-\mathbf{r}'|} d^3\mathbf{r}d^3\mathbf{r}',$$

This expression is an example of how E_0 is given as a **local density functional approximation** (LDA). The term local means that the energy is given as a functional (i.e., a function of ρ) which depends only on $\rho(\mathbf{r})$ at points in space but not on $\rho(\mathbf{r})$ at more than one point in space.

Unfortunately, the Thomas-Fermi energy functional does not produce results that are of sufficiently high accuracy to be of great use in chemistry. What is missing in this theory are a. the exchange energy and b. the correlation energy; moreover, the kinetic energy is treated only in the approximate manner described.

In the book by Parr and Yang, it is shown how Dirac was able to address the exchange energy for the 'uniform electron gas' (N Coulomb **interacting** electrons moving in a uniform positive background charge whose magnitude balances the charge of the N electrons). If the exact expression for the exchange energy of the uniform electron gas is applied on a local level, one obtains the commonly used Dirac **local density approximation to the exchange energy**:

$$E_{\text{ex, Dirac}}[\rho] = -C_x \int \sqrt[3]{\rho(\mathbf{r})}^4 d^3\mathbf{r},$$

with $C_x = \frac{3}{4} | \text{sqr}t[3] | \frac{3}{\pi} = 0.7386$ in atomic units. Adding this exchange energy to the Thomas-Fermi total energy $E_{0,TF}[\rho]$ gives the so-called Thomas-Fermi-Dirac (TFD) energy functional.

Because electron densities vary rather strongly spatially near the nuclei, corrections to the above approximations to $T[\rho]$ and $E_{\text{ex,Dirac}}$ are needed. One of the more commonly used so-called **gradient-corrected** approximations is that invented by Becke, and referred to as the Becke88 exchange functional:

$$E_{\text{ex}}(\text{Becke88}) = E_{\text{ex,Dirac}}[\rho] - \gamma \int x^2 \sqrt[3]{\rho^4} \left[\frac{1}{1 + 6\gamma x \text{csch}(x)} \right] d\mathbf{r},$$

where $x = \frac{1}{\sqrt[3]{\rho^4}} |\nabla \rho|$, and γ is a parameter chosen so that the above exchange energy can best reproduce the known exchange energies of specific electronic states of the inert gas atoms (Becke finds γ to equal 0.0042). A common gradient correction to the earlier $T[\rho]$ is called the **Weizsacker correction** and is given by

$$\delta T_{\text{Weizsacker}} = \frac{1}{72} \frac{\hbar}{m_e} \int \frac{|\nabla \rho(\mathbf{r})|^2}{\rho(\mathbf{r})} d\mathbf{r}.$$

Although the above discussion suggests how one might compute the ground-state energy once the ground-state density $\rho(\mathbf{r})$ is given, one still needs to know how to obtain ρ . Kohn and Sham (KS) introduced a set of so-called KS orbitals obeying the following equation:

$$\left[-\frac{1}{2} \nabla^2 + V(\mathbf{r}) + \frac{e^2}{2} \int \frac{\rho(\mathbf{r}')}{|\mathbf{r} - \mathbf{r}'|} d\mathbf{r}' + U_{xc}(\mathbf{r}) \right] \phi_j = \epsilon_j \phi_j,$$

where the so-called exchange-correlation potential $U_{xc}(\mathbf{r}) = \delta E_{xc} \frac{[\rho]}{\delta \rho(\mathbf{r})}$ could be obtained by functional differentiation if the exchange-correlation energy functional $E_{xc}[\rho]$ were known. KS also showed that the KS orbitals $\{\phi_j\}$ could be used to compute the density ρ by simply adding up the orbital densities multiplied by orbital occupancies n_j :

$$\rho(\mathbf{r}) = \sum_j n_j |\phi_j(\mathbf{r})|^2.$$

(here $n_j = 0, 1$, or 2 is the occupation number of the orbital ϕ_j in the state being studied) and that the kinetic energy should be calculated as

$$T = \sum_j n_j \langle \phi_j(\mathbf{r}) | -\frac{1}{2} \nabla^2 | \phi_j(\mathbf{r}) \rangle.$$

The same investigations of the idealized 'uniform electron gas' that identified the Dirac exchange functional, found that the correlation energy (per electron) could also be written exactly as a **function** of the electron density ρ of the system, but only in two limiting cases- the high-density limit (large ρ) and the low-density limit. There still exists no exact expression for the correlation energy even for the uniform electron gas that is valid at arbitrary values of ρ . Therefore, much work has been devoted to creating efficient and accurate interpolation formulas connecting the low- and high- density uniform electron gas expressions. One such expression is

$$E_c[\rho] = \int \rho(\mathbf{r}) \epsilon_c(\rho) d\mathbf{r},$$

where

$$\epsilon_c(\rho) = \frac{A}{2} \left[\ln \left(\frac{x}{X} \right) + \frac{2b}{Q \tan^{-1} \left(\frac{Q}{2x+b} \right)} - \frac{bx_0}{X_0} \left[\ln \left(\frac{(x-x_0)^2}{X} + \frac{2(b+x_0)}{Q \tan^{-1} \left(\frac{Q}{2x+b} \right)} \right) \right] \right]$$

is the correlation energy per electron. Here $x = \sqrt{r_s}$, $X = x^2 + bx + c$, $X_0 = x_0^2 + bx_0 + c$ and $Q = \sqrt{(4c - b^2)}$, $A = 0.0621814$, $x_0 = -0.409286$, $b = 13.0720$, and $c = 42.7198$. The parameter r_s is how the density ρ enters since $\frac{4}{3}\pi r_s^3$ is equal to $\frac{1}{\rho}$; that is, r_s is the radius of a sphere whose volume is the effective volume occupied by one electron. A reasonable approximation to the full $E_{xc}[\rho]$ would contain the Dirac (and perhaps gradient corrected) exchange functional plus the above $E_C[\rho]$, but there are many alternative approximations to the exchange-correlation energy functional. Currently, many workers are doing their best to “cook up” functionals for the correlation and exchange energies, but no one has yet invented functionals that are so reliable that most workers agree to use them.

To summarize, in implementing any DFT, one usually proceeds as follows:

1. An atomic orbital basis is chosen in terms of which the KS orbitals are to be expanded.
2. Some initial guess is made for the LCAO-KS expansion coefficients $C_{jj,a} : \phi_j = \sum_a C_{j,a} \chi_a$.
3. The density is computed as $\rho(\mathbf{r}) = \sum_j n_j |\phi_j(\mathbf{r})|^2$. Often, $\rho(\mathbf{r})$ is expanded in an atomic orbital basis, which need not be the same as the basis used for the ϕ_j , and the expansion coefficients of ρ are computed in terms of those of the ϕ_j . It is also common to use an atomic orbital basis to expand $\sqrt[3]{\rho(\mathbf{r})}$ which, together with ρ , is needed to evaluate the exchange-correlation functional's contribution to E_0 .
4. The current iteration's density is used in the KS equations to determine the Hamiltonian $\left[-\frac{1}{2} \nabla^2 + V(\mathbf{r}) + \frac{e^2}{2} \int \frac{\rho(\mathbf{r}')}{|\mathbf{r} - \mathbf{r}'|} d\mathbf{r}' + U_{xc}(\mathbf{r}) \right]$ whose “new” eigenfunctions $\{\phi_j\}$ and eigenvalues $\{\epsilon_j\}$ are found by solving the KS equations.
5. These new ϕ_j are used to compute a new density, which, in turn, is used to solve a new set of KS equations. This process is continued until convergence is reached (i.e., until the ϕ_j used to determine the current iteration's ρ are the same ϕ_j that arise as solutions on the next iteration).
6. Once the converged $\rho(\mathbf{r})$ is determined, the energy can be computed using the earlier expression

$$E[\rho] = \sum_j n_j \langle \phi_j(\mathbf{r}) | -\frac{1}{2} \nabla^2 | \phi_j(\mathbf{r}) \rangle + \int V(\mathbf{r}) \rho(\mathbf{r}) d\mathbf{r} + \frac{e^2}{2} \int \rho(\mathbf{r}) \frac{\rho(\mathbf{r}')}{|\mathbf{r} - \mathbf{r}'|} d\mathbf{r} d\mathbf{r}' + E_{xc}[\rho].$$

In closing this section, it should once again be emphasized that this area is currently undergoing explosive growth and much scrutiny. As a result, it is nearly certain that many of the specific functionals discussed above will be replaced in the near future by improved and more rigorously justified versions. It is also likely that extensions of DFT to excited states (many workers are actively pursuing this) will be placed on more solid ground and made applicable to molecular systems. Because the computational effort involved in these approaches scales much less strongly with basis set size than for conventional (SCF, MCSCF, CI, etc.) methods, density functional methods offer great promise and are likely to contribute much to quantum chemistry in the next decade.

This page titled [19.4: Further Details on Implementing Multiconfigurational Methods](#) is shared under a [CC BY-NC-SA 4.0](#) license and was authored, remixed, and/or curated by [Jack Simons](#) via [source content](#) that was edited to the style and standards of the LibreTexts platform.

CHAPTER OVERVIEW

20: Response Theory

Many physical properties of a molecule can be calculated as expectation values of a corresponding quantum mechanical operator. The evaluation of other properties can be formulated in terms of the "response" (i.e., derivative) of the electronic energy with respect to the application of an external field perturbation.

[20.1: Calculations of Properties Other Than the Energy](#)

[20.2: Ab Initio, Semi-Empirical, and Empirical Force Field Methods](#)

This page titled [20: Response Theory](#) is shared under a [CC BY-NC-SA 4.0](#) license and was authored, remixed, and/or curated by [Jack Simons](#) via [source content](#) that was edited to the style and standards of the LibreTexts platform.

20.1: Calculations of Properties Other Than the Energy

There are, of course, properties other than the energy that are of interest to the practicing chemist. Dipole moments, polarizabilities, transition probabilities among states, and vibrational frequencies all come to mind. Other properties that are of importance involve operators whose quantum numbers or symmetry indices label the state of interest. Angular momentum and point group symmetries are examples of the latter properties; for these quantities the properties are precisely specified once the quantum number or symmetry label is given (e.g., for a 3P state, the average value of L^2 is $\langle ^3P | L^2 | ^3P \rangle = \hbar^2 1(1+1) = 2\hbar^2$).

Although it may be straightforward to specify what property is to be evaluated, often computational difficulties arise in carrying out the calculation. For some ab initio methods, these difficulties are less severe than for others. For example, to compute the electric dipole transition matrix element $\langle \Psi_2 | \mathbf{r} | \Psi_1 \rangle$ between two states Ψ_1 and Ψ_2 , one must evaluate the integral involving the one-electron dipole operator $\mathbf{r} = \sum_j e\mathbf{r}_j - \sum_a eZ_a\mathbf{R}_a$; here the first sum runs over the N electrons and the second sum runs over the

nuclei whose charges are denoted Z_a . To evaluate such transition matrix elements in terms of the Slater-Condon rules is relatively straightforward as long as Ψ_1 and Ψ_2 are expressed in terms of Slater determinants involving a single set of orthonormal spin-orbitals. If Ψ_1 and Ψ_2 have been obtained, for example, by carrying out separate MCSCF calculations on the two states in question, the energy optimized spin-orbitals for one state will not be the same as the optimal spin-orbitals for the second state. As a result, the determinants in Ψ_1 and those in Ψ_2 will involve spin-orbitals that are not orthonormal to one another. Thus, the SC rules can not immediately be applied. Instead, a transformation of the spin-orbitals of Ψ_1 and Ψ_2 to a single set of orthonormal functions must be carried out. This then expresses Ψ_1 and Ψ_2 in terms of new Slater determinants over this new set of orthonormal spinorbitals, after which the SC rules can be exploited.

In contrast, if Ψ_1 and Ψ_2 are obtained by carrying out a CI calculation using a single set of orthonormal spin-orbitals (e.g., with Ψ_1 and Ψ_2 formed from two different eigenvectors of the resulting secular matrix), the SC rules can immediately be used to evaluate the transition dipole integral.

Formulation of Property Calculations as Responses

Essentially all experimentally measured properties can be thought of as arising through the **response** of the system to some externally applied perturbation or disturbance. In turn, the calculation of such properties can be formulated in terms of the response of the energy E or wavefunction Ψ to a perturbation. For example, molecular dipole moments μ are measured, via electric-field deflection, in terms of the change in energy

$$\Delta E = \mu \cdot \mathbf{E} + \frac{1}{2} \mathbf{E} \cdot \alpha \cdot \mathbf{E} + \frac{1}{6} \mathbf{E} \cdot \mathbf{E} \cdot \mathbf{E} \cdot \beta + \dots$$

caused by the application of an external electric field \mathbf{E} which is spatially inhomogeneous, and thus exerts a force

$$\mathbf{F} = -\nabla \Delta E$$

on the molecule proportional to the dipole moment (good treatments of response properties for a wide variety of wavefunction types (i.e., SCF, MCSCF, MPPT/MBPT, etc.) are given in **Second Quantization Based Methods in Quantum Chemistry**, P. Jørgensen and J. Simons, Academic Press, New York (1981) and in **Geometrical Derivatives of Energy Surfaces and Molecular Properties**, P. Jørgensen and J. Simons, Eds., NATO ASI Series, Vol. 166, D. Reidel, Dordrecht (1985)).

To obtain expressions that permit properties other than the energy to be evaluated in terms of the state wavefunction Ψ , the following strategy is used:

1. The perturbation $V = H - H^0$ appropriate to the particular property is identified. For dipole moments (μ), polarizabilities (α), and hyperpolarizabilities (β), V is the interaction of the nuclei and electrons with the external electric field

$$V = \sum_a Z_a e \mathbf{R}_a \cdot \mathbf{E} - \sum_j e \mathbf{r}_j \cdot \mathbf{E}.$$

For vibrational frequencies, one needs the derivatives of the energy E with respect to deformation of the bond lengths and angles of the molecule, so V is the sum of all changes in the electronic Hamiltonian that arise from displacements $\delta \mathbf{R}_a$ of the atomic centers

$$V = \sum_a (\nabla \mathbf{R}_a H) \cdot \delta \mathbf{R}_a.$$

2. A power series expansion of the state energy E , computed in a manner consistent with how Ψ is determined (i.e., as an expectation value for SCF, MCSCF, and CI wavefunctions or as $\langle \Phi | H | \Psi \rangle$ for MPPT/MBPT or as $\langle \Phi | e^{-T} H e^T \Phi \rangle$ for CC wavefunctions), is carried out in powers of the perturbation V :

$$E = E^0 + E^{(1)} + E^{(2)} + E^{(3)} + \dots$$

In evaluating the terms in this expansion, the dependence of $H = H^0 + V$ and of Ψ (which is expressed as a solution of the SCF, MCSCF, ..., or CC equations for H **not** for H^0) must be included.

3. The desired physical property must be extracted from the power series expansion of ΔE in powers of V .

The MCSCF Response Case

The Dipole Moment

To illustrate how the above developments are carried out and to demonstrate how the results express the desired quantities in terms of the original wavefunction, let us consider, for an MCSCF wavefunction, the response to an external electric field. In this case, the Hamiltonian is given as the conventional one- and two-electron operators H^0 to which the above one-electron electric dipole perturbation V is added. The MCSCF wavefunction Ψ and energy E are assumed to have been obtained via the MCSCF procedure with $H = H^0 + \lambda V$, where λ can be thought of as a measure of the strength of the applied electric field. The terms in the expansion of $E(\lambda)$ in powers of λ :

$$E = E(\lambda = 0) + \lambda \left(\frac{dE}{d\lambda} \right)_0 + \frac{1}{2} \lambda^2 \left(\frac{d^2E}{d\lambda^2} \right)_0 + \dots$$

are obtained by writing the total derivatives of the MCSCF energy functional with respect to λ and evaluating these derivatives at $\lambda = 0$ (which is indicated by the subscript $(\dots)_0$ on the above derivatives):

$$\begin{aligned} E(\lambda = 0) &= \langle \Psi(\lambda = 0) | H^0 | \Psi(\lambda = 0) \rangle = E^0, \\ \left(\frac{dE}{d\lambda} \right)_0 &= \langle \Psi(\lambda = 0) | V | \Psi(\lambda = 0) \rangle + 2 \sum_J \left(\frac{\partial C_J}{\partial \lambda} \right)_0 \left\langle \frac{\partial \Psi}{\partial C_J} | H^0 | \Psi(\lambda = 0) \right\rangle + 2 \\ &\quad \sum_{i,a} \left(\frac{\partial C_{a,i}}{\partial \lambda} \right)_0 \left\langle \frac{\partial \Psi}{\partial C_{a,i}} | H^0 | \Psi(\lambda = 0) \right\rangle + \dots \\ &\quad \dots + 2 \sum_\nu \left(\frac{\partial \chi_\nu}{\partial \lambda} \right)_0 \left\langle \frac{\partial \Psi}{\partial \chi_\nu} | H^0 | \Psi(\lambda = 0) \right\rangle, \end{aligned}$$

and so on for higher order terms. The factors of 2 in the last three terms come through using the hermiticity of H^0 to combine terms in which derivatives of Ψ occur.

The first-order correction can be thought of as arising from the response of the wavefunction (as contained in its LCAO-MO and CI amplitudes and basis functions χ_ν) plus the response of the Hamiltonian to the external field. Because the MCSCF energy functional has been made stationary with respect to variations in the C_J and $C_{i,a}$ amplitudes, the second and third terms above vanish:

$$\begin{aligned} \frac{\partial E}{\partial C_J} &= 2 \left\langle \frac{\partial \Psi}{\partial C_J} | H^0 | \Psi(\lambda = 0) \right\rangle = 0, \\ \frac{\partial E}{\partial C_{a,i}} &= 2 \left\langle \frac{\partial \Psi}{\partial C_{a,i}} | H^0 | \Psi(\lambda = 0) \right\rangle = 0. \end{aligned}$$

If, as is common, the atomic orbital bases used to carry out the MCSCF energy optimization are not explicitly dependent on the external field, the third term also vanishes because $\left(\frac{\partial \chi_\nu}{\partial \lambda} \right)_0 = 0$. Thus for the MCSCF case, the first-order response is given as the average value of the perturbation over the wavefunction with $\lambda l = 0$:

$$\left(\frac{dE}{d\lambda} \right)_0 = \langle \Psi(\lambda = 0) | V | \Psi(\lambda = 0) \rangle.$$

For the external electric field case at hand, this result says that the field-dependence of the state energy will have a linear term equal to

$$\langle \Psi(\lambda=0) | V | \Psi(\lambda=0) \rangle = \langle \Psi | \sum_a Z_a e \mathbf{R}_a \cdot \mathbf{e} - \sum_j e \mathbf{r}_j \cdot \mathbf{e} | \Psi \rangle,$$

where \mathbf{e} is a unit vector in the direction of the applied electric field (the magnitude of the field λ having already been removed in the power series expansion). Since the dipole moment is determined experimentally as the energy's slope with respect to field strength, this means that the dipole moment is given as:

$$\mu = \langle \Psi | \sum_a Z_a e \mathbf{R}_a - \sum_j e \mathbf{r}_j | \Psi \rangle.$$

The Geometrical Force

These same techniques can be used to determine the response of the energy to displacements $\delta \mathbf{R}_a$ of the atomic centers. In such a case, the perturbation is

$$V = \sum_a \delta \mathbf{R}_a \cdot \nabla_{\mathbf{R}_a} \left(- \sum_i \frac{(\mathbf{r}_i - \mathbf{R}_a)}{|\mathbf{r}_i - \mathbf{R}_a|} \right) = - \sum_a Z_a e^2 \delta \mathbf{R}_a \cdot \sum_i \frac{(\mathbf{r}_i - \mathbf{R}_a)}{|\mathbf{r}_i - \mathbf{R}_a|^3}.$$

Here, the one-electron operator $\sum_i \frac{(\mathbf{r}_i - \mathbf{R}_a)}{|\mathbf{r}_i - \mathbf{R}_a|}$ is referred to as 'the HellmannFeynman' force operator; it is the derivative of the Hamiltonian with respect to displacement of center-a in the x, y, or z direction. The expressions given above for $E(\lambda=0)$ and $(\frac{dE}{d\lambda})_0$ can once again be used, but with the Hellmann-Feynman form for V . Once again, for the MCSCF wavefunction, the variational optimization of the energy gives

$$\langle \frac{\partial \Psi}{\partial C_J} | H^0 | \Psi(\lambda=0) \rangle = \langle \frac{\partial \Psi}{\partial C_{a,i}} | H^0 | \Psi(\lambda=0) \rangle = 0.$$

However, because the atomic basis orbitals are attached to the centers, and because these centers are displaced in forming V , it is no longer true that $(\frac{\partial \chi_\nu}{\partial \lambda})_0 = 0$; the variation in the wavefunction caused by movement of the basis functions now contributes to the firstorder energy response. As a result, one obtains

$$()_0 = - \sum_a Z_a e^2 \delta \mathbf{R}_a \cdot \langle \Psi | \sum_i \frac{(\mathbf{r}_i - \mathbf{R}_a)}{|\mathbf{r}_i - \mathbf{R}_a|^3} | \Psi \rangle + 2 \sum_a \delta \mathbf{R}_a \cdot \sum_\nu (\nabla_{\mathbf{R}_a} \chi_\nu)_0 \langle \frac{\partial \Psi}{\partial \chi_\nu} | H^0 | \Psi(\lambda=0) \rangle.$$

The first contribution to the **force**

$$\mathbf{F}_a = -Z_a e^2 \langle \Psi | \sum_i \frac{(\mathbf{r}_i - \mathbf{R}_a)}{|\mathbf{r}_i - \mathbf{R}_a|^3} | \Psi \rangle + 2 \sum_\nu (\nabla_{\mathbf{R}_a} \chi_\nu)_0 \langle \frac{\partial \Psi}{\partial \chi_\nu} | H^0 | \Psi(\lambda=0) \rangle$$

along the x, y, and z directions for center-a involves the expectation value, with respect to the MCSCF wavefunction with $\lambda = 0$, of the Hellmann-Feynman force operator. The second contribution gives the forces due to infinitesimal displacements of the basis functions on center-a. The evaluation of the latter contributions can be carried out by first realizing that

$$\Psi = \sum_J C_J | \phi_{J1} \phi_{J2} \phi_{J3} \dots \phi_{Jn} \dots \phi_{JN} |$$

with

$$\phi_j = \sum_\mu C_{\mu,j} \chi_\mu$$

involves the basis orbitals through the LCAO-MO expansion of the ϕ_j s. So the derivatives of the basis orbitals contribute as follows:

$$\sum_\nu (\nabla_{\mathbf{R}_a} \chi_\nu) \langle \frac{\partial \Psi}{\partial \chi_\nu} | = \sum_J \sum_{j,\nu} C_J C_{\nu,j} \langle \phi_{J1} \phi_{J2} \phi_{J3} \dots \nabla_{\mathbf{R}_a} \chi_\nu \dots \phi_{JN} |.$$

Each of these factors can be viewed as combinations of CSFs with the same C_J and $C_{n,j}$ coefficients as in Ψ but with the j^{th} spin-orbital involving basis functions that have been differentiated with respect to displacement of center-a. It turns out that such derivatives of Gaussian basis orbitals can be carried out analytically (giving rise to new Gaussians with one higher and one lower l-quantum number). When substituted into $\sum_{\nu} (\nabla_{\mathbf{R}_a} \chi_{\nu})_0 \langle \frac{\partial \Psi}{\partial \chi_{\nu}} | H^0 | \Psi(\lambda = 0) \rangle$, these basis derivative terms yield

$$\sum_{\nu} (\nabla_{\mathbf{R}_a} \chi_{\nu})_0 \langle \frac{\partial \Psi}{\partial \chi_{\nu}} | H^0 | \Psi(\lambda = 0) \rangle = \sum_J \sum_{j,\nu} C_J C_{\nu,j} \langle \phi_{J1} \phi_{J2} \phi_{J3} \dots \nabla_{\mathbf{R}_a} \chi_{\nu} \dots \phi_{JN} | H^0 | \Psi \rangle,$$

whose evaluation via the Slater-Condon rules is straightforward. It is simply the expectation value of H^0 with respect to Ψ (with the same density matrix elements that arise in the evaluation of Ψ 's energy) **but** with the one- and two-electron integrals over the atomic basis orbitals involving one of these differentiated functions:

$$\begin{aligned} \langle \chi_{\mu} \chi_{\nu} | g | \chi_{\gamma} \chi_{\delta} \rangle &\implies \nabla_{\mathbf{R}_a} \langle \chi_{\mu} \chi_{\nu} | g | \chi_{\gamma} \chi_{\delta} \rangle = \\ &= \langle \nabla_{\mathbf{R}_a} \chi_{\mu} \chi_{\nu} | g | \chi_{\gamma} \chi_{\delta} \rangle + \langle \chi_{\mu} \nabla_{\mathbf{R}_a} \chi_{\nu} | g | \chi_{\gamma} \chi_{\delta} \rangle + \langle \chi_{\mu} \chi_{\nu} | g | \nabla_{\mathbf{R}_a} \chi_{\gamma} \chi_{\delta} \rangle + \langle \chi_{\mu} \chi_{\nu} | g | \chi_{\gamma} \nabla_{\mathbf{R}_a} \chi_{\delta} \rangle. \end{aligned}$$

In summary, the force \mathbf{F}_a felt by the nuclear framework due to a displacement of center-a along the x, y, or z axis is given as

$$\mathbf{F}_a = -Z_a e^2 \langle \Psi | \sum_i \frac{(\mathbf{r}_i - \mathbf{R}_a)}{|\mathbf{r}_i - \mathbf{R}_a|^3} | \Psi \rangle + (\nabla_{\mathbf{R}_a} \langle \Psi | H^0 | \Psi \rangle),$$

where the second term is the energy of Ψ but with all atomic integrals replaced by integral derivatives: $\langle \chi_{\mu} \chi_{\nu} | g | \chi_{\gamma} \chi_{\delta} \rangle \implies \nabla_{\mathbf{R}_a} \langle \chi_{\mu} \chi_{\nu} | g | \chi_{\gamma} \chi_{\delta} \rangle$.

Responses for Other Types of Wavefunctions

It should be stressed that the MCSCF wavefunction yields especially compact expressions for responses of E with respect to an external perturbation because of the variational conditions

$$\langle \frac{\partial \Psi}{\partial C_J} | H^0 | \Psi(\lambda = 0) \rangle = \langle \frac{\partial \Psi}{\partial C_{a,i}} | H^0 | \Psi(\lambda = 0) \rangle = 0$$

that apply. The SCF case, which can be viewed as a special case of the MCSCF situation, also admits these simplifications. However, the CI, CC, and MPPT/MBPT cases involve additional factors that arise because the above variational conditions do not apply (in the CI case, $\langle \frac{\partial \Psi}{\partial C_J} | H^0 | \Psi(\lambda = 0) \rangle = 0$ still applies, but the orbital condition $\langle \frac{\partial \Psi}{\partial C_{a,i}} | H^0 | \Psi(\lambda = 0) \rangle = 0$ does not because the orbitals are not varied to make the CI energy functional stationary).

Within the CC, CI, and MPPT/MBPT methods, one must evaluate the so-called responses of the C_I and $C_{a,i}$ coefficients $\left(\frac{\partial C_J}{\partial \lambda} \right)_0$ and $\left(\frac{\partial C_{a,i}}{\partial \lambda} \right)_0$ that appear in the full energy response as (see above) $2 \sum_J \left(\frac{\partial C_J}{\partial \lambda} \right)_0 \langle \frac{\partial \Psi}{\partial C_J} | H^0 | \Psi(\lambda = 0) \rangle + 2 \sum_{i,a} \left(\frac{\partial C_{a,i}}{\partial \lambda} \right)_0 \langle \frac{\partial \Psi}{\partial C_{a,i}} | H^0 | \Psi(\lambda = 0) \rangle$. To do so requires solving a set of response equations that are obtained by differentiating whatever equations govern the C_I and $C_{a,i}$ coefficients in the particular method (e.g., CI, CC, or MPPT/MBPT) with respect to the external perturbation. In the geometrical derivative case, this amounts to differentiating with respect to x, y, and z displacements of the atomic centers. These response equations are discussed in **Geometrical Derivatives of Energy Surfaces and Molecular Properties**, P. Jørgensen and J. Simons, Eds., NATO ASI Series, Vol. 166, D. Reidel, Dordrecht (1985). Their treatment is somewhat beyond the scope of this text, so they will not be dealt with further here.

The Use of Geometrical Energy Derivatives

1. Gradients as Newtonian Forces The first energy derivative is called the gradient \mathbf{g} and is the negative of the force \mathbf{F} (with components along the a^{th} center denoted \mathbf{F}_a) experienced by the atomic centers $\mathbf{F} = -\mathbf{g}$. These forces, as discussed in Chapter 16, can be used to carry out classical trajectory simulations of molecular collisions or other motions of large organic and biological molecules for which a quantum treatment of the nuclear motion is prohibitive. The second energy derivatives with respect to the x, y, and z directions of centers a and b (for example, the x, y component for centers a and b is

$H_{a,b} = \left(\frac{\partial^2 E}{\partial x_a \partial y_b} \right)$ form the Hessian matrix \mathbf{H} . The elements of \mathbf{H} give the local curvatures of the energy surface along the

3N cartesian directions. The gradient and Hessian can be used to systematically locate local minima (i.e., stable geometries) and transition states that connect one local minimum to another. At each of these stationary points, all forces and thus all elements of the gradient \mathbf{g} vanish. At a local minimum, the \mathbf{H} matrix has 5 or 6 zero eigenvalues corresponding to translational and rotational displacements of the molecule (5 for linear molecules; 6 for non-linear species) and 3N-5 or 3N-6 positive eigenvalues. At a transition state, \mathbf{H} has one negative eigenvalue, 5 or 6 zero eigenvalues, and 3N-6 or 3N-7 positive eigenvalues.

2. Transition State Rate Coefficients The transition state theory of Eyring or its extensions due to Truhlar and coworkers (see, for example, D. G. Truhlar and B. C. Garrett, Ann. Rev. Phys. Chem. 35, 159 (1984)) allow knowledge of the Hessian matrix at a transition state to be used to compute a rate coefficient k_{rate} appropriate to the chemical reaction for which the transition state applies. More specifically, the geometry of the molecule at the transition state is used to compute a rotational partition function Q_{rot}^\ddagger in which the principal moments of inertia I_a , I_b , and I_c (see Chapter 13) are those of the transition state (the ‡ symbol is, by convention, used to label the transition state):

$$Q_{\text{rot}}^\ddagger = \prod_{n=a,b,c} \sqrt{\frac{8\pi^2 I_n kT}{h^2}},$$

where k is the Boltzmann constant and T is the temperature in $^\circ\text{K}$. The eigenvalues $\{\omega_\alpha\}$ of the mass weighted Hessian matrix (see below) are used to compute, for each of the 3N-7 vibrations with real and positive ω_α values, a vibrational partition function that is combined to produce a transition-state vibrational partition function:

$$Q_{\text{vib}}^\ddagger = \prod_{\alpha=1, 3N-7} \frac{e^{-\frac{\hbar\omega_\alpha}{2kT}}}{1 - e^{-\frac{\hbar\omega_\alpha}{kT}}}.$$

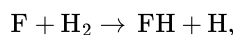
The electronic partition function of the transition state is expressed in terms of the activation energy (the energy of the transition state relative to the electronic energy of the reactants) E^\ddagger as:

$$Q_{\text{electronic}}^\ddagger = \omega^\ddagger e^{-\frac{E^\ddagger}{kT}}$$

where ω^\ddagger is the degeneracy of the electronic state at the transition state geometry. In the original Eyring version of transition state theory (TST), the rate coefficient k_{rate} is then given by:

$$k_{\text{rate}} = \frac{kT}{h} \omega^\ddagger e^{-\frac{E^\ddagger}{kT}} \frac{Q_{\text{rot}}^\ddagger Q_{\text{vib}}^\ddagger}{Q_{\text{reactants}}}$$

where $Q_{\text{reactants}}$ is the conventional partition function for the reactant materials. For example, in a biomolecular reaction such as:



the reactant partition function

$$Q_{\text{reactants}} = Q_{\text{F}} Q_{\text{H}_2}$$

is written in terms of the translational and electronic (the degeneracy of the ^2P state produces the 2 (3) overall degeneracy factor) partition functions of the F atom

$$Q_{\text{F}} = 2 \sqrt{\frac{2\pi m_{\text{F}} kT}{h^2}}$$

and the translational, electronic, rotational, and vibrational partition functions of the H_2 molecule

$$Q_{\text{H}_2} = \sqrt{\frac{2\pi m_{\text{H}_2} kT}{h^2}} \frac{8\pi^2 I_{\text{H}_2} kT}{2h^2} \frac{e^{-\frac{\hbar\omega_{\text{H}_2}}{2kT}}}{1 - e^{-\frac{\hbar\omega_{\text{H}_2}}{kT}}}.$$

The factor of 2 in the denominator of the H₂ molecule's rotational partition function is the "symmetry number" that must be inserted because of the identity of the two H nuclei. The overall rate coefficient k_{rate} (with units sec^{-1} because this is a rate per collision pair) can thus be expressed entirely in terms of energetic, geometrical, and vibrational information about the reactants and the transition state. Even within the extensions to Eyring's original model, such is the case. The primary difference in the more modern theories is that the transition state is identified not as the point on the potential energy surface at which the gradient vanishes and there is one negative Hessian eigenvalue. Instead, a so-called variational transition state (see the above reference by Truhlar and Garrett) is identified. The geometry, energy, and local vibrational frequencies of this transition state are then used to compute, must like outlined above, k_{rate} .

3. Harmonic Vibrational Frequencies It is possible (see, for example, J. Nichols, H. L. Taylor, P. Schmidt, and J. Simons, J. Chem. Phys. 92, 340 (1990) and references therein) to remove from \mathbf{H} the zero eigenvalues that correspond to rotation and translation and to thereby produce a Hessian matrix whose eigenvalues correspond only to internal motions of the system. After doing so, the number of negative eigenvalues of \mathbf{H} can be used to characterize the nature of the stationary point (local minimum or transition state), and \mathbf{H} can be used to evaluate the local harmonic vibrational frequencies of the system. The relationship between \mathbf{H} and vibrational frequencies can be made clear by recalling the classical equations of motion in the Lagrangian formulation:

$$\frac{d}{dt} \left(\frac{\partial L}{\partial \dot{q}_j} \right) - \left(\frac{\partial L}{\partial q_j} \right) = 0,$$

where q_j denotes, in our case, the 3N cartesian coordinates of the N atoms, and \dot{q}_j is the velocity of the corresponding coordinate. Expressing the Lagrangian L as kinetic energy minus potential energy and writing the potential energy as a local quadratic expansion about a point where \mathbf{g} vanishes, gives

$$L = \frac{1}{2} \sum_j m_j \dot{q}_j^2 - E(0) - \frac{1}{2} \sum_{j,k} q_j H_{j,k} q_k.$$

Here, $E(0)$ is the energy at the stationary point, m_j is the mass of the atom to which q_j applies, and the $H_{j,k}$ are the elements of \mathbf{H} along the x, y, and z directions of the various atomic centers. Applying the Lagrangian equations to this form for L gives the equations of motion of the q_j coordinates:

$$m_j \ddot{q}_j = - \sum_k H_{j,k} q_k.$$

To find solutions that correspond to local harmonic motion, one assumes that the coordinates q_j oscillate in time according to

$$q_j(t) = q_j \cos(\omega t).$$

Substituting this form for $q_j(t)$ into the equations of motion gives

$$m_j \omega^2 q_j = \sum_k H_{j,k} q_k.$$

Defining

$$q'_j = q_j \sqrt{m_j}$$

and introducing this into the above equation of motion yields

$$\omega^2 q'_j = \sum_k H'_{j,k} q'_k,$$

where

$$H'_{j,k} = H_{j,k} \frac{1}{\sqrt{m_j m_k}}$$

is the so-called **mass-weighted Hessian** matrix. The squares of the desired harmonic vibrational frequencies ω^2 are thus given as eigenvalues of the mass-weighted Hessian \mathbf{H}' :

$$\mathbf{H}' \mathbf{q}'_\alpha = \omega_\alpha^2 \mathbf{q}'_\alpha$$

The corresponding eigenvector, $\{q'_{\alpha,j}\}$ gives, when multiplied by $\frac{1}{\sqrt{m_j}}$, the atomic displacements that accompany that particular harmonic vibration. At a transition state, one of the ω_α^2 will be negative and $3N-6$ or $3N-7$ will be positive.

4. Reaction Path Following The Hessian and gradient can also be used to trace out 'streambeds' connecting local minima to transition states. In doing so, one utilizes a local harmonic description of the potential energy surface

$$E(\mathbf{x}) = E(0) + \mathbf{x} \cdot \mathbf{g} + \frac{1}{2} \mathbf{x} \cdot \mathbf{H} \cdot \mathbf{x} + \dots,$$

where \mathbf{x} represents the (small) step away from the point $\mathbf{x} = \mathbf{0}$ at which the gradient \mathbf{g} and Hessian \mathbf{H} have been evaluated. By expressing \mathbf{x} and \mathbf{g} in terms of the eigenvectors \mathbf{v}_α of \mathbf{H}

$$\begin{aligned} \mathbf{H} \mathbf{v}_\alpha &= \lambda_\alpha \mathbf{v}_\alpha, \\ \mathbf{x} &= \sum_\alpha \langle \mathbf{v}_\alpha | \mathbf{x} \rangle \mathbf{v}_\alpha = \sum_\alpha x_\alpha \mathbf{v}_\alpha, \\ \mathbf{g} &= \sum_\alpha \langle \mathbf{v}_\alpha | \mathbf{g} \rangle \mathbf{v}_\alpha = \sum_\alpha g_\alpha \mathbf{v}_\alpha, \end{aligned}$$

the energy change $E(\mathbf{x}) - E(0)$ can be expressed in terms of a sum of independent changes along the eigendirections:

$$E(\mathbf{x}) - E(0) = \sum_\alpha \left[x_\alpha g_\alpha + \frac{1}{2} x_\alpha^2 \lambda_\alpha \right] + \dots$$

Depending on the signs of g_α and of λ_α , various choices for the displacements x_α will produce increases or decreases in energy:

1. If λ_α is positive, then a step x_α 'along' g_α (i.e., one with $x_\alpha g_\alpha$ positive) will generate an energy increase. A step 'opposed to' g_α will generate an energy decrease if it is short enough that $x_\alpha g_\alpha$ is larger in magnitude than $\frac{1}{2} x_\alpha^2 \lambda_\alpha$, otherwise the energy will increase.
2. If λ_α is negative, a step opposed to g_α will generate an energy decrease. A step along g_α will give an energy increase if it is short enough for $x_\alpha g_\alpha$ to be larger in magnitude than $\frac{1}{2} x_\alpha^2 \lambda_\alpha$, otherwise the energy will decrease. Thus, to proceed downhill in all directions (such as one wants to do when searching for local minima), one chooses each x_α in opposition to g_α and of small enough length to guarantee that the magnitude of $x_\alpha g_\alpha$ exceeds that of $\frac{1}{2} x_\alpha^2 \lambda_\alpha$ for those modes with $\lambda_\alpha > 0$. To proceed uphill along a mode with $\lambda_\alpha < 0$ and downhill along all other modes with $\lambda_\alpha > 0$, one chooses x_α 'along' g_α with x_α short enough to guarantee that $x_\alpha g_\alpha$ is larger in magnitude than $\frac{1}{2} x_\alpha^2 \lambda_\alpha$, and one chooses the other x_α opposed to g_α and short enough that $x_\alpha g_\alpha$ is larger in magnitude than $\frac{1}{2} x_\alpha^2 \lambda_\alpha$. Such considerations have allowed the development of highly efficient potential energy surface 'walking' algorithms (see, for example, J. Nichols, H. L. Taylor, P. Schmidt, and J. Simons, J. Chem. Phys. 92, 340 (1990) and references therein) designed to trace out streambeds and to locate and characterize, via the local harmonic frequencies, minima and transition states. These algorithms form essential components of most modern ab initio, semi-empirical, and empirical computational chemistry software packages.

This page titled [20.1: Calculations of Properties Other Than the Energy](#) is shared under a [CC BY-NC-SA 4.0](#) license and was authored, remixed, and/or curated by [Jack Simons](#) via [source content](#) that was edited to the style and standards of the LibreTexts platform.

20.2: Ab Initio, Semi-Empirical, and Empirical Force Field Methods

Ab Initio Methods

Most of the techniques described in this Chapter are of the **ab initio** type. This means that they attempt to compute electronic state energies and other physical properties, as functions of the positions of the nuclei, from first principles without the use or knowledge of experimental input. Although perturbation theory or the variational method may be used to generate the working equations of a particular method, and although finite atomic orbital basis sets are nearly always utilized, these approximations do not involve 'fitting' to known experimental data. They represent approximations that can be systematically improved as the level of treatment is enhanced.

Semi-Empirical and Fully Empirical Methods

Semi-empirical methods, such as those outlined in Appendix F, use experimental data or the results of **ab initio** calculations to determine some of the matrix elements or integrals needed to carry out their procedures. Totally empirical methods attempt to describe the internal electronic energy of a system as a function of geometrical degrees of freedom (e.g., bond lengths and angles) in terms of analytical 'force fields' whose parameters have been determined to 'fit' known experimental data on some class of compounds. Examples of such parameterized force fields were presented in Section III. A of Chapter 16.

Strengths and Weaknesses

Each of these tools has advantages and limitations. **Ab initio** methods involve intensive computation and therefore tend to be limited, for practical reasons of computer time, to smaller atoms, molecules, radicals, and ions. Their CPU time needs usually vary with basis set size (M) as at least M^4 ; correlated methods require time proportional to at least M^5 because they involve transformation of the atomic-orbital-based two-electron integrals to the molecular orbital basis. As computers continue to advance in power and memory size, and as theoretical methods and algorithms continue to improve, **ab initio** techniques will be applied to larger and more complex species. When dealing with systems in which qualitatively new electronic environments and/or new bonding types arise, or excited electronic states that are unusual, **ab initio** methods are essential. Semi-empirical or empirical methods would be of little use on systems whose electronic properties have not been included in the data base used to construct the parameters of such models.

On the other hand, to determine the stable geometries of large molecules that are made of conventional chemical units (e.g., CC, CH, CO, etc. bonds and steric and torsional interactions among same), fully empirical force-field methods are usually quite reliable and computationally very fast. Stable geometries and the relative energetic stabilities of various conformers of large macromolecules and biopolymers can routinely be predicted using such tools if the system contains only conventional bonding and common chemical building blocks. These empirical potentials usually do not contain sufficient flexibility (i.e., their parameters and input data do not include enough knowledge) to address processes that involve rearrangement of the electronic configurations. For example, they can not treat:

1. Electronic transitions, because knowledge of the optical oscillator strengths and of the energies of excited states is absent in most such methods;
2. Concerted chemical reactions involving simultaneous bond breaking and forming, because to do so would require the force-field parameters to evolve from those of the reactant bonding to those for the product bonding as the reaction proceeds;
3. Molecular properties such as dipole moment and polarizability, although in certain fully empirical models, bond dipoles and lone-pair contributions have been incorporated (although again only for conventional chemical bonding situations).

Semi-empirical techniques share some of the strengths and weaknesses of **ab initio** and of fully empirical methods. They treat at least the valence electrons explicitly, so they are able to address questions that are inherently electronic such as electronic transitions, dipole moments, polarizability, and bond breaking and forming. Some of the integrals involving the Hamiltonian operator and the atomic basis orbitals are performed **ab initio**; others are obtained by fitting to experimental data. The computational needs of semiempirical methods lie between those of the **ab initio** methods and the force-field techniques. As with the empirical methods, they should never be employed when qualitatively new electronic bonding situations are encountered because the data base upon which their parameters were determined contain, by assumption, no similar bonding cases.

This page titled [20.2: Ab Initio, Semi-Empirical, and Empirical Force Field Methods](#) is shared under a [CC BY-NC-SA 4.0](#) license and was authored, remixed, and/or curated by [Jack Simons](#) via [source content](#) that was edited to the style and standards of the LibreTexts platform.

21: Problem Sets

Your page has been created!

Remove this content and add your own.

Edit page

Click the Edit page button in your user bar. You will see a suggested structure for your content. Add your content and hit Save.

Tips:

[Drag and drop](#)

Drag one or more image files from your computer and drop them onto your browser window to add them to your page.

[Classifications](#)

Tags are used to link pages to one another along common themes. Tags are also used as markers for the dynamic organization of content in the CXone Expert framework.

[Working with templates](#)

CXone Expert [templates](#) help guide and organize your documentation, making it flow easier and more uniformly. Edit existing templates or create your own.

 [Visit for all help topics.](#)

This page titled [21: Problem Sets](#) is shared under a [CC BY-NC-SA 4.0](#) license and was authored, remixed, and/or curated by [Jack Simons](#) via [source content](#) that was edited to the style and standards of the LibreTexts platform.

CHAPTER OVERVIEW

22: Problems

Topic hierarchy

22.1: The Basic Tools of Quantum Mechanics

22.1.1: i. Review Exercises

22.1.2: ii. Exercises

22.1.3: iii. Problems 1-10

22.1.4: iv. Problems 11-18

22.1.5: v. Review Exercise Solutions

22.1.6: vi. Exercise Solutions

22.2: Simple Molecular Orbital Theory

22.2.1: i. Review Exercises

22.2.2: ii. Exercises

22.2.3: iii. Problems

22.2.4: iv. Review Exercises Solutions

22.2.5: v. Exercise Solution

22.2.6: vi. Problem Solutions

22.3: Electronic Configurations, Term Symbols, and States

22.3.1: i. Review Exercises

22.3.2: ii. Exercises

22.3.3: iii. Problems

22.3.4: iv. Review Exercise Solutions

22.3.5: v. Exercise Solutions

22.3.6: vi. Problem Solutions

22.4: Molecular Rotation and Vibration

22.4.1: i. Exercises

22.4.2: ii. Problems

22.4.3: iii. Exercise Solutions

22.4.4: iv. Problem Solutions

22.5: Time Dependent Processes

22.5.1: i. Exercises

22.5.2: ii. Problems

22.5.3: iii. Exercise Solutions

22.5.4: iv. Problem Solutions

22.6: More Quantitative Aspects of Electronic Structure Calculations

22.6.1: i. Review Exercises

22.6.2: i. Review Exercises-

22.6.3: ii. Exercises

22.6.4: iii. Problems

22.6.5: iv. Review Exercise Solutions

22.6.6: v. Exercise Solutions

22.6.7: vi. Problem Solutions

This page titled [22: Problems](#) is shared under a [CC BY-NC-SA 4.0](#) license and was authored, remixed, and/or curated by [Jack Simons](#) via [source content](#) that was edited to the style and standards of the LibreTexts platform.

SECTION OVERVIEW

22.1: The Basic Tools of Quantum Mechanics

Topic hierarchy

22.1.1: i. Review Exercises

22.1.2: ii. Exercises

22.1.3: iii. Problems 1-10

22.1.4: iv. Problems 11-18

22.1.5: v. Review Exercise Solutions

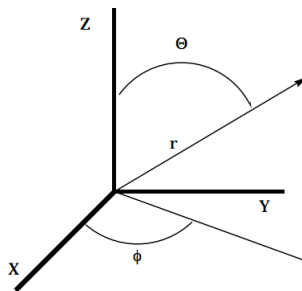
22.1.6: vi. Exercise Solutions

This page titled [22.1: The Basic Tools of Quantum Mechanics](#) is shared under a [CC BY-NC-SA 4.0](#) license and was authored, remixed, and/or curated by [Jack Simons](#) via [source content](#) that was edited to the style and standards of the LibreTexts platform.

22.1.1: i. Review Exercises

Q1

Transform (using the coordinate system provided below) the following functions accordingly:



a. from Cartesian to spherical polar coordinates

$$3x + y - 4z = 12$$

b. from Cartesian to cylindrical coordinates

$$y^2 + z^2 = 9$$

c. from spherical polar to Cartesian coordinates

$$r = 2 \sin \theta \cos \phi$$

Q2

Perform a separation of variables and indicate the general solution for the following expressions:

a. $9x + 16y \frac{\partial y}{\partial x} = 0$

b. $2y + \frac{\partial y}{\partial x} + 6 = 0$

Q3

Find the eigenvalues and corresponding eigenvectors of the following matrices:

a. $\begin{bmatrix} -1 & 2 \\ 2 & 2 \end{bmatrix}$

b. $\begin{bmatrix} -2 & 0 & 0 \\ 0 & -1 & 2 \\ 0 & 2 & 2 \end{bmatrix}$

Q4

For the hermitian matrix in review exercise 3a show that the eigenfunctions can be normalized and that they are orthogonal.

Q5

For the hermitian matrix in review exercise 3b show that the pair of degenerate eigenvalues can be made to have orthonormal eigenfunctions.

Q6

Solve the following second order linear differential equation subject to the specified "boundary conditions":

$$\frac{d^2 x}{dt^2} + k^2 x(t) = 0$$

where $x(t=0) = L$ and $\left. \frac{dx}{dt} \right|_{t=0} = 0$.

This page titled [22.1.1.1: i. Review Exercises](#) is shared under a [CC BY-NC-SA 4.0](#) license and was authored, remixed, and/or curated by [Jack Simons](#) via [source content](#) that was edited to the style and standards of the LibreTexts platform.

22.1.2: ii. Exercises

Q1

Replace the following classical mechanical expressions with their corresponding quantum mechanical operators.

- K.E. = $\frac{mv^2}{2}$ in three-dimensional space.
- $\mathbf{p} = m\mathbf{v}$, a three-dimensional Cartesian vector.
- y-component of angular momentum: $L_y = zp_x - xp_z$.

Q2

Transform the following operators into the specified coordinates:

- $\mathbf{L}_x = \frac{\hbar}{i} \left(y \frac{\partial}{\partial z} - z \frac{\partial}{\partial y} \right)$ from Cartesian to spherical polar coordinates.
- $\mathbf{L}_z = \frac{\hbar}{i} \frac{\partial}{\partial \phi}$ from spherical polar to Cartesian coordinates.

Q3

Match the eigenfunctions in column B to their operators in column A. What is the eigenvalue for each eigenfunction?

Column A	Column B
i. $(1-x^2) \frac{d^2}{dx^2} - x \frac{d}{dx}$	$4x^4 - 12x^2 + 3$
ii. $\frac{d^2}{dx^2}$	$5x^4$
iii. $x \frac{d}{dx}$	$e^{3x} + e^{-3x}$
iv. $\frac{d^2}{dx^2} - 2x \frac{d}{dx}$	$x^2 - 4x + 2$
v. $x \frac{d^2}{dx^2} + (1-x) \frac{d}{dx}$	$4x^3 - 3x$

Q4

Show that the following operators are Hermitian.

- \mathbf{P}_x
- \mathbf{L}_x

Q5

For the following basis of functions ($\Psi_{2p_{-1}}$, Ψ_{2p_0} , and Ψ_{2p_1}), construct the matrix representation of the \mathbf{L}_x operator (use the ladder operator representation of \mathbf{L}_x). Verify that the matrix is Hermitian. Find the eigenvalues and corresponding eigenvectors. Normalize the eigenfunctions and verify that they are orthogonal.

$$\Psi_{2p_{-1}} = \frac{1}{8\sqrt{\pi}} \sqrt{\frac{Z}{a}} re^{\frac{-Zr}{2a}} \sin\theta e^{-i\phi}$$

$$\Psi_{2p_0} = \frac{1}{\sqrt{\pi}} \sqrt{\frac{Z}{2a}} re^{\frac{-Zr}{2a}} \cos\theta$$

$$\Psi_{2p_1} = \frac{1}{8\sqrt{\pi}} \sqrt{\frac{Z}{a}} re^{\frac{-Zr}{2a}} \sin\theta e^{i\phi}$$

Q6

Using the set of eigenstates (with corresponding eigenvalues) from the preceding problem, determine the probability for observing a z-component of angular momentum equal to $1\hbar$ if the state is given by the \mathbf{L}_x eigenstate with $0\hbar$ \mathbf{L}_x eigenvalue.

Q7

Use the following definitions of the angular momentum operators:

$$\mathbf{L}_x = \frac{\hbar}{i} \left(y \frac{\partial}{\partial z} - z \frac{\partial}{\partial y} \right), \mathbf{L}_y = \frac{\hbar}{i} \left(z \frac{\partial}{\partial x} - x \frac{\partial}{\partial z} \right), \mathbf{L}_z = \frac{\hbar}{i} \left(x \frac{\partial}{\partial y} - y \frac{\partial}{\partial x} \right)$$

and $\mathbf{L}^2 = \mathbf{L}_x^2 + \mathbf{L}_y^2 + \mathbf{L}_z^2$, and the relationships:

$[\mathbf{x}, \mathbf{p}_x] = i\hbar$, $[\mathbf{y}, \mathbf{p}_y] = i\hbar$, and $[\mathbf{z}, \mathbf{p}_z] = i\hbar$, to demonstrate the following operator identities:

- $[\mathbf{L}_x, \mathbf{L}_y] = i\hbar \mathbf{L}_z$,
- $[\mathbf{L}_y, \mathbf{L}_z] = i\hbar \mathbf{L}_x$,
- $[\mathbf{L}_z, \mathbf{L}_x] = i\hbar \mathbf{L}_y$,
- $[\mathbf{L}_x, \mathbf{L}^2] = 0$,
- $[\mathbf{L}_y, \mathbf{L}^2] = 0$,
- $[\mathbf{L}_z, \mathbf{L}^2] = 0$.

Q8

In exercise 7 above you determined whether or not many of the angular momentum operators commute. Now, examine the operators below along with an appropriate given function. Determine if the given function is simultaneously an eigenfunction of **both** operators. Is this what you expected?

- $\mathbf{L}_z, \mathbf{L}^2$, with function: $Y_0^0(\theta, \phi) = \frac{1}{\sqrt{4\pi}}$.
- $\mathbf{L}_x, \mathbf{L}_z$, with function: $Y_0^0(\theta, \phi) = \frac{1}{\sqrt{4\pi}}$.
- $\mathbf{L}_z, \mathbf{L}^2$, with function: $Y_1^0(\theta, \phi) = \frac{3}{\sqrt{4\pi}} \cos\theta$.
- $\mathbf{L}_x, \mathbf{L}_z$, with function: $Y_1^0(\theta, \phi) = \frac{3}{\sqrt{4\pi}} \cos\theta$.

Q9

For a "particle in a box" constrained along two axes, the wavefunction $\Psi(x,y)$ as given in the text was:

$$\Psi(x, y) = \sqrt{\frac{1}{2L_x}} \sqrt{\frac{1}{2L_y}} \left[e^{\left(\frac{in_x\pi x}{L_x}\right)} - e^{\left(\frac{-in_x\pi x}{L_x}\right)} \right] \left[e^{\left(\frac{in_y\pi y}{L_y}\right)} - e^{\left(\frac{-in_y\pi y}{L_y}\right)} \right],$$

with n_x and $n_y = 1, 2, 3, \dots$. Show that this wavefunction is normalized.

Q10

Using the same wavefunction, $\Psi(x,y)$, given in exercise 9 show that the expectation value of \mathbf{p}_x vanishes.

Q11

Calculate the expectation value of the \mathbf{x}^2 operator for the first two states of the harmonic oscillator. Use the $v=0$ and $v=1$ harmonic oscillator wavefunctions given below which are normalized such that $\int_{-\infty}^{\infty} \Psi(x)^2 dx = 1$. Remember that

$$\Psi_0 = \sqrt{\frac{\alpha}{\pi}} e^{\left(-\frac{\alpha x^2}{2}\right)} \text{ and } \Psi_1 = \sqrt{\frac{4\alpha^3}{\pi}} x e^{\left(-\frac{\alpha x^2}{2}\right)}.$$

Q12

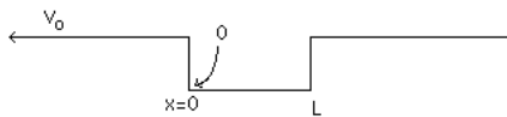
For each of the one-dimensional potential energy graphs shown below, determine:

- whether you expect symmetry to lead to a separation into odd and even solutions,
- whether you expect the energy will be quantized, continuous, or both, and
- the boundary conditions that apply at each boundary (merely stating that Ψ and/or $\frac{\partial \Psi}{\partial x}$ is continuous is all that is necessary).

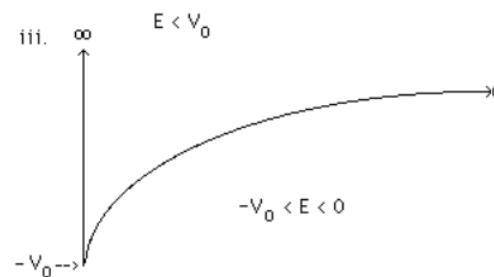
i.



ii.



iii.



Q13

Consider a particle of mass m moving in the potential:

$$\begin{array}{lll} V(x) = \infty & \text{for } x < 0 & \text{Region I} \\ V(x) = 0 & \text{for } 0 \leq x \leq L & \text{Region II} \\ V(x) = V(V > 0) & \text{for } x > L & \text{Region III} \end{array}$$

- Write the general solution to the Schrödinger equation for the regions I, II, III, assuming a solution with energy $E < V$ (i.e. a bound state).
- Write down the wavefunction matching conditions at the interface between regions I and II and between II and III.
- Write down the boundary conditions on Ψ for $x \rightarrow \pm\infty$.
- Use your answers to a. - c. to obtain an algebraic equation which must be satisfied for the bound state energies, E .
- Demonstrate that in the limit $V \rightarrow \infty$, the equation you obtained for the bound state energies in d. gives the energies of a particle in an infinite box; $E_n = \frac{n^2 \hbar^2 \pi^2}{2mL^2}$; $n = 1, 2, 3, \dots$

This page titled [22.1.2: ii. Exercises](#) is shared under a [CC BY-NC-SA 4.0](#) license and was authored, remixed, and/or curated by [Jack Simons](#) via [source content](#) that was edited to the style and standards of the LibreTexts platform.

22.1.3: iii. Problems 1-10

Q1

A particle of mass m moves in a one-dimensional box of length L , with boundaries at $x = 0$ and $x = L$. Thus, $V(x) = 0$ for $0 \leq x \leq L$, and $V(x) = \infty$. The normalized eigenfunctions of the Hamiltonian for this system are given by $\Psi_n(x) = \sqrt{\frac{2}{L}} \sin \frac{n\pi x}{L}$, with $E_n = \frac{n^2 \pi^2 \hbar^2}{2mL^2}$, where the quantum number n can take on the values $n=1,2,3,\dots$

- Assuming that the particle is in an eigenstate, $\Psi_n(x)$, calculate the probability that the particle is found somewhere in the region $0 \leq x \leq \frac{L}{4}$. Show how this probability depends on n .
- For what value of n is there the largest probability of finding the particle in $0 \leq x \leq \frac{L}{4}$?
- Now assume that Ψ is a superposition of two eigenstates, $\Psi = a\Psi_n + b\Psi_m$, at time $t = 0$. What is Ψ at time t ? What energy expectation value does Ψ have at time t and how does this relate to its value at $t = 0$?
- For an experimental measurement which is capable of distinguishing systems in state Ψ_n from those in Ψ_m , what fraction of a large number of systems each described by Ψ will be observed to be in Ψ_n ? What energies will these experimental measurements find and with what probabilities?
- For those systems originally in $\Psi = a\Psi_n + b\Psi_m$ which were observed to be in Ψ_n at time t , what state (Ψ_n , Ψ_m , or whatever) will they be found in if a second experimental measurement is made at a time t' later than t ?
- Suppose by some method (which need not concern us at this time) the system has been prepared in a nonstationary state (that is, it is not an eigenfunction of \mathbf{H}). At the time of a measurement of the particle's energy, this state is specified by the normalized wavefunction $\Psi = \sqrt{\frac{30}{L^5}} x(L-x)$ for $0 \leq x \leq L$, and $\Psi = 0$ elsewhere. What is the probability that a measurement of the energy of the particle will give the value $E_n = \frac{n^2 \pi^2 \hbar^2}{2mL^2}$ for any given value of n ?
- What is the expectation value of \mathbf{H} , i.e. the average energy of the system, for the wavefunction Ψ given in part f?

Q2

Show that for a system in a non-stationary state, $\Psi = \sum_j C_j \Psi_j e^{-\frac{iE_j t}{\hbar}}$, the average value of the energy does **not** vary with time but the expectation values of other properties **do** vary with time.

Q3

A particle is confined to a one-dimensional box of length L having infinitely high walls and is in its lowest quantum state. Calculate: $\langle x \rangle$, $\langle x^2 \rangle$, $\langle p \rangle$, and $\langle p^2 \rangle$. Using the definition $\Delta A = \sqrt{\langle A^2 \rangle - \langle A \rangle^2}$, to define the uncertainty, ΔA , calculate Δx and Δp . Verify the Heisenberg uncertainty principle that $\Delta x \Delta p \geq \frac{\hbar}{2}$.

It has been claimed that as the quantum number n increases, the motion of a particle in a box becomes more classical. In this problem you will have an opportunity to convince yourself of this fact.

- For a particle of mass m moving in a one-dimensional box of length L , with ends of the box located at $x = 0$ and $x = L$, the classical probability density can be shown to be independent of x and given by $P(x)dx = \frac{dx}{L}$ regardless of the energy of the particle. Using this probability density, evaluate the probability that the particle will be found within the interval from $x = 0$ to $x = \frac{L}{4}$.
- Now consider the quantum mechanical particle-in-a-box system. Evaluate the probability of finding the particle in the interval from $x = 0$ to $x = \frac{L}{4}$ for the system in its n th quantum state.
- Take the limit of the result you obtained in part b as $n \rightarrow \infty$. How does your result compare to the classical result you obtained in part a?

Q5

According to the rules of quantum mechanics as we have developed them, if Ψ is the state function, and ϕ_n are the eigenfunctions of a linear, Hermitian operator, \mathbf{A} , with eigenvalues a_n , $\mathbf{A}\phi_n = a_n\phi_n$, then we can expand Ψ in terms of the complete set of

eigenfunctions of \mathbf{A} according to $\Psi = \sum_n c_n \phi_n$, where $c_n = \int \phi_n^* \Psi d\tau$. Furthermore, the probability of making a measurement of the property corresponding to \mathbf{A} and obtaining a value a_n is given by $|c_n|^2$, provided both Ψ and ϕ_n are properly normalized. Thus, $P(a_n) = |c_n|^2$. These rules are perfectly valid for operators which take on a discrete set of eigenvalues, but must be generalized for operators which can have a continuum of eigenvalues. An example of this latter type of operator is the momentum

operator, $\mathbf{p}(-x)$, which has eigenfunctions given by $\phi_p(x) = A e^{\frac{ipx}{\hbar}}$ where p is the eigenvalue of the \mathbf{p}_x operator and A is a normalization constant. Here p can take on any value, so we have a continuous spectrum of eigenvalues of \mathbf{p}_x . The obvious generalization to the equation for Ψ is to convert the sum over discrete states to an integral over the continuous spectrum of states:

$$\Psi(x) = \int_{-\infty}^{+\infty} C(p) \phi_p(x) dp = \int_{-\infty}^{+\infty} C(p) A e^{\frac{ipx}{\hbar}} dp$$

The interpretation of $C(p)$ is now the desired generalization of the equation for the probability $P(p)dp = |C(p)|^2 dp$. This equation states that the probability of measuring the momentum and finding it in the range from p to $p+dp$ is given by $|C(p)|^2 dp$.

Accordingly, the probability of measuring p and finding it in the range from p_1 to p_2 is given by $\int_{p_1}^{p_2} P(p) dp = \int_{p_1}^{p_2} C(p)^* C(p) dp$.

$C(p)$ is thus the probability amplitude for finding the particle with momentum between p and $p+dp$. This is the **momentum representation** of the wavefunction. Clearly we must require $C(p)$ to be normalized, so that $\int_{-\infty}^{+\infty} C(p)^* C(p) dp = 1$. With this

restriction we can derive the normalization constant $A = \frac{1}{\sqrt{\pi\hbar}}$, giving a direct relationship between the wavefunction in coordinate space, $\Psi(x)$, and the wavefunction in momentum space, $C(p)$:

$$\Psi(x) = \frac{1}{\sqrt{2\pi\hbar}} \int_{-\infty}^{+\infty} C(p) e^{\frac{ipx}{\hbar}} dp,$$

and by the Fourier integral theorem:

$$C(p) = \frac{1}{\sqrt{2\pi\hbar}} \int_{-\infty}^{+\infty} \Psi(x) e^{\frac{ipx}{\hbar}} dx.$$

Lets use these ideas to solve some problems focusing our attention on the harmonic oscillator; a particle of mass m moving in a one-dimensional potential described by $V(x) = \frac{kx^2}{2}$.

a. Write down the Schrödinger equation in the coordinate representation.

b. Now lets proceed by attempting to write the Schrödinger equation in the momentum representation. Identifying the kinetic energy operator \mathbf{T} , in the momentum representation is quite straitforward $\mathbf{T} = \frac{\mathbf{p}^2}{2m} = -\text{Error!}$. Writing the potential, $V(x)$, in the momentum representation is not quite as straightforward. The relationship between position and momentum is realized in their commutation relation $[\mathbf{x}, \mathbf{p}] = i\hbar$, or $(\mathbf{x}\mathbf{p} - \mathbf{p}\mathbf{x}) = i\hbar$ This commutation relation is easily verified in the coordinate representation leaving \mathbf{x} untouched ($\mathbf{x} = x$.) and using the above definition for \mathbf{p} . In the momentum representation we want to leave \mathbf{p} untouched ($\mathbf{p} = p$.) and define the operator \mathbf{x} in such a manner that the commutation relation is still satisfied. Write the operator \mathbf{x} in the momentum representation. Write the full Hamiltonian in the momentum representation and hence the Schrödinger equation in the momentum representation.

c. Verify that Ψ as given below is an eigenfunction of the Hamiltonian in the coordinate representation. What is the energy of the system when it is in this state? Determine the normalization constant C , and write down the normalized ground state wavefunction in coordinate space.

$$\Psi(x) = C e^{\left(-\sqrt{mk} \frac{x^2}{2\hbar}\right)}.$$

d. Now consider Ψ in the momentum representation. Assuming that an eigenfunction of the Hamiltonian may be found of the form $\Psi(p) = Ce^{-\alpha p^2}$, substitute this form of Ψ into the Schrödinger equation in the momentum representation to find the value of α which makes this an eigenfunction of \mathbf{H} having the same energy as $\Psi(x)$ had. Show that this $\Psi(p)$ is the proper fourier transform of $\Psi(x)$. The following integral may be useful:

$$\int_{-\infty}^{+\infty} e^{-\beta x^2} \cos(bx) dx = \sqrt{\frac{\pi}{\beta}} e^{-\frac{b^2}{4\beta}}.$$

since this Hamiltonian has no degenerate states, you may conclude that $\Psi(x)$ and $\Psi(p)$ represent the same state of the system if they have the same energy.

Q6

The energy states and wavefunctions for a particle in a 3-dimensional box whose lengths are L_1, L_2 , and L_3 are given by

$$E(n_1, n_2, n_3) = \frac{h^2}{8m} \left[\left(\frac{n_1}{L_1} \right)^2 + \left(\frac{n_2}{L_2} \right)^2 + \left(\frac{n_3}{L_3} \right)^2 \right] \text{ and}$$

$$\Psi(n_1, n_2, n_3) = \sqrt{\frac{2}{L_1}} \sqrt{\frac{2}{L_2}} \sqrt{\frac{2}{L_3}} \sin \left(\frac{n_2 \pi y}{L_2} \right) \sin \left(\frac{n_3 \pi z}{L_3} \right).$$

These wavefunctions and energy levels are sometimes used to model the motion of electrons in a central metal atom (or ion) which is surrounded by six ligands.

- Show that the lowest energy **level** is nondegenerate and the second energy **level** is triply degenerate if $L_1 = L_2 = L_3$. What values of n_1, n_2 , and n_3 characterize the **states** belonging to the triply degenerate level?
- For a box of volume $V = L_1 L_2 L_3$, show that for three electrons in the box (two in the nondegenerate lowest "orbital", and one in the next), a lower **total** energy will result if the box undergoes a rectangular distortion ($L_1 = L_2 \neq L_3$). **which preserves the total volume** than if the box remains undistorted (hint: if V is fixed and $L_1 = L_2$, then $L_3 = \frac{V}{L_1^2}$ and L_1 is the only "variable").
- Show that the degree of distortion (ratio of L_3 to L_1) which will minimize the total energy is $L_3 = \sqrt{2} L_1$. How does this problem relate to Jahn-Teller distortions? Why (in terms of the property of the central atom or ion) do we do the calculation with fixed volume?
- By how much (in eV) will distortion lower the energy (from its value for a cube, $L_1 = L_2 = L_3$) if $V = 8 \text{ \AA}^3$ and $\frac{h^2}{8m} = 6.01 \times 10^{-27} \text{ erg cm}^2$. $1 \text{ eV} = 1.6 \times 10^{-12} \text{ erg}$

Q7

The wavefunction $\Psi = Ae^{-a|x|}$ is an exact eigenfunction of some one-dimensional Schrödinger equation in which x varies from $-\infty$ to $+\infty$. The value of a is: $a = (2\text{\AA})^{-1}$. For now, the potential $V(x)$ in the Hamiltonian $\left(\text{H} = -\frac{\hbar^2}{2m} \frac{d^2}{dx^2} + V(x) \right)$ for which $\Psi(x)$ is an eigenfunction is unknown.

- Find a value of A which makes $\Psi(x)$ normalized. Is this value unique? What units does $\Psi(x)$ have?
- Sketch the wavefunction for positive and negative values of x , being careful to show the behavior of its slope near $x = 0$. Recall that $|x|$ is defined as:

$$|x| = \begin{cases} x & \text{if } x > 0 \\ -x & \text{if } x < 0 \end{cases}$$

- Show that the derivative of $\Psi(x)$ undergoes a discontinuity of magnitude $2\sqrt{a}$ as x goes through $x = 0$. What does this fact tell you about the potential $V(x)$?
- Calculate the expectation value of $|x|$ for the above normalized wavefunction (obtain a numerical value and give its units). What does this expectation value give a measure of?

- e. The potential $V(x)$ appearing in the Schrödinger equation for which $\Psi = Ae^{-a|x|}$ is an exact solution is given by $V(x) = \frac{\hbar^2 a}{m} \delta(x)$. Using this potential, compute the expectation value of the Hamiltonian $\left(\mathbf{H} = -\frac{\hbar}{2m} \frac{d^2}{dx^2} + V(x) \right)$ for your normalized wavefunction. Is $V(x)$ an attractive or repulsive potential? Does your wavefunction correspond to a bound state? Is $\langle H \rangle$ use $\frac{\hbar^2}{2m} = 6.06 \times 10^{-28} \text{ erg cm}^2$ and $1\text{eV} = 1.6 \times 10^{-12} \text{ erg}$.
- f. Transform the wavefunction, $\Psi = Ae^{-a|x|}$, from coordinate space to momentum space.
- g. What is the ratio of the probability of observing a momentum equal to $2a\hbar$ to the probability of observing a momentum equal to $-a\hbar$?

Q8

The π -orbitals of benzene, C_6H_6 , may be modeled very crudely using the wavefunctions and energies of a particle on a ring. Let's first treat the particle on a ring problem and then extend it to the benzene system.

- a. Suppose that a particle of mass m is constrained to move on a circle (of radius r) in the xy plane. Further assume that the particle's potential energy is constant (zero is a good choice). Write down the Schrödinger equation in the normal cartesian coordinate representation. Transform this Schrödinger equation to cylindrical coordinates where $x = r\cos(\phi)$, $y = r\sin(\phi)$, and $z = z$ ($z = 0$ in this case). Taking r to be held constant, write down the general solution, $\Phi(\phi)$, to this Schrödinger equation. The "boundary" conditions for this problem require that $\Phi(\phi) = \Phi(\phi + 2\pi)$. Apply this boundary condition to the general solution. This results in the quantization of the energy levels of this system. Write down the final expression for the normalized wavefunction and quantized energies. What is the physical significance of these quantum numbers which can have both positive and negative values? Draw an energy diagram representing the first five energy levels.
- b. Treat the six π -electrons of benzene as particles free to move on a ring of radius 1.40 \AA , and calculate the energy of the lowest electronic transition. Make sure the Pauli principle is satisfied! What wavelength does this transition correspond to? Suggest some reasons why this differs from the wavelength of the lowest observed transition in benzene, which is 2600 \AA .

Q9

A diatomic molecule constrained to rotate on a flat surface can be modeled as a planar rigid rotor (with eigenfunctions, $\Phi(\phi)$, analogous to those of the particle on a ring) with fixed bond length r . At $t = 0$, the rotational (orientational) probability distribution is observed to be described by a wavefunction $\Psi(\phi, 0) = \sqrt{\frac{4}{3\pi}} \cos^2 \phi$. What values, and with what probabilities, of the rotational angular momentum, $\left(-i\hbar \frac{\partial}{\partial \phi} \right)$, could be observed in this system? Explain whether these probabilities would be time dependent as $\Psi(\phi, 0)$ evolves into $\Psi(\phi, t)$.

Q10

A particle of mass m moves in a potential given by $V(x, y, z) = \frac{k}{2}(x^2 + y^2 + z^2) = \text{frac}{k}{2}r^2$.

- a. Write down the time-independent Schrödinger equation for this system.
- b. Make the substitution $\Psi(x, y, z) = X(x)Y(y)Z(z)$ and separate the variables for this system.
- c. What are the solutions to the resulting equations for $X(x)$, $Y(y)$, and $Z(z)$?
- d. What is the general expression for the quantized energy levels of this system, in terms of the quantum numbers n_x , n_y , and n_z , which correspond to $X(x)$, $Y(y)$, and $Z(z)$?
- e. What is the degree of degeneracy of a state of energy

$$E = 5.5\hbar\sqrt{\frac{k}{m}} \text{ for this system?}$$

- f. An alternative solution may be found by making the substitution $\Psi(r, \theta, \phi) = F(r)G(\theta, \phi)$. In this substitution, what are the solutions for $G(\theta, \phi)$?
- g. Write down the differential equation for $F(r)$ which is obtained when the substitution $\Psi(r, \theta, \phi) = F(r)G(\theta, \phi)$ is made. Do not solve this equation.

This page titled [22.1.3; iii. Problems 1-10](#) is shared under a [CC BY-NC-SA 4.0](#) license and was authored, remixed, and/or curated by [Jack Simons](#) via [source content](#) that was edited to the style and standards of the LibreTexts platform.

22.1.4: iv. Problems 11-18

Q11

Consider an N_2 molecule, in the ground vibrational level of the ground electronic state, which is bombarded by 100 eV electrons. This leads to the ionization of the N_2 molecule to form N_2^+ . In this problem we will attempt to calculate the vibrational distribution of the newly-formed N_2^+ ions, using a somewhat simplified approach.

a. Calculate (according to classical mechanics) the velocity (in cm/sec) of a 100 eV electron, ignoring any relativistic effects. Also calculate the amount of time required for a 100 eV electron to pass an N_2 molecule, which you may estimate as having a length of 2 Å.

b. The radial Schrödinger equation for a diatomic molecule treating vibration as a harmonic oscillator can be written as:

$$-\frac{\hbar^2}{2\mu r^2} \left(\frac{\partial}{\partial r} \left(r^2 \frac{\partial \Psi}{\partial r} \right) \right) + \frac{k}{2} (r - r_e)^2 \Psi = E \Psi,$$

Substituting $\Psi(r) = \frac{F(r)}{r}$, this equation can be rewritten as:

$$-\frac{\hbar^2}{2\mu} \frac{\partial^2}{\partial r^2} F(r) + \frac{k}{2} (r - r_e)^2 \Psi = E \Psi,$$

The vibrational Hamiltonian for the ground electronic state of the N_2 molecule within this approximation is given by:

$$\mathbf{H}(N_2) = -\frac{\hbar^2}{2\mu} \frac{d^2}{dr^2} + \frac{k_{N_2}}{2} (r - r_{N_2})^2,$$

where r_{N_2} and k_{N_2} have been measured experimentally to be:

$$r_{N_2} = 1.09796 \text{ Å}; k_{N_2} = 2.294 \times 10^6 \frac{\text{g}}{\text{sec}^2}.$$

The vibrational Hamiltonian for the N_2^+ ion, however, is given by :

$$\mathbf{H}(N_2^+) = -\frac{\hbar^2}{2\mu} \frac{d^2}{dr^2} + \frac{k_{N_2}^+}{2} (r - r_{N_2}^+)^2,$$

where $r_{N_2}^+$ and $k_{N_2}^+$ have been measured experimentally to be:

$$r_{N_2}^+ = 1.11642 \text{ Å}; k_{N_2}^+ = 2.009 \times 10^6 \frac{\text{g}}{\text{sec}^2}$$

In both systems the reduced mass is $\mu = 1.1624 \times 10^{-23} \text{ g}$. Use the above information to write out the ground state vibrational wavefunctions of the N_2 and N_2^+ molecules, giving explicit values for any constants which appear in them. Note: For this problem use the "normal" expression for the ground state wavefunction of a harmonic oscillator. You need not solve the differential equation for this system.

c. During the time scale of the ionization event (which you calculated in part a), the vibrational wavefunction of the N_2 molecule has effectively no time to change. As a result, the newly-formed N_2^+ ion finds itself in a vibrational state which is **not** an eigenfunction of the **new** vibrational Hamiltonian, $\mathbf{H}(N_2^+)$. Assuming that the N_2 molecule was originally in its $v=0$ vibrational state, calculate the probability that the N_2^+ ion will be produced in its $v=0$ vibrational state.

Q12

The force constant, k , of the C-O bond in carbon monoxide is $1.87 \times 10^6 \frac{\text{g}}{\text{sec}^2}$. Assume that the vibrational motion of CO is purely harmonic and use the reduced mass $\mu = 6.857 \text{ amu}$.

a. Calculate the spacing between vibrational energy levels in this molecule, in units of ergs and cm^{-1} .

b. Calculate the uncertainty in the internuclear distance in this molecule, assuming it is in its ground vibrational level. Use the ground state vibrational wavefunction ($\Psi_{v=0}$), and calculate $\langle x \rangle$, $\langle x^2 \rangle$, and $\Delta x = \sqrt{\langle x^2 \rangle - \langle x \rangle^2}$.

c. Under what circumstances (i.e. large or small values of k ; large or small values of μ) is the uncertainty in internuclear distance large? Can you think of any relationship between this observation and the fact that helium remains a liquid down to absolute zero?

Q13

Suppose you are given a trial wavefunction of the form:

$$\phi = \frac{Z_e^3}{\pi a_0^3} e^{\left(\frac{-Z_e r_1}{a_0}\right)} e^{\left(\frac{-Z_e r_2}{a_0}\right)}$$

to represent the electronic structure of a two-electron ion of nuclear charge Z and suppose that you were also lucky enough to be **given** the variational integral, W , (instead of asking you to derive it!):

$$W = \left(Z_e^2 - 2ZZ_e + \frac{5}{8}Z_e \right) \frac{e^2}{a_0}.$$

- Find the optimum value of the variational parameter Z_e for an arbitrary nuclear charge Z by setting $\frac{dW}{dZ_e} = 0$. Find both the optimal value of Z_e and the resulting value of W .
- The total energies of some two-electron atoms and ions have been experimentally determined to be:

$Z = 1$	H^-	-14.35eV
$Z = 2$	He	-78.98eV
$Z = 3$	Li^+	-198.02eV
$Z = 4$	Be^{+2}	-371.5eV
$Z = 5$	B^{+3}	-599.3eV
$Z = 6$	C^{+4}	-881.6eV
$Z = 7$	N^{+5}	-1218.3eV
$Z = 8$	O^{+6}	-1609.5eV

Using your optimized expression for W , calculate the estimated total energy of each of these atoms and ions. Also calculate the percent error in your estimate for each ion. What physical reason explains the decrease in percentage error as Z increases?

- In 1928, when quantum mechanics was quite young, it was not known whether the isolated, gas-phase hydride ion, H^- , was stable with respect to dissociation into a hydrogen atom and an electron. Compare your estimated total energy for H^- to the ground state energy of a hydrogen atom and an isolated electron (system energy = -13.60 eV), and show that this simple variational calculation erroneously predicts H^- to be unstable. (More complicated variational treatments give a ground state energy of H^- of -14.35 eV , in agreement with experiment.)

Q14

A particle of mass m moves in a one-dimensional potential given by $H = -\frac{\hbar^2}{2m} \frac{d^2}{dx^2} + a|x|$, where the absolute value function is defined by $|x| = x$ if $x \geq 0$ and $|x| = -x$ if $x \leq 0$.

- Use the normalized trial wavefunction $\phi = \sqrt[4]{\frac{2b}{\pi}} e^{-bx^2}$ to estimate the energy of the ground state of this system, using the variational principle to evaluate $W(b)$.
- Optimize b to obtain the best approximation to the ground state energy of this system, using a trial function of the form of ϕ , as given above. The numerically calculated exact ground state energy is $0.808616 \sqrt[3]{\hbar^2 \sqrt{m} \sqrt{a}^2}$. What is the percent error in your value?

Q15

The harmonic oscillator is specified by the Hamiltonian:

$$H = -\frac{\hbar^2}{2m} \frac{d^2}{dx^2} + \frac{1}{2}kx^2.$$

Suppose the ground state solution to this problem were unknown, and that you wish to approximate it using the variational theorem. Choose as your trial wavefunction,

$$\phi = \sqrt{\frac{15}{16}} \sqrt[3]{a^5} (a^2 - x^2) \text{ for } -a < x < a$$

$$\phi = 0 \text{ for } |x| \geq a$$

where a is an arbitrary parameter which specifies the range of the wavefunction. Note that ϕ is properly normalized as given.

a. Calculate $\lim_{a \rightarrow \infty} \int_{-\infty}^{+\infty} \phi^* \mathbf{H} \phi dx$ and show it to be given by:

$$\int_{-\infty}^{+\infty} \phi^* \mathbf{H} \phi dx = \frac{5}{4} \frac{\hbar^2}{ma^2} + \frac{ka^2}{14}.$$

b. Calculate $\int_{-\infty}^{+\infty} \phi^* \mathbf{H} \phi dx$ for $a = b \sqrt[4]{\frac{\hbar^2}{km}}$ with $b = 0.2, 0.4, 0.6, 0.8, 1.0, 1.5, 2.0, 2.5, 3.0, 4.0$, and 5.0 , and plot the result.

c. To find the best approximation to the true wavefunction and its energy, find the minimum of $\int_{-\infty}^{+\infty} \phi^* \mathbf{H} \phi dx$ by setting $\frac{d}{da} \int_{-\infty}^{+\infty} \phi^* \mathbf{H} \phi dx = 0$ and solving for a . Substitute this value into the expression for $\int_{-\infty}^{+\infty} \phi^* \mathbf{H} \phi dx$ given in part a. to obtain the best approximation for the energy of the ground state of the harmonic oscillator.

d. What is the percent error in your calculated energy of part c. ?

Q16

Einstein told us that the (relativistic) expression for the energy of a particle having rest mass m and momentum p is $E^2 = m^2 c^4 + p^2 c^2$.

a. Derive an expression for the relativistic kinetic energy operator which contains terms correct through one higher order than the "ordinary" $E = mc^2 + \frac{p^2}{2m}$.

b. Using the first order correction as a perturbation, compute the first-order perturbation theory estimate of the energy for the 1s level of a hydrogen-like atom (general Z). Show the Z dependence of the result.

$$\text{Note: } \Psi(r)_{1s} = \sqrt{\frac{Z^3}{a}} \sqrt{\frac{1}{\pi}} e^{-\frac{Zr}{a}} \text{ and } E_{1s} = -\frac{Z^2 m e^4}{2 \hbar^2}$$

c. For what value of Z does this first-order relativistic correction amount to 10% of the unperturbed (non-relativistic) 1s energy?

Q17

Consider an electron constrained to move on the surface of a sphere of radius r . The Hamiltonian for such motion consists of a kinetic energy term only $\mathbf{H}_0 = \frac{\mathbf{L}^2}{2m_e r_0^2}$, where \mathbf{L} is the orbital angular momentum operator involving derivatives with respect to

the spherical polar coordinates (θ, ϕ) . \mathbf{H}_0 has the complete set of eigenfunctions $\psi_{lm}^{(0)} = Y_{lm}(\theta, \phi)$.

a. Compute the zeroth order energy levels of this system.

b. A uniform electric field is applied along the z -axis, introducing a perturbation $V = -e\epsilon z = -e\epsilon r_0 \cos\theta$, where ϵ is the strength of the field. Evaluate the correction to the energy of the lowest level through second order in perturbation theory, using the identity

$$\cos\theta Y_{lm}(\theta, \phi) = \sqrt{\frac{(l+m+1)(l-m+1)}{(2l+1)(2l+3)}} Y_{l+1,m}(\theta, \phi) + \sqrt{\frac{(l+m)(l-m)}{(2l+1)(2l-1)}} Y_{l-1,m}(\theta, \phi).$$

Note that this identity enables you to utilize the orthonormality of the spherical harmonics.

c. The electric polarizability α gives the response of a molecule to an externally applied electric field, and is defined by $\alpha = -\frac{\partial^2 E}{\partial^2 \epsilon} \Big|_{\epsilon=0}$ where E is the energy in the presence of the field and ϵ is the strength of the field. Calculate α for this system.

d. Use this problem as a model to estimate the polarizability of a hydrogen atom, where $r_0 = a_0 = 0.529 \text{ \AA}$, and a cesium atom, which has a single 6s electron with $r_0 \approx 2.60 \text{ \AA}$. The corresponding experimental values are $\alpha_H = 0.6668 \text{ \AA}^3$ and $\alpha_{Cs} = 59.6 \text{ \AA}^3$.

Q18

An electron moving in a conjugated bond framework can be viewed as a particle in a box. An externally applied electric field of strength ϵ interacts with the electron in a fashion described by the perturbation $V = e\epsilon \left(x - \frac{L}{2}\right)$, where x is the position of the electron in the box, e is the electron's charge, and L is the length of the box.

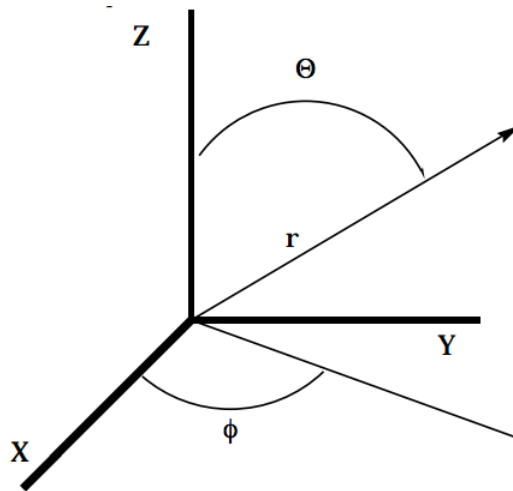
- Compute the first order correction to the energy of the $n=1$ state and the first order wavefunction for the $n=1$ state. In the wavefunction calculation, you need only compute the contribution to $\Psi_1^{(1)}$ made by $\Psi_2^{(0)}$. Make a rough (no calculation needed) sketch of $\Psi_1^{(0)} + \Psi_1^{(1)}$ as a function of x and physically interpret the graph.
- Using your answer to part a. compute the induced dipole moment caused by the polarization of the electron density due to the electric field effect $\mu_{\text{induced}} = -e \int \Psi^* \left(x - \frac{L}{2}\right) \Psi dx$. You may neglect the term proportional to ϵ^2 ; merely obtain the term linear in ϵ .
- Compute the polarizability, α , of the electron in the $n=1$ state of the box, and explain physically why α should depend as it does upon the length of the box L . Remember that $\alpha = \left. \frac{\partial \mu}{\partial \epsilon} \right|_{\epsilon=0}$.

This page titled [22.1.4: iv. Problems 11-18](#) is shared under a [CC BY-NC-SA 4.0](#) license and was authored, remixed, and/or curated by [Jack Simons](#) via [source content](#) that was edited to the style and standards of the LibreTexts platform.

22.1.5: v. Review Exercise Solutions

Q1

The general relationships are as follows:



$$\begin{aligned} x &= r \sin \theta \cos \phi & r^2 &= x^2 + y^2 + z^2 \\ y &= r \sin \theta \sin \phi & \sin \theta &= \frac{\sqrt{x^2 + y^2}}{\sqrt{x^2 + y^2 + z^2}} \\ z &= r \cos \theta & \cos \theta &= \frac{z}{\sqrt{x^2 + y^2 + z^2}} \\ & & \tan \phi &= \frac{y}{x} \end{aligned}$$

a.

$$\begin{aligned} 3x + y - 4z &= 12 \\ 3(r \sin \theta \cos \phi) + \sin \theta \sin \phi - 4(r \cos \theta) &= 12 \\ r(3 \sin \theta \cos \phi + \sin \theta \sin \phi - 4 \cos \theta) &= 12 \end{aligned}$$

b.

$$\begin{aligned} x &= r \cos \phi & r^2 &= x^2 + y^2 \\ y &= r \sin \phi & \tan \phi &= \frac{y}{x} \\ z &= z & y^2 + z^2 &= 9 \\ & & r^2 \sin^2 \phi + z^2 &= 9 \end{aligned}$$

c.

$$\begin{aligned} r &= 2 \sin \theta \cos \phi \\ r &= 2 \left(\frac{x}{r} \right) \\ r^2 &= 2x \\ x^2 + y^2 + z^2 &= 2x \\ x^2 - 2x + y^2 + z^2 &= 0 \\ x^2 - 2x + 1 + y^2 + z^2 &= 1 \\ (x - 1)^2 + y^2 + z^2 &= 1 \end{aligned}$$

Q2

a.

$$\begin{aligned}
 9x + 16y \frac{\partial y}{\partial x} &= 0 \\
 16y dy &= -9x dx \\
 \frac{16}{2} y^2 &= -\frac{9}{2} x^2 + c \\
 16y^2 &= -9x^2 + c' \\
 \frac{y^2}{9} + \frac{x^2}{16} &= c'' \text{ (general equation for an ellipse)}
 \end{aligned}$$

b.

$$\begin{aligned}
 2y + \frac{\partial y}{\partial x} + 6 &= 0 \\
 2y + 6 &= -\frac{dy}{dx} \\
 -2dx &= -\frac{dy}{2dx} \\
 -2dx &= \frac{dy}{y+3} \\
 -2x &= \ln(y+3) + c \\
 c'e^{-2x} &= y+3 \\
 y &= c'e^{-2x} - 3
 \end{aligned}$$

Q3

a. First determine the eigenvalues:

$$\begin{aligned}
 \det \begin{bmatrix} -1-\lambda & 2 \\ 2 & 2-\lambda \end{bmatrix} &= 0 \\
 (-1-\lambda)(2-\lambda) - 2^2 &= 0 \\
 -2 + \lambda - 2\lambda + \lambda^2 - 4 &= 0 \\
 \lambda^2 - \lambda - 6 &= 0 \\
 (\lambda - 3)(\lambda + 2) &= 0 \\
 \lambda = 3 \text{ or } \lambda = -2.
 \end{aligned}$$

Next, determine the eigenvectors. First, the eigenvector associated with eigenvalue -2:

$$\begin{aligned}
 \begin{bmatrix} -1 & 2 \\ 2 & 2 \end{bmatrix} \begin{bmatrix} C_{11} \\ C_{21} \end{bmatrix} &= -2 \begin{bmatrix} C_{11} \\ C_{21} \end{bmatrix} \\
 -C_{11} + 2C_{21} &= -2C_{11} \\
 C_{11} &= -2C_{21}
 \end{aligned}$$

(Note: The second row offers no new information, e.g. $2C_{11} + 2C_{21} = -2C_{21}$)

$$C_{11}^2 + C_{21}^2 = 1 \text{ (from normalization)}$$

$$(-2C_{21})^2 + C_{21}^2 = 1$$

$$4C_{21}^2 + C_{21}^2 = 1$$

$$5C_{21}^2 = 1$$

$$C_{21}^2 = 0.2$$

$$C_{21} = \sqrt{0.2}$$

(again the second row offers no new information)

$$C_{12}^2 + C_{22}^2 = 1$$

$$0.25C_{22}^2 + C_{22}^2 = 1$$

$$1.25C_{22}^2 = 1$$

$$C_{22}^2 = 0.8$$

$$C_{22} = \sqrt{0.8} = 2\sqrt{0.2}, \text{ and therefore } C_{12} = \sqrt{0.2}.$$

Therefore the eigenvector matrix becomes:

$$\begin{bmatrix} -2\sqrt{0.2} & \sqrt{0.2} \\ \sqrt{0.2} & 2\sqrt{0.2} \end{bmatrix}$$

b. First determine the eigenvalues:

$$\det \begin{bmatrix} -2-\lambda & 0 & 0 \\ 0 & -1-\lambda & 2 \\ 0 & 2 & 2-\lambda \end{bmatrix} = 0$$

$$\det [-2-\lambda] \det \begin{bmatrix} -1-\lambda & 2 \\ 2 & 2-\lambda \end{bmatrix} = 0$$

From 3a, the solutions then become -2, -2, and 3. Next, determine the eigenvectors. First the eigenvector associated with eigenvalue 3 (the third root):

$$\begin{bmatrix} -2 & 0 & 0 \\ 0 & -1 & 2 \\ 0 & 2 & 2 \end{bmatrix} \begin{bmatrix} C_{11} \\ C_{21} \\ C_{31} \end{bmatrix} = 3 \begin{bmatrix} C_{11} \\ C_{21} \\ C_{31} \end{bmatrix}$$

$$-2C_{13} = 3C_{13} \text{ (row one)}$$

$$C_{13} = 0$$

$$-C_{23} + 2C_{33} = 3C_{23} \text{ (row two)}$$

$$2C_{33} = 2C_{23}$$

$$C_{33} = 2C_{23} \text{ (again the third row offers no new information)}$$

$$C_{13}^2 + C_{23}^2 + C_{33}^2 = 1 \text{ (from normalization)}$$

$$0 + C_{23}^2 + (2C_{23})^2 = 1$$

$$5C_{23}^2 = 1$$

$$C_{23} = \sqrt{0.2}, \text{ and therefore } C_{33} = \sqrt{0.2}.$$

Next, find the pair of eigenvectors associated with the degenerate eigenvalue of -2. First, root one eigenvector one:

$$\begin{aligned}
 -2C_{11} &= -2C_{11} \text{ (no new information from row one)} \\
 -C_{21} + 2C_{31} &= -2C_{21} \text{ (row two)} \\
 C_{21} &= -2C_{31} \text{ (again the third row offers no new information)} \\
 C_{11}^2 + C_{21}^2 + C_{31}^2 &= 1 \text{ (from normalization)} \\
 C_{11}^2 + (-2C_{31})^2 + C_{31}^2 &= 1 \\
 C_{11}^2 + 5C_{31}^2 &= 1 \\
 C_{11} &= \sqrt{1 - 5C_{31}^2}
 \end{aligned}$$

Note: There are now two equations with three unknowns. Second, root two eigenvector two:

$$\begin{aligned}
 -2C_{12} &= -2C_{12} \text{ (no new information from row one)} \\
 -C_{21} + 2C_{31} &= -2C_{21} \text{ (row two)} \\
 C_{21} &= -2C_{31} \text{ (again the third row offers no new information)} \\
 C_{11}^2 + C_{21}^2 + C_{31}^2 &= 1 \text{ (from normalization)} \\
 C_{12}^2 + (-2C_{32})^2 + C_{32}^2 &= 1 \\
 C_{12}^2 + 5C_{32}^2 &= 1 \\
 C_{12} &= \sqrt{1 - 5C_{32}^2}
 \end{aligned}$$

Note: Again there are now two equations with three unknowns.

$$C_{11}C_{12} + C_{21}C_{22} + C_{31}C_{32} = 0 \text{ (from orthogonalization)}$$

Now there are five equations with six unknowns.

$$\begin{aligned}
 &\text{Arbitrarily choose } C_{11} = 0 \\
 C_{11} &= 0 = \sqrt{1 - 5C_{31}^2} \\
 5C_{31}^2 &= 1 \\
 C_{31} &= \sqrt{0.2} \\
 C_{21} &= -2\sqrt{0.2} \\
 C_{11}C_{12} + C_{21}C_{22} + C_{31}C_{32} &= 0 \text{ (from orthogonalization)} \\
 0 + -2\sqrt{0.2}(-2C_{32}) + \sqrt{0.2}C_{32} &= 0 \\
 5C_{32} &= 0 \\
 C_{32} = 0, C_{22} = 0, \text{ and } C_{12} &= 1
 \end{aligned}$$

Therefore the eigenvector matrix becomes:

$$\begin{bmatrix} 0 & 1 & 0 \\ -2\sqrt{0.2} & 0 & \sqrt{0.2} \\ \sqrt{0.2} & 0 & 2\sqrt{0.2} \end{bmatrix}$$

Q4

Show: $\langle \phi_1 | \phi_1 \rangle = 1$, $\langle \phi_2 | \phi_2 \rangle = 1$, and $\langle \phi_1 | \phi_2 \rangle = 0$

$$\begin{aligned}
 \langle \phi_1 | \phi_1 \rangle &\stackrel{?}{=} 1 \\
 (-2\sqrt{0.2})^2 + (\sqrt{0.2})^2 &\stackrel{?}{=} 1 \\
 4(0.2) + 0.2 &\stackrel{?}{=} 1 \\
 0.8 + 0.2 &\stackrel{?}{=} 1 \\
 1 &= 1 \\
 \langle \phi_2 | \phi_2 \rangle &\stackrel{?}{=} 1 \\
 (\sqrt{0.2})^2 + (2\sqrt{0.2})^2 &\stackrel{?}{=} 1 \\
 0.2 + 4(0.2) &\stackrel{?}{=} 1 \\
 0.2 + 0.8 &\stackrel{?}{=} 1 \\
 1 &= 1 \\
 \langle \phi_1 | \phi_2 \rangle = \langle \phi_2 | \phi_1 \rangle &\stackrel{?}{=} 0 \\
 -2\sqrt{0.2}\sqrt{0.2} &\stackrel{?}{=} 2\sqrt{0.2}\sqrt{0.2} \\
 -2(0.2) + 2(0.2) &\stackrel{?}{=} 0 \\
 -0.4 + 0.4 &\stackrel{?}{=} 0 \\
 0 &= 0
 \end{aligned}$$

Q5

Show (for the degenerate eigenvalue; $\lambda = -2$): $\langle \phi_2 | \phi_2 \rangle = 1$, $\langle \phi_2 | \phi_1 \rangle = 0$, and $\langle \phi_1 | \phi_2 \rangle = 0$

$$\begin{aligned}
 \langle \phi_1 | \phi_1 \rangle &\stackrel{?}{=} 1 \\
 0 + (-2\sqrt{0.2})^2 + (\sqrt{0.2})^2 &\stackrel{?}{=} 1 \\
 4(0.2) + 0.2 &\stackrel{?}{=} 1 \\
 0.8 + 0.2 &\stackrel{?}{=} 1 \\
 1 &= 1 \\
 \langle \phi_1 | \phi_2 \rangle &\stackrel{?}{=} 0 \\
 1^2 + 0 + 0 &\stackrel{?}{=} 0 \\
 1 &= 0 \\
 \langle \phi_1 | \phi_2 \rangle = \langle \phi_2 | \phi_1 \rangle &\stackrel{?}{=} 0 \\
 (0)(1) + (-2\sqrt{0.2})(0) + (\sqrt{0.2})(0) &\stackrel{?}{=} 0
 \end{aligned}$$

Q6

Suppose the solution is of the form $x(t) = e^{\alpha t}$, with α unknown. Inserting this trial solution into the differential equation results in the following:

$$\begin{aligned}
 \frac{d^2}{dt^2} e^{\alpha t} + k^2 e^{\alpha t} &= 0 \\
 \alpha^2 e^{\alpha t} + k^2 e^{\alpha t} &= 0 \\
 (\alpha^2 + k^2) x(t) &= 0 \\
 (\alpha^2 + k^2) &= 0 \\
 \alpha^2 &= -k^2 \\
 \alpha &= \pm i k
 \end{aligned}$$

\therefore Solutions are of the form e^{-ikt} , e^{ikt} , or a combination of both: $x(t) = C_1 e^{ikt} + C_2 e^{-ikt}$.

Euler's formula also states that: $e^{\pm i\theta} = \cos\theta \pm i\sin\theta$, so the previous equation for $x(t)$ can also be written as:

$$\begin{aligned}x(t) &= C_1 [\cos(kt) + i\sin(kt)] + C_2 [\cos(kt) - i\sin(kt)] \\x(t) &= (C_1 + C_2) \cos(kt) + (C_1 - C_2) i\sin(kt), \text{ or alternatively} \\x(t) &= C_3 \cos(kt) + C_4 \sin(kt).\end{aligned}$$

We can determine these coefficients by making use of the "boundary conditions".

$$\begin{aligned}\text{at } t = 0, x(0) &= L \\x(0) &= C_3 \cos(0) + C_4 \sin(0) = L \\C_3 &= L \\ \text{at } t = 0, \frac{dx(0)}{dt} &= 0 \\\frac{d}{dt}x(t) &= \frac{d}{dt}(C_3 \cos(kt) + C_4 \sin(kt)) \\\frac{d}{dt}x(t) &= -C_3 k \sin(kt) + C_4 k \cos(kt) \\\frac{d}{dt}x(0) = 0 &= -C_3 k \sin(0) + C_4 k \cos(0) \\C_4 k &= 0 \\C_4 &= 0\end{aligned}$$

∴ The solution is of the form: $x(t) = L \cos(kt)$

This page titled [22.1.5: v. Review Exercise Solutions](#) is shared under a [CC BY-NC-SA 4.0](#) license and was authored, remixed, and/or curated by [Jack Simons](#) via [source content](#) that was edited to the style and standards of the LibreTexts platform.

22.1.6: vi. Exercise Solutions

Q1

$$K.E. = \frac{mv^2}{2} = \left(\frac{m}{m}\right) \frac{dmv^2}{2} = \frac{(mv)^2}{2m} = \frac{p^2}{2m} \quad (22.1.6.1)$$

$$K.E. = \frac{1}{2m}(p_x^2 + p_y^2 + p_z^2) \quad (22.1.6.2)$$

a.

$$K.E. = \frac{1}{2m} \left[\left(\hbar \frac{\partial}{\partial x} \right)^2 + \left(\frac{\hbar}{i} \frac{\partial}{\partial y} \right)^2 + \left(\frac{\hbar}{i} \frac{\partial}{\partial z} \right)^2 \right] \quad (22.1.6.3)$$

$$K.E. = \frac{-\hbar^2}{2m} \left[\frac{\partial^2}{\partial x^2} + \frac{\partial^2}{\partial y^2} + \frac{\partial^2}{\partial z^2} \right] \quad (22.1.6.4)$$

$$\mathbf{p} = m\mathbf{v} = \mathbf{i}p_x + \mathbf{j}p_y + \mathbf{k}p_z \quad (22.1.6.5)$$

b.

$$\mathbf{p} = \left[\mathbf{i} \left(\frac{\hbar}{i} \frac{\partial}{\partial x} \right) + \mathbf{j} \left(\frac{\hbar}{i} \frac{\partial}{\partial y} \right) + \left(\frac{\hbar}{i} \frac{\partial}{\partial z} \right) \right] \quad (22.1.6.6)$$

where i, j, and k are unit vectors along the x, y, and z axes.

$$L_y = zp_x - xp_z \quad (22.1.6.7)$$

c.

$$L_y = z \left(\frac{\hbar}{i} \frac{\partial}{\partial x} \right) - x \left(\frac{\hbar}{i} \frac{\partial}{\partial z} \right) \quad (22.1.6.8)$$

Q2

First derive the general formulas for $\frac{\partial}{\partial x}$, $\frac{\partial}{\partial y}$, $\frac{\partial}{\partial z}$ in terms of r, θ , and ϕ , and $\frac{\partial}{\partial r}$, $\frac{\partial}{\partial \theta}$, and $\frac{\partial}{\partial \phi}$ in terms of x, y, and z. The general relationships are as follows:

$$x = r \sin \theta \cos \phi \quad r^2 = x^2 + y^2 + z^2 \quad (22.1.6.9)$$

$$y = r \sin \theta \sin \phi \quad \sin \theta = \frac{\sqrt{x^2 + y^2}}{\sqrt{x^2 + y^2 + z^2}} \quad (22.1.6.10)$$

$$z = r \cos \theta \quad \cos \theta = \frac{z}{\sqrt{x^2 + y^2 + z^2}} \quad (22.1.6.11)$$

$$\tan \phi = \frac{y}{x} \quad (22.1.6.12)$$

First $\frac{\partial}{\partial x}$, $\frac{\partial}{\partial y}$, and $\frac{\partial}{\partial z}$ from the chain rule:

$$\frac{\partial}{\partial x} = \left(\frac{\partial r}{\partial x} \right)_{y,z} \frac{\partial}{\partial r} + \left(\frac{\partial \theta}{\partial x} \right)_{y,z} \frac{\partial}{\partial \theta} + \left(\frac{\partial \phi}{\partial x} \right)_{y,z} \frac{\partial}{\partial \phi}, \quad (22.1.6.13)$$

$$\frac{\partial}{\partial y} = \left(\frac{\partial r}{\partial y} \right)_{x,z} \frac{\partial}{\partial r} + \left(\frac{\partial \theta}{\partial y} \right)_{x,z} \frac{\partial}{\partial \theta} + \left(\frac{\partial \phi}{\partial y} \right)_{x,z} \frac{\partial}{\partial \phi}, \quad (22.1.6.14)$$

$$\frac{\partial}{\partial z} = \left(\frac{\partial r}{\partial z} \right)_{x,y} \frac{\partial}{\partial r} + \left(\frac{\partial \theta}{\partial z} \right)_{x,y} \frac{\partial}{\partial \theta} + \left(\frac{\partial \phi}{\partial z} \right)_{x,y} \frac{\partial}{\partial \phi}, \quad (22.1.6.15)$$

Evaluation of the many "coefficients" gives the following:

$$\left(\frac{\partial r}{\partial x} \right)_{y,z} = \sin \theta \cos \phi, \quad \left(\frac{\partial \theta}{\partial x} \right)_{y,z} = \frac{\cos \theta \cos \phi}{r}, \quad \left(\frac{\partial \phi}{\partial x} \right)_{y,z} = -\frac{\sin \phi}{r \sin \theta} \quad (22.1.6.16)$$

$$\left(\frac{\partial r}{\partial y} \right)_{x,z} = \sin \theta \sin \phi, \quad \left(\frac{\partial \theta}{\partial y} \right)_{x,z} = \frac{\cos \theta \sin \phi}{r}, \quad \left(\frac{\partial \phi}{\partial y} \right)_{x,z} = \frac{\cos \phi}{r \sin \theta} \quad (22.1.6.17)$$

$$\left(\frac{\partial r}{\partial z} \right)_{x,y} = \cos \theta, \quad \left(\frac{\partial \theta}{\partial z} \right)_{x,y} = -\frac{\sin \theta}{r}, \quad \text{and} \quad \left(\frac{\partial \phi}{\partial z} \right)_{x,y} = 0. \quad (22.1.6.18)$$

Upon substitution of these "coefficients":

$$\frac{\partial}{\partial x} = \sin \theta \cos \phi \frac{\partial}{\partial r} + \frac{\cos \theta \cos \phi}{r} \frac{\partial}{\partial \theta} - \frac{\sin \phi}{r \sin \theta} \frac{\partial}{\partial \phi}, \quad (22.1.6.19)$$

$$\frac{\partial}{\partial y} = \sin \theta \sin \phi \frac{\partial}{\partial r} + \frac{\cos \theta \sin \phi}{r} \frac{\partial}{\partial \theta} + \frac{\cos \phi}{r \sin \theta} \frac{\partial}{\partial \phi}, \quad \text{and} \quad (22.1.6.20)$$

$$\frac{\partial}{\partial z} = \cos \theta \frac{\partial}{\partial r} - \frac{\sin \theta}{r} \frac{\partial}{\partial \theta} + 0 \frac{\partial}{\partial \phi}, \quad (22.1.6.21)$$

Next $\frac{\partial}{\partial r}$, $\frac{\partial}{\partial \theta}$, and $\frac{\partial}{\partial \phi}$ from the chain rule:

$$\frac{\partial}{\partial r} = \left(\frac{\partial x}{\partial r}\right)_{\theta,\phi} \frac{\partial}{\partial x} + \left(\frac{\partial y}{\partial r}\right)_{\theta,\phi} \frac{\partial}{\partial y} + \left(\frac{\partial z}{\partial r}\right)_{\theta,\phi} \frac{\partial}{\partial z}, \quad (22.1.6.22)$$

$$\frac{\partial}{\partial \theta} = \left(\frac{\partial x}{\partial \theta}\right)_{r,\phi} \frac{\partial}{\partial x} + \left(\frac{\partial y}{\partial \theta}\right)_{r,\phi} \frac{\partial}{\partial y} + \left(\frac{\partial z}{\partial \theta}\right)_{r,\phi} \frac{\partial}{\partial z}, \text{ and} \quad (22.1.6.23)$$

$$\frac{\partial}{\partial \phi} = \left(\frac{\partial x}{\partial \phi}\right)_{r,\theta} \frac{\partial}{\partial x} + \left(\frac{\partial y}{\partial \phi}\right)_{r,\theta} \frac{\partial}{\partial y} + \left(\frac{\partial z}{\partial \phi}\right)_{r,\theta} \frac{\partial}{\partial z}. \quad (22.1.6.24)$$

Again evaluation of the the many "coefficients" results in:

$$\left(\frac{\partial x}{\partial r}\right)_{\theta,\phi} = \frac{x}{\sqrt{x^2+y^2+z^2}}, \quad \left(\frac{\partial y}{\partial r}\right)_{\theta,\phi} = \frac{y}{\sqrt{x^2+y^2+z^2}}, \quad \left(\frac{\partial z}{\partial r}\right)_{\theta,\phi} = \frac{z}{\sqrt{x^2+y^2+z^2}} \quad (22.1.6.25)$$

$$\left(\frac{\partial x}{\partial \theta}\right)_{r,\phi} = \frac{xz}{\sqrt{x^2+y^2}}, \quad \left(\frac{\partial y}{\partial \theta}\right)_{r,\phi} = \frac{yz}{\sqrt{x^2+y^2}}, \quad \left(\frac{\partial z}{\partial \theta}\right)_{r,\phi} = -\sqrt{x^2+y^2} \quad (22.1.6.26)$$

$$\left(\frac{\partial x}{\partial \phi}\right)_{r,\theta} = -y, \quad \left(\frac{\partial y}{\partial \phi}\right)_{r,\theta} = x, \quad \text{and} \quad \left(\frac{\partial z}{\partial \phi}\right)_{r,\theta} = 0 \quad (22.1.6.27)$$

Upon substitution of these "coefficients":

$$\frac{\partial}{\partial r} = \frac{x}{\sqrt{x^2+y^2+z^2}} \frac{\partial}{\partial x} + \frac{y}{\sqrt{x^2+y^2+z^2}} \frac{\partial}{\partial y} + \frac{z}{\sqrt{x^2+y^2+z^2}} \frac{\partial}{\partial z} \quad (22.1.6.28)$$

$$\frac{\partial}{\partial \theta} = \frac{xz}{\sqrt{x^2+y^2}} \frac{\partial}{\partial x} + \frac{yz}{\sqrt{x^2+y^2}} \frac{\partial}{\partial y} - \sqrt{x^2+y^2} \frac{\partial}{\partial z} \quad (22.1.6.29)$$

$$\frac{\partial}{\partial \phi} = -y \frac{\partial}{\partial x} + x \frac{\partial}{\partial y} + 0 \frac{\partial}{\partial z}. \quad (22.1.6.30)$$

Note, these many "coefficients" are the elements which make up the Jacobian matrix used whenever one wishes to transform a function from one coordinate representation to another. One very familiar result should be in transforming the volume element $dx dy dz$ to $r^2 \sin \theta dr d\theta d\phi$. For example:

$$\int f(x, y, z) dx dy dz = \int f(x(r, \theta, \phi), y(r, \theta, \phi), z(r, \theta, \phi)) \begin{vmatrix} \left(\frac{\partial x}{\partial r}\right)_{\theta,\phi} & \left(\frac{\partial x}{\partial \theta}\right)_{r,\phi} & \left(\frac{\partial x}{\partial \phi}\right)_{r,\theta} \\ \left(\frac{\partial y}{\partial r}\right)_{\theta,\phi} & \left(\frac{\partial y}{\partial \theta}\right)_{r,\phi} & \left(\frac{\partial y}{\partial \phi}\right)_{r,\theta} \\ \left(\frac{\partial z}{\partial r}\right)_{\theta,\phi} & \left(\frac{\partial z}{\partial \theta}\right)_{r,\phi} & \left(\frac{\partial z}{\partial \phi}\right)_{r,\theta} \end{vmatrix} dr d\theta d\phi$$

a.

$$L_x = \frac{\hbar}{i} \left[y \frac{\partial}{\partial z} - z \frac{\partial}{\partial y} \right] \quad (22.1.6.31)$$

$$L_x = \frac{\hbar}{i} \left[r \sin \theta \sin \phi \left(\cos \theta \frac{\partial}{\partial r} - \frac{\sin \theta}{r} \frac{\partial}{\partial \theta} \right) \right] - \frac{\hbar}{i} \left[r \cos \theta \left(\sin \theta \sin \phi \frac{\partial}{\partial r} + \frac{\cos \theta \sin \phi}{r} \frac{\partial}{\partial \theta} + \frac{\cos \phi}{r \sin \theta} \frac{\partial}{\partial \phi} \right) \right] \quad (22.1.6.32)$$

$$L_x = -\frac{\hbar}{i} \left(\sin \phi \frac{\partial}{\partial \theta} + \cot \theta \cos \phi \frac{\partial}{\partial \phi} \right) \quad (22.1.6.33)$$

b.

$$L_z = \frac{\hbar}{i} \frac{\partial}{\partial \phi} = -i\hbar \frac{\partial}{\partial \phi} \quad (22.1.6.34)$$

$$L_z = \frac{\hbar}{i} \left(-y \frac{\partial}{\partial x} + x \frac{\partial}{\partial y} \right) \quad (22.1.6.35)$$

Q3

	B	B'	B''	(22.1.6.36)
i.	$4x^4 - 12x^2 + 3$	$16x^3 - 24x$	$48x^2 - 24$	(22.1.6.37)
ii.	$5x^4$	$20x^3$	$60x^2$	(22.1.6.38)
iii.	$e^{3x} + e^{-3x}$	$3(e^{3x} - e^{-3x})$	$9(e^{3x} + e^{-3x})$	(22.1.6.39)
iv.	$x^2 - 4x + 2$	$2x - 4$	2	(22.1.6.40)
v.	$4x^3 - 3$	$12x^2 - 3$	$24x$	(22.1.6.41)

B(v.) is an eigenfunction of A(i.):

$$\begin{aligned}
 (1-x^2) \frac{d^2}{dx^2} - x \frac{d}{dx} B(v.) &= & (22.1.6.42) \\
 &= (1-x^2)(24x) - x(12x^2-3) & (22.1.6.43) \\
 &= 24x - 24x^3 - 12x^3 + 3x & (22.1.6.44) \\
 &= -36x^3 + 27x & (22.1.6.45) \\
 &= -9(4x^3 - 3x) \text{ (eigenvalue is -9)} & (22.1.6.46)
 \end{aligned}$$

B(iii.) is an eigenfunction of A(ii.):

$$\begin{aligned}
 \frac{d^2}{dx^2} B(iii.) &= & (22.1.6.47) \\
 &= 9(e^{3x} + e^{-3x}) \text{ (eigenvalue is 9)} & (22.1.6.48)
 \end{aligned}$$

B(ii.) is an eigenfunction of A(iii.):

$$\begin{aligned}
 x \frac{d}{dx} B(ii.) &= & (22.1.6.49) \\
 &= x(20x^3) & (22.1.6.50) \\
 &= 20x^4 & (22.1.6.51) \\
 &= 4(5x^4) \text{ (eigenvalue is 4)} & (22.1.6.52)
 \end{aligned}$$

B(i.) is an eigenfunction of A(vi.):

$$\begin{aligned}
 \frac{d^2}{dx^2} - 2x \frac{d}{dx} B(i.) &= & (22.1.6.53) \\
 &= (48x^2 - 24) - 2x(16x^3 - 24x) & (22.1.6.54) \\
 &= 48x^2 - 24 - 32x^4 + 48x^2 & (22.1.6.55) \\
 &= -32x^4 + 6x^2 - 24 & (22.1.6.56) \\
 &= -8(4x^4 - 12x^2 + 3) \text{ (eigenvalue is -8)} & (22.1.6.57)
 \end{aligned}$$

B(iv.) is an eigenfunction of A(v.):

$$\begin{aligned}
 x \frac{d^2}{dx^2} - (1-x) \frac{d}{dx} B(iv.) &= & (22.1.6.58) \\
 &= x(2) + (1-x)(2x-4) & (22.1.6.59) \\
 &= 2x + 2x - 4 - 2x^2 + 4x & (22.1.6.60) \\
 &= -2x^2 + 8x - 4 & (22.1.6.61) \\
 &= -2(x^2 - 4x + 2) \text{ (eigenvalue is -2)} & (22.1.6.62)
 \end{aligned}$$

Q4

Show that:

$$\int f^* \mathbf{A} g d\tau = \int g(\mathbf{A} f)^* d\tau$$

a. Suppose f and g are functions of x and evaluate the integral on the left hand side by "integration by parts":

$$\int f(x)^* \left(-i\hbar \frac{\partial}{\partial x} \right) g(x) dx$$

$$\text{let } dv = \frac{\partial}{\partial x} g(x) dx \text{ and } u = -i\hbar f(x)^*$$

$$v = g(x) du = -i\hbar \frac{\partial}{\partial x} f(x)^* dx$$

$$\text{Now, } \int u dv = uv - \int v du,$$

so:

$$f(x)^* \left(-i\hbar \frac{\partial}{\partial x} \right) g(x) dx = -i\hbar f(x)^* g(x) + i\hbar \int g(x) \frac{\partial}{\partial x} f(x)^* dx.$$

Note that in, principle, it is impossible to prove hermiticity **unless** you are given knowledge of the type of function on which the operator is acting. Hermiticity requires (as can be seen in this example) that the term $-i\hbar f(x)^* g(x)$ vanish when evaluated at the integral limits. This, in general, will occur for the "well behaved" functions (e.g., in **bound state** quantum chemistry, the wavefunctions will vanish as the distances among particles approaches infinity). So, in proving the hermiticity of an operator, one must be careful to specify the behavior of the functions on which the operator is considered to act. This means that an operator may be hermitian for one class of functions and non-hermitian for another class of functions. If we assume that f and g vanish at the boundaries, then we have

$$\int f(x)^* \left(-i\hbar \frac{\partial}{\partial x} \right) g(x) dx = \int g(x) \left(-i\hbar \frac{\partial}{\partial x} (f(x))^* \right) dx$$

b. Suppose f and g are functions of y and z and evaluate the integral on the left hand side by "integration by parts" as in the previous exercise:

$$\int f(y, z)^* \left[-i\hbar \left(y \frac{\partial}{\partial z} - z \frac{\partial}{\partial y} \right) \right] g(y, z) dy dz = \int f(y, z)^* \left[-i\hbar \left(y \frac{\partial}{\partial z} \right) \right] g(y, z) dy dz - \int f(y, z)^* \left[-i\hbar \left(z \frac{\partial}{\partial y} \right) \right] g(y, z) dy dz$$

For the first integral, $\int f(z)^* \left(-i\hbar y \frac{\partial}{\partial z} \right) g(z) dz$,

$$\text{let } dv = \frac{\partial}{\partial z} g(z) dz \quad u = -i\hbar y f(z)^* \quad (22.1.6.63)$$

$$v = g(z) \quad du = -i\hbar y \frac{\partial}{\partial z} (f(z)^*) dz \quad (22.1.6.64)$$

so:

$$\int f(z)^* \left(-i\hbar y \frac{\partial}{\partial z} \right) g(z) dz = -i\hbar y f(z)^* g(z) + i\hbar y \int g(z) \frac{\partial}{\partial z} f(z)^* dz = \int g(z) \left(-i\hbar y \frac{\partial}{\partial z} f(z)^* \right) dz.$$

For the second integral, $\int f(y)^* \left(-i\hbar y \frac{\partial}{\partial y} \right) g(y) dy$,

$$\text{let } dv = \frac{\partial}{\partial y} g(y) dy \quad u = -i\hbar y f(y)^* \quad (22.1.6.65)$$

$$v = g(y) \quad du = -i\hbar \frac{\partial}{\partial y} f(y)^* dy \quad (22.1.6.66)$$

so:

$$\begin{aligned} \int f(y)^* \left(-i\hbar z \frac{\partial}{\partial y} \right) g(y) dy &= -i\hbar z f(y)^* g(y) + i\hbar z \int g(y) \frac{\partial}{\partial y} f(y)^* dy = \int g(y) \left(-i\hbar z \frac{\partial}{\partial y} f(y)^* \right) dy. \\ \int f(y, z)^* \left[-i\hbar \left(y \frac{\partial}{\partial z} - z \frac{\partial}{\partial y} \right) \right] g(y, z) dy dz &= \int g(z) \left(-i\hbar y \frac{\partial}{\partial z} f(z)^* \right) dz - \int g(y) \left(-i\hbar z \frac{\partial}{\partial y} f(y)^* \right) dy \\ &= \int g(y, z) \left(-i\hbar \left(y \frac{\partial}{\partial z} - z \frac{\partial}{\partial y} \right) f(y, z)^* \right) dy dz. \end{aligned}$$

Again we have had to assume that the functions f and g vanish at the boundary.

Q5

$$L_+ = L_x + iL_y$$

$$L_- = L_x - iL_y, \text{ so}$$

$$L_+ + L_- = 2L_x, \text{ or } L_x = \frac{1}{2}(L_+ + L_-)$$

$$L_+ Y_{l,m} = \sqrt{l(l+1) - m(m+1)} \hbar T_{l,m+1}$$

$$L_- Y_{l,m} = \sqrt{l(l+1) - m(m-1)} \hbar T_{l,m-1}$$

Using these relationships:

$$L_- \Psi_{2p-1} = 0, L_- \Psi_{2p_0} = \sqrt{2}\hbar \Psi_{2p-1}, L_- \Psi_{2p+1} = \sqrt{2}\hbar \Psi_{2p_0}$$

$$L_+ \Psi_{2p-1} = \sqrt{2}\hbar \Psi_{2p_0}, L_+ \Psi_{2p_0} = \sqrt{2}\hbar \Psi_{2p+1}, L_+ \Psi_{2p+1} = 0, \text{ and the following } L_x \text{ matrix elements can be evaluated:}$$

$$L_x(1, 1) = \langle \Psi_{2p-1} | \frac{1}{2}(L_+ + L_-) | \Psi_{2p-1} \rangle = 0$$

$$L_x(1, 2) = \langle \Psi_{2p-1} | \frac{1}{2}(L_+ + L_-) | \Psi_{2p_0} \rangle = \frac{\sqrt{2}}{2}\hbar$$

$$L_x(1, 3) = \langle \Psi_{2p_{-1}} | \frac{1}{2}(\mathbf{L}_+ + \mathbf{L}_-) | \Psi_{2p_{+1}} \rangle = 0$$

$$L_x(2, 1) = \langle \Psi_{2p_0} | \frac{1}{2}(\mathbf{L}_+ + \mathbf{L}_-) | \Psi_{2p_{-1}} \rangle = \frac{\sqrt{2}}{2}\hbar$$

$$L_x(2, 2) = \langle \Psi_{2p_0} | \frac{1}{2}(\mathbf{L}_+ + \mathbf{L}_-) | \Psi_{2p_0} \rangle = 0$$

$$L_x(2, 3) = \langle \Psi_{2p_0} | \frac{1}{2}(\mathbf{L}_+ + \mathbf{L}_-) | \Psi_{2p_{+1}} \rangle = \frac{\sqrt{2}}{2}\hbar$$

$$L_x(3, 1) = \langle \Psi_{2p_{+1}} | \frac{1}{2}(\mathbf{L}_+ + \mathbf{L}_-) | \Psi_{2p_{-1}} \rangle = 0$$

$$L_x(3, 2) = \langle \Psi_{2p_{+1}} | \frac{1}{2}(\mathbf{L}_+ + \mathbf{L}_-) | \Psi_{2p_0} \rangle = \frac{\sqrt{2}}{2}\hbar$$

$$L_x(3, 3) = 0$$

This matrix:

$$\begin{bmatrix} 0 & \frac{\sqrt{2}}{2}\hbar & 0 \\ \frac{\sqrt{2}}{2}\hbar & 0 & \frac{\sqrt{2}}{2}\hbar \\ 0 & \frac{\sqrt{2}}{2}\hbar & 0 \end{bmatrix} \quad (22.1.6.67)$$

, can now be diagonalized:

$$\begin{vmatrix} 0 - \lambda & \frac{\sqrt{2}}{2}\hbar & 0 \\ \frac{\sqrt{2}}{2}\hbar & 0 & \frac{\sqrt{2}}{2}\hbar \\ 0 & \frac{\sqrt{2}}{2}\hbar & 0 \end{vmatrix} \quad (22.1.6.68) =$$

$$\begin{vmatrix} 0 - \lambda & \frac{\sqrt{2}}{2}\hbar \\ \frac{\sqrt{2}}{2}\hbar & 0 - \lambda \end{vmatrix} \quad (22.1.6.69) (-$$

$$\begin{vmatrix} \frac{\sqrt{2}}{2}\hbar & \frac{\sqrt{2}}{2}\hbar \\ 0 & 0 - \lambda \end{vmatrix} \quad (22.1.6.70) \left($$

Expanding these determinants yields:

$$\left(\lambda^2 - \frac{\hbar^2}{2}\right)(-\lambda) - \frac{\sqrt{2}\hbar}{2}(-\lambda)\left(\frac{\sqrt{2}\hbar}{2}\right) = 0$$

$$-\lambda(\lambda^2 - \hbar^2) = 0$$

$$-\lambda(\lambda - \hbar)(\lambda + \hbar) = 0$$

with roots: $0, \hbar$, and $-\hbar$

Next, determine the corresponding eigenvectors:

For $\lambda = 0$

$$\begin{bmatrix} 0 & \frac{\sqrt{2}}{2}\hbar & 0 \\ \frac{\sqrt{2}}{2}\hbar & 0 & \frac{\sqrt{2}}{2}\hbar \\ 0 & \frac{\sqrt{2}}{2}\hbar & 0 \end{bmatrix} \quad (22.1.6.71) \left[$$

$$\frac{\sqrt{2}}{2}\hbar C_{21} = 0 \text{ (row one)}$$

$$C_2 1 = 0$$

$$\frac{\sqrt{2}}{2}\hbar C_{11} + \frac{\sqrt{2}}{2}\hbar C_{31} = 0 \text{ (row two)}$$

$$C_{11} + C_{31} = 0$$

$$C_{11} = -C_{31}$$

$$C_{11}^2 + C_{21}^2 + C_{31}^2 = 1 \text{ (normalization)}$$

$$C_{11}^2 + (-C_{11})^2 = 1$$

$$2C_{11}^2 = 1$$

$$C_{11} = \frac{1}{\sqrt{2}}, C_{21} = 0, \text{ and } C_{31} = -\frac{1}{\sqrt{2}}$$

For $\lambda = 1\hbar$:

$$\begin{bmatrix} 0 & \frac{\sqrt{2}}{2}\hbar & 0 \\ \frac{\sqrt{2}}{2}\hbar & 0 & \frac{\sqrt{2}}{2}\hbar \\ 0 & \frac{\sqrt{2}}{2}\hbar & 0 \end{bmatrix} \quad (22.1.6.72) \quad \left[\right.$$

$$\frac{\sqrt{2}}{2}\hbar C_{22} = \hbar C_{12} \text{ (row one)}$$

$$C_{12} = \frac{\sqrt{2}}{2}C_{22}$$

$$\frac{\sqrt{2}}{2}\hbar C_{12} + \frac{\sqrt{2}}{2}\hbar C_{32} = \hbar C_{22} \text{ (row two)}$$

$$\frac{\sqrt{2}}{2} \cdot \frac{\sqrt{2}}{2}C_{22} + \frac{\sqrt{2}}{2}C_{32} = C_{22}$$

$$\frac{1}{2}C_{22} + \frac{\sqrt{2}}{2}C_{32} = C_{22}$$

$$\frac{\sqrt{2}}{2}C_{32} = \frac{1}{2}C_{22}$$

$$C_{32} = \frac{\sqrt{2}}{2}C_{22}$$

$$C_{12}^2 + C_{22}^2 + C_{32}^2 = 1 \text{ (normalization)}$$

$$\left(\frac{\sqrt{2}}{2}C_{22}\right)^2 + C_{22}^2 + \left(\frac{\sqrt{2}}{2}C_{22}\right)^2 = 1$$

$$\frac{1}{2}C_{22}^2 + C_{22}^2 + \frac{1}{2}C_{22}^2 = 1$$

$$2C_{22}^2 = 1$$

$$C_{22} = \frac{\sqrt{2}}{2}$$

$$C_{12} = \frac{1}{2}, C_{22} = \frac{\sqrt{2}}{2}, \text{ and } C_{32} = \frac{1}{2}$$

For $\lambda = -1\hbar$

$$\begin{bmatrix} 0 & \frac{\sqrt{2}}{2}\hbar & 0 \\ \frac{\sqrt{2}}{2}\hbar & 0 & \frac{\sqrt{2}}{2}\hbar \\ 0 & \frac{\sqrt{2}}{2}\hbar & 0 \end{bmatrix} \quad (22.1.6.73) \quad \left[\right.$$

$$\frac{\sqrt{2}}{2}\hbar C_{23} = -\hbar C_{13} \text{ (row one)}$$

$$C_{13} = -\frac{\sqrt{2}}{2}C_{23}$$

$$\frac{\sqrt{2}}{2}\hbar C_{13} + \frac{\sqrt{2}}{2}\hbar C_{33} = -\hbar C_{23} \text{ (row two)}$$

$$\frac{\sqrt{2}}{2}\left(-\frac{\sqrt{2}}{2}C_{23}\right) + \frac{\sqrt{2}}{2}C_{33} = -C_{23}$$

$$-\frac{1}{2}C_{23} + \frac{\sqrt{2}}{2}C_{33} = -C_{23}$$

$$\frac{\sqrt{2}}{2}C_{33} = -\frac{1}{2}C_{23}$$

$$C_{33} = -\frac{\sqrt{2}}{2}C_{23}$$

$$C_{13}^2 + C_{23}^2 + C_{33}^2 = 1 \text{ (normalization)}$$

$$\left(-\frac{\sqrt{2}}{2}C_{23}\right)^2 + C_{23}^2 + \left(-\frac{\sqrt{2}}{2}C_{23}\right)^2 = 1$$

$$\frac{1}{2}C_{23}^2 + C_{23}^2 + \frac{1}{2}C_{23}^2 = 1$$

$$2C_{23}^2 = 1$$

$$C_{23} = \frac{\sqrt{2}}{2}$$

$$C_{13} = -\frac{1}{2}, C_{23} = \frac{\sqrt{2}}{2}, \text{ and } C_{33} = -\frac{1}{2}$$

Show: $\langle\phi_1|\phi_1\rangle = 1$, $\langle\phi_2|\phi_2\rangle = 1$, $\langle\phi_3|\phi_3\rangle = 1$, $\langle\phi_1|\phi_2\rangle = 0$, $\langle\phi_1|\phi_3\rangle = 0$, and $\langle\phi_2|\phi_3\rangle = 0$.

$$\langle\phi_1|\phi_1\rangle \stackrel{?}{=} 1$$

$$\left(\frac{\sqrt{2}}{2}\right)^2 + 0 + \left(-\frac{\sqrt{2}}{2}\right)^2 \stackrel{?}{=} 1$$

$$\frac{1}{2} + \frac{1}{2} \stackrel{?}{=} 1$$

$$1 = 1$$

$$\langle\phi_2|\phi_2\rangle \stackrel{?}{=} 1$$

$$\left(\frac{1}{2}\right)^2 + \left(\frac{\sqrt{2}}{2}\right)^2 + \left(\frac{1}{2}\right)^2 \stackrel{?}{=} 1$$

$$\frac{1}{4} + \frac{1}{2} + \frac{1}{4} \stackrel{?}{=} 1$$

$$1 = 1$$

$$\langle\phi_3|\phi_3\rangle \stackrel{?}{=} 1$$

$$\left(-\frac{1}{2}\right)^2 + \left(\frac{\sqrt{2}}{2}\right)^2 + \left(-\frac{1}{2}\right)^2 \stackrel{?}{=} 1$$

$$\frac{1}{4} + \frac{1}{2} + \frac{1}{4} \stackrel{?}{=} 1$$

$$1 = 1$$

$$\langle\phi_1|\phi_2\rangle = \langle\phi_2|\phi_1\rangle \stackrel{?}{=} 0$$

$$\left(\frac{\sqrt{2}}{2}\right)\left(\frac{1}{2}\right) + (0)\left(\frac{\sqrt{2}}{2}\right) + \left(-\frac{\sqrt{2}}{2}\right)\left(\frac{1}{2}\right) \stackrel{?}{=} 0$$

$$\left(\frac{\sqrt{2}}{4}\right) - \left(\frac{\sqrt{2}}{4}\right) \stackrel{?}{=} 0$$

$$0 = 0$$

$$\langle \phi_1 | \phi_3 \rangle = \langle \phi_3 | \phi_1 \rangle \stackrel{?}{=} 0$$

$$\left(\frac{\sqrt{2}}{2}\right)\left(-\frac{1}{2}\right) + (0)\left(\frac{\sqrt{2}}{2}\right) + \left(-\frac{\sqrt{2}}{2}\right)\left(-\frac{1}{2}\right) \stackrel{?}{=} 0$$

$$\left(-\frac{\sqrt{2}}{4}\right) + \left(\frac{\sqrt{2}}{4}\right) \stackrel{?}{=} 0$$

$$0 = 0$$

$$\langle \phi_2 | \phi_3 \rangle = \langle \phi_3 | \phi_2 \rangle \stackrel{?}{=} 0$$

$$\left(\frac{1}{2}\right)\left(-\frac{1}{2}\right) + \left(\frac{\sqrt{2}}{2}\right)\left(\frac{\sqrt{2}}{2}\right) + \left(\frac{1}{2}\right)\left(-\frac{1}{2}\right) \stackrel{?}{=} 0$$

$$\left(-\frac{1}{4}\right) + \left(\frac{1}{2}\right) + \left(-\frac{1}{4}\right) \stackrel{?}{=} 0$$

$$0 = 0$$

Q6

$$P_{2p+1} = |\langle \phi_{2p+1} | \Phi_{L_x}^{0\hbar} \rangle|^2$$

$$\Psi_{L_x}^{0\hbar} = \frac{1}{\sqrt{2}} \phi_{2p-1} - \frac{1}{\sqrt{2}} \phi_{2p+1}$$

$$P_{2p+1} = \left| -\frac{1}{\sqrt{2}} \langle \phi_{20+1} | \phi_{2p+1} \rangle \right|^2 = \frac{1}{2} \text{ (or 50\%)}$$

Q7

It is useful here to use some of the general commutator relations found in Appendix C.V.

a.

$$\begin{aligned} [L_x, L_y] &= [yp_z - zp_y, zp_x - xp_z] \\ &= [yp_z, zp_x] - [yp_z, xp_z] - [zp_y, zp_x] + [zp_y, xp_z] \\ &= [y, z]p_xp_z + z[y, p_x]p_z + y[p_z, z]p_x + yz[p_z, p_x] \\ &\quad - [y, x]p_zp_x - x[y, p_z]p_x - y[p_z, x]p_x - yx[p_z, p_x] \\ &\quad - [z, z]p_xp_y - z[z, p_x]p_y - z[p_y, z]p_x - zz[p_y, p_x] \\ &\quad + [z, x]p_zp_y + x[z, p_z]p_y + z[p_y, x]p_z + zx[p_y, p_z] \end{aligned}$$

As can be easily ascertained, the only non-zero terms are:

$$\begin{aligned} [L_x, L_y] &= y[p_z, Z]p_x + x[z, p_z]p_y \\ &= y(i\hbar)p_x + x(i\hbar)p_y \\ &= i\hbar(-yp_x + xp_y) \\ &= i\hbar L_z \end{aligned}$$

b.

$$\begin{aligned} [L_y, L_z] &= [zp_x - xp_z, xp_y - yp_z] \\ &= [zp_x, xp_y] - [zp_x, yp_z] - [xp_z, xp_y] + [xp_z, yp_z] \\ &= [z, x]p_yp_x + x[z, p_y]p_x + z[p_x, x]p_y + zx[p_x, p_z] \\ &\quad - [z, y]p_xp_x - y[z, p_x]p_x - z[p_x, y]p_x - zy[p_x, p_x] \\ &\quad - [x, x]p_yp_z - x[x, p_y]p_z - x[p_z, x]p_y - xx[p_z, p_y] \\ &\quad + [x, y]p_xp_z + y[x, p_x]p_z + x[p_z, y]p_x + xy[p_z, p_x] \end{aligned}$$

Again, as can be easily ascertained, the only non-zero terms are:

$$\begin{aligned}
 [L_y, L_z] &= z[p_x, x]p_y + y[x, p_x]p_z \\
 &= z(-i\hbar)p_y + y(i\hbar)p_z \\
 &= i\hbar(-zp_y + yp_z) \\
 &= i\hbar L_x
 \end{aligned}$$

c.

$$\begin{aligned}
 [L_z, L_x] &= [xp_y - yp_x, yp_z - zp_y] \\
 &= [xp_y, yp_z] - [xp_y, zp_y] - [yp_x, yp_z] + [yp_x, zp_y] \\
 &= [x, y]p_zp_y + y[x, p_z]p_y + x[p_y, y]p_z + xy[p_y, p_z] \\
 &\quad - [x, z]p_y p_y - z[x, p_y]p_y - x[p_y, z]p_y - xz[p_y, p_y] \\
 &\quad - [y, y]p_zp_x - z[y, p_y]p_x - y[p_x, y]p_z - yz[p_x, p_z] \\
 &\quad + [y, z]p_y p_x + z[y, p_y]p_x + y[p_x, z]p_y + yz[p_x, p_z]
 \end{aligned}$$

Again, as can be easily ascertained, the only non-zero terms are:

$$\begin{aligned}
 [L_z, L_x] &= x[p_y, y]p_z + z[y, p_y]p_x \\
 &= x(-i\hbar)p_z + z(i\hbar)p_x \\
 &= i\hbar(-xp_z + zp_x) \\
 &= i\hbar L_y
 \end{aligned}$$

d.

$$\begin{aligned}
 [L_x, L^2] &= [L_x, L_x^2 + L_y^2 + L_z^2] \\
 &= [L_x, L_x^2] + [L_x, L_y^2] + [L_x, L_z^2] \\
 &= [L_x, L_x^2] + [L_x, L_z^2] \\
 &= [L_x, L_y]L_y + L_y[L_x, L_y] + [L_x, L_z]L_z + L_z[L_x, L_z] \\
 &= (i\hbar L_z)L_y + L_y(i\hbar L_z) + (-i\hbar L_y)L_z + L_z(-i\hbar L_y) \\
 &= (i\hbar)(-L_zL_x - L_xL_z + L_xL_z + L_zL_x) \\
 &= (i\hbar)([L_z, L_y] + [L_y, L_z]) = 0
 \end{aligned}$$

e.

$$\begin{aligned}
 [L_y, L^2] &= [L_y, L_x^2 + L_y^2 + L_z^2] \\
 &= [L_y, L_x^2] + [L_y, L_y^2] + [L_y, L_z^2] \\
 &= [L_z, L_x^2] + [L_z, L_y^2] \\
 &= [L_y, L_x]L_x + L_x[L_y, L_x] + [L_y, L_z]L_z + L_z[L_y, L_z] \\
 &= (-i\hbar L_z)L_x + L_x(-i\hbar L_z) + (i\hbar L_x)L_z + L_z(i\hbar L_x) \\
 &= (i\hbar)(-L_zL_x - L_xL_z + L_xL_z + L_zL_x) \\
 &= (i\hbar)([L_x, L_z] + [L_z, L_x]) = 0
 \end{aligned}$$

f.

$$\begin{aligned}
 [L_z, L^2] &= [L_z, L_x^2 + L_y^2 + L_z^2] \\
 &= [L_z, L_x^2] + [L_z, L_y^2] + [L_z, L_z^2] \\
 &= [L_z, L_x^2] + [L_z, L_y^2] \\
 &= [L_z, L_x]L_x + L_x[L_z, L_x] + [L_z, L_y]L_y + L_y[L_z, L_y] \\
 &= (i\hbar L_y)L_x + L_x(i\hbar L_y) + (-i\hbar L_x)L_y + L_y(-i\hbar L_x) \\
 &= (i\hbar)(L_yL_x + L_xL_y - L_xL_y - L_yL_x)
 \end{aligned}$$

$$(i\hbar)([L_y, L_x] + [L_x, L_y]) = 0$$

Q8

Use the general angular momentum relationships:

$$J^2|j, m\rangle = \hbar^2(j(j+1))|j, m\rangle$$

$$J_z|j, m\rangle = \hbar m|j, m\rangle,$$

and the information used in exercise 5, namely that:

$$\mathbf{L}_x = \frac{1}{2}(\mathbf{L}_+ + \mathbf{L}_-)$$

$$\mathbf{L}_+ Y_{l,m} = \sqrt{l(l+1) - m(m+1)} \hbar Y_{l,m+1}$$

$$[\text{L}_-, Y_{l,m}] = \sqrt{l(l+1) - m(m-1)} \hbar Y_{l,m-1}$$

Given that:

$$Y_{0,0}(\theta, \phi) = \frac{1}{\sqrt{4\pi}} = |0, 0\rangle$$

$$Y_{1,0}(\theta, \phi) = \sqrt{\frac{3}{4\pi}} \cos\theta = |1, 0\rangle.$$

a.

$$\mathbf{L}_z|0, 0\rangle = 0$$

$$[\text{L}^2, \mathbf{L}_z]|0, 0\rangle = 0$$

Since L^2 and L_z commute you would expect $|0, 0\rangle$ to be simultaneous eigenfunctions of both.

b.

$$\mathbf{L}_x|0, 0\rangle = 0$$

$$\mathbf{L}_z|0, 0\rangle = 0$$

L_x and L_z **do not** commute. It is unexpected to find a simultaneous eigenfunction ($|0, 0\rangle$) of both ... for sure these operators do not have the same full set of eigenfunctions.

c.

$$\mathbf{L}_z|1, 0\rangle = 0$$

$$\mathbf{L}^2|1, 0\rangle = 2\hbar^2|1, 0\rangle$$

Again since L^2 and L_z commute you would expect $|1, 0\rangle$ to be simultaneous eigenfunctions of both.

d.

$$\mathbf{L}_x|1, 0\rangle = \frac{\sqrt{2}}{2}\hbar|1, -1\rangle + \frac{\sqrt{2}}{2}\hbar|1, 1\rangle$$

$$\mathbf{L}_z|1, 0\rangle = 0$$

Again, L_x and L_z **do not** commute. Therefore it is expected to find differing sets of eigenfunctions for both.

Q9

For

$$\Psi(x, y) = \sqrt{\left(\frac{1}{2L_x}\right)\left(\frac{1}{2L_y}\right)} \left[e^{\left(\frac{in_x\pi x}{L_x}\right)} - e^{\left(\frac{-in_x\pi x}{L_x}\right)} \right] \left[e^{\left(\frac{in_y\pi y}{L_y}\right)} - e^{\left(\frac{-in_y\pi y}{L_y}\right)} \right]$$

$$\langle \Psi(x, y) | \Psi(x, y) \rangle \stackrel{?}{=} 1$$

Let: $a_x = \frac{n_x\pi}{L_x}$, and $a_y = \frac{n_y\pi}{L_y}$ and using Euler's formula, expand the exponentials into Sin and Cos terms.

$$\begin{aligned}\Psi(x, y) &= \sqrt{\left(\frac{1}{2L_x}\right)\left(\frac{1}{2L_y}\right)} [\cos(a_x x) + i \sin(a_x x) - \cos(a_x x) + i \sin(a_x x)] [\cos(a_y y) + i \sin(a_y y) - \cos(a_y y) \\ &\quad + i \sin(a_y y)] \\ \Psi(x, y) &= \sqrt{\left(\frac{1}{2L_x}\right)\left(\frac{1}{2L_y}\right)} 2i \sin(a_x x) 2i \sin(a_y y) \\ \Psi(x, y) &= \sqrt{\left(-\frac{2}{L_x}\right)\left(\frac{2}{L_y}\right)} \sin(a_x x) \sin(a_y y) \\ \langle \Psi(x, y) | \Psi(x, y) \rangle &= \int \left(\sqrt{\left(-\frac{2}{L_x}\right)\left(\frac{2}{L_y}\right)} \sin(a_x x) \sin(a_y y) \right)^2 dx dy \\ &= \left(\frac{2}{L_x}\right) \left(\frac{2}{L_y}\right) \int \sin^2(a_x x) \sin^2(a_y y) dx dy\end{aligned}$$

Using the integral:

$$\begin{aligned}\int_0^L \sin^2 \frac{n\pi x}{L} dx &= \frac{L}{2}, \\ \langle \Psi(x, y) | \Psi(x, y) \rangle &= \left(\frac{2}{L_x}\right) \left(\frac{2}{L_y}\right) \left(\frac{L_x}{2}\right) \left(\frac{L_y}{2}\right) = 1\end{aligned}$$

Q10

$$\begin{aligned}\langle \Psi(x, y) | p_x | \Psi(x, y) \rangle &= \left(\frac{2}{L_y}\right) \int_0^{L_y} \sin^2(a_y y) dy \left(\frac{2}{L_x}\right) \int_0^{L_x} \sin(a_x x) \left(-i\hbar \frac{\partial}{\partial x}\right) \sin(a_x x) dx = \left(\frac{-i\hbar 2a_x}{L_x}\right) \int_0^{L_x} \sin \\ &\quad (a_x x) \cos(a_x x) dx\end{aligned}$$

But the integral:

$$\begin{aligned}\int_0^{L_x} \cos(a_x x) \sin(a_x x) dx &= 0, \\ \therefore \langle \Psi(x, y) | p_x | \Psi(x, y) \rangle &= 0\end{aligned}$$

Q11

$$\langle \Psi_0 | x^2 | \Psi_0 \rangle = \sqrt{\frac{\alpha}{\pi}} \int_{-\infty}^{\infty} \left(e^{-\frac{1}{2}\alpha x^2} \right) (x^2) \left(e^{-\frac{1}{2}\alpha x^2} \right) dx = 2\sqrt{\frac{\alpha}{\pi}} \int_0^{\infty} x^2 e^{-\frac{1}{2}\alpha x^2} dx$$

Using the integral:

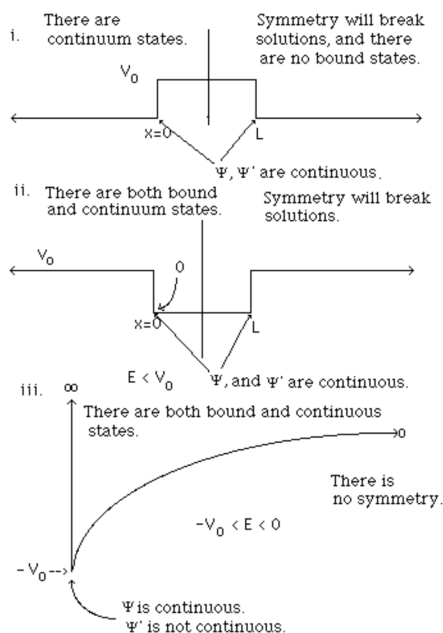
$$\begin{aligned}\int_0^{\infty} x^{2n} e^{-\beta x^2} dx &= \frac{1 \cdot 3 \cdots (2n-1)}{2^{n+1}} \sqrt{\left(\frac{\pi}{\beta^{2n+1}}\right)} \\ \langle \Psi_0 | x^2 | \Psi_0 \rangle &= 2\sqrt{\frac{\alpha}{\pi}} \left(\frac{1}{2^2}\right) \sqrt{\frac{\pi}{\alpha^3}} \\ \langle \Psi_0 | x^2 | \Psi_0 \rangle &= \left(\frac{1}{2\alpha}\right) \\ \langle \Psi_1 | x^2 | \Psi_1 \rangle &= \sqrt{\frac{4\alpha^3}{\pi}} \int_{-\infty}^{\infty} \left(x e^{-\frac{1}{2}\alpha x^2} \right) (x^2) \left(x e^{-\frac{1}{2}\alpha x^2} \right) dx \\ &= 2\sqrt{\frac{4\alpha^3}{\pi}} \int_0^{\infty} x^4 e^{-\frac{1}{2}\alpha x^2} dx\end{aligned}$$

Using the previously defined integral:

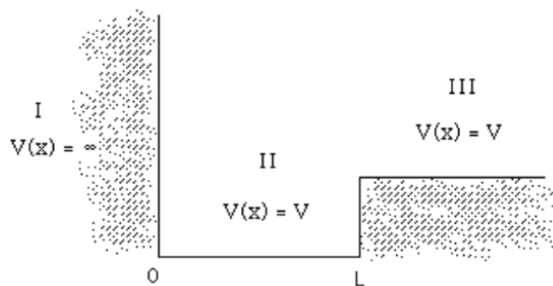
$$\langle \Psi_1 | x^2 | \Psi_1 \rangle = 2 \sqrt{\frac{4\alpha^3}{\pi}} \left(\frac{3}{2^3} \right) \sqrt{\frac{\pi}{\alpha^5}}$$

$$\langle \Psi_1 | x^2 | \Psi_1 \rangle = \left(\frac{3}{2\alpha} \right)$$

Q12



Q13



a.

$$\Psi_I(x) = 0$$

$$\Psi_{II}(x) = Ae^{i\sqrt{\frac{2mE}{\hbar^2}}x} + Be^{-i\sqrt{\frac{2mE}{\hbar^2}}x}$$

$$\Psi_{III}(x) = A'e^{i\sqrt{\frac{2m(V-E)}{\hbar^2}}x} + B'e^{-i\sqrt{\frac{2m(V-E)}{\hbar^2}}x}$$

b.

$$I \leftrightarrow II$$

$$\Psi_I(0) = \Psi_{II}(0)$$

$$\Psi_I(0) = 0 = \Psi_{II}(0) = Ae^{i\sqrt{\frac{2mE}{\hbar^2}}(0)} + Be^{-i\sqrt{\frac{2mE}{\hbar^2}}(0)}$$

$$0 = A + B$$

$$B = -A$$

$$\Psi_I'(0) = \Psi_{II}'(0)$$

(this gives no useful information since $\Psi_I'(x)$ does not exist at $x = 0$)

$$I \leftrightarrow II$$

$$\Psi_{II}(L) = \Psi_{III}(L)$$

$$Ae^{i\sqrt{\frac{2mE}{\hbar^2}}L} + Be^{-i\sqrt{\frac{2mE}{\hbar^2}}L} = A'e^{i\sqrt{\frac{2m(V-E)}{\hbar^2}}L} + B'e^{-i\sqrt{\frac{2m(V-E)}{\hbar^2}}L}$$

$$\Psi_{II}'(L) = \Psi_{III}'(L)A \left(e^{i\sqrt{\frac{2mE}{\hbar^2}}L} \right) + B \left(e^{-i\sqrt{\frac{2mE}{\hbar^2}}L} \right) = A' \left(e^{i\sqrt{\frac{2m(V-E)}{\hbar^2}}L} \right) + B' \left(e^{-i\sqrt{\frac{2m(V-E)}{\hbar^2}}L} \right)$$

$$\Psi_{II}'(L) = \Psi_{III}'(L)$$

$$A \left(i\sqrt{\frac{2mE}{\hbar^2}} \right) e^{i\sqrt{\frac{2mE}{\hbar^2}}L} - B \left(i\sqrt{\frac{2mE}{\hbar^2}} \right) e^{-i\sqrt{\frac{2mE}{\hbar^2}}L}$$

$$= A' \left(i\sqrt{\frac{2m(V-E)}{\hbar^2}} \right) e^{i\sqrt{\frac{2m(V-E)}{\hbar^2}}L} - B' \left(i\sqrt{\frac{2m(V-E)}{\hbar^2}} \right) e^{-i\sqrt{\frac{2m(V-E)}{\hbar^2}}L}$$

c.

$$asx \rightarrow -\infty, \Psi_I(x) = 0$$

$$asx \rightarrow \infty, \Psi_{III}(x) = 0 \therefore A' = 0$$

d. Rewrite the equations for $\Psi_I(0)$, $\Psi_{II}(0)$, $\Psi_{II}(L) = \Psi_{III}(L)$, and $\Psi_{II}'(L) = \Psi_{III}'(L)$ using the information in 13c:

$$B = -A(\text{eqn. 1})$$

$$Ae^{i\sqrt{\frac{2mE}{\hbar^2}}L} + Be^{-i\sqrt{\frac{2mE}{\hbar^2}}L} = B'e^{i\sqrt{\frac{2m(V-E)}{\hbar^2}}L}$$

(eqn. 2)

$$A \left(i\sqrt{\frac{2mE}{\hbar^2}} \right) e^{i\sqrt{\frac{2mE}{\hbar^2}}L} - B \left(i\sqrt{\frac{2mE}{\hbar^2}} \right) e^{-i\sqrt{\frac{2mE}{\hbar^2}}L} = -B' \left(i\sqrt{\frac{2m(V-E)}{\hbar^2}} \right) e^{-i\sqrt{\frac{2m(V-E)}{\hbar^2}}L}$$

substitution (eqn. 1) into (eqn. 2)

$$Ae^{i\sqrt{\frac{2mE}{\hbar^2}}L} - Ae^{-i\sqrt{\frac{2mE}{\hbar^2}}L} = B'e^{i\sqrt{\frac{2m(V-E)}{\hbar^2}}L}$$

$$A \left[\cos\left(\sqrt{\frac{2mE}{\hbar^2}}L\right) + i\sin\left(\sqrt{\frac{2mE}{\hbar^2}}L\right) \right] - A \left[\cos\left(\sqrt{\frac{2mE}{\hbar^2}}L\right) - i\sin\left(\sqrt{\frac{2mE}{\hbar^2}}L\right) \right] = B'e^{-i\sqrt{\frac{2m(V-E)}{\hbar^2}}L}$$

$$2Ai\sin\left(\sqrt{\frac{2mE}{\hbar^2}}L\right) = B'e^{-i\sqrt{\frac{2m(V-E)}{\hbar^2}}L}$$

$$\sin\left(\sqrt{\frac{2mE}{\hbar^2}}L\right) = \frac{B'}{2Ai}e^{-i\sqrt{\frac{2m(V-E)}{\hbar^2}}L} \quad (\text{eqn. 4})$$

substituting (eqn. 1) into (eqn. 3):

$$A \left(i\sqrt{\frac{2mE}{\hbar^2}} \right) e^{i\sqrt{\frac{2mE}{\hbar^2}}L} + A \left(i\sqrt{\frac{2mE}{\hbar^2}} \right) e^{-i\sqrt{\frac{2mE}{\hbar^2}}L} = -B' \left(i\sqrt{\frac{2m(V-E)}{\hbar^2}} \right) e^{-i\sqrt{\frac{2m(V-E)}{\hbar^2}}L}$$

$$A \left(i \sqrt{\frac{2mE}{\hbar^2}} \right) \left(\cos \left(\sqrt{\frac{2mE}{\hbar^2}} L \right) + i \sin \left(\sqrt{\frac{2mE}{\hbar^2}} L \right) \right) \\ + A \left(i \sqrt{\frac{2mE}{\hbar^2}} \right) \left(\cos \left(\sqrt{\frac{2mE}{\hbar^2}} L \right) - i \sin \left(\sqrt{\frac{2mE}{\hbar^2}} L \right) \right)$$

This page titled [22.1.6: vi. Exercise Solutions](#) is shared under a [CC BY-NC-SA 4.0](#) license and was authored, remixed, and/or curated by [Jack Simons](#) via [source content](#) that was edited to the style and standards of the LibreTexts platform.

SECTION OVERVIEW

22.2: Simple Molecular Orbital Theory

Topic hierarchy

22.2.1: i. Review Exercises

22.2.2: ii. Exercises

22.2.3: iii. Problems

22.2.4: iv. Review Exercises Solutions

22.2.5: v. Exercise Solution

22.2.6: vi. Problem Solutions

This page titled [22.2: Simple Molecular Orbital Theory](#) is shared under a [CC BY-NC-SA 4.0](#) license and was authored, remixed, and/or curated by [Jack Simons](#) via [source content](#) that was edited to the style and standards of the LibreTexts platform.

22.2.1: i. Review Exercises

Q1

Draw qualitative shapes of the (1) s, (3) p and (5) d "tangent sphere" atomic orbitals (note that these orbitals represent only the angular portion and **do not** contain the radial portion of the hydrogen like atomic wavefunctions) Indicate with \pm the relative signs of the wavefunctions and the position(s) (if any) of any nodes.

Q2

Define the symmetry adapted "core" and "valence" orbitals of the following systems:

- i. NH_3 in the C_{3v} point group,
- ii. H_2O in the C_{2v} point group,
- iii. H_2O_2 (cis) in the C_2 point group,
- iv. N in $D_{\infty h}$, D_{2h} , C_{2v} , and C_s point groups,
- v. N_2 in $D_{\infty h}$, D_{2h} , C_{2v} , and C_s point groups.

Q3

Plot the radial portions of the 4s, 4p, 4d, and 4f hydrogen like atomic wavefunctions.

Q4

Plot the radial portions of the 1s, 2s, 2p, 3s, and 3p hydrogen like atomic wavefunctions for the Si atom using screening concepts for any inner electrons.

This page titled [22.2.1: i. Review Exercises](#) is shared under a [CC BY-NC-SA 4.0](#) license and was authored, remixed, and/or curated by [Jack Simons](#) via [source content](#) that was edited to the style and standards of the LibreTexts platform.

22.2.2: ii. Exercises

1. In quantum chemistry it is quite common to use combinations of more familiar and easy-to-handle "basis functions" to approximate atomic orbitals. Two common types of basis functions are the Slater type orbitals (STO's) and gaussian type orbitals (GTO's). STO's have the normalized form:

$$\left(\frac{2\xi}{a_0}\right)^{n+\frac{1}{2}} \left(\frac{1}{(2n)!}\right)^{\frac{1}{2}} r^{n-1} e^{\left(\frac{-\xi r}{a_0}\right)} Y_{l,m}(\theta, \phi),$$

whereas GTO's have the form:

$$N r^1 e^{(-\xi r^2)} Y_{l,m}(\theta, \phi).$$

Orthogonalize (using Löwdin (symmetric) orthogonalization) the following 1s (core), 2s (valence), and 3s (Rydberg) STO's for the Li atom given:

$$Li_{1s}\xi = 2.6906$$

$$Li_{2s}\xi = 0.6396$$

$$Li_{3s}\xi = 0.1503.$$

Express the three resultant orthonormal orbitals as linear combinations of these three normalized STO's.

2. Calculate the expectation value of r for each of the orthogonalized 1s, 2s, and 3s Li orbitals found in Exercise 1.
3. Draw a plot of the radial probability density (e.g., $r^2 [R_{nl}(r)]^2$ with R referring to the radial portion of the STO) versus r for each of the orthonormal Li s orbitals found in Exercise 1.

This page titled [22.2.2: ii. Exercises](#) is shared under a [CC BY-NC-SA 4.0](#) license and was authored, remixed, and/or curated by [Jack Simons](#) via [source content](#) that was edited to the style and standards of the LibreTexts platform.

22.2.3: iii. Problems

Q1

Given the following orbital energies (in hartrees) for the N atom and the coupling elements between two like atoms (these coupling elements are the Fock matrix elements from standard ab-initio minimum-basis SCF calculations), calculate the molecular orbital energy levels and 1-electron wavefunctions. Draw the orbital correlation diagram for formation of the N_2 molecule. Indicate the symmetry of each atomic and molecular orbital. Designate each of the molecular orbitals as bonding, non-bonding, or antibonding.

$$\begin{aligned}
 N_{1s} &= -15.31^* \\
 N_{2s} &= -0.86^* \\
 N_{2p} &= -0.48^* \\
 N_{2\sigma_g} \text{ Fock matrix}^* \\
 \begin{bmatrix} -6.52 & & \\ -6.22 & -7.06 & \\ 3.61 & 4.00 & -3.92 \end{bmatrix} \\
 N_{2\pi_g} \text{ For Matrix}^* \\
 [0.28] \\
 N_{2\sigma_u} \text{ For Matrix}^* \\
 \begin{bmatrix} 1.02 & & \\ -0.60 & -7.59 & \\ 0.02 & 7.42 & -8.53 \end{bmatrix} \\
 N_{2\pi_u} \text{ Fock matrix}^* \\
 [-0.58]
 \end{aligned}
 \tag{22.2.3.1}$$

$$\tag{22.2.3.2}$$

*The Fock matrices (and orbital energies) were generated using standard STO3G minimum basis set SCF calculations. The Fock matrices are in the orthogonal basis formed from these orbitals.

Q2

Given the following valence orbital energies for the C atom and H_2 molecule draw the orbital correlation diagram for formation of the CH_2 molecule (via a C_{2v} insertion of C into H_2 resulting in bent CH_2). Designate the symmetry of each atomic and molecular orbital in both their highest point group symmetry and in that of the reaction path (C_{2v}).

$$\begin{aligned}
 C_{1s} &= -10.91^* & H_{2\sigma_g} &= -0.58^* & (22.2.3.3) \\
 C_{2s} &= -0.60^* & H_{2\sigma_u} &= 0.67^* & (22.2.3.4) \\
 C_{2p} &= -0.33^* & & & (22.2.3.5)
 \end{aligned}$$

*The orbital energies were generated using standard STO3G minimum basis set SCF calculations.

Q3

Using the empirical parameters given below for C and H (taken from Appendix F and "The HMO Model and its Applications" by E. Heilbronner and H. Bock, Wiley- Interscience, NY, 1976), apply the Hückel model to ethylene in order to determine the valence electronic structure of this system. Note that you will be obtaining the 1-electron energies and wavefunctions by solving the **secular equation** (as you **always** will when the energy is dependent upon a set of linear parameters like the MO coefficients in the LCAO- MO approach) using the definitions for the matrix elements found in Appendix F.

$$\begin{aligned}
 C\alpha_{2p\pi} &= -11.4eV \\
 C\alpha_{sp^2} &= -14.7eV
 \end{aligned}$$

$$H\alpha_s = -13.6eV$$

$$C - C\beta_{2p\pi-2\pi} = -1.2eV$$

$$C - C\beta_{sp^2-2p^2} = -5.0eV$$

$$C - H\beta_{sp^2-s} = -4.0eV$$

- Determine the C=C (2π) 1-electron molecular orbital energies and wavefunctions. Calculate the $\pi \rightarrow \pi^*$ transition energy for ethylene within this model.
- Determine the C-C (sp^2) 1-electron molecular orbital energies and wavefunctions.
- Determine the C-H (sp^2-s) 1-electron molecular orbital energies and wavefunctions (note that appropriate choice of symmetry will reduce this 8x8 matrix down to 4 2x2 matrices; that is, you are encouraged to symmetry adapt the atomic orbitals before starting the Hückel calculation). Draw a qualitative orbital energy diagram using the HMO energies you have calculated.

Q4Q5

Using the empirical parameters given below for B and H (taken from Appendix F and "The HMO Model and its Applications" by E. Heilbronner and H. Bock, Wiley- Interscience, NY, 1976), apply the Hückel model to borane (BH_3) in order to determine the valence electronic structure of this system.

$$B\alpha_{2p\pi} = -8.5eV$$

$$B\alpha_{sp^2} = -10.7eV$$

$$H\alpha_s = -13.6eV$$

$$B - H\beta_{sp^2-s} = -3.5eV$$

Determine the symmetries of the resultant molecular orbitals in the D_{3h} point group. Draw a qualitative orbital energy diagram using the HMO energies you have calculated.

Q5

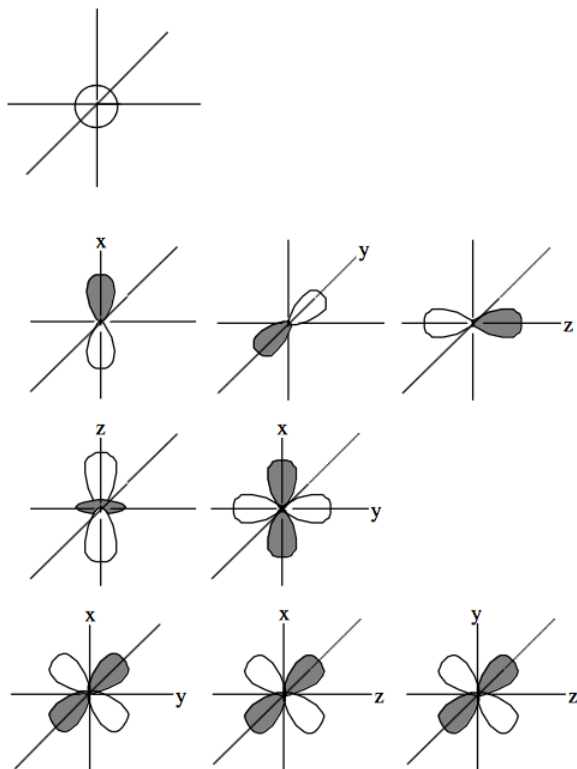
Qualitatively analyze the electronic structure (orbital energies and 1-electron wavefunctions) of PF_5 . Analyze only the 3s and 3p electrons of P and the **one** 2p bonding electron of each F. Proceed with a D_{3h} analysis in the following manner:

- Symmetry adapt the top and bottom F atomic orbitals.
- Symmetry adapt the three (trigonal) F atomic orbitals.
- Symmetry adapt the P 3s and 3p atomic orbitals.
- Allow these three sets of D_{3h} orbitals to interact and draw the resultant orbital energy diagram. Symmetry label each of these molecular energy levels. Fill this energy diagram with 10 "valence" electrons.

This page titled [22.2.3: iii. Problems](#) is shared under a [CC BY-NC-SA 4.0](#) license and was authored, remixed, and/or curated by [Jack Simons](#) via [source content](#) that was edited to the style and standards of the LibreTexts platform.

22.2.4: iv. Review Exercises Solutions

1.



2. i. In ammonia the only "core" orbital is the N 1s and this becomes an a_1 orbital in C_{3v} symmetry. The N 2s orbitals and 3 H 1s orbitals become 2 a_1 and an e set of orbitals. The remaining N 2p orbitals also become 1 a_1 and a set of e orbitals. The total valence orbitals in C_{3v} symmetry are 3 a_1 and 2e orbitals.

ii. In water the only core orbital is the O 1s and this becomes an a_1 orbital in C_{2v} symmetry. Placing the molecule in the yz plane allows us to further analyze the remaining valence orbitals as: O $2p_z = a_1$, O $2p_y$ as b_2 , and O $2p_x$ as b_1 . The H 1s + H 1s combination is an a_1 whereas the H 1s - H 1s combination is a b_2 .

iii. Placing the oxygens of H_2O_2 in the yz plane (z bisecting the oxygens) and the (cis) hydrogens distorted slightly in +x and -x directions allows us to analyze the orbitals as follows. The core O 1s + O 1s combination is an a orbital whereas the O 1s - O 1s combination is an orbital. The valence orbitals are: O2s+O2s= a , O2s-O2s= b , O $2p_x$ + O $2p_x$ = b , O $2p_x$ - O $2p_x$ = a , O $2p_y$ + O $2p_y$ = a , O $2p_y$ - O $2p_y$ = b , O $2p_z$ + O $2p_z$ = b , O $2p_z$ - O $2p_z$ = a , H 1s + H 1s = a , and finally the H 1s - H 1s = b .

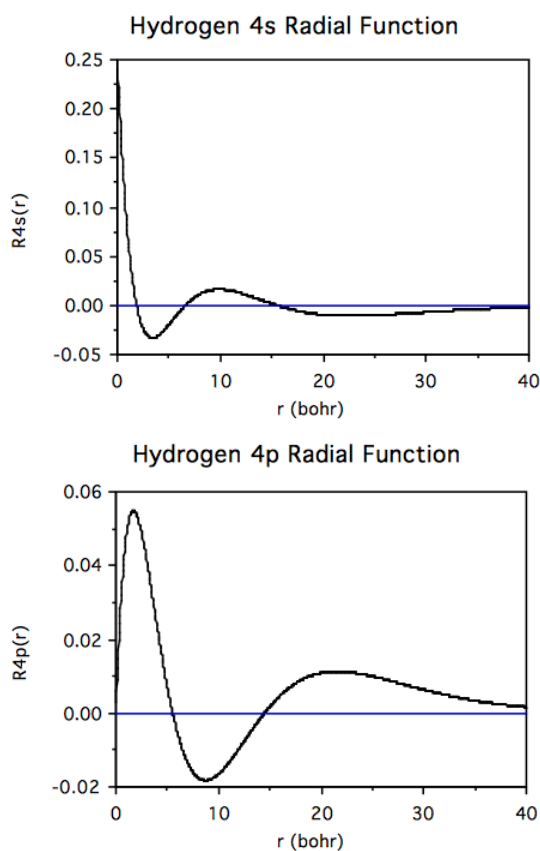
iv. For the next two problems we will use the convention of choosing the z axis as principal axis for the $D_{\infty h}$, D_{2h} , and C_{2v} point groups and the xy plane as the horizontal reflection plane in C_s symmetry.

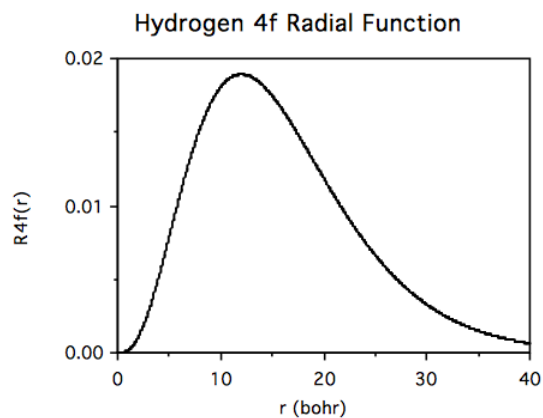
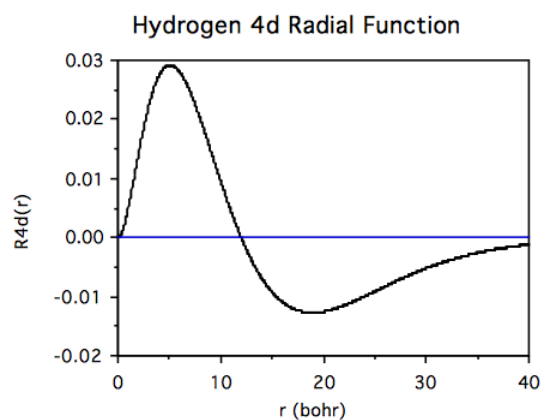
	$D_{\infty h}$	D_{2h}	C_{2v}	C_s	(22.2.4.1)
N1s	σ_g	a_g	a_1	a'	(22.2.4.2)
N2s	σ_g	a_g	a_1	a'	(22.2.4.3)
N2p _x	π_{xu}	b_{3u}	b_1	a'	(22.2.4.4)
N2p _y	π_{yu}	b_{2u}	b_2	a'	(22.2.4.5)
N2p _z	σ_u	b_{1u}	a_1	a''	(22.2.4.6)

v. The Nitrogen molecule is in the yz plane for all point groups except the C_s in which case it is placed in the xy plane.

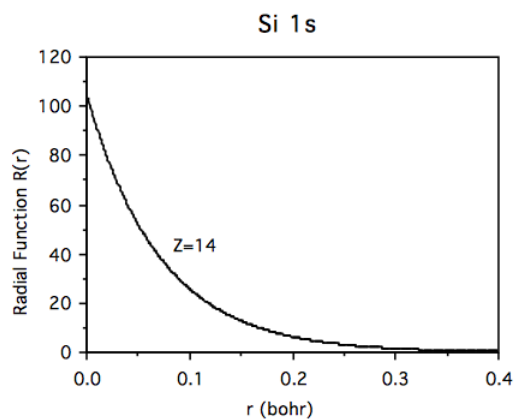
	$D_{\infty h}$	D_{2h}	C_{2v}	C_s	(22.2.4.7)
$N1s + N1s$	σ_g	a_g	a_1	a'	(22.2.4.8)
$N1s - N1s$	σ_u	b_{1u}	b_2	a'	(22.2.4.9)
$N2s + N2s$	σ_g	a_g	a_1	a'	(22.2.4.10)
$N2s - N2s$	σ_u	b_{1u}	b_2	a'	(22.2.4.11)
$N2p_x + N2p_x$	π_{xu}	b_{3u}	b_1	a'	(22.2.4.12)
$N2p_x - N2p_x$	π_{xg}	b_{2g}	a_2	a'	(22.2.4.13)
$N2p_y + N2p_y$	π_{yu}	b_{2u}	a_1	a'	(22.2.4.14)
$N2p_y - N2p_y$	π_{yg}	b_{3g}	b_2	a'	(22.2.4.15)
$N2p_z + N2p_z$	σ_u	b_{1u}	b_2	a''	(22.2.4.16)
$N2p_z - N2p_z$	σ_g	a_g	a_1	a''	(22.2.4.17)

3.

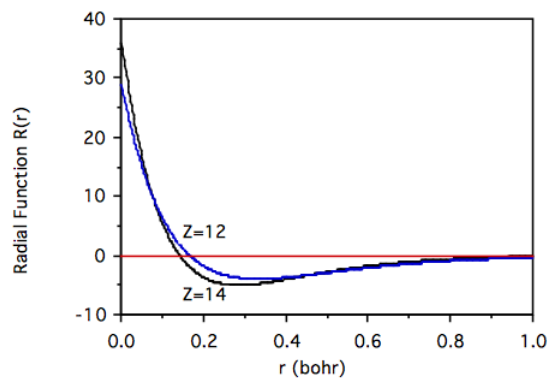




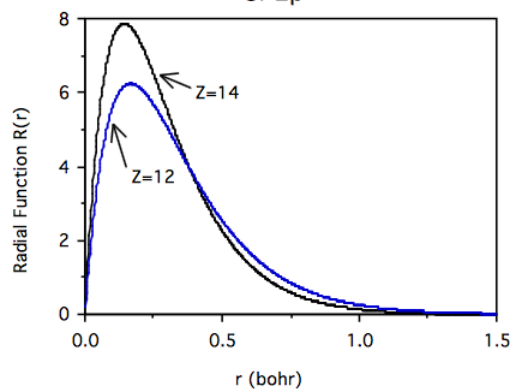
4.



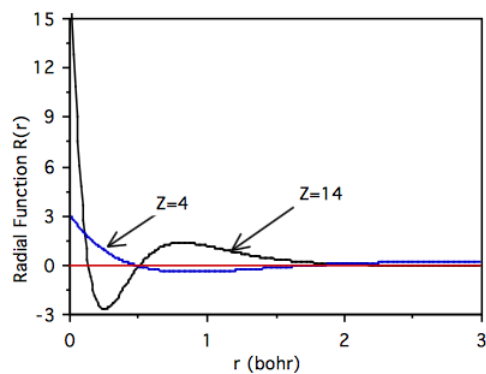
Si 2s



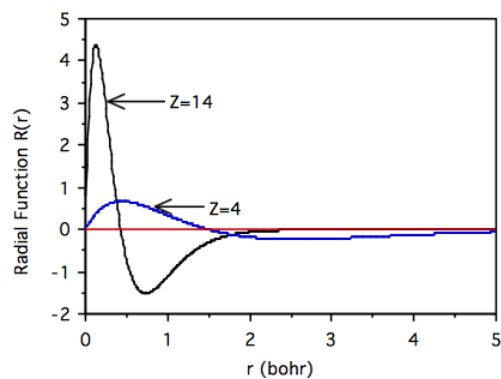
Si 2p



Si 3s



Si 3p



This page titled [22.2.4: iv. Review Exercises Solutions](#) is shared under a [CC BY-NC-SA 4.0](#) license and was authored, remixed, and/or curated by [Jack Simons](#) via [source content](#) that was edited to the style and standards of the LibreTexts platform.

22.2.5: v. Exercise Solution

1. Two Slater type orbitals, i and j, centered on the same point results in the following overlap integrals:

$$S_{ij} = \int_0^{2\pi} \int_0^\pi \int_0^\infty \left(\frac{2\xi_i}{a_0} \right)^{n_i + \frac{1}{2}} \sqrt{\frac{1}{(2n_i)!}} r^{(n_i-1)} e^{\left(\frac{-\xi_i r}{a_0} \right)} Y_{l_i, m_i}(\theta, \phi) \left(\frac{2\xi_j}{a_0} \right)^{n_j + \frac{1}{2}} \sqrt{\frac{1}{(2n_j)!}} r^{(n_j-1)} e^{\left(\frac{-\xi_j r}{a_0} \right)} Y_{l_j, m_j}(\theta, \phi) r^2 \sin\theta dr d\theta d\phi.$$

For these s orbitals $l = m = 0$ and $Y_{0,0}(\theta, \phi) = \frac{1}{\sqrt{4\pi}}$. Performing the integrations over θ and ϕ yields 4π which then cancels with these Y terms. The integral then reduces to:

$$\begin{aligned} S_{ij} &= \left(\frac{2\xi_i}{a_0} \right)^{n_i + \frac{1}{2}} \sqrt{\frac{1}{(2n_i)!}} \left(\frac{2\xi_j}{a_0} \right)^{n_j + \frac{1}{2}} \sqrt{\frac{1}{(2n_j)!}} \int_0^\infty r^{(n_i-1+n_j-1)} e^{\left(\frac{-(\xi_i + \xi_j)r}{a_0} \right)} r^2 dr \\ &= \left(\frac{2\xi_i}{a_0} \right)^{n_i + \frac{1}{2}} \sqrt{\frac{1}{(2n_i)!}} \left(\frac{2\xi_j}{a_0} \right)^{n_j + \frac{1}{2}} \sqrt{\frac{1}{(2n_j)!}} \int_0^\infty r^{(n_i-1+n_j-1)} e^{\left(\frac{-(\xi_i + \xi_j)r}{a_0} \right)} r^2 dr \end{aligned}$$

Using integral equation (4) the integral then reduces to:

$$S_{ij} = \left(\frac{2\xi_i}{a_0} \right)^{n_i + \frac{1}{2}} \sqrt{\frac{1}{(2n_i)!}} \left(\frac{2\xi_j}{a_0} \right)^{n_j + \frac{1}{2}} \sqrt{\frac{1}{(2n_j)!}} (n_i + n_j)! \left(\frac{a_0}{\xi_i + \xi_j} \right)^{n_i + n_j + 1}.$$

We then substitute in the values for each of these constants:

for $i=1$; $n=1$, $l=m=0$, and $\xi = 2.6906$

for $i=2$; $n=2$, $l=m=0$, and $\xi = 0.6396$

for $i=3$; $n=3$, $l=m=0$, and $\xi = 0.1503$.

Evaluating each of these matrix elements we obtain:

$$S_{11} = (12.482992)(0.707107)(12.482992)(0.707107)(2.00)(0.006417) = 1.000000$$

$$S_{21} = S_{12} = (1.850743)(0.204124)(12.482992)(0.707107)(6.00)(0.008131) = 0.162673$$

$$S_{22} = (1.850743)(0.204124)(1.850743)(0.204124)(24.00)(0.291950) = 1.00$$

$$S_{31} = S_{13} = (0.0144892)(0.037268)(12.482992)(0.707107)(24.00)(0.005404) = 0.000635$$

$$S_{32} = S_{23} = (0.014892)(0.037268)(1.850743)(0.204124)(120.00)(4.116872) = 0.103582$$

$$S_{33} = (0.014892)(0.037268)(0.014892)(0.037268)(720.00)(4508.968136) = 1.00$$

$$S = \begin{bmatrix} 1.000000 & & \\ 0.162673 & 1.000000 & \\ 0.000635 & 0.103582 & 1.000000 \end{bmatrix}$$

We now solve the matrix eigenvalue problem $S U = \lambda U$.

The eigenvalues, λ , of this overlap matrix are:

[0.807436 0.999424 1.193139],

and the corresponding eigenvectors, U , are:

$$\begin{bmatrix} 0.596540 & -0.537104 & -0.596372 \\ -0.707634 & -0.001394 & 0.706578 \\ 0.378675 & 0.843515 & -0.380905 \end{bmatrix} \quad (22.2.5.1)$$

The $\lambda^{-\frac{1}{2}}$ matrix becomes:

$$\lambda^{-\frac{1}{2}} = \begin{bmatrix} 1.112874 & 0.000000 & 0.000000 \\ 0.000000 & 1.000288 & 0.000000 \\ 0.000000 & 0.000000 & 0.915492 \end{bmatrix}.$$

Back transforming into the original eigenbasis gives $S^{-\frac{1}{2}}$, e.g.

$$S^{-\frac{1}{2}} = U \lambda^{-\frac{1}{2}} U^T$$

$$S^{-\frac{1}{2}} = \begin{bmatrix} 1.010194 & & \\ -0.083258 & 1.014330 & \\ 0.006170 & -0.052991 & 1.004129 \end{bmatrix}$$

The old ao matrix can be written as:

$$C = \begin{bmatrix} 1.000000 & 0.000000 & 0.000000 \\ 0.000000 & 1.000000 & 0.000000 \\ 0.000000 & 0.000000 & 1.000000 \end{bmatrix}$$

The new ao matrix (which now gives each ao as a linear combination of the original aos) then becomes:

$$C' = S^{-\frac{1}{2}} C = \begin{bmatrix} 1.010194 & -0.083258 & 0.006170 \\ -0.083258 & 1.014330 & -0.052991 \\ 0.006170 & -0.052991 & 1.004129 \end{bmatrix}$$

These new aos have been constructed to meet the orthonormalization requirement $C'^T S C' = 1$ since:

$$\left(S^{-\frac{1}{2}} C \right)^T S S^{-\frac{1}{2}} C = C^T S^{-\frac{1}{2}} S S^{-\frac{1}{2}} C = C^T C = 1.$$

But, it is always good to check our result and indeed:

$$C'^T S C' = \begin{bmatrix} 1.000000 & 0.000000 & 0.000000 \\ 0.000000 & 1.000000 & 0.000000 \\ 0.000000 & 0.000000 & 1.000000 \end{bmatrix}$$

2. The least time consuming route here is to evaluate each of the needed integrals first. These are evaluated analogous to exercise 1, letting χ_i denote each of the individual Slater Type Orbitals.

$$\int_0^{\infty} \chi_i r \chi_j r^2 dr = \langle r \rangle_{ij} \quad (22.2.5.2)$$

$$= \left(\frac{2\xi_i}{a_0} \right)^{n_i + \frac{1}{2}} \sqrt{\frac{1}{(2n_i)!}} \left(\frac{2\xi_j}{a_0} \right)^{n_j + \frac{1}{2}} \sqrt{\frac{1}{(2n_j)!}} \int_0^{\infty} r^{(n_i + n_j + 1)} e^{\left(-\frac{(\xi_i + \xi_j)r}{a_0} \right)} dr \quad (22.2.5.3)$$

Once again using integral equation (4) the integral reduces to:

$$= \left(\frac{2\xi_i}{a_0} \right)^{n_i + \frac{1}{2}} \sqrt{\frac{1}{(2n_i)!}} \left(\frac{2\xi_j}{a_0} \right)^{n_j + \frac{1}{2}} \sqrt{\frac{1}{(2n_j)!}} \int_0^{\infty} r^{(n_i + n_j + 1)} e^{\left(-\frac{(\xi_i + \xi_j)r}{a_0} \right)} dr$$

Again, upon substituting in the values for each of these constants, evaluation of these expectation values yields:

$$\langle r \rangle_{11} = (12.482992)(0.707107)(12.482992)(0.707107)(6.00)(0.001193) = 0.557496$$

$$\langle r \rangle_{21} = \langle r \rangle_{12} = (1.850743)(0.204124)(12.482992)(0.707107)(24.00)(0.002441) = 0.195391$$

$$\langle r \rangle_{22} = (1.850743)(0.204124)(1.850743)(0.204124)(120.00)(0.228228) = 3.908693$$

$$\langle r \rangle_{31} = \langle r \rangle_{13} = (0.014892)(0.0337268)(12.482992)(0.707107)(120.00)(0.001902) = 0.001118$$

$$\langle r \rangle_{32} = \langle r \rangle_{23} = (0.014892)(0.0337268)(1.850743)(0.204124)(720.00)(5.211889) = 0.786798$$

$$\langle r \rangle_{33} = (0.014892)(0.0337268)(0.014892)(0.0337268)(5040.00)(14999.893999) = 23.286760$$

$$\int_0^{\infty} \chi_i r \chi_j r^2 dr = \langle r \rangle_{ij} \begin{bmatrix} 0.557496 \\ 0.195391 & 3.908693 \\ 0.001118 & 0.786798 & 23.286760 \end{bmatrix}$$

Using these integrals one then proceeds to evaluate the expectation values of each of the orthogonalized aos, χ'_n , as:

$$\int_0^{\infty} \chi'_n r \chi'_n r^2 dr = \sum_{i=1}^3 \sum_{j=1}^3 C'_{ni} C'_{nj} \langle r \rangle_{ij}.$$

This results in the following expectation values (in atomic units):

$$\int_0^{\infty} \chi'_{1s} r \chi'_{1s} r^2 dr = 0.563240 \text{ bohr} \quad (22.2.5.4)$$

$$\int_0^{\infty} \chi'_{2s} r \chi'_{2s} r^2 dr = 3.973199 \text{ bohr} \quad (22.2.5.5)$$

$$\int_0^{\infty} \chi'_{3s} r \chi'_{3s} r^2 dr = 23.406622 \text{ bohr} \quad (22.2.5.6)$$

3. The radial density for each orthogonalized orbital, χ'_n , assuming integrations over θ and ϕ have already been performed can be written as:

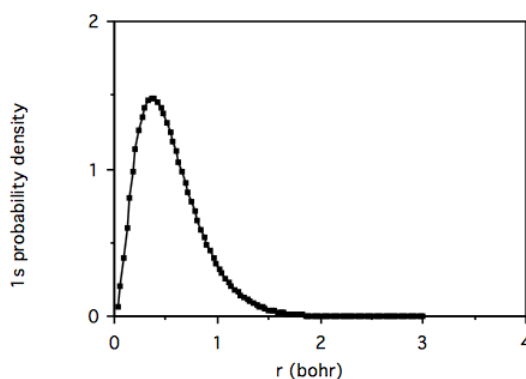
$$\int_0^{\infty} \chi'_n \chi'_n r^2 dr = \sum_{i=1}^3 \sum_{j=1}^3 C'_{ni} C'_{nj}$$

$\int_0^{\infty} R_i R_j r^2 dr$, where R_i and R_j are the radial portions of the individual Slater Type Orbitals, e.g.,

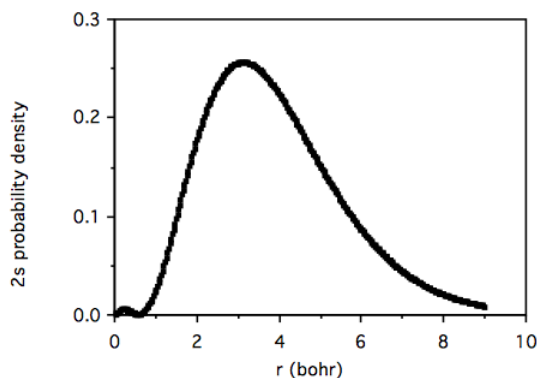
$$R_i R_j r^2 = \left(\frac{2\xi_i}{a_0} \right)^{n_i + \frac{1}{2}} \sqrt{\frac{1}{(2n_i)!}} \left(\frac{2\xi_j}{a_0} \right)^{n_j + \frac{1}{2}} \sqrt{\frac{1}{(2n_j)!}} r^{(n_i + n_j)} e^{-\frac{(\xi_i + \xi_j)r}{a_0}}$$

Therefore a plot of the radial probability for a given orthogonalized atomic orbital, n, will be: $\sum_{i=1}^3 \sum_{j=1}^3 C'_{ni} C'_{nj} R_i R_j r^2$ vs. r.

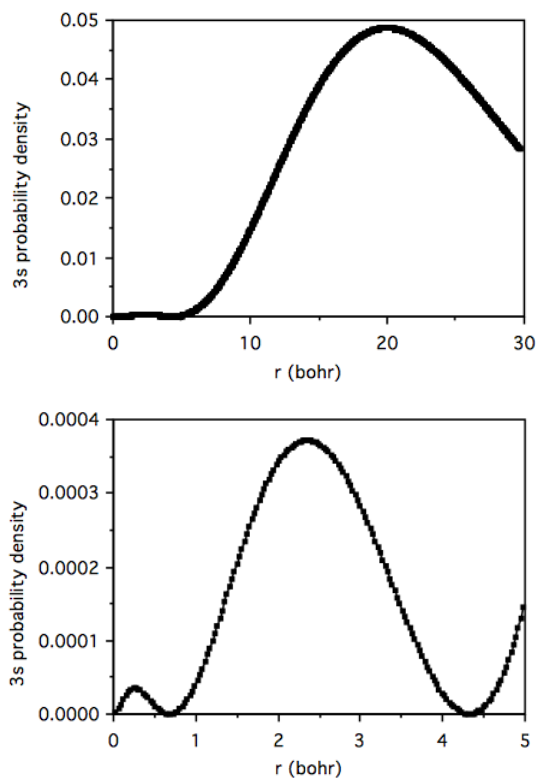
Plot the orthogonalized 1s orbital probability density vs r; note there are no nodes.



Plot of the orthogonalized 2s orbital probability density vs r; note there is one node.



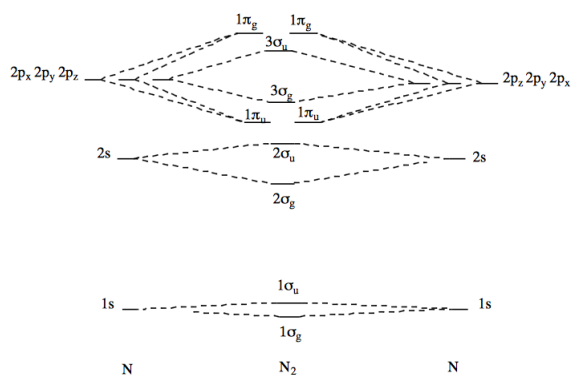
Plot of the orthogonalized 3s orbital probability density vs r; note there are two nodes in the 0-5 bohr region but they are not distinguishable as such. A duplicate plot with this nodal region expanded follows.



This page titled [22.2.5: v. Exercise Solution](#) is shared under a [CC BY-NC-SA 4.0](#) license and was authored, remixed, and/or curated by [Jack Simons](#) via [source content](#) that was edited to the style and standards of the LibreTexts platform.

22.2.6: vi. Problem Solutions

1.



The above diagram indicates how the SALC-AOs are formed from the 1s, 2s, and 2p N atomic orbitals. It can be seen that there are $3\sigma_g$, $3\sigma_u$, $1\pi_{ux}$, $1\pi_{uy}$, $1\pi_{gx}$, and $1\pi_{gy}$ SALC - AOs. The Hamiltonian matrices (Fock matrices) are given. Each of these can be diagonalized to give the following MO energies:

$3\sigma_g$; -15.52, -1.45, and -0.54 (hartrees)

$3\sigma_u$; -15.52, -0.72, and 1.13

$1\pi_{ux}$; -0.58

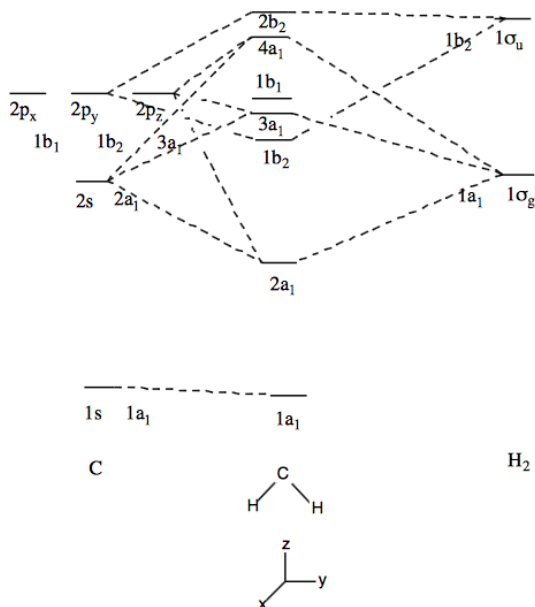
$1\pi_{uy}$; -0.58

$1\pi_{gx}$; 0.28

$1\pi_{gy}$; 0.28

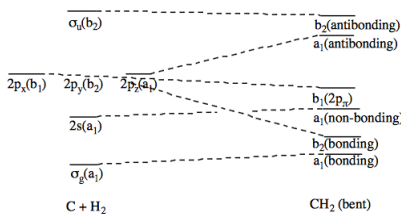
It can be seen that the $3\sigma_g$ orbitals are bonding, the $3\sigma_u$ orbitals are antibonding, the $1\pi_{ux}$ and $1\pi_{uy}$ orbitals are bonding, and the $1\pi_{gx}$ and $1\pi_{gy}$ orbitals are antibonding. The eigenvectors one obtains are in the orthogonal basis and therefore pretty meaningless. Back transformation into the original basis will generate the expected results for the $1e^-$ MOs (expected combinations of SALC-AOs).

2. Using these approximate energies we can draw the following MO diagram:

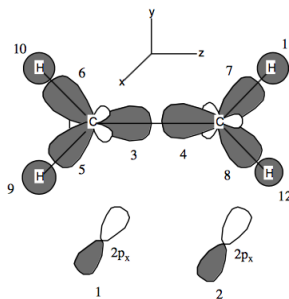


This MO diagram is **not** an orbital correlation diagram but can be used to help generate one. The energy levels on each side (C and H_2) can be "superimposed" to generate the left side of the orbital correlation diagram and the center CH_2 levels can be used to form the right side. Ignoring the core levels this generates the following orbital correlation diagram.

Orbital-correlation diagram for the reaction $C + H_2 \rightarrow CH_2$ (bent)



3.



Using D_{2h} symmetry and labeling the orbitals ($f_1 - f_{12}$) as shown above proceed by using the orbitals to define a reducible representation which may be subsequently reduced to its irreducible components. Use projectors to find the SALC-AOs for these irreps.

3. a. The $2P_x$ orbitals on each carbon form the following reducible representation:

$$\begin{array}{ccccccc} D_{2h} & E & C_2(z) & C_2(y) & C_2(x) & i & \sigma(xy) \sigma(xz) \sigma(yz) \\ \Gamma_{2p_x} & 2 & -2 & 0 & 0 & 0 & 0 \quad 2 \quad -2 \end{array} \quad \begin{array}{l} (22.2.6.1) \\ (22.2.6.2) \end{array}$$

The number of irreducible representations may be found by using the following formula:

$$n_{irrep} = \frac{1}{g} \sum_R \chi_{red}(R) \chi_{irrep}(R),$$

where g = the order of the point group (8 for D_{2h}).

$$n_{A_g} = \frac{1}{8} \sum_R \Gamma_{2p_x}(R) A_g(R) \quad (22.2.6.3)$$

$$= \frac{1}{8} [(2)(1) + (-2)(1) + (0)(1) + (0)(1) + (0)(1) + (0)(1) + (2)(1) + (-2)(1)] = 0 \quad (22.2.6.4)$$

Similarly,

$$n_{B_{1g}} = 0 \quad (22.2.6.5)$$

$$n_{B_{2g}} = 1 \quad (22.2.6.6)$$

$$n_{B_{3g}} = 0 \quad (22.2.6.7)$$

$$n_{A_u} = 0 \quad (22.2.6.8)$$

$$n_{B_{1u}} = 0 \quad (22.2.6.9)$$

$$n_{B_{2u}} = 0 \quad (22.2.6.10)$$

$$n_{B_{3u}} = 1 \quad (22.2.6.11)$$

Projectors using the formula:

$$P_{irrep} = \sum_R \chi_{irrep}(R) R,$$

may be used to find the SALC-AOs for these irreducible representations.

$$P_{B_{2g}} = \sum_R \chi_{B_{2g}}(R) R,$$

$$P_{B_{2g}} = (1)E f_1 + (-1)C_2(z) f_1 + (1)C_2(y) f_1 + (-1)C_2(x) f_1 + (1)i f_1 + (-1)\sigma(xy) f_1 + (1)\sigma(xz) f_1 + (-1)\sigma(yz) f_1 \quad (22.2.6.12)$$

$$= (1)f_1 + (-1)f_1 + (1)f_1 + (-1)f_1 + (1)f_1 + (-1)f_1 + (1)f_1 + (-1)f_1 \quad (22.2.6.13)$$

$$= f_1 + f_1 - f_1 - f_1 - f_1 - f_1 + f_1 + f_1 \quad (22.2.6.14)$$

$$= 4f_1 - 4f_2 \quad (22.2.6.15)$$

Normalization of this SALC-AO (and representing the SALC-AOs with ϕ) yields:

$$\begin{aligned} \int N(f_1 - f_2) N(f_1 - f_2) d\tau &= 1 \\ N^2 \left(\int f_1 f_1 d\tau - \int f_1 f_2 d\tau - \int f_2 f_1 d\tau + \int f_2 f_2 d\tau \right) &= 1 \\ N^2(1 + 1) &= 1 \\ 2N^2 &= 1 \\ N &= \frac{1}{\sqrt{2}} \end{aligned}$$

$$\phi_{1b_{3y}} = \frac{1}{\sqrt{2}}(f_1 - f_2).$$

The B_{3u} SALC-AO may be found in a similar fashion:

$$\begin{aligned} P_{B_{3u}} f_1 &= (1)f_1 + (-1)f_1 + (-1)f_2 + (1)f_2 + (-1)f_2 + (1)f_2 + (1)f_1 + (-1)f_1 & (22.2.6.16) \\ &= f_1 + f_1 + f_2 + f_2 + f_2 + f_2 + f_1 + f_1 & (22.2.6.17) \\ &= 4f_1 + 4f_2 & (22.2.6.18) \end{aligned}$$

Normalization of this SALC-AO yields:

$$\phi_{1b_{3u}} = \frac{1}{\sqrt{2}}(f_1 + f_2).$$

Since there are only two SALC-AOs and both are of different symmetry types these SALC-AOs are MOs and the 2x2 Hamiltonian matrix reduces to 2 1x1 matrices.

$$H_{1b_{3y}, 1b_{3y}} = \int \frac{1}{\sqrt{2}}(f_1 - f_2) H \frac{1}{\sqrt{2}}(f_1 - f_2) d\tau \quad (22.2.6.19)$$

$$= \frac{1}{2} \left(\int f_1 H f_1 d\tau - 2 \int f_1 H f_2 d\tau + \int f_2 H f_2 d\tau \right) \quad (22.2.6.20)$$

$$= \frac{1}{2} (\alpha_{2p\pi} - 2\beta_{2p\pi-2p\pi} + \alpha_{2p\pi}) \quad (22.2.6.21)$$

$$= \alpha_{2p\pi} - \beta_{2p\pi-2p\pi} \quad (22.2.6.22)$$

$$= -11.4 - (-1.2) = -10.2 \quad (22.2.6.23)$$

$$H_{1b_{3u}, 1b_{3u}} = \int \frac{1}{\sqrt{2}}(f_1 + f_2) H \frac{1}{\sqrt{2}}(f_1 + f_2) d\tau \quad (22.2.6.24)$$

$$= \frac{1}{2} \left(\int f_1 H f_1 d\tau + 2 \int f_1 H f_2 d\tau + \int f_2 H f_2 d\tau \right) \quad (22.2.6.25)$$

$$= \frac{1}{2} (\alpha_{2p\pi} + 2\beta_{2p\pi-2p\pi} + \alpha_{2p\pi}) \quad (22.2.6.26)$$

$$= \alpha_{2p\pi} + \beta_{2p\pi-2p\pi} \quad (22.2.6.27)$$

$$= -11.4 + (-1.2) = -12.6 \quad (22.2.6.28)$$

This results in a $\pi \rightarrow \pi^*$ splitting of 2.4 eV.

3. b. The sp^2 orbitals forming the C-C bond generate the following reducible representation:

$$\begin{array}{ccccccc} D_{2h} & E & C_2(z) & C_2(y) & C_2(x) & i & \sigma(xy) & \sigma(xz) & \sigma(yz) \\ \Gamma_{C_{sp}^2}^2 & 2 & 2 & 0 & 0 & 0 & 0 & 2 & 2 \end{array} \quad (22.2.6.29)$$

This reducible representation reduces to $1A_g$ and $1B_{1u}$ irreducible representations.

Projectors are used to find the SALC-AOs for these irreducible representations.

$$\begin{aligned} P_{A_g} f_3 &= (1)Ef_3 + (1)C_2(z)f_3 + (1)C_2(y)f_3 + (1)C_2(x)f_3 + (1)if_3 + (1)\sigma(xy)f_3 + (1)\sigma(xz)f_3 + (1)\sigma(yz)f_3 & (2) \\ (1)f_3 + (1)f_3 + (1)f_4 + (1)f_4 + (1)f_4 + (1)f_4 + (1)f_3 + (1)f_3 & & (2) \\ &= 4f_3 + 4f_4 & (2) \end{aligned}$$

Normalization of this SALC-AO yields:

$$\phi_{1a_g} = \frac{1}{\sqrt{2}}(f_3 + f_4).$$

The B_{1u} SALC-AO may be found in a similar fashion:

$$\begin{aligned} P_{B_{1u}} f_3 &= (1)f_3 + (1)f_3 + (-1)f_4 + (-1)f_4 + (-1)f_4 + (-1)f_4 + (1)f_3 + (1)f_3 & (22.2.6.34) \\ &= 4f_3 - 4f_4 & (22.2.6.35) \end{aligned}$$

Normalization of this SALC-AOs yields:

$$\phi_{1b_{1u}} = \frac{1}{\sqrt{2}}(f_3 - f_4).$$

Again since there are only two SALC-AOs and both are of different symmetry types these SALC-AOs are MOs and the 2x2 Hamiltonian matrix reduces to 2 1x1 matrices.

$$H_{1a_g, 1a_g} = \int \frac{1}{\sqrt{2}}(f_3 + f_4) H \frac{1}{\sqrt{2}}(f_3 + f_4) d\tau \quad (22.2.6.36)$$

$$= \frac{1}{2} \left(\int f_3 H f_3 d\tau + 2 \int f_3 H f_4 d\tau + \int f_4 H f_4 d\tau \right) \quad (22.2.6.37)$$

$$= \frac{1}{2} (\alpha_{sp^2} + 2\beta_{sp^2-sp^2} + \alpha_{sp^2}) \quad (22.2.6.38)$$

$$= \alpha_{sp^2} + \beta_{sp^2-sp^2} \quad (22.2.6.39)$$

$$= -14.7 + (-5.0) = -19.7 \quad (22.2.6.40)$$

$$H_{1b_{1u}, 1b_{1u}} = \int \frac{1}{\sqrt{2}}(f_3 - f_4) H \frac{1}{\sqrt{2}}(f_3 - f_4) d\tau \quad (22.2.6.41)$$

$$= \frac{1}{2} \left(\int f_3 H f_3 d\tau - 2 \int f_3 H f_4 d\tau + \int f_4 H f_4 d\tau \right) \quad (22.2.6.42)$$

$$= \frac{1}{2} (\alpha_{sp^2} - 2\beta_{2p^2-2p^2} + \alpha_{sp^2}) \quad (22.2.6.43)$$

$$= \alpha_{sp^2} - \beta_{sp^2-sp^2} \quad (22.2.6.44)$$

$$= -14.7 - (-5.0) = -9.7 \quad (22.2.6.45)$$

3. c. The C sp^2 orbitals and the H s orbitals forming the C-H bonds generate the following reducible representation:

$$\begin{array}{ccccccc} D_{2h} & E & C_2(z) & C_2(y) & C_2(x) & i & \sigma(xy) & \sigma(xz) & \sigma(yz) \\ \Gamma_{sp^2-s} & 8 & 0 & 0 & 0 & 0 & 0 & 0 & 8 \end{array} \quad (22.2.6.46)$$

This reducible representation reduces to $2A_g$, $2B_{3g}$, $2B_{1u}$, and $2B_{2u}$ irreducible representation.

Projectors are used to find the SALC-AOs for these irreducible representations.

$$\begin{aligned} P_{A_g} f_6 &= (1)E f_6 + (1)C_2(z) f_6 + (1)C_2(y) f_6 + (1)C_2(x) f_6 + (1)i f_6(1)\sigma(xy) f_6 + (1)\sigma(xz) f_6 + (1)\sigma(yz) f_6 & (22.2.6.48) \\ &= (1)f_6 + (1)f_5 + (1)f_7 + (1)f_8 + (1)f_8 + (1)f_7 + (1)f_5 + (1)f_6 & (22.2.6.49) \\ &= 2f_5 + 2f_6 + 2f_7 + 2f_8 & (22.2.6.50) \end{aligned}$$

Normalization yields: $\phi_{2a_g} = \frac{1}{2}(f_5 + f_6 + f_7 + f_8)$.

$$\begin{aligned} P_{A_g} f_{10} &= (1)E f_{10} + (1)C_2(z) f_{10} + (1)C_2(y) f_{10} + (1)C_2(x) f_{10} + (1)i f_{10}(1)\sigma(xy) f_{10} + (1)\sigma(xz) f_{10} + (1)\sigma(yz) f_{10} & (22.2.6.51) \\ &= (1)f_{10} + (1)f_9 + (1)f_{11} + (1)f_{12} + (1)f_{12} + (1)f_{11} + (1)f_9 + (1)f_{10} & (22.2.6.52) \\ &= 2f_9 + 2f_{10} + 2f_{11} + 2f_{12} & (22.2.6.53) \end{aligned}$$

Normalization yields: $\phi_{3a_g} = \frac{1}{2}(f_9 + f_{10} + f_{11} + f_{12})$.

$$\begin{aligned} P_{B_{3g}} f_6 &= (1)f_6 + (-1)f_5 + (-1)f_7 + (1)f_8 + (1)f_8 + (-1)f_7 + (-1)f_5 + (1)f_6 & (22.2.6.54) \\ &= -2f_5 + 2f_6 - 2f_7 + 2f_8 & (22.2.6.55) \end{aligned}$$

Normalization yields: $\phi_{1b_{3g}} = \frac{1}{2}(-f_5 + f_6 - f_7 + f_8)$.

$$\begin{aligned} P_{B_{3g}} f_{10} &= (1)f_{10} + (-1)f_9 + (-1)f_{11} + (1)f_{12} + (1)f_{12} + (-1)f_{11} + (-1)f_9 + (1)f_{10} & (22.2.6.56) \\ &= -2f_9 + 2f_{10} - 2f_{11} + 2f_{12} & (22.2.6.57) \end{aligned}$$

Normalization yields: $\phi_{2b_{3g}} = \frac{1}{2}(-f_9 + f_{10} - f_{11} + f_{12})$.

$$\begin{aligned} P_{B_{1g}} f_6 &= (1)f_6 + (1)f_5 + (-1)f_7 + (-1)f_8 + (-1)f_8 + (-1)f_7 + (1)f_5 + (1)f_6 & (22.2.6.58) \\ &= 2f_5 + 2f_6 - 2f_7 - 2f_8 & (22.2.6.59) \end{aligned}$$

Normalization yields: $\phi_{2b_{1g}} = \frac{1}{2}(f_5 + f_6 - f_7 - f_8)$.

$$\begin{aligned} P_{B_{1g}} f_{10} &= (1)f_{10} + (1)f_9 + (-1)f_{11} + (-1)f_{12} + (-1)f_{12} + (-1)f_{11} + (1)f_9 + (1)f_{10} & (22.2.6.60) \\ &= 2f_9 + 2f_{10} - 2f_{11} - 2f_{12} & (22.2.6.61) \end{aligned}$$

Normalization yields: $\phi_{3b_{1g}} = \frac{1}{2}(f_9 + f_{10} - f_{11} - f_{12})$.

$$P_{B_{2u}} f_6 = (1)f_6 + (-1)f_5 + (1)f_7 + (-1)f_8 + (-1)f_8 + (1)f_7 + (-1)f_5 + (1)f_6 = -2f_5 + 2f_6 + 2f_7 - 2f_8 \quad (22.2.6.62)$$

Normalization yields: $\phi_{1b_{2u}} = \frac{1}{2}(-f_5 + f_6 - f_7 - f_8)$.

$$P_{B_{2u}} f_{10} = (1)f_{10} + (-1)f_9 + (1)f_{11} + (-1)f_{12} + (-1)f_{12} + (1)f_{11} + (-1)f_9 + (1)f_{10} = -2f_9 + 2f_{10} + 2f_{11} - 2f_{12} \quad (22.2.6.63)$$

Normalization yields: $\phi_{2b_{2u}} = \frac{1}{2}(-f_9 + f_{10} + f_{11} - f_{12})$.

Each of these four 2x2 symmetry blocks generate identical Hamiltonian matrices. This will be demonstrated for the B_{3g} symmetry, the others proceed analogously:

$$H_{1b_{3g}, 1b_{3g}} = \int \frac{1}{2}(-f_5 + f_6 - f_7 + f_8) H \frac{1}{2}(-f_5 + f_6 - f_7 + f_8) d\tau \quad (22.2.6.64)$$

$$= \frac{1}{4} \left[\int f_5 H f_5 d\tau - \int f_5 H f_6 d\tau + \int f_5 H f_7 d\tau - \int f_5 H f_8 d\tau \right. \quad (22.2.6.65)$$

$$\left. - \int f_6 H f_5 d\tau + \int f_6 H f_6 d\tau - \int f_6 H f_7 d\tau + \int f_6 H f_8 d\tau \right. \quad (22.2.6.66)$$

$$\left. + \int f_7 H f_5 d\tau - \int f_7 H f_6 d\tau + \int f_7 H f_7 d\tau - \int f_7 H f_8 d\tau \right. \quad (22.2.6.67)$$

$$\left. - \int f_8 H f_5 d\tau + \int f_8 H f_6 d\tau - \int f_8 H f_7 d\tau + \int f_8 H f_8 d\tau \right] \quad (22.2.6.68)$$

$$= \frac{1}{4} [\beta_{sp^2-s} - 0 + 0 - 0 - 0 + \beta_{sp^2-s} - 0 + 0 + 0 - 0 + \beta_{sp^2-s} - 0 - 0 + 0 - 0 + \beta_{sp^2-s}] = \beta_{sp^2-s} \quad (22.2.6.69)$$

$$H_{1b_{3g}, 2b_{3g}} = \int \frac{1}{2}(-f_5 + f_6 - f_7 + f_8) H \frac{1}{2}(-f_9 + f_{10} - f_{11} + f_{12}) d\tau \quad (22.2.6.70)$$

$$= \frac{1}{4} \left[\int f_5 H f_9 d\tau - \int f_5 H f_{10} d\tau + \int f_5 H f_{11} d\tau - \int f_5 H f_{12} d\tau \right. \quad (22.2.6.71)$$

$$\left. - \int f_6 H f_9 d\tau + \int f_6 H f_{10} d\tau - \int f_6 H f_{11} d\tau + \int f_6 H f_{12} d\tau \right. \quad (22.2.6.72)$$

$$\left. + \int f_7 H f_9 d\tau - \int f_7 H f_{10} d\tau + \int f_7 H f_{11} d\tau - \int f_7 H f_{12} d\tau \right. \quad (22.2.6.73)$$

$$\left. - \int f_8 H f_9 d\tau + \int f_8 H f_{10} d\tau - \int f_8 H f_{11} d\tau + \int f_8 H f_{12} d\tau \right] \quad (22.2.6.74)$$

$$= \frac{1}{4} [\beta_{sp^2-s} - 0 + 0 - 0 - 0 + \beta_{sp^2-s} - 0 + 0 + 0 - 0 + \beta_{sp^2-s} - 0 - 0 + 0 - 0 + \beta_{sp^2-s}] = \beta_{sp^2-s} \quad (22.2.6.75)$$

$$H_{2b_{3g}, 2b_{3g}} = \int \frac{1}{2}(-f_9 + f_{10} - f_{11} + f_{12}) H \frac{1}{2}(-f_9 + f_{10} - f_{11} + f_{12}) d\tau \quad (22.2.6.76)$$

$$= \frac{1}{4} \left[\int f_9 H f_9 d\tau - \int f_9 H f_{10} d\tau + \int f_9 H f_{11} d\tau - \int f_9 H f_{12} d\tau \right. \quad (22.2.6.77)$$

$$\left. - \int f_{10} H f_9 d\tau + \int f_{10} H f_{10} d\tau - \int f_{10} H f_{11} d\tau + \int f_{10} H f_{12} d\tau \right. \quad (22.2.6.78)$$

$$\left. + \int f_{11} H f_9 d\tau - \int f_{11} H f_{10} d\tau + \int f_{11} H f_{11} d\tau - \int f_{11} H f_{12} d\tau \right. \quad (22.2.6.79)$$

$$\left. - \int f_{12} H f_9 d\tau + \int f_{12} H f_{10} d\tau - \int f_{12} H f_{11} d\tau + \int f_{12} H f_{12} d\tau \right] \quad (22.2.6.80)$$

$$= \frac{1}{4} [\alpha_s - 0 + 0 - 0 - 0 + \alpha_s - 0 + 0 + 0 - 0 + \alpha_s - 0 - 0 + 0 - 0 + \alpha_s] = \alpha_s \quad (22.2.6.81)$$

This matrix eigenvalue problem then becomes:

$$\begin{vmatrix} \alpha_{sp^2} - \epsilon & \beta_{sp^2-s} \\ \beta_{sp^2-s} & \alpha_s - \epsilon \end{vmatrix} = 0$$

$$\begin{vmatrix} -14.7 - \epsilon & -4.0 \\ -4.0 & -13.6 \end{vmatrix} = 0$$

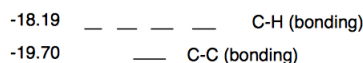
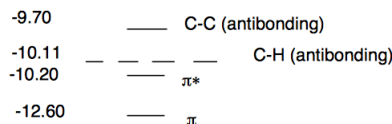
Solving this yields eigenvalues of:

$$\begin{vmatrix} -18.19 & -10.11 \end{vmatrix} \quad (22.2.6.82)$$

and corresponding eigenvectors:

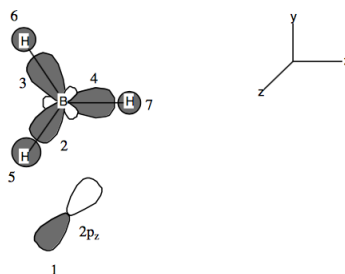
$$\begin{vmatrix} -0.7537 & -0.6572 \\ -0.6572 & 0.7537 \end{vmatrix} \quad (22.2.6.83)$$

This results in an orbital energy diagram:



For the ground state of ethylene you would fill the bottom 3 levels (the C-C, C-H, and π bonding orbitals), with 12 electrons.

4.



Using the hybrid atomic orbitals as labeled above (functions $f_1 - f_7$) and the D_{3h} point group symmetry it is easiest to construct three sets of reducible representations:

- the B $2p_z$ orbital (labeled function 1)
- the 3 B sp^2 hybrids (labeled functions 2 - 4)
- the 3 H 1s orbitals (labeled functions 5 - 7).

i. The B $2p_z$ orbital generates the following irreducible representation:

$$\begin{matrix} D_{3h} & E & 2C_3 & 3C_2 & \sigma_h & 2S_3 & 3\sigma_v \\ \Gamma_{2p_z} & 1 & 1 & -1 & -1 & -1 & 1 \end{matrix} \quad (22.2.6.84)$$

This irreducible representation is A_2'' and is its own SALC-AO.

ii. The B sp^2 orbitals generate the following reducible representation:

$$\begin{vmatrix} D_{3h} & E & 2C_3 & 3C_2 & \sigma_h & 2S_3 & 3\sigma_v \\ \Gamma_{2p} & 3 & 0 & 1 & 3 & 0 & 1 \end{vmatrix}$$

This reducible representation reduces to $1A_1'$ and $1E'$ irreducible representations.

Projectors are used to find the SALC-AOs for these irreducible representations.

Define: $C_3 = 120$ degree rotations, $C_3' = 240$ degree rotation,

$C_2 =$ rotation around f_4 , $C_2' =$ rotation around f_2 , and

$C_2'' =$ rotation around f_3 . S_3 and S_3' are defined analogous

to C_3 and C_3' with accompanying horizontal reflection.

$\sigma_v =$ a reflection plane through f_4 , $\sigma_v' =$ a reflection plane

through f_2 , and $\sigma_v'' =$ a reflection plane through f_3

$$P_{A_1'} f_2 = (1)E f_2 + (1)C_3 f_2 + (1)C_3' f_2 + (1)C_2 f_2 + (1)C_2' f_2 + (1)C_2'' f_2 + (1)\sigma_h f_2 + (1)S_3 f_2 + (1)S_3' f_2 + (1)\sigma_v f_2 + (1)\sigma_v' f_2 + (1)\sigma_v'' f_2$$

$$= (1)f_2 + (1)f_3 + (1)f_4 + (1)f_3 + (1)f_2 + (1)f_4 + (1)f_2 + (1)f_3 + (1)f_4 + (1)f_3 + (1)f_2 + (1)\sigma f_4$$

$$= 4f_2 + 4f_3 + 4f_4$$

$$\text{Normalization yields: } \phi_{1e'} = \frac{1}{\sqrt{6}}(2f_2 - f_3 - f_4).$$

To find the second e' (orthogonal to the first), projection of f_3 yields $(2f_3 - f_2 - f_4)$ and projection on f_4 yields $(2f_4 - f_2 - f_3)$. Neither of these functions are orthogonal to the first, but a combination of the two $(2f_4 - f_2 - f_4) - (2f_3 - f_2 - f_3)$ yields a function which is orthogonal to the first.

Normalization yields: $\phi_{2e'} = \frac{1}{\sqrt{2}}(f_3 - f_4)$.

iii. The H 1s orbitals generate the following reducible representation:

$$D_{3h} \quad E \quad 2C_3 \quad 3C_2 \quad \sigma_h \quad 2S_3 \quad 3\sigma_v \quad (22.2.6.86)$$

$$\Gamma_{sp^2} \quad 3 \quad 0 \quad 1 \quad 3 \quad 0 \quad 1 \quad (22.2.6.87)$$

This reducible representation reduces to $1A'_1$ and $1E'$ irreducible representations exactly like part ii. and in addition the projectors used to find the SALC-AOs for these irreducible representations is exactly analogous to part ii.

$$\phi_{2a'_1} = \frac{1}{\sqrt{3}}(f_5 + f_6 + f_7)$$

$$\phi_{3e'} = \frac{1}{\sqrt{6}}(2f_5 - f_6 - f_7).$$

$$\phi_{4e'} = \frac{1}{\sqrt{2}}(f_6 - f_7).$$

So, there are $1A'_2$, $2A'_1$ and $2E'$ orbitals. Solving the Hamiltonian matrix for each symmetry block yields:

A'_2 Block:

$$H_{1a_2, 1a_2} = \int f_1 H f_1 d\tau \quad (22.2.6.88)$$

$$= \alpha_{2p\pi} \quad (22.2.6.89)$$

$$= -8.5 \quad (22.2.6.90)$$

A'_1 Block:

$$H_{1a_1', 1a_1'} = \int \frac{1}{\sqrt{3}}(f_2 + f_3 + f_4) H \frac{1}{\sqrt{3}}(f_2 + f_3 + f_4) d\tau = \frac{1}{3} \left[\int f_2 H f_2 d\tau + \int f_2 H f_3 d\tau + \int f_2 H f_4 d\tau + \right. \quad (22.2.6.91)$$

$$+ \int f_3 H f_2 d\tau + \int f_3 H f_3 d\tau + \int f_3 H f_4 d\tau + \quad (22.2.6.92)$$

$$+ \int f_4 H f_2 d\tau + \int f_4 H f_3 d\tau + \int f_4 H f_4 d\tau \left. \right] \quad (22.2.6.93)$$

$$= \frac{1}{3} [\alpha_{sp^2} + 0 + 0 + 0 + \alpha_{sp^2} + 0 + 0 + 0 + \alpha_{sp^2}] = \alpha_{sp^2} \quad (22.2.6.94)$$

$$H_{1e_1', 2e_1'} = \int \frac{1}{\sqrt{3}}(f_2 + f_3 + f_4) H \frac{1}{\sqrt{3}}(f_5 + f_6 + f_7) d\tau = \frac{1}{3} \left[\int f_2 H f_5 d\tau + \int f_2 H f_6 d\tau + \int f_2 H f_7 d\tau + \right. \quad (22.2.6.95)$$

$$+ \int f_3 H f_5 d\tau + \int f_3 H f_6 d\tau + \int f_3 H f_7 d\tau + \quad (22.2.6.96)$$

$$+ \int f_4 H f_5 d\tau + \int f_4 H f_6 d\tau + \int f_4 H f_7 d\tau \left. \right] \quad (22.2.6.97)$$

$$= \frac{1}{3} [\beta_{sp^2-s} + 0 + 0 + 0 + \beta_{sp^2-s} + 0 + 0 + 0 + \beta_{sp^2-s}] = \beta_{sp^2-s} \quad (22.2.6.98)$$

$$H_{2a_1', 2a_1'} = \int \frac{1}{\sqrt{3}}(f_5 + f_6 + f_7) H \frac{1}{\sqrt{3}}(f_5 + f_6 + f_7) d\tau = \frac{1}{3} \left[\int f_5 H f_5 d\tau + \int f_5 H f_6 d\tau + \int f_5 H f_7 d\tau + \right. \quad (22.2.6.99)$$

$$+ \int f_6 H f_5 d\tau + \int f_6 H f_6 d\tau + \int f_6 H f_7 d\tau + \quad (22.2.6.100)$$

$$+ \int f_7 H f_5 d\tau + \int f_7 H f_6 d\tau + \int f_7 H f_7 d\tau \left. \right] \quad (22.2.6.101)$$

$$= \frac{1}{3} [\alpha_s + 0 + 0 + 0 + \alpha_s + 0 + 0 + 0 + \alpha_s] = \alpha_s \quad (22.2.6.102)$$

This matrix eigenvalue problem then becomes:

$\begin{vmatrix} \alpha_{sp^2-s} & \beta_{sp^2-s} \\ \beta_{sp^2-s} & \alpha_s - \epsilon \end{vmatrix}$

$$\quad (22.2.6.103)$$

$\& = \& 0$

$$\quad (22.2.6.104)$$

$\& = \& 0$

Solving this yields eigenvalues of:

$$\quad (22.2.6.105)$$

and corresponding eigenvectors:

$$\quad (22.2.6.106)$$

E' Block:

This 4x4 symmetry block factors to two 2x2 blocks: where one 2x2 block includes the SALC-AOs

$$\phi_{e'} = \frac{1}{\sqrt{6}}(2f_2 - f_3 - f_4) \quad (22.2.6.107)$$

$$\phi_{e'} = \frac{1}{\sqrt{6}}(2f_5 - f_6 - f_7), \quad (22.2.6.108)$$

and the other includes the SALC-AOs

$$\phi_{e'} = \frac{1}{\sqrt{2}}(f_3 - f_4) \quad (22.2.6.109)$$

$$\phi_{e'} = \frac{1}{\sqrt{2}}(f_6 - f_7). \quad (22.2.6.110)$$

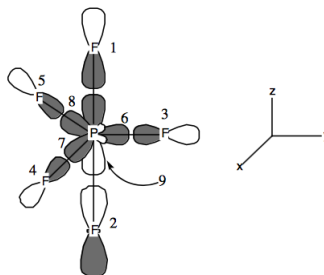
Both of these 2x2 matrices are identical to the A_1' 2x2 array and therefore yield identical energies and MO coefficients. This results in an orbital energy diagram:

$$\begin{array}{c} -8.36 \quad \text{---} \quad \text{---} \quad \text{---} \quad a_1', e' \\ -8.5 \quad \text{---} \quad a_2'' \end{array}$$

$$-15.94 \quad \text{---} \quad \text{---} \quad \text{---} \quad a_1', e'$$

For the ground state of BH_3 you would fill the bottom level (B-H bonding), a_1' and e' orbitals, with 6 electrons.

5.



5. a. The two F p orbitals (top and bottom) generate the following reducible representation:

$$\begin{array}{c|ccccc} D_{3h} & E & 2C_3 & 3C_2 & \sigma_h & 2S_3 3\sigma_v \\ \Gamma_p & 2 & 2 & 0 & 0 & 0 \end{array} \quad \begin{array}{l} (22.2.6.111) \\ (22.2.6.112) \end{array}$$

This reducible representation reduces to $1A_1'$ and $1A_2''$ irreducible representations. Projectors may be used to find the SALC-AOs for these irreducible representations.

$$\phi_{a_1'} = \frac{1}{\sqrt{2}}(f_1 - f_2) \quad (22.2.6.113)$$

$$\phi_{a_2''} = \frac{1}{\sqrt{2}}(f_1 + f_2) \quad (22.2.6.114)$$

5. b. The three trigonal F p orbitals generate the following reducible representation:

$$\begin{array}{c|ccccc} D_{3h} & E & 2C_3 & 3C_2 & \sigma_h & 2S_3 3\sigma_v \\ \Gamma_p & 3 & 0 & 1 & 3 & 0 \end{array} \quad \begin{array}{l} (22.2.6.115) \\ (22.2.6.116) \end{array}$$

This reducible representation reduces to $1A_1'$ and $1E'$ irreducible representations. Projectors may be used to find the SALC-AOs for these irreducible representations (but they are exactly analogous to the previous few problems):

$$\phi_{a_1'} = \frac{1}{\sqrt{3}}(f_3 + f_4 + f_5) \quad (22.2.6.117)$$

$$\phi_{e'} = \frac{1}{\sqrt{6}}(2f_3 - f_4 - f_5) \quad (22.2.6.118)$$

$$\phi_{e'} = \frac{1}{\sqrt{2}}(f_4 - f_5). \quad (22.2.6.119)$$

5. c. The 3 P sp^2 orbitals generate the following reducible representation:

$$\begin{array}{c|ccccc} D_{3h} & E & 2C_3 & 3C_2 & \sigma_h & 2S_3 3\sigma_v \\ \Gamma_p & 3 & 0 & 1 & 3 & 0 \end{array} \quad \begin{array}{l} (22.2.6.120) \\ (22.2.6.121) \end{array}$$

This reducible representation reduces to $1A_1'$ and $1E'$ irreducible representations. Again, projectors may be used to find the SALC-AOs for these irreducible representations.(but again they are exactly analogous to the previous few problems):

$$\phi_{a_1'} = \frac{1}{\sqrt{3}}(f_6 + f_7 + f_8) \quad (22.2.6.122)$$

$$\phi_{e'} = \frac{1}{\sqrt{6}}(2f_6 - f_7 - f_8) \quad (22.2.6.123)$$

$$\phi_{e'} = \frac{1}{\sqrt{2}}(f_7 - f_8). \quad (22.2.6.124)$$

The leftover P p_z orbital generate the following irreducible representation:

$$\begin{array}{c|ccccc} D_{3h} & E & 2C_3 & 3C_2 & \sigma_h & 2S_3 3\sigma_v \\ \Gamma_p & 1 & 1 & -1 & -1 & -1 \end{array} \quad \begin{array}{l} (22.2.6.125) \\ (22.2.6.126) \end{array}$$

This irreducible representation is an A_2''

$$\phi_{a_2''} = f_9.$$

Drawing an energy level diagram using these SALC-AOs would result in the following:

$$\begin{array}{r}
 \text{--- } a_1^* \\
 \text{--- } a_2^* \\
 \text{--- } e^* \\
 \text{--- } a_1 \\
 \text{--- } e' \\
 \text{--- } a_2' \\
 \text{--- } a_1'
 \end{array}$$

This page titled [22.2.6: vi. Problem Solutions](#) is shared under a [CC BY-NC-SA 4.0](#) license and was authored, remixed, and/or curated by [Jack Simons](#) via [source content](#) that was edited to the style and standards of the LibreTexts platform.

SECTION OVERVIEW

22.3: Electronic Configurations, Term Symbols, and States

Topic hierarchy

22.3.1: i. Review Exercises

22.3.2: ii. Exercises

22.3.3: iii. Problems

22.3.4: iv. Review Exercise Solutions

22.3.5: v. Exercise Solutions

22.3.6: vi. Problem Solutions

This page titled [22.3: Electronic Configurations, Term Symbols, and States](#) is shared under a [CC BY-NC-SA 4.0](#) license and was authored, remixed, and/or curated by [Jack Simons](#) via [source content](#) that was edited to the style and standards of the LibreTexts platform.

22.3.1: i. Review Exercises

Q1

For the given orbital occupations (configurations) of the following systems, determine all possible states (all possible allowed combinations of spin and space states). There is no need to form the determinantal wavefunctions simply label each state with its proper term symbol. One method commonly used is Harry Grays "box method" found in **Electrons and Chemical Bonding**.

- | | | | |
|-----|--------|---|------------|
| a.) | CH_2 | $1a_1^2 2a_1^2 1b_2^2 3a_1^1 1b_1^1$ | (22.3.1.1) |
| b.) | B_2 | $1\sigma_g^2 1\sigma_u^2 2\sigma_u^2 1\pi_u^1 2\pi_u^1$ | (22.3.1.2) |
| c.) | O_2 | $1\sigma_g^2 1\sigma_u^2 2\sigma_g^2 2\sigma_u^2 1\pi_u^4 3\sigma_g^2 1\pi_g^2$ | (22.3.1.3) |
| d.) | Ti | $1s^2 2s^2 2p^6 3s^2 3p^6 4s^2 d^1 4d^1$ | (22.3.1.4) |
| e.) | Ti | $1s^2 2s^2 2p^6 3s^2 3p^6 4s^2 3d^2$ | (22.3.1.5) |

This page titled [22.3.1: i. Review Exercises](#) is shared under a [CC BY-NC-SA 4.0](#) license and was authored, remixed, and/or curated by [Jack Simons](#) via [source content](#) that was edited to the style and standards of the LibreTexts platform.

22.3.2: ii. Exercises

Q1

Show that the configuration (determinant) corresponding to the $Li^+ 1s(\alpha)1s(\alpha)$ state vanishes.

Q2

Construct the 3 triplet and 1 singlet wavefunctions for the $Li^+ 1s^1 2s^1$ configuration. Show that each state is a proper eigenfunction of S^2 and S_z (use raising and lowering operators for S^2)

Q3

Construct wavefunctions for each of the following states of CH_2 :

$$a.) \quad {}^1B_1(1_{a1}^2 2_{a1}^2 1_{b2}^2 3_{a1}^1 1_{b1}^1) \quad (22.3.2.1)$$

$$b.) \quad {}^3B_1(1_{a1}^2 2_{a1}^2 1_{b2}^2 3_{a1}^1 1_{b1}^1) \quad (22.3.2.2)$$

$$c.) \quad {}^1A_1(1_{a1}^2 2_{a1}^2 1_{b2}^2 3_{a1}^2) \quad (22.3.2.3)$$

Q4

Construct wavefunctions for each state of the $1\sigma^2 2\sigma^2 3\sigma^2 1\pi^2$ configuration of NH.

Q5

Construct wavefunctions for each state of the $1s^1 2s^1 3s^1$ configuration of Li.

Q6

Determine all term symbols that arise from the $1s^2 2s^2 2p^2 3d^1$ configuration of the excited N atom.

Q7

Calculate the energy (using Slater Condon rules) associated with the π valence electrons for the following states of the C atom.

- i. ${}^3P(M_L = 1, M_S = 1)$,
- ii. ${}^3P(M_L = 0, M_S = 0)$,
- iii. ${}^1S(M_L = 0, M_S = 0)$, and
- iv. ${}^1D(M_L = 0, M_S = 0)$.

Q8

Calculate the energy (using Slater Condon rules) associated with the π valence electrons for the following states of the NH molecule.

- i. ${}^1\Delta(M_L = 2, M_S = 0)$,
- ii. ${}^1\Sigma(M_L = 0, M_S = 0)$, and
- iii. ${}^3\Sigma(M_L = 0, M_S = 0)$.

This page titled [22.3.2: ii. Exercises](#) is shared under a [CC BY-NC-SA 4.0](#) license and was authored, remixed, and/or curated by [Jack Simons](#) via [source content](#) that was edited to the style and standards of the LibreTexts platform.

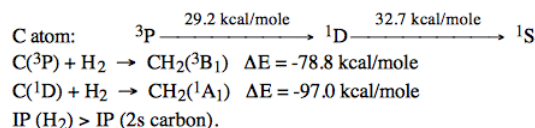
22.3.3: iii. Problems

Q1

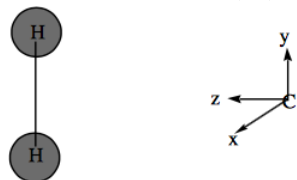
Let us investigate the reactions:



under an assumed C_{2v} reaction pathway utilizing the following information:



- Write down (first in terms of $2p_{1,0,-1}$ orbitals and then in terms of $2p_{x,y,z}$ orbitals) the:
 - three Slater determinant (SD) wavefunctions belonging to the 3P state all of which have $M_S = 1$,
 - five 1D SD wavefunctions, and
 - one 1S SD wavefunction.
- Using the coordinate system shown below, label the hydrogen orbitals σ_g, σ_u and the carbon $2s, 2p_x, 2p_y, sp_z$, orbitals as $a_1, b_1(x), b_2(y)$, or a_2 . Do the same for the $\sigma, \sigma, \sigma^*, \sigma^*, n$, and p_π orbitals of CH_2 .



- Draw an orbital correlation diagram for the $CH_2 \rightarrow H_2 + C$ reactions. Try to represent the relative energy orderings of the orbitals correctly.
- Draw (on graph paper) a configuration correlation diagram for $CH_2(^3B_1) \rightarrow H_2 + C$ showing **all** configurations which arise from the $C(^3P) + H_2$ products. You can assume the doubly excited configurations like much (~ 100 kcal / mole) above their parent configurations.
- Repeat step d. for $CH_2(^1A_1) \rightarrow H_2 + C$ again showing all configurations which arise from the $C(^1D) + H_2$ products.
- Do you expect the reaction $C(^3P) + H_2 \rightarrow CH_2$ to have a large activation barrier? About how long? What state of CH_2 is produced in this reaction? Would distortions away from C_{2v} symmetry be expected to raise or lower the activation barrier? Show how one could estimate where along the reaction path the barrier top occurs.
- Would $C(^1D) + H_2 \rightarrow CH_2$ be expected to have a larger or smaller barrier than you found for the 3PC reaction?

Q2

The decomposition of the ground-state single carbene, \triangle , to produce acetylene and 1D carbon is known to occur with an activation energy equal to the reaction endothermicity. However, when triplet carbene decomposes to acetylene and ground-state (triplet) carbon, the activation energy exceeds this reaction's endothermicity. Construct orbital, configuration, and state correlation diagrams which permit you to explain the above observations. Indicate whether single configuration or configuration interaction wavefunctions would be required to describe the above singlet and triplet decomposition processes.

Q3

We want to carry out a configuration interaction calculation on H_2 at $R=1.40$ au. A minimal basis consisting of normalized $1s$ Slater orbitals with $\xi=1.0$ gives rise to the following overlap (S), one-electron (h), and two-electron atomic integrals:

$$\begin{aligned} \langle 1S_A | 1S_B \rangle &= 0.753 \equiv S, \\ \langle 1S_A | h | 1S_A \rangle &= -1.110, \quad \langle 1S_B | h | S_A \rangle = -0.968, \end{aligned}$$

$$\langle 1S_A 1S_A | h | 1S_A 1S_A \rangle = 0.625 \equiv \langle AA | AA \rangle$$

$$\langle AA | BB \rangle = 0.323, \langle AB | AB \rangle = 0.504, \text{ and}$$

$$\langle AA | AB \rangle = 0.426.$$

- a. The normalized and orthogonal molecular orbitals we will use for this minimal basis will be determined purely by symmetry:

$$\sigma_g = \frac{(1S_A + 1S_B)}{\sqrt{2 + 2S}}, \text{ and}$$

$$\sigma_u = \frac{(1S_A - 1S_B)}{\sqrt{2 + 2S}}$$

Show that these orbitals are indeed orthogonal.

- b. Evaluate (using the one- and two- electron atomic integrals given above) the unique one- and two- electron integrals over this molecular orbital basis (this is called a transformation from the ao to the mo basis). For example, evaluate $\langle u|h|u \rangle$, $\langle uu|uu \rangle$, $\langle gu|gu \rangle$, ect.
- c. Using the two $1 \sum_g^+$ configurations σ_g^2 , and σ_u^2 , show that the elements of the 2x2 configuration interaction Hamiltonian matrix are -1.805, 0.140, and -0.568.
- d. Using **this** configuration interaction matrix, find the configuration interaction (CI) approximation to the ground and excited state energies and wavefunctions.
- e. Evaluate and make a rough sketch of the polarized orbitals which result from the above ground state σ_g^2 and σ_u^2 CI wavefunction.

This page titled [22.3.3: iii. Problems](#) is shared under a [CC BY-NC-SA 4.0](#) license and was authored, remixed, and/or curated by [Jack Simons](#) via [source content](#) that was edited to the style and standards of the LibreTexts platform.

22.3.4: iv. Review Exercise Solutions

Q1

a. For non-degenerate point groups one can simply multiply the representations (since only one representation will be obtained):

$$a_1 \otimes b_1 = b_1$$

Constructing a "box" in this case is unnecessary since it would only contain a single row. Two unpaired electrons will result in a singlet ($S=0$, $M_S=0$), and three triplets ($S=1$, $M_S=1$, $S=1$, $M_S=0$, $S=1$, $M_S=-1$). The states will be: $^3B_1(M_S=1)$, $^3B_1(M_S=0)$, ($^3B_1(M_S=-1)$), and $^1B_1(M_S=0)$.

b. Remember that when coupling non-equivalent linear molecule angular momenta, one simply adds the individual L_z values and vector couples the electron spin. So, in this case ($1\pi_u^1 2\pi_u^1$), we have M_L values of 1+1, 1-1, -1+1, and -1-1 (2,0,0, and -2). The term symbol Δ is used to denote the spatially doubly degenerate level ($M_L = \pm 2$) and there are two distinct spatially non-degenerate levels denote by the term symbol $\Sigma(M_L = 0)$. Again, two unpaired electrons will result in a singlet ($S = 0$, $M_S = 0$), and three triplets ($S = 1$, $M_S = 1$; $S = 1$, $M_S = 0$; $S = 1$, $M_S = -1$). The states generated are then:

$$^1\Delta(M_L = 2); \text{ one state } (M_S = 0),$$

$$^1\Delta(M_L = -2); \text{ one state } (M_S = 0),$$

$$^3\Delta(M_L = 2); \text{ one state } (M_S = 1, 0, \text{ and } -1),$$

$$^3\Delta(M_L = -2); \text{ one state } (M_S = 1, 0, \text{ and } -1),$$

$$^1\Sigma(M_L = 0); \text{ one state } (M_S = 0),$$

$$^1\Sigma(M_L = 0); \text{ one state } (M_S = 0),$$

$$^3\Sigma(M_L = 0); \text{ one state } (M_S = 1, 0, \text{ and } -1), \text{ and}$$

$$^3\Sigma(M_L = 0); \text{ one state } (M_S = 1, 0, \text{ and } -1)$$

c. Constructing the "box" for two equivalent π electrons one obtains:

M_S	M_L	2	1	0
1				$ \pi_1\alpha\pi_{-1}\alpha $
0		$ \pi_1\alpha\pi_1\beta $		$ \pi_1\alpha\pi_{-1}\beta ,$ $ \pi_{-1}\alpha\pi_1\beta $

From this "box" one obtains six states:

$$^1\Delta(M_L = 2); \text{ one state } (M_S = 0),$$

$$^1\Delta(M_L = -2); \text{ one state } (M_S = 0),$$

$$^1\Delta(M_L = 0); \text{ one state } (M_S = 0),$$

$$^3\Delta(M_L = 0); \text{ three states } (M_S = 1, 0, \text{ and } -1),$$

d. It is not necessary to construct a "box" when coupling non-equivalent angular momenta since the vector coupling results in a range from the sum of the two individual angular momenta to the absolute value of their difference. In this case, $3d^1 4d^1$, $L=4, 3, 2, 1, 0$, and $S=1, 0$. The term symbols are: $^3G, ^1G, ^3F, ^1F, ^3D, ^1D, ^3P, ^1P, ^3S$, and 1S . The L and S angular momenta can be vector coupled to produce further splitting into levels:

$$J = L + S \dots |L - S|.$$

Denoting J as a term symbol subscript one can identify all the levels and the subsequent $(2J + 1)$ states:

$$^3G_5 \text{ (11 states),}$$

$$^3G_4 \text{ (9 states),}$$

$$^3G_3 \text{ (7 states),}$$

$$^1G_4 \text{ (9 states),}$$

$$^3F_4 \text{ (9 states),}$$

$$^3F_3 \text{ (7 states),}$$

$$^3F_2 \text{ (5 states),}$$

$$^1F_3 \text{ (7 states),}$$

$$^3D_3 \text{ (7 states),}$$

$$^3D_2 \text{ (5 states),}$$

$$^3D_1 \text{ (3 states),}$$

1D_2 (5 states),

3P_2 (5 states),

3P_1 (3 states),

3P_0 (1 states),

1P_1 (3 states),

3S_1 (3 states), and

1S_0 (1 states).

e. Construction of a "box" for the two equivalent d electrons generates (note the "box" has been turned side ways for convenience):

M_L	M_S	1	0
4			$ d_2\alpha d_2\beta $
3		$ d_2\alpha d_1\alpha $	$ d_2\alpha d_1\beta , d_2\beta d_1\alpha $
2		$ d_2\alpha d_0\alpha $	$ d_2\alpha d_0\beta , d_1\alpha d_1\beta , d_2\beta d_0\alpha $
1		$ d_1\alpha d_0\alpha , d_2\alpha d_{-1}\alpha $	$ d_1\alpha d_0\beta , d_1\beta d_0\alpha , d_2\alpha d_{-1}\beta , d_2\beta d_{-1}\alpha $
0		$ d_2\alpha d_{-2}\alpha , d_1\alpha d_{-1}\alpha $	$ d_2\alpha d_{-2}\beta , d_2\beta d_{-2}\alpha , d_1\alpha d_{-1}\beta , d_1\beta d_{-1}\alpha , d_0\alpha d_0\beta $

The term symbols are: 1G , 3F , 1D , 3P , and 1S . The L and S angular momenta can be vector coupled to produce further splitting into levels:

1G_4 (9 states),

3F_4 (9 states),

3F_3 (7 states),

3F_2 (5 states),

1D_2 (5 states),

3P_2 (5 states),

3P_1 (3 states),

3P_0 (1 states), and

1S_0 (1 states).

This page titled [22.3.4: iv. Review Exercise Solutions](#) is shared under a [CC BY-NC-SA 4.0](#) license and was authored, remixed, and/or curated by [Jack Simons](#) via [source content](#) that was edited to the style and standards of the LibreTexts platform.

22.3.5: v. Exercise Solutions

Q1

Constructing the Slater determinant corresponding to the "state" $1s(\alpha)1s(\alpha)$ with the rows labeling the orbitals and the columns labeling the electrons gives:

$$|1s\alpha 1s\alpha| = \frac{1}{\sqrt{2}} \begin{vmatrix} 1s\alpha(1) & 1s\alpha(2) \\ 1s\alpha(1) & 1s\alpha(2) \end{vmatrix} \quad (22.3.5.1)$$

$$= \frac{1}{\sqrt{2}}(1s\alpha(1)1s\alpha(2) - 1s\alpha(1)1s\alpha(2)) \quad (22.3.5.2)$$

$$= 0 \quad (22.3.5.3)$$

Q2

Starting with the $M_S = 1$ 3S state which in a "box" for this $M_L = 0$, $M_S = 1$ case would contain only one product function; $|1s\alpha 2s\alpha|$ and applying S_- gives:

$$S_-^2 S(S=1, M_S=1) = \sqrt{1(1+1) - 1(1-1)} \hbar^3 S(S=1, M_S=0) \quad (22.3.5.4)$$

$$= \hbar\sqrt{2}^3 S(S=1, M_S=0) \quad (22.3.5.5)$$

$$= (S_-(1) + S_-(2)) |1s\alpha 2s\alpha| \quad (22.3.5.6)$$

$$= S_-(1)|1s\alpha 2s\alpha| + S_-(2)|1s\alpha 2s\alpha| \quad (22.3.5.7)$$

$$= \hbar\sqrt{\frac{1}{2}\left(\frac{1}{2}+1\right) - \frac{1}{2}\left(\frac{1}{2}-1\right)} [|1s\beta 2s\alpha| + |1s\alpha 2s\beta|] \quad (22.3.5.8)$$

$$= \hbar(|1s\beta 2s\alpha| + |1s\alpha 2s\beta|) \quad (22.3.5.9)$$

$$\text{So, } \hbar\sqrt{2}^3 S(S=1, M_S=0) = \hbar(|1s\beta 2s\alpha| + |1s\alpha 2s\beta|) \quad (22.3.5.10)$$

$$^3S(S=1, M_S=0) = \frac{1}{\sqrt{2}}(|1s\beta 2s\alpha| + |1s\alpha 2s\beta|) \quad (22.3.5.11)$$

The three triplet states are then:

$$^3S(S=1, M_S=1) = |1s\alpha 2s\alpha|, \quad (22.3.5.12)$$

$$^3S(S=1, M_S=0) = \frac{1}{\sqrt{2}}(|1s\beta 2s\alpha| + |1s\alpha 2s\beta|), \text{ and} \quad (22.3.5.13)$$

$$^3S(S=1, M_S=-1) = |1s\beta 2s\beta|. \quad (22.3.5.14)$$

The single state which must be constructed orthogonal to the three singlet states (and in particular to the $^3S(S=0, M_S=0)$ state) can be seen to be:

$$^1S(S=0, M_S=0) = \frac{1}{\sqrt{2}}(|1s\beta 2s\alpha| - |1s\alpha 2s\beta|).$$

Applying S^2 and S_z to each of these states gives:

$$S_z |1s\alpha 2s\alpha| = (S_z(1) + S_z(2)) |1s\alpha 2s\alpha| \quad (22.3.5.15)$$

$$= S_z(1)|1s\alpha 2s\alpha| + S_z(2)|1s\alpha 2s\alpha| \quad (22.3.5.16)$$

$$= \hbar\left(\frac{1}{2}\right)|1s\alpha 2s\alpha| + \hbar\left(\frac{1}{2}\right)|1s\alpha 2s\alpha| \quad (22.3.5.17)$$

$$= \hbar|1s\alpha 2s\alpha| \quad (22.3.5.18)$$

$$S^2 |1s\alpha 2s\alpha| = (S_-S_+ + S_z^2 + \hbar S_z) |1s\alpha 2s\alpha| \quad (22.3.5.19)$$

$$= S_-S_+ |1s\alpha 2s\alpha| + S_z^2 |1s\alpha 2s\alpha| + \hbar S_z |1s\alpha 2s\alpha| \quad (22.3.5.20)$$

$$= 0 + \hbar^2 |1s\alpha 2s\alpha| + \hbar^2 |1s\alpha 2s\alpha| \quad (22.3.5.21)$$

$$= 2\hbar^2 |1s\alpha 2s\alpha| \quad (22.3.5.22)$$

$$S_z \frac{1}{\sqrt{2}}(|1s\beta 2s\alpha| + |1s\alpha 2s\beta|) = (S_z(1) + S_z(2)) \frac{1}{\sqrt{2}}(|1s\beta 2s\alpha| + |1s\alpha 2s\beta|) \quad (22.3.5.23)$$

$$= \frac{1}{\sqrt{2}}(S_z(1) + S_z(2)) |1s\beta 2s\alpha| + \frac{1}{\sqrt{2}}(S_z(1) + S_z(2)) |1s\alpha 2s\beta| \quad (22.3.5.24)$$

$$= \frac{1}{\sqrt{2}}\left(\hbar\left(-\frac{1}{2}\right) + \hbar\left(\frac{1}{2}\right)\right) |1s\beta 2s\alpha| + \frac{1}{\sqrt{2}}\left(\hbar\left(\frac{1}{2}\right) + \hbar\left(-\frac{1}{2}\right)\right) |1s\alpha 2s\beta| \quad (22.3.5.25)$$

$$= 0\hbar - \frac{1}{\sqrt{2}}(|1s\beta 2s\alpha| + |1s\alpha 2s\beta|) \quad (22.3.5.26)$$

$$\begin{aligned}
 S^2 \frac{1}{\sqrt{2}} (|1s\beta 2s\alpha\rangle + |1s\alpha 2s\beta\rangle) &= (S_- S_+ + S_z^2 + \hbar S_z) \frac{1}{\sqrt{2}} (|1s\beta 2s\alpha\rangle + |1s\alpha 2s\beta\rangle) & (22.3.5.27) \\
 &= S_- S_+ \frac{1}{\sqrt{2}} (|1s\beta 2s\alpha\rangle + |1s\alpha 2s\beta\rangle) & (22.3.5.28) \\
 &= \frac{1}{\sqrt{2}} (S_- (S_+ (1) + S_+ (2)) |1s\beta 2s\alpha\rangle + S_- (S_+ (1) + S_+ (2)) |1s\alpha 2s\beta\rangle) & (22.3.5.29) \\
 &= \frac{1}{\sqrt{2}} (S_- \hbar |1s\alpha 2s\alpha\rangle + S_- \hbar |1s\alpha 2s\alpha\rangle) & (22.3.5.30) \\
 &= 2\hbar \frac{1}{\sqrt{2}} ((S_- (1) + S_- (2)) |1s\alpha 2s\alpha\rangle) & (22.3.5.31) \\
 &= 2\hbar \frac{1}{\sqrt{2}} (\hbar |1s\beta 2s\alpha\rangle + \hbar |1s\alpha 2s\beta\rangle) & (22.3.5.32) \\
 &= 2\hbar^2 \frac{1}{\sqrt{2}} (|1s\beta 2s\alpha\rangle + |1s\alpha 2s\beta\rangle) & (22.3.5.33)
 \end{aligned}$$

$$\begin{aligned}
 S^2 |1s\beta 2s\beta\rangle &= (S_+ S_- + S_z^2 - \hbar S_z) |1s\beta 2s\beta\rangle & (22.3.5.34) \\
 &= S_+ S_- |1s\beta 2s\beta\rangle |1s\beta 2s\beta\rangle - \hbar S_z |1s\beta 2s\beta\rangle & (22.3.5.35) \\
 &= 0 + \hbar^2 |1s\beta 2s\beta\rangle + \hbar^2 |1s\beta 2s\beta\rangle & (22.3.5.36) \\
 &= 2\hbar^2 |1s\beta 2s\beta\rangle & (22.3.5.37)
 \end{aligned}$$

$$\begin{aligned}
 S_z \frac{1}{\sqrt{2}} (|1s\beta 2s\alpha\rangle - |1s\alpha 2s\beta\rangle) &= (S_z (1) + S_z (2)) \frac{1}{\sqrt{2}} (|1s\beta 2s\alpha\rangle - |1s\alpha 2s\beta\rangle) & (22.3.5.38) \\
 &= \frac{1}{\sqrt{2}} (S_z (1) + S_z (2)) |1s\beta 2s\alpha\rangle - \frac{1}{\sqrt{2}} (S_z (1) + S_z (2)) |1s\alpha 2s\beta\rangle & (22.3.5.39) \\
 &= \frac{1}{\sqrt{2}} \left(\hbar \left(-\frac{1}{2} \right) + \hbar \left(\frac{1}{2} \right) \right) |1s\beta 2s\alpha\rangle - \frac{1}{\sqrt{2}} \left(\hbar \left(\frac{1}{2} \right) + \hbar \left(-\frac{1}{2} \right) \right) |1s\alpha 2s\beta\rangle & (22.3.5.40) \\
 &= 0\hbar \frac{1}{\sqrt{2}} (|1s\beta 2s\alpha\rangle - |1s\alpha 2s\beta\rangle) & (22.3.5.41)
 \end{aligned}$$

$$\begin{aligned}
 S^2 \frac{1}{\sqrt{2}} (|1s\beta 2s\alpha\rangle - |1s\alpha 2s\beta\rangle) &= (S_- S_+ S_z^2 + \hbar S_z) \frac{1}{\sqrt{2}} (|1s\beta 2s\alpha\rangle - |1s\alpha 2s\beta\rangle) & (22.3.5.42) \\
 &= S_- S_+ \frac{1}{\sqrt{2}} (|1s\beta 2s\alpha\rangle - |1s\alpha 2s\beta\rangle) & (22.3.5.43) \\
 &= \frac{1}{\sqrt{2}} (S_- (S_+ (1) + S_+ (2)) |1s\beta 2s\alpha\rangle - S_- (S_+ (1) + S_+ (2)) |1s\alpha 2s\beta\rangle) & (22.3.5.44) \\
 &= \frac{1}{\sqrt{2}} (S_- \hbar |1s\alpha 2s\alpha\rangle - S_- \hbar |1s\alpha 2s\alpha\rangle) & (22.3.5.45) \\
 &= 0\hbar \frac{1}{\sqrt{2}} ((S_- (1) + S_- (2)) |1s\alpha 2s\alpha\rangle) & (22.3.5.46) \\
 &= 0\hbar \frac{1}{\sqrt{2}} (\hbar |1s\beta 2s\alpha\rangle - \hbar |1s\alpha 2s\beta\rangle) & (22.3.5.47) \\
 &= 0\hbar^2 \frac{1}{\sqrt{2}} (|1s\beta 2s\alpha\rangle - |1s\alpha 2s\beta\rangle) & (22.3.5.48)
 \end{aligned}$$

Q3

a. Once the spatial symmetry has been determined by multiplication of the irreducible representations, the spin coupling is identical to exercise 2 and gives the result:

$$\frac{1}{\sqrt{2}} (|3_{a1}\alpha 1b_1\beta\rangle - |3_{a1}\beta 1b_1\alpha\rangle)$$

b. There are three states here (again analogous to exercise 2):

$$1.) |3_{a1}\alpha 1b_1\alpha\rangle, \quad (22.3.5.49)$$

$$2.) \frac{1}{\sqrt{2}} (|3_{a1}\alpha 1b_1\beta\rangle + |3_{a1}\beta 1b_1\alpha\rangle), \text{ and} \quad (22.3.5.50)$$

$$3.) |3_{a1}\beta 1b_1\beta\rangle \quad (22.3.5.51)$$

c.

$$|3_{a1}\alpha 3_{a1}\beta\rangle$$

Q4

As shown in review exercise 1c, for two equivalent π electrons one obtains six states:

$${}^1\Delta(M_L = 2); \text{ one state } (M_S = 0), \quad (22.3.5.52)$$

$${}^1\Delta(M_L = -2); \text{ one state } (M_S = 0), \quad (22.3.5.53)$$

$${}^1\Sigma(M_L = 0); \text{ one state } (M_S = 0), \text{ and} \quad (22.3.5.54)$$

$${}^3\Sigma(M_L = 0); \text{ three states } (M_S = 1, 0, \text{ and } -1). \quad (22.3.5.55)$$

By inspecting the "box" in review exercise 1c, it should be fairly straightforward to write down the wavefunctions for each of these:

$$^1\Delta(M_L = 2); |\pi_1\alpha\pi_1\beta| \quad (22.3.5.56)$$

$$^1\Delta(M_L = -2); |\pi_1\alpha\pi_1\beta| \quad (22.3.5.57)$$

$$^1\Sigma(M_L = 0); \frac{1}{\sqrt{2}}(|\pi_1\beta\pi_{-1}\alpha| - |\pi_1\alpha\pi_{-1}\beta|) \quad (22.3.5.58)$$

$$^3\Sigma(M_L = 0, M_S = 1); |\pi_1\alpha\pi_{-1}\alpha| \quad (22.3.5.59)$$

$$^3\Sigma(M_L = 0, M_S = 0); \frac{1}{\sqrt{2}}(|\pi_1\beta\pi_{-1}\alpha| + |\pi_1\alpha\pi_{-1}\beta|) \quad (22.3.5.60)$$

$$^3\Sigma(M_L = 0, M_S = -1); |\pi_1\beta\pi_{-1}\beta| \quad (22.3.5.61)$$

Q5

We can conveniently couple another s electron to the states generate from the $1s^1 2s^1$ configuration in exercise 2:

$$^3S(L = 0, S = 1) \text{ with } 3s^1(L = 0, S = \frac{1}{2}) \text{ giving:} \quad (22.3.5.62)$$

$$L = 0, S = \frac{3}{2}, ^4S(4 \text{ states}) \text{ and } ^2S(2 \text{ states}). \quad (22.3.5.63)$$

$$^1S(L = 0, S = 0) \text{ with } 3s^1(L = 0, S = \frac{1}{2}) \text{ giving:} \quad (22.3.5.64)$$

$$L = 0, S = \frac{1}{2}, ^2S(2 \text{ states}). \quad (22.3.5.65)$$

Constructing a "box" for this case would yield:

M_S	M_L	0
$\frac{3}{2}$		$ 1s\alpha 2s\alpha 3s\alpha $
$\frac{1}{2}$		$ 1s\alpha 2s\alpha 3s\beta , 1s\alpha 2s\beta 3s\alpha , 1s\beta 2s\alpha 3s\alpha $

One can immediately identify the wavefunctions for two of the quartets (they are single entries):

$$^4S(S = \frac{3}{2}, M_S = \frac{3}{2}): |1s\alpha 2s\alpha 3s\alpha| \quad (22.3.5.66)$$

$$^4S(S = \frac{3}{2}, M_S = -\frac{3}{2}): |1s\beta 2s\beta 3s\beta| \quad (22.3.5.67)$$

Applying S_- to $^4S(S = \frac{3}{2}, M_S = -\frac{3}{2})$ yields:

$$S_-^4S(S = \frac{3}{2}, M_S = \frac{3}{2}) = \hbar\sqrt{\frac{3}{2}\left(\frac{3}{2}+1\right) - \frac{3}{2}\left(\frac{3}{2}-1\right)}^4 S(S = \frac{3}{2}, M_S = \frac{1}{2}) \quad (22.3.5.68)$$

$$= \hbar\sqrt{3}^4 S(S = \frac{3}{2}, M_S = \frac{1}{2}) \quad (22.3.5.69)$$

$$S_-|1s\alpha 2s\alpha 3s\alpha| = \hbar(|1s\beta 2s\alpha 3s\alpha| + |1s\alpha 2s\beta 3s\alpha| + |1s\alpha 2s\alpha 3s\beta|) \quad (22.3.5.70)$$

$$\text{So, } ^4S(S = \frac{3}{2}, M_S = \frac{1}{2}) = \frac{1}{\sqrt{3}}(|1s\beta 2s\alpha 3s\alpha| + |1s\alpha 2s\beta 3s\alpha| + |1s\alpha 2s\alpha 3s\beta|) \quad (22.3.5.71)$$

Applying S_+ to $^4S(S = \frac{3}{2}, M_S = -\frac{3}{2})$ yields:

Applying S_+ to $^4S(S = \frac{3}{2}, M_S = -\frac{3}{2})$ yields:

$$S_+^4S(S = \frac{3}{2}, M_S = -\frac{3}{2}) = \hbar\sqrt{\frac{3}{2}\left(\frac{3}{2}+1\right) - \frac{3}{2}\left(\frac{3}{2}-1\right)}^4 S(S = \frac{3}{2}, M_S = -\frac{1}{2}) \quad (22.3.5.72)$$

$$= \hbar\sqrt{3}^4 S(S = \frac{3}{2}, M_S = -\frac{1}{2}) \quad (22.3.5.73)$$

$$S_+|1s\beta 2s\beta 3s\beta| = \hbar(|1s\alpha 2s\beta 3s\beta| + |1s\beta 2s\alpha 3s\beta| + |1s\beta 2s\beta 3s\alpha|) \quad (22.3.5.74)$$

$$\text{So, } ^4S(S = \frac{3}{2}, M_S = -\frac{1}{2}) = \frac{1}{\sqrt{3}}(|1s\alpha 2s\beta 3s\beta| + |1s\beta 2s\alpha 3s\beta| + |1s\beta 2s\beta 3s\alpha|) \quad (22.3.5.75)$$

Applying S_+ to $^4S(S = \frac{3}{2}, M_S = -\frac{3}{2})$ yields:

It only remains to construct the doublet states which are orthogonal to these quartet states. Recall that the orthogonal combinations for systems having three equal components (for example when symmetry adapting the 3 sp^2 hybrids in C_{2v} or D_{3h} symmetry) give results of $++$, $+-$, and $0+$. Notice that the quartets are the $+++$ combinations and therefore the doublets can be recognized as:

$$\begin{aligned}
 {}^2S(S = \frac{1}{2}, M_S = -\frac{1}{2}) &= \frac{1}{\sqrt{6}}(|1s\beta 2s\alpha 3s\alpha| + |1s\alpha 2s\beta 3s\alpha| - 2|1s\alpha 2s\alpha 3s\beta|) & (22.3.5.76) \\
 {}^2S(S = \frac{1}{2}, M_S = -\frac{1}{2}) &= \frac{1}{\sqrt{2}}(|1s\beta 2s\alpha 3s\alpha| - |1s\alpha 2s\beta 3s\alpha| + 0|1s\alpha 2s\alpha 3s\beta|) & (22.3.5.77) \\
 {}^2S(S = \frac{1}{2}, M_S = -\frac{1}{2}) &= \frac{1}{\sqrt{6}}(|1s\alpha 2s\beta 3s\beta| + |1s\beta 2s\alpha 3s\beta| - 2|1s\beta 2s\beta 3s\alpha|) & (22.3.5.78) \\
 {}^2S(S = \frac{1}{2}, M_S = -\frac{1}{2}) &= \frac{1}{\sqrt{3}}(|1s\alpha 2s\beta 3s\beta| - |1s\beta 2s\alpha 3s\beta| + 0|1s\beta 2s\beta 3s\alpha|) & (22.3.5.79)
 \end{aligned}$$

Q6

As illustrated in this chapter a p^2 configuration (two equivalent p electrons) gives rise to the term symbols: 3P , 1D , and 1S . Coupling an additional electron ($3d^1$) to this p^2 configuration will give the desired $1s^2 2s^2 2p^2 3d^1$ term symbols:

$${}^3P(L = 1, S = 1) \text{ with } {}^1D(L = 2, S = \frac{1}{2}) \text{ generates;} \quad (22.3.5.80)$$

$$L = 3, 2, 1, \text{ and } S = \frac{3}{2}, \frac{1}{2} \text{ with term symbols } {}^4F, {}^2F, {}^4D, {}^2D, {}^4P, \text{ and } {}^2S, \quad (22.3.5.81)$$

$${}^1S(L = 0, S = 0) \text{ with } {}^1D(L = 2, S = \frac{1}{2}) \text{ generates;} \quad (22.3.5.82)$$

$$L = 2 \text{ and } S = \frac{1}{2} \text{ with term symbol } {}^2D. \quad (22.3.5.83)$$

Q7

The notation used for the Slater Condon rules will be the same as used in the test:

(a.) zero (spin orbital) difference;

$$\langle |F + G| \rangle = \langle \phi_i | f | \phi_i \rangle + \sum_{i>j} (\langle \phi_i \phi_j | g | \phi_i \phi_j \rangle - \langle \phi_i \phi_j | g | \phi_j \phi_i \rangle) \quad (22.3.5.84)$$

$$= \sum_i f_{ii} + \sum_{i>j} (g_{ijij} - g_{ijji}) \quad (22.3.5.85)$$

(b.) one (spin orbital) difference ($\phi_p \neq \phi_{p'}$);

$$\langle |F + G| \rangle = \langle \phi_p | f | \phi_{p'} \rangle + \sum_{j \neq p, p'} (\langle \phi_p \phi_j | g | \phi_{p'} \phi_j \rangle - \langle \phi_p \phi_j | g | \phi_j \phi_{p'} \rangle) \quad (22.3.5.86)$$

$$= f_{pp'} + \sum_{j \neq p, p'} (g_{pj p' j} - g_{p j p' j}) \quad (22.3.5.87)$$

(c.) two (spin orbital) differences ($\phi_p \neq \phi_{p'}$ and $\phi_q \neq \phi_{q'}$);

$$\langle |F + G| \rangle = \langle \phi_p \phi_q | g | \phi_{p'} \phi_{q'} \rangle - \langle \phi_p \phi_q | g | \phi_j \phi_{p'} \rangle \quad (22.3.5.88)$$

$$= g_{pq q' p'} - g_{pq q' p'} \quad (22.3.5.89)$$

(d.) three or more (spin orbital) differences;

$$\langle |F + G| \rangle = 0$$

i. ${}^3P(M_L = 1, M_S = 1) = |p_1 \alpha p_0 \alpha|$

$$\langle |p_1 \alpha p_0 \alpha | H | p_1 \alpha p_0 \alpha | \rangle =$$

Error!. Using the Slater Condon rule (a.) above (SCa):

$$\langle |10| H | 10| \rangle = f_{11} + f_{00} + g_{1010} - g_{1001}$$

ii. ${}^3P(M_L = 0, M_S = 0) = \frac{1}{\sqrt{2}}(|p_1 \alpha p_{-1} \beta| + |p_1 \beta p_{-1} \alpha|)$

$$\langle {}^3P(M_L = 0, M_S = 0) | H | {}^3P(M_L = 0, M_S = 0) \rangle = \quad (22.3.5.90)$$

$$= \frac{1}{2} (\langle |p_1 \alpha p_{-1} \beta | H | p_1 \alpha p_{-1} \beta | \rangle + \langle |p_1 \alpha p_{-1} \beta | H | p_1 \beta p_{-1} \alpha | \rangle + \langle |p_1 \beta p_{-1} \alpha | H | p_1 \alpha p_{-1} \beta | \rangle + \langle |p_1 \beta p_{-1} \alpha | H | p_1 \beta p_{-1} \alpha | \rangle) \quad (22.3.5.91)$$

Evaluating each matrix element gives:

$$\langle |p_1 \alpha p_{-1} \beta | H | p_1 \alpha p_{-1} \beta | \rangle = f_{1\alpha 1\alpha} + f_{-1\beta -1\beta} + g_{1\alpha -1\beta 1\alpha -1\beta} - g_{1\alpha -1\beta -1\beta 1\alpha} (SCA) \quad (22.3.5.92)$$

$$= f_{11} + f_{-1-1} + g_{1-11-1} - 0 \quad (22.3.5.93)$$

$$\langle |p_1 \alpha p_{-1} \beta | H | p_1 \beta p_{-1} \alpha | \rangle = g_{1\alpha -1\beta 1\beta -1\alpha} - g_{1\alpha -1\beta -1\alpha 1\beta} (SCc) \quad (22.3.5.94)$$

$$= 0 - g_{1-1-11} \quad (22.3.5.95)$$

$$\langle |p_1 \beta p_{-1} \alpha | H | p_1 \alpha p_{-1} \beta | \rangle = g_{1\beta -1\alpha 1\alpha -1\beta} - g_{1\beta -1\alpha -1\beta 1\alpha} (SCc) \quad (22.3.5.96)$$

$$= 0 - g_{1-1-11} \quad (22.3.5.97)$$

$$\langle |p_1 \beta p_{-1} \alpha | H | p_1 \beta p_{-1} \alpha | \rangle = f_{1\beta 1\beta} + f_{-1\alpha -1\alpha} + g_{1\beta -1\alpha 1\beta -1\alpha} - g_{1\beta -1\alpha -1\alpha 1\beta} (SCa) \quad (22.3.5.98)$$

$$= f_{11} + f_{-1-1} + g_{1-11-1} - 0 \quad (22.3.5.99)$$

Substitution of these expressions give:

$$\langle {}^3P(M_L = 0, M_S = 0) | H | {}^3P(M_L = 0, M_S = 0) \rangle = \frac{1}{2} (f_{11} + f_{-1-1} + g_{1-11-1} - g_{1-11-1} - g_{1-11-1} + f_{11} + f_{-1-1} + g_{1-11-1}) \quad (22.3.5.100)$$

$$= f_{11} + f_{-1-1} + g_{1-11-1} - g_{1-11-1} \quad (22.3.5.101)$$

$$\text{iii. } {}^1S(M_L = 0, M_S = 0); \frac{1}{\sqrt{3}}(|p_0\alpha p_0\beta\rangle - |p_1\alpha p_{-1}\beta\rangle - |p_{-1}\alpha p_1\beta\rangle)$$

$$\begin{aligned} \langle {}^1S(M_L = 0, M_S = 0) | H | {}^1S(M_L = 0, M_S = 0) \rangle &= \frac{1}{3} \left(\langle p_0\alpha p_0\beta | H | p_0\alpha p_0\beta \rangle - \langle p_0\alpha p_0\beta | H | p_1\alpha p_{-1}\beta \rangle - \langle p_0\alpha p_0\beta | H | p_{-1}\alpha p_1\beta \rangle \right. \\ &\quad + \langle p_1\alpha p_{-1}\beta | H | p_1\alpha p_{-1}\beta \rangle + \langle p_1\alpha p_{-1}\beta | H | p_{-1}\alpha p_1\beta \rangle \\ &\quad - \langle p_{-1}\alpha p_1\beta | H | p_0\alpha p_0\beta \rangle + \langle p_{-1}\alpha p_1\beta | H | p_1\alpha p_{-1}\beta \rangle \\ &\quad \left. + \langle p_{-1}\alpha p_1\beta | H | p_{-1}\alpha p_1\beta \rangle \right) \end{aligned} \quad (22)$$

Evaluating each matrix element gives:

$$\begin{aligned} \langle p_0\alpha p_0\beta | H | p_0\alpha p_0\beta \rangle &= f_{0\alpha 0\alpha} + f_{0\beta 0\beta} + g_{0\alpha 0\beta 0\alpha 0\beta} - g_{0\alpha 0\beta 0\alpha 0\beta} (SCa) & (22.3.5.106) \\ &= f_{00} + f_{00} + g_{0000} - 0 & (22.3.5.107) \\ \langle p_0\alpha p_0\beta | H | p_1\alpha p_{-1}\beta \rangle &= \langle p_1\alpha p_{-1}\beta | H | p_0\alpha p_0\beta \rangle & (22.3.5.108) \\ &= g_{0\alpha 0\beta 1\alpha -1\beta} - g_{0\alpha 0\beta -1\beta 1\alpha} (SCc) & (22.3.5.109) \\ &= g_{001-1} - 0 & (22.3.5.110) \\ \langle p_0\alpha p_0\beta | H | p_{-1}\alpha p_1\beta \rangle &= \langle p_{-1}\alpha p_1\beta | H | p_0\alpha p_0\beta \rangle & (22.3.5.111) \\ &= g_{0\alpha 0\beta -1\alpha 1\beta} - g_{0\alpha 0\beta 1\beta -1\alpha} (SCc) & (22.3.5.112) \\ &= g_{00-11} - 0 & (22.3.5.113) \\ \langle p_1\alpha p_{-1}\beta | H | p_1\alpha p_{-1}\beta \rangle &= f_{1\alpha 1\alpha} + f_{-1\beta -1\beta} + g_{1\alpha -1\beta 1\alpha -1\beta} - g_{1\alpha -1\beta -1\beta 1\alpha} (SCa) & (22.3.5.114) \\ &= f_{11} + f_{-1-1} + g_{11-11} - 0 & (22.3.5.115) \\ \langle p_1\alpha p_{-1}\beta | H | p_{-1}\alpha p_1\beta \rangle &= \langle p_{-1}\alpha p_1\beta | H | p_1\alpha p_{-1}\beta \rangle & (22.3.5.116) \\ &= g_{1\alpha -\beta -1\alpha 1\beta} - g_{1\alpha -1\beta 1\beta -1\alpha} (SCc) & (22.3.5.117) \\ &= g_{1-1-11} - 0 & (22.3.5.118) \\ \langle p_{-1}\alpha p_1\beta | H | p_{-1}\alpha p_1\beta \rangle &= f_{-1\alpha -1\alpha} + f_{1\beta 1\beta} + g_{-1\alpha 1\beta -1\alpha 1\beta} - g_{-1\alpha 1\beta 1\beta -1\alpha} (SCa) & (22.3.5.119) \\ &= f_{-1-1} + f_{11} + g_{-11-11} - 0 & (22.3.5.120) \end{aligned}$$

Substitution of these expressions give:

$$\langle {}^1S(M_L = 0, M_S = 0) | H | {}^1S(M_L = 0, M_S = 0) \rangle \quad (22.3.5.121)$$

$$= \frac{1}{3} (f_{00} + f_{00} + g_{0000} - g_{001-1} - g_{00-11} - g_{001-1} + f_{11} + f_{-1-1} + g_{11-11} + g_{1-1-11} - g_{00-11} + g_{1-1-11} + f_{-1-1} + f_{11} + g_{-11-11}) \quad (22.3.5.122)$$

$$= \frac{1}{3} (2f_{00} + 2f_{11} + 2f_{-1-1} + g_{0000} - 4g_{001-1} + 2g_{11-11} + 2g_{1-1-11}) \quad (22.3.5.123)$$

$$\text{iv. } {}^1D(M_L = 0, M_S = 0) = \frac{1}{\sqrt{6}}(2|p_0\alpha p_0\beta\rangle + |p_1\alpha p_{-1}\beta\rangle + |p_{-1}\alpha p_1\beta\rangle)$$

Evaluating $\langle {}^1D(M_L = 0, M_S = 0) | H | {}^1D(M_L = 0, M_S = 0) \rangle$ we note that all the Slater Condon matrix elements generated are the same as those evaluated in part iii. (the sign for the wavefunction components and the multiplicative factor of two for one of the components, however, are different).

$$\langle {}^1D(M_L = 0, M_S = 0) | H | {}^1D(M_L = 0, M_S = 0) \rangle \quad (22.3.5.124)$$

$$\frac{1}{6} (4f_{00} + 4f_{00} + 4g_{0000} + 2g_{001-1} + 2g_{00-11} + 2g_{001-1} + f_{11} + f_{-1-1} + g_{11-11} + g_{1-1-11} + 2g_{00-11} + g_{1-1-11} + f_{-1-1} + f_{11} + g_{-11-11}) \quad (22.3.5.125)$$

$$= \frac{1}{6} (8f_{00} + 2f_{11} + 2f_{-1-1} + 4g_{0000} + 8g_{001-1} + 2g_{11-11} + 2g_{1-1-11}) \quad (22.3.5.126)$$

Q8

$$\text{i. } {}^{\Delta}(M_L = 2, M_S = 0) = |\pi_1\alpha\pi_1\beta\rangle$$

$$\langle {}^{\Delta}(M_L = 2, M_S = 0) | H | {}^{\Delta}(M_L = 2, M_S = 0) \rangle \quad (22.3.5.127)$$

$$= \langle \pi_1\alpha\pi_1\beta | H | \pi_1\alpha\pi_1\beta \rangle \quad (22.3.5.128)$$

$$= f_{1\alpha 1\alpha} + f_{1\beta 1\beta} + g_{1\alpha 1\beta 1\alpha 1\beta} - g_{1\alpha 1\beta 1\beta 1\alpha} (SCa) \quad (22.3.5.129)$$

$$= f_{11} + f_{11} + g_{1111} - 0 \quad (22.3.5.130)$$

$$= 2f_{11} + g_{1111} \quad (22.3.5.131)$$

$$\text{ii. } {}^1\Sigma(M_L = 0, M_S = 0) = \frac{1}{\sqrt{2}}(|\pi_1\alpha\pi_{-1}\beta\rangle - |\pi_1\beta\pi_{-1}\alpha\rangle)$$

$$\begin{aligned} \langle {}^1\Sigma(M_L = 0, M_S = 0) | H | {}^1\Sigma(M_L = 0, M_S = 0) \rangle &= \frac{1}{2} (\langle \pi_1\alpha\pi_{-1}\beta | H | \pi_1\alpha\pi_{-1}\beta \rangle - \langle \pi_1\alpha\pi_{-1}\beta | H | \pi_1\beta\pi_{-1}\alpha \rangle - \langle \pi_1\beta\pi_{-1}\alpha | H | \pi_1\alpha\pi_{-1}\beta \rangle + \langle \pi_1\beta\pi_{-1}\alpha | H | \pi_1\beta\pi_{-1}\alpha \rangle) \end{aligned}$$

Evaluating each matrix element gives:

$$\begin{aligned}
 \langle \pi_1 \alpha \pi_{-1} \beta | H | \pi_1 \alpha \pi_{-1} \beta \rangle &= f_{1\alpha 1\alpha} + f_{-1\beta -1\beta} + g_{1\alpha -1\beta 1\alpha -1\beta} - g_{1\alpha -1\beta -1\beta 1\alpha} (SCa) & (22.3.5.134) \\
 &= f_{11} + f_{-1-1} + g_{1-11-1} - 0 & (22.3.5.135) \\
 \langle \pi_1 \alpha \pi_{-1} \beta | H | \pi_1 \beta \pi_{-1} \alpha \rangle &= g_{1\alpha -1\beta 1\beta -1\alpha} - g_{1\alpha -1\beta -1\alpha 1\beta} (SCc) & (22.3.5.136) \\
 &= 0 - g_{1-1-11} & (22.3.5.137) \\
 \langle \pi_1 \beta \pi_{-1} \alpha | H | \pi_1 \alpha \pi_{-1} \beta \rangle &= 0 - g_{1-1-11} & (22.3.5.138) \\
 \langle \pi_1 \beta \pi_{-1} \alpha | H | \pi_1 \beta \pi_{-1} \beta \rangle &= f_{1\beta 1\beta} + f_{-1\alpha -1\alpha} + g_{1\beta -1\alpha 1\beta -1\alpha} - g_{1\beta -1\alpha -1\alpha 1\beta} (SCa) & (22.3.5.139) \\
 &= f_{11} + f_{-1-1} + g_{1-11-1} - 0 & (22.3.5.140)
 \end{aligned}$$

Substitution of these expressions give:

$$\begin{aligned}
 \langle {}^3 \sum (M_L = 0, M_S = 0) | H | {}^3 \sum (M_L = 0, M_S = 0) \rangle &= \frac{1}{2} (f_{11} + f_{-1-1} + g_{1-11-1} + g_{1-1-11} + g_{1-1-11} + f_{11} + f_{-1-1} + g_{1-11-1}) & (22.3.5.141) \\
 &= f_{11} + f_{-1-1} + g_{1-11-1} + g_{1-1-11} & (22.3.5.142)
 \end{aligned}$$

$$\begin{aligned}
 \text{iii. } {}^3 \sum (M_L = 0, M_S = 0) &= \frac{1}{\sqrt{2}} (|\pi_1 \alpha \pi_{-1} \beta\rangle + |\pi_1 \beta \pi_{-1} \alpha\rangle) \\
 \langle {}^3 \sum (M_L = 0, M_S = 0) | H | {}^3 \sum (M_L = 0, M_S = 0) \rangle &= \frac{1}{2} (\langle \pi_1 \alpha \pi_{-1} \beta | H | \pi_1 \alpha \pi_{-1} \beta \rangle + \langle \pi_1 \alpha \pi_{-1} \beta | H | \pi_1 \beta \pi_{-1} \alpha \rangle + \langle \pi_1 \beta \pi_{-1} \alpha | H | \pi_1 \alpha \pi_{-1} \beta \rangle + \langle \pi_1 \beta \pi_{-1} \alpha | H | \pi_1 \beta \pi_{-1} \alpha \rangle)
 \end{aligned}$$

Evaluating each matrix element gives:

$$\begin{aligned}
 \langle \pi_1 \alpha \pi_{-1} \beta | H | \pi_1 \alpha \pi_{-1} \beta \rangle &= f_{1\alpha 1\alpha} + f_{-1\beta -1\beta} + g_{1\alpha -1\beta 1\alpha -1\beta} - g_{1\alpha -1\beta -1\beta 1\alpha} (SCa) & (22.3.5.145) \\
 &= f_{11} + f_{-1-1} + g_{1-11-1} - 0 & (22.3.5.146) \\
 \langle \pi_1 \alpha \pi_{-1} \beta | H | \pi_1 \beta \pi_{-1} \alpha \rangle &= g_{1\alpha -1\beta 1\beta -1\alpha} - g_{1\alpha -1\beta -1\alpha 1\beta} (SCc) & (22.3.5.147) \\
 &= 0 - g_{1-1-11} & (22.3.5.148) \\
 \langle \pi_1 \beta \pi_{-1} \alpha | H | \pi_1 \alpha \pi_{-1} \beta \rangle &= f_{1\beta 1\beta} + f_{-1\alpha -1\alpha} + g_{1\beta -1\alpha 1\beta -1\alpha} - g_{1\beta -1\alpha -1\alpha 1\beta} (SCa) & (22.3.5.149) \\
 &= f_{11} + f_{-1-1} + g_{1-11-1} - 0 & (22.3.5.150)
 \end{aligned}$$

Substitution of these expressions give:

$$\begin{aligned}
 \langle {}^3 \sum (M_L = 0, M_S = 0) | H | {}^3 \sum (M_L = 0, M_S = 0) \rangle & & (22.3.5.151) \\
 = \frac{1}{2} (f_{11} + f_{-1-1} + g_{1-11-1} - g_{1-1-11} + f_{11} + f_{-1-1} + g_{1-11-1}) & & (22.3.5.152) \\
 = f_{11} + f_{-1-1} + g_{1-11-1} - g_{1-1-11} & & (22.3.5.153)
 \end{aligned}$$

This page titled 22.3.5: v. Exercise Solutions is shared under a CC BY-NC-SA 4.0 license and was authored, remixed, and/or curated by Jack Simons via source content that was edited to the style and standards of the LibreTexts platform.

22.3.6: vi. Problem Solutions

Q1

a. All the Slater determinants have in common the $|1s\alpha 1s\beta 2s\alpha 2s\beta|$ "core" and hence this component will not be written out explicitly for each case.

$${}^3P(M_L = 1, M_S = 1) = |p_1\alpha p_0\alpha| \quad (22.3.6.1)$$

$$= \left| \frac{1}{\sqrt{2}}(p_x + ip_y)\alpha(p_z)\alpha \right| \quad (22.3.6.2)$$

$$= \frac{1}{\sqrt{2}}(|p_x\alpha p_z\alpha| + i|p_y\alpha p_z\alpha|) \quad (22.3.6.3)$$

$${}^3P(M_L = 0, M_S = 1) = |p_1\alpha p_{-1}\alpha| \quad (22.3.6.4)$$

$$= \left| \frac{1}{\sqrt{2}}(p_x + ip_y)\alpha \right| \quad (22.3.6.5)$$

$$\frac{1}{\sqrt{2}}(p_x - ip_y)\alpha = \frac{1}{2}(|p_x\alpha p_x\alpha| - i|p_x\alpha p_y\alpha| + i|p_y\alpha p_x\alpha| + |p_y\alpha p_y\alpha|) \quad (22.3.6.6)$$

$$= \frac{1}{2}(0 - i|p_x\alpha p_y\alpha|) \quad (22.3.6.7)$$

$$= -i|p_x\alpha p_y\alpha| \quad (22.3.6.8)$$

$${}^3P(M_L = -1, M_S = 1) = |p_{-1}\alpha p_0\alpha| \quad (22.3.6.9)$$

$$= \left| \frac{1}{\sqrt{2}}(p_x - ip_y)\alpha(p_z)\alpha \right| \quad (22.3.6.10)$$

$$= \frac{1}{\sqrt{2}}(|p_x\alpha p_z\alpha| - i|p_y\alpha p_z\alpha|) \quad (22.3.6.11)$$

As you can see, the symmetries of each of these states cannot be labeled with a single irreducible representation of the C_{2v} point group. For example, $|p_x\alpha p_z\alpha|$ is xz (B_1) and $|p_y\alpha p_z\alpha|$ is yz (B_2) and hence the ${}^3P(M_L, M_S = 1)$ functions are degenerate for the C atom and any combination of these functions would also be degenerate. Therefore we can choose new combinations which can be labeled with "pure" C_{2v} point group labels.

$${}^3P(xz, M_S = 1) = |p_x\alpha p_z\alpha| \quad (22.3.6.12)$$

$$= \frac{1}{\sqrt{2}}({}^3P(M_L = 1, M_S = 1) + {}^3P(M_L = -1, M_S = 1)) = {}^3B_1 \quad (22.3.6.13)$$

$${}^3P(yx, M_S = 1) = |p_y\alpha p_x\alpha| \quad (22.3.6.14)$$

$$= \frac{1}{i}({}^3P(M_L = 0, M_S = 1)) = {}^3A_2 \quad (22.3.6.15)$$

$${}^3P(yz, M_S = 1) = |p_y\alpha p_z\alpha| \quad (22.3.6.16)$$

$$= \frac{1}{i\sqrt{2}}({}^3P(M_L = 1, M_S = 1) - {}^3P(M_L = -1, M_S = 1)) = {}^3B_2 \quad (22.3.6.17)$$

Now we can do likewise for the five degenerate 1D states:

$$\begin{aligned}
 {}^1D(M_L = 2, M_S = 0) &= |p_1\alpha p_1\beta| & (22.3.6.18) \\
 &= \left| \frac{1}{\sqrt{2}}(p_x + ip_y)\alpha \frac{1}{\sqrt{2}}(p_x + ip_y)\beta \right| & (22.3.6.19) \\
 &= \frac{1}{2}(|p_x\alpha p_x\beta| + i|p_x\alpha p_y\beta| + i|p_y\alpha p_x\beta| - |p_y\alpha p_y\beta|) & (22.3.6.20) \\
 {}^1D(M_L = -2, M_S = 0) &= |p_{-1}\alpha p_{-1}\beta| & (22.3.6.21) \\
 &= \left| \frac{1}{\sqrt{2}}(p_x - ip_y)\alpha \frac{1}{\sqrt{2}}(p_x - ip_y)\beta \right| & (22.3.6.22) \\
 &= \frac{1}{2}(|p_x\alpha p_x\beta| - i|p_x\alpha p_y\beta| - i|p_y\alpha p_x\beta| - |p_y\alpha p_y\beta|) & (22.3.6.23) \\
 {}^1D(M_L = 1, M_S = 0) &= \frac{1}{\sqrt{2}}(|p_0\alpha p_1\beta| - |p_0\beta p_1\alpha|) & (22.3.6.24) \\
 &= \frac{1}{\sqrt{2}} \left(|(p_z)\alpha \frac{1}{\sqrt{2}}(p_x + ip_y)\beta| - |(p_z)\beta \frac{1}{\sqrt{2}}(p_x + ip_y)\alpha| \right) & (22.3.6.25) \\
 &= \frac{1}{2}(|p_z\alpha p_x\beta| + i|p_z\alpha p_y\beta| - |p_z\beta p_x\alpha| - i|p_z\beta p_y\alpha|) & (22.3.6.26) \\
 {}^1D(M_L = -1, M_S = 0) &= \frac{1}{\sqrt{2}}(|p_0\alpha p_{-1}\beta| - |p_0\beta p_{-1}\alpha|) & (22.3.6.27) \\
 &= \frac{1}{\sqrt{2}} \left(|(p_z)\alpha \frac{1}{\sqrt{2}}(p_x - ip_y)\beta| - |(p_z)\beta \frac{1}{\sqrt{2}}(p_x - ip_y)\alpha| \right) & (22.3.6.28) \\
 &= \frac{1}{2}(|p_z\alpha p_x\beta| - i|p_z\alpha p_y\beta| - |p_z\beta p_x\alpha| + i|p_z\beta p_y\alpha|) & (22.3.6.29) \\
 {}^1D(M_L = 0, M_S = 0) &= \frac{1}{\sqrt{6}}(2|p_0\alpha p_0\beta| + |p_1\alpha p_{-1}\beta| + |p_{-1}\alpha p_1\beta|) & (22.3.6.30) \\
 &= \frac{1}{\sqrt{6}} \left(2|p_z\alpha p_z\beta| + \left| \frac{1}{\sqrt{2}}(p_x + ip_y)\alpha \frac{1}{\sqrt{2}}(p_x - ip_y)\beta \right| + \left| \frac{1}{\sqrt{2}}(p_x - ip_y)\alpha \frac{1}{\sqrt{2}}(p_x + ip_y)\beta \right| \right) & (22.3.6.31) \\
 &= \frac{1}{\sqrt{6}} \left(2|p_z\alpha p_z\beta| + \frac{1}{2}(|p_x\alpha p_x\beta| - i|p_x\alpha p_y\beta| + i|p_y\alpha p_x\beta| + |p_y\alpha p_y\beta|) \right. & (22.3.6.32) \\
 &\quad \left. + \frac{1}{2}(|p_x\alpha p_x\beta| + i|p_x\alpha p_y\beta| - i|p_y\alpha p_x\beta| + |p_y\alpha p_y\beta|) \right) \\
 &= \frac{1}{\sqrt{6}}(2|p_z\alpha p_z\beta| + |p_x\alpha p_x\beta| + |p_y\alpha p_y\beta|) & (22.3.6.33)
 \end{aligned}$$

Analogous to the three 3p states we can also choose combinations of the five degenerate 1D states which can be labeled with "pure" C_{2v} point group labels:

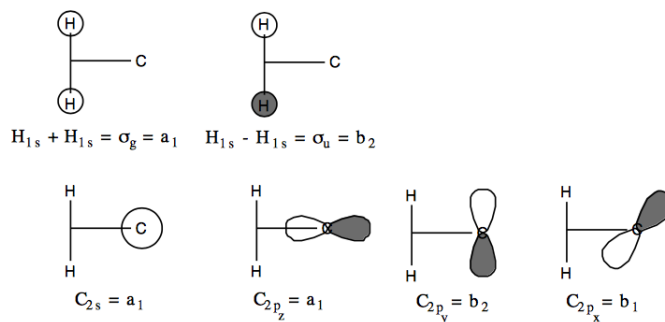
$$\begin{aligned}
 {}^1D(x - yy, M_S = 0) &= |p_x\alpha p_x\beta| - |p_y\alpha p_y\beta| & (22.3.6.34) \\
 &= ({}^1D(M_L = 2, M_S = 0) + {}^1D(M_L = -2, M_S = 0)) = {}^1A_1 & (22.3.6.35) \\
 {}^1D(yx, M_S = 0) &= |p_x\alpha p_y\beta| + |p_y\alpha p_x\beta| & (22.3.6.36) \\
 &= \frac{1}{i}({}^1D(M_L = 2, M_S = 0) - {}^1D(M_L = -2, M_S = 0)) = {}^1A_2 & (22.3.6.37) \\
 {}^1D(zx, M_S = 0) &= |p_z\alpha p_y\beta| - |p_z\beta p_y\alpha| & (22.3.6.38) \\
 &= ({}^1D(M_L = 1, M_S = 0) + {}^1D(M_L = -1, M_S = 0)) = {}^1B_1 & (22.3.6.39) \\
 {}^1D(zy, M_S = 0) &= |p_z\alpha p_y\beta| - |p_z\beta p_y\alpha| & (22.3.6.40) \\
 &= \frac{1}{i}({}^1D(M_L = 1, M_S = 0) - {}^1D(M_L = -1, M_S = 0)) = {}^1B_2 & (22.3.6.41) \\
 {}^1D(2zz + xx + yy, M_S = 0) &= \frac{1}{\sqrt{6}}(2|p_z\alpha p_z\beta| + |p_x\alpha p_x\beta| + |p_y\alpha p_y\beta|) & (22.3.6.42) \\
 &= {}^1D(M_L = 0, M_S = 0) = {}^1A_1 & (22.3.6.43)
 \end{aligned}$$

The only state left is the 1S :

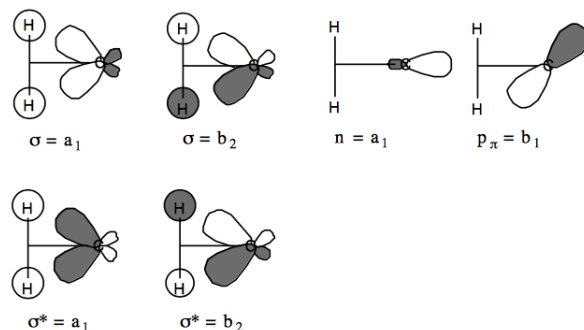
$$\begin{aligned}
 {}^1S(M_L = 0, M_S = 0) &= \frac{1}{\sqrt{3}}(|p_0\alpha p_0\beta| - |p_1\alpha p_{-1}\beta| - |p_{-1}\alpha p_1\beta|) & (22.3.6.44) \\
 &= \frac{1}{\sqrt{3}} \left(|p_z\alpha p_z\beta| - \left| \frac{1}{\sqrt{2}}(p_x + ip_y)\alpha \frac{1}{\sqrt{2}}(p_x - ip_y)\beta \right| - \left| \frac{1}{\sqrt{2}}(p_x - ip_y)\alpha \frac{1}{\sqrt{2}}(p_x + ip_y)\beta \right| \right) & (22.3.6.45) \\
 &= \frac{1}{\sqrt{3}} \left(|p_z\alpha p_z\beta| - \frac{1}{2}(|p_x\alpha p_x\beta| - i|p_x\alpha p_y\beta| + i|p_y\alpha p_x\beta| + |p_y\alpha p_y\beta|) \right. & (22.3.6.46) \\
 &\quad \left. + \frac{1}{2}(|p_x\alpha p_x\beta| + i|p_x\alpha p_y\beta| - i|p_y\alpha p_x\beta| + |p_y\alpha p_y\beta|) \right) \\
 &= \frac{1}{\sqrt{3}}(|p_z\alpha p_z\beta| - |p_x\alpha p_x\beta| - |p_y\alpha p_y\beta|) & (22.3.6.47)
 \end{aligned}$$

Each of the components of this state are A_1 and hence this state has A_1 symmetry.

b. Forming SALC-AOs from the C and H atomic orbitals would generate the following:

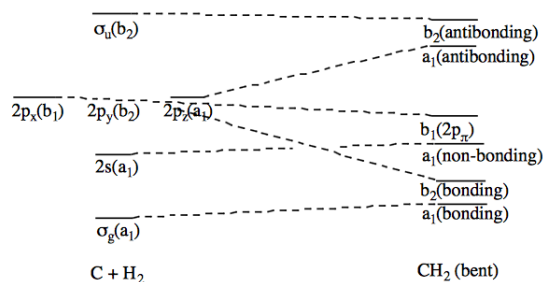


The bonding, nonbonding, and antibonding orbitals of CH_2 can be illustrated in the following manner:



c.

Orbital-correlation diagram for the reaction $C + H_2 \rightarrow CH_2$ (bent)



d. - e. It is necessary to determine how the wave functions found in part a. correlate with states of the CH_2 molecule:

$$^3P(xz, M_S = 1); ^3B_1 = \sigma_g^2 s^2 p_x p_z \rightarrow \sigma^2 n^2 p_\pi \sigma^* \quad (22.3.6.48)$$

$$^3P(yx, M_S = 1); ^3A_2 = \sigma_g^2 s^2 p_x p_y \rightarrow \sigma^2 n^2 p_\pi \sigma \quad (22.3.6.49)$$

$$^3P(yz, M_S = 1); ^3B_2 = \sigma_g^2 s^2 p_y p_z \rightarrow \sigma^2 n^2 \sigma \sigma^* \quad (22.3.6.50)$$

$$^1D(xx - yy, M_S = 0); ^1A_1 \rightarrow \sigma^2 n^2 p_\pi^2 - \sigma^2 n^2 \sigma^2 \quad (22.3.6.51)$$

$$^1D(yx, M_S = 0); ^1A_2 \rightarrow \sigma^2 n^2 \sigma p_\pi \quad (22.3.6.52)$$

$$^1D(zx, M_S = 0); ^1B_1 \rightarrow \sigma^2 n^2 \sigma^* p_\pi \quad (22.3.6.53)$$

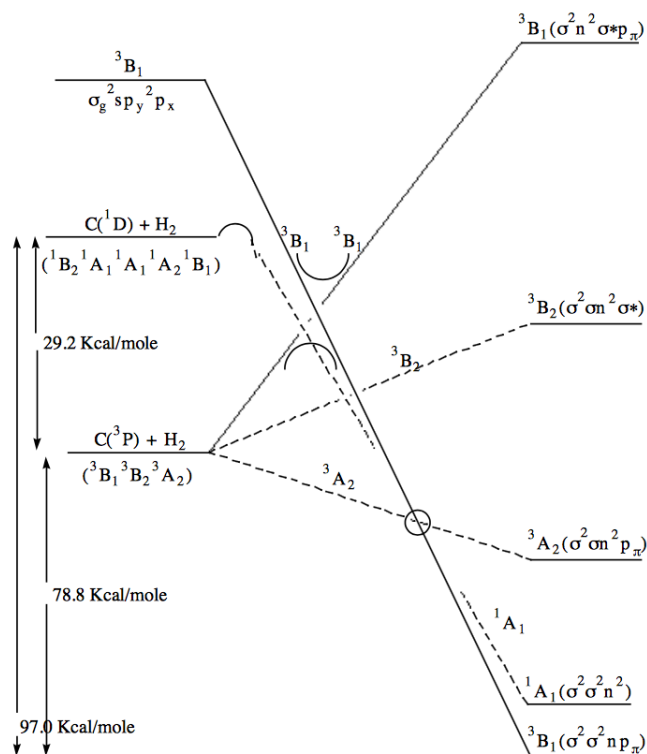
$$^1D(zy, M_S = 0); ^1B_2 \rightarrow \sigma^2 n^2 \sigma^* \sigma \quad (22.3.6.54)$$

$$^1D(2zz + xx + yy, M_S = 0); ^1A_1 \rightarrow 2\sigma^2 n^2 \sigma^* \sigma^2 + \sigma^2 n^2 p_\pi^2 + \sigma^2 n^2 \sigma^2 \quad (22.3.6.55)$$

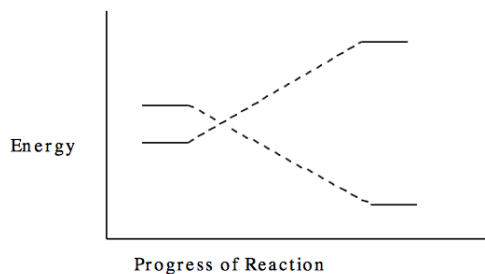
Note, the $C + H_2$ state to which the lowest $^1A_1(\sigma^2 n^2 \sigma^2)CH_2$ state decomposes would be $\sigma_g^2 s^2 p_y^2$. This state ($\sigma_g^2 s^2 p_y^2$) cannot be obtained by a simple combination of the 1D states. In order to obtain pure $\sigma_g^2 s^2 p_y^2$ it is necessary to combine 1S with 1D . For example,

$$\sigma_g^2 s^2 p_y^2 = \frac{1}{6} \left(\sqrt{6} ^1D(0, 0) - 2\sqrt{3} ^1S(0, 0) \right) - \frac{1}{2} (^1D(2, 0) + ^1D(-2, 0)) .$$

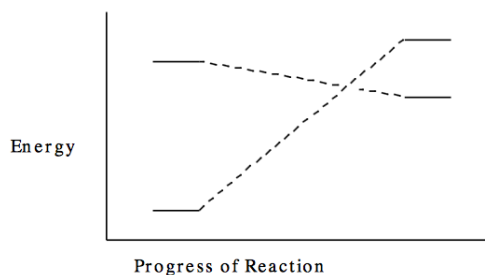
This indicates that a CCD must be drawn with a barrier near the 1D asymptote to represent the fact that $^1A_1 CH_2$ correlates with a mixture of 1D and 1S carbon plus hydrogen. The $C + H_2$ state to which the lowest $^3B_1(\sigma^2 n^2 \sigma^2 p_\pi)CH_2$ state decomposes would be $\sigma_g^2 s^2 p_y^2 p_x$.



f. If you follow the 3B_1 component of the $C(^3P) + H_2$ (since it leads to the ground state products) to 3B_1CH_2 you must go over an approximately 20 Kcal/mole barrier. Of course this path produces 3B_1CH_2 product. Distortions away from C_{2v} symmetry, for example to $C-s$ symmetry, would make the a_1 and b_2 orbitals identical in symmetry (a'). The b_1 orbitals would maintain their identity group going to a'' symmetry. Thus 3B_1 and 3A_2 (both $^3A''$ in C_s symmetry and odd under reflection through the molecular plane) can mix. The system could thus follow the 3A_2 component of the $C(^3P) + H_2$ surface to the place (marked with a circle on the CCD) where it crosses the 3B_1 surface upon which it then moves and continues to products. As a result, the barrier would be lowered. You can estimate when the barrier occurs (late or early) using thermodynamic information for the reaction (i.e. slopes and asymptotic energies). For example, an early barrier would be obtained for a reaction with the characteristics:



and a late barrier would be obtained for a reaction with the characteristics:



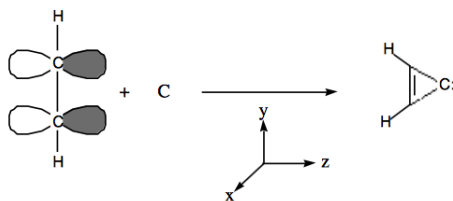
This relation between reaction endothermicity or exothermicity is known as the Hammond postulate. Note that the $C(^3P_1) + H_2 \rightarrow CH_2$ reaction of interest here (see the CCD) has an early barrier.

g. The reaction $C(^1D) + H_2 \rightarrow CH_2(^1A_1)$ should have no symmetry barrier (this can be recognized by the following the $^1A_1(C(^1D) + H_2)$ reactants down to the $^1A_1(CH_2)$ products on the CCD).

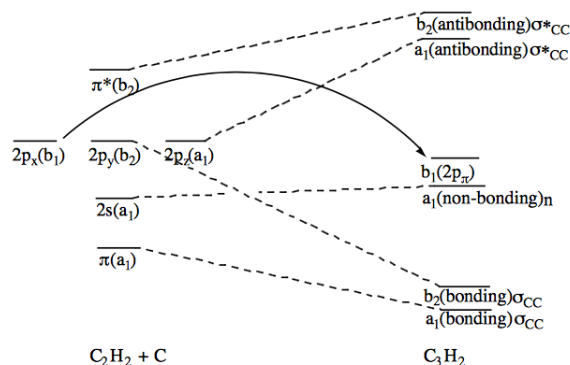
Q2

This problem in many respects is analogous to problem 1.

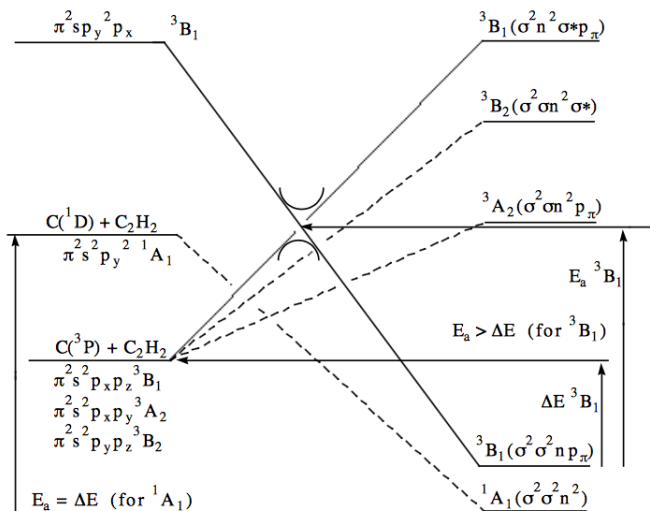
The 3B_1 surface certainly requires a two configuration CI wavefunction; the $\sigma^2\sigma^2np_x(\pi^2p_y^2sp_x)$ and the $\sigma^2n^2p_x\sigma^*(\pi^2s^2p_xp_z)$. The 1A_1 surface could use the $\sigma^2\sigma^2\sigma^2n^2(\pi^2s^2p_y^2)$ only but once again there is a combination of 1D determinants which gives purely this configuration ($\pi^2s^2p_y^2$). Thus mixing of both 1D and 1S determinants are necessary to yield the required $\pi^2s^2p_y^2$ configuration. Hence even the 1A_1 surface would require a multiconfigurational wavefunction for adequate description.



Orbital-correlation diagram for the reaction $C_2H_2 + C \rightarrow C_3H_2$



Configuration correlation diagram for the reaction $C_2H_2 + C \rightarrow C_3H_2$.



Q3

a.

$$\langle \sigma_g | \sigma_g \rangle = \left\langle \frac{1s_A + 1s_B}{\sqrt{2 + 2S}} \middle| \frac{1s_A + 1s_B}{\sqrt{2 + 2S}} \right\rangle \quad (22.3.6.56)$$

$$= \frac{1}{2 + 2S} (\langle 1s_A | 1s_A \rangle + \langle 1s_A | 1s_B \rangle + \langle 1s_B | 1s_A \rangle + \langle 1s_B | 1s_B \rangle) \quad (22.3.6.57)$$

$$= (0.285)((1.000) + (0.753) + (0.753) + (1.000)) \quad (22.3.6.58)$$

$$= 0.999 \approx 1 \quad (22.3.6.59)$$

$$\begin{aligned}
 \langle \sigma_g | \sigma_u \rangle &= \left\langle \frac{1s_A + 1s_B}{\sqrt{2+2S}} \left| \frac{1s_A - 1s_B}{\sqrt{2-2S}} \right. \right\rangle & (22.3.6.60) \\
 &= \frac{\langle 1s_A | 1s_A \rangle + \langle 1s_A | 1s_B \rangle + \langle 1s_B | 1s_A \rangle + \langle 1s_B | 1s_B \rangle}{\sqrt{2+2S}\sqrt{2-2S}} & (22.3.6.61) \\
 &= (1.434)(0.534)((1.000) - (0.753) + (0.753) - (1.000)) & (22.3.6.62) \\
 &= 0 & (22.3.6.63) \\
 \langle \sigma_u | \rangle &= \left\langle \frac{1s_A - 1s_B}{\sqrt{2-2S}} \left| \frac{1s_A - 1s_B}{\sqrt{2-2S}} \right. \right\rangle & (22.3.6.64) \\
 &= \frac{\langle 1s_A | 1s_A \rangle - \langle 1s_A | 1s_B \rangle - \langle 1s_B | 1s_A \rangle + \langle 1s_B | 1s_B \rangle}{2-2S} & (22.3.6.65) \\
 &= (2.024)((1.000) - (0.753) - (0.753) + (1.000)) & (22.3.6.66) \\
 &= 1.000 & (22.3.6.67)
 \end{aligned}$$

b.

$$\begin{aligned}
 \langle \sigma_g | h | \sigma_g \rangle &= \left\langle \frac{1s_A + 1s_B}{\sqrt{2+2S}} \left| h \right| \frac{1s_A + 1s_B}{\sqrt{2+2S}} \right\rangle & (22.3.6.68) \\
 &= \frac{\langle 1s_A | h | 1s_A \rangle + \langle 1s_A | h | 1s_B \rangle + \langle 1s_B | h | 1s_A \rangle + \langle 1s_B | h | 1s_B \rangle}{2+2S} & (22.3.6.69) \\
 &= (0.285)((-1.110) + (-0.968) + (-0.968) + (-1.110)) & (22.3.6.70) \\
 &= -1.184 & (22.3.6.71) \\
 \langle \sigma_u | h | \sigma_u \rangle &= \left\langle \frac{1s_A - 1s_B}{\sqrt{2-2S}} \left| h \right| \frac{1s_A - 1s_B}{\sqrt{2-2S}} \right\rangle & (22.3.6.72) \\
 &= \frac{\langle 1s_A | h | 1s_A \rangle - \langle 1s_A | h | 1s_B \rangle - \langle 1s_B | h | 1s_A \rangle + \langle 1s_B | h | 1s_B \rangle}{2-2S} & (22.3.6.73) \\
 &= (2.024)((-1.110) + (0.968) + (0.968) + (-1.110)) & (22.3.6.74) \\
 &= -0.575 & (22.3.6.75) \\
 \langle \sigma_g \sigma_g | h | \sigma_g \sigma_g \rangle &\equiv \langle gg | gg \rangle = \frac{1}{2+2S} \frac{1}{2+2S} & (22.3.6.76) \\
 &= \frac{1}{(2+2S)^2} (\langle AA | AA \rangle + \langle AA | AB \rangle + \langle AA | BA \rangle + \langle AA | BB \rangle + \langle AB | AA \rangle + \langle AB | AB \rangle + \langle AB | BA \rangle + \langle AB | BB \rangle + & (22.3.6.77) \\
 &\quad \langle BA | AA \rangle + \langle BA | AB \rangle + \langle BA | BA \rangle + \langle BA | BB \rangle + \langle BB | AA \rangle + \langle BB | BA \rangle + \langle BB | BA \rangle + \langle BB | BB \rangle) & (22.3.6.78) \\
 &= (0.081)((0.625) + (0.426) + (0.426) + (0.323) + (0.426) + (0.504) + (0.323) + (0.426) + & (22.3.6.79) \\
 &\quad (0.426) + (0.323) + (0.504) + (0.426) + (0.323) + (0.426) + (0.426) + (0.625)) & (22.3.6.80) \\
 &= 0.564 & (22.3.6.81) \\
 \langle uu | uu \rangle &= \frac{1}{2-2S} \frac{1}{2-2S} & (22.3.6.82) \\
 &= \frac{1}{(2-2S)^2} (\langle AA | AA \rangle - \langle AA | AB \rangle - \langle AA | BA \rangle + \langle AA | BB \rangle - \langle BA | AA \rangle + \langle BA | AB \rangle + \langle BA | BA \rangle - \langle BA | BB \rangle & (22.3.6.83) \\
 &\quad + \langle BB | AA \rangle - \langle BB | AB \rangle - \langle BB | BA \rangle + \langle BB | BB \rangle) & (22.3.6.84) \\
 &= (4.100)((0.625) - (0.426) - (0.426) + (0.323) - (0.426) + (0.504) + (0.323) - (0.426) - & (22.3.6.85) \\
 &\quad (0.426) + (0.323) + (0.504) - (0.426) + (0.323) - (0.426) - (0.426) + (0.625)) & (22.3.6.86) \\
 &= 0.582 & (22.3.6.87) \\
 & & (22.3.6.88) \\
 & & (22.3.6.89)
 \end{aligned}$$

$$\begin{aligned}
 \langle gg|uu \rangle &= \frac{1}{2+2S} \frac{1}{2-2S} & (22.3.6.90) \\
 &= \frac{1}{2+2S} \frac{1}{2-2S} \langle (1s_A + 1s_B)(1s_A + 1s_B) | (1s_A - 1s_B)(1s_A - 1s_B) \rangle & (22.3.6.91) \\
 &= \frac{1}{2+2S} \frac{1}{2-2S} & (22.3.6.92) \\
 &= \frac{1}{2+2S} \frac{1}{2-2S} \langle (AA|AA) - \langle AA|AB \rangle - \langle AA|BA \rangle + \langle AA|BB \rangle + \langle AB|AA \rangle - \langle AB|AB \rangle - \langle AB|BA \rangle + \langle AB|BB \rangle + & (22.3.6.93) \\
 &\quad + \langle BA|AA \rangle - \langle BA|AB \rangle - \langle BA|BA \rangle + \langle BA|BB \rangle + \langle BB|AA \rangle - \langle BB|AB \rangle - \langle BB|BA \rangle + \langle BB|BB \rangle \rangle & (22.3.6.94) \\
 &= (0.285)(2.024)((0.625) - (0.426) - (0.426) + (0.323) + (0.426) - (0.504) - (0.323) + (0.426) + & (22.3.6.95) \\
 &\quad + (0.426) - (0.323) - (0.504) - (0.426) + (0.323) - (0.426) - (0.426) + (0.625)) & (22.3.6.96) \\
 &= 0.140 & (22.3.6.97) \\
 \langle gu|gu \rangle &= \frac{1}{2+2S} \frac{1}{2-2S} & (22.3.6.98) \\
 &= \frac{1}{2+2S} \frac{1}{2-2S} \langle (1s_A + 1s_B)(1s_A - 1s_B) | (1s_A + 1s_B)(1s_A - 1s_B) \rangle & (22.3.6.99) \\
 &= \frac{1}{2+2S} \frac{1}{2-2S} & (22.3.6.100) \\
 &= \frac{1}{2+2S} \frac{1}{2-2S} \langle (AA|AA) - \langle AA|AB \rangle + \langle AA|BA \rangle - \langle AA|BB \rangle - \langle AB|AA \rangle + \langle AB|AB \rangle - \langle AB|BA \rangle + \langle AB|BB \rangle & (22.3.6.101) \\
 &\quad + \langle BA|AA \rangle - \langle BA|AB \rangle + \langle BA|BA \rangle - \langle BA|BB \rangle - \langle BB|AA \rangle + \langle BB|AB \rangle - \langle BB|BA \rangle + \langle BB|BB \rangle \rangle & (22.3.6.102) \\
 &= (0.285)(2.024)((0.625) - (0.426) + (0.426) - (0.323) - (0.426) + (0.504) - (0.323) + (0.426) + \dots & (22.3.6.103) \\
 &\quad \dots + (0.426) - (0.323) + (0.504) - (0.426) - (0.323) + (0.426) - (0.426) + (0.625)) & (22.3.6.104) \\
 &= 0.557 & (22.3.6.105)
 \end{aligned}$$

Note, that $\langle gg|gu \rangle = \langle uu|ug \rangle = 0$ from symmetry considerations, but this can be easily verified. For example,

$$\begin{aligned}
 \langle gg|gu \rangle &= \frac{1}{\sqrt{2+2S}} \frac{1}{\sqrt{(2-2S)^3}} & (22.3.6.106) \\
 &= \frac{1}{\sqrt{2+2S}} \frac{1}{\sqrt{(2-2S)^3}} \langle (1s_A + 1s_B)(1s_A + 1s_B) | (1s_A + 1s_B)(1s_A - 1s_B) \rangle & (22.3.6.107) \\
 &= \frac{1}{\sqrt{2+2S}} \frac{1}{\sqrt{(2-2S)^3}} \langle (AA|AA) - \langle AA|AB \rangle + \langle AA|BA \rangle - \langle AA|BB \rangle & (22.3.6.109) \\
 &\quad + \langle AB|AA \rangle - \langle AB|AB \rangle + \langle AB|BA \rangle - \langle AB|BB \rangle + & (22.3.6.110) \\
 &\quad + \langle BA|AA \rangle - \langle BA|AB \rangle + \langle BA|BA \rangle - \langle BA|BB \rangle + & (22.3.6.111) \\
 &\quad + \langle BB|AA \rangle - \langle BB|AB \rangle + \langle BB|BA \rangle - \langle BB|BB \rangle \rangle & (22.3.6.112) \\
 &= \frac{1}{\sqrt{2+2S}} \frac{1}{\sqrt{(2-2S)^3}} (0.534)(2.880)((0.625) - (0.426) + (0.426) - (0.323) + (0.426) - (0.504) + (0.323) - (0.426) + \dots & (22.3.6.113) \\
 &\quad \dots + (0.426) - (0.323) + (0.504) - (0.426) + (0.323) - (0.426) + (0.426) - (0.625)) & (22.3.6.114) \\
 &= 0.000 & (22.3.6.115)
 \end{aligned}$$

c. We can now set up the configuration interaction Hamiltonian matrix. The elements are evaluated by using the Slater-Condon rules as shown in the text.

$$\begin{aligned}
 H_{11} &= \langle \sigma_g \alpha \sigma_g \beta | H | \sigma_g \alpha \sigma_g \beta \rangle & (22.3.6.116) \\
 &= 2f_{\sigma_g \sigma_g} + g_{\sigma_g \sigma_g \sigma_g \sigma_g} & (22.3.6.117) \\
 &= 2(-1.184) + 0.564 = -1.804 & (22.3.6.118) \\
 H_{21} &= \langle \sigma_g \alpha \sigma_g \beta | H | \sigma_u \alpha \sigma_u \beta \rangle & (22.3.6.119) \\
 &= g_{\sigma_g \sigma_g \sigma_u \sigma_u} & (22.3.6.120) \\
 &= 0.140 & (22.3.6.121) \\
 H_{22} &= \langle \sigma_u \alpha \sigma_u \beta | H | \sigma_u \alpha \sigma_u \beta \rangle & (22.3.6.122) \\
 &= 2f_{\sigma_u \sigma_u} + g_{\sigma_u \sigma_u \sigma_u \sigma_u} & (22.3.6.123) \\
 &= 2(-0.575) + 0.582 = -0.568 & (22.3.6.124)
 \end{aligned}$$

d. Solving this eigenvalue problem:

$$\begin{aligned}
 \begin{vmatrix} -1.804 - \epsilon & 0.140 \\ 0.140 & -0.568 - \epsilon \end{vmatrix} &= 0 & (22.3.6.125) \\
 (-1.804 - \epsilon)(-0.568 - \epsilon) - (0.140)^2 &= 0 & (22.3.6.126) \\
 1.025 + 1.804\epsilon + 0.568\epsilon + \epsilon^2 - 0.0196 &= 0 & (22.3.6.127) \\
 \epsilon^2 + 2.372\epsilon + 1.005 &= 0 & (22.3.6.128) \\
 \epsilon &= \frac{-2.372 \pm \sqrt{(2.372)^2 - 4(1)(1.005)}}{(2)(1)} & (22.3.6.129) \\
 &= -1.186 \pm 0.634 & (22.3.6.130) \\
 &= -1.820, \text{ and } -0.552. & (22.3.6.131)
 \end{aligned}$$

Solving for the coefficients:

$$\begin{bmatrix} -1,804 - \varepsilon & 0.140 \\ 0.140 & -0.568 - \varepsilon \end{bmatrix} \begin{bmatrix} C_1 \\ C_2 \end{bmatrix} = \begin{bmatrix} 0 \\ 0 \end{bmatrix} \quad (22.3.6.132)$$

For the first eigenvalue this becomes:

$$\begin{bmatrix} -1.804 + 1.820 & 0.140 \\ 0.140 & -0.568 + 1.820 \end{bmatrix} \begin{bmatrix} C_1 \\ C_2 \end{bmatrix} = \begin{bmatrix} 0 \\ 0 \end{bmatrix} \quad (22.3.6.133)$$

$$\begin{bmatrix} 0.016 & 0.140 \\ 0.140 & 1.252 \end{bmatrix} \begin{bmatrix} C_1 \\ C_2 \end{bmatrix} = \begin{bmatrix} 0 \\ 0 \end{bmatrix} \quad (22.3.6.134)$$

$$(0.140)(C_1) + (1.252)(C_2) = 0 \quad (22.3.6.135)$$

$$C_1 = -8.943C_2 \quad (22.3.6.136)$$

$$C_1^2 + C_2^2 = 1 \text{ (from normalization)} \quad (22.3.6.137)$$

$$(-8.943C_2)^2 + C_2^2 = 1 \quad (22.3.6.138)$$

$$80.975C_2^2 = 1 \quad (22.3.6.139)$$

$$C_2 = 0.111, C_1 = -0.994 \quad (22.3.6.140)$$

For the second eigenvalue this becomes:

$$\begin{bmatrix} -1.804 + 0.552 & 0.140 \\ 0.140 & -0.568 + 0.552 \end{bmatrix} \begin{bmatrix} C_1 \\ C_2 \end{bmatrix} = \begin{bmatrix} 0 \\ 0 \end{bmatrix} \quad (22.3.6.141)$$

$$\begin{bmatrix} -1.252 & 0.140 \\ 0.140 & -0.016 \end{bmatrix} \begin{bmatrix} C_1 \\ C_2 \end{bmatrix} = \begin{bmatrix} 0 \\ 0 \end{bmatrix} \quad (22.3.6.142)$$

$$(-1.252)(C_1) + (0.140)(C_2) = 0 \quad (22.3.6.143)$$

$$C_1 = 0.112C_2 \quad (22.3.6.144)$$

$$C_1^2 + C_2^2 = 1 \text{ (from normalization)} \quad (22.3.6.145)$$

$$(0.112C_2)^2 + C_2^2 = 1 \quad (22.3.6.146)$$

$$1.0125C_2^2 = 1 \quad (22.3.6.147)$$

$$C_2 = 0.994, C_1 = 0.111 \quad (22.3.6.148)$$

e. The polarized orbitals, R_{\pm} , are given by:

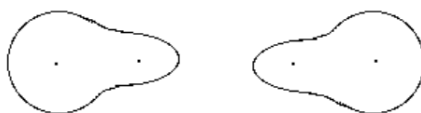
$$R_{\pm} = \sigma_g \pm \sqrt{\frac{C_2}{C_1}} \sigma_u \quad (22.3.6.149)$$

$$R_{\pm} = \sigma_g \pm \sqrt{\frac{0.111}{0.994}} \sigma_u \quad (22.3.6.150)$$

$$R_{\pm} = \sigma_g \pm 0.334\sigma_u \quad (22.3.6.151)$$

$$R_+ = \sigma_g + 0.334\sigma_u \text{ (left polarized)} \quad (22.3.6.152)$$

$$R_- = \sigma_g - 0.334\sigma_u \text{ (right polarized)} \quad (22.3.6.153)$$



R_+ Left Polarized

R_- Right Polarized

This page titled 22.3.6: vi. Problem Solutions is shared under a CC BY-NC-SA 4.0 license and was authored, remixed, and/or curated by Jack Simons via source content that was edited to the style and standards of the LibreTexts platform.

SECTION OVERVIEW

22.4: Molecular Rotation and Vibration

Topic hierarchy

[22.4.1: i. Exercises](#)

[22.4.2: ii. Problems](#)

[22.4.3: iii. Exercise Solutions](#)

[22.4.4: iv. Problem Solutions](#)

This page titled [22.4: Molecular Rotation and Vibration](#) is shared under a [CC BY-NC-SA 4.0](#) license and was authored, remixed, and/or curated by [Jack Simons](#) via [source content](#) that was edited to the style and standards of the LibreTexts platform.

22.4.1: i. Exercises

Q1

Consider the molecules CCl_4 , $CHCl_3$, and CH_2Cl_2 .

- What kind of rotor are they (symmetric top, ect; do not bother with oblate, or near-prolate, etc.)
- Will they show pure rotational spectra?
- Assume that ammonia shows a pure rotational spectrum. If the rotational constants are 9.44 and 6.20 cm^{-1} , use the energy expression:

$$E = (A - B)K^2 + BJ(J + 1),$$

to calculate the energies (in cm^{-1}) of the first three lines (i.e., those with lowest K, J quantum number for the absorbing level) in the absorption spectrum (ignoring higher order terms in the energy expression).

Q2

The molecule $^{11}B^{16}O$ has a vibrational frequency $\omega_e = 1885 \text{ cm}^{-1}$, a rotational constant $B - e = 1,78 \text{ cm}^{-1}$, and a bond energy from the bottom of the potential well of $D_e^0 = 8.28 \text{ eV}$.

Use integral atomic masses in the following:

- In the approximation that the molecule can be represented as a Morse oscillator, calculate the bond length, R_e in angstroms, the centrifugal distortion constant, D_e in cm^{-1} , the anharmonicity constant, $\omega_e X_e$ in cm^{-1} , the zero-point corrected bond energy, D_0^0 in eV, the vibrational rotation interaction constant, α_e in cm^{-1} , and the vibrational state specific rotation constants, B_0 and B_1 in cm^{-1} . Use the vibration-rotation energy expression for a Morse oscillator:

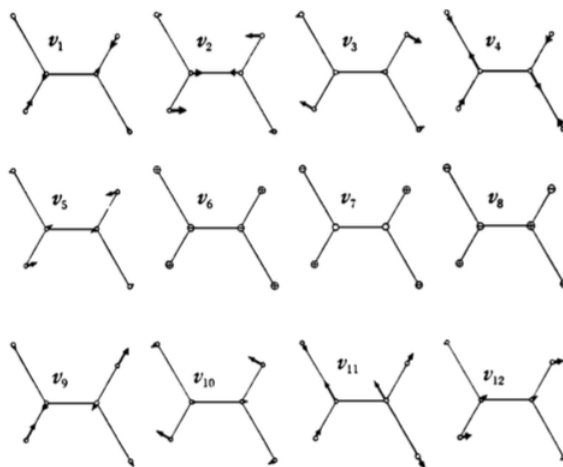
$$E = \hbar\omega_e \left(v + \frac{1}{2} \right) - \hbar\omega_e X_e \left(v + \frac{1}{2} \right)^2 + B_v J(J + 1) - D_e J^2(J + 1)^2, \text{ where} \quad (22.4.1.1)$$

$$B_v = B_e - \alpha_e \left(v + \frac{1}{2} \right), \alpha_e = \frac{-6B_e^2}{\hbar\omega_e} + \frac{6\sqrt{B_e^3 \hbar\omega_e X_e}}{\hbar\omega_e}, \text{ and } D_e = \frac{4B_e^3}{\hbar\omega_e^2} \quad (22.4.1.2)$$

- Will this molecule show a pure rotation spectrum? A vibration-rotation spectrum? Assume that it does, what are the energies (in cm^{-1}) of the first three lines in the P branch ($\Delta v = +1, \Delta J = -1$) of the fundamental absorption?

Q3

Consider trans- $C_2H_2Cl_2$. The vibrational normal modes of this molecule are shown below. What is the symmetry of the molecule? Label each of the modes with the appropriate irreducible representation.

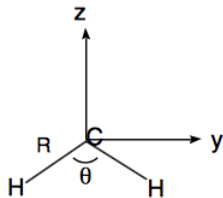


This page titled [22.4.1: i. Exercises](#) is shared under a [CC BY-NC-SA 4.0](#) license and was authored, remixed, and/or curated by [Jack Simons](#) via [source content](#) that was edited to the style and standards of the LibreTexts platform.

22.4.2: ii. Problems

Q1

Suppose you are given two molecules (one is CH_2 and the other is CH_2^- but you don't know which is which). Both molecules have C_{2v} symmetry. The CH bond length of molecule I is 1.121 Å and for molecule II it is 1.076 Å. The bond angle of molecule I is 104° and for molecule II it is 136° .



a. Using a coordinate system centered on the C nucleus as shown above (the molecule is in the YZ plane), compute the moment of inertia tensors of both species (I and II). The definitions of the components of the tensor are, for example:

$$I_{xx} = \sum_j m_j (y_j^2 + z_j^2) - M(Y^2 + Z^2) \quad (22.4.2.1)$$

$$I_{xy} = -\sum_j m_j x_j y_j - MXY \quad (22.4.2.2)$$

Here, m_j is the mass of the nucleus j , M is the mass of the entire molecule, and X, Y, Z are the coordinates of the center of mass of the molecule. Use Å for distances and amu's for masses.

b. Find the principal moment of inertia I_a, I_b, I_c for both compounds (in amu Å² units) and convert these values into rotational constants $A, B,$ and C in cm^{-1} using, for example,

$$A = \frac{h}{8\pi^2 c I_a}.$$

c. Both compounds are "nearly prolate tops" whose energy levels can be well approximated using the prolate top formula:

$$E = (A - B)K^2 + BJ(J + 1),$$

if one uses for the B constant the average of the B and C values determined earlier. Thus, take B and C values (for each compound) and average them to produce an effective B constant to use in the above energy formula. Write down (in cm^{-1} units) the energy formula for both species. What values are J and K allowed to assume? What is the degeneracy of the level labeled by a given J and K ?

d. Draw a picture of both compounds and show the directions of the three principle axes (a, b, c). On these pictures show the kind of rotational motion associated with the quantum number K .

e. Given that the electrical **transition** moment vector $\vec{\mu}$ connecting species I and II is directed along the Y axis, what are the selection rules J and K ?

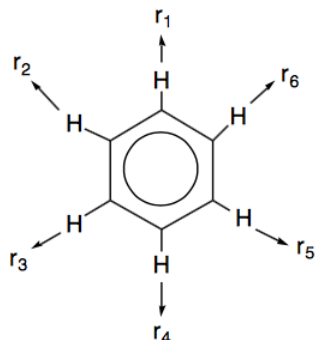
f. Suppose you are given the photoelectron spectrum of CH_2^- . In this spectrum $J_j = J_i + 1$ transitions are called R-branch absorptions and those obeying $J_j = J_i - 1$ are called P-branch transitions. The spacing between lines can increase or decrease as functions of J_i depending on the changes in the moment of inertia for the transition. If spacings grow closer and closer, we say that the spectrum exhibits a so-called band head formation. In the photoelectron spectrum that you are given, a rotational analysis of the vibrational lines in this spectrum is carried out and it is found that the R-branches show band head formation but the P-branches do not. Based on this information, determine which compound I or II is the CH_2^- anion. Explain your reasoning.

g. At what J value (of the absorbing species) does the band head occur and at what rotational energy difference?

Q2

Let us consider the vibrational motions of benzene. To consider all of the vibrational modes of benzene we should attach a set of displacement vectors in the x, y, and z directions to each atom in the molecule (giving 36 vectors in all), and evaluate how these transform under the symmetry operations of D_{6h} . For this problem, however, let's only inquire about the C-H stretching vibrations.

a. Represent the C-H stretching motion on each C-H bond by an outward-directed vector on each H atom, designated r_i :



These vectors form the basis for a reducible representation. Evaluate the characters for this reducible representation under the symmetry operations of the D_{6h} group.

b. Decompose the reducible representation you obtained in part a. into its irreducible components. These are the symmetries of the various C-H stretching vibrational modes in benzene.

c. The vibrational state with zero quanta in each of the vibrational modes (the ground vibrational state) of any molecule always belongs to the totally symmetric representation. For benzene the ground vibrational state is therefore of A_{1g} symmetry. An excited state which has one quantum of vibrational excitation in a mode which is of a given symmetry species has the same symmetry species as the mode which is excited (because the vibrational wave functions are given as Hermite polynomials in the stretching coordinate). Thus, for example, excitation (by one quantum) of a vibrational mode of A_{2u} symmetry gives a wavefunction of A_{2u} symmetry. To resolve the question of what vibrational modes may be excited by the absorption of infrared radiation we must examine the x, y, and z components of the transition dipole integral for initial and final state wave functions ψ_i and ψ_f , respectively:

$$|\langle \psi_f | x | \psi_i \rangle|, |\langle \psi_f | y | \psi_i \rangle|, \text{ and } |\langle \psi_f | z | \psi_i \rangle|.$$

Using the information provided above, which of the C-H vibrational modes of benzene will be infrared-active, and how will the transitions be polarized? How many C-H vibrations will you observe in the infrared spectrum of benzene?

d. A vibrational mode will be active in Raman spectroscopy only if one of the following integrals is nonzero:

$$|\langle \psi_f | xy | \psi_i \rangle|, |\langle \psi_f | xz | \psi_i \rangle|, |\langle \psi_f | yz | \psi_i \rangle|, \quad (22.4.2.3)$$

$$|\langle \psi_f | x^2 | \psi_i \rangle|, |\langle \psi_f | y^2 | \psi_i \rangle|, \text{ and } |\langle \psi_f | z^2 | \psi_i \rangle|. \quad (22.4.2.4)$$

Using the fact that the quadratic operators transform according to the irreducible representations:

$$(x^2 + y^2, z^2) \Rightarrow A_{1g} \quad (22.4.2.5)$$

$$(xz, yz) \Rightarrow E_{1g} \quad (22.4.2.6)$$

$$(x^2 - y^2, xy) \Rightarrow E_{2g} \quad (22.4.2.7)$$

Determine which of the C-H vibrational modes will be Raman-active.

e. Are there any of the C-H stretching vibrational motions of benzene which cannot be observed in either infrared or Raman spectroscopy? Give the irreducible representation label for these unobservable modes.

Q3

In treating the vibrational and rotational motion of a diatomic molecule having reduced mass μ , equilibrium bond length r_e and harmonic force constant k , we are faced with the following radial Schrödinger equation:

$$\frac{-\hbar^2}{2\mu r^2} \frac{d}{dr} \left(r^2 \frac{dR}{dr} \right) + \frac{J(J+1)\hbar^2}{2\mu r^2} R + \frac{1}{2} k(r-r_e)^2 R = ER$$

a. Show that the substitution $R = \frac{F}{r}$ leads to:

$$\frac{-\hbar^2}{2\mu} F'' + \frac{J(J+1)\hbar^2}{2\mu r^2} F + \frac{1}{2} k(r-r_e)^2 F = EF$$

b. Taking $r = r_e + \Delta r$ and expanding $\frac{1}{(1+x)^2} = 1 - 2x + 3x^2 + \dots$,

show that so-called vibration-rotation coupling term $\frac{J(J+1)\hbar^2}{2\mu r^2}$ can be approximated (for small Δr) by $\frac{J(J+1)\hbar^2}{2\mu r_e^2} \left(1 - \frac{2\Delta r}{r_e} + \frac{3\Delta r^2}{r_e^2} \right)$.

Keep terms only through order Δr^2 .

c. Show that, through terms of order Δr^2 , the above equation for F can be rearranged to yield a new equation of the form:

$$\frac{-\hbar^2}{2\mu} F'' + \frac{1}{2} \bar{k}(r - \bar{r}_e)^2 F = \left(E - \frac{J(J+1)\hbar^2}{2\mu r_e^2} + \Delta \right) F$$

Give explicit expressions for how the modified force constant \bar{k} , bond length \bar{r}_e , and energy shift Δ depend on J , k , r_e and μ .

d. Given the above modified vibrational problem, we can now conclude that the modified energy levels are:

$$E = \hbar \sqrt{\frac{\bar{k}}{\mu}} \left(v + \frac{1}{2} \right) + \frac{J(J+1)\hbar^2}{2\mu r_e^2} - \Delta.$$

Explain how the conclusion is "obvious", how for $J = 0$, $k = \bar{k}$, and $\Delta = 0$, we obtain the usual harmonic oscillator energy levels. Describe how the energy levels would be expected to vary as J increases from zero and explain how these changes arise from changes in k and r_e . Explain in terms of physical forces involved in the rotating-vibrating molecule why r_e and k are changed by rotation.

This page titled [22.4.2: ii. Problems](#) is shared under a [CC BY-NC-SA 4.0](#) license and was authored, remixed, and/or curated by [Jack Simons](#) via [source content](#) that was edited to the style and standards of the LibreTexts platform.

22.4.3: iii. Exercise Solutions

Q1

- a. CCl_4 is tetrahedral and therefore is a spherical top. $CHCl_3$ has C_{3v} symmetry and therefore is a symmetric top. CH_2Cl_2 has C_{2v} symmetry and therefore is an asymmetric top.
- b. CCl_4 has such high symmetry that it will not exhibit pure rotational spectra. $CHCl_3$ and CH_2Cl_2 will both exhibit pure rotation spectra.
- c. NH_3 is a symmetric top (oblate). Use the given energy expression,

$$E = (A - B)K^2 + BJ(J + 1),$$

$A = 6.20 \text{ cm}^{-1}$, $B = 9.44 \text{ cm}^{-1}$, selection rules $\Delta J = \pm 1$, and the fact that $\vec{\mu}_0$ lies along the figure axis such that $\Delta K = 0$, to give:

$$\Delta E = 2B(J + 1) = 2B, 4B, \text{ and } 6B (J = 0, 1, \text{ and } 2).$$

So, lines are at 18.88 cm^{-1} , 37.76 cm^{-1} , and 56.64 cm^{-1} .

Q2

To convert between cm^{-1} and energy, multiply by $hc = 6.62618 \times 10^{-34} \text{ J sec} (2.997925 \times 10^{10} \text{ cm sec}^{-1}) = 1.9865 \times 10^{-23} \text{ J cm}$

Let all quantities in cm^{-1} be designated with a bar,

e.g. $\bar{B}_e = 1.78 \text{ cm}^{-1}$.

a.

$$hc\bar{B}_e = \frac{\hbar^2}{2\mu R_e^2} \quad (22.4.3.1)$$

$$R_e = \frac{\hbar}{\sqrt{2\mu hc\bar{B}_e}}, \quad (22.4.3.2)$$

$$\mu = \frac{m_B m_O}{m_B + m_O} = \frac{(11)(16)}{(11+16)} \times 1.66056 \times 10^{-27} \text{ kg} \quad (22.4.3.3)$$

$$= 1.0824 \times 10^{-26} \text{ kg} \quad (22.4.3.4)$$

$$hc\bar{B}_e = hc(1.78 \text{ cm}^{-1} = 3.5359 \times 10^{-23} \text{ J} \quad (22.4.3.5)$$

$$R_e = \frac{1.05459 \times 10^{-34} \text{ J sec}}{\sqrt{(2)(1.0824 \times 10^{-26} \text{ kg})(3.5359 \times 10^{-23} \text{ J})}} \quad (22.4.3.6)$$

$$R_e = 1.205 \times 10^{-10} \text{ m} = 1.205 \text{ \AA} \quad (22.4.3.7)$$

$$D_e = \frac{4B_e^3}{\hbar\omega_e^2}, \bar{D}_e = \frac{4\bar{B}_e^3}{\bar{\omega}_e^2} = \frac{(4)(1.78 \text{ cm}^{-1})^3}{(4)(66782.2 \text{ cm}^{-1})} = 6.35 \times 10^{-6} \text{ cm}^{-1} \quad (22.4.3.8)$$

$$\omega_e x_e = \frac{\hbar\omega_e^2}{4D_e^0}, \omega_e \bar{x}_e = \frac{\bar{\omega}_e^2}{4\bar{D}_e^0} = \frac{(1885 \text{ cm}^{-1})^2}{(4)(66782.2 \text{ cm}^{-1})} = 13.30 \text{ cm}^{-1}. \quad (22.4.3.9)$$

$$D_0^0 = D_e^0 - \frac{\hbar\omega_e}{2} + \frac{\hbar\omega_e x_e}{4}, \bar{D}_0^0 = \bar{D}_e^0 - \frac{\omega_e}{2} + \frac{\omega_e \bar{x}_e}{4} \quad (22.4.3.10)$$

$$= 66782.2 - \frac{1885}{2} + \frac{13.3}{4} \quad (22.4.3.11)$$

$$= 65843.0 \text{ cm}^{-1} = 8.16 \text{ eV}. \quad (22.4.3.12)$$

$$\alpha_e = \frac{-6B_e^2}{\hbar\omega_e} + \frac{6\sqrt{B_e^3 \hbar\omega_e x_e}}{\hbar\omega_e} \quad (22.4.3.13)$$

$$\bar{\alpha}_e = \frac{-6\bar{B}_e^2}{\bar{\omega}_e} + \frac{6\sqrt{\bar{B}_e^3 \omega_e \bar{x}_e}}{\bar{\omega}_e} \quad (22.4.3.14)$$

$$\bar{\alpha}_e = \frac{(-6)(1.78)^2}{(1885)} + \frac{6\sqrt{(1.78)^3(13.3)}}{(1885)} = 0.0175 \text{ cm}^{-1}. \quad (22.4.3.15)$$

$$B_0 = B_e - \alpha_e \left(\frac{1}{2} \right), \bar{B}_0 = \bar{B}_e - \bar{\alpha}_e \left(\frac{1}{2} \right) = 1.78 - \frac{0.0175}{2} \quad (22.4.3.16)$$

$$= 1.77 \text{ cm}^{-1} \quad (22.4.3.17)$$

$$B_1 = B_e - \alpha_e \left(\frac{3}{2} \right), \bar{B}_1 = \bar{B}_e - \bar{\alpha}_e \left(\frac{3}{2} \right) = 1.78 - 0.0175(1.5) \quad (22.4.3.18)$$

$$= 1.75 \text{ cm}^{-1} \quad (22.4.3.19)$$

b. The molecule has a dipole moment and so it should have a pure rotational spectrum. In addition, the dipole moment should change with R and so it should have a vibration rotation spectrum.

The first three lines correspond to $J = 1 \rightarrow 0, J = 2 \rightarrow 1, J = 3 \rightarrow 2$

$$E = \hbar\omega_e \left(v + \frac{1}{2} \right) - \hbar\omega_e x_e \left(v + \frac{1}{2} \right)^2 + B_v J(J+1) - D_v J^2(J+1)^2 \quad (22.4.3.20)$$

$$\Delta E = \hbar\omega_e - 2\hbar\omega_e x_e - B_0 J(J+1) + B_1 J(J-1) - 4D_e J^3 \quad (22.4.3.21)$$

$$\Delta \bar{E} = \bar{\omega}_e - 2\omega_e \bar{x}_e - \bar{B}_0 J(J+1) + \bar{B}_1 J(J-1) - 4\bar{D}_e J^3 \quad (22.4.3.22)$$

$$\Delta \bar{E} = 1885 - 2(13.3) - 1.77 J(J+1) + 1.75 J(J-1) - 4(6.35 \times 10^{-6}) J^3 \quad (22.4.3.23)$$

$$= 1858.4 - 1.77 J(J+1) + 1.75 J(J-1) - 2.54 \times 10^{-5} J^3 \quad (22.4.3.24)$$

$$\Delta \bar{E}(J=1) = 1854.9 \text{ cm}^{-1} \quad (22.4.3.25)$$

$$\Delta \bar{E}(J=2) = 1851.3 \text{ cm}^{-1} \quad (22.4.3.26)$$

$$\Delta \bar{E}(J=3) = 1847.7 \text{ cm}^{-1} \quad (22.4.3.27)$$

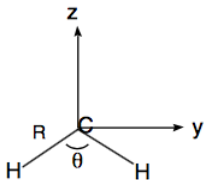
Q3

The $C_2H_2Cl_2$ molecule has a σ_h plane of symmetry (plane of molecule) a C_2 axis (\perp to plane), and inversion symmetry, this result in C_{2h} symmetry. Using C_{2h} symmetry labels the modes can be labeled as follows: $\nu_1, \nu_2, \nu_3, \nu_4$, and ν_5 are a_g , ν_6 and ν_7 are a_u , ν_8 is b_g , and $\nu_9, \nu_{10}, \nu_{11}$, and ν_{12} are b_u .

This page titled [22.4.3: iii. Exercise Solutions](#) is shared under a [CC BY-NC-SA 4.0](#) license and was authored, remixed, and/or curated by [Jack Simons](#) via [source content](#) that was edited to the style and standards of the LibreTexts platform.

22.4.4: iv. Problem Solutions

Q1



Molecule I

$$R_{CH} = 1.121 \text{ \AA}$$

$$\angle_{HCH} = 104^\circ$$

$$y_H = R \sin\left(\frac{\theta}{2}\right) = \pm 0.8834$$

$$z_H = R \cos\left(\frac{\theta}{2}\right) = -0.2902$$

Center of Mass (COM):

$$Z = \frac{12(0) - 2R \cos\left(\frac{\theta}{2}\right)}{14} = -0.0986$$

Molecule II

$$R_{CH} = 1.076 \text{ \AA}$$

$$\angle_{HCH} = 136^\circ$$

$$y_H = \pm 0.9976$$

$$z_H = -0.4031$$

clearly, $X = Y = 0$,

$$Z = -0.0576$$

(22.4.4.1)

(22.4.4.2)

(22.4.4.3)

(22.4.4.4)

(22.4.4.5)

(22.4.4.6)

(22.4.4.7)

a.

$$I_{xx} = \sum_j m_j (y_j^2 + z_j^2) - M(Y^2 + Z^2) \quad (22.4.4.8)$$

$$T_{xy} = -\sum_j m_j x_j y_j - MXY \quad (22.4.4.9)$$

$$I_{xx} = 2(1.121)^2 - 14(-0.0986)^2 \quad I_{xx} = 2(1.076)^2 - 14(-0.0576)^2 \quad (22.4.4.10)$$

$$= 2.377 \quad = 2.269 \quad (22.4.4.11)$$

$$I_{yy} = 2(0.6902)^2 - 14(-0.0986)^2 \quad I_{yy} = 2(0.4031)^2 - 14(-0.0576)^2 \quad (22.4.4.12)$$

$$= 0.8167 \quad = 0.2786 \quad (22.4.4.13)$$

$$I_{zz} = 2(0.8834)^2 \quad I_{zz} = 2(0.9976)^2 \quad (22.4.4.14)$$

$$= 1.561 \quad = 1.990 \quad (22.4.4.15)$$

$$I_{xz} = I_{yz} = I_{xy} = 0 \quad (22.4.4.16)$$

b. Since the moment of inertia tensor is already diagonal, the principal moments of inertia have already been determined to be

$$(I_a \langle I_b \langle I_c) : \quad (22.4.4.17)$$

$$I_{yy} \langle I_{zz} \langle I_{xx} \quad I_{yy} \langle I_{zz} \langle I_{xx} \quad (22.4.4.18)$$

$$0.8167 \langle 1.561 \langle 2.377 \quad 0.2786 \langle 1.990 \langle 2.269 \quad (22.4.4.19)$$

$$\text{Using the formula: } A = \frac{h}{8\pi^2 c I_a} = \frac{6.62 \times 10^{-27}}{8\pi^2 (3 \times 10^{10}) I_a}$$

$$A = \frac{16.84}{I_a} \text{cm}^{-1}$$

similarly, $B = \cdot \text{cm}^{-1}$, and $C = \frac{16.84}{I_c} \text{cm}^{-1}$.

So,

$$\text{Molecule I} \qquad \text{Molecule II} \qquad (22.4.4.20)$$

$$y \Rightarrow A = 20.62 \qquad y \Rightarrow A = 60.45 \qquad (22.4.4.21)$$

$$z \Rightarrow B = 10.79 \qquad z \Rightarrow B = 8.46 \qquad (22.4.4.22)$$

$$x \Rightarrow C = 7.08 \qquad x \Rightarrow C = 7.42 \qquad (22.4.4.23)$$

c. Averaging B + C:

$$B = B \frac{B+C}{2} = 8.94 \qquad B = \frac{B+C}{2} = 7.94 \qquad (22.4.4.24)$$

$$A - B = 11.68 \qquad A - B = 52.51 \qquad (22.4.4.25)$$

Using the Prolate top formula

$$E = (A - B)K^2 + BJ(J+1),$$

$$\text{Molecule I} \qquad \text{Molecule II} \qquad (22.4.4.26)$$

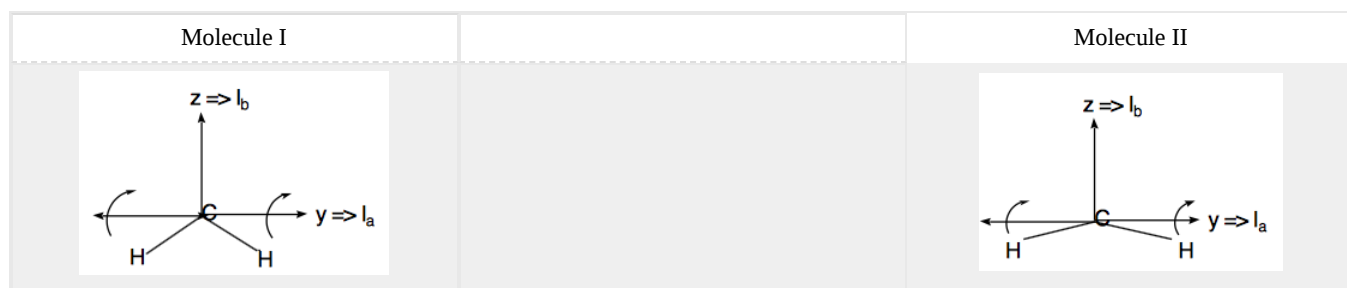
$$E = 11.68K^2 + 8.94J(J+1) \qquad E = 52.51K^2 + 7.94J(J+1) \qquad (22.4.4.27)$$

Levels: $J = 0, 1, 2, \dots$ and $K = 0, 1, \dots J$

For a given level defined by J and K , there are M_J degeneracies given by: $(2J + 1) \times$

$$\begin{cases} 1 \text{ for } K = 0 \\ 2 \text{ for } K \neq 0 \end{cases} \qquad (22.4.4.28)$$

d.



e. Since $\vec{\mu}$ is along Y, $\Delta K = 0$ since K describes rotation about the y axis.

Therefore $\Delta J = \pm 1$

f. **Assume** molecule I is CH_2^- and molecule II is CH_2 . Then, $\Delta E = E_{J_j}(\text{CH}_2)$, where:

$E(\text{CH}_2) = 52.51K^2 + 7.94J(J+1)$, and $E(\text{CH}_2^-) = 11.68K^2 + 8.94J(J+1)$

For R-branches: $J_j = J_i + 1$, $\Delta K = 0$;

$$\begin{aligned}
 \Delta E_R &= E_{J_i}(CH_2) - E_{J_i}(CH_2) & (22.4.4.29) \\
 &= 7.94(J_i + 1)(J_i + 1 + 1) - 8.94J_i(J_i + 1) & (22.4.4.30) \\
 &= (J_i + 1)\{7.94(J_i + 1 + 1) - 8.94J_i\} & (22.4.4.31) \\
 &= (J_i + 1)\{(7.94 - 8.94)J_i + 2(7.94)\} & (22.4.4.32) \\
 &= (J_i + 1)\{-J_i + 15.88\} & (22.4.4.33)
 \end{aligned}$$

For P-branches: $J_j - 1, \Delta K = 0$;

$$\begin{aligned}
 \Delta E_P &= E_{J_i}(CH_2) - E_{J_i}(CH_2) & (22.4.4.34) \\
 &= 7.94(J_i - 1)(J_i - 1 + 1) - 8.94J_i(J_i + 1) & (22.4.4.35) \\
 &= J_i\{7.94(J_i - 1) - 8.94(J_i + 1)\} & (22.4.4.36) \\
 &= J_i\{(7.94 - 8.94)J_i - 7.94 - 8.94\} & (22.4.4.37) \\
 &= J_i\{-J_i - 16.88\} & (22.4.4.38)
 \end{aligned}$$

This indicates that the R branch lines occur at energies which grow closer and closer together as J increases (since the $15.88 - J_i$ term will cancel). The P branch lines occur at energies which lie more and more negative (i.e. to the left of the origin). So, you can predict that if molecule I is CH_2^- and molecule II is CH_2 then the R-branch has a band head and the P-branch does not. This is observed therefore our assumption was correct:

molecule I is CH_2^- and molecule II is CH_2 .

g. The band head occurs when $\frac{d(\Delta E_R)}{dJ} = 0$.

$$\frac{d(\Delta E_R)}{dJ} = \frac{d}{dJ}[(J_i + 1)\{-J_i + 15.88\}] = 0 \quad (22.4.4.39)$$

$$= \frac{d}{dJ}(-J_i^2 - J_i + 15.88J_i + 15.88) = 0 \quad (22.4.4.40)$$

$$= -2J_i + 14.88 = 0 \quad (22.4.4.41)$$

$$\therefore J_i = 7.44, \text{ so } J = 7 \text{ or } 8. \quad (22.4.4.42)$$

At $J = 7.44$:

$$\Delta E_R = (J + 1)\{-J + 15.88\} \quad (22.4.4.43)$$

$$\Delta E_R = (7.44 + 1)\{-7.44 + 15.88\} = (8.44)(8.44) = 71.2\text{cm}^{-1} \text{ above the origin.} \quad (22.4.4.44)$$

Q2

a.

D _{6h}	E	2C ₆	2C ₃	C ₂	3C ₂ '	3C ₂ "	i	2S ₃	2S ₆	σ _h	3σ _d	3σ _v		
A _{1g}	1	1	1	1	1	1	1	1	1	1	1	1	R _z	x ² +y ² , z ²
A _{2g}	1	1	1	1	-1	-1	1	1	1	1	-1	-1		
B _{1g}	1	-1	1	-1	1	-1	1	-1	1	-1	1	-1		
B _{2g}	1	-1	1	-1	-1	1	1	-1	1	-1	-1	1		
E _{1g}	2	1	-1	-2	0	0	2	1	-1	-2	0	0	(R _x , R _y)	(xz, yz) (x ² -y ² , xy)
E _{2g}	2	-1	-1	2	0	0	2	-1	-1	2	0	0		
A _{1u}	1	1	1	1	1	1	-1	-1	-1	-1	-1	-1	z	
A _{2u}	1	1	1	1	-1	-1	-1	-1	-1	-1	1	1		
B _{1u}	1	-1	1	-1	1	-1	-1	1	-1	1	-1	1		
B _{2u}	1	-1	1	-1	-1	1	-1	1	-1	1	1	-1		
E _{1u}	2	1	-1	-2	0	0	-2	-1	1	2	0	0	(x, y)	
E _{2u}	2	-1	-1	2	0	0	-2	1	1	-2	0	0		
Γ _{C-H}	6	0	0	0	0	2	0	0	0	6	2	0		

b. The number of irreducible representations may be found by using the following formula:

$$n_{irrep} = \frac{1}{g} \sum_R \xi_{red}(R) \xi_{irrep}(R), \quad (22.4.4.45)$$

where g = the order of the point group (24 for D_{6h}). (22.4.4.46)

$$n_{A_{1g}} = \frac{1}{24} \sum_R \Gamma_{C-H}(R) A_{1g}(R) \quad (22.4.4.47)$$

$$= \frac{1}{24} \{ (1)(6)(1) + (2)(0)(1) + (2)(0)(1) + (1)(0)(1) + \dots \quad (22.4.4.48)$$

$$+ (3)(0)(1) + (3)(2)(1) + (1)(0)(1) + (2)(0)(1) + \dots \quad (22.4.4.49)$$

$$+ (2)(0)(1) + (1)(6)(1) + (3)(2)(1) + (3)(0)(1) \} \quad (22.4.4.50)$$

$$= 1 \quad (22.4.4.51)$$

$$n_{A_{2g}} = \frac{1}{24} \{ (1)(6)(1) + (2)(0)(1) + (2)(0)(1) + (1)(0)(1) + \dots \quad (22.4.4.52)$$

$$+ (3)(0)(-1) + (3)(2)(-1) + (1)(0)(1) + (2)(0)(1) + \dots \quad (22.4.4.53)$$

$$+ (2)(0)(1) + (1)(6)(1) + (3)(2)(-1) + (3)(0)(-1) \} \quad (22.4.4.54)$$

$$= 0 \quad (22.4.4.55)$$

$$n_{B_{1g}} = \frac{1}{24} \{ (1)(6)(1) + (2)(0)(-1) + (2)(0)(1) + (1)(0)(-1) + \dots \quad (22.4.4.56)$$

$$+ (3)(0)(1) + (3)(2)(-1) + (1)(0)(1) + (2)(0)(-1) + \dots \quad (22.4.4.57)$$

$$+ (2)(0)(1) + (1)(6)(-1) + (3)(2)(1) + (3)(0)(-1) \} \quad (22.4.4.58)$$

$$= 0 \quad (22.4.4.59)$$

$$n_{B_{2g}} = \frac{1}{24} \{ (1)(6)(1) + (2)(0)(-1) + (2)(0)(1) + (1)(0)(-1) + \dots \quad (22.4.4.60)$$

$$+ (3)(0)(-1) + (3)(2)(1) + (1)(0)(1) + (2)(0)(-1) + \dots \quad (22.4.4.61)$$

$$+ (2)(0)(1) + (1)(6)(-1) + (3)(2)(-1) + (3)(0)(1) \} \quad (22.4.4.62)$$

$$= 0 \quad (22.4.4.63)$$

$$n_{E_{1g}} = \frac{1}{24} \{ (1)(6)(2) + (2)(0)(1) + (2)(0)(-1) + (1)(0)(-2) + \dots \quad (22.4.4.64)$$

$$+ (3)(0)(0) + (3)(2)(0) + (1)(0)(2) + (2)(0)(1) + \dots \quad (22.4.4.65)$$

$$+ (2)(0)(-1) + (1)(6)(-2) + (3)(2)(0) + (3)(0)(0) \} \quad (22.4.4.66)$$

$$= 0 \quad (22.4.4.67)$$

$$n_{E_{2g}} = \frac{1}{24} \{ (1)(6)(2) + (2)(0)(-1) + (2)(0)(-1) + (1)(0)(2) + \dots \quad (22.4.4.68)$$

$$+ (3)(0)(0) + (3)(2)(0) + (1)(0)(2) + (2)(0)(-1) + \dots \quad (22.4.4.69)$$

$$\begin{aligned}
 & + (2)(0)(-1) + (1)(6)(2) + (3)(2)(0) + (3)(0)(0) \} & (22.4.4.70) \\
 = & 0 & (22.4.4.71) \\
 n_{A_{1u}} = & \frac{1}{24} \{ (1)(6)(1) + (2)(0)(1) + (2)(0)(1) + (1)(0)(1) + \dots & (22.4.4.72) \\
 & + (3)(0)(1) + (3)(2)(1) + (1)(0)(-1) + (2)(0)(-1) + \dots & (22.4.4.73) \\
 & + (2)(0)(-1) + (1)(6)(-1) + (3)(2)(-1) + (3)(0)(-1) \} & (22.4.4.74) \\
 = & 0 & (22.4.4.75) \\
 n_{A_{2u}} = & \frac{1}{24} \{ (1)(6)(1) + (2)(0)(1) + (2)(0)(1) + (1)(0)(1) + \dots & (22.4.4.76) \\
 & + (3)(0)(-1) + (3)(2)(-1) + (1)(0)(-1) + (2)(0)(-1) + \dots & (22.4.4.77) \\
 & + (2)(0)(-1) + (1)(6)(-1) + (3)(2)(1) + (3)(0)(1) \} & (22.4.4.78) \\
 = & 0 & (22.4.4.79) \\
 n_{B_{1u}} = & \frac{1}{24} \{ (1)(6)(1) + (2)(0)(-1) + (2)(0)(1) + (1)(0)(-1) + \dots & (22.4.4.80) \\
 & + (3)(0)(1) + (3)(2)(-1) + (1)(0)(-1) + (2)(0)(1) + \dots & (22.4.4.81) \\
 & + (2)(0)(-1) + (1)(6)(1) + (3)(2)(-1) + (3)(0)(1) \} & (22.4.4.82) \\
 = & 0 & (22.4.4.83) \\
 n_{B_{2u}} = & \frac{1}{24} \{ (1)(6)(1) + (2)(0)(-1) + (2)(0)(1) + (1)(0)(-1) + \dots & (22.4.4.84) \\
 & + (3)(0)(-1) + (3)(2)(1) + (1)(0)(-1) + (2)(0)(1) + \dots & (22.4.4.85) \\
 & + (2)(0)(-1) + (1)(6)(1) + (3)(2)(1) + (3)(0)(-1) \} & (22.4.4.86) \\
 = & 1 & (22.4.4.87) \\
 n_{E_{1u}} = & \frac{1}{24} \{ (1)(6)(2) + (2)(0)(1) + (2)(0)(-1) + (1)(0)(-2) + \dots & (22.4.4.88) \\
 & + (3)(0)(0) + (3)(2)(0) + (1)(0)(-2) + (2)(0)(-1) + \dots & (22.4.4.89) \\
 & + (2)(0)(1) + (1)(6)(2) + (3)(2)(0) + (3)(0)(0) \} & (22.4.4.90) \\
 = & 1 & (22.4.4.91) \\
 n_{E_{2u}} = & \frac{1}{24} \{ (1)(6)(2) + (2)(0)(-1) + (2)(0)(-1) + (1)(0)(2) + \dots & (22.4.4.92) \\
 & + (3)(0)(0) + (3)(2)(0) + (1)(0)(-2) + (2)(0)(1) + \dots & (22.4.4.93) \\
 & + (2)(0)(1) + (1)(6)(-2) + (3)(2)(0) + (3)(0)(0) \} & (22.4.4.94) \\
 = & 0 & (22.4.4.95)
 \end{aligned}$$

We see that $\Gamma_{C-H} = A_{1g} \oplus E_{2g} \oplus B_{2u} \oplus E_{1u}$

c. x and $y \Rightarrow E_{1u}$, $z \Rightarrow A_{2u}$, so, the ground state A_{1g} level can be excited to the degenerate E_{1u} level by coupling through the x or y transition dipoles. Therefore E_{1u} is infrared active and \perp polarized.

d. $(x^2 + y^2, z^2) \Rightarrow A_{1g}$, $(xz, yz) \Rightarrow E_{1g}$, $(x^2 - y^2, xy) \Rightarrow E_{2g}$, so, the ground state A_{1g} level can be excited to the degenerate E_{2g} level by coupling through the $x^2 - y^2$ or xy transitions or be excited to the degenerate A_{1g} level by coupling through the xz or yz transitions. Therefore A_{1g} and E_{2g} are Raman active.

Q3

a.

$$\frac{d}{dr} \left(\frac{F}{r} \right) = \frac{F'}{r} - \frac{F}{r^2} \quad (22.4.4.96)$$

$$r^2 \frac{d}{dr} \left(\frac{F}{r} \right) = rF' - F \quad (22.4.4.97)$$

$$\frac{d}{dr} \left(r^2 \frac{d}{dr} \left(\frac{F}{r} \right) \right) = F' - F' + rF'' \quad (22.4.4.98)$$

So,

$$\frac{-\hbar^2}{2\mu r^2} \frac{d}{dr} \left(r^2 \frac{d}{dr} \left(\frac{F}{r} \right) \right) = \frac{-\hbar^2}{2\mu} \frac{F''}{r} \quad (22.4.4.99)$$

Rewriting the radial Schrödinger equation with the substitution: $R = \frac{F}{r}$ gives:

$$\frac{-\hbar^2}{2\mu r^2} \frac{d}{dr} \left(r^2 \frac{d(Fr^{-1})}{dr} \right) + \frac{J(J+1)\hbar^2}{2\mu r^2} \left(\frac{F}{r} \right) + \frac{1}{2} k(r-r_e)^2 \left(\frac{F}{r} \right) = \left(\frac{F}{r} \right)$$

Using the above derived identity gives:

$$\frac{-\hbar^2}{2\mu} \frac{F''}{r} + \frac{J(J+1)\hbar^2}{2\mu r^2} \left(\frac{F}{r} \right) + \frac{1}{2} k(r-r_e)^2 \left(\frac{F}{r} \right) = E \left(\frac{F}{r} \right)$$

Cancelling out an r^{-1} :

$$\frac{-\hbar^2}{2\mu} F'' + \frac{J(J+1)\hbar^2}{2\mu r^2} F + \frac{1}{2} k(r-r_e)^2 F = EF$$

b.

$$\frac{1}{r^2} = \frac{1}{(r_e + \Delta r)^2} = \frac{1}{r_e^2 \left(1 + \frac{\Delta r}{r_e} \right)} \approx \frac{1}{r_e^2} \left(1 - \frac{2\Delta r}{r_e} + \frac{3\Delta r^2}{r_e^2} \right)$$

So,

$$\frac{J(J+1)\hbar^2}{2\mu r^2} \approx \frac{J(J+1)\hbar^2}{2\mu r_e^2} \left(1 - \frac{2\Delta r}{r_e} + \frac{3\Delta r^2}{r_e^2} \right)$$

c. Using this substitution we now have:

$$\frac{-\hbar^2}{2\mu} F'' + \frac{J(J+1)\hbar^2}{2\mu r_e^2} \left(1 - \frac{2\Delta r}{r_e} + \frac{3\Delta r^2}{r_e^2} \right) F + \frac{1}{2} k(r-r_e)^2 F = EF$$

Now, regroup the terms which are linear and quadratic in $\Delta r = r - r_e$:

$$\begin{aligned} & \frac{1}{2} k \Delta r^2 + \frac{J(J+1)\hbar^2}{2\mu r_e^2} \frac{3}{r_e^2} \Delta r^2 - \frac{J(J+1)\hbar^2}{2\mu r_e^2} \frac{2}{r_e} \Delta r \\ &= \left(\frac{1}{2} k + \frac{J(J+1)\hbar^2}{2\mu r_e^2} \frac{3}{r_e^2} \right) \Delta r^2 - \left(\frac{J(J+1)\hbar^2}{2\mu r_e^2} \frac{2}{r_e} \right) \Delta r \end{aligned}$$

Now, we must complete the square:

$$a\Delta r^2 - b\Delta r = a\left(\Delta r - \frac{b}{2a}\right)^2 - \frac{b^2}{4a}.$$

So,

$$\left(\frac{1}{2}k + \frac{J(J+1)\hbar^2}{2\mu r_e^2} \frac{3}{r_e^2}\right) \left(\Delta r - \frac{\frac{J(J+1)\hbar^2}{2\mu r_e^2} \frac{1}{r_e}}{\frac{1}{2}k + \frac{J(J+1)\hbar^2}{2\mu r_e^2} \frac{3}{r_e^2}}\right)^2 - \frac{\left(\frac{J(J+1)\hbar^2}{2\mu r_e^2} \frac{1}{r_e}\right)^2}{\frac{1}{2}k + \frac{J(J+1)\hbar^2}{2\mu r_e^2} \frac{3}{r_e^2}}$$

Now, redefine the first term as $\frac{1}{2}\bar{k}$, second term as $(r - \bar{r}_e)^2$, and the third term as $-\Delta$ giving:

$$\frac{1}{2}\bar{k}(r - \bar{r}_e)^2 - \Delta$$

From:

$$\frac{-\hbar^2}{2\mu}F'' + \frac{J(J+1)\hbar^2}{2\mu r_e^2} \left(1 - \frac{2\Delta r}{r_e} + \frac{3\Delta r^2}{r_e^2}\right) F + \frac{1}{2}k(r - r_e)^2 F = EF, \quad (22.4.4.100)$$

$$\frac{-\hbar^2}{2\mu}F'' + \frac{J(J+1)\hbar^2}{2\mu r_e^2} F + \left(\frac{J(J+1)\hbar^2}{2\mu r_e^2} \left(-\frac{2\Delta r}{r_e} + \frac{3\Delta r^2}{r_e^2}\right) + \frac{1}{2}k\Delta r^2\right) F = EF \quad (22.4.4.101)$$

and making the above substitution result in:

$$\frac{-\hbar^2}{2\mu}F'' + \frac{J(J+1)\hbar^2}{2\mu r_e^2} F + \left(\frac{1}{2}\bar{k}(r - \bar{r}_e)^2 - \Delta\right) F = EF,$$

or,

$$\frac{-\hbar^2}{2\mu}F'' + \frac{1}{2}\bar{k}(r - \bar{r}_e)^2 F = \left(E - \frac{J(J+1)\hbar^2}{2\mu r_e^2} + \Delta\right) F.$$

d. Since the above is nothing but a harmonic oscillator differential equation in x with force constant \bar{k} and equilibrium bond length \bar{r}_e , we know that:

$$\frac{-\hbar^2}{2\mu}F'' + \frac{1}{2}\bar{k}(r - \bar{r}_e)^2 F = \varepsilon F, \text{ has energy levels:} \quad (22.4.4.102)$$

$$\varepsilon = \hbar\sqrt{\frac{\bar{k}}{\mu}} \left(v + \frac{1}{2}\right), v = 0, 1, 2, \dots \quad (22.4.4.103)$$

So,

$$E + \Delta - \frac{J(J+1)\hbar^2}{2\mu r_e^2} = \varepsilon \quad (22.4.4.104)$$

tell us that:

$$E = \hbar \sqrt{\frac{\bar{k}}{\mu} \left(v + \frac{1}{2} \right)} + \frac{J(J+1)\hbar^2}{2\mu r_e^2} - \Delta. \quad (22.4.4.105)$$

As J increases, \bar{r}_e increases because of the centrifugal force pushing the two atoms apart. On the other hand \bar{k} increases which indicates that the molecule finds it more difficult to stretch against both the centrifugal and Hooke's Law (spring) Harmonic force field. The total energy level (labeled by J and v) will equal a rigid rotor component $\frac{J(J+1)\hbar^2}{2\mu r_e^2}$ plus a Harmonic oscillator part $\hbar \sqrt{\frac{\bar{k}}{\mu} \left(v + \frac{1}{2} \right)}$ (which has a force constant \bar{k} which increases with J).

This page titled [22.4.4: iv. Problem Solutions](#) is shared under a [CC BY-NC-SA 4.0](#) license and was authored, remixed, and/or curated by [Jack Simons](#) via [source content](#) that was edited to the style and standards of the LibreTexts platform.

SECTION OVERVIEW

22.5: Time Dependent Processes

Topic hierarchy

22.5.1: i. Exercises

22.5.2: ii. Problems

22.5.3: iii. Exercise Solutions

22.5.4: iv. Problem Solutions

This page titled [22.5: Time Dependent Processes](#) is shared under a [CC BY-NC-SA 4.0](#) license and was authored, remixed, and/or curated by [Jack Simons](#) via [source content](#) that was edited to the style and standards of the LibreTexts platform.

22.5.1: i. Exercises

Q1

Time dependent perturbation theory provides an expression for the radiative lifetime of an excited electronic state, given by τ_R :

$$\tau_R = \frac{3\hbar^4 c^3}{4(E_i - E_f)^3 |\mu_{fi}|^2},$$

where i refers to the excited state, f refers to the lower state, and μ_{fi} is the transition dipole.

a. Evaluate the z-component of the transition dipole for the $2p_z \rightarrow 1s$ transition in a hydrogenic atom of nuclear charge Z, given:

$$\psi_{1s} = \frac{1}{\sqrt{\pi}} \left(\frac{Z}{a_0} \right)^{3/2} e^{-Zr/a_0}, \text{ and } \psi_{2p_z} = \frac{1}{4\sqrt{2\pi}} \left(\frac{Z}{a_0} \right)^{5/2} r \cos\theta e^{-Zr/2a_0}$$

Express your answer in units of ea_0 .

b. Use symmetry to demonstrate that the x- and y-components of μ_{fi} are zero, i.e.

$$\langle 2p_z | ex | 1s \rangle = \langle 2p_z | ey | 1s \rangle = 0.$$

c. Calculate the radiative lifetime τ_R of a hydrogenlike atom in its $2p_z$ state. Use the relation $e^2 = \frac{\hbar^2}{m_e a_0}$ to simplify our results.

Q2

Consider a case in which the complete set of states $\{\phi_k\}$ for a Hamiltonian is known.

a. If the system is initially in the state m at time $t=0$ when a constant perturbation V is suddenly turned on, find the probability amplitudes $C_k^{(2)}(t)$ and $C_m^{(2)}(t)$, to second order in V, that describe the system being in a different state k or the same state m at time t.

b. If the perturbation is turned on adiabatically, what are $C_k^{(2)}(t)$ and $C_m^{(2)}(t)$?

Here, consider that the initial time is $t_0 \rightarrow -\infty$, and the potential is $V e^{\eta t}$, where the positive parameter η is allowed to approach zero $\eta \rightarrow 0$ in order to describe the adiabatically (i.e., slowly) turned on perturbation.

c. Compare the results of parts a. and b. and explain any differences.

d. Ignore first order contributions (assume they vanish) and evaluate the transition rates $\frac{d}{dt} |C_k^{(2)}(t)|^2$ for the results of part b. by taking the limits $\eta \rightarrow 0^+$, to obtain the adiabatic results.

Q3

If a system is initially in a state m, conservation of probability requires that the total probability of transitions out of state m be obtainable from the decrease in the probability of being in state m. Prove this to the lowest order by using the results of exercise 2, i.e. show that: $|C_m|^2 = 1 - \sum_{k \neq m} |C_k|^2$.

This page titled [22.5.1: i. Exercises](#) is shared under a [CC BY-NC-SA 4.0](#) license and was authored, remixed, and/or curated by [Jack Simons](#) via [source content](#) that was edited to the style and standards of the LibreTexts platform.

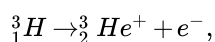
22.5.2: ii. Problems

Q1

Consider an interaction or perturbation which is carried out suddenly (instantaneously, e.g., within an interval of time Δt which is small compared to the natural period ω_{nm}^{-1} corresponding to the transition from state m to state n), and after that is turned off adiabatically (i.e., extremely slowly as $V e^{\eta t}$). The transition probability in this case is given as:

$$T_{nm} \approx \frac{|\langle n|V|m\rangle|^2}{\hbar^2 \omega_{nm}^2}$$

where V corresponds to the maximum value of the interaction when it is turned on. This formula allows one to calculate the transition probabilities under the action of sudden perturbations which are small in absolute value whenever perturbation theory is applicable. Let's use this "sudden approximation" to calculate the probability of excitation of an electron under a sudden change of the charge of the nucleus. Consider the reaction:



and assume the tritium atom has its electron initially in a 1s orbital.

- Calculate the transition probability for the transition $1s \rightarrow 2s$ for this reaction using the above formula for the transition probability.
- Suppose that at time $t = 0$ the system is in a state which corresponds to the wavefunction φ_m , which is an eigenfunction of the operator H_0 . At $t = 0$, the sudden change of the Hamiltonian occurs (now denoted as H and remains unchanged). Calculate the same $1s \rightarrow 2s$ transition probability as in part a., only this time as the square of the magnitude of the coefficient, $A_{1s,2s}$ using the expansion:

$$\Psi(r, 0) = \varphi_m(r) = \sum_n A_{nm} \psi_n(r), \text{ where } A_{nm} = \int \varphi_m(r) \psi_n(r) d^3r$$

Note, that the eigenfunctions of H are ψ_n with eigenvalues E_n . Compare this "exact" value with that obtained by perturbation theory in part a.

Q2

The methyl iodide molecule is studied using microwave (pure rotational) spectroscopy. The following integral governs the rotational selection rules for transitions labeled $J, M, K \rightarrow J', M', K'$:

$$I = \langle D_{M'K'}^{J'} | \vec{\epsilon} \cdot \vec{\mu} | D_{MK}^J \rangle.$$

The dipole moment $\vec{\mu}$ lies along the molecule's C_3 symmetry axis. Let the electric field of the light $\vec{\epsilon}$ define the lab-fixed Z -direction.

- Using the fact that $\cos\beta = D_{00}^{1*}$, show that

$$I = 8\pi^2 \mu \epsilon (-1)^{(M+K)} \begin{pmatrix} J' & 1 & J \\ M & 0 & M \end{pmatrix} \begin{pmatrix} J' & 1 & J \\ K & 0 & K \end{pmatrix} \delta_{M'M} \delta_{K'K}$$

- What restrictions does this result place on $\Delta J = J' - J$? Explain physically why the K quantum number can not change.

Q3

Consider the molecule BO.

- What are the total number of possible electronic states which can be formed by combination of ground state B and O atoms?
- What electron configurations of the molecule are likely to be low in energy? Consider all reasonable orderings of the molecular

orbitals. What are the states corresponding to these configurations?

c. What are the bond orders in each of these states?

d. The true ground state of BO is $^2\Sigma$. Specify the \pm and u/g symmetries for this state.

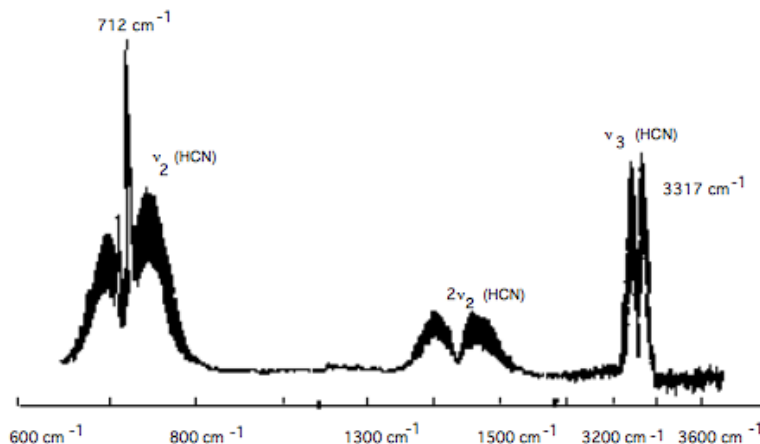
e. Which of the excited states you derived above will radiate to the $^2\Sigma$ ground state? Consider electric dipole, magnetic dipole, and electric quadrupole radiation.

f. Does ionization of the molecule to form a cation lead to a stronger, weaker, or equivalent bond strength?

g. Assuming that the energies of the molecular orbitals do not change upon ionization, what are the ground state, the first excited state, and the second excited state of the positive ion?

h. Considering only these states, predict the structure of the photoelectron spectrum you would obtain for ionization of BO.

Q4



The above figure shows part of the infrared absorption spectrum of HCN gas. The molecule has a CH stretching vibration, a bending vibration, and a CN stretching vibration.

a. Are any of the vibrations of linear HCN degenerate?

b. To which vibration does the group of peaks between 600 cm⁻¹ and 800 cm⁻¹ belong?

c. To which vibration does the group of peaks between 3200 cm⁻¹ and 3400 cm⁻¹ belong?

d. What are the symmetries (σ , π , δ) of the CH stretch, CN stretch, and bending vibrational motions?

e. Starting with HCN in its 0,0,0 vibrational level, which fundamental transitions would be infrared active under parallel polarized light (i.e., z-axis polarization):

i. 000 → 001?

ii. 000 → 100?

iii. 000 → 010?

f. Which transitions would be active when perpendicular polarized light is used?

g. Why does the 712 cm⁻¹ transition have a Q-branch, whereas that near 3317 cm⁻¹ has only P- and R-branches?

This page titled [22.5.2: ii. Problems](#) is shared under a [CC BY-NC-SA 4.0](#) license and was authored, remixed, and/or curated by [Jack Simons](#) via [source content](#) that was edited to the style and standards of the LibreTexts platform.

22.5.3: iii. Exercise Solutions

Q1

a. Evaluate the z-component of μ_{fi} :

$$\mu_{fi} = \langle 2p_z | e r \cos \theta | 1s \rangle, \text{ where } \psi_{1s} = \frac{1}{\sqrt{\pi}} \left(\frac{Z}{a_0} \right)^{\frac{3}{2}} e^{-\frac{Zr}{a_0}}, \text{ and } \psi_{2p_z} = \frac{1}{4\sqrt{2\pi}} \left(\frac{Z}{a_0} \right)^{\frac{5}{2}} r \cos \theta e^{-\frac{Zr}{2a_0}} \quad (22.5.3.1)$$

$$\mu_{fi} = \frac{1}{4\sqrt{2\pi}} \left(\frac{Z}{a_0} \right)^{\frac{5}{2}} \frac{1}{\sqrt{\pi}} \left(\frac{Z}{a_0} \right)^{\frac{3}{2}} \langle r \cos \theta e^{-\frac{Zr}{2a_0}} | e r \cos \theta | e^{-\frac{Zr}{a_0}} \rangle \quad (22.5.3.2)$$

$$= \frac{e}{4\pi\sqrt{2}} \left(\frac{Z}{a_0} \right)^4 \int_0^\infty r^2 dr \int_0^\pi \sin \theta d\theta \int_0^{2\pi} d\varphi \left(r^2 e^{-\frac{Zr}{2a_0}} e^{-\frac{Zr}{a_0}} \right) \cos^2 \theta \quad (22.5.3.3)$$

$$= \frac{e}{4\pi\sqrt{2}} 2\pi \left(\frac{Z}{a_0} \right)^4 \int_0^\infty \left(r^4 e^{-\frac{3Zr}{2a_0}} \right) dr \int_0^\pi \sin \theta \cos^2 \theta d\theta \quad (22.5.3.4)$$

Using integral equation 4 to integrate over r and equation 17 to integrate over θ we obtain:

$$= \frac{e}{4\pi\sqrt{2}} 2\pi \left(\frac{Z}{a_0} \right)^4 \frac{4}{\left(\frac{3Z}{2a_0} \right)^5} \left(\frac{-1}{3} \right) \cos^3 \theta \Big|_0^\pi \quad (22.5.3.5)$$

$$= \frac{e}{4\pi\sqrt{2}} 2\pi \left(\frac{Z}{a_0} \right)^4 \frac{2^5 a_0^5}{3^5 Z^5} \left(\frac{-1}{3} \right) ((-1)^3 - (1)^3) \quad (22.5.3.6)$$

$$= \frac{e}{\sqrt{2}} \frac{2^8 a_0}{3^5 Z} = \frac{e a_0}{Z} \frac{2^8}{\sqrt{2} 3^5} = 0.7499 \frac{e a_0}{Z} \quad (22.5.3.7)$$

b. Examine the symmetry of the integrands for $\langle 2p_z | e x | 1s \rangle$ and $\langle 2p_z | e y | 1s \rangle$.

Function	Symmetry
$2p_z$	- 1
x	+ 1
1s	+ 1
y	+ 1

Under this operation the integrand of $\langle 2p_z | e x | 1s \rangle$ is $(-1)(1)(1) = -1$ (it is antisymmetric) and hence $\langle 2p_z | e x | 1s \rangle = 0$.

Similarly, under this operation the integrand of $\langle 2p_z | e y | 1s \rangle$ is $(-1)(1)(1) = -1$ (it is antisymmetric) and hence $\langle 2p_z | e y | 1s \rangle = 0$.

c.

$$\tau_R = \frac{3\hbar^4 c^3}{4 \left(\frac{3}{8} \left(\frac{e^2}{a_0} \right) Z^2 \right)^3 \left(\left(\frac{e a_0}{Z} \right) \frac{2^8}{\sqrt{2} 3^5} \right)^2}, \quad (22.5.3.8)$$

$$= \frac{3\hbar^4 c^3}{4 \frac{3^3}{8^3} \left(\frac{e^6}{a_0^3} \right) Z^6 \left(\frac{e^2 a_0^2}{Z^2} \right) \frac{2^{16}}{(2)^3 10}} \quad (22.5.3.9)$$

$$= \frac{\hbar^4 c^3 3^8 a_0}{e^8 Z^4 2^8} \quad (22.5.3.10)$$

$$\text{Inserting } e^2 = \frac{\hbar^2}{m_e a_0} \text{ we obtain :} \quad (22.5.3.11)$$

$$\tau_R = \frac{\hbar^4 c^3 3^8 a_0 m_e^4 a_0^4}{\hbar^8 Z^4 2^8} = \frac{3^8 c^3 a_0^5 m_e^4}{2^8 \hbar^4 Z^4} \quad (22.5.3.12)$$

$$= 25.6289 \frac{c^3 a_0^5 m_e^4}{\hbar^4 Z^4} \quad (22.5.3.13)$$

$$= 256,289 \left(\frac{1}{Z^4} \right) x \frac{(2.998 \times 10^{10} \text{ cm sec}^{-1})^3 (0.529177 \times 10^{-8} \text{ cm})^5 (9.109 \times 10^{-28} \text{ g})^4}{(1.0546 \times 10^{-27} \text{ g cm}^2 \text{ sec}^{-1})^4} \quad (22.5.3.14)$$

$$= 1.595 \times 10^{-9} \text{ sec } x \left(\frac{1}{Z^4} \right) \quad (22.5.3.15)$$

So, for example:

Atom	τ_R
H	1.595 ns
He ⁺	99.7 ps
Li ⁺²	19.7 ps
Be ⁺³	6.23 ps
Ne ⁺⁹	159 fs

Q2

a. $H = H_0 + \lambda H'(t)$, $H'(t) = V\theta(t)$, $H_0\varphi_k = E_k\varphi_k$, $\omega_k = \frac{E_k}{\hbar}$, $i\hbar\frac{\partial\psi}{\partial t} = H\psi$

let $\psi(r, t) = i\hbar \sum_j c_j(t) \varphi_j e^{-i\omega_j t}$ and insert into the above expression:

$$i\hbar \sum_j [\dot{c}_j - i\omega_j c_j] e^{-i\omega_j t} \varphi_j = i\hbar \sum_j c_j(t) e^{-i\omega_j t} (H_0 + \lambda H'(t)) \varphi_j \quad (22.5.3.16)$$

$$\sum_j [i\hbar \dot{c}_j + E_j c_j - c_j E_j - c_j \lambda H'] e^{-i\omega_j t} \varphi_j = 0 \quad (22.5.3.17)$$

$$\sum_j [i\hbar \dot{c}_j \langle m | j \rangle - c_j \lambda \langle m | H' | j \rangle] e^{-i\omega_j t} = 0 \quad (22.5.3.18)$$

$$i\hbar \dot{c}_m e^{-i\omega_m t} = \sum_j c_j \lambda H'_{mj} e^{-i\omega_j t} \quad (22.5.3.19)$$

So, $\quad (22.5.3.20)$

$$\dot{c}_m = \frac{1}{i\hbar} \sum_j c_j \lambda H'_{mj} e^{-i(\omega_j - \omega_m)t} \quad (22.5.3.21)$$

Going back a few equations and multiplying from the left by φ_k instead of φ_m we obtain:

$$\sum_j [i\hbar \dot{c}_j \langle k | j \rangle - c_j \lambda \langle k | H' | j \rangle] e^{-i\omega_j t} = 0 \quad (22.5.3.22)$$

$$i\hbar \dot{c}_k e^{-i\omega_k t} = \sum_j c_j \lambda H'_{kj} e^{-i\omega_j t} \quad (22.5.3.23)$$

So, $\quad (22.5.3.24)$

$$\dot{c}_k = \frac{1}{i\hbar} \sum_j c_j \lambda H'_{kj} e^{-i\omega_j t} \quad (22.5.3.25)$$

Now, let: $\quad (22.5.3.26)$

$$c_m = c_m^{(0)} + c_m^{(1)} \lambda + c_m^{(2)} \lambda^2 + \dots \quad (22.5.3.27)$$

$$c_k = c_k^{(0)} + c_k^{(1)} \lambda + c_k^{(2)} \lambda^2 + \dots \quad (22.5.3.28)$$

and substituting into above we obtain: $\quad (22.5.3.29)$

$$\dot{c}_m^{(0)} + \dot{c}_m^{(1)} \lambda + \dot{c}_m^{(2)} \lambda^2 + \dots = \frac{1}{i\hbar} \sum_j [c_j^{(0)} + c_j^{(1)} \lambda + c_j^{(2)} \lambda^2 + \dots] \lambda H'_{mj} e^{-i(\omega_j - \omega_m)t} \quad (22.5.3.30)$$

first order: (22.5.3.31)

$$\dot{c}_m^{(0)} = 0 \Rightarrow c_m^{(0)} = 1 \quad (22.5.3.32)$$

second order: $\dot{c}_m^{(1)} = \frac{1}{i\hbar} \sum_j c_j^{(0)} H'_{mj} e^{-i(\omega_{jm})t}$ (22.5.3.33)

$(n+1)^{st}$ order: (22.5.3.34)

$$\dot{c}_m^{(n)} = \frac{1}{i\hbar} \sum_j c_j^{(n-1)} H'_{mj} e^{-i(\omega_{jm})t} \quad (22.5.3.35)$$

Similarly: (22.5.3.36)

first order: (22.5.3.37)

$$\dot{c}_k^{(0)} = 0 \Rightarrow c_{k \neq m}^{(0)} = 0 \quad (22.5.3.38)$$

second order: (22.5.3.39)

$$\dot{c}_k^{(1)} = \frac{1}{i\hbar} \sum_j c_j^{(0)} H'_{kj} e^{-i(\omega_{jk})t} \quad (22.5.3.40)$$

$(n+1)^{st}$ order: (22.5.3.41)

$$\dot{c}_k^{(n)} = \frac{1}{i\hbar} \sum_j c_j^{(n-1)} H'_{kj} e^{-i(\omega_{jk})t} \quad (22.5.3.42)$$

So, (22.5.3.43)

$$\dot{c}_m^{(1)} = \frac{1}{i\hbar} c_m^{(0)} H'_{mm} e^{-i(\omega_{mm})t} = \frac{1}{i\hbar} H'_{mm} \quad (22.5.3.44)$$

$$c_m^{(1)}(t) = \frac{1}{i\hbar} \int_0^t dt' V_{mm} = \frac{V_{mm}t}{i\hbar} \quad (22.5.3.45)$$

and similarly, (22.5.3.46)

$$\dot{c}_k^{(1)} = \frac{1}{i\hbar} c_m^{(0)} H'_{km} e^{-i(\omega_{mk})t} = \frac{1}{i\hbar} H'_{km} e^{-i(\omega_{mk})t} \quad (22.5.3.47)$$

$$c_k^{(1)}(t) = \frac{1}{i\hbar} V_{km} \int_0^t dt' e^{-i(\omega_{mk})t'} = \frac{V_{km}}{\hbar\omega_{mk}} [e^{-i(\omega_{mk})t} - 1] \quad (22.5.3.48)$$

$$\dot{c}_m^{(2)} = \frac{1}{i\hbar} \sum_j c_j^{(1)} H'_{mj} e^{-i(\omega_{jm})t} \quad (22.5.3.49)$$

$$\dot{c}_m^{(2)} = \sum_{j \neq m} \frac{1}{i\hbar} \frac{V_{jm}}{\hbar\omega_{mj}} [e^{-i(\omega_{mj})t} - 1] H'_{mj} e^{-i(\omega_{jm})t} + \frac{1}{i\hbar} \frac{V_{mm}t}{i\hbar} H'_{mm} \quad (22.5.3.50)$$

$$c_m^{(2)} = \sum_{j \neq m} \frac{1}{i\hbar} \frac{V_{jm}V_{mj}}{\hbar\omega_{mj}} \int_0^t dt' e^{-i(\omega_{jm})t'} [e^{-i(\omega_{mj})t'} - 1] - \frac{V_{mm}V_{mm}}{\hbar^2} \int_0^t t' dt' \quad (22.5.3.51)$$

$$= \sum_{j \neq m} \frac{V_{jm}V_{mj}}{i\hbar^2\omega_{mj}} \int_0^t dt' [1 - e^{-i(\omega_{jm})t'}] - \frac{|V_{mm}|^2}{\hbar^2} \frac{t^2}{2} \quad (22.5.3.52)$$

$$= \sum_{j \neq m} \frac{V_{jm}V_{mj}}{i\hbar^2\omega_{mj}} \left(t - \frac{e^{-i(\omega_{jm})t} - 1}{-i\omega_{jm}} \right) - \frac{|V_{mm}|^2}{\hbar^2} \frac{t^2}{2} \quad (22.5.3.53)$$

$$= \sum_{j \neq m} \frac{V_{jm}V_{mj}}{\hbar^2\omega_{mj}^2} (e^{-i(\omega_{jm})t} - 1) + \sum_{j \neq m} \frac{V_{jm}V_{mj}}{i\hbar^2\omega_{mj}} t - \frac{|V_{mm}|^2}{2\hbar^2} \quad (22.5.3.54)$$

Similarly, (22.5.3.55)

$$\dot{c}_k^{(2)} = \frac{1}{i\hbar} \sum_j c_j^{(1)} H'_{kj} e^{-i(\omega_{jk})t} \quad (22.5.3.56)$$

$$= \sum_{j \neq m} \frac{1}{i\hbar} \frac{V_{jm}}{\hbar\omega_{mj}} [e^{-i(\omega_{mj})t} - 1] H'_{kj} e^{-i(\omega_{jk})t} + \frac{1}{i\hbar} \frac{V_{mm}t}{i\hbar} H'_{km} e^{-i(\omega_{mk})t} \quad (22.5.3.57)$$

$$c_k^{(2)}(t) = \sum_{j \neq m} \frac{V_{jm}V_{kj}}{i\hbar^2\omega_{mj}} \int_0^t dt' e^{-i(\omega_{jk})t'} [e^{-i(\omega_{mj})t'} - 1] - \frac{V_{mm}V_{km}}{\hbar^2} \int_0^t t' dt' e^{-i(\omega_{mk})t'} \quad (22.5.3.58)$$

$$= \sum_{j \neq m} \frac{V_{jm}V_{kj}}{i\hbar^2\omega_{mj}} \left(\frac{e^{-i(\omega_{mj}+\omega_{jk})t} - 1}{-i\omega_{mk}} - \frac{e^{-i(\omega_{jk})t} - 1}{-i\omega_{jk}} \right) - \frac{V_{mm}V_{km}}{\hbar^2} \left[e^{-i(\omega_{mk})t} \left(\frac{t'}{-i\omega_{mk}} - \frac{1}{-(i\omega_{mk})^2} \right) \right]_0^t \quad (22.5.3.59)$$

$$= \sum_{j \neq m} \frac{V_{jm}V_{kj}}{\hbar^2\omega_{mj}} \left(\frac{e^{-i(\omega_{mk})t} - 1}{\omega_{mk}} - \frac{e^{-i(\omega_{jk})t} - 1}{\omega_{jk}} \right) + \frac{V_{mm}V_{km}}{\hbar^2\omega_{mk}} \left[e^{-i(\omega_{mk})t} \left(\frac{t'}{i} - \frac{1}{\omega_{mk}} \right) \right]_0^t \quad (22.5.3.60)$$

$$= \sum_{j \neq m} \frac{V_{jm}V_{kj}}{E_m - E_j} \left(\frac{e^{-i(\omega_{mk})t} - 1}{E_m - E_k} - \frac{e^{-i(\omega_{jk})t} - 1}{E_j - E_k} \right) + \frac{V_{mm}V_{km}}{\hbar(E_m - E_k)} \left[e^{-i(\omega_{mk})t} \left(\frac{t}{i} - \frac{1}{\omega_{mk}} \right) + \frac{1}{\omega_{mk}} \right] \quad (22.5.3.61)$$

So, the overall amplitudes c_m , and c_k , to second order are:

$$c_m(t) = 1 + \frac{V_{mm}t}{i\hbar} + \sum_{j \neq m}' \frac{V_{jm}V_{mj}}{i\hbar(E_m - E_j)}t + \sum_{j \neq m}' \frac{V_{jm}V_{mj}}{\hbar^2(E_m - E_j)^2}(e^{-i(\omega_{mk})t} - 1) - \frac{|V_{mm}|^2 t^2}{2\hbar^2} \quad (22.5.3.62)$$

$$c_k(t) = \frac{V_{km}}{(E_m - E_k)}[e^{-i(\omega_{mk})t} - 1] + \frac{V_{mm}V_{km}}{(E_m - E_k)^2}[1 - e^{-i(\omega_{mk})t}] + \frac{V_{mm}V_{km}}{(E_m - E_k)}\frac{t}{\hbar i}e^{-i(\omega_{mk})t} + \sum_{j \neq m}' \frac{V_{jm}V_{kj}}{E_m - E_j} \left(\frac{e^{-i(\omega_{mk})t} - 1}{E_m - E_k} - \frac{e^{-i(\omega_{jk})t} - 1}{E_j - E_k} \right) \quad (22.5.3.63)$$

b. The perturbation equations still hold:

$$\dot{c}_m^{(n)} = \frac{1}{i\hbar} \sum_j c_j^{(n-1)} H'_{mj} e^{-i(\omega_{jm})t}; \dot{c}_k^{(n)} = \frac{1}{i\hbar} \sum_j c_j^{(n-1)} H'_{kj} e^{-i(\omega_{jk})t} \quad (22.5.3.64)$$

$$\text{So, } c_m^{(0)} = 1 \text{ and } c_k^{(0)} = 0 \quad (22.5.3.65)$$

$$\dot{c}_m^{(1)} = \frac{1}{i\hbar} H'_{mm} \quad (22.5.3.66)$$

$$c_m^{(1)} = \frac{1}{i\hbar} V_{mm} \int_{-\infty}^t dt' e^{-i(\omega)t'} = \frac{V_{mm}}{i\hbar(-i\omega_{mk} + \eta)} [e^{-i(\omega_{mk} + \eta)t}] \quad (22.5.3.67)$$

$$= \frac{V_{mm}}{E_m - E_k + i\hbar\eta} [e^{-i(\omega_{mk} + \eta)t}] \quad (22.5.3.68)$$

$$\dot{c}_m^{(2)} = \sum_{j \neq m}' \frac{1}{i\hbar} \frac{V_{jm}}{E_m - E_j + i\hbar\eta} e^{-i(\omega_{mj} + \eta)t} V_{mj} e^{\eta t} e^{-i(\omega_{jm})t} + \frac{1}{i\hbar} \frac{V_{mm} e^{\eta t}}{i\hbar\eta} V_{mm} e^{\eta t} \quad (22.5.3.69)$$

$$c_m^{(2)} = \sum_{j \neq m}' \frac{1}{i\hbar} \frac{V_{jm}V_{mj}}{E_m - E_j + i\hbar\eta} \int_{-\infty}^t e^{2\eta t'} dt' - \frac{|V_{mm}|^2}{2\hbar^2 \eta^2} \int_{-\infty}^t e^{2\eta t'} dt' = \sum_{j \neq m}' \frac{V_{jm}V_{mj}}{i\hbar 2\eta(E_m - E_j + i\hbar\eta)} e^{2\eta t} - \frac{|V_{mm}|^2}{2\hbar^2 \eta^2} e^{2\eta t} \quad (22.5.3.70)$$

$$\dot{c}_k^{(2)} = \sum_{j \neq m}' \frac{1}{i\hbar} \frac{V_{jm}}{E_m - E_j + i\hbar\eta} e^{-i(\omega_{mj} + \eta)t} H'_{kj} e^{-i(\omega_{jk})t} \quad (22.5.3.71)$$

c. In part a. the $c^{(2)}(t)$ grow linearly with time (for $V_{mm} = 0$) while in part b. they remain finite for $\eta > 0$. The result in part a. is due to the sudden turning on of the field.
d.

$$|c_k(t)|^2 = \left| \sum_j \frac{V_{jm}V_{kj} e^{-i(\omega_{mk} + 2\eta)t}}{(E_m - E_j + i\hbar\eta)(E_m - E_k + 2i\hbar\eta)} \right|^2 \quad (22.5.3.72)$$

$$= \sum_{j,j'} \frac{V_{kj}V_{k'j'} V_{jm}V_{j'm} e^{4\eta t}}{[(E_m - E_j)(E_m - E_{j'}) + i\hbar\eta(E_j - E_{j'}) + \hbar^2 \eta^2] [(E_m - E_k)^2 + 4\hbar^2 \eta^2]} \quad (22.5.3.73)$$

$$\text{Now, look at the limit as } \eta \rightarrow 0^+: \quad (22.5.3.74)$$

$$\frac{d}{dt} |c_k(t)|^2 \neq 0 \text{ when } E_m = E_k \quad (22.5.3.75)$$

$$\lim_{\eta \rightarrow 0^+} \frac{4\eta}{((E_m - E_k)^2 + 4\hbar^2 \eta^2)} \alpha \delta(E_m - E_k) \quad (22.5.3.76)$$

$$\text{So, the final result is the } 2^{nd} \text{ order golden rule expression:} \quad (22.5.3.77)$$

$$\frac{d}{dt} |c_k(t)|^2 \frac{2\pi}{\hbar} \delta(E_m - E_k) \lim_{\eta \rightarrow 0^+} \left| \frac{V_{jm}V_{kj}}{(E_j - E_m - i\hbar\eta)} \right|^2 \quad (22.5.3.78)$$

Q3

For the sudden perturbation case:

$$|c_m(t)|^2 = 1 + \sum_j' \frac{V_{jm}V_{mj}}{(E_m - E_j)^2} [e^{-i(\omega_{jm})t} - 1 + e^{i(\omega_{jm})t} - 1] + O(V^3) \quad (22.5.3.79)$$

$$|c_m(t)|^2 = 1 + \sum_j' \frac{V_{jm}V_{mj}}{(E_m - E_j)^2} [e^{-i(\omega_{jm})t} + e^{i(\omega_{jm})t} - 2] + O(V^3) \quad (22.5.3.80)$$

$$|c_k(t)|^2 = \frac{V_{km}V_{mk}}{(E_m - E_k)^2} [-e^{-i(\omega_{mk})t} - e^{i(\omega_{mk})t} + 2] + O(V^3) \quad (22.5.3.81)$$

$$1 - \sum_{k \neq m}' |c_k(t)|^2 = 1 - \sum_k' \frac{V_{km}V_{mk}}{(E_m - E_k)^2} [-e^{-i(\omega_{mk})t} - e^{i(\omega_{mk})t} + 2] + O(V^3) \quad (22.5.3.82)$$

$$= 1 + \sum_k' \frac{V_{km}V_{mk}}{(E_m - E_k)^2} [e^{-i(\omega_{mk})t} + e^{i(\omega_{mk})t} - 2] + O(V^3) \quad (22.5.3.83)$$

\therefore to order V^2 , $|c_m(t)|^2 = 1 - \sum_k' |c_k(t)|^2$, with no assumptions made regarding V_{mm} .

For the adiabatic perturbation case:

$$|c_m(t)|^2 = 1 + \sum_{j \neq m}' \left[\frac{V_{jm} V_{mj} e^{2\eta t}}{i\hbar 2\eta (E_m - E_j + i\hbar\eta)} + \frac{V_{jm} V_{mj} e^{2\eta t}}{-i\hbar 2\eta (E_m - E_j - i\hbar\eta)} \right] + O(V^3) \quad (22.5.3.84)$$

$$= 1 + \sum_{j \neq m}' \frac{1}{i\hbar 2\eta} \left[\frac{1}{(E_m - E_j + i\hbar\eta)} - \frac{1}{(E_m - E_j - i\hbar\eta)} \right] V_{jm} V_{mj} e^{2\eta t} + O(V^3) \quad (22.5.3.85)$$

$$= 1 + \sum_{j \neq m}' \frac{1}{i\hbar 2\eta} \left[\frac{-2i\hbar\eta}{(E_m - E_j)^2 + \hbar^2\eta^2} \right] V_{jm} V_{mj} e^{2\eta t} + O(V^3) \quad (22.5.3.86)$$

$$= 1 - \sum_{j \neq m}' \left[\frac{V_{jm} V_{mj} e^{2\eta t}}{(E_m - E_j)^2 + \hbar^2\eta^2} \right] + O(V^3) \quad (22.5.3.87)$$

$$|c_k(t)|^2 = \frac{V_{km} V_{mk}}{(E_m - E_k)^2 + \hbar^2\eta^2} e^{2\eta t} + O(V^3) \quad (22.5.3.88)$$

\therefore to order V^2 , $|c_m(t)|^2 = 1 - \sum_k' |c_k(t)|^2$, with no assumptions made regarding V_{mm} for this case as well.

This page titled [22.5.3: iii. Exercise Solutions](#) is shared under a [CC BY-NC-SA 4.0](#) license and was authored, remixed, and/or curated by [Jack Simons](#) via [source content](#) that was edited to the style and standards of the LibreTexts platform.

22.5.4: iv. Problem Solutions

Q1

a. $T_{nm} \approx \frac{|\langle n|V|m \rangle|^2}{\hbar^2 \omega_{nm}^2}$

evaluating $\langle 1s|V|2s \rangle$ (using only the radial portions of the 1s and 2s wavefunctions since the spherical harmonics will integrate to unity) where $V = (e^2/r)$:

$$\langle 1s|V|2s \rangle = \int 2 \left(\frac{Z}{a_0} \right)^{\frac{3}{2}} e^{-\frac{Zr}{a_0}} \frac{1}{r} \frac{1}{\sqrt{2}} \left(\frac{Z}{a_0} \right)^{\frac{3}{2}} \left(1 - \frac{Zr}{2a_0} \right) e^{-\frac{Zr}{2a_0}} r^2 dr \quad (22.5.4.1)$$

$$\langle 1s|V|2s \rangle = \frac{2}{\sqrt{2}} \left(\frac{Z}{a_0} \right)^3 \left[\int r e^{-\frac{3Zr}{2a_0}} dr - \int \frac{Zr^2}{2a_0} e^{-\frac{3Zr}{2a_0}} dr \right] \quad (22.5.4.2)$$

Using integral equation 4 for two integration we obtain:

$$\langle 1s|V|2s \rangle = \frac{2}{\sqrt{2}} \left(\frac{Z}{a_0} \right)^3 \left[\frac{1}{\left(\frac{3Z}{2a_0} \right)^2} - \left(\frac{Z}{2a_0} \right) \frac{2}{\left(\frac{3Z}{2a_0} \right)} \right] \quad (22.5.4.3)$$

$$\langle 1s|V|2s \rangle = \frac{2}{\sqrt{2}} \left(\frac{Z}{a_0} \right)^3 \left[\frac{2^2 a_0^2}{3^2 Z^2} - \frac{2^3 a_0^2}{3^3 Z^2} \right] \quad (22.5.4.4)$$

$$\langle 1s|V|2s \rangle = \frac{2}{\sqrt{2}} \left(\frac{Z}{a_0} \right)^3 \left[\frac{(3)2^2 a_0^2 - 2^3 a_0^2}{3^3 Z^2} \right] = \frac{8Z}{\sqrt{227} a_0} \quad (22.5.4.5)$$

$$\text{Now,} \quad (22.5.4.6)$$

$$E_n = -\frac{Z^2 e^2}{n^2 2a_0}, E_{1s} = -\frac{Z^2 e^2}{2a_0}, E_{2s} = -\frac{Z^2 e^2}{8a_0}, E_{2s} - E_{1s} = \frac{3Z^2 e^2}{8a_0} \quad (22.5.4.7)$$

$$\text{So,} \quad (22.5.4.8)$$

$$T_{mn} = \frac{\left(\frac{8Z}{\sqrt{227} a_0} \right)^2}{\left(\frac{3Z^2}{8a_0} \right)} = \frac{2^6 Z^2 2^6 a_0^2}{(2)3^8 a_0^2 Z^4} = \frac{2^{11}}{3^8 Z^2} = 0.312 \text{ (for } Z=1) \quad (22.5.4.9)$$

b. $\varphi_m(r) = \varphi_{1s} = 2 \left(\frac{Z}{a_0} \right)^{\frac{3}{2}} e^{-\frac{Zr}{a_0}} Y_{00}$

The orthogonality of the spherical harmonics results in only s-states having non-zero values for A_{nm} . We can then drop the Y_{00} (integrating this term will only result in unity) in determining the value of $A_{1s,2s}$.

$$\psi_n(r) = \psi_{2s} = \frac{1}{\sqrt{2}} \left(\frac{Z}{a_0} \right)^{\frac{3}{2}} \left(1 - \frac{Zr}{2a_0} \right) e^{-\frac{Zr}{2a_0}} \quad (22.5.4.10)$$

$$\text{Remember for } \varphi_{1s} Z=1 \text{ and or } \psi_{2s} Z=2 \quad (22.5.4.11)$$

$$A_{nm} = \int 2 \left(\frac{Z}{a_0} \right)^{\frac{3}{2}} e^{-\frac{Zr}{a_0}} \frac{1}{\sqrt{2}} \left(\frac{Z+1}{a_0} \right)^{\frac{3}{2}} \left(1 - \frac{(Z+1)r}{2a_0} \right) e^{-\frac{(Z+1)r}{2a_0}} r^2 dr \quad (22.5.4.12)$$

$$A_{nm} = \frac{2}{\sqrt{2}} \left(\frac{Z}{a_0} \right)^{\frac{3}{2}} \left(\frac{Z+1}{a_0} \right)^{\frac{3}{2}} \int e^{-\frac{(3Z+1)r}{2a_0}} \left(1 - \frac{(Z+1)r}{2a_0} \right) r^2 dr \quad (22.5.4.13)$$

$$A_{nm} = \frac{2}{\sqrt{2}} \left(\frac{Z}{a_0} \right)^{\frac{3}{2}} \left(\frac{Z+1}{a_0} \right)^{\frac{3}{2}} \left[\int r^2 e^{-\frac{(3Z+1)r}{2a_0}} dr - \int \frac{(Z+1)r^3}{2a_0} e^{-\frac{(3Z+1)r}{2a_0}} dr \right] \quad (22.5.4.14)$$

Evaluating these integrals using integral equation 4 we obtain:

$$A_{nm} = \frac{2}{\sqrt{2}} \left(\frac{Z}{a_0} \right)^{\frac{3}{2}} \left[\frac{2}{\left(\frac{3Z+1}{2a_0} \right)^3} - \left(\frac{Z+1}{2a_0} \right) \frac{(3)(2)}{\left(\frac{3Z+1}{2a_0} \right)^4} \right] \quad (22.5.4.15)$$

$$A_{nm} = \frac{2}{\sqrt{2}} \left(\frac{Z}{a_0} \right)^{\frac{3}{2}} \left(\frac{Z+1}{a_0} \right)^{\frac{3}{2}} \left[\frac{2^4 a_0^3}{(3Z+1)^3} - (Z+1) \frac{(3)2^4 a_0^3}{(3Z+1)^4} \right] \quad (22.5.4.16)$$

$$A_{nm} = \frac{2}{\sqrt{2}} \left(\frac{Z}{a_0} \right)^{\frac{3}{2}} \left(\frac{Z+1}{a_0} \right)^{\frac{3}{2}} \left[\frac{-2^5 a_0^3}{(3Z+1)^4} \right] \quad (22.5.4.17)$$

$$A_{nm} = -2 \frac{[2^3 Z(Z+1)]^{\frac{3}{2}}}{(3Z+1)^4} \quad (22.5.4.18)$$

The transition probability is the square of this amplitude:

$$T_{nm} = \left(-2 \frac{[2^3 Z(Z+1)]^{\frac{3}{2}}}{(3Z+1)^4} \right)^2 = \frac{2^{11} Z^3 (Z+1)^3}{(3Z+1)^8} = 0.25 \text{ (for } Z = 1\text{)}.$$

The difference in these two results (parts a. and b.) will become negligible at large values of Z when the perturbation becomes less significant as in the case of $Z = 1$.

Q2

$\vec{\epsilon}$ is along Z (lab fixed), and $\vec{\mu}$ is along z (the C-I module fixed bond). The angle between Z and z is β :

$$\vec{\epsilon} \cdot \vec{\mu} = \epsilon \mu \cos \beta = \epsilon \mu D_{00}^{1*}(\alpha \beta \gamma)$$

So,

$$I = \langle D_{M'K'}^{J'} | \vec{\epsilon} \dot{\vec{\mu}} | D_{MK}^J \rangle = \int D_{M'K'}^{J'} \vec{\epsilon} \dot{\vec{\mu}} D_{MK}^J \sin \beta d\beta d\gamma d\alpha \quad (22.5.4.19)$$

$$= \epsilon \mu \int D_{M'K'}^{J'} D_{00}^{1*} D_{MK}^J \sin \beta d\beta d\gamma d\alpha. \quad (22.5.4.20)$$

Now use: (22.5.4.21)

$$D_{M'n'}^{J'*} D_{00}^{1*} = \sum_{jmn} \langle J' M' 10 | jm \rangle^* D_{mn}^{j*} \langle jn | J' K' 10 \rangle^*, \quad (22.5.4.22)$$

to obtain: (22.5.4.23)

$$I = \epsilon \mu \sum_{jmn} \langle J' M' 10 | jm \rangle^* \langle jn | J' K' 10 \rangle^* \int D_{mn}^{j*} D_{MK}^J \sin \beta d\beta d\gamma d\alpha. \quad (22.5.4.24)$$

Now use: (22.5.4.25)

$$\int D_{mn}^{j*} D_{MK}^J \sin \beta d\beta d\gamma d\alpha = \frac{8\pi^2}{2J+1} \delta_{Jj} \delta_{Mm} \delta_{Kn}, \quad (22.5.4.26)$$

to obtain: (22.5.4.27)

$$I = \epsilon \mu \frac{8\pi^2}{2J+1} \sum_{jmn} \langle J' M' 10 | jm \rangle^* \langle jn | J' K' 10 \rangle^* \delta_{Jj} \delta_{Mm} \delta_{Kn} \quad (22.5.4.28)$$

$$= \epsilon \mu \frac{8\pi^2}{2J+1} \langle J' M' 10 | JM \rangle^* \langle JK | J' K' 10 \rangle. \quad (22.5.4.29)$$

We use: (22.5.4.30)

$$\langle JK | J' K' 10 \rangle = \sqrt{2J+1} (-i)^{J'-1+K} \begin{pmatrix} J' & 1 & J \\ K' & 0 & K \end{pmatrix} \quad (22.5.4.31)$$

and, (22.5.4.32)

$$\langle J' M' 10 | JM \rangle = \sqrt{2J+1} (-i)^{(J'-1)+M} \begin{pmatrix} J' & 1 & J \\ M' & 0 & M \end{pmatrix} \quad (22.5.4.33)$$

to give: (22.5.4.34)

$$I = \epsilon \mu \frac{8\pi^2}{2J+1} \sqrt{2J+1} (-i)^{(J'-1)+M} \begin{pmatrix} J' & 1 & J \\ M' & 0 & M \end{pmatrix} \sqrt{2J+1} (-i)^{(J'-1)+K} \begin{pmatrix} J' & 1 & J \\ K' & 0 & K \end{pmatrix} \quad (22.5.4.35)$$

$$= \epsilon \mu 8\pi^2 (-i)^{(J'-1)+M+J'-1+K} \begin{pmatrix} J' & 1 & J \\ M' & 0 & M \end{pmatrix} \begin{pmatrix} J' & 1 & J \\ K' & 0 & K \end{pmatrix} \quad (22.5.4.36)$$

$$= \epsilon \mu 8\pi^2 (-i)^{(M+K)} \begin{pmatrix} J' & 1 & J \\ M' & 0 & M \end{pmatrix} \begin{pmatrix} J' & 1 & J \\ K' & 0 & K \end{pmatrix} \quad (22.5.4.37)$$

The 3-J symbols vanish unless: $K' + 0 = K$ and $M' + 0 = M$.

So,

$$I = \epsilon \mu 8\pi^2 (-i)^{(M+K)} \begin{pmatrix} J' & 1 & J \\ M & 0 & M \end{pmatrix} \begin{pmatrix} J' & 1 & J \\ K & 0 & K \end{pmatrix} \delta_{M'M} \delta_{K'K}$$

b. $\begin{pmatrix} J' & 1 & J \\ M & 0 & M \end{pmatrix}$ and $\begin{pmatrix} J' & 1 & J \\ K & 0 & K \end{pmatrix}$ vanish unless $J' = J + 1, J, J - 1$; $\Delta J = \pm 1, 0$

The K quantum number can not change because the dipole moment lies along the molecule's C_3 axis and the light's electric field thus can exert no torque that twists the molecule about this axis. As a result, the light can not induce transitions that excite the molecule's spinning motion about this axis.

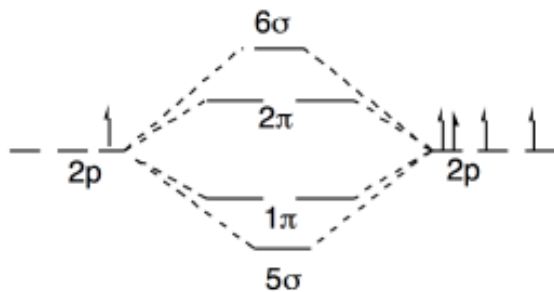
Q3

a. B atom: $as^2 2s^2 2p^1$, 2P ground state $L = 1, S = \frac{1}{2}$, gives degeneracy $((2L + 1)(2S + 1))$ of 6.

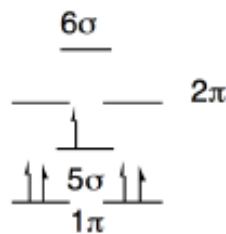
O atom: $1s^2 2s^2 2p^4$, 3P ground state $L = 1, S = 1$, gives a degeneracy $((2L + 1)(2S + 1))$ of 9.

The total number of states formed is then $(6)(9) = 54$.

b. We need only consider the p orbitals to find the low lying molecular states:



Which, in reality look like this:



This is the correct ordering to give a $^2\Sigma^+$ ground state. The only low-lying electron configurations are $1\pi^35\sigma^2$ or $1\pi^45\sigma^1$. These lead to $^2\Pi$ and $^2\Sigma^+$ states, respectively.

c. The bond orders in both states are $2\frac{1}{2}$.

d. The $^2\Sigma$ is + and g/u cannot be specified since this is a heteronuclear molecule.

e. Only one excited state, the $^2\Pi$, is spin-allowed to radiate to the $^2\Sigma^+$. Consider symmetries of transition moment operators that arise in the E1, E2 and M1 contributions to the transition rate

Electric dipole allowed: $z \rightarrow \Sigma^+$, $x, y \rightarrow \Pi$, \therefore the $^2\Pi \rightarrow ^2\Sigma^+$ is electric dipole allowed via a perpendicular band.

Magnetic dipole allowed: $R_z \rightarrow \Sigma^-$, $R_{x,y} \rightarrow \Pi$, \therefore the $^2\Pi \rightarrow ^2\Sigma^+$ is magnetic dipole allowed.

Electric quadrupole allowed: $x^2 + y^2, z^2 \rightarrow \Sigma^+$, $xy, yz \rightarrow \Pi$, $x^2 - y^2, xy \rightarrow \Delta$, \therefore the $^2\Pi \rightarrow ^2\Sigma^+$ is electric quadrupole allowed as well.

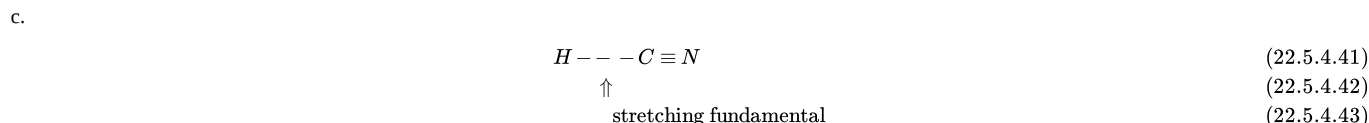
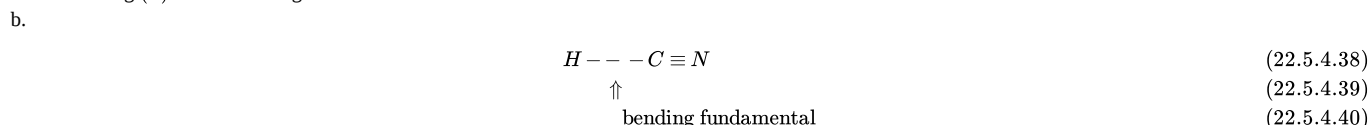
f. Since ionization will remove a bonding electron, the BO^+ bond is weaker than the BO bond.

g. The ground state BO^+ is $^1\Sigma^+$ corresponding to a $1\pi^4$ electron configuration. An electron configuration of $1\pi^35\sigma^1$ leads to a $^3\Pi$ and a $^1\Pi$ state. The $^3\Pi$ will be lower in energy. A $1\pi^25\sigma^2$ configuration will lead to higher lying states of $^3\Sigma^-$, $^1\Delta$, and $^1\Sigma^+$.

h. There should be 3 bands corresponding to formation of BO^+ in the $^1\Sigma^+$, $^3\Pi$, and $^1\Pi$ states. Since each of these involves removing a bonding electron, the Franck-Condon integrals will be appreciable for several vibrational levels, and thus a vibrational progression should be observed.

Q4

a. The bending (π) vibration is degenerate.



d. CH stretch (ν_3 in figure) is σ CN stretch is σ and HCN (ν_2 in figure) bend is π .

e. Under z (σ) light the CN stretch and the CH stretch can be excited, since $\psi_0 = \sigma$, $\psi_1 = \sigma$ and $z = \sigma$ provides coupling.

f. Under x,y (π) light the HCN bend can be excited, since $\psi_0 = \sigma$, $\psi_1 = \pi$ and $x,y = \pi$ provides coupling.

g. The bending vibration is active under (x,y) perpendicular polarized light. $\Delta J = 0, \pm 1$ are the selection rules for \perp transitions. The CH stretching vibration is active under (z) \parallel polarized light. $\Delta J = \pm 1$ are the selection rules for \parallel transitions.

This page titled 22.5.4: iv. Problem Solutions is shared under a CC BY-NC-SA 4.0 license and was authored, remixed, and/or curated by Jack Simons via source content that was edited to the style and standards of the LibreTexts platform.

SECTION OVERVIEW

22.6: More Quantitative Aspects of Electronic Structure Calculations

Topic hierarchy

22.6.1: i. Review Exercises

22.6.2: i. Review Exercises-

22.6.3: ii. Exercises

22.6.4: iii. Problems

22.6.5: iv. Review Exercise Solutions

22.6.6: v. Exercise Solutions

22.6.7: vi. Problem Solutions

This page titled [22.6: More Quantitative Aspects of Electronic Structure Calculations](#) is shared under a [CC BY-NC-SA 4.0](#) license and was authored, remixed, and/or curated by [Jack Simons](#) via [source content](#) that was edited to the style and standards of the LibreTexts platform.

22.6.1: i. Review Exercises

Q1

Contrast Slater type orbitals (STOs) with Gaussian type orbitals (GTOs).

This page titled [22.6.1: i. Review Exercises](#) is shared under a [CC BY-NC-SA 4.0](#) license and was authored, remixed, and/or curated by [Jack Simons](#) via [source content](#) that was edited to the style and standards of the LibreTexts platform.

22.6.2: i. Review Exercises-

Your page has been created!

Remove this content and add your own.

Edit page

Click the Edit page button in your user bar. You will see a suggested structure for your content. Add your content and hit Save.

Tips:

[Drag and drop](#)

Drag one or more image files from your computer and drop them onto your browser window to add them to your page.

[Classifications](#)

Tags are used to link pages to one another along common themes. Tags are also used as markers for the dynamic organization of content in the CXone Expert framework.

[Working with templates](#)

CXone Expert [templates](#) help guide and organize your documentation, making it flow easier and more uniformly. Edit existing templates or create your own.

 [Visit for all help topics.](#)

This page titled [22.6.2: i. Review Exercises-](#) is shared under a [CC BY-NC-SA 4.0](#) license and was authored, remixed, and/or curated by [Jack Simons](#) via [source content](#) that was edited to the style and standards of the LibreTexts platform.

22.6.3: ii. Exercises

Q1

By expanding the molecular orbitals $\{\phi_k\}$ as linear combinations of atomic orbitals $\{\chi_\mu\}$,

$$\phi_k = \sum_{\mu} c_{\mu k} \chi_{\mu}$$

show how the canonical Hartree-Fock (HF) equations:

$$F\phi_i = \epsilon_i \phi_i$$

reduce to the matrix eigenvalue-type equation of the form given in the text:

$$\sum_{\nu} F_{\mu\nu} C_{\nu i} = \epsilon_i \sum_{\nu} S_{\mu\nu} C_{\nu i}$$

where:

$$F_{\mu\nu} = \langle \chi_{\mu} | h | \chi_{\nu} \rangle + \sum_{\delta\kappa} [\gamma_{\delta\kappa} \langle \chi_{\mu} \chi_{\delta} | g | \chi_{\nu} \chi_{\kappa} \rangle - \gamma_{\delta\kappa}^{ex} \langle \chi_{\mu} \chi_{\delta} | g | \chi_{\kappa} \chi_{\nu} \rangle], \quad (22.6.3.1)$$

$$S_{\mu\nu} = \langle \chi_{\mu} | \chi_{\nu} \rangle, \gamma_{\delta\kappa} = \sum_{i=occ} C_{\delta i} C_{\kappa i}, \quad (22.6.3.2)$$

$$\text{and } \gamma_{\delta\kappa}^{ex} = \sum_{\substack{i=occ \\ \text{and} \\ \text{same spin}}} C_{\delta i} C_{\kappa i}. \quad (22.6.3.3)$$

Note that the sum over i in $\gamma_{\delta\kappa}$ and $\gamma_{\delta\kappa}^{ex}$ is a sum over spin orbitals. In addition, show that this Fock matrix can be further reduced for the closed shell case to:

$$F_{\mu\nu} = \langle \chi_{\mu} | h | \chi_{\nu} \rangle + \sum_{\delta\kappa} P_{\delta\kappa} \left[\langle \chi_{\mu} \chi_{\delta} | g | \chi_{\nu} \chi_{\kappa} \rangle - \frac{1}{2} \langle \chi_{\mu} \chi_{\delta} | g | \chi_{\kappa} \chi_{\nu} \rangle \right],$$

where the charge bond order matrix, P, is defined to be:

$$P_{\delta\kappa} = \sum_{i=occ} 2C_{\delta i} C_{\kappa i},$$

where the sum over i here is a sum over orbitals not spin orbitals.

Q2

Show that the HF total energy for a closed-shell system may be written in terms of integrals over the orthonormal HF orbitals as:

$$E(\text{SCF}) = 2 \sum_k^{occ} \langle \phi_k | h | \phi_k \rangle + \sum_{kl}^{occ} [2 \langle k1 | g k1 \rangle - \langle k1 | g | 1k \rangle] + \sum_{\mu>\nu} \frac{Z_{\mu} Z_{\nu}}{R_{\mu\nu}}.$$

Q3

Show that the HF total energy may alternatively be expressed as:

$$E(\text{SCF}) = \sum_k^{occ} (\epsilon_k + \langle \phi_k | h | \phi_k \rangle) + \sum_{\mu>\nu} \frac{Z_{\mu} Z_{\nu}}{R_{\mu\nu}}$$

where the ϵ_k refer to the HF orbital energies.

This page titled [22.6.3: ii. Exercises](#) is shared under a [CC BY-NC-SA 4.0](#) license and was authored, remixed, and/or curated by [Jack Simons](#) via [source content](#) that was edited to the style and standards of the LibreTexts platform.

22.6.4: iii. Problems

Q1

This problem will be concerned with carrying out an SCF calculation for the HeH^+ molecule in the $1\sum_g^+(1\sigma^2)$ ground state. The one- and two-electron integrals (in atomic units) needed to carry out this SCF calculation at $R = 1.4$ a.u. using Slater type orbitals with orbital exponents of 1.6875 and 1.0 for the He and H, respectively are:

$$S_{11} = 1.0, \quad S_{22} = 1.0, \quad S_{12} = 0.5784 \quad (22.6.4.1)$$

$$h_{11} = -2.6442, \quad h_{22} = -1.7201, \quad h_{12} = -1.5113, \quad (22.6.4.2)$$

$$g_{1111} = 1.0547, \quad g_{1121} = 0.4744, \quad g_{1212} = 0.5664, \quad (22.6.4.3)$$

$$g_{2211} = 0.2469, \quad g_{2221} = 0.3504, \quad g_{2222} = 0.6250, \quad (22.6.4.4)$$

where 1 refers to $1s_{\text{He}}$ and 2 to $1s_{\text{H}}$. Note that the two-electrons integrals are given in Dirac notation. Parts a. - d. should be done by hand. Any subsequent parts can make use of the QMIC software provided.

- Using $\phi_1 \approx 1s_{\text{He}}$ for the initial guess of the occupied molecular orbital, form a 2x2 Fock matrix. Use the equation derived above in question 1 for $F_{\mu\nu}$.
- Solve the Fock matrix eigenvalue equations given above to obtain the orbital energies and an improved occupied molecular orbital. In so doing, note that $\langle \phi_1 | \phi_1 \rangle = 1 = C_1^T S C_1$ gives the needed normalization condition for the expansion coefficients of the ϕ_1 in the atomic orbital basis.
- Determine the total SCF energy using the result of exercise 3 above at this step of the iterative procedure. When will this energy agree with that obtained by using the alternative expression for $E(\text{SCF})$ given in exercise 2?
- Obtain the new molecular orbital, ϕ_1 , from the solution of the matrix eigenvalue problem (part b).
- A new Fock matrix and related total energy can be obtained with this improved choice of molecular orbital, ϕ_1 . This process can be continued until a convergence criterion has been satisfied. Typical convergence criteria include: no significant change in the molecular orbitals or the total energy (or both) from one iteration to the next. Perform this iterative procedure for the HeH^+ system until the difference in total energy between two successive iterations is less than 10^{-5} a.u.
- Show, by comparing the difference between the SCF total energy at one iteration and the converged SCF total energy, that the convergence of the above SCF approach is primarily linear (or first order).
- Is the SCF total energy calculated at each iteration of the above SCF procedure (via exercise 3) an upper bound to the exact ground-state total energy?
- Using the converged self-consistent set of molecular orbitals, ϕ_1 and ϕ_2 , calculate the one- and two-electron integrals in the molecular orbital basis. Using the equations for $E(\text{SCF})$ in exercises 2 and 3 calculate the converged values of the orbital energies making use of these integrals in the mo basis.
- Does this SCF wavefunction give rise (at $R \rightarrow \infty$) to proper dissociation products?

Q2

This problem will continue to address the same HeH^+ molecular system as above, extending the analysis to include "correlation effects." We will use the one- and two-electron integrals (same geometry) in the converged (to 10^{-5} au) SCF molecular orbital basis which we would have obtained after 7 iterations above. The **converged** mos you would have obtained in problem 1 are:

$$\phi_1 = \begin{bmatrix} -0.89997792 \\ -0.15843012 \end{bmatrix} \quad \phi_2 = \begin{bmatrix} -0.83233180 \\ 1.21558030 \end{bmatrix}$$

- Carry out a two configuration CI calculation using the $1\sigma^2$ and $2\sigma^2$ configurations first by obtaining an expression for the CI matrix elements $H_{ij}(i, j = 1\sigma^2, 2\sigma^2)$ in terms of one- and two-electron integrals, and secondly by showing that the resultant CI matrix is (ignoring the nuclear repulsion term):

$$\begin{bmatrix} -4.2720 & 0.1261 \\ 0.1261 & -2.0149 \end{bmatrix}$$

- b. Obtain the two CI energies and eigenvectors for the matrix found in a part a.
- c. Show that the lowest energy CI wavefunction is equivalent to the following two-determinant (single configuration) wavefunction:

$$\frac{1}{2} \left[\left| \left(\frac{1}{a} \frac{1}{2} \phi_1 + b \frac{1}{2} \phi_2 \right) \alpha \left(\frac{1}{a} \frac{1}{2} \phi_1 - b \frac{1}{2} \phi_2 \right) \beta \right| + \left| \left(\frac{1}{a} \frac{1}{2} \phi_1 - b \frac{1}{2} \phi_2 \right) \alpha \left(\frac{1}{a} \frac{1}{2} \phi_1 + b \frac{1}{2} \phi_2 \right) \beta \right| \right]$$

involving the polarized orbitals: $\frac{1}{a} \frac{1}{2} \phi_1 \pm b \frac{1}{2} \phi_2$, where $a = 0.9984$ and $b = 0.0556$.

- d. Expanding the CI list to 3 configurations by adding the $1\sigma 2\sigma$ to the original $1\sigma^2$ and $2\sigma^2$ configurations of part a above. First, express the proper singlet spin-coupled $1\sigma 2\sigma$ configuration as a combination of Slater determinants and then compute all elements of this 3x3 matrix.
- e. Obtain all eigenenergies and corresponding normalized eigenvectors for this CI problem.
- f. Determine the excitation energies and transition moments for HeH^+ using the full CI result of part e above. The nonvanishing matrix elements of the dipole operator $\mathbf{r}(x,y,z)$ in the atomic basis are:

$$\langle 1_{SH} | z | 1_{SHe} \rangle = 0.2854 \text{ and } \langle 1_{SH} | z | 1_{SH} \rangle = 1.4$$

First determine the matrix elements of \mathbf{r} in the SCF orbital basis then determine the excitation energies and transition moments from the ground state to the two excited singlet states of HeH^+ .

- g. Now turning to perturbation theory, carry out a RSPT calculation of the first-order wavefunction $|1\sigma^2\rangle^{(1)}$ for the case in which the zeroth-order wavefunction is taken to be the $1\sigma^2$ Slater determinant. Show that the first-order wavefunction is given by:

$$|1\sigma^2\rangle^{(1)} = -0.0442|2\sigma^2\rangle.$$

- h. Why does the $|1\sigma 2\sigma\rangle$ configuration not enter into the first-order wavefunction?
- i. Normalize the resultant wavefunction that contains zeroth- plus first-order parts and compare it to the wavefunction obtained in the two-configuration CI study of part b.
- j. Show that the second-order RSPT correlation energy, $E^{(2)}$, of HeH^+ is -0.0056 a.u. How does this compare with the correlation energy obtained from the two- configuration CI study of part b?

Q3

Using the QMIC programs, calculate the SCF energy of HeH^+ using the same geometry as in problem 1 and the STO3G basis set provided in the QMIC basis set library. How does this energy compare to that found in problem 1? Run the calculation again with the 3- 21G basis basis provided. How does this energy compare to the STO3G and the energy found using STOs in problem 1?

Q4

Generate SCF potential energy surfaces for HeH^+ and H_2 using the QMIC software provided. Use the 3-21G basis set and generate points for geometries of $R = 1.0, 1.2, 1.4, 1.6, 1.8, 2.0, 2.5$, and 10.0 . Plot the energies vs. geometry for each system. Which system dissociates properly?

Q5

Generate CI potential energy surfaces for the 4 states of H_2 resulting from a CAS calculation with 2 electrons in the lowest 2 SCF orbitals ($1\sigma_g$ and $1\sigma_u$). Use the same geometries and basis set as in problem 4. Plot the energies vs. geometry for each system. Properly label and characterize each of the states (e.g., repulsive, dissociate properly, etc.).

This page titled [22.6.4: iii. Problems](#) is shared under a [CC BY-NC-SA 4.0](#) license and was authored, remixed, and/or curated by [Jack Simons](#) via [source content](#) that was edited to the style and standards of the LibreTexts platform.

22.6.5: iv. Review Exercise Solutions

Q1

Slater type orbitals (STOs) are "hydrogen-like" in that they have a normalized form of:

$$\left(\frac{2\xi}{a_0}\right)^{n+\frac{1}{2}} \left(\frac{1}{(2n)!}\right)^{\frac{1}{2}} r^{n-1} e^{\left(\frac{-\xi r}{a_0}\right)} Y_{l,m}(\theta, \phi),$$

where as gaussian type orbitals GTOs have the form:

$$N' x^a y^b z^c e^{(-\alpha r^2)},$$

where a, b, and c are quantum numbers each ranging from zero upward in unit steps. So, STOs give "better" overall energies and properties that depend on the shape of the wavefunction near the nuclei (e.g., Fermi contact ESR hyperfine constants) but they are more difficult to use (two-electron integrals are more difficult to evaluate; especially the 4- center variety which have to be integrated numerically). GTOs on the other hand are easier to use (more easily integrable) but improperly describe the wavefunction near the nuclear centers because of the so-called cusp condition (they have zero slope at $R = 0$, whereas 1s STOs have non-zero slopes there).

This page titled [22.6.5: iv. Review Exercise Solutions](#) is shared under a [CC BY-NC-SA 4.0](#) license and was authored, remixed, and/or curated by [Jack Simons](#) via [source content](#) that was edited to the style and standards of the LibreTexts platform.

22.6.6: v. Exercise Solutions

Q1

$$F\phi_i = \varepsilon_i \phi_j = h\phi_i + \sum_j [J_j - K_j] \phi_i$$

Let the closed shell Fock potential be written as:

$$V_{ij} = \sum_k (2\langle ik|jk\rangle - \langle ik|kj\rangle), \text{ and the } 1e^- \text{ component as:} \quad (22.6.6.1)$$

$$h_{ij} = \langle \phi_i | -\frac{1}{2}\nabla^2 - \sum_A \frac{Z_A}{|r - R_A|} | \phi_j \rangle, \text{ and the delta as:} \quad (22.6.6.2)$$

$$\delta_{ij} = \langle i|j\rangle, \text{ so that: } h_{ij} + V_{ij} = \delta_{ij}\varepsilon_i \quad (22.6.6.3)$$

$$\text{using: } \phi_i = \sum_\mu C_{\mu i} \chi_\mu, \phi_j = \sum_\nu C_{\nu j} \chi_\nu, \text{ and } \phi_k = \sum_\gamma C_{\gamma k} \chi_\gamma \quad (22.6.6.4)$$

, and transforming from the mo to ao basis we obtain:

$$V_{ij} = \sum_{k\mu\gamma\nu\kappa} C_{\mu i} C_{\gamma k} C_{\nu j} C_{\kappa k} (2\langle \mu\gamma|\nu\kappa\rangle - \langle \mu\gamma|\kappa\nu\rangle) \quad (22.6.6.5)$$

$$= \sum_{k\mu\gamma\nu\kappa} (C_{\gamma k} C_{\kappa k}) (C_{\mu i} C_{\nu j}) (2\langle \mu\gamma|\nu\kappa\rangle - \langle \mu\gamma|\kappa\nu\rangle) \quad (22.6.6.6)$$

$$= \sum_{\mu\nu} (C_{\mu i} C_{\nu j}) V_{\mu\nu} \text{ where,} \quad (22.6.6.7)$$

$$V_{\mu\nu} = \sum_{\gamma\kappa} P_{\gamma\kappa} (2\langle \mu\gamma|\nu\kappa\rangle - \langle \mu\gamma|\kappa\nu\rangle), \text{ and } P_{\gamma\kappa} = \sum_k (C_{\gamma k} C_{\kappa k}), \quad (22.6.6.8)$$

$$h_{ij} = \sum_{\mu\nu} (C_{\mu i} C_{\nu j}) h_{\mu\nu}, \text{ where} \quad (22.6.6.9)$$

$$h_{\mu\nu} = \langle \chi_\mu | -\frac{1}{2}\nabla^2 - \sum_A \frac{Z_A}{|r - R_A|} | \chi_\nu \rangle, \text{ and} \quad (22.6.6.10)$$

$$\delta_{ij} = \langle i|j\rangle = \sum_{\mu\nu} (C_{\mu i} S_{\mu\nu} C_{\nu j}). \quad (22.6.6.11)$$

SO, $h_{ij} + V_{ij} = \delta_{ij}\varepsilon_j$ becomes:

$$\sum_{\mu\nu} (C_{\mu i} C_{\nu j}) h_{\mu\nu} + \sum_{\mu\nu} (C_{\mu i} C_{\nu j}) V_{\mu\nu} = \sum_{\mu\nu} (C_{\mu i} S_{\mu\nu} C_{\nu j}) \varepsilon_j, \quad (22.6.6.12)$$

$$\sum_{\mu\nu} (C_{\mu i} S_{\mu\nu} C_{\nu j}) \varepsilon_j - \sum_{\mu\nu} (C_{\mu i} C_{\nu j}) h_{\mu\nu} - \sum_{\mu\nu} (C_{\mu i} C_{\nu j}) V_{\mu\nu} = 0 \text{ for all } i, j \quad (22.6.6.13)$$

$$\sum_{\mu\nu} C_{\mu i} [\varepsilon_j S_{\mu\nu} - h_{\mu\nu} - V_{\mu\nu}] C_{\nu j} = 0 \text{ for all } i, j \quad (22.6.6.14)$$

$$\text{Therefore,} \quad (22.6.6.15)$$

$$\sum_\nu [h_{\mu\nu} + V_{\mu\nu} - \varepsilon_j S_{\mu\nu}] C_{\nu j} = 0 \quad (22.6.6.16)$$

This is FC = SCE.

Q2

The Slater Condon rule for zero (spin orbital) difference with N electrons in N spin orbitals is:

$$E = \langle |H + G| \rangle = \sum_i^N \langle \phi_i | h | \phi_i \rangle + \sum_{i>j}^N (\langle \phi_i \phi_j | g | \phi_i \phi_j \rangle - \langle \phi_i \phi_j | g | \phi_j \phi_i \rangle) \quad (22.6.6.17)$$

$$= \sum_i h_{ii} + \sum_{i>j} (g_{ijji} - g_{ijji}) \quad (22.6.6.18)$$

$$= \sum_i h_{ii} + \frac{1}{2} \sum_{ij} (g_{ijij} - g_{ijji}) \quad (22.6.6.19)$$

If all orbitals are doubly occupied and we carry out the spin integration we obtain:

$$E = 2 \sum_i^{occ} h_{ii} + \sum_{ij}^{occ} (2g_{ijij} - g_{ijji}),$$

where i and j now refer to orbitals (not spin-orbitals).

Q3

If the occupied orbitals obey $F\phi_k = \varepsilon_k \phi_k$, then the expression for E in problem 2 above can be rewritten as.

$$E = \sum_i^{occ} \left(h_{ii} + \sum_j^{occ} (2g_{ijij} - g_{ijji}) \right) + \sum_i^{occ} h_{ii}$$

We recognize the closed shell Fock operator expression and rewrite this as

$$E = \sum_i^{occ} F_{ii} + \sum_i^{occ} h_{ii} = \sum_i^{occ} (\varepsilon_i + h_{ii})$$

This page titled [22.6.6: v. Exercise Solutions](#) is shared under a [CC BY-NC-SA 4.0](#) license and was authored, remixed, and/or curated by [Jack Simons](#) via [source content](#) that was edited to the style and standards of the LibreTexts platform.

22.6.7: vi. Problem Solutions

1. We will use the QMIC software to do this problem. Lets just start from the beginning. Get the starting "guess" mo coefficients on disk. Using the program MOCOEFs it asks us for the first and second mo vectors. We input 1, 0 for the first mo (this means that the first mo is 1.0 times the He 1s orbital plus 0.0 times the H 1s orbital; this bonding mo is more likely to be heavily weighted on the atom having the higher nuclear charge) and 0, 1 for the second. Our beginning mo-ao array looks like:

$$\begin{bmatrix} 1.0 & 0.0 \\ 0.0 & 1.0 \end{bmatrix} \quad (22.6.7.1)$$

and is placed on disk in a file we choose to call "mocoefs.dat". We also put the ao integrals on disk using the program RW_INTS. It asks for the unique one- and two- electron integrals and places a canonical list of these on disk in a file we choose to call "ao_integrals.dat". At this point it is useful for us to step back and look at the set of equations which we wish to solve: FC = SCE. The QMIC software does not provide us with a so-called generalized eigenvalue solver (one that contains an overlap matrix; or metric), so in order to use the diagonalization program that is provided we must transform this equation (FC = SCE) to one that looks like (F'C' = C'E). We do that in the following manner:

Since S is symmetric and positive definite we can find an $S^{-\frac{1}{2}}$ such that $S^{-\frac{1}{2}} S^{-\frac{1}{2}} = 1$, $S^{-\frac{1}{2}} S = S^{+\frac{1}{2}}$, etc. rewrite FC = SCE by inserting unity between FC and multiplying the whole equation on the left by $S^{-\frac{1}{2}}$. This gives:

$$S^{-\frac{1}{2}} F S^{-\frac{1}{2}} S^{+\frac{1}{2}} C = S^{-\frac{1}{2}} S C E = S^{+\frac{1}{2}} C E$$

Letting:

$$F' = S^{-\frac{1}{2}} F S^{-\frac{1}{2}} \quad (22.6.7.2)$$

$$C' = S^{+\frac{1}{2}} C, \text{ and inserting expressions above give:} \quad (22.6.7.3)$$

$$F' C' = C' E \quad (22.6.7.4)$$

Note, that to get the next iterations mo coefficients we must calculate C from C':

$C' = S^{+\frac{1}{2}} C$, so, multiplying through on the left by $S^{-\frac{1}{2}}$ gives:

$$S^{-\frac{1}{2}} C' = S^{-\frac{1}{2}} S^{+\frac{1}{2}} C = C$$

This will be the method we will use to solve our fock equations.

Find $S^{-\frac{1}{2}}$ by using the program FUNCT_MAT (this program generates a function of a matrix). This program will ask for the elements of the S array and write to disk a file (name of your choice ... a good name might be "shalf") containing the $S^{-\frac{1}{2}}$ array. Now we are ready to begin the iterative Fock procedure.

a. Calculate the Fock matrix, F, using program FOCK which reads in the mo coefficients from "mocoefs.dat" and the integrals from "ao_integrals.dat" and writes the resulting Fock matrix to a user specified file (a good filename to use might be something like "fock1").

b. Calculate $F' = S^{-\frac{1}{2}} F S^{-\frac{1}{2}}$ using the program UTMATU which reads in F and $S^{-\frac{1}{2}}$ from files on the disk and writes F' to a user specified file (a good filename to use might be something like "fock1p"). Diagonalize F' using the program DIAG. This program reads in the matrix to be diagonalized from a user specified filename and writes the resulting eigenvectors to disk using a user specified filename (a good filename to use might be something like "coef1p"). You may wish to choose the option to write the eigenvalues (Fock orbital

energies) to disk in order to use them at a later time in program FENERGY. Calculate C by back transforming e.g. $C = S^{-\frac{1}{2}} C'$. This is accomplished by using the program MATXMAT which reads in two matrices to be multiplied from user specified files and writes the product to disk using a user specified filename (a good filename to use might be something like "mocoefs.dat").

c. The QMIC program FENERGY calculates the total energy, using the result of exercises 2 and 3;

$$\sum_{kl} 2\langle k|h|k\rangle + 2\langle k1|1k\rangle - \langle k1|1k\rangle + \sum_{\mu>\nu} \frac{Z_{\mu}Z_{\nu}}{R_{\mu\nu}}, \text{ and } \sum_k \varepsilon_k + \langle k|h|k\rangle + \sum_{\mu>\nu} \frac{Z_{\mu}Z_{\nu}}{R_{\mu\nu}}.$$

This is the conclusion of one iteration of the Fock procedure ... you may continue by going back to part a. and proceeding onward.

d. and e. Results for the successful convergence of this system using the supplied QMIC software is as follows (this is alot of bloody detail but will give the user assurance that they are on the right track; alternatively one could switch to the QMIC program SCF and allow that program to iteratively converge the Fock equations):

The one-electron AO integrals:

$$\begin{bmatrix} -2.644200 & -1.511300 \\ -1.511300 & -1.720100 \end{bmatrix}$$

The two-electron AO integrals:

1	1	1	1	1.054700	(22.6.7.5)
2	1	1	1	0.4744000	(22.6.7.6)
2	1	2	1	0.5664000	(22.6.7.7)
2	2	1	1	0.2469000	(22.6.7.8)
2	2	2	1	0.3504000	(22.6.7.9)
2	2	2	2	0.6250000	(22.6.7.10)

The "initial" MO-AO coefficients:

$$\begin{bmatrix} 1.000000 & 0.000000 \\ 0.000000 & 1.000000 \end{bmatrix}$$

AO overlap matrix (S):

$$\begin{bmatrix} 1.000000 & 0.578400 \\ 0.578400 & 1.000000 \end{bmatrix}$$

$$S^{-\frac{1}{2}} \begin{bmatrix} 1.168032 & -0.3720709 \\ -0.3720709 & 1.168031 \end{bmatrix}$$

ITERATION 1

The charge bond order matrix

$$\begin{bmatrix} 1.000000 & 0.000000 \\ 0.000000 & 0.000000 \end{bmatrix}$$

The Fock matrix (F):

$$\begin{bmatrix} -1.589500 & -1.036900 \\ -1.036900 & -0.8342001 \end{bmatrix}$$

$$S^{-\frac{1}{2}} F S^{-\frac{1}{2}}$$

$$\begin{bmatrix} -1.382781 & -0.5048679 \\ -0.5048678 & -0.4568883 \end{bmatrix}$$

The eigenvalues of this matrix (Fock orbital energies) are:

$$[-1.604825 \quad -0.2348450]$$

Their corresponding eigenvectors ($C = S^{-\frac{1}{2}} * C'$) are:

$$\begin{bmatrix} -0.9153809 & -0.4025888 \\ -0.4025888 & 0.9153810 \end{bmatrix}$$

The "new" MO-AO coefficients ($C = S^{-\frac{1}{2}} * C'$)

$$\begin{bmatrix} -0.9194022 & -0.8108231 \\ -0.1296498 & 1.218985 \end{bmatrix}$$

The one-electron MO integrals:

$$\begin{bmatrix} -2.624352 & -0.1644336 \\ -0.1644336 & -1.306845 \end{bmatrix}$$

The two-electron MO integrals:

1	1	1	1	0.9779331	(22.6.7.11)
2	1	1	1	0.1924623	(22.6.7.12)
2	1	2	1	0.5972075	(22.6.7.13)
2	2	1	1	0.1170838	(22.6.7.14)
2	2	2	1	-0.0007945194	(22.6.7.15)
2	2	2	2	0.6157323	(22.6.7.16)

The closed shell Fock energy from formula:

$$\sum_{kl} 2 \langle k|h|k \rangle + 2 \langle k1|k1 \rangle - \langle k1|1k \rangle + \sum_{\mu>\nu} \frac{Z_{\mu}Z_{\nu}}{R_{\mu\nu}} = -2.84219933$$

from formula:

$$\sum_k \varepsilon_k + \langle k|h|k \rangle + \sum_{\mu>\nu} \frac{Z_{\mu}Z_{\nu}}{R_{\mu\nu}} = -2.80060530$$

the difference is:

$$-0.04159403$$

 ITERATION 2

The change bond order matrix:

$$\begin{bmatrix} 0.8453005 & 0.1192003 \\ 0.1192003 & 0.01680906 \end{bmatrix}$$

The Fock matrix:

$$\begin{bmatrix} -1.624673 & -1.083623 \\ -1.083623 & -0.8772071 \end{bmatrix}$$

$$S^{-\frac{1}{2}} F S^{-\frac{1}{2}}$$

$$\begin{bmatrix} -1.396111 & -0.5411037 \\ -0.5411037 & -0.4798213 \end{bmatrix}$$

The eigenvalues of this matrix (Fock orbital energies) are:

$$[-1.646972 \quad -0.2289599]$$

Their corresponding eigenvectors ($C' = S^{-\frac{1}{2}} * C$) are:

$$\begin{bmatrix} -0.9072427 & -0.4206074 \\ -0.4206074 & 0.9072427 \end{bmatrix}$$

The "new" MO-AO coefficients ($C = S^{-\frac{1}{2}} * C'$):

$$\begin{bmatrix} -0.9031923 & -0.8288413 \\ -0.1537240 & 1.216184 \end{bmatrix}$$

The one-electron MO integrals:

$$\begin{bmatrix} -2.617336 & -0.1903475 \\ -0.1903475 & -1.313861 \end{bmatrix}$$

The two-electron MO integrals:

1	1	1	1	0.9626070	(22.6.7.17)
2	1	1	1	0.1949828	(22.6.7.18)
2	1	2	1	0.6048143	(22.6.7.19)
2	2	1	1	0.1246907	(22.6.7.20)
2	2	2	1	0.003694540	(22.6.7.21)
2	2	2	2	0.6158437	(22.6.7.22)

The closed shell Fock energy from formula:

$$\sum_{kl} 2\langle k|h|k\rangle + 2\langle kl|kl\rangle - \langle kl|lk\rangle + \sum_{\mu>\nu} \frac{Z_{\mu}Z_{\nu}}{R_{\mu\nu}} = -2.84349298$$

from formula:

$$\sum_k \varepsilon_k + \langle k|h|k\rangle + \sum_{\mu>\nu} \frac{Z_{\mu}Z_{\nu}}{R_{\mu\nu}} = -2.83573675$$

the difference is:

$$-0.00775623$$

 ITERATION 3

The charge bond order matrix:

$$\begin{bmatrix} -1.631153 & -1.091825 \\ -1.091825 & -0.8853514 \end{bmatrix}$$

$$S^{-\frac{1}{2}} F S^{-\frac{1}{2}}$$

$$\begin{bmatrix} -1.398951 & -0.5470731 \\ -0.5470730 & -0.4847007 \end{bmatrix}$$

The eigenvalues of this matrix (Fock orbital energies) are:

$$[-1.654745 \quad -0.2289078]$$

Their corresponding eigenvectors ($C' = S^{-\frac{1}{2}} * C$) are:

$$\begin{bmatrix} -0.9058709 & -0.4235546 \\ -0.4235545 & 0.9058706 \end{bmatrix}$$

The "new" MM-AO coefficients ($C = S^{-\frac{1}{2}} * C'$):

$$\begin{bmatrix} -0.9004935 & -0.8317733 \\ -0.1576767 & 1.215678 \end{bmatrix}$$

The one-electron MO integrals:

$$\begin{bmatrix} -2.616086 & -0.1945811 \\ -0.1945811 & -1.315112 \end{bmatrix}$$

The two-electron MO integrals:

1	1	1	1	0.9600707	(22.6.7.23)
2	1	1	1	0.1953255	(22.6.7.24)
2	1	2	1	0.6060572	(22.6.7.25)
2	2	1	1	0.1259332	(22.6.7.26)
2	2	2	1	0.004475587	(22.6.7.27)
2	2	2	2	0.6158972	(22.6.7.28)

The closed shell Fock energy from formula:

$$\sum_{kl} 2\langle k|h|k\rangle + 2\langle kl|kl\rangle - \langle kl|lk\rangle + \sum_{\mu>\nu} \frac{Z_{\mu}Z_{\nu}}{R_{\mu\nu}} = -2.84353018$$

from formula:

$$\sum_k \epsilon_k + \langle k|h|k\rangle + \sum_{\mu>\nu} \frac{Z_{\mu}Z_{\nu}}{R_{\mu\nu}} = -2.84225941$$

the difference is:

$$-0.00127077$$

ITERATION 4

The charge bond order matrix:

$$\begin{bmatrix} 0.8108885 & -1.093155 \\ -1.093155 & -0.8866909 \end{bmatrix}$$

The Fock matrix:

$$\begin{bmatrix} -1.632213 & -1.093155 \\ -1.093155 & -0.8866909 \end{bmatrix}$$

$$S^{-\frac{1}{2}} F S^{-\frac{1}{2}}$$

$$\begin{bmatrix} -1.399426 & -0.5480287 \\ -0.5480287 & -0.4855191 \end{bmatrix}$$

The eigenvalues of this matrix (Fock orbital energies) are:

$$[-1.656015 \quad -0.2289308]$$

Their corresponding eigenvectors ($C' = S^{-1/2} * C$) are:

$$\begin{bmatrix} -0.9056494 & -0.4240271 \\ -0.4240271 & 0.9056495 \end{bmatrix}$$

The "new" MO-AO coefficients ($C = S^{-1/2} * C'$):

$$[-0.9000589 \quad -0.8322428 \quad -0.1583111 \quad 1.215595]$$

The one-electron MO integrals:

$$\begin{bmatrix} -2.615881 & -0.1952594 \\ -0.1952594 & -1.315315 \end{bmatrix}$$

The two-electron MO integrals:

1	1	1	1	0.9596615	(22.6.7.29)
2	1	1	1	0.1953781	(22.6.7.30)
2	1	2	1	0.6062557	(22.6.7.31)
2	2	1	1	0.1261321	(22.6.7.32)
2	2	2	1	0.004601604	(22.6.7.33)
2	2	2	2	0.6159065	(22.6.7.34)

The closed shell Fock energy from formula:

$$\sum_{kl} 2 \langle k|h|k \rangle + 2 \langle kl|kl \rangle - \langle kl|lk \rangle + \sum_{\mu>\nu} \frac{Z_\mu Z_\nu}{R_{\mu\nu}} = -2.84352922$$

from formula:

$$\sum_k \varepsilon_k + \langle k|h|k \rangle + \sum_{\mu>\nu} \frac{Z_\mu Z_\nu}{R_{\mu\nu}} = -2.84332418$$

the difference is:

$$-0.00020504$$

ITERATION 5

The charge bond order matrix:

$$\begin{bmatrix} 0.8101060 & 0.1424893 \\ 0.1424893 & 0.02506241 \end{bmatrix}$$

The Fock matrix:

$$\begin{bmatrix} -1.632385 & -1.093368 \\ -1.093368 & -0.8869066 \end{bmatrix}$$

$$S^{-1/2} F S^{-1/2}$$

$$\begin{bmatrix} -1.399504 & -0.5481812 \\ -0.5481813 & -0.4856516 \end{bmatrix}$$

The eigenvalues of this matrix (Fock orbital energies) are:

$$[-1.656219 \quad -0.2289360]$$

Their corresponding eigenvectors ($C' = S^{-\frac{1}{2}} * C$) are:

$$\begin{bmatrix} -0.9056138 & -0.4241026 \\ -0.4241028 & 0.9056141 \end{bmatrix}$$

The "new" MO-AO coefficients ($C = S^{-\frac{1}{2}} * C'$):

$$\begin{bmatrix} -0.8999892 & -0.8323179 \\ -0.1584127 & 1.215582 \end{bmatrix}$$

The one-electron MO integrals:

$$\begin{bmatrix} -2.615847 & -0.1953674 \\ -0.1953674 & -1.315348 \end{bmatrix}$$

The two-electron MO integrals:

1	1	1	1	0.9595956	(22.6.7.35)
2	1	1	1	0.1953862	(22.6.7.36)
2	1	2	1	0.6062872	(22.6.7.37)
2	2	1	1	0.1261639	(22.6.7.38)
2	2	2	1	0.004621811	(22.6.7.39)
2	2	2	2	0.6159078	(22.6.7.40)

The closed shell Fock energy from formula:

$$\sum_{kl} 2 \langle k|h|k \rangle + 2 \langle kl|kl \rangle - \langle kl|lk \rangle + \sum_{\mu>\nu} \frac{Z_{\mu} Z_{\nu}}{R_{\mu\nu}} = -2.84352779$$

from formula:

$$\sum_k \varepsilon_k + \langle k|h|k \rangle + \sum_{\mu>\nu} \frac{Z_{\mu} Z_{\nu}}{R_{\mu\nu}} = -2.84349489$$

the difference is:
-0.00003290

ITERATION 6

The charge bond order matrix:

$$\begin{bmatrix} 0.8099805 & 0.1425698 \\ 0.1425698 & 0.02509460 \end{bmatrix}$$

The Fock matrix:

$$\begin{bmatrix} -1.632412 & -1.093402 \\ -1.093402 & -0.8869413 \end{bmatrix}$$

$$S^{-\frac{1}{2}} F S^{-\frac{1}{2}}$$

$$\begin{bmatrix} -1.399517 & -0.5482056 \\ -0.5482056 & -0.4856730 \end{bmatrix}$$

The eigenvalues of this matrix (Fock orbital energies) are:

$$[-1.656253 \quad -0.2289375]$$

Their corresponding eigenvectors ($C' = S^{-\frac{1}{2}} * C$) are:

$$\begin{bmatrix} -0.9056085 & -0.4241144 \\ -0.4241144 & 0.9056086 \end{bmatrix}$$

The "new" MO-AO coefficients ($C = S^{-\frac{1}{2}} * C'$):

$$\begin{bmatrix} 0.8999786 & -0.8323296 \\ -0.15842831 & 1.215580 \end{bmatrix}$$

The one-electron MO integrals:

$$\begin{bmatrix} -2.615843 & -0.1953846 \\ -0.1953846 & -1.315353 \end{bmatrix}$$

The two-electron MO integrals:

1	1	1	1	0.9595859	(22.6.7.41)
2	1	1	1	0.1953878	(22.6.7.42)
2	1	2	1	0.6062925	(22.6.7.43)
2	2	2	1	0.004625196	(22.6.7.44)
2	2	2	2	0.6159083	(22.6.7.45)

The closed shell Fock energy from formula:

$$\sum_{kl} 2\langle k|h|k\rangle 2\langle kl|kl\rangle - \langle kl|lk\rangle + \sum_{\mu>\nu} \frac{Z_\mu Z_\nu}{R_{\mu\nu}} = -2.84352827$$

from formula:

$$\sum_k \varepsilon_k + \langle k|h|k\rangle + \sum_{\mu>\nu} \frac{Z_\mu Z_\nu}{R_{\mu\nu}} = -2.84352398$$

the difference is:
-0.00000429

ITERATION 7

The charge bond order matrix:

$$\begin{bmatrix} 0.8099616 & 0.1425821 \\ 0.1425821 & 0.02509952 \end{bmatrix}$$

The Fock matrix:

$$\begin{bmatrix} -1.632416 & -1.093407 \\ -1.093407 & -0.8869464 \end{bmatrix}$$

$$S^{-\frac{1}{2}} F S^{-\frac{1}{2}}$$

$$\begin{bmatrix} -1.399519 & -0.5482093 \\ -0.5482092 & -0.4856761 \end{bmatrix}$$

The eigenvalues of this matrix (Fock orbital energies) are:

$$[-1.656257 \quad -0.2289374]$$

Their corresponding eigenvectors ($C' = S^{-\frac{1}{2}} * C$) are:

$$\begin{bmatrix} -0.9056076 & -0.4241164 \\ -0.4241164 & 0.9056077 \end{bmatrix}$$

The "new" MO-AO coefficients ($C = S^{-\frac{1}{2}} * C'$):

$$\begin{bmatrix} -0.8999770 & -0.8323317 \\ -0.1584310 & 1.215580 \end{bmatrix}$$

The one-electron MO integrals:

$$\begin{bmatrix} -2.615843 & -0.1953876 \\ -0.1953876 & -1.315354 \end{bmatrix}$$

The two-electron MO integrals:

1	1	1	1	0.9595849	(22.6.7.46)
2	1	1	1	0.1953881	(22.6.7.47)
2	1	2	1	0.6062936	(22.6.7.48)
2	2	1	1	0.1261697	(22.6.7.49)
2	2	2	1	0.004625696	(22.6.7.50)
2	2	2	2	0.6159083	(22.6.7.51)

The closed shell Fock energy from formula:

$$\sum_{kl} 2\langle k|h|k\rangle + 2\langle kl|kl\rangle - \langle kl|lk\rangle + \sum_{\mu>\nu} \frac{Z_{\mu}Z_{\nu}}{R_{\mu\nu}} = -2.84352922$$

from formula:

$$\sum_k \varepsilon_k + \langle k|h|k\rangle + \sum_{\mu>\nu} \frac{Z_{\mu}Z_{\nu}}{R_{\mu\nu}} = -2.84352827$$

the difference is:

$$-0.00000095$$

 ITERATION 8

The charge bond order matrix:

$$\begin{bmatrix} 0.8099686 & 0.1425842 \\ 0.1425842 & 0.02510037 \end{bmatrix}$$

The Fock matrix:

$$\begin{bmatrix} -1.632416 & -1.093408 \\ -1.093408 & -0.8869470 \end{bmatrix}$$

$$S \frac{1}{2} F S \frac{1}{2}$$

$$\begin{bmatrix} -1.399518 & -0.5482103 \\ -0.5482102 & -0.4856761 \end{bmatrix}$$

The eigenvalues of this matrix (Fock orbital energies) are:

$$[-1.656258 - 0.2289368]$$

Their corresponding eigenvectors ($C = S^{-\frac{1}{2}} * C'$) are:

$$\begin{bmatrix} -0.9056074 & -0.4241168 \\ -0.4241168 & 0.9056075 \end{bmatrix}$$

The "new" MO-AO coefficients ($C = S^{-\frac{1}{2}} * C'$):

$$\begin{bmatrix} -0.8999765 & -0.8323320 \\ -0.1584315 & 1.215579 \end{bmatrix}$$

The one-electron MO integrals:

$$\begin{bmatrix} -2.615842 & -0.1953882 \\ -0.1953882 & -1.315354 \end{bmatrix}$$

The two-electron MO integrals:

1	1	1	1	0.9595841	(22.6.7.52)
2	1	1	1	0.1953881	(22.6.7.53)
2	1	2	1	0.6062934	(22.6.7.54)
2	2	1	1	0.1261700	(22.6.7.55)
2	2	2	1	0.004625901	(22.6.7.56)
2	2	2	2	0.6159081	(22.6.7.57)

The closed shell Fock energy from formula:

$\left[\sum_k \varepsilon_k + \langle k|h|k \rangle + 2 \langle k|kl|kl \rangle - \langle k|lk|kl \rangle + \sum_{\mu>\nu} \frac{Z_\mu Z_\nu}{R_{\mu\nu}} \right] = -2.84352827$ from formula:

$$\sum_k \varepsilon_k + \langle k|h|k \rangle + \sum_{\mu>\nu} \frac{Z_\mu Z_\nu}{R_{\mu\nu}} = -2.84352827$$

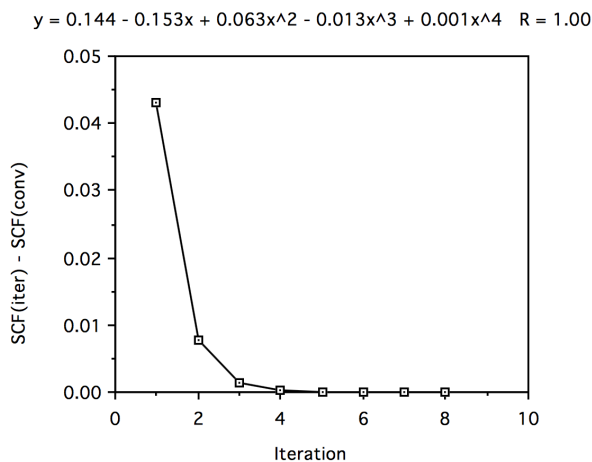
the difference is:

$$0.00000000$$

f. In looking at the energy convergence we see the following:

Iteration	Formula 1	Formula 2
1	-2.84219933	-2.80060530
2	-2.84349298	-2.83573675
3	-2.84353018	-2.84225941
4	-2.84352922	-2.84332418
5	-2.84352779	-2.84349489
6	-2.84352827	-2.84352827
7	-2.84352922	-2.84352827
8	-2.84352827	-2.84352827

f. If you look at the energy difference (SCF at iteration n - SCF converged) and plot this data versus iteration number, and do a 5th order polynomial fit, we see the following:



In looking at the polynomial fit we see that the convergence is primarily linear since the coefficient of the linear term is much larger than those of the cubic and higher terms.

g. The converged SCF total energy calculated using the result of exercise 3 is an upper bound to the ground state energy, but, during the iterative procedure it is not. At convergence, the expectation value of the Hamiltonian for the Hartree Fock determinant is given by the equation in exercise 3.

h. The one- and two- electron integrals in the MO basis are given above (see part e iteration 8). The orbital energies are found using the result of exercise 2 and 3 to be:

$$E(SCF) = \sum_k \varepsilon_k + \langle k|h|k \rangle + \sum_{\mu>\nu} \frac{Z_\mu Z_\nu}{R_{\mu\nu}} \quad (22.6.7.58)$$

$$E(SCF) = \sum_{kl} 2 \langle k|h|k \rangle + 2 \langle kl|kl \rangle - \langle kl|lk \rangle + \sum_{\mu>\nu} \frac{Z_\mu Z_\nu}{R_{\mu\nu}} \quad (22.6.7.59)$$

$$\text{so, } \varepsilon_k = \langle k|h|k \rangle + \sum_1^{occ} (2 \langle kl|kl \rangle - \langle kl|lk \rangle) \quad (22.6.7.60)$$

$$\varepsilon_1 = h_{11} + 2 \langle 11|11 \rangle - \langle 11|11 \rangle \quad (22.6.7.61)$$

$$= -2.615842 + 0.9595841 \quad (22.6.7.62)$$

$$= -1.656258 \quad (22.6.7.63)$$

$$\varepsilon_2 = h_{22} + 2 \langle 21|21 \rangle - \langle 21|12 \rangle \quad (22.6.7.64)$$

$$= -1.315354 + 2 * 0.6062934 - 0.1261700 \quad (22.6.7.65)$$

$$= -0.2289372 \quad (22.6.7.66)$$

i. Yes, the $1\sigma^2$ configuration does dissociate properly because at $R \rightarrow \infty$ the lowest energy state is $\text{He} + H^+$, which also has a $1\sigma^2$ orbital occupancy (i.e., $1s^2$ on He and $1s^0$ on H^+).

1. At convergence the mo coefficients are:

$$\phi_1 = \begin{bmatrix} -0.8999765 \\ -0.1584315 \end{bmatrix} \quad \phi_2 = \begin{bmatrix} -0.8323320 \\ 1.215579 \end{bmatrix}$$

and the integrals in this MO basis are:

$$\begin{aligned} h_{11} &= -2.615842 & h_{21} &= -0.1953882 & h_{22} &= -1.315354 & (22.6.7.67) \\ g_{1111} &= 0.9595841 & g_{2111} &= 0.1953881 & g_{2121} &= 0.6062934 & (22.6.7.68) \\ g_{2211} &= 0.1261700 & g_{2221} &= 0.04625901 & g_{2222} &= 0.6159081 & (22.6.7.69) \end{aligned}$$

a.

$$H = \begin{bmatrix} \langle 1\sigma^2 | H | 1\sigma^2 \rangle & \langle 1\sigma^2 | H | 2\sigma^2 \rangle \\ \langle 2\sigma^2 | H | 1\sigma^2 \rangle & \langle 2\sigma^2 | H | 2\sigma^2 \rangle \end{bmatrix} = \begin{bmatrix} 2h_{11} + g_{1111} & g_{1122} \\ g_{1122} & 2h_{22} + g_{2222} \end{bmatrix} \quad (22.6.7.70)$$

$$= \begin{bmatrix} 2 * -2.615842 + 0.9595841 & 0.1261700 \\ 0.126170 & 2 * -1.315354 + 0.6159081 \end{bmatrix} \quad (22.6.7.71)$$

$$= \begin{bmatrix} -4.272100 & 0.126170 \\ 0.126170 & -2.014800 \end{bmatrix} \quad (22.6.7.72)$$

b. The eigenvalues are $E_1 = -4.279131$ and $E_2 = -2.007770$. The corresponding eigenvectors are:

$$C_1 = \begin{bmatrix} -0.99845123 \\ 0.05563439 \end{bmatrix}, C_2 = \begin{bmatrix} 0.05563438 \\ 0.99845140 \end{bmatrix}$$

c.

$$\frac{1}{2} \left[\left| (\sqrt{a}\phi_1 + \sqrt{b}\phi_2) \alpha (\sqrt{a}\phi_1 - \sqrt{b}\phi_2) \beta \right| + \left| (\sqrt{a}\phi_1 - \sqrt{b}\phi_2) \alpha (\sqrt{a}\phi_1 + \sqrt{b}\phi_2) \beta \right| \right] \quad (22.6.7.73)$$

$$= \frac{1}{2\sqrt{2}} [(\sqrt{a}\phi_1 + \sqrt{b}\phi_2)(\sqrt{a}\phi_1 - \sqrt{b}\phi_2) + (\sqrt{a}\phi_1 - \sqrt{b}\phi_2)(\sqrt{a}\phi_1 + \sqrt{b}\phi_2)] (\alpha\beta - \beta\alpha) \quad (22.6.7.74)$$

$$= \frac{1}{\sqrt{2}} (a\phi_1\phi_1 - b\phi_2\phi_2)(\alpha\beta - \beta\alpha) \quad (22.6.7.75)$$

$$= a|\phi_1\alpha\phi_1\beta| - b|\phi_2\alpha\phi_2\beta|. \quad (\text{note from part b. } a = 0.9984 \text{ and } b = 0.0556) \quad (22.6.7.76)$$

d. The third configuration $|1\sigma 2\sigma\rangle = \frac{1}{\sqrt{2}} [|1\alpha 2\beta\rangle - |1\beta 2\alpha\rangle]$

Adding this configuration to the previous 2x2 CI results in the following 3x3 'full' CI:

$$H = \begin{bmatrix} \langle 1\sigma^2 | H | 1\sigma^2 \rangle & \langle 1\sigma^2 | H | 2\sigma^2 \rangle & \langle 1\sigma^2 | H | 1\sigma 2\sigma \rangle \\ \langle 2\sigma^2 | H | 1\sigma^2 \rangle & \langle 2\sigma^2 | H | 2\sigma^2 \rangle & \langle 2\sigma^2 | H | 1\sigma 2\sigma \rangle \\ \langle 1\sigma 2\sigma | H | 1\sigma^2 \rangle & \langle 2\sigma^2 | H | 1\sigma 2\sigma \rangle & \langle 1\sigma 2\sigma | H | 1\sigma 2\sigma \rangle \end{bmatrix} \quad (22.6.7.77)$$

$$= \begin{bmatrix} 2h_{11} + g_{1111} & g_{1122} & \frac{1}{\sqrt{2}} [2h_{12} + 2g_{2111}] \\ g_{1122} & 2h_{22} + g_{2222} & \frac{1}{\sqrt{2}} [2h_{12} + 2g_{2221}] \\ \frac{1}{\sqrt{2}} [2h_{12} + 2g_{2111}] & \frac{1}{\sqrt{2}} [2h_{12} + 2g_{2221}] & h_{11} + h_{22} + g_{2121} + g_{2211} \end{bmatrix} \quad (22.6.7.78)$$

Evaluating the new matrix elements:

$$H_{12} = H_{21} = \sqrt{2} * (-0.1953882 + 0.1953881) = 0.0 \quad (22.6.7.79)$$

$$H_{23} = H_{32} = \sqrt{2} * (-0.1953882 + 0.004626) = -0.269778 \quad (22.6.7.80)$$

$$H_{33} = -2.615842 - 1.315354 + 0.606293 + 0.126170 \quad (22.6.7.81)$$

$$= -3.198733 \quad (22.6.7.82)$$

$$= \begin{bmatrix} -4.272100 & 0.126170 & 0.0 \\ 0.126170 & -2.014800 & -0.269778 \\ 0.0 & -0.269778 & -3.198733 \end{bmatrix} \quad (22.6.7.83)$$

e. The eigenvalues are $E_1 = -4.279345$, $E_2 = -3.256612$ and $E_3 = -1.949678$. The corresponding eigenvectors are:

$$\begin{bmatrix} -0.99825280 \\ 0.05732290 \\ 0.01431085 \end{bmatrix}, C_2 = \begin{bmatrix} -0.05302767 \\ -0.20969283 \\ -0.9774200 \end{bmatrix}, C_3 = \begin{bmatrix} -0.05302767 \\ -0.97608540 \\ 0.21082004 \end{bmatrix}$$

f.

We need the non-vanishing matrix elements of the dipole operator in the mo basis. These can be obtained by calculating them by hand. They are more easily obtained by using the TRANS program. Put the $1e^-$ ao integrals on disk by running the program RW_INTS. In this case you are inserting $z_{11} = 0.0$, $z_{21} = 0.2854$, and $z_{22} = 1.4$ (insert 0.0 for all the $2e^-$ integrals) ... call the output file "ao_dipole.ints" for example. The converged MO-AO coefficients should be in a file ("mocoefs.dat" is fine). The transformed integrals can be written to a file (name of your choice) for example "mo_dipole.ints". These matrix elements are:

$$Z_{11} = 0.11652690, z_{21} = -0.54420990, z_{22} = 1.49117320$$

The excitation energies are $E_2 - E_1 = -3.256612 - -4.279345 = 1.022733$, and $E_3 - E_1 = -1.949678 - -4.279345 = 2.329667$. Using the Slater-Condon rules to obtain the matrix elements between configurations we get:

$$H_z = \begin{bmatrix} \langle 1\sigma^2 | z | 1\sigma^2 \rangle & \langle 1\sigma^2 | z | 2\sigma^2 \rangle & \langle 1\sigma^2 | z | \sigma 2\sigma \rangle \\ \langle 2\sigma^2 | z | 1\sigma^2 \rangle & \langle 2\sigma^2 | z | 2\sigma^2 \rangle & \langle 2\sigma^2 | z | \sigma 2\sigma \rangle \\ \langle \sigma 2\sigma | z | 1\sigma^2 \rangle & \langle \sigma 2\sigma | z | 2\sigma^2 \rangle & \langle \sigma 2\sigma | z | \sigma 2\sigma \rangle \end{bmatrix} \quad (22.6.7.84)$$

$$= \begin{bmatrix} 2z_{11} & 0 & \frac{1}{\sqrt{2}}[2z_{12}] \\ 0 & 2z_{22} & \frac{1}{\sqrt{2}}[2z_{12}] \\ \frac{1}{\sqrt{2}}[2z_{12}] & \frac{1}{\sqrt{2}}[2z_{12}] & z_{11} + z_{22} \end{bmatrix} \quad (22.6.7.85)$$

$$\begin{bmatrix} 0.233054 & 0 & -0.769629 \\ 0 & 2.982346 & -0.769629 \\ -0.769629 & -0.769629 & 1.607700 \end{bmatrix} \quad (22.6.7.86)$$

Now, $\langle \Psi_1 | z | \Psi_2 \rangle = C_1^T H_z C_2$, (this can be accomplished with the program UTMATU)

$$= \begin{bmatrix} -0.99825280 \\ 0.05732290 \\ 0.01431085 \end{bmatrix}^T \begin{bmatrix} 0.233054 & 0 & -0.769629 \\ 0 & 2.982346 & -0.769629 \\ -0.769629 & -0.769629 & 1.607700 \end{bmatrix} \begin{bmatrix} -0.02605343 \\ -0.20969283 \\ -0.9774200 \end{bmatrix} \quad (22.6.7.87)$$

$$= -0.757494 \quad (22.6.7.88)$$

and, $\langle \Psi_1 | z | \Psi_3 \rangle = C_1^T H_z C_3$

$$= \begin{bmatrix} -0.99825280 \\ 0.05732290 \\ 0.01431085 \end{bmatrix}^T \begin{bmatrix} 0.233054 & 0 & -0.769629 \\ 0 & 2.982346 & -0.769629 \\ -0.769629 & -0.769629 & 1.607700 \end{bmatrix} \begin{bmatrix} -0.05302767 \\ -0.97698540 \\ 0.21082004 \end{bmatrix} \quad (22.6.7.89)$$

g.

Using the converged coefficients the orbital energies obtained from solving the Fock equations are $\varepsilon_1 = -1.656258$ and $\varepsilon_2 = -0.228938$. The resulting expression for the RSPT first-order wavefunction becomes:

$$|1\sigma^2\rangle^{(1)} = -\frac{g_{2211}}{2(\varepsilon_2 - \varepsilon_1)} |2\sigma^2\rangle \quad (22.6.7.90)$$

$$|1\sigma^2\rangle^{(1)} = -\frac{0.126170}{2(-0.228938 + 1.656258)} |2\sigma^2\rangle \quad (22.6.7.91)$$

$$|1\sigma^2\rangle^{(1)} = -0.0441982 |2\sigma^2\rangle \quad (22.6.7.92)$$

h. As you can see from part c., the matrix element $\langle 1\sigma^2 | H | 1\sigma 2\sigma \rangle = 0$ (this is also a result of the Brillouin theorem) and hence this configuration does not enter into the first-order wavefunction.

i.

$$|0\rangle = |1\sigma^2\rangle - 0.0441982 |2\sigma^2\rangle. \text{ To normalize we divide by:} \quad (22.6.7.93)$$

$$\sqrt{1 + (0.0441982)^2} = 1.0009762 \quad (22.6.7.94)$$

$$|0\rangle = 0.999025 |1\sigma^2\rangle - 0.044155 |2\sigma^2\rangle \quad (22.6.7.95)$$

In the 2x2 CI we obtained:

$$|0\rangle = 0.99845123 |1\sigma^2\rangle - 0.05563439 |2\sigma^2\rangle \quad (22.6.7.96)$$

j. The expression for the 2nd order RSPT is:

$$E^{(2)} = -\frac{|g_{2211}|^2}{2(\varepsilon_2 - \varepsilon_1)} = -\frac{0.126170^2}{2(-0.228938 + 1.656258)} \quad (22.6.7.97)$$

$$= -0.005576 \text{ au} \quad (22.6.7.98)$$

Comparing the 2x2 CI energy obtained to the SCF result we have:

$$-4.279131 - (-4.272102) = -0.007029 \text{ au}$$

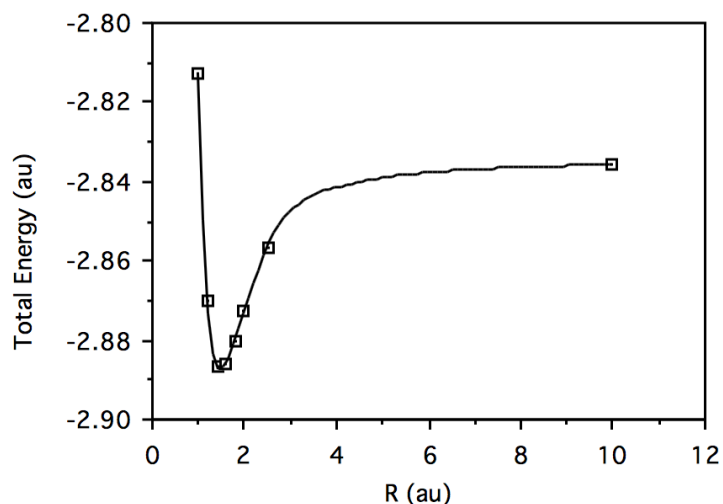
2.	STO total energy:	-2.8435283	(22.6.7.99)
	STO3G total energy	-2.8340561	(22.6.7.100)
	3-21G total energy	-2.8864405	(22.6.7.101)

The STO3G orbitals were generated as a best fit of 3 primitive gaussians (giving 1 CGTO) to the STO. So, STO3G can at best reproduce the STO result. The 3-21G orbitals are more flexible since there are 2 CGTOs per atom. This gives 4 orbitals (more parameters to optimize) and a lower total energy.

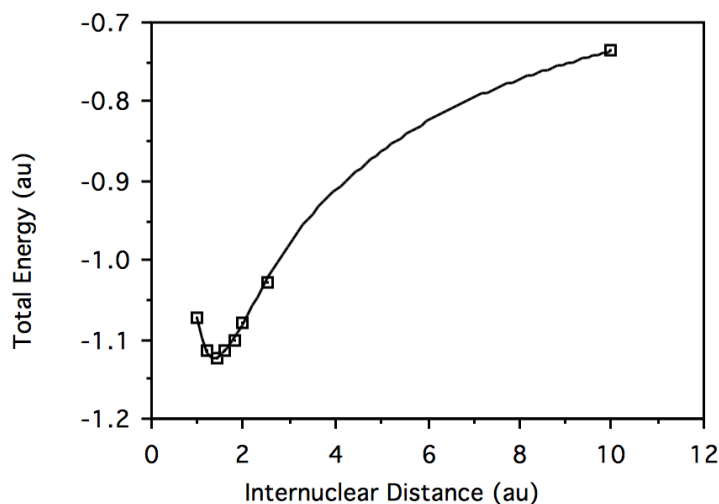
3.	R	HeH ⁺ Energy	H ₂ Energy

1.0	-2.812787056	-1.071953297
1.2	-2.870357513	-1.113775015
1.4	-2.886440516	-1.122933507
1.6	-2.886063576	-1.115567684
1.8	-2.880080938	-1.099872589
2.0	-2.872805595	-1.080269098
2.5	-2.856760263	-1.026927710
10.0	-2.835679293	-0.7361705303

Plotting total energy vs. geometry for HeH^+ :



Plotting total energy vs. geometry for H_2 :



For HeH^+ at $R = 10.0$ au, the eigenvalues of the converged Fock matrix and the corresponding converged MO-AO coefficients are:

$-0.1003571E+01$	$-0.4961988E+00$	$0.5864846E+00$	$0.1981702E+01$	(22.6.7.102)
$0.4579189E+00$	$-0.8245406E-05$	$0.1532163E-04$	$0.1157140E+01$	(22.6.7.103)
$0.6572777E+00$	$-0.4580946E-05$	$-0.6822942E-05$	$-0.1056716E+01$	(22.6.7.104)
$-0.1415438E-05$	$0.3734069E+00$	$0.1255539E+01$	$-0.1669342E-04$	(22.6.7.105)
$0.11127780.71732444E+00$		$-0.1096019E010.2031348E-04$		(22.6.7.106)

Notice that this indicates that orbital 1 is a combination of the s functions on He only (dissociating properly to $He + H^+$).

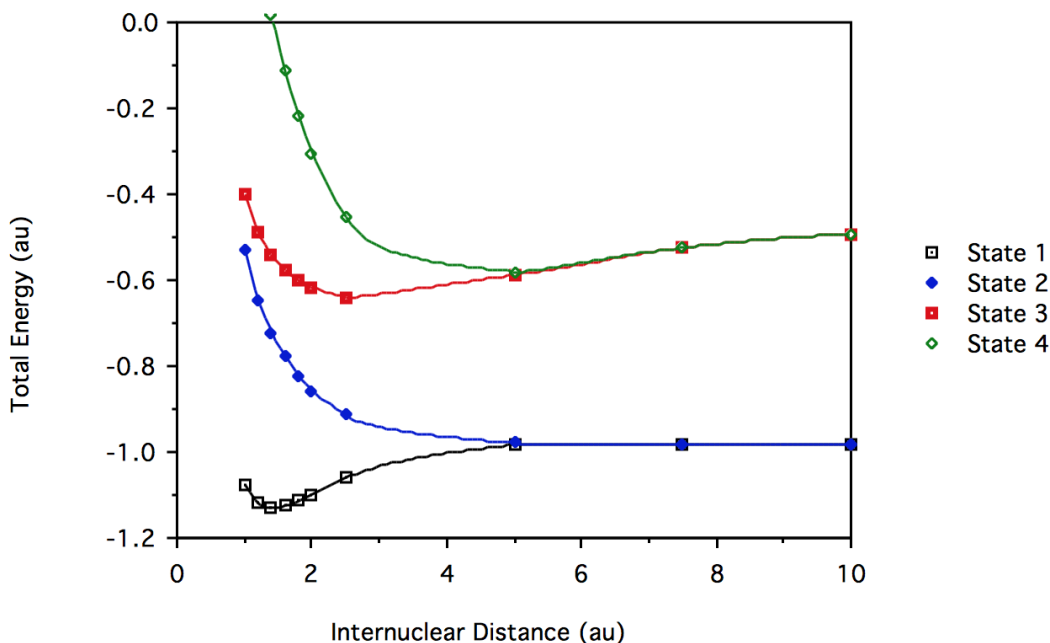
For H_2 at $R = 10.0$ au, the eigenvalues of the converged Fock matrix and the corresponding converged MO-AO coefficients are:

$-0.2458041E+00$	$-0.1456223E+00$	$0.1137235E+01$	$0.1137825E+01$	(22.6.7.107)
$0.1977649E+00$	$-0.1978204E+00$	$0.1006458E+01$	$-0.7903225E+00$	(22.6.7.108)
$0.56325666E+00$	$-0.5628273E+00$	$-0.8179120E+00$	$0.6424941E+00$	(22.6.7.109)
$0.1976312E+00$	$0.1979216E+00$	$0.7902887E+00$	$0.1006491E+01$	(22.6.7.110)
$0.5629326E+00$	$0.5631776E+00$	$-0.6421731E+00$	$-0.6421731E+00$	$-0.8181460E+00$ (22.6.7.111)

Notice that this indicates that the orbital 1 is a combination of the s functions on both H atoms (dissociating improperly; equal probabilities of H_2 dissociating to two neutral atoms or to a proton plus hydride ion).

1. The H_2 CI result"

R	$^1 \sum_g^+$	$^3 \sum_u^+$	$^1 \sum_u^+$	$^1 \sum_g^+$
1.0	-1.074970	-0.5323429	-0.3997412	0.3841676
1.2	-1.118442	-0.6450778	-0.4898805	0.1763018
1.4	-1.129904	-0.7221781	-0.5440346	0.0151913
1.6	-1.125582	-0.7787328	-0.5784428	-0.1140074
1.8	-1.113702	-0.8221166	-0.6013855	-0.2190144
2.0	-1.098676	-0.8562555	-0.6172761	-0.3044956
2.5	-1.060052	-0.9141968	-0.6384557	-0.4530645
5.0	-0.9835886	-0.9790545	-0.5879662	-0.5802447
7.5	-0.9806238	-0.9805795	-0.5247415	-0.5246646
10.0	-0.989598	-0.9805982	-0.4914058	-0.4913532



For H_2 at $R = 1.4$ au, the eigenvalues of the Hamiltonian matrix and the corresponding determinant amplitudes are:

determinant	-1.129904	-0.722178	-0.544035	0.015191
$ 1\sigma_g\alpha 1\sigma_g\beta $	0.99695	0.00000	0.00000	0.07802
$ 1\sigma_g\beta 1\sigma_u\alpha $	0.00000	0.70711	0.70711	0.00000
$ 1\sigma_g\alpha 1\sigma_u\beta $	0.00000	0.70711	-0.70711	0.00000
$ \sigma_u\alpha 1\sigma_u\beta $	-0.07802	0.00000	0.00000	0.99695

This shows, as expected, the mixing of the first $^1 \sum_g^+ (1\sigma_g^2)$ and the 2nd $^1 \sum_g^+ (1\sigma_u^2)$ determinants, the

$$^3 \sum_u^+ = \left(\frac{1}{\sqrt{2}} (|1\sigma_g\beta 1\sigma_u\alpha| + |1\sigma_g\alpha 1\sigma_u\beta|) \right),$$

$$\text{and the } {}^1\sum_u^+ = \left(\frac{1}{\sqrt{2}} (|\sigma_g\beta 1\sigma_u\alpha| - |\sigma_g\alpha 1\sigma_u\beta|) \right).$$

Also notice that the ${}^1\sum_g^+$ state is the bonding (0.99695 - 0.07802) combination (note specifically the + - combination) and the second ${}^1\sum_g^+$ state is the antibonding combination (note specifically the + + combination). The + + combination always gives a higher energy than the + - combination. Also notice that the 1st and 2nd states (${}^1\sum_g^+$ and ${}^3\sum_u^+$) are dissociating to proton/anion combinations. The difference in these energies is the ionization potential of H minus the electron affinity of H.

This page titled [22.6.7: vi. Problem Solutions](#) is shared under a [CC BY-NC-SA 4.0](#) license and was authored, remixed, and/or curated by [Jack Simons](#) via [source content](#) that was edited to the style and standards of the LibreTexts platform.

Index

A

Atomic Configuration Wavefunctions

[10.5: Atomic Configuration Wavefunctions](#)

atomic term symbols

[10.3: Coupling of Angular Momenta](#)

[10.4: Atomic Term Symbols and Wavefunctions](#)

atomic units

[17.4: Atomic Units](#)

B

Brillouin Theorem

[18.7: Observations on Orbitals and Orbital Energies](#)

C

configuration interaction

[19.2: Different Methods](#)

Configuration Interaction Method

[19.4: Further Details on Implementing Multiconfigurational Methods](#)

D

Density Functional Theory

[19.4: Further Details on Implementing Multiconfigurational Methods](#)

E

exchange correlation potential

[19.4: Further Details on Implementing Multiconfigurational Methods](#)

F

Fermi energy

[19.4: Further Details on Implementing Multiconfigurational Methods](#)

Fock equations

[18.1: Optimization of the Energy for a Multiconfiguration Wavefunction](#)

Fock operator

[18.2: The Single-Determinant Wavefunction](#)

H

Hessian

[20.1: Calculations of Properties Other Than the Energy](#)

I

integrated density of states

[19.4: Further Details on Implementing Multiconfigurational Methods](#)

K

Koopmans' Theorem

[18.7: Observations on Orbitals and Orbital Energies](#)

L

LCAO

[18.5: The LCAO-MO Expansion](#)

LS Coupling

[10.4: Atomic Term Symbols and Wavefunctions](#)

M

MCSCF method

[19.4: Further Details on Implementing Multiconfigurational Methods](#)

O

Orbital Correlation Diagram

[6.2: Orbital Correlation Diagrams - Origins of the Woodward-Hoffmann Rules](#)

Orbital Energies

[18.7: Observations on Orbitals and Orbital Energies](#)

P

perturbation theory

[2.2: Perturbation Theory](#)

R

reference function

[19.4: Further Details on Implementing Multiconfigurational Methods](#)

reference space

[19.4: Further Details on Implementing Multiconfigurational Methods](#)

S

Schrödinger equation

[1.3: The Schrödinger Equation](#)

secular equations

[18.1: Optimization of the Energy for a Multiconfiguration Wavefunction](#)

Slater determinant wavefunction

[18.2: The Single-Determinant Wavefunction](#)

spin contamination

[19.1: Introduction to Multi-Determinant Wavefunctions](#)

Spin Impurity Problem

[18.3: The Unrestricted Hartree-Fock Spin Impurity Problem](#)

T

Time Correlation Functions

[15.4: Time Correlation Function Expressions for Transition Rates](#)

V

Vector Coupling

[10.3: Coupling of Angular Momenta](#)

W

Weizsacker correction

[19.4: Further Details on Implementing Multiconfigurational Methods](#)

Glossary

Sample Word 1 | Sample Definition 1

Detailed Licensing

Overview

Title: [Quantum Mechanics in Chemistry \(Simons and Nichols\)](#)

Webpages: 163

Applicable Restrictions: Noncommercial

All licenses found:

- [CC BY-NC-SA 4.0](#): 94.5% (154 pages)
- [Undeclared](#): 5.5% (9 pages)

By Page

- [Quantum Mechanics in Chemistry \(Simons and Nichols\) - CC BY-NC-SA 4.0](#)
 - [Front Matter - Undeclared](#)
 - [TitlePage - Undeclared](#)
 - [InfoPage - Undeclared](#)
 - [Table of Contents - Undeclared](#)
 - [Licensing - Undeclared](#)
 - [1: The Basic Tools of Quantum Mechanics - CC BY-NC-SA 4.0](#)
 - [1.1: Operators - CC BY-NC-SA 4.0](#)
 - [1.2: Wavefunctions - CC BY-NC-SA 4.0](#)
 - [1.3: The Schrödinger Equation - CC BY-NC-SA 4.0](#)
 - [1.4: Free-Particle Motion in Two Dimensions - CC BY-NC-SA 4.0](#)
 - [1.5: Particles in Boxes - CC BY-NC-SA 4.0](#)
 - [1.6: One Electron Moving About a Nucleus - CC BY-NC-SA 4.0](#)
 - [1.7: Harmonic Vibrational Motion - CC BY-NC-SA 4.0](#)
 - [1.8: Rotational Motion for a Rigid Diatomic Molecule - CC BY-NC-SA 4.0](#)
 - [1.9: The Physical Relevance of Wavefunctions, Operators and Eigenvalues - CC BY-NC-SA 4.0](#)
 - [2: Approximation Methods - CC BY-NC-SA 4.0](#)
 - [2.E: Approximation Methods \(Exercises\) - CC BY-NC-SA 4.0](#)
 - [2.1: The Variational Method - CC BY-NC-SA 4.0](#)
 - [2.2: Perturbation Theory - CC BY-NC-SA 4.0](#)
 - [3: Nuclear Motion - CC BY-NC-SA 4.0](#)
 - [3.E: Exercises - CC BY-NC-SA 4.0](#)
 - [3.1: The Born-Oppenheimer Separation of Electronic and Nuclear Motions - CC BY-NC-SA 4.0](#)
 - [3.2: Time Scale Separation - CC BY-NC-SA 4.0](#)
 - [3.3: Vibration/Rotation States for Each Electronic Surface - CC BY-NC-SA 4.0](#)
 - [3.4: Rotation and Vibration of Diatomic Molecules - CC BY-NC-SA 4.0](#)
 - [3.5: Separation of Vibration and Rotation - CC BY-NC-SA 4.0](#)
 - [3.6: The Rigid Rotor and Harmonic Oscillator - CC BY-NC-SA 4.0](#)
 - [3.7: The Morse Oscillator - CC BY-NC-SA 4.0](#)
 - [3.8: Rotation of Polyatomic Molecules - CC BY-NC-SA 4.0](#)
 - [3.9: Rotation of Linear Molecules - CC BY-NC-SA 4.0](#)
 - [3.10: Rotation of Non-Linear Molecules - CC BY-NC-SA 4.0](#)
 - [3.11: Chapter Summary - CC BY-NC-SA 4.0](#)
 - [4: Atomic Orbitals - CC BY-NC-SA 4.0](#)
 - [4.1: Shapes of Atomic Orbitals - CC BY-NC-SA 4.0](#)
 - [4.2: Directions of Atomic Orbitals - CC BY-NC-SA 4.0](#)
 - [4.3: Sizes and Energies - CC BY-NC-SA 4.0](#)
 - [5: Molecular Orbitals - CC BY-NC-SA 4.0](#)
 - [5.1: Orbital Interaction Topology - CC BY-NC-SA 4.0](#)
 - [5.2: Orbital Symmetry - CC BY-NC-SA 4.0](#)
 - [5.3: Linear Molecules - CC BY-NC-SA 4.0](#)
 - [5.4: Atoms - CC BY-NC-SA 4.0](#)
 - [6: Quantum Mechanics in Reactions - CC BY-NC-SA 4.0](#)
 - [6.1: Reduction in Symmetry Along Reaction Paths - CC BY-NC-SA 4.0](#)
 - [6.2: Orbital Correlation Diagrams - Origins of the Woodward-Hoffmann Rules - CC BY-NC-SA 4.0](#)
 - [7: Further Characterization of Molecular Orbitals - CC BY-NC-SA 4.0](#)
 - [7.1: The LCAO-MO Expansion and the Orbital-Level Schrödinger Equation - CC BY-NC-SA 4.0](#)
 - [7.2: Determining the Effective Potential - CC BY-NC-SA 4.0](#)
 - [7.3: The Hückel Parameterization - CC BY-NC-SA 4.0](#)
 - [7.4: The Extended Hückel Method - CC BY-NC-SA 4.0](#)
 - [8: Electronic Configurations - CC BY-NC-SA 4.0](#)

- 8.1: Orbitals Do Not Provide the Complete Picture; Their Occupancy By the N Electrons Must Be Specified - CC BY-NC-SA 4.0
- 8.2: Even N-Electron Configurations are Not Mother Nature's True Energy States - CC BY-NC-SA 4.0
- 8.3: Mean-Field Models - CC BY-NC-SA 4.0
- 8.4: Configuration Interaction (CI) Describes the Correct Electronic States - CC BY-NC-SA 4.0
- 8.5: Summary - CC BY-NC-SA 4.0
- 9: Symmetry of Electronic Wavefunctions - CC BY-NC-SA 4.0
 - 9.1: Electronic Configurations - CC BY-NC-SA 4.0
 - 9.2: Antisymmetric Wavefunctions - CC BY-NC-SA 4.0
- 10: Angular Momentum and Group Symmetries of Electronic Wavefunctions - CC BY-NC-SA 4.0
 - 10.1: Angular Momentum Symmetry and Strategies for Angular Momentum Coupling - CC BY-NC-SA 4.0
 - 10.2: Electron Spin Angular Momentum - CC BY-NC-SA 4.0
 - 10.3: Coupling of Angular Momenta - CC BY-NC-SA 4.0
 - 10.4: Atomic Term Symbols and Wavefunctions - CC BY-NC-SA 4.0
 - 10.5: Atomic Configuration Wavefunctions - CC BY-NC-SA 4.0
 - 10.6: Inversion Symmetry - CC BY-NC-SA 4.0
 - 10.7: Review of Atomic Cases - CC BY-NC-SA 4.0
- 11: Evaluating the Matrix Elements of N-electron Wavefunctions - CC BY-NC-SA 4.0
 - 11.5: Evaluating the Matrix Elements of N-electron Wavefunctions (Summary) - CC BY-NC-SA 4.0
 - 11.1: Configuration State Functions can Express the Full N-Electron Wavefunction - CC BY-NC-SA 4.0
 - 11.2: The Slater-Condon Rules Give Expressions for the Operator Matrix Elements Among the CSFs - CC BY-NC-SA 4.0
 - 11.3: The Slater-Condon Rules - CC BY-NC-SA 4.0
 - 11.4: Examples of Applying the Slater-Condon Rules - CC BY-NC-SA 4.0
- 12: Quantum Mechanical Picture of Bond Making and Breaking Reactions - CC BY-NC-SA 4.0
 - 12.1: Concepts of Configuration and State Energies - CC BY-NC-SA 4.0
 - 12.2: Mixing of Covalent and Ionic Configurations - CC BY-NC-SA 4.0
 - 12.3: Various Types of Configuration Mixing - CC BY-NC-SA 4.0
- 13: Molecular Rotation and Vibration - CC BY-NC-SA 4.0
 - 13.1: Rotational Motions of Rigid Molecules - CC BY-NC-SA 4.0
 - 13.2: Vibrational Motion Within the Harmonic Approximation - CC BY-NC-SA 4.0
 - 13.3: Anharmonicity - CC BY-NC-SA 4.0
- 14: Time-dependent Quantum Dynamics - CC BY-NC-SA 4.0
 - 14.1: Time-Dependent Vector Potentials - CC BY-NC-SA 4.0
 - 14.2: Time-Dependent Perturbation Theory - CC BY-NC-SA 4.0
 - 14.3: Application to Electromagnetic Perturbations - CC BY-NC-SA 4.0
 - 14.4: The "Long-Wavelength" Approximation - CC BY-NC-SA 4.0
 - 14.5: The Kinetics of Photon Absorption and Emission - CC BY-NC-SA 4.0
- 15: Spectroscopy - CC BY-NC-SA 4.0
 - 15.1: Rotational Transitions - CC BY-NC-SA 4.0
 - 15.2: Vibration-Rotation Transitions - CC BY-NC-SA 4.0
 - 15.3: Electronic-Vibration-Rotation Transitions - CC BY-NC-SA 4.0
 - 15.4: Time Correlation Function Expressions for Transition Rates - CC BY-NC-SA 4.0
- 16: Collisions and Scattering - CC BY-NC-SA 4.0
 - 16.1: One Dimensional Scattering - CC BY-NC-SA 4.0
 - 16.2: Multichannel Problems - CC BY-NC-SA 4.0
 - 16.3: Classical Treatment of Nuclear Motion - CC BY-NC-SA 4.0
 - 16.4: Wavepackets - CC BY-NC-SA 4.0
- 17: Higher Order Corrections to Electronic Structure - CC BY-NC-SA 4.0
 - 17.1: Orbitals, Configurations, and the Mean-Field Potential - CC BY-NC-SA 4.0
 - 17.2: Electron Correlation Requires Moving Beyond a Mean-Field Model - CC BY-NC-SA 4.0
 - 17.3: Moving from Qualitative to Quantitative Models - CC BY-NC-SA 4.0
 - 17.4: Atomic Units - CC BY-NC-SA 4.0
- 18: Multiconfiguration Wavefunctions - CC BY-NC-SA 4.0
 - 18.1: Optimization of the Energy for a Multiconfiguration Wavefunction - CC BY-NC-SA 4.0
 - 18.2: The Single-Determinant Wavefunction - CC BY-NC-SA 4.0
 - 18.3: The Unrestricted Hartree-Fock Spin Impurity Problem - CC BY-NC-SA 4.0
 - 18.4: Atomic Orbital Basis Sets - CC BY-NC-SA 4.0

- 18.5: The LCAO-MO Expansion - CC BY-NC-SA 4.0
- 18.6: The Roothaan Matrix SCF Process - CC BY-NC-SA 4.0
- 18.7: Observations on Orbitals and Orbital Energies - CC BY-NC-SA 4.0
- 19: Multi-Determinant Wavefunctions - CC BY-NC-SA 4.0
 - 19.1: Introduction to Multi-Determinant Wavefunctions - CC BY-NC-SA 4.0
 - 19.2: Different Methods - CC BY-NC-SA 4.0
 - 19.3: Strengths and Weaknesses of Various Methods - CC BY-NC-SA 4.0
 - 19.4: Further Details on Implementing Multiconfigurational Methods - CC BY-NC-SA 4.0
- 20: Response Theory - CC BY-NC-SA 4.0
 - 20.1: Calculations of Properties Other Than the Energy - CC BY-NC-SA 4.0
 - 20.2: Ab Initio, Semi-Empirical, and Empirical Force Field Methods - CC BY-NC-SA 4.0
- 21: Problem Sets - CC BY-NC-SA 4.0
- 22: Problems - CC BY-NC-SA 4.0
 - 22.1: The Basic Tools of Quantum Mechanics - CC BY-NC-SA 4.0
 - 22.1.1: i. Review Exercises - CC BY-NC-SA 4.0
 - 22.1.2: ii. Exercises - CC BY-NC-SA 4.0
 - 22.1.3: iii. Problems 1-10 - CC BY-NC-SA 4.0
 - 22.1.4: iv. Problems 11-18 - CC BY-NC-SA 4.0
 - 22.1.5: v. Review Exercise Solutions - CC BY-NC-SA 4.0
 - 22.1.6: vi. Exercise Solutions - CC BY-NC-SA 4.0
 - 22.2: Simple Molecular Orbital Theory - CC BY-NC-SA 4.0
 - 22.2.1: i. Review Exercises - CC BY-NC-SA 4.0
 - 22.2.2: ii. Exercises - CC BY-NC-SA 4.0
 - 22.2.3: iii. Problems - CC BY-NC-SA 4.0
 - 22.2.4: iv. Review Exercises Solutions - CC BY-NC-SA 4.0
 - 22.2.5: v. Exercise Solution - CC BY-NC-SA 4.0
 - 22.2.6: vi. Problem Solutions - CC BY-NC-SA 4.0
- 22.3: Electronic Configurations, Term Symbols, and States - CC BY-NC-SA 4.0
 - 22.3.1: i. Review Exercises - CC BY-NC-SA 4.0
 - 22.3.2: ii. Exercises - CC BY-NC-SA 4.0
 - 22.3.3: iii. Problems - CC BY-NC-SA 4.0
 - 22.3.4: iv. Review Exercise Solutions - CC BY-NC-SA 4.0
 - 22.3.5: v. Exercise Solutions - CC BY-NC-SA 4.0
 - 22.3.6: vi. Problem Solutions - CC BY-NC-SA 4.0
- 22.4: Molecular Rotation and Vibration - CC BY-NC-SA 4.0
 - 22.4.1: i. Exercises - CC BY-NC-SA 4.0
 - 22.4.2: ii. Problems - CC BY-NC-SA 4.0
 - 22.4.3: iii. Exercise Solutions - CC BY-NC-SA 4.0
 - 22.4.4: iv. Problem Solutions - CC BY-NC-SA 4.0
- 22.5: Time Dependent Processes - CC BY-NC-SA 4.0
 - 22.5.1: i. Exercises - CC BY-NC-SA 4.0
 - 22.5.2: ii. Problems - CC BY-NC-SA 4.0
 - 22.5.3: iii. Exercise Solutions - CC BY-NC-SA 4.0
 - 22.5.4: iv. Problem Solutions - CC BY-NC-SA 4.0
- 22.6: More Quantitative Aspects of Electronic Structure Calculations - CC BY-NC-SA 4.0
 - 22.6.1: i. Review Exercises - CC BY-NC-SA 4.0
 - 22.6.2: i. Review Exercises - CC BY-NC-SA 4.0
 - 22.6.3: ii. Exercises - CC BY-NC-SA 4.0
 - 22.6.4: iii. Problems - CC BY-NC-SA 4.0
 - 22.6.5: iv. Review Exercise Solutions - CC BY-NC-SA 4.0
 - 22.6.6: v. Exercise Solutions - CC BY-NC-SA 4.0
 - 22.6.7: vi. Problem Solutions - CC BY-NC-SA 4.0
- Back Matter - *Undeclared*
 - Index - *Undeclared*
 - Glossary - *Undeclared*
 - Detailed Licensing - *Undeclared*